DEFORMATION OF PARTIALLY PRESTRESSED CONCRETE BEAMS UNDER SERVICE LOADS

by

KUAN HONG LEE

A thesis submitted in accordance with the requirements

for the Degree of Doctor of Philosophy

Department of Civil Engineering

The University of Leeds

July, 1984

To my parents

Acknowledgements

I gratefully acknowledge the facilities provided for this investigation by Professor A.R. Cusens, Head of Civil Engineering Department at the University of Leeds. I am also indebted to Dr. E.W. Bennett for his constructive criticism, encouragement and helpful supervision throughout the course of this research.

I would also like to express my thanks to: the Technical Staff for their assistance in the preparation of tests, my friends, Dr. C.J. Tay and Mr. K.Y Chu for their help during the experiment.

I would like to extend my sincere thanks to my friend, Mr. H.S. Lai for his ready assistance, from the tests to the preparation of this thesis, in this three years of research. I also thank Mrs. V. Grant for typing part of this thesis and Mr. Duxbury for taking the photographs.

I am also indebted to my parents, brothers and sisters for their encouragement and support.

The scholarship provided by the University of Leeds is also gratefully acknowledged.

K.H. Lee (Leeds)

ABSTRACT

Nine tests were carried out on partially prestressed concrete beams in which 50 per cent of the service load was sustained for a period of up to 46 days during which time the load was increased to the full service load up to seven times in intermittent short-term cycles. One cycle of short-term loading was carried out at intervals of about five days. Three additional beams were tested under the sustained load alone.

An analytical method was developed for calculating short-term deflection of cracked prestressed concrete members by integration of the curvature, using the recommendation in CP110 Appendix A to take account of the "tension stiffening" effect of the concrete between cracks. This was extended to predict long-term deflection by considering the effect of creep and shrinkage in the analysis of the cracked sections.

A separate section of the thesis describes a comparative study of three alternative partial prestressing parameters: Hypothetical tensile stress, Degree of Prestress and Partial Prestressing Ratio. The relationship of each of these parameters to the serviceability criteria was considered. The Degree of Prestress was concluded to be the most suitable parameter for design purposes and a suitable design approach is recommended.

TABLE OF CONTENTS

NOTATIONS

A_c	Area of concrete
A_p	Area of prestressing tendon
A_s	Area of non-prestressed tension reinforcement
A_{eq}	Equivalent area of prestressed steel having strength equal to the combined strength of the prestressing tendons and non-prestressed tension reinforcement
a	Deflection
b	Breadth of upper flange
b_i	Breadth of lower flange
b_w	Breadth of web
b_1	$b_1 = (1 - b_w/b)$
b_2	$b_2 = (b_i/b - b_w/b)$
c_c	Creep coefficient
DEG	Degree of Prestress
d	Effective depth of tension reinforcement
d_p	Effective depth of tendons
d_s	Effective depth of non-prestressed tension reinforcement
d_1	$d_1 = 3d/h$
d_2	$d_2 = d_p/h$
d_3	$d_3 = d_{s/h}$
e	Eccentricity of prestressing force with respect to centroid of concrete section
E_c	Modulus of elasticity of concrete
E_s	Modulus of elasticity of steel
F	Load or force generally
F_{se}	Total effective force in non-prestressed tension reinforcement after losses
f_a	Increase of stress from the point of decompression, at the level of soffit

f_c	Concrete stress at the top surface generally
f_{cp}	Effective prestress in concrete at the level of tendon
f_{cr}	Stress in non-prestressed reinforcement in a cracked section immediately after cracking
f_{cs}	Effective prestress in concrete at the level of non-prestressed reinforcement
f_{cu}	Compressive strength of concrete
f_{c1}	Concrete stress at top surface under instantaneous load
f_{c2}	Final concrete stress at top surface under sustained loading
f_{inf}	Effective prestress in concrete at the soffit
f_{pe}	Effective prestress in tendon
f_{pu}	Ultimate stress of tendons
f_{se}	Effective stress in non-prestressed steel
f_{s2}	Total increase of stress in tendons under sustained loading
f_{s2}''	Total increase of stress in non-prestressed reinforcement under sustained loading
f_{tc}	Concrete tensile strength - modulus of rupture
f_t	Split cylinder concrete tensile strength
f_y	Yield stress of non-prestressed steel
Hyp	Hypothetical tensile stress
h	Overall depth of section
h_b	Thickness of bottom flange
h_f	Thickness of upper flange
h_1	$h_1 = h_{f/h}$
h_2	$h_2 = h_{b/h}$
I_{cr}	Second moment of area of a cracked section
I_g	Second moment of area of an uncracked concrete section
L	Span of the beam
M	Bending moment generally

M_{cr}	Cracking moment
M_d	Moment causing decompression at the soffit
M_{g+q}	Bending moment due to live and dead loads (service moment)
M_{max}	Maximum bending moment
M_{min}	Minimum moment acting on a prestressed section
M_{rep}	Repeated load
M_u	Ultimate bending moment generally
$(M_u)_p$	Ultimate moment of resistance contributed by tendons alone
$(M_u)_{p+s}$	Ultiment of resistance provided by prestressed and non-prestressed reinforcement
P	Load generally
P_{cr}	Cracking load
P_e	Total effective force in tendons after losses
P_{rep}	Repeated load
PPR	Partial prestressing ratio
P_u	Ultimate load
x	Depth of neutral axis generally
x_1	Initial depth of stress/strain neutral axis under instantaneous load
x_2	Final depth of stress neutral axis under long-term loading
x_3	Final depth of strain neutral axis under long-term loading
Z_{inf}	Section modulus for lowest (inferior) point in concrete section
z'	Depth of the centroid of the compression force in concrete
α	Modular ratio of steel to concrete
β	Curvature distribution coefficient
ϵ_{cs}	Concrete shrinkage strain

ε_{sm}	Average steel strain
ξ	$\xi = x/h$
ρ_p	$\rho_p = A_p/bh$
ρ_s	$\rho_s = A_s/bh$

Abbreviations:

ACI	American Concrete Institute
CEB	Comité Euro-International du Béton
BS CP110	Code of Practice CP110: 1972
FIP	Federation International de la Precontrainte

LIST OF TABLES

PART I

GENERAL INTRODUCTION AND REVIEW OF PREVIOUS WORKS

CHAPTER ONE

Introduction

1.1 General

The development of reinforced concrete was based on the concept of combining two materials, with concrete which is strong in compression resisting the compressive stresses and steel resisting the tensile stresses. Prestressed concrete was later introduced by Freyssinet as a new material which put concrete into precompression by tensioning steel, so that it could resist both the tensile and compressive stresses. He thus formulated the design criterion of permitting no tensile stress in the concrete. Emperger and Abeles advocated a third method of combining concrete and steel in which limited tensile stresses or even hair cracks would be permitted in concrete, which Abeles termed "Partially Prestressed Concrete" to distinguish it from "fully prestressed concrete".

Partially prestressed concrete, therefore, occupies the complete spectrum between the two extremes. The conventional reinforced concrete in which none of the reinforcement is prestressed represents one extreme while the other extreme, commonly known as "fully prestressed" concrete, consists of reinforcement all of which is prestressed.

Decades have gone by since the development of

prestressed concrete by Freyssinet. More and more partially prestressed concrete structures have been built. Today, partial prestressing is accepted world wide, at least implicitly, in most of the engineering codes of practice (6,17,36,57,62) and a number of prominent researchers have already drawn attention to its potential (8,14,18,60,61).

1.2 Classification of Concrete Structures

In most of the current codes of practice, concrete structures are divided into several classes or types on the basis of either the nominal concrete tensile stresses at service load or the incremental reinforcement stresses. In the current British Code CP110 (6), the classification comprises the following categories:

Class 1 : Prestressed concrete in which no tensile stresses are permitted in concrete under service load,

Class 2 : Prestressed concrete in which limited tensile stresses less than the concrete tensile strength are permitted under service load,

Class 3 : Prestressed concrete in which cracks of limited width are permitted and

Class 4 : Conventional reinforced concrete without prestressed reinforcement in which cracks of limited width are permitted under service load.

Class 2 and Class 3 members, particularly the latter, are referred to as partially prestressed. In the present study, the main concern is with Class 3 structures.

1.3 Advantages and Disadvantages of Partial Prestressing

The availability of a wider range of stresses at the critical points in partially prestressed concrete members, can lead to less prestressed steel than required for fully prestressed concrete or shallow sections and a smaller total amount of steel than required for reinforced concrete. The primary factor in favour of partial prestressing is therefore economy.

It is commonly known that at the ultimate limit state, there is basically no difference between ordinary reinforced, partially prestressed or fully prestressed concrete. The distinctive behaviour of partially prestressed concrete therefore occurs under service load.

Other advantages of partial prestressing are as follows:-

(a) By prestressing part of the reinforcement, the downward deflection is normally smaller than ordinary reinforced concrete and the initial upward camber is smaller than for fully prestressed concrete. The ability to control cambers or deflection by varying the level of prestress is of considerable value in cases where the camber of long-span prestressed elements might otherwise be a

problem.

(b) Non-prestressed reinforcement serves the dual purpose of contributing to the ultimate strength and controlling crack formation and crack width.

(c) Cracks of a width which would otherwise be unpleasing and subject to corrosion risk, can be controlled by prestressing part of the reinforcement.

(d) The ductility of members at ultimate load is increased thereby avoiding sudden failure. This feature is of particular value in design for seismic conditions.

The main disadvantages, on the other hand, are higher losses of prestress in concrete due to the presence of a larger amount of steel and the absorption of a higher proportion of the initial prestress by the non-prestressed reinforcement.

1.4 Purpose of Investigation

The present investigation was carried out to add to the existing knowledge of partially prestressed concrete. As Professor Sabnis (Howard University) put it in a recent private communication: the tests provided additional information to the "...much needed data on partially prestressed concrete".

This research was carried out in two phases. The first was to study the deflection of partially prestressed concrete beams under service load and the second phase was

to investigate the relative usefulness of some partial prestressing design parameters.

In Phase One, an experimental programme consisting of nine tests of partially prestressed concrete beams was carried out. An analytical method of calculating the deflection of cracked prestressed concrete beams was developed and the calculated deflection compared with the experimental results. Various design codes and standards are examined in detail and predicted values using these codes are compared with the experimental results.

The three proposed partial prestressing parameters are the main subject of study in Phase Two. The performance of these parameters is studied in relation to the variable known to govern crack width and deflection and a suitable design parameter is recommended for partially prestressed concrete.

The detailed objectives of the investigations and methods adopted are given in Chapters Three and Nine.

1.5 Outline of Thesis

The thesis is divided into three parts. The general introduction and the review of previous research and current design recommendations form Part I.

Part II consists of Chapters Three to Eignt and is

concerned with the deflection of partially prestressed concrete beams with pretensioned tendons.

The objectives of the study and the methods of calculating deflection as recommended in various codes of practice are described in Chapter Three.

Chapter Four is devoted to the analysis of cracked sections under short-term and long-term loading in which the effects of creep and shrinkage are taken into account.

The analytical methods of calculating the deflection of cracked prestressed concrete beam by integration of curvature are described in Chapter Five.

The experimental programme including the materials used and the fabrication of beams is described in detail in Chapter Six.

In Chapter Seven, the behaviour of the beams under test is described and discussed. These results are then compared with the deflection calculated by the methods described in Chapter Five. Deflections calculated using the empirical formulae recommended in other codes of practice are also compared with the experimental results and discussed.

The conclusions of the investigation described in Part II are given in Chapter Eight and recommendations for further research are made.

Part III (Chapters Nine to Eleven) of the thesis is devoted to the study of partial prestressing design parameters.

The objectives of the study and the method of analysis are described in detail in Chapter Nine.

The results of the analysis of the parameters are given and discussed in Chapter Ten.

The conclusions of the investigation described in Part III are given in Chapter Eleven and a simple design procedure is also recommended.

CHAPTER TWO

Early History and Review of Design Procedures and Previous Research

2.1 Early History

The idea of prestressing concrete was not successfully applied until the introduction of high tensile strength wire in the mid-1920s; because of excessive losses due to creep. Freyssinet who was pioneering this new technique regarded prestressing as a means of eliminating undesirable cracks and allows beams to function as homogeneous materials. However, Emperger who was a reinforced concrete expert came forward with a different view of prestressing, he regarded prestressing as a method of controlling crack width in reinforced concrete while permitting higher service load.

In the years that followed, Abeles further developed and endorsed this new concept of prestressing. The term "Partial Prestressing" was first introduced by him, to distinguish this new concept of permitting tensile stress or even hair cracks under service load, from that of "full prestressing" where no tensile stress is permitted (1). The idea of permitting tensile stresses in concrete under service load means that less prestressing force would be required and either all the reinforcement be tensioned to a lesser degree or only part of the reinforcement tensioned. Abeles also advocated the use of high tensile strength wire

as non-prestressed steel whilst maintaining the same ultimate resistance. He claimed that a saving could thus be achieved in the amount of steel required, even allowing for the higher unit cost of high tensile wire (2). In ordinary reinforced concrete, this same high strength steel could be used to achieve the same ultimate strength of the beam but only in the expense of excessive deflection and crack width. By applying prestressing force, the excessive deflection and crack width could be reduced to an acceptable level.

This new concept of partial prestressing was received with considerable criticisms from many experts in prestressed concrete. Mautner (3) criticised Abeles's suggestion as amounting to the giving up of the many advantages of a homogeneous and perfectly elastic material for the sake of simplicity and economy which he claimed was non-existent. Freyssinet (4) dubiously exclaimed that "... relative to a state of load, a structure either is, or is not, prestressed. There is no half-way house between reinforced and prestressed concrete; any intermediate systems are equally bad as reinforced structures or as prestressed structures and of no interest." Having received such a strong critism from Freyssinet, the development of partial prestressing was thus slow.

Abeles, however, was convinced that it would be possible to keep the deflection and crack width of partially prestressed concrete members within an acceptable limit provided the reinforcement was well distributed and bonded.

2.2 Review of The Proposed Design Procedures

2.2.1 Hypothetical Tensile Stress (HYP)

The hypothetical or fictitious tensile stress is the tensile stress in the concrete which would be developed if the concrete section were to remain uncracked. The resultant tensile stress is the difference between the bending stress at the tensile face, calculated by assuming an uncracked section, and the prestress after accounting for all the losses (Fig.2.1).

This approach was originally proposed by Abeles (5) as an index of the degree of cracking of a partially prestressed section and has been adopted in the British Standard, CP110 (6). The allowable hypothetical tensile stress is specified with reference to the following:-

a) the permissible crack width depending on the environment to which the member is likely to be subjected,

b) the concrete strength,

c) the distribution of the tendons,

d) the percentage of non-prestressed reinforcement and

e) the depth of the section.

In a number of recent publications, Bennett (7-9) has demonstrated a design approach for partially prestressed concrete by using the hypothetical tensile stress as an index of the level of prestressing. The proposed basic design steps are summarised as follows:-

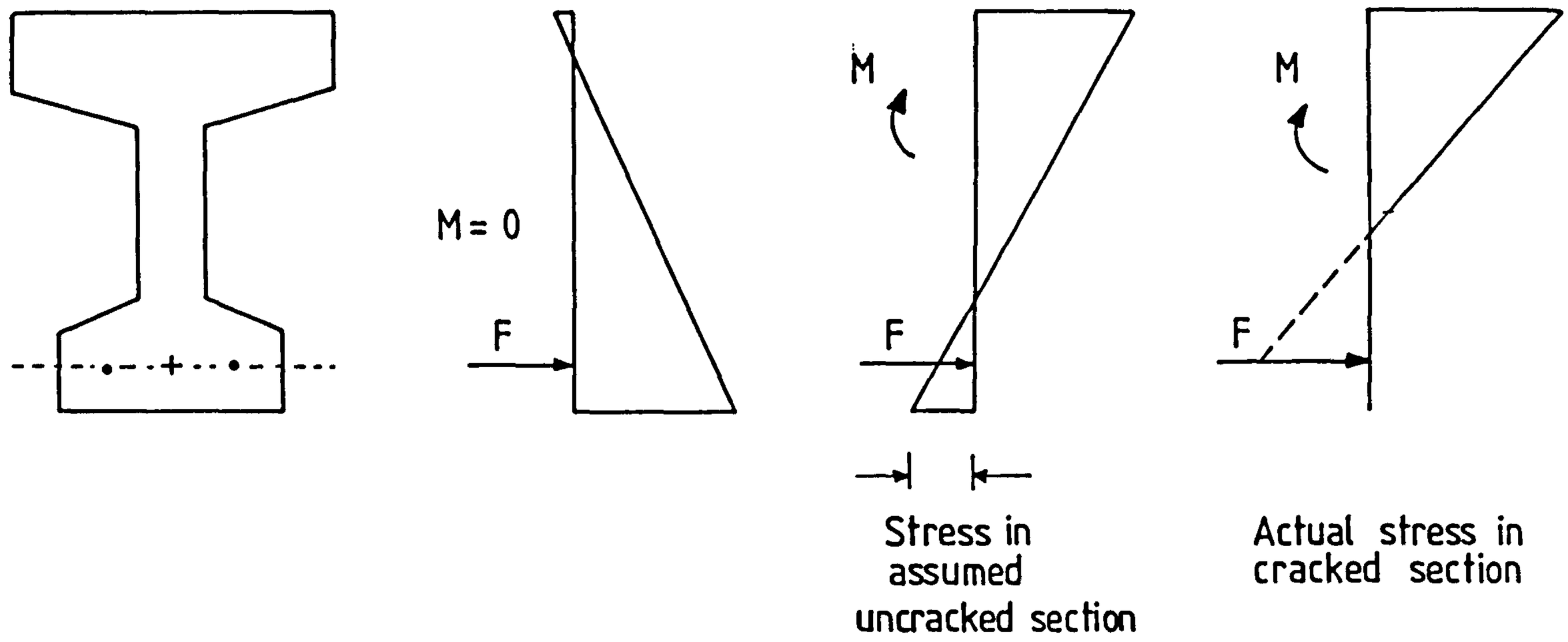

Fig. 2.1 Hypothetical Tensile Stress

1) Select a suitable value of hypothetical tensile stress corresponding approximately to the degree of cracking permitted. This value may be obtained from CP110 (6) or some of the recommended crack width equations (10-12). The minimum section modulus of the required section subject to tensile bending stress may then be obtained from the same formulae as for the design of Class 1 and Class 2 members (13); the permissible tensile stress being replaced by the allowable hypothetical tensile stress.

2) Determine the concrete cross section and calculate its dimensional properties.

3) Calculate the prestress required at the extreme top and bottom faces and hence the magnitude and position of the prestressing force. The number of tendons required is then known.

4) Calculate the amount of non-prestressed reinforcement required to satisfy the ultimate limit state condition:

$$M_u = Z (A_p f_{pu} + A_s f_y)$$

5) Serviceability limit state conditions are then checked. If necessary, calculate the stresses in the tendons or non-prestressed reinforcement and check the deflection and crack width.

Based on the results of some tests on rectangular

beams, Abeles (5,20) proposed a design approach in terms of the permissible tensile stresses (hypothetical tensile stress) for the two limiting crack widths of 0.1mm and 0.2mm. The present British Standard CP110 (6,22) recommendations are similar to these proposals in which the type of steel and the shape of cross section are not accounted for; although there is a provision for increasing the permissible hypothetical tensile stress in proportion to the area of non-prestressed steel expressed as a percentage of the cross sectional area of the concrete.

However, there was doubt about the relationship of the nominal tensile stress and the main serviceability design criteria: crack width. Stevens (21) tested thirteen partially prestressed concrete beams and observed that the maximum widths of cracks were in good agreement with the formula: $w = 3.3ce$ where c is the cover in inches and e is the average strain of the reinforcement steel.

Bennett and Chandrasekhar (11) conducted tests on thirty-seven beams and found that crack width was closely related to the stress in the steel after cracking, which in turn was largely dependent on the total area of the steel, whereas the hypothetical tensile stress was comparatively insensitive to the actual area of the steel. Bennett and Veerasubramaniam (23,24) tested thirty-seven partially prestressed concrete beams of varying shapes and reaffirmed Chandrasekhar (11,12) test results that the width of flexural cracks was better related to the stress increment

in the non-prestressed reinforcement than the nominal tensile stress. The crack width, however, was found to be independent of the shape of the cross section.

Martino and Nilson (10) collected experimental data from various investigators to study the sensitivity of the crack width to a number of parameters including the increase of stress in the non-prestressed reinforcement and the nominal concrete tensile stress. They concluded that a considerably higher degree of correlation was shown between the crack width and the incremental steel stresses than between the crack width and the hypothetical tensile stress, indicating that the latter would be less reliable as a crack width predictor.

The suitability of the hypothetical tensile stress as the only criterion for the design of all partially prestressed concrete sections, was again questioned following the analyses performed by Siriaksorn and Naaman (14,15) which showed that the hypothetical tensile stress could vary between 3 N/sq.mm to 23 N/sq.mm to cause the same crack width (0.2mm).

Nevertheless, the main advantage of the "hypothetical tensile stress" design approach is its simplicity which allows partially prestressed concrete beams to be designed according to the familiar procedure already well established for fully prestressed concrete.

2.2.2 Partial Prestressing Ratio (PPR)

The term "Partial Prestressing Ratio" was proposed by Naaman (14-16) to quantify the amount of prestressing in a partially prestressed beam. It is defined as the ratio of the ultimate resisting moment contributed by the prestressing steel to the total ultimate resisting moment taking account of both prestressed and non-prestressed reinforcement:

$$PPR = \frac{(M_u)_p}{(M_u)_{p+s}}$$

Assuming that both types of steel are located at the same level, the above equation can be approximately expressed as follow:-

$$PPR = \frac{A_p f_{pu}}{A_s f_y + A_p f_{pu}}$$

Effectively, the Partial Prestressing Ratio is thus the ratio of the tensile force in the prestressing steel at ultimate capacity to the tensile force in the total steel.

The value of the Partial Prestressing Ratio (PPR) is unity when the member is fully prestressed ($A_s = 0$) and at the other extreme of an ordinary reinforced concrete beam, it is always zero ($A_p = 0$). According to the definition, PPR is always one for beams without non-prestressed reinforcement independently of whether or not cracking is assumed under service load. Thus, a fully prestressed beam in which cracking is allowed under service load still has a value of PPR equal to one.

Based on the ultimate strength requirements, the Partial Prestressing Ratio provides a unified treatment of the full range of sections based on ultimate flexural capacity. Naaman believed that it was logical to propose a design procedure based on ultimate strength since at this state, fully prestressed, partially prestressed and ordinary reinforced concrete members have similar behaviour.

Besides being useful as a definition of partial prestressing and as an index of the level of prestress, the Partial Prestressing Ratio also serves as an extra equation in the analysis of a cracked section. In order to satisfy the ultimate moment criterion, there are generally two unknown quantities in the dimensioning of ordinary reinforced concrete or fully prestressed concrete, e.g. A_s or A_p and the depth of the neutral axis. As two equations of equilibrium (force and moment) are available at the ultimate load, the two unknowns can be easily determined. However, three unknowns exist in a partially prestressed section, namely, A_p , A_s and the depth of the neutral axis; thus, a third equation is essential and the Partial Prestressing Ratio can be easily selected to provide the required equation.

The design procedure based on the ultimate strength conditions suggested by Naaman, can be summarised in the following steps:-

1) Select the concrete section and the material properties.

The concrete section may be selected from the standard precast sections available.

2) Choose a suitable Partial Prestressing Ratio. Typical values which normally satisfy the serviceability criteria have been recommended by Naaman (14-16) and may be used as a first approximation.

3) Calculate the required ultimate moment of resistance M_u and determine the effective reinforcement ratio. For a rectangular section where d is the level of the total reinforcement, the effective reinforcement ratio is:-

$$\frac{A_p f_{pu} + A_s f_y}{bdf_{cu}} = \frac{M_u}{0.87\ bdf_{cu}(d - \frac{x}{2})}$$

4) Another equation is obtained from the equilibrium of forces at ultimate load,

$$0.4\ f_{cu}\ bx = 0.87\ (A_p f_{pu} + A_s f_y)$$

5) Areas of the tendons and the non-prestressed steel can then be calculated by solving the three equations in steps 2, 3 and 4.

6) Check the section at serviceability limit state. The stresses in the steel and concrete are checked. If necessary, the deflection and crack width are then calculated. The procedure is repeated from step 2 with a different value of PPR, if the serviceability requirements are not met.

2.2.3 Degree of Prestress

It is well known that the main advantage of prestressing a member lies in its superior structural behaviour under service load. At the ultimate state, however, there is no appreciable difference in structural behaviour between a prestressed, non-prestressed or partially prestressed structure. Bachmann (17,18), therefore, proposed a definition of prestressing based on the service load behaviour of the member. He suggested the term "Degree of Prestress" (DEG) as a measure of the level of prestress and is defined as:

$$DEG = \frac{M_d}{M_{g+q}}$$

where M_d is the decompression moment, the moment which produces zero stress at the extreme bottom fibre of a member, (Fig.2.2). The degree of prestress, thus, gives a measure of that proportion of the total service moment under which the maximum tensile fibre stress is zero.

Like "Partial Prestressing Ratio", the value of the "Degree of Prestress" is always zero for ordinary reinforced concrete, while its value is always one if the section is fully prestressed. However, for a fully prestressed concrete member (without non-prestressed reinforcement) which is designed to develop tensile stress under service load, it may be classified as "fully prestressed" according to the definition of Partial Prestressing Ratio, but not according to the Degree of Prestress. On the other hand, for a

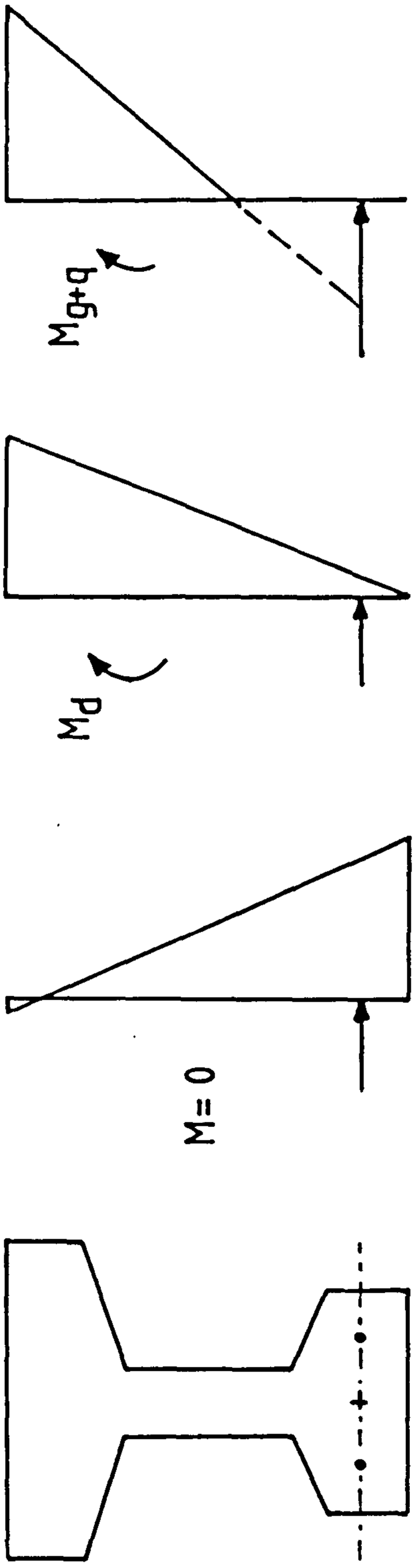

Fig. 2.2 Decompression moment in The Degree of Prestress

prestressed concrete member reinforced with both types of steel and designed to be under permanent compression, DEG = 1.0 (fully prestressed) while PPR is less than one.

Bachmann suggested that the design method for partially prestressed concrete should allow a smooth transition between reinforced and fully prestressed concrete design, and should be a unified procedure, applicable to all classes of concrete structures. An outline of the proposed design procedure based on the serviceability state, is given in the following steps:

1) Choose a desired degree of prestressing based on the design requirements. If minimum cost or area of the steel is the main factor, the optimum values of the degree of prestress suggested by Bachmann and described later in this Chapter, can be used. The decompression moment for which the section is to be prestressed can then be calculated,

$$M_d = (DEG)\, M_{g+q}$$

2) With a pre-selected section, calculate the necessary prestressing force which together with the decompression moment, produces zero stress at the extreme bottom fibre. It can be calculated by applying the usual rules for prestressed concrete design. The required area of prestressed reinforcement can then be found.

3) Determine the additional area of non-prestressed

reinforcement required to satisfy the ultimate conditions (Fig.2.3).

4) Check the stresses in the concrete under the service load and if necessary, calculate the stresses in the reinforcement by an appropriate cracked section theory which may be similar to that described in Chapter Four.

The main advantage of using the "degree of prestress" as a definition of partially prestressed concrete is its reference to the serviceability state which helps the engineer to forsee whether the amount of prestress chosen will, for instance, be sufficient to cover a certain proportion of the total service load. In order to arrive at the minimum total area of the steel, Bachmann suggested a value of 0.6 for a rectangular section and 0.82 for an I-section. Considering the relative cost of the prestressed to non-prestressed steel to be approximately 3:1, Leonhardt (19) found that for the most economical design, the degree of prestress should lie between 0.45 and 0.6 depending on the type of cross section.

2.3 Review of Previous Research on Deflection

One of the main advantages of partial prestressing is the ability to control deflection, but the lack of understanding of the behaviour under service load has limited its application. While the elastic theory for predicting the deflection of fully prestressed members has

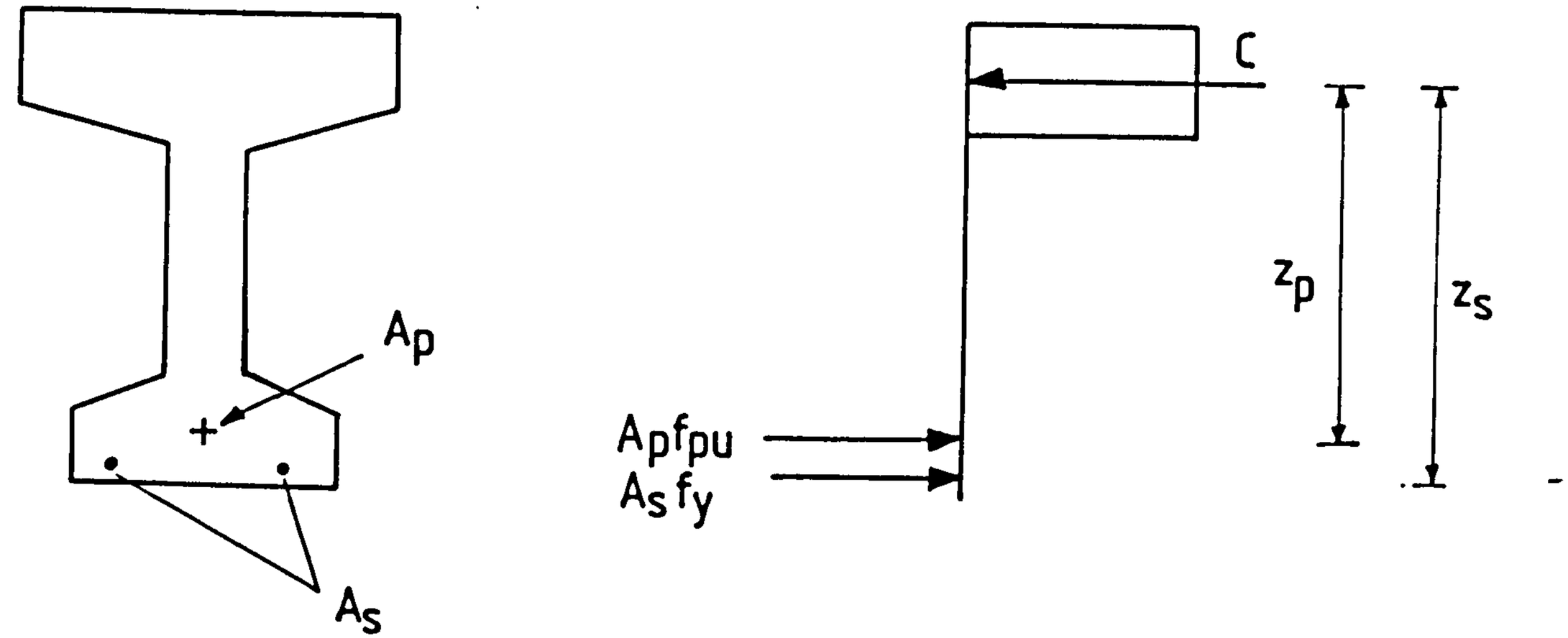

Fig. 2.3 Internal forces at ultimate state

been well established, the analytical method of calculating deflection of partially prestressed members is still at its infancy. Most of the previous research on partially prestressed concrete has been concentrated on the problems of corrosion and crack width. Nevertheless, the problem of deflection and the parameters affecting it have been a regular feature of the discussions.

Abeles

Most of the early tests were conducted by Abeles and few were directly related to deflection. The only issue concerning deflection was the choice of the type of steel for non-prestressed reinforcement. Abeles (2,5,25,26) advocated the use of high tensile steel of the same quality as the prestressing tendons. He argued that because of shrinkage and creep, a compressive force develops in the non-prestressed steel which increases with a larger cross sectional area of the non-prestressed steel and thus, reduces the total effective prestressing force. On the other hand, with larger amount of low strength steel, the stiffness is improved and consequently the downward deflection is considerably reduced.

Bennett et al

Bennett and collegues at the University of Leeds carried out extensive research on partially prestressed concrete, particularly Class 3 members as defined in the

British Code CP110 (6).

Bennett and Dave (20,21) tested forty rectangular beams in which the amount of reinforcement and the level of prestress were varied. The tests represented a complete range between fully prestressed concrete and conventional reinforced concrete. Eight beams were tested by sustaining the full design load for periods of between 276 and 600 days; nine beams were subjected to fatigue loading and the remaining were short-term tests.

They observed the typical behaviour of partially prestressed concrete beams; after cracking, the load-deflection curves for all the beams with the same amount of reinforcement had about the same increased slope although higher cracking loads were naturally observed in beams with greater prestress.

The deflection of the beams under sustained loads was reported to have increased to about 2.6 times the initial deflection at the end of the tests. It should be pointed out that the loads sustained represented the full design service load which is not normally encountered in practical cases.

In 1970, Bennett and Chandrasekhar (11,12) carried out more tests on partially prestressed concrete beams. Thirty-six rectangular beams of varying levels of prestress and reinforcement were tested. Among the parameters studied were

the types of non-prestressed reinforcement (deformed bars, prestressing wires and strands) and the nature of the loading.

It was concluded from the tests that the use of lower grade steel as non-prestressed reinforcement would effect a substantial reduction in the prestress in concrete compared with the use of lower amount of high strength steel. However, the deflection of all the beams other than those reinforced with deformed bars was found to exceed the limit specified in the code, during the second cycle of loading, indicating the effect of non-prestressed reinforcement on the deflection. The lower amount of steel was reported to be the reason for the reduced stiffness observed in beams reinforced with strands and wires at all stages of loading after cracking.

The deflections of the beams tested under sustained loading (full design load) were found to increase with time although at a progressively reducing rate. At the end of nearly 400 days of sustained loading, the maximum increase in the deflection was found to be 150 percent of the initial instantaneous deflection under static load.

In 1971, Bennett and Veerasubramanian (23,24) tested thirty-seven beams with varying degree of prestress and levels of reinforcement. The main parameter studied was the effect of non-rectangular section (shape) on the behaviour of partially prestressed concrete beams. All the beams were

reinforced with deformed bars and tests were performed under static short-term loading only.

Apart from the results that confirmed previous researchers' findings, they concluded that the composite T and T-beams were stiffer than the I and the rectangular beams. The presence of a larger area of non-prestressed reinforcement was again found to have increased the stiffness of the cracked beams.

Branson et al

Branson has been investigating the problem of deflection of reinforced concrete beams since 1960s and more recently he has extended his research to partially prestressed concrete.

Branson and Shaikh (27) carried out tests on twelve partially prestressed concrete beams with pretensioned tendons, to study the effect of both the quality (type) and quantity of non-tensioned steel on the behaviour of the beams. They found that the effect of using the transformed section properties was important in partially prestressed concrete.

They also observed that the deflections of the beams with more non-prestressed steel were considerably less than the deflections under the corresponding loads of identical beams containing smaller amounts of non-prestressed steel.

This finding confirmed the results of the investigations carried out by Bennett et al.

Branson and Kripanarayanan (29) carried out further tests on fifteen beams under static and repeated loadings. Based on the results of tests Branson (29,59) suggested an empirical expression for computing the deflection of beams under repeated cycles of loading. The effective second moment of area, commonly known as "I-effective", as defined in the ACI code (57), was modified and given as follows:

$$I_{rep} = \phi I_e + (1 - \phi) I_g$$

where I_{rep} is used to compute the recovery during the unloading part of the cycle as well as the reloading up to the maximum load in the previous cycle.

$$\phi = (P_u - P_{rep})/(P_u - P_{cr})$$

$$= (M_u - M_{rep})/(M_u - M_{cr})$$

This method appeared to be applicable to repeated loading with increasing maximum load in every cycle. It mainly accounts for residual deflection due to cracking alone. The cumulative residual deflection due to repeated cycles of loading with the same maximum load was not considered.

More recently, Branson and Trost (30,49,58) tested four beams under time-dependent repeated cycles of loading. The rate of loading and unloading was deliberately reduced and three to eight hours were taken to test the beams in three

or four cycles. In each cycle the beam was loaded up to a maximum load higher than the previous cycle.

The experimental results in the first cycle were reported to be in good agreement with the deflection calculated by the "I-effective" method proposed by Branson. This method has been adopted in the ACI code (57) and will be described in Chapter Three.

In the Branson and Trost tests, the maximum load in each cycle was higher than the previous cycles and cracking and creep were therefore the two main causes of the increased deflection. A simple method for estimating the time-dependent effect of creep and cracking under a limited number of load cycles on deflection had been proposed:

For single or first loading cycle,

$$\text{Deflection, } a = k_r C_t \text{ (initial } a \text{)}$$

where k_r is a reduction factor for the effect of compression steel and downward movement of the neutral axis with time.

For repeated loading cycles,

$$a = k_r C_t \text{ (initial } a \text{)} + F_{rep} \text{ (initial } a \text{)}$$

where F_{rep} is a factor that takes into account the increased deflection due to the effect of cracking under repeated loading cycles, given as the ratio of this increased deflection to the initial deflection. It appeared that the latter equation was not applicable to repeated cycles of

loading with the same maximum load in every cycle.

It is evident from the review and literature search that there has been a considerable number of tests on partially prestressed concrete beams and comparisons have been made with the deflections calculated by using some of the empirical formulae, but so far few analytical methods have been investigated. It is also clear that most of the tests so far have been carried out either with a few cycles of short-term or slow loading or under sustained load. It is considered important to investigate the type of loading that is most likely to occur in practice.

PART II

INVESTIGATION OF DEFLECTION

CHAPTER THREE

Programme of Research

3.1 Introduction

The excessive deflection of building structures may cause considerable damage. Doors and window frames become distorted and their proper functioning is impeded, finishes crack or buckle, tiles lift and the floor level is affected. Most important of all is the effect on the users. Any obvious deflection which detracts from the appearance of a structure cause irritation and may even be viewed as a sign of danger of collapse.

In the past, this problem did not greatly concern practising engineers because low design stresses together with deeper and shorter span members produced relatively small deflection. Until recently, therefore, deflections were rarely checked by calculation, and when this was done the basis was the elastic theory using the properties of the uncracked concrete sections.

With the introduction of prestressed concrete, high grade concrete and high strength steel, it has been possible to design for shallower and longer spans. Design engineers are, therefore, faced with problems of the control and prediction of deflection and camber.

3.2 Present Design Recommendations on Deflection

3.2.1 British Standard CP110

In the British Code CP110, provisions for deflection are given according to defined classes of structures. Reinforced concrete members are required to satisfy basic span/depth ratios, compliance with which normally results in satisfactory deflection and calculation of deflection is thus generally not required. The deflection of prestressed concrete members subject only to small tensile stresses in the concrete (Class 1 and 2) is to be calculated using elastic analysis based on the uncracked concrete section properties and the modulus of elasticity of the concrete. The long-term deflection due to prestressing force, dead load and sustained load is also calculated using elastic analysis based on uncracked concrete section properties, but using an 'effective' modulus of elasticity allowing for creep of the concrete.

For Class 3 prestressed concrete (partially prestressed) members in which some cracking of the concrete is permitted, it is recommended that the deflection should be calculated using elastic analysis as for Class 1 and Class 2 members, provided the permanent load is less than or equal to 25 per cent of the total design imposed load. Where the permanent load is greater than 25 per cent of the design load, the basic span/depth ratios are to be complied with unless detailed calculations based on the moment curvature relationship are made.

Where such calculations are required, CP110 Appendix A gives a suitable method. The approach used is to assess the curvatures of sections along the member, under the appropriate moments and then calculate the deflection from the integrated curvatures. The curvatures of the cracked sections are to be calculated by applying the usual assumptions of linear strain distributions and elastic compressive stress in concrete. The stress in the concrete in tension is assumed to have a value of zero at the level of neutral axis and a short-term value of 1.0N/mm2 at the centroid of the tension steel, reducing to 0.55N/mm2 in the long-term. In assessing long-term deflection, the Code also recommends the use of reduced 'effective' modulus of elasticity for calculating the curvatures of the sections.

In a number of recent publications, Bennett (7,8) has discussed how the above method may be extended to partially prestressed concrete members.

3.2.2 ACI 318 - 83

Like the British Code CP110, the ACI Code recommends the usual method of elastic analysis using the uncracked concrete section properties for the computation of short-term deflection of uncracked prestressed concrete members. For long-term loading, the Code specifies that the additional long-term deflection should be computed taking into account the stresses in concrete and steel under sustained load and including the effect of creep and

shrinkage of concrete and relaxation of steel.

The calculation of the deflection of reinforced concrete members is not essential if the basic span/depth ratios are complied with. Where, however, short-term deflection is to be computed, the code recommends the use of what has become known as the "I-effective" method. The deflection is calculated using the modulus of elasticity of the concrete and the "effective" second moment of area of the member, I_e, where I_e is defined as follows:-

$$I_e = \left(\frac{M_{cr}}{M_{max}}\right)^3 I_g + \left[1 - \left(\frac{M_{cr}}{M_{max}}\right)^3\right] I_{cr}$$

Fig.3.1 shows that the value of I_e lies between the values of the gross second moment of area of the uncracked section I_g and the second moment of area of the totally cracked section, I_{cr}.

The additional long-term deflection is to be calculated by multiplying the short-term deflection caused by the sustained load, by the factor:-

$$\lambda = \frac{\xi}{1 + 50p'}$$

where p' is the ratio of the compressive reinforcement and ξ is a time-dependent factor for sustained loads.

No special provision is given for the calculation of

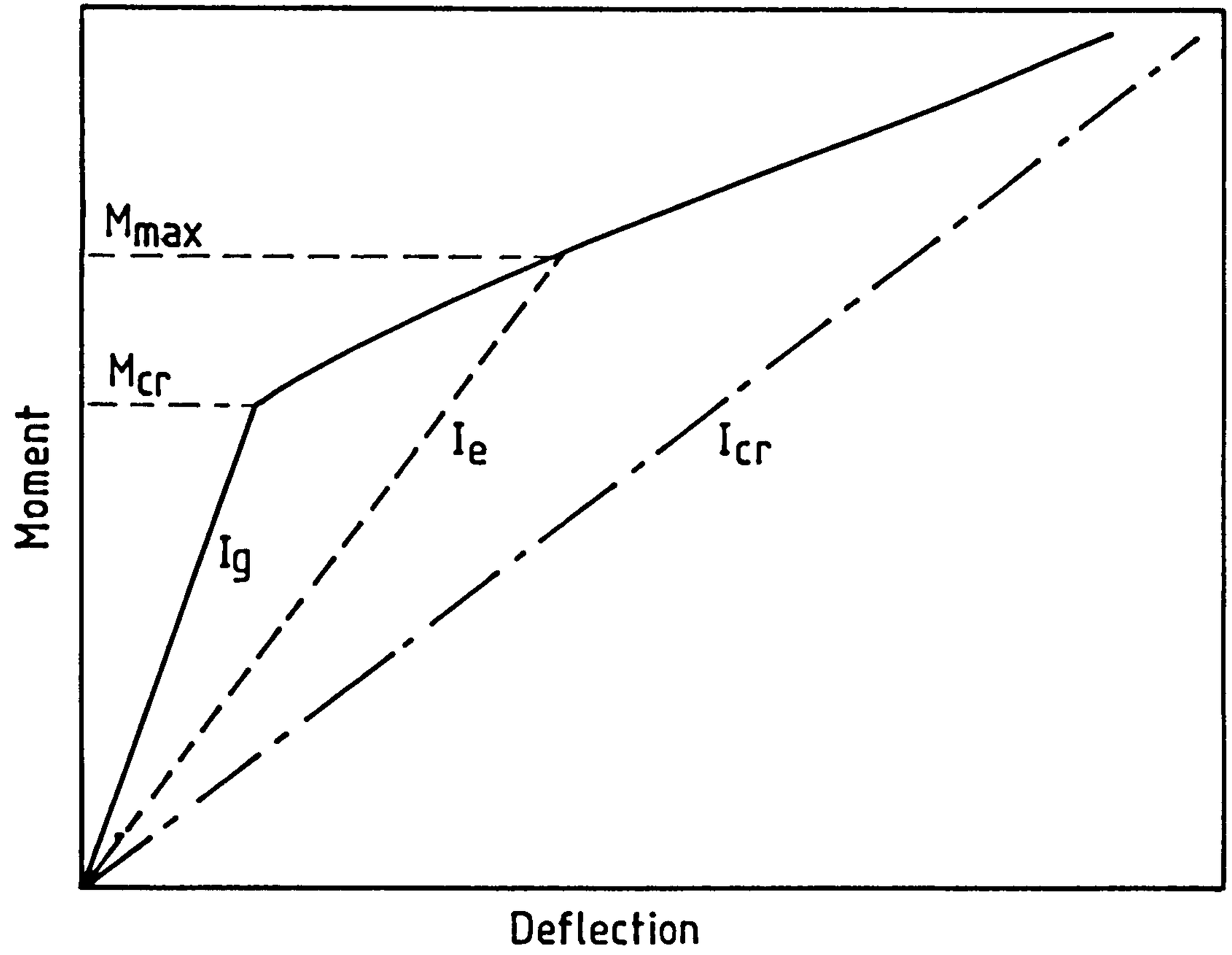

Fig. 3.1 Typical moment deflection curve showing range of I-effective

deflection of cracked prestressed concrete members. However, a number of recent publications (14,15,30) have recommended the extension of the I-effective method to cracked prestressed concrete members, with slight modifications:-

$$I_e = \left(\frac{M_{cr} - Pe}{M_{max} - Pe}\right)^3 I_g + \left[1 - \left(\frac{M_{cr} - Pe}{M_{max} - Pe}\right)^3\right] I_{cr}$$

3.2.3 CEB - FIP Model Code

In this Model Code, calculation of deflection of cracked members (State II) requires numerical integration of curvatures along the member similar to the recommendations of CP110, Appendix A. The effect of 'tension stiffening', however, is treated differently. According to the recommendation of the Model Code, the strain of the reinforcement at the crack is reduced by an amount, which depends on the degree of cracking, bond properties and the type of loading, to give the average strain of the bonded reinforcement. This is further discussed in Chapter Five.

For uncracked members (State I), the recommendation is effectively the usual elastic analysis using the modulus of elasticity of the concrete and the transformed concrete section properties.

3.3 Development of an Analytical Method

It is not usually necessary to calculate deflection in ordinary reinforced concrete design provided that the basic

span/depth ratios set down in the codes of practice have been complied with. For uncracked prestressed concrete members (Class 1 and 2 as defined in B.S.CP110), the calculation of deflection is simple and quite accurate using the conventional linear analysis. However, with partially prestressed concrete members (Class 3), the calculation for the cracked sections is more complicated. Moreover, a member is usually only partially cracked and a calculation based on the curvature of the cracked section often overestimates the actual deflection. For example, a simply supported beam under uniform load normally cracks in the mid-span region but sections near the supports remain uncracked. Recently, several empirical formulae (15,30) based on test results have been proposed with the aim of simplifying an otherwise complicated analysis.

Most of the present codes of practice consider deflection of the members as one of the important design criteria particularly in partially prestressed concrete in which control of deflection is one of the advantages claimed. Although some of the empirical formulae predict approximately correct deflection when compared with tests (30), it is important to develop an analytical method and hence an analytically based semi-empirical formula for calculating deflection in order to increase the confidence of practising engineers in designing partially prestressed concrete members. Lack of such confidence and understanding of the behaviour of partially prestressed concrete is considered to be the main reason for the slow acceptance of

this class of prestressed concrete among designers although provisions were made in the British Code more than ten years ago.

CP110 has recommended a general analytical method for calculating the deflection of cracked members. One of the objectives of the present research is to develop an analytical method for the calculation of deflection of partially prestressed concrete members based on this method.

In the analysis of deflection, the member is divided into elements and for each individual element, the curvature is analysed either by the modified reinforced concrete theory for the cracked section or by the elastic theory if uncracked. The deflection of each point along the member is then computed by integrating the curvatures over the whole span. The procedures are complicated, and a computer program was therefore developed for this part of the work.

Subsequently, using the same method, an analytical procedure for the calculation of long-term deflection was also developed taking into account the effects of creep, shrinkage and relaxation of steel.

3.4 Experimental Programme

3.4.1 Parameters Studied

The previous investigations of the various parameters affecting the deflection of partially prestressed concrete

members are reviewed in Section 2.2. It has been found that there are many parameters affecting deflection which cannot all be studied in this research. The major parameters considered were as follows:-

i) reinforcement ratio or amount of reinforcement

ii) degree or level of prestress

iii) loading procedure

All the rest of the parameters were kept constant as far as practicable. All the beams were of I-section and strands were used as the prestressing tendons as they were considered to be most common in use. The pretensioning process was used throughout.

3.4.2 Loading Procedures

Most of the tests conducted by other researchers (12,24) on partially prestressed beams were either short-term loading tests or long-term sustained loading tests under full 'design' load. However, in practical cases, only a certain proportion of the design load is permanent while the remaining live load is applied at intervals. Also, previous tests have indicated that part of the residual deflection after each cycle of loading is non-recoverable. It was therefore decided to study the effect of cycles of loading (representing live load) on the maximum and on the permanent deflection.

For this purpose, the beams were tested under a

combination of sustained load and short-term intermittent cycles of loading. The beams were first subjected to one cycle of loading to service load in which cracking occurred in all cases. Immediately after unloading the beams were submitted to a sustained load equal to one half of the service load (representing the permanent load). Intermittent cycles of loading (representing live load) were applied in addition to the sustained load to bring the total load to the level of the full service load. This intermittent load cycles were applied at intervals of about five days so that the recovery could be observed and the total duration of each test was about 30 days.

3.5 Summary of the Objectives of Study

The objectives of this part of the research can be summarized as follows:-

i) to develop an analytical method for the calculation of both long-term and short-term deflection of partially prestressed concrete members.

ii) to study the deflection of partially prestressed concrete beams under a combination of sustained load and short-term intermittent loading i.e. the effect of cycles of intermittent loading on the maximum and on the permanent deflection.

CHAPTER FOUR

Analysis of Cracked Sections

4.1 Introduction and Review

The stresses in both the prestressed and non-prestressed reinforcement greatly influence the flexural strength, crack width and deflection of partially prestressed concrete members. The flexural strength is dependent on the maximum stresses that can be developed in the tendons and the non-prestressed reinforcement. Chandrasekhar and Veerasubramaniam (11,12,23,24) found that crack width is related to the reinforcement stresses and this has been verified by Nilson et al (10). The curvature of a cracked section, which is a function of the steel strain, is also related to the reinforcement stresses. An accurate method of calculating deflection, therefore, requires an accurate analysis of these stresses at the cracked sections.

By proper modification, the analytical procedure for ordinary reinforced concrete based on the linear elastic theory can be used to analyse cracked prestressed concrete sections. In a cracked prestressed section, the position of the neutral axis is obtained by taking account of the compressive action of the prestressing force and the section is thus, stiffer than the corresponding cracked non-prestressed (ordinary) reinforced concrete section.

Many researchers have attempted to apply reinforced concrete cracked section analysis to cracked prestressed beams with non-prestressed reinforcement. Chandrasekhar (12) proposed a method for rectangular sections and Veerasubramaniam (23) modified it to include flanged sections with reinforcement at different levels. By comparing the calculated stresses with test results, they concluded that the modified reinforced concrete analysis was reasonably accurate under service load, but under-estimated the steel stresses as soon as the response of the concrete became non-linear

More recently, Nilson (42) proposed another method of calculating reinforcement stresses which is also based on the reinforced concrete theory. Basically, the member is treated as ordinary reinforced concrete subjected to pure bending and axial load. The axial force is also equal to a fictitious force acting at the level of tendons and causes zero stress state (decompression of the entire concrete section) in the concrete. The member is then analysed using the transformed section properties. The utilization of this concept of decompression has recently been emphasized by Moustafa (43), Nielson (44) and Naaman (14,15). The determination of decompression force, however, is complicated by the fact that prestress continues to change with time due to creep and shrinkage of concrete and relaxation of the prestressing steel, as rightly pointed out by Tadros (45). The method as proposed by Nilson (42) also ignored the compressive stresses induced in the non-

prestressed reinforcement which may be significant, particularly in partially prestressed concrete members.

The analysis of cracked sections presented in this Chapter is based on the method proposed by Chandrasekhar and Veerasubramaniam but with further modifications and improvements. The analytical expressions derived here included a further modification to allow for the compressive forces induced in the non-prestressed reinforcement after losses. The effect is significant when the amount of non-prestressed reinforcement is considerable. The compressive stresses contributed by the bottom flange in the I-section when the neutral axis is in the bottom flange are also taken into account and are found to be significant when the beam has a thick bottom flange.

The cubic equation derived by Chandrasekhar and Veerasubramaniam (12,23), to find the position of the neutral axis, required an iterative process to obtain the reinforcement stresses. This has been improved by using the 'reference force' (the total force in the reinforcement when the concrete at a reference level ceases to be compressive), so that the reinforcement stresses can be obtained directly without the process of iteration.

The analysis of the cracked section under instantaneous load or moment is then extended to analyse sections under sustained load (with creep effect) and undergoing shrinkage. Although the three effects are combined at any stage, they

are treated individually. Three separate analytical expressions were derived and presented in this Chapter: analysis of cracked section under instantaneous load, analysis of cracked section with the effect of creep and cracked section with the effect of shrinkage.

4.2 Cracked Sections Under Instantaneous Load

Many experts (16,18,45) have recognised that the behaviour of a cracked partially prestressed concrete member at ultimate state is similar to the corresponding conventional reinforced concrete member, but under serviceability conditions, the former type of member is stiffer because of the presence of an additional compressive force. For an ordinary reinforced concrete member, the neutral axis of bending is the same as the centroid of the cracked transformed section. Thus, the point of zero stress (neutral axis) in the section coincides with its centroid. The situation, however, is different for partially prestressed sections, as their point of zero stress can vary in the section depending on the magnitude of the applied moment and/or the axial prestressing force. Nevertheless, it is convenient to adopt reinforced concrete theory, with appropriate modifications to account for the additional compressive force, to analyse a cracked prestressed section under serviceability conditions.

The basic assumptions made in the following analysis are :-

1) Plane sections remain plane at any stage of loading.

2) The stress - strain relationships of concrete and steel are linear and elastic.

3) Stresses and strains at any level in the cross-section of the beam and in the prestressed and non-prestressed steel are proportional to the distance from the neutral axis.

4) Concrete cannot withstand any tension.

5) There is perfect bond between steel and concrete.

In the recent Concrete Society Report (9), it was found convenient to refer the reinforcement stresses of a cracked section to a reference load at which the stress in the concrete ceases to be compressive. For a virgin concrete member (concrete that has not been subjected to any external applied load), cracks are not expected to appear until the tensile stress in the concrete exceed its strength and thus, the cracked phase may be taken to commence after the tensile strength is exceeded. On subsequent cycles of loading or unloading, although cracks may close or re-open at a slightly lower load than at the point of decompression, it has been commonly accepted that in normal structures, the cracked phase may be taken to begin at the load at which the stress in the concrete ceases to be compressive at the soffit. The stresses of a cracked section should, preferably, refer to this load as reference load. The Concrete Society Report (9), however, showed that it is more convenient to use the load at which the concrete stress is zero at the level of the reinforcement instead of at the point of decompression at the soffit. For rigorous analysis

where the two types of reinforcement are located at different levels and the cracked phase is considered to begin at the point of decompression, it was found simpler to use two reference loads.

In the analysis presented in this Chapter, P_o is defined as the force in the prestressing steel (after accounted for losses), and F_{so} is defined as the total force in the ordinary reinforcement, when the concrete stress is zero at the respective level. Referring to Fig.4.1, the reference forces are defined as follows:-

$$P_o = P_e + \alpha f_{cp} A_p$$

$$F_{so} = F_{se} + \alpha f_{cs} A_s$$

The analysis of uncracked sections and the calculation of prestress, was based on the simple elastic theory assuming homogeneous concrete sections. The stresses in the steel, before the section is considered cracked, are thus obtained by multiplying the stress in the concrete by the modular ratio and adding the initial effective stress.

The stress and strain distributions of a cracked section based on the above assumptions are shown in Fig.4.2. By equating the conditions of equilibrium, the following equations can be obtained:-

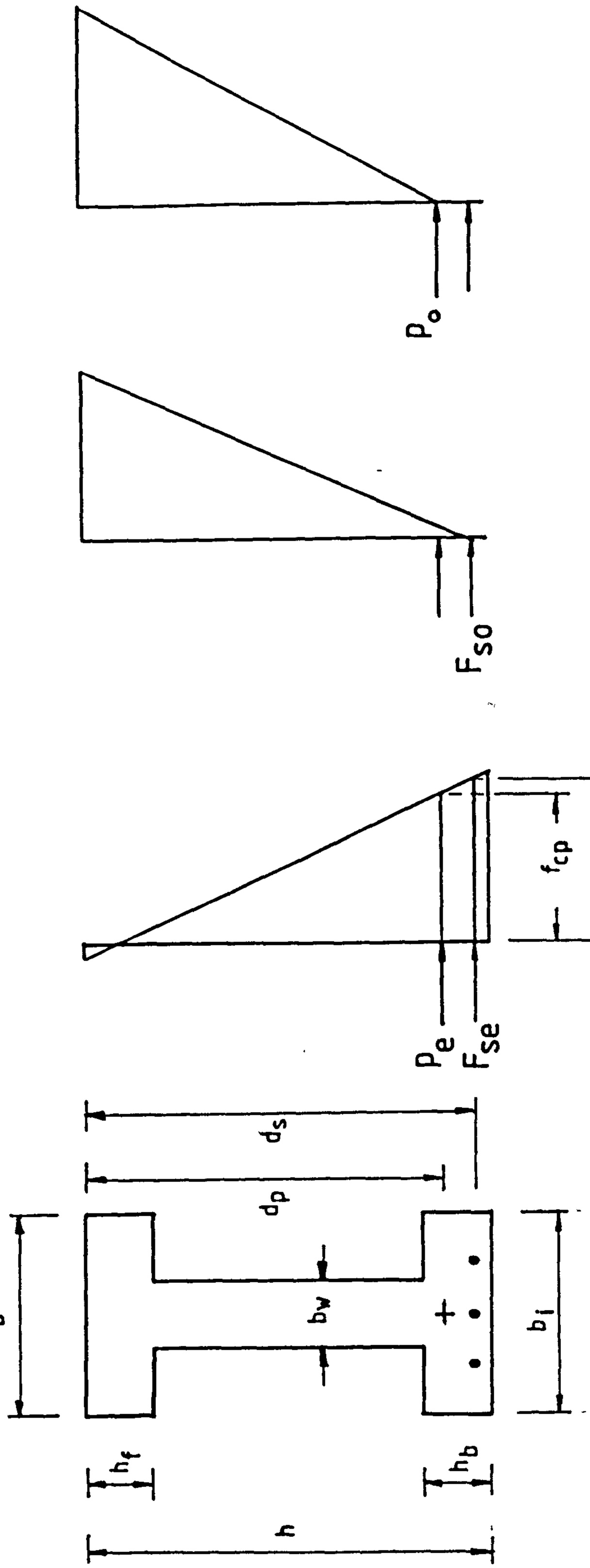

Fig. 4.1 Reference stresses at loads effective prestress stress reference forces in the analysis of cracked section

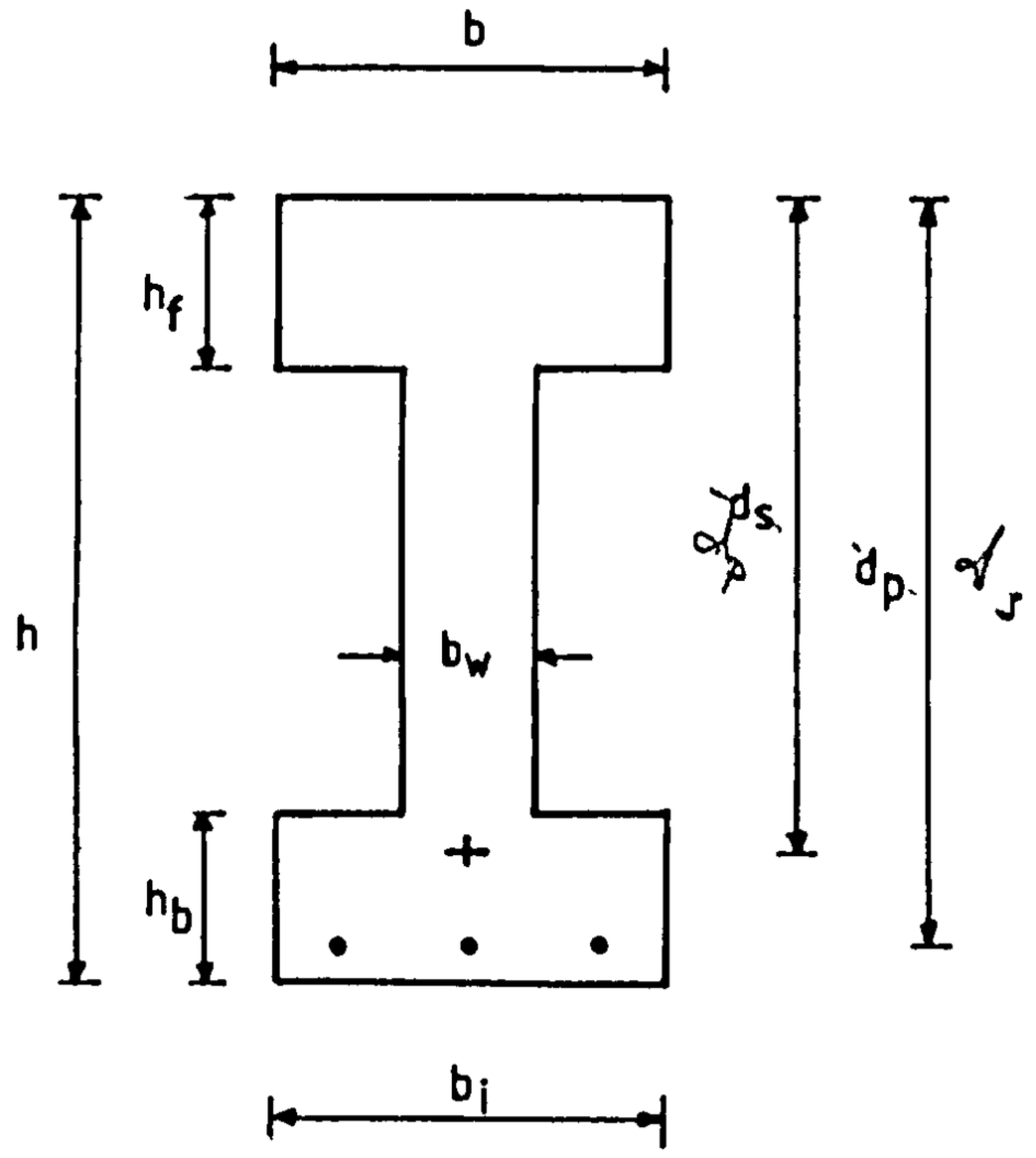

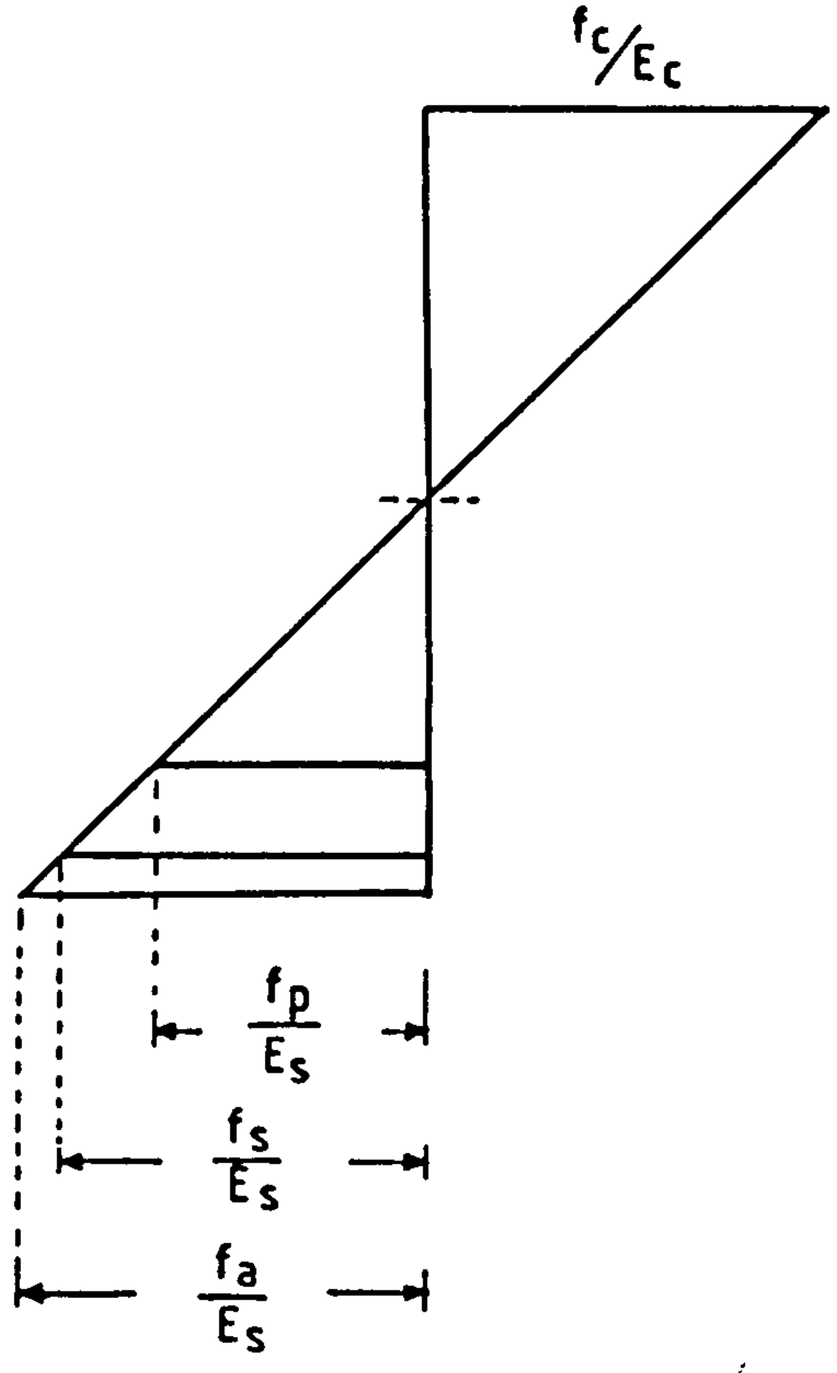

strain in cracked section

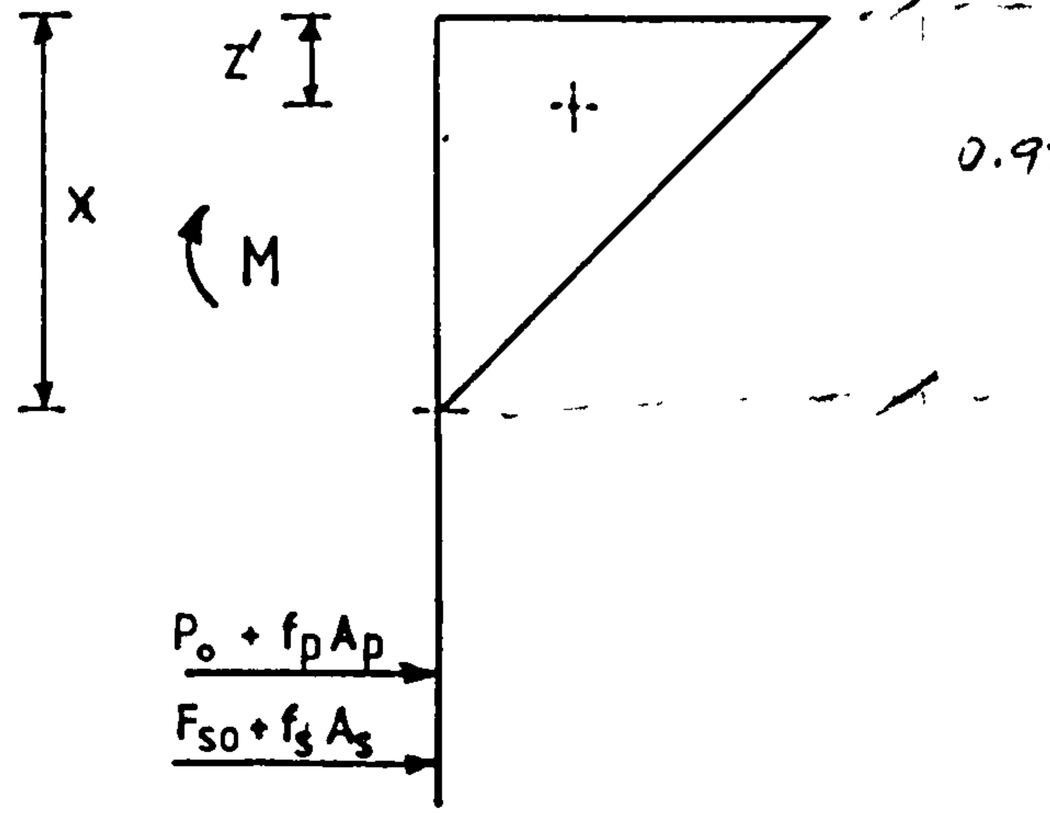

stress in cracked section

Reason for not using rectangular stress block is that it isn't at failure or near failure but at elastic serviceability state.

Fig. 4.2 Stress and strain distributions of a cracked section

1) From the condition of strain compatibility,

$$f_a = \alpha f_c \left(\frac{h - x}{x}\right) \qquad \text{... Eqn (4.1)}$$

2) From the equilibrium of forces,

$$P_o + F_{so} + \left[A_p \left(\frac{d_p - x}{h - x}\right) + A_s \left(\frac{d_s - x}{h - x}\right)\right] f_a$$

$$= \frac{bx}{2} f_c - \frac{(b - b_w)(x - h_f)^2}{2x} f_c^{\,*} + \frac{(b_i - b_w)(h_b - h + x)^2}{2x} f_c^{\,**}$$

... Eqn (4.2)

3) From the equilibrium of moments, about centroid of compression

$$M = \left[P_o + f_a A_p \left(\frac{d_p - x}{h - x}\right)\right] (d_p - z')$$

$$+ \left[F_{so} + f_a A_s \left(\frac{d_s - x}{h - x}\right)\right] (d_s - z') \qquad \text{... Eqn (4.3)}$$

where

$$\frac{z'}{h} = \frac{\xi^3 - b_1(\xi - h_1)^2(\xi + 2h_1) + b_2(h_2 - 1 + \xi)^2(\xi - 2h_2 + 2)}{3\left[\xi^2 - b_1(\xi - h_1)^2 + b_2(h_2 - 1 + \xi)^2\right]}$$

Solve this / Solved

M = external applied moment

$$\xi = \frac{x}{h}$$

$b_1 = (1 - b_w/b)$ $\qquad h_1 = h_f/h$

$b_2 = (b_i/b - b_w/b)$ $\qquad h_2 = h_b/h$

The above expressions apply generally to all the shapes of the sections. The terms with * and ** exist provided the neutral axis, x, is below the top flange, or in the bottom flange for the latter symbol.

f_a and f_c are eliminated from Eqns.(4.1),(4.2) and (4.3). The final equation, in terms of the ratio of the depth of the neutral axis to the depth of the section, can be expressed in the following form:-

$$A\,\xi^3 + B\,\xi^2 + C\,\xi + D = 0$$

where

$$A = (1 - b_1 + b_2)$$

$$B = 3K(1 - b_1 + b_2) + 3(b_1 d_2 - b_2 d_2 - d_2)$$

$$C = 6b_1 h_1 K + 3b_1 h_1^2 - 6b_1 h_1 d_2 + 6\alpha\rho_p K + 6\alpha\rho_s K$$
$$- 6\alpha\rho_s(d_2 - d_3) + b_2[6K(h_2 - 1) - 3h_2^2 + 6h_2 - 3$$
$$- 6d_2 h_2 + 6d_2]$$

$$D = b_1 h_1^2[3d_2 - 2h_1 - 3K] - 6\alpha K[\rho_p d_2 + \rho_s d_3]$$
$$+ 6\alpha\rho_s(d_2 - d_3)d_3 + 3b_2 K[h_2^2 - 2h_2 + 1]$$
$$+ b_2[6h_2^2 - 6h_2 - 2h_2^3 + 2 + 6d_2 h_2 - 3d_2 h_2^2 - 3d_2]$$

and $K = \dfrac{M + F_{so}(d_p - d_s)}{(P_o + F_{so})h}$

P_o & F_{so} must be known before $\frac{a}{h}$ can be found!

$d_1 = \dfrac{3d}{h}$ $\quad \alpha = \dfrac{E_s}{E_c}$ $\quad f_s = \dfrac{A_s}{bh}$

$d_2 = d_p/h$ $\quad \rho_p = \dfrac{A_p}{bh}$

$d_3 = d_s/h$

By solving the above cubic equation with any value of the applied moment, M, the position of the neutral axis can be computed for the beam whose sectional and material properties and the initial stresses in the concrete and steel before the application of load are known.

The stress at the reference level, f_a , can then be calculated from equation (4.1). The increase of stresses and the final stresses in the tendons and the non-prestressed steel, after decompression at the respective level, are given by the following expressions:-

$$F_p = P_o + \left(\frac{d_p - x}{h - x}\right) f_a A_p \qquad \text{... Eqn.(4.4)}$$

$$F_s = F_{so} + \left(\frac{d_s - x}{h - x}\right) f_a A_s \qquad \text{... Eqn.(4.5)}$$

The computation steps involved in the analysis of reinforcement stresses are listed below:-

1) Calculate the transformed section properties in which the area of reinforcement is taken into account.
2) From the given effective stresses in both types of reinforcement, compute the reference forces, P_o and F_{so}.
3) With the given applied moment, solve the cubic equation either by the Newton-Raphson method or by the computer packages (NAG library routines), to obtain the position of the neutral axis.
4) Compute the increase of stresses and hence the total stresses in the prestressed and non-prestressed steel (Eqns.4.4 and 4.5).

A computer program has been developed which includes the analysis of a cracked section as described above. The complete program was developed for calculating the deflection of partially prestressed concrete members as described in Chapter Five. The program is listed in Appendix A.

4.3 Cracked Section with Creep Effect

The primary factor that hindered the early development of prestressed concrete was the loss of prestress and creep was later found to be the major cause of this loss. Creep in prestressed concrete, as is understood today, is the result of compressive stress in the concrete; it induces a shortening strain in the concrete, in excess of the elastic strain, increasing with time and leading to a loss of stress in the bonded tendons. In some cases of fully prestressed members where the proportion of dead load is small, creep may cause an undesirably large increase in the upward camber. In other cases, where the dead load is large, excessive deflection may be the result.

However, the effect of creep on a cracked prestressed section is not yet fully understood, although there are indications from test results (12,46) that the long-term deflection increased as a result of creep. A number of sustained loading tests were carried out at Leeds University in the 1960s and 1970s. Dave (46) and Chandrasekhar (12) found that there was only a slight increase in the

reinforcement stresses of their beams, while the final deflection increased to more than three times its initial value. Similar results were obtained by Glanville and Thomas (32), as early as 1939, from tests on reinforced concrete beams under sustained load. According to Glanville and Thomas, there are two distinct neutral surfaces in a beam subjected to sustained loading, one of zero stress, the other of zero strain. This arises from the fact that an increase in the strain in concrete leads to an increased stress in the steel and a consequent lowering of the neutral axis when an increasing depth of concrete is brought into compression. As a result, the elastic strain distribution changes, but the creep strain is not removed, so that at the level of the new neutral axis of stress a tensile strain will remain. At some level above this axis, there will be a fibre of zero strain at any time although there will be a stress acting (Fig.4.3).

The above argument, put forward by Glanville and Thomas (32), was based on two assumptions:-

1) that the concrete on the tension side deforms as a result of creep in the same way as the concrete in compression,
2) there is no complete recovery of creep when the load causing that creep is removed.

In this Section, an analytical method of calculating the reinforcement stresses in a cracked prestressed concrete section under sustained load is described. The theory presented by Glanville and Thomas (32) for analysing

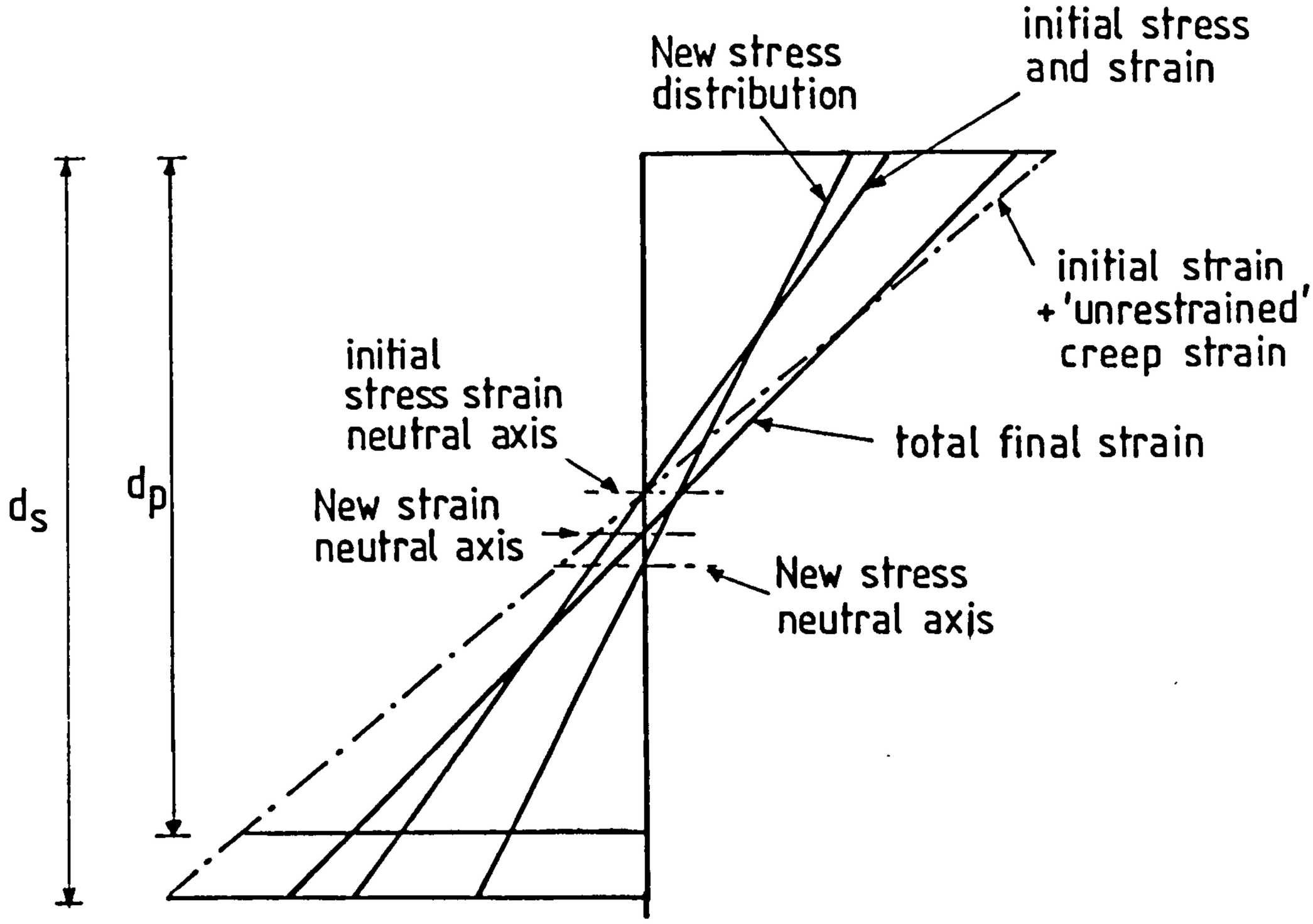

Fig.4.3 Stress strain distributions of a cracked section under sustained load, according to Glanville and Thomas

ordinary reinforced concrete section is modified and adapted for the analysis of a cracked prestressed section. The assumptions made in the analysis are as follows:-

1) Plane section remain plane at any time and stage of loading.
2) The stress-strain relationship of steel is linear and elastic.
3) The strain at any level in the cross section of the beam and in the prestressed and non-prestressed steel are proportional to the distance from the neutral axis of the strain.
4) The 'elastic strain' of the concrete is proportional to the 'elastic stress'.
5) The total strain at any level is equal to the sum of the 'elastic strain' and the 'unrestrained' creep at the corresponding level
6) Unrestrained creep is assumed to be proportional to the initial stress in the concrete.
7) Concrete cannot withstand any tension and creep therefore, only occurs under compressive stress. This is the main difference from the assumption (1) made by Glanville and Thomas, in which concrete both in tension and compression was assumed to exhibit creep. This is considered unreasonable because of the common assumption that concrete cannot withstand any tension and therefore creep cannot occur below the level of the neutral axis where tensile stresses are ignored.
8) There is perfect bond between steel and concrete.

The analysis of a cracked section at the start of sustained loading (instantaneous load), is similar to that described in Section 4.2 for short-term loading. The reference forces introduced in that analysis are again used in the present analysis with the same notations.

The stress and strain distributions based on the above assumptions are given in Fig.4.4. In this analysis, the initial stress and strain distributions are calculated by the method described in Section 4.2 and are therefore taken as known values. At any time under sustained load, the equilibrium conditions can be expressed as follows:-

1) Strain Compatibility

$$\frac{f_{s2}}{E_s} = \left(\frac{f_{c2}}{E_c} + \frac{c_c f_{c1}}{E_c}\right)\left(\frac{d_p - x_3}{x_3}\right) \quad \ldots \text{Eqn (4.6)}$$

$$\frac{f_{s2}''}{E_s} = \left(\frac{f_{c2}}{E_c} + \frac{c_c f_{c1}}{E_c}\right)\left(\frac{d_s - x_3}{x_3}\right) \quad \ldots \text{Eqn (4.7)}$$

2) Equilibrium of Forces

$$F_{so} + P_o + A_p f_{s2} + A_s f_{s2}''$$

$$= \frac{bx_3}{2}(f_{c2} + c_c f_{c1}) - (f_{c2} + c_c f_{c1})\frac{(b-b_w)(x_3-h_f)^2}{2x_3}$$

$$+ \frac{(b_i-b_w)(h_b-h+x_3)^2}{2x_3}(f_{c2} + c_c f_{c1}) - \frac{bx_1}{2} c_c f_{c1}$$

$$+ (b-b_w)\frac{(x_1-h_f)^2}{2x_1} c_c f_{c1} - (b_i-b_w)\frac{(h_b-h+x_1)^2}{2x_1} c_c f_{c1}$$

$$\ldots \text{Eqn (4.8)}$$

3) Moment Equilibrium

$$M = \frac{bx_3}{2}(f_{c2} + c_c f_{c1})(d - \frac{x_3}{3})$$

$$- (b - b_w)\frac{(x_3 - h_f)^2}{2x_3}(f_{c2} + c_c f_{c1})(d - \frac{x_3}{3} - \frac{2}{3}h_f)$$

$$+ (b_i - b_w)\frac{(h_b - h + x_3)^2}{2x_3}(f_{c2} + c_c f_{c1})$$

$$(d - \frac{x_3}{3} + \frac{2h_b}{3} - \frac{2h}{3}) - \frac{bx_1}{2} c_c f_{c1}(d - \frac{x_1}{3})$$

$$+ (b - b_w)\frac{(x_1 - h_f)^2}{2x_1} c_c f_{c1}(d - \frac{x_1}{3} - \frac{2h_f}{3})$$

$$- (b_i - b_w)\frac{(h_b - h + x_1)^2}{2x_1} c_c f_{c1}(d - \frac{x_1}{3}$$

$$+ \frac{2h_b}{3} - \frac{2h}{3}) \qquad \ldots \text{ Eqn (4.9)}$$

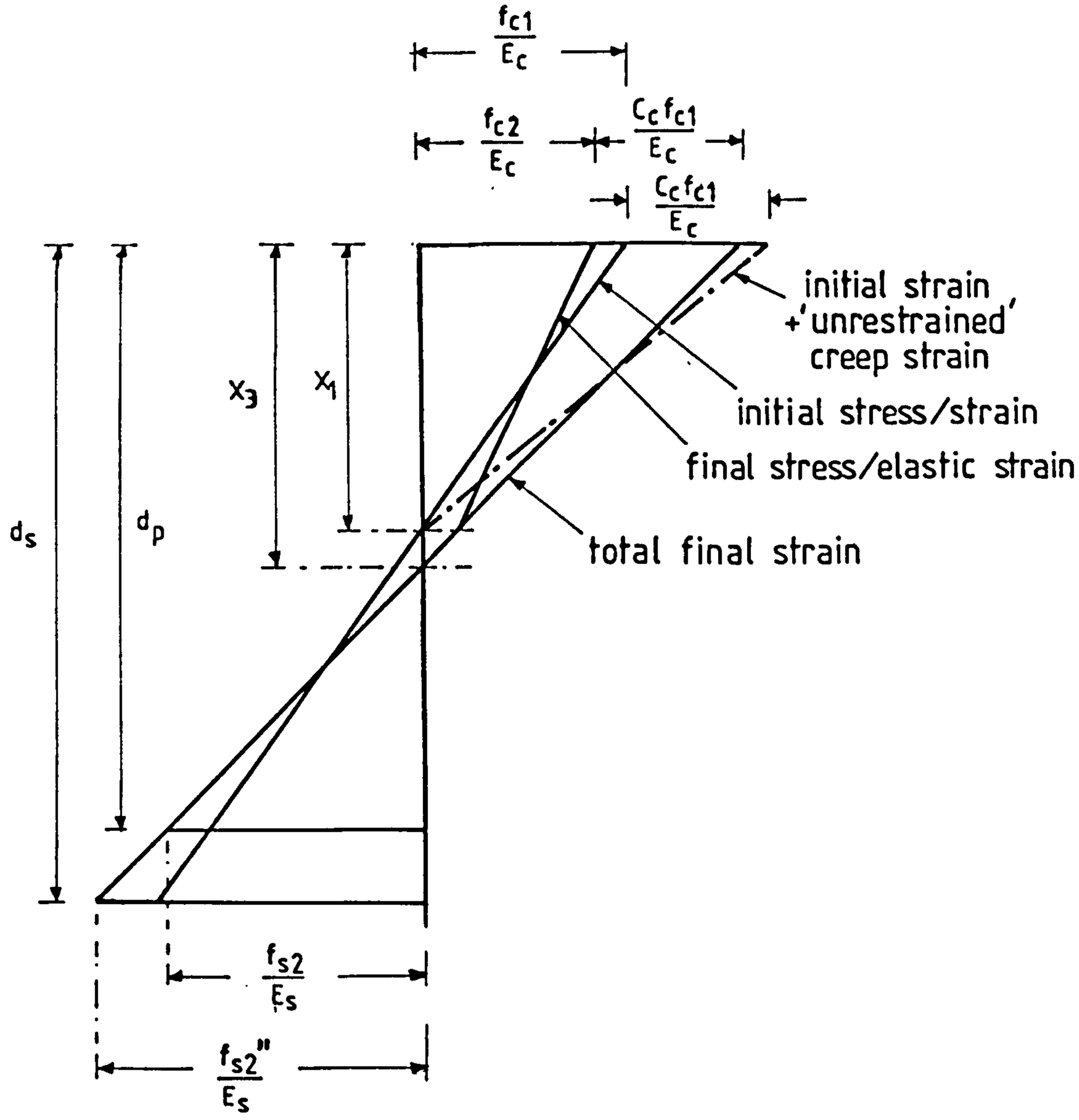

Fig. 4.4 Stress strain distributions of a cracked prestressed section under sustained load (with creep effect alone)

Substitute Eqn.(4.6) and Eqn.(4.7) into Eqn.(4.8), Eqn.(4.9) is then divided by the new equation to give the cubic equation in the following form:-

$$A\left(\frac{x_3}{h}\right)^3 + B\left(\frac{x_3}{h}\right)^2 + C\left(\frac{x_3}{h}\right) + D = 0$$

where

$$A = (1 - b_1 + b_2)$$

$$B = K(1 - b_1) + (b_1 d_1 - d_1) + (K - d_1)d_2$$

$$C = b_1[2h_1 K + 3h_1^2 - 2h_1 d_1] + 2\alpha K(\rho_p + \rho_s)$$

$$+ b_2[2K(h_2 - 1) - (2h_2 d_1 + 3h_2^2 - 6h_2 - 2d_1 + 3)]$$

$$D = b_1[(h_1^2 d_1 - 2h_1^3) - h_1^2 K] - 2\alpha K[\rho_p d_2 + \rho_s d_3]$$

$$- b_2[K(2h_2 - h_2^2 - 1) + (h_2^2 d_1 - 2h_2 d_1 + 2h_2^3 - 6h_2^2$$

$$+ 6h_2 + d_1 - 2)]$$

and $K = \dfrac{3(M + K_2)}{(F_{so} + P_o + K_1)h}$

$$\frac{K_1}{b} = \frac{x_1}{2}K_3 - b_1\frac{(x_1 - h_f)^2}{2x_1}K_3 + b_2\frac{(h_b - h + x_1)^2}{2x_1}K_3$$

$$\frac{K_2}{b} = \frac{x_1}{2}K_3\left(d - \frac{x_1}{3}\right) - b_1\frac{(x_1 - h_f)^2}{2x_1}K_3\left(d - \frac{x_1}{3} - \frac{2h_f}{3}\right)$$

$$+ b_2\frac{(h_b - h + x_1)^2}{2x_1}K_3\left(d - \frac{x_1}{3} + \frac{2h_b}{3} - \frac{2h}{3}\right)$$

$$K_3 = c_c f_{c1}$$

By solving the cubic equation with the same data as provided for the analysis of the cracked section under short-term load, the new position of the neutral axis can be obtained provided the creep coefficient at the time considered is known.

The new stresses in the prestressed and non-prestressed reinforcement can then be computed from Eqns.(4.6) and (4.7). The computation steps involved in the analysis of reinforcement stresses are briefly described below:-

1) With a given sustained load, analyse the cracked section subjected to the instantaneous load as described in Section 4.2
2) Assume the effective forces of the prestressed and non-prestressed reinforcement act at the level of the centroid of the total reinforcement area, d.
3) With a given value of creep coefficient, solve the cubic equation to obtain the new position of the neutral axis.
4) Calculate the final stresses in the prestressed and non-prestressed reinforcement.
5) Calculate the new level, d, at which the effective forces act. If the difference between this new value and the assumed level in step (2), is greater than the tolerance, all the steps from (3) are repeated by assuming the effective forces act at the level of the new depth, d.

In the present analysis, the position of the neutral axis and the reinforcement stresses are calculated in one step, in which the changes of concrete stresses between the

initial time and the time considered, are ignored. It also appears from the analysis that the compressive stresses of the concrete are reduced with time, and therefore, the magnitude of creep which is proportional to the stress should be reduced at the same time. A more rigorous analysis, which cannot be presented in this thesis because of complexity and the time involved, should take these decreasing stresses into account by analysing the section in a number of steps extending over the time considered. This is illustrated diagrammatically in Fig.4.5.

The analytical method described here has been programmed into Leed University Amdahl Computer and formed part of a package for analysing deflection of partially prestressed concrete beams. The main program is listed in Appendix A.

4.4 Cracked Section with Shrinkage Effect Irrelevant to my analysis

Concrete contracts on drying whether or not it is subjected to load; it is thus described as undergoing shrinkage. The magnitudes of shrinkage and creep are of the same order as the elastic strain under the usual range of stress, so that the various types of strains must be at all time taken into account. It is, commonly known (31) that shrinkage takes place over a long period of time, although at a decreasing rate. It is, therefore, important to account for the effect when analysing cracked prestressed sections and the long-term deflection of the beam.

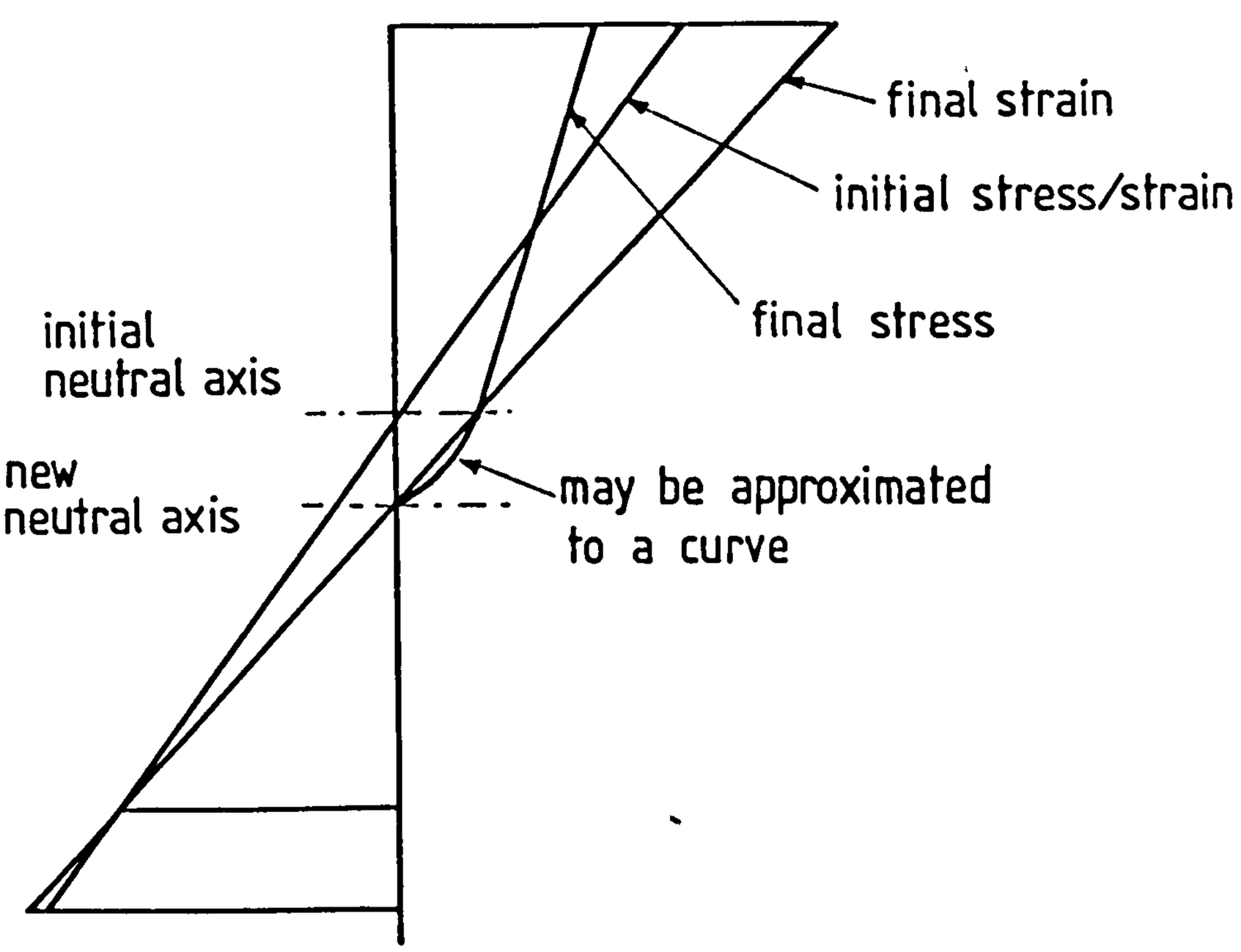

Fig.4.5 Stress strain distributions of a cracked section under sustained load, in multiple steps analysis

Like creep, concrete shrinkage reduces the tensile stresses in the tendons of fully prestressed members, hence resulting in the loss of prestress. The same effect can be expected in the uncracked regions of partially prestressed or ordinary reinforced concrete beams. In cracked sections, however, due to shrinkage and creep, reinforcement stresses are increased slightly over a period of time under sustained load. The position of neutral axis of strain is also correspondingly lowered.

Based on the same approach for the analysis of cracked prestressed section with creep effect described in Section 4.3, a method is described here to analyse the same cracked section with the effect of shrinkage alone. The basic assumptions in the analysis are given below:

1) Plane section remain plane at any stages of loading.
2) The stress strain relationship of steel is linear and elastic.
3) The strains at any level in the cross section of the beam and in the prestressed and non-prestressed steel are proportional to the distance from the neutral surface of strain.
4) The 'elastic strain' of the concrete is proportional to the 'elastic stress'.
5) The total strain (resultant strain) is equal to the sum of the 'elastic strain' and the 'unrestrained shrinkage' strain at the time considered.
6) Shrinkage is independent of the concrete stresses and

is, therefore, the same at any level of the section.

7) The stresses in the prestressed and non-prestressed steel at a cracked section are not affected by shrinkage that occurs in the adjacent sections (between the cracks) which are uncracked.

8) Concrete cannot withstand any tension.

9) Shrinkage does not occur at any level below the neutral axis of strain.

10) There is perfect bond between steel and concrete.

The stress and strain distributions at any given time under sustained load are given in Fig.4.6. The expressions for calculating the new position of neutral axis and the reinforcement stresses with the sole effect of shrinkage were derived from the following equilibrium conditions:

1) Strain Compatibility

$$\frac{f_{s2}}{E_s} = \left(\frac{f_{c2}}{E_c} + \varepsilon_{cs}\right)\left(\frac{d_p - x_3}{x_3}\right) \qquad \ldots \text{ Eqn (4.10)}$$

$$\frac{f_{s2}''}{E_s} = \left(\frac{f_{c2}}{E_c} + \varepsilon_{cs}\right)\left(\frac{d_s - x_3}{x_3}\right) \qquad \ldots \text{ Eqn (4.11)}$$

and

$$\frac{x_2}{f_{c2}/E_c} = \frac{x_3}{\frac{f_{c2}}{E_c} + \varepsilon_{cs}} \qquad \ldots \text{ Eqn (4.12)}$$

substitute Eqn (4.12) into Eqns (4.10) and 4.11),

$$f_{s2} = \alpha f_{c2} \left(\frac{d_p - x_2}{x_2}\right) - E_s \varepsilon_{cs} \quad \text{... Eqn (4.13)}$$

$$f_{s2}'' = \alpha f_{c2} \left(\frac{d_s - x_2}{x_2}\right) - E_s \varepsilon_{cs} \quad \text{... Eqn (4.14)}$$

2) Equilibrium of Forces

$$P_o + F_{so} + A_p f_{s2} + A_s f_{s2}''$$

$$= \frac{bx_2}{2} f_{c2} - \frac{(b - b_w)(x_2 - h_f)^2}{2x_2} f_{c2} + (b_i - b_w) \frac{(h_b - h + x_2)^2}{2x_2} f_{c2}$$

... Eqn (4.15)

3) Equilibrium of Moments

$$M = (P_o + A_p f_{s2})(d_p - z') + (F_{so} + A_s f_{s2}'')(d_s - z')$$

... Eqn (4.16)

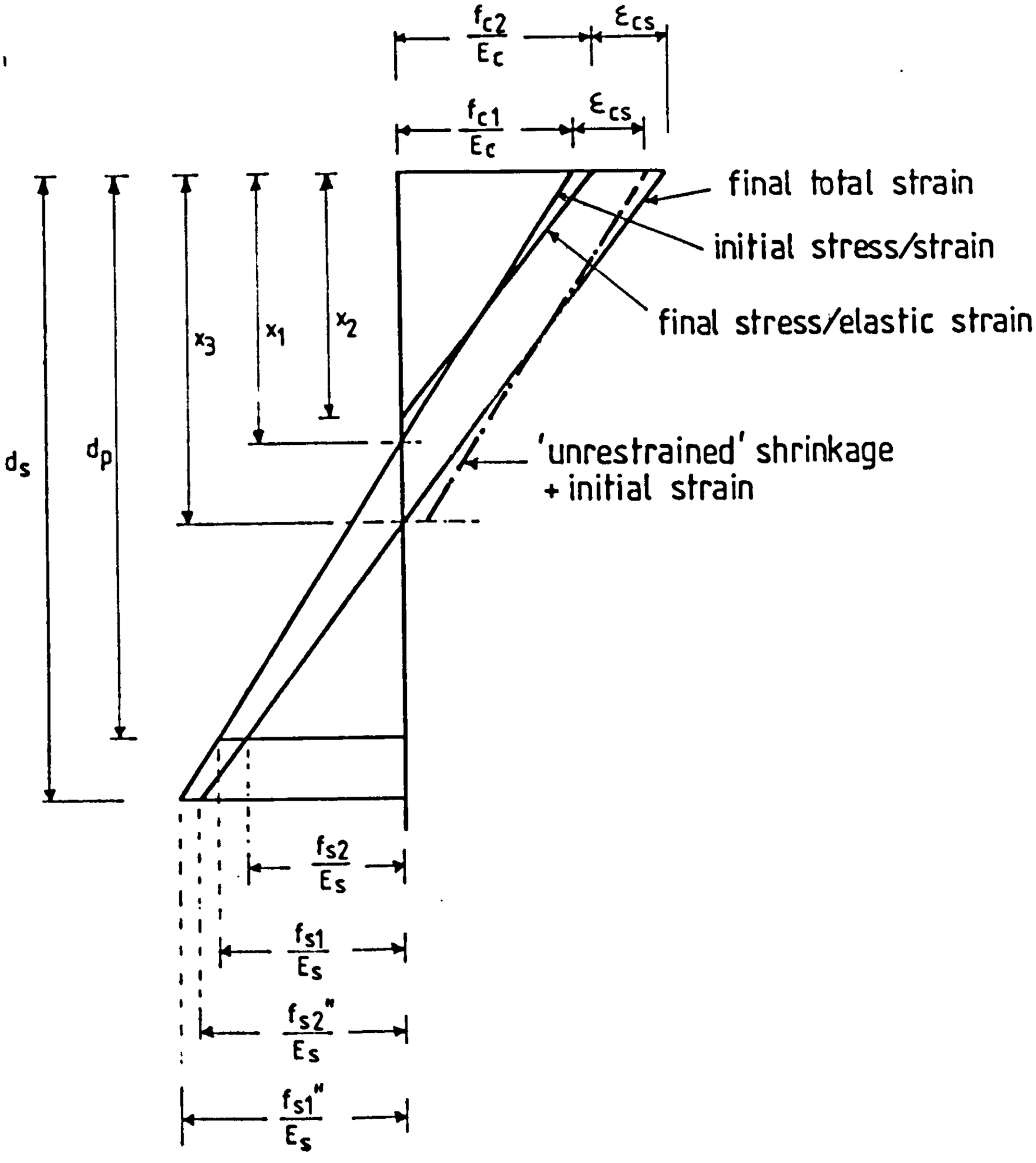

Fig.4.6 Stress, strain distributions of a cracked prestressed section under sustained load (with shrinkage effect alone)

Substitute Eqns.(4.13) and (4.14) into Eqn.(4.15) and then substitute the resultant equation into Eqn.(4.16). This new equation is then divided by the new Eqn.(4.15) to obtain the cubic equation in the form of:

$$A\left(\frac{x_2}{h}\right)^3 + B\left(\frac{x_2}{h}\right)^2 + C\left(\frac{x_2}{h}\right) + D = 0$$

where

$$A = (1 - b_1) + b_2$$

$$B = 3K(1 - b_1) - 3(1 - b_1)d_2 + 3b_2(K - d_2)$$

$$C = b_1(6Kh_1 - 6h_1d_2 + 3h_1^2) + 6\alpha K(\rho_p + \rho_s)$$

$$- 6\alpha\rho_s(d_2 - d_3) + b_2K(6h_2 - 6)$$

$$+ b_2(6d_2 - 6h_2d_2 - 3h_2^2 + 6h_2 - 3)$$

$$D = b_1(3h_1^2d_2 - 2h_1^3 - 3h_1^2K) - 6\alpha K(\rho_p d_2 + \rho_s d_3)$$

$$+ 6\alpha\rho_s d_3(d_2 - d_3) + 6b_2K(3h_2^2 + 3 - 6h_2)$$

$$+ b_2(6h_2d_2 - 3h_2^2d_2 - 3d_2 + 6h_2^2 - 6h_2 - 2h_2^3 + 2)$$

and

$$K = \frac{M + (F_{so} - A_s E_s \varepsilon_{cs})(d_p - d_s)}{[P_o + F_{so} - E_s \varepsilon_{cs}(A_p + A_s)]h}$$

By solving the cubic equation with the same data provided in the analysis of the cracked section under instantaneous load, the new position of neutral axis of stresses, x_2, can be obtained for the section when the concrete shrinkage, ε_{cs}, at the time considered is known. The concrete stresses at the top fibre and the position of neutral axis of the the total strain can then be computed by substituting x_2 into the original equations. Subsequently, the increase of stresses and the final total stresses in the prestressed and non-prestressed reinforcement can be calculated from Eqns.(4.10) and (4.11)

The analysis presented here is limited to a single step computation. A more rigorous analysis would be to analyse the section in multiple steps in which the original stress distribution is replaced, in each step, with a new stress distribution at a small interval of time. This analysis, in fact, slightly under estimates the increase of stresses in the reinforcement as the effect of shrinkage on the adjacent sections is ignored. Theoretically, the effect of shrinkage on the adjacent sections is to increase the stresses in the reinforcement of the cracked section when the adjacent uncracked sections contract.

This analysis also formed part of a computer program for the analysis of long-term deflection of partially prestressed concrete beam by integration of curvature. The program is listed in Appendix B.

CHAPTER FIVE

Analysis of Deflection

5.1 Introduction

The importance of developing an analytical method for predicting the deflection of partially prestressed concrete members has been discussed in Chapter Three. The analysis described in this Chapter is applicable to beams with bonded tendons, simply supported and either loaded at two points or by a uniformly distributed load.

The analysis of the deflection of a cracked prestressed concrete member is complicated because the member, if simply supported, is normally cracked around the mid-span region where the maximum moment occurs, while sections near the supports remain uncracked (Fig.5.1). The stresses of the uncracked sections can be calculated by the normal prestressed concrete theory assuming homogeneous sections while the cracked sections can be analysed by the more rigorous modified reinforced concrete theory. The analysis of reinforcement stresses at the cracks has been described in Chapter Four and hence the curvatures at the cracks can be calculated. The analysis of the deflection, however, requires the average strain which includes the uncracked sections between the cracks. In these sections, the curvatures are reduced by the effect which is generally known as "tension stiffening". This effect is discussed in

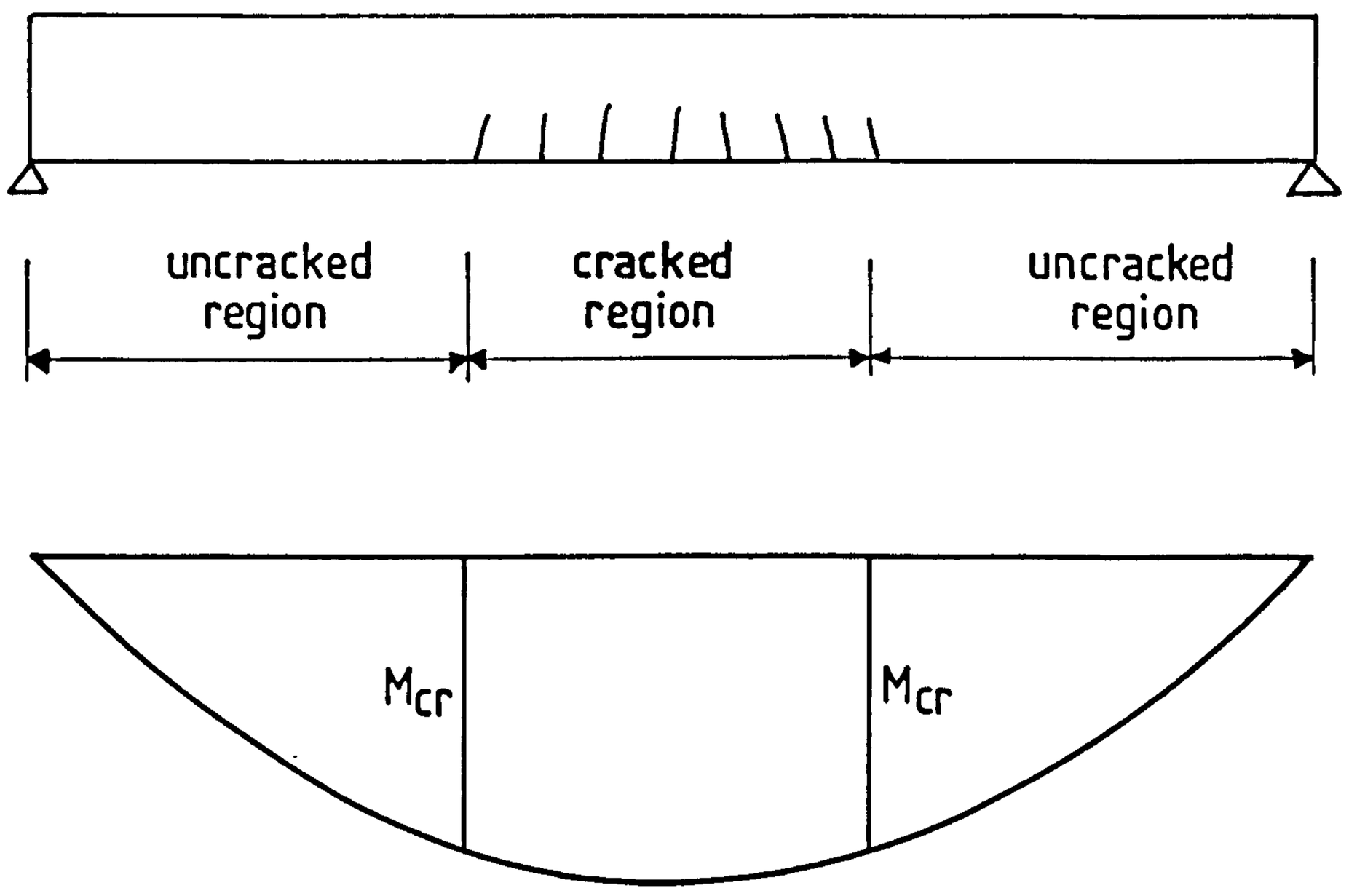

Fig. 5.1 Typical partially prestressed concrete beam and bending moment diagram under uniformly distributed load.

detail in Section 5.2.

Two analytical methods are presented in this Chapter, one for the calculation of short-term deflection and one for the long-term deflection of partially prestressed concrete members. Computer programs were developed for these purposes and are listed in Appendices A and B.

5.2 Evaluation of Tension Stiffening

The analysis of cracked prestressed concrete sections based on the conventional linear theory of reinforced concrete has been well established and generally gives acceptably accurate values of tensile stresses in both the prestressed and non-prestressed reinforcement (12,23). The stresses, however, become less along the length of the steel between two adjacent cracks where some tensile resistance is contributed by the concrete below the neutral axis. Thus, the average strain at the level of the steel is less than the steel strain in a crack. This effect is commonly known as "tension stiffening" and must be accounted for in the analysis of deflection.

It has been generally accepted in reinforced and prestressed concrete and can be legitimately assumed in partially prestressed concrete, that the steel reinforcement and the concrete surrounding it behave linearly provided the concrete stresses are less than the tensile strength. When this strength is exceeded on the tension face of the member,

cracks form up to a level very close to the neutral axis as calculated from the conventional theory ignoring tensile stresses. All the forces being carried by the concrete prior to the development of these cracks must, therefore, transfer to the steel which crosses the crack interface.

However, little evidence is yet available regarding the distribution of stresses along the bonded bar between the two adjacent cracks, which is obviously related to the bond properties. Qualitatively, according to Goto (33), at advanced levels of strain and with deformed steel, a pattern of internal cracking develops as shown in Fig.5.2. Radial thrusts develop from the bar deformations and must be resisted by a ring or hoop tension in the concrete. As strain and radial thrusts increase, a stage can be reached for bars close to the surface where the ring tension causes longitudinal splitting. At this stage, the tension stiffening effect will dissipate completely.

A number of empirical expressions have been proposed (34-36,50) for reinforced concrete structures, to account for this effect. Basically, the average steel stress f_{sm} is calculated from the expression:-

$$f_{sm} = f_s - d(f_s)$$

where f_s is the steel stress at the crack without any contribution of concrete tensile stress, $d(f_s)$ is the average reduction of steel stress due to tension stiffening effect.

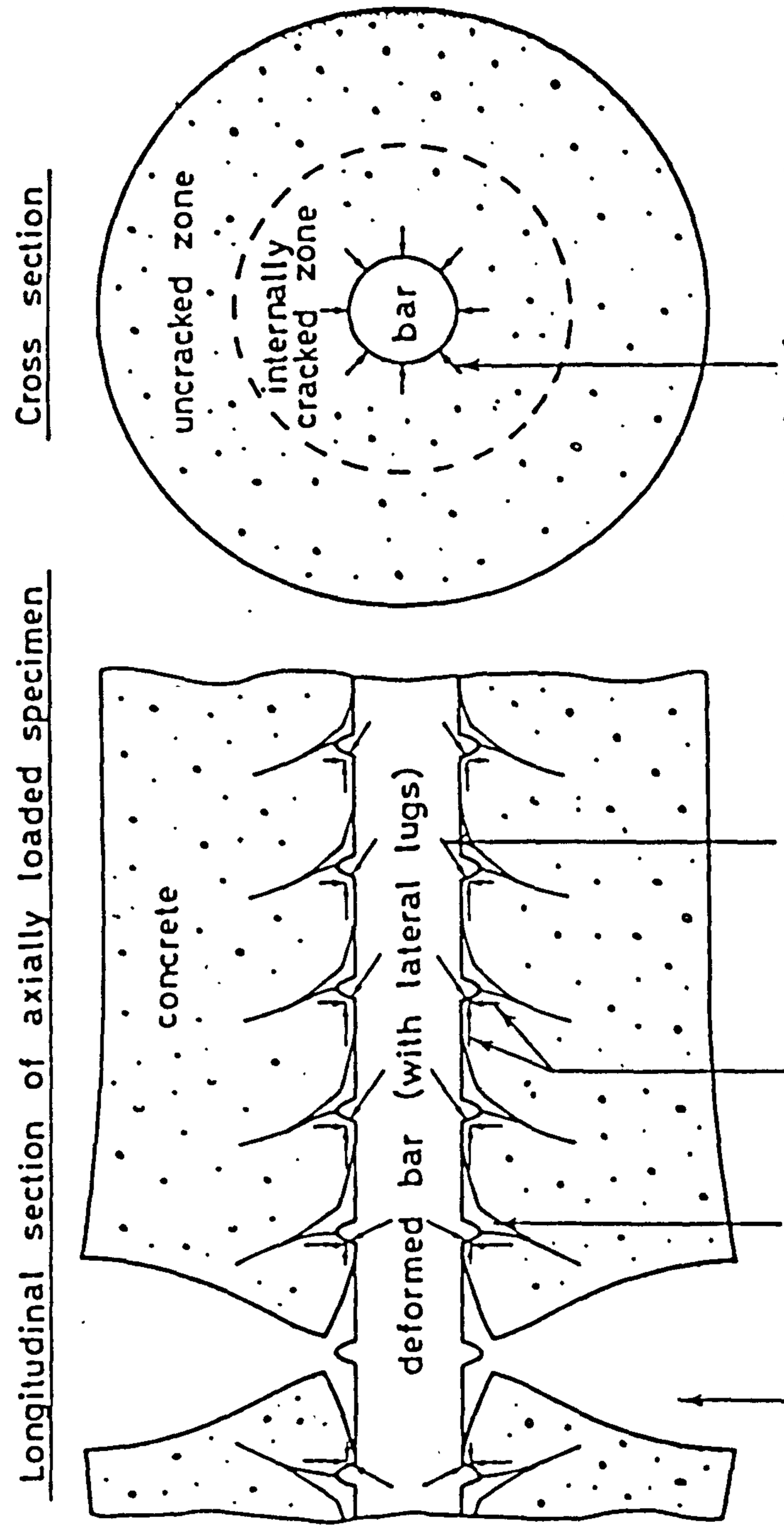

Fig. 5.2 Cracking of concrete around reinforcing steel according to Goto

From equilibrium conditions, $d(f_s)$ can be expressed as:-

$$d(f_s) = cf_t \frac{A_c}{A_s}$$

where C is an empirical factor

f_t is the concrete tensile strength

A_c is the effective area of the concrete around the tension steel contributing to tension stiffening.

A_s is the area of the reinforcement.

By studying the experimental evidence from tests on reinforced concrete beams, Rao and Subrahmanyam (34) found that the reduction in stress due to tension stiffening is reduced when the applied force increases. The following empirical expression was suggested based on the experimental data,

$$f_{sm} = f_s - 0.18\left(\frac{f_{cr}}{f_s}\right) \frac{f_{tc}\, bd}{A_s}$$

where the ratio $\frac{f_{cr}}{f_s}$ signifies the degree of cracking.

The equation was further modified for the CEB-FIP Model Code (36) in which the average steel strain is expressed as:-

$$\varepsilon_{sm} = \frac{f_s}{E_s}\left[1 - \beta_1\beta_2\left(\frac{f_{cr}}{f_s}\right)^2\right] \nless 0.4 \frac{f_s}{E_s}$$

where β_1 denotes a coefficient which characterises the bond properties of the bars

β_2 denotes a coefficient representing the influence of the duration of the application or repetition of the loads.

β_2 = 1 at first loading,

β_2 = 0.5 for loads applied in a sustained manner or for a large number of load cycles.

The expression is shown diagrammatically in Fig.5.3.

The British Code CP110, however, accounts for the tension stiffening effect by assuming that the concrete stresses vary from zero at the neutral axis to a value of 1.0 N/sq.mm (for short term loading) at the centroid of the tension steel. This enables the curvatures at the uncracked sections between the cracks to be calculated. CP110 however, does not give guidance regarding the variation of the curvatures between the uncracked sections between the cracks and the sections at the crack. Bennett in a number of recent publications (7,8) suggested that the curvatures be linearly distributed. Fig.5.4 illustrates the assumed stress distribution at the sections between cracks, according to CP110.

5.3 Analysis of Short-term Deflection

The analytical method of calculating the deflection of partially prestressed concrete members described in this Chapter is based on the CP110 Appendix A recommendation. The deflection at any point or the deflected profile of the beam is calculated by integrating the curvatures of the sections

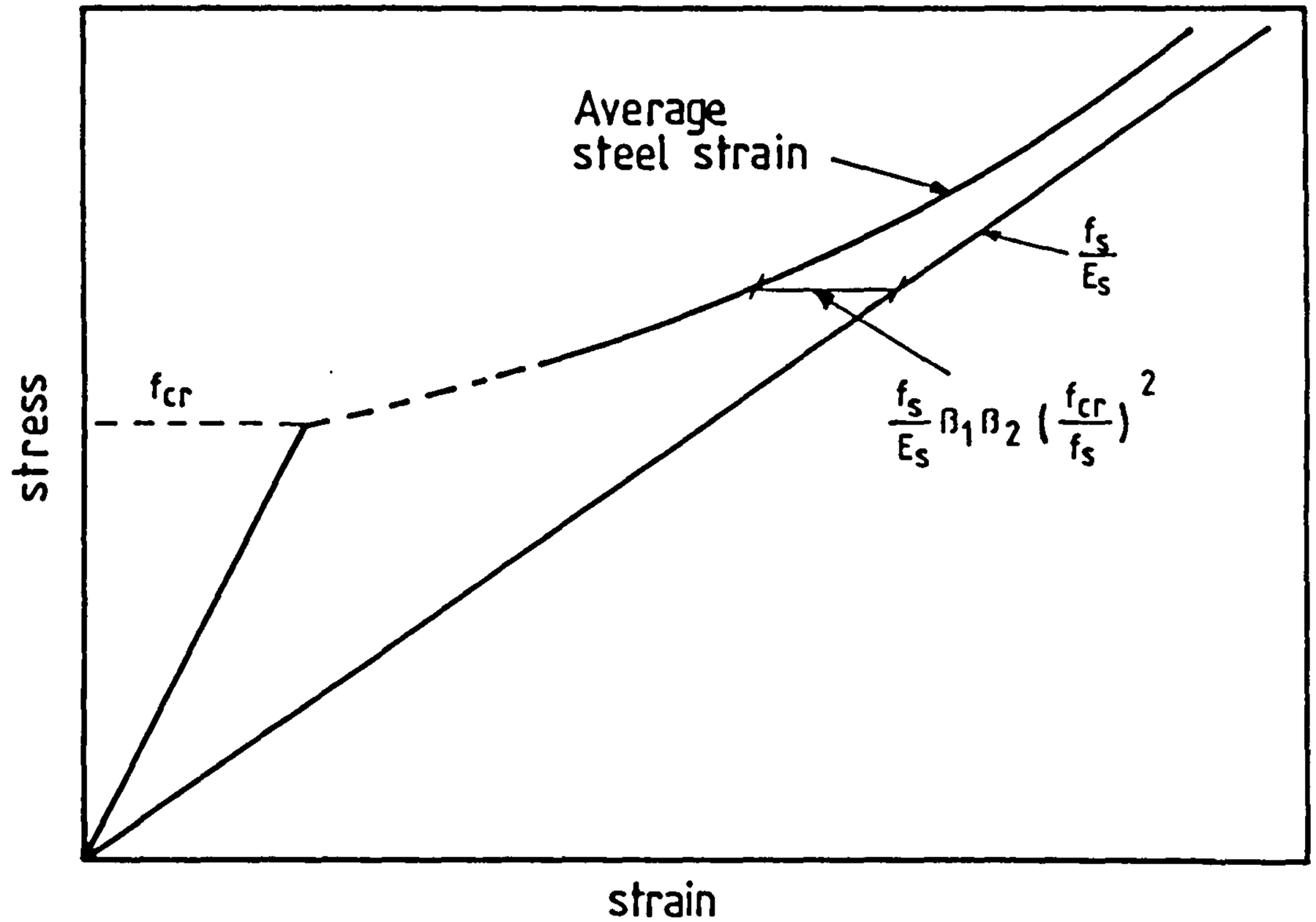

Fig. 5.3 Average steel strain according to CEB/FIP Model Code

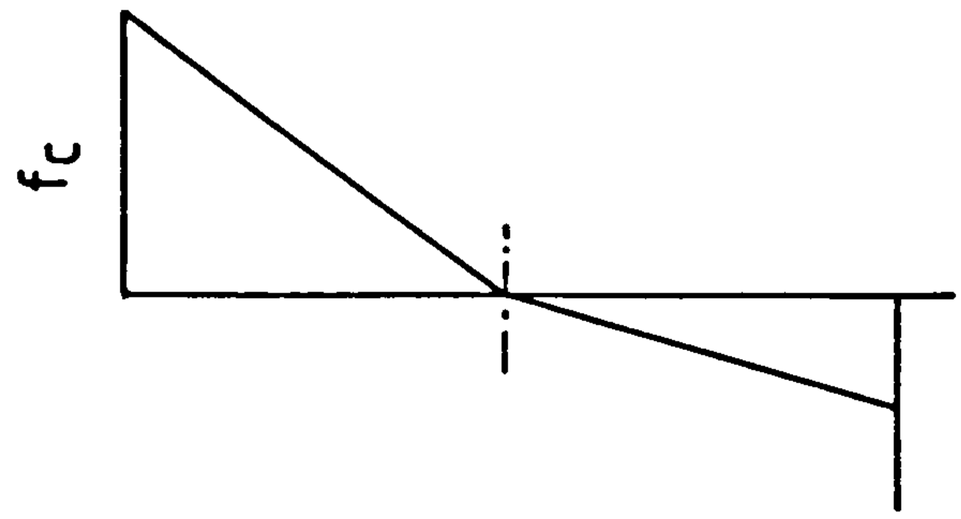

Fig. 5.4 Stress distributions at sections between cracks according to CP110

over the whole span.

The member is divided into small elements or sections and for each section, strain is obtained from the calculated stress distribution. At the cracked region (Fig.5.1), sections are analysed by the method described in Chapter Four, Section 4.2., in which the reinforcement stresses are analysed by the modified reinforced concrete theory. The calculated stresses and thus the strain of the reinforcement, together with the stress and strain at the top of the section, enables the curvature to be calculated from the expression:-

$$\frac{1}{r} = \frac{\varepsilon_{top} + \varepsilon_{bottom}}{h} \qquad \text{... Eqn (5.1)}$$

where r is the radius of curvature

h is the depth of the section

However, due to the effect of "tension stiffening" discussed in Section 5.1, the curvatures of the sections between the cracks are reduced. Several empirical expressions have been proposed to account for this effect while the the recommendation of the British Code CP110 is that the tensile stress of the concrete at the centroid of the tension steel be assumed to have a value of 1.0 N/sq.mm under short-term loading, Fig.5.4. The latter recommendation regarding tension stiffening effect has been adopted in the analysis presented in this Chapter. The average curvature of the uncracked section between the cracks is therefore given

by:-

$$\frac{1}{r_{uncr}} = \frac{f_c + 1}{E_c d} \quad (N/mm^2) \qquad \text{... Eqn (5.2)}$$

where f_c is the compressive stress at the top of the beam, assumed to be the same as at the cracks.

The average curvature is thus intermediate between the two values given by Eqns.(5.1) and (5.2), depending on the longitudinal distribution of the curvature between cracks, (Fig.5.5).

$$\frac{1}{r_{av}} = \frac{1}{r_{uncr}} + \beta\left(\frac{1}{r_{cr}} - \frac{1}{r_{uncr}}\right) \qquad \text{... Eqn (5.3)}$$

where β is a distribution coefficient. Referring to Eqn.(5.3), $\beta = 1$ represents complete loss of tension stiffening when the average curvature is also the curvatures at the cracks. The CP110, however, does not give guidance on the distribution coefficient. Bennett (7,8) suggested a linear distribution which means that $\beta = 0.5$. In the present research, several values of the coefficient were studied and compared with test results. The comparisons are discussed in Chapter Seven.

In the uncracked regions (for example, sections near the supports of a simply supported beam), stresses and strains are calculated by the normal prestressed concrete theory. The curvatures are again calculated by Eqn.(5.1).

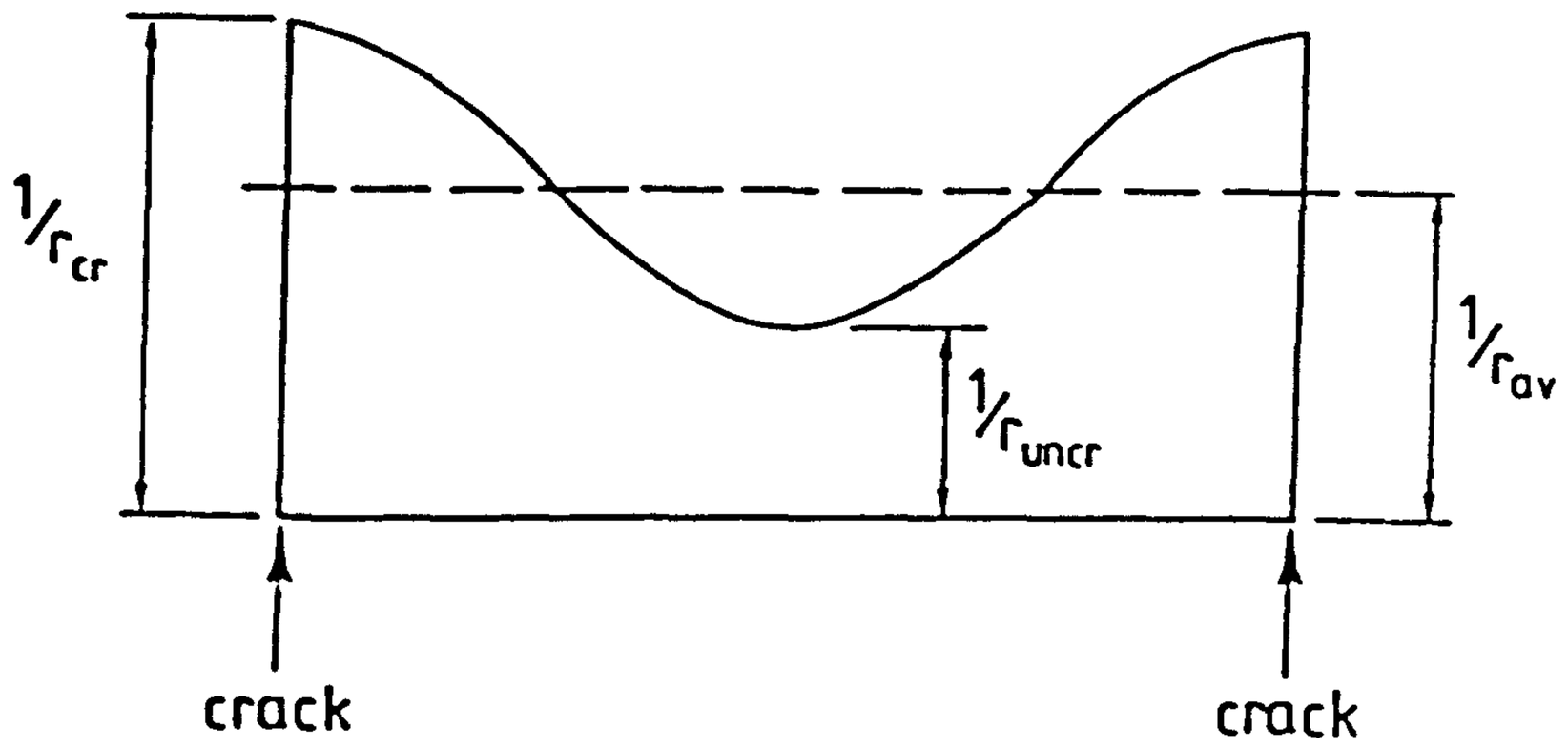

Fig.5.5 Distribution of curvature between cracks

The deflection y, at any point at a distance x along the beam and hence the deflected profile can then be calculated by numerical integration of the curvature equation:-

$$\frac{1}{r} = \frac{d^2y}{dx^2} \qquad \text{... Eqn (5.4)}$$

Applying Eqn(5.4) in the analysis of deflection by computer, it has been found convenient to integrate the curvatures numerically on the basis of the conjugate beam theory for which purpose the beam is divided into a finite number of short elements over each of which the moment, and hence the curvature is assumed to be constant. A computer program has been developed which is capable of calculating deflection at any point over the whole span of the beam. The program is listed in Appendix A.

The computation steps involved in the analysis of deflection described above, are as follows:-

1) From the given dimensions of the beam, the uncracked section properties are calculated based on the transformed concrete area.
2) With the given load, calculate the bending moments and the bending stress at the soffit of every section over the whole span.
3) Starting from the first section near the support, calculate the effective prestress at the soffit from the given effective prestressing force and based on the

uncracked (homogeneous) concrete section.

4) The resultant of the bending stress and prestress is then compared with the given tensile strength (for first load cycle) or zero stress of the concrete (for second or subsequent cycles of loading).

5) (i) If the resultant stresses at the soffit are less than the tensile strength or zero, depending on the cycle of loading, the sections are analysed by assuming them to be uncracked. Curvatures are then calculated by Eqn.(5.1).

   (ii) Otherwise, the sections are analysed as cracked by the method described in Section 4.2. The average curvature is then computed by Eqn.(5.3).

6) Steps 3, 4 and 5 are repeated for all the elemental sections over the whole span (or half span if the beam and the loading are symmetrical).

7) The curvatures of all the sections are then integrated according to the conjugate beam theory and hence the deflection at any point along the beam can be calculated.

5.4 Analysis of Long-term Deflection

The creep and shrinkage of concrete and the relaxation of steel are known to be the major factors affecting the time-dependent increase of deflection of partially prestressed concrete members under sustained loading. For low relaxation steel such as the seven-wire strands used in the experimental programme, the total relaxation was

predicted, from tests conducted by the manufacturer, not to exceed 5.6 per cent of the initial stress. The tests also estimated that a relaxation of 3.2 per cent of the initial stress occurred in the first 30 days. It was, therefore, decided to assume that all the loss due to relaxation occurred before the commencement of the beam tests, and to ignore the continuing small loss in the long-term tests. The effects of creep and shrinkage of concrete on the long-term deflection of partially prestressed beams under sustained load, were considered separately. The total increase of deflection was then taken to be the sum of the increase of deflection due to each of these two effects. Thus, two similar computer programs were developed and are given in Appendices A and B.

The analysis is again based on the CP110 Appendix A recommendation in which the curvature is to be calculated by Eqn.(5.1). The deflected profile of the beam is also calculated by integrating the curvatures of the sections over the whole span.

The member is divided into elements or sections and for each element, strain is obtained by analysing the reinforcement stresses which accounts for the non-elastic strains induced by the concrete creep or shrinkage. In the cracked region, the sections are analysed by the methods described either in Section 4.3 (for the case with creep effect) or Section 4.4 (for the case with shrinkage effect). The concrete stress (at the level of the centroid of the

tensioned steel), at the uncracked sections between cracks, is reduced to 0.55 N/sq.mm for the long-term deflection calculation. The curvature of the uncracked section is, therefore, given by (for the case with creep effect):-

$$\frac{1}{r_{uncr}}' = \frac{(c_c f_{c1} + f_{c2}) + 0.55}{E_c d} \qquad \text{... Eqn (5.5)}$$

where f_{c2} is the new stress at the top of the beam

$c_c f_{c1}$ is the 'unrestrained' creep

The average curvature in the cracked region is then calculated using Eqn.(5.3) where β is a distribution factor.

In the uncracked regions near the supports, sections are analysed by the "Imaginary and balancing forces" method demonstrated by Bennett (13). The compressive forces induced by creep or shrinkage in the reinforcement are "balanced" by an equal and opposite force at the level of the steel. This force causes a change of concrete stress and thus the total strain at the time considered is taken to be the sum of the reduced 'elastic' strain and the 'unrestrained' creep or shrinkage. The common assumptions that creep is proportional to the concrete stress and that the magnitude of shrinkage is constant over the section, are adopted in the analysis.

The deflected profile is again calculated by integrating the curvatures of the sections, based on the conjugate beam theory.

The analytical procedures involved in the calculation of the long-term deflection are listed in the following steps:-

1) Given the load sustained on the beam, analyse the short-term stresses and strains (as described in Section 5.3) of all the sections under the applied moment at each section.

2) Estimate the magnitude of the specific creep and the concrete shrinkage over the time considered. These values can either be obtained from standard text books, codes of practice (6,51) or from tests on plain concrete specimens.

3) Starting from the first section nearest to the support, analyse the section according to the analysis as described in Section 4.4 (for the case with creep effect) or Section 4.5 (for the case with shrinkage effect), if it was cracked under short-term load. If however, the section was uncracked, calculate the new stress and strain by the 'imaginary and balancing forces' method (13).

4) The curvatures of the uncracked sections are calculated by Eqn.(5.1) while the average curvatures of the cracked sections are computed by Eqn.(5.3) and (5.5).

5) The deflection at any point along the beam is then calculated by integration of the curvatures.

6) The deflection obtained with the effect of creep alone is then added to the increase of deflection calculated separately with the effect of shrinkage. This is then taken to be the long-term deflection.

In any case, when the calculated new neutral axis in Step (3) falls below the level of the soffit (i.e. the section is in full compression), the curvature is re-calculated by assuming it was uncracked and thus using the "imaginary and balancing forces" method.

In view of the complexity of the procedures involved, a separate computer program was developed for the calculation of long-term deflection with the effect of shrinkage alone. This is given in Appendix B.

CHAPTER SIX

Design and Fabrication of The Beams and Test Procedures

6.1 General

In this chapter, the design and fabrication of the beams, together with the testing procedures, are described in detail. The tests consisted of a series of nine partially prestressed concrete beams subjected to a combination of long-term and short-term loading. In addition, three duplicate beams were tested under long-term loading alone.

6.2 Test Beams

6.2.1 Shape and Dimensions

A total of twelve beams were tested of which three were control tests. Although shape of the section is an important parameter affecting deflection, it had already been studied elsewhere (23,24), so that it was not necessary to include it again in this programme. All the beams were, therefore, of a similar I-section which was considered to be typical of common practice.

It was also considered necessary to test beams of dimensions and span comparable with those in practice and of maximum possible size to be handled in the laboratory. Span/effective ratio was designed to be near the maximum allowable in the British Standard CP110 (6). All the beams

were, therefore, cast 6.3m long for a test span of 6.0m. The depth of all the beams was 305mm and hence, the span/effective depth ratio was approximately 22 while the permissible ratio in the code is 20, excluding the modification factor for tension reinforcement (Fig.6.1). The flange breadth was 150mm; the breadth of the web and the thickness of the bottom flange was 50mm while the top flange was 55mm thick. Thus, the size of the beams was of the same order as some of the smaller members used in building construction. They may also be regarded as models of bridge beams.

6.2.2 Reinforcement Level

The test beams can be divided into three series based on the level of reinforcement; the tensile force developed at failure and the 'design' ultimate moment (calculated according to B.S. CP110) being almost the same for all the beams at each level. For rectangular prestressed concrete members, the British Code represents the degree of reinforcement by the dimensionless quantity $A_s f_y / bd_e f_{cu}$, but there is no simplified form available for non-rectangular sections. The 'design' ultimate moment for the three levels of reinforcement varies from 55.2kNm to 71.9kNm and the actual values are given in Table 6.1. The three levels of reinforcement chosen correspond to the tensile forces provided by 6, 5 and 4, 7.94mm seven-wires strands in a fully prestressed beam without non-prestressed reinforcement. The force developed in one strand at ultimate

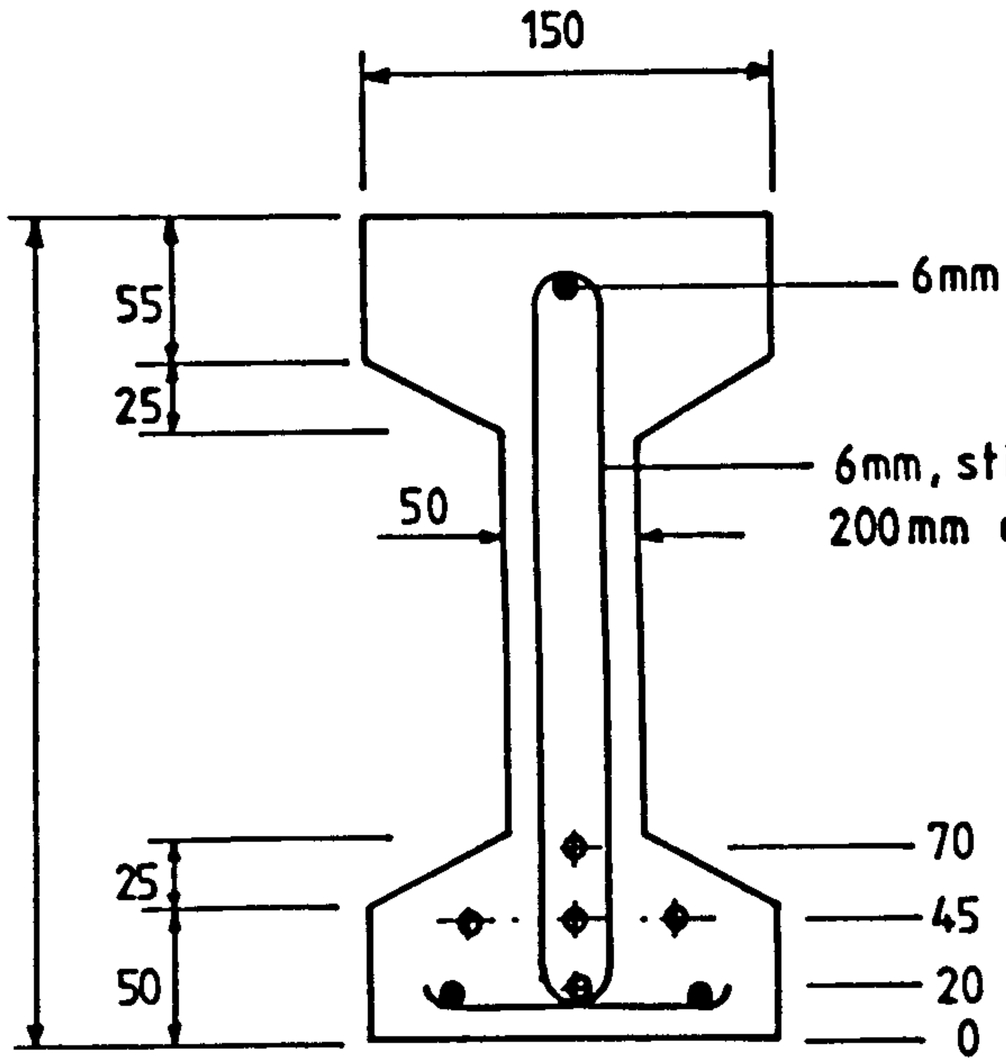

Beam S1.5.2

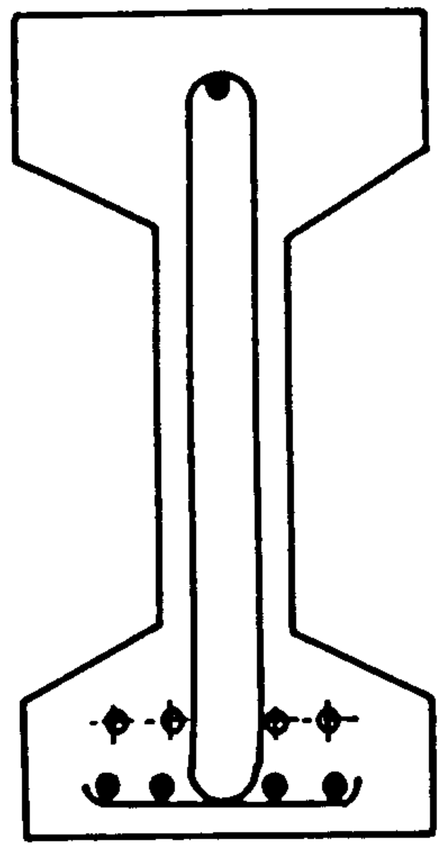

Beam S1.4.4

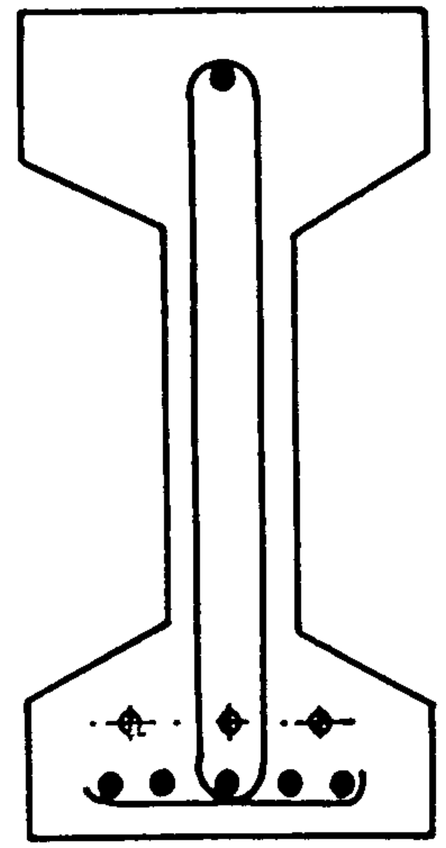

Beams S1.3.5
S1.3.5S

◆ 7.9 mm strand

● 10mm non-prestressed steel

all dimensions in mm

Fig. 6.1 Cross-section of beams, 1

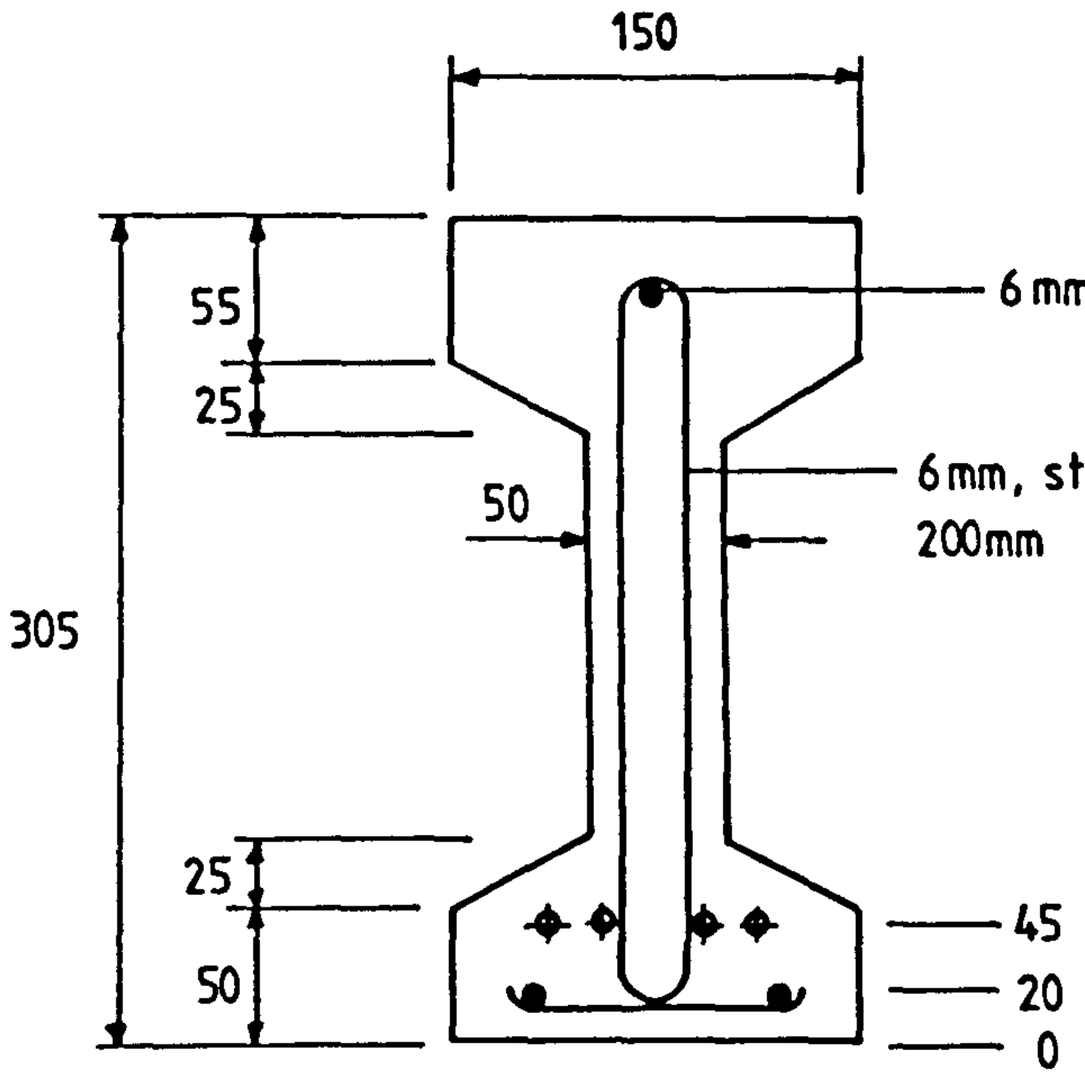

Beam S2.4.2

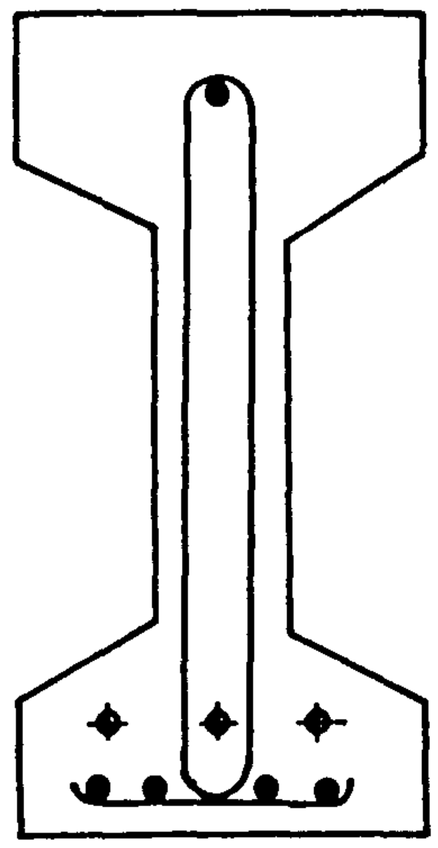

Beams S2.3.4
S2.3.4S

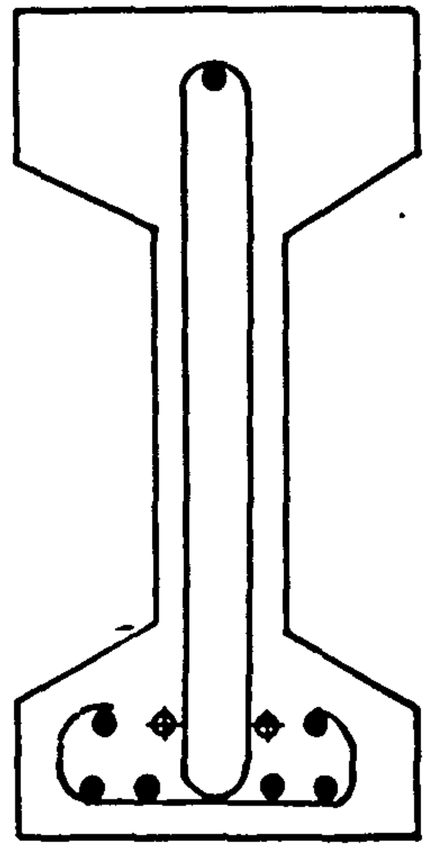

Beam S2.2.6

Fig. 6.1 (Continue), 2

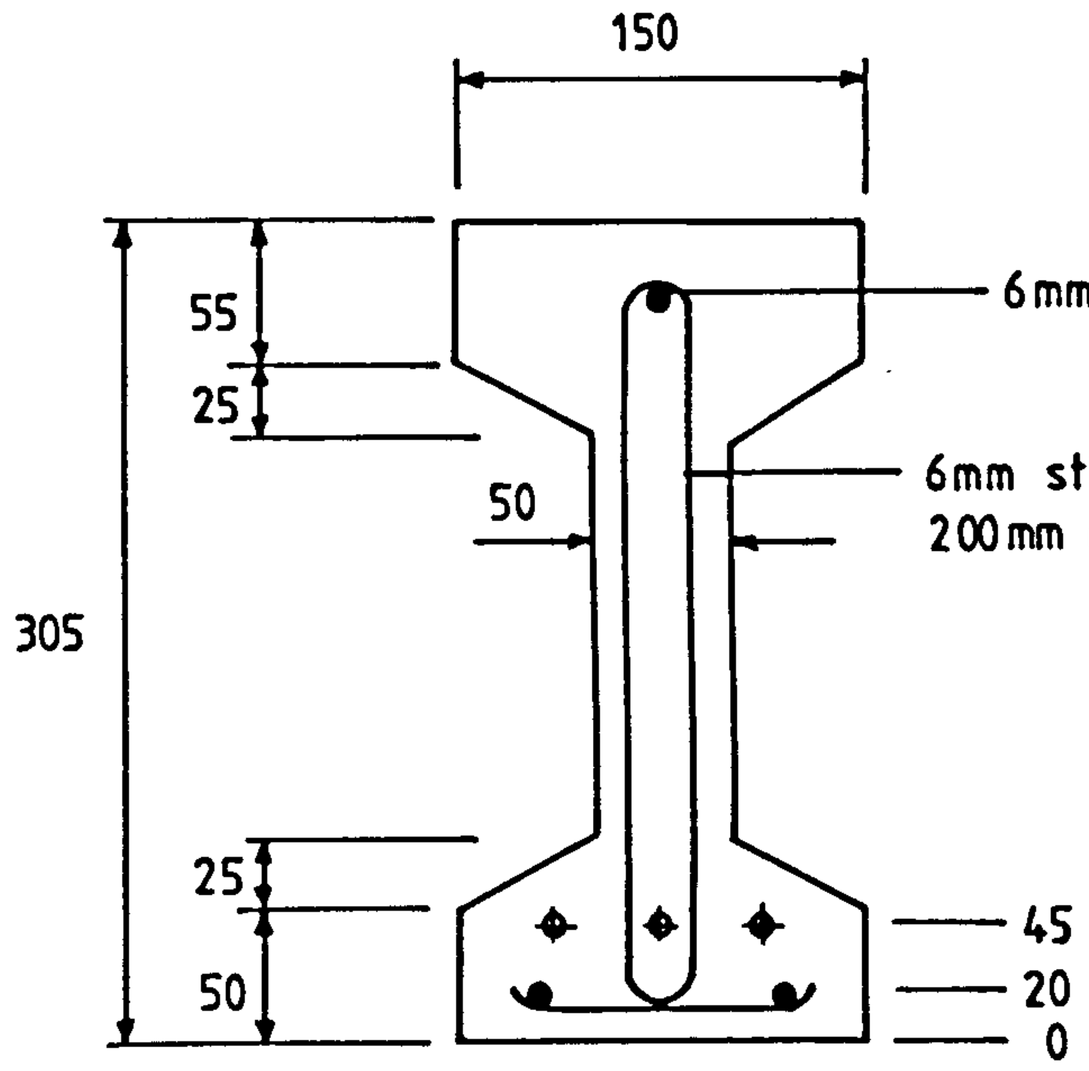

Beams S3.3.2
S3.3.2S

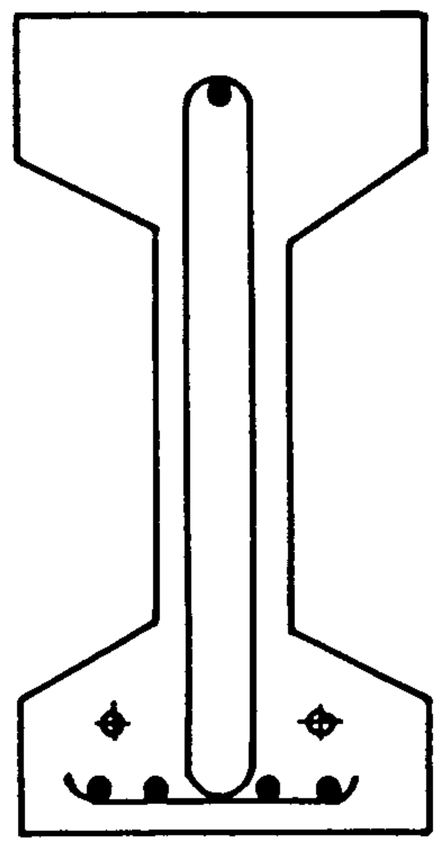

Beam S3.2.4

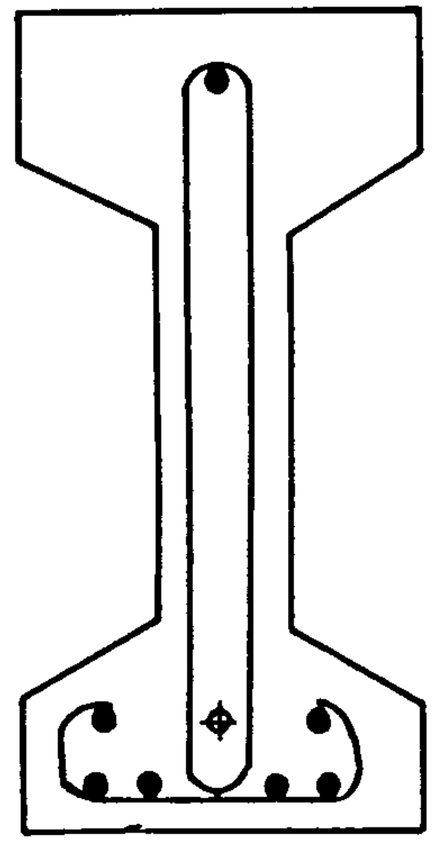

Beam S3.1.6

Fig. 6.1 (Continue), 3

Beam References	PPR	DEG	Total strength of reinforcement at ultimate (kN)	'Design' ultimate moment (kNm)	'Design' service moment (kNm)	Service moment in tests (kNm)
S1.5.2	0.83	0.69	363.0	69.92	46.61	47.38
S1.4.4	0.65	0.56	365.8	71.89	47.93	47.38
S1.3.5	0.53	0.42	337.3	70.59	47.06	47.38
S2.4.2	0.79	0.62	303.0	64.34	42.89	43.82
S2.3.4	0.59	0.47	305.8	66.29	44.19	43.82
S2.2.6	0.39	0.32	308.7	66.68	44.45	43.82
S3.3.2	0.74	0.58	243.0	55.25	38.53	36.70
S3.2.4	0.49	0.38	245.8	57.30	38.20	36.70
S3.1.6	0.24	0.20	248.6	57.80	36.83	36.70

Table 6.1: Levels of Prestress and Reinforcement

load is approximately equal to that of two 10mm cold-worked deformed bars. The numbers of tendons and non-prestressed reinforcement for each beam are given in Table 6.2 and Fig.6.1

6.2.3 Level of Prestress

The level of prestress in the beams at each level of reinforcement was varied by altering the number of strands prestressed and replacing the unstressed strands by two 10mm cold-worked deformed bars (replaced by one bar in beam S1.3.5). For example, for the beams with the lowest level of reinforcement (series 3 in Table 6.2), the level of prestress was varied by stressing three, two and one strands respectively in the three beams. Similar variation in the other levels of reinforcement (series 1 and 3 in Table 6.2) provided a range of levels of prestress with 25 to 83 per cent of the total reinforcement being prestressed. The series of beams, therefore, covers five levels of prestress corresponding to 5,4,3,2 and 1 strand in the beams (Table 6.2) and each strand was stressed initially to 1291.4 N/mm2 (70 per cent of the characteristic ultimate strength). The levels of prestress can also be represented by the dimensionless ratios which are better known as the 'degree of prestress' (17,18) and the 'partial prestressing ratio' (14-16). The calculated values are given in Table 6.1.

In order to accommodate the wide range of the level of prestress, a high strength concrete was used so that the

	Number of 7.9 mm strands				Number of 10 mm bars		
Distance from bottom mm	20	45	70	Total	20	45	Total
Beam Reference							
S1.5.2	1	3	1	5	2	-	2
S1.4.4	-	4	-	4	4	-	4
S1.3.5	-	3	-	3	5	-	5
S2.4.2	-	4	-	4	2	-	2
S2.3.4	-	3	-	3	4	-	4
S2.2.6	-	2	-	2	4	2	6
S3.3.2	-	3	-	3	2	-	2
S3.2.4	-	2	-	2	4	-	4
S3.1.6	-	1	-	1	4	2	6

Table 6.2: Position of Strands and Bars in Beams

prestress in concrete at the highest level did not exceed the permissible values at transfer specified in the British Standard CP110.

6.2.4 Type of Prestressing

The type of prestressing, viz. pretensioning or post-tensioning is one of the parameters affecting the deflection of partially prestressed concrete members. However, this parameter was not studied in this research and was therefore, kept constant. All the beams were pretensioned because this form of prestressing is most commonly used in precast beams.

6.2.5 Ultimate and Service Moment

The 'design' ultimate moment for each beam was calculated according to CP110 with the materials safety factors of 1.5 for concrete and 1.15 for steel. The dead load moment was assumed to be equal to the live load moment and thus the service moment was two-third of the 'design' ultimate moment. Table 6.1 shows the actual values of the 'design' ultimate and service moment.

6.2.6 Other Details

The concrete grade was 60 as specified in CP110 for all the beams in the test programme. All the beams had 6mm diameter high-yield hot-rolled bars bent as stirrups and

were designed to take the maximum shear on the beam with the highest amount of tensile reinforcement, thus ensuring a flexural failure.

6.2.7 Beam References

A simple system dividing a beam reference into three parts with "full-stops", was adopted to designate the beams, Table 6.2. The first part chosen designated the level of reinforcement. Thus, all the beam references with S1 (series 1) had the highest level of reinforcement and were of approximately equal ultimate moment. Similarly for S2 (series 2) with medium and S3 (series 3) with the lowest level of reinforcement. The numeral in the second part corresponds to the number of prestressed strands in the beam. In the third part, the numeral corresponds to the number of non-prestressed bars in the beam and the letter 'S', where added, signifies that the beam was subjected to sustained loading only.

6.3 Materials

6.3.1 Concrete

All the beams were cast in the laboratory of the Civil Engineering Department, University of Leeds. The grade of concrete used was 60 N/mm2 as specified in CP110 and the actual strength obtained for each beam is given in Table 6.3. Since the beams were tested at different ages (varying from 21 to 97 days), the average compressive strength for

Beam reference	Calculated tensile stress in concrete (uncracked section) N/mm²		Strength of Concrete			Modulus of Elasticity (4) (kN/mm²)
			Compressive (1) (N/mm²)	Tensile (N/mm²)		
	1/2 service moment	service moment		Split Cylinder (2)	Flexural (3)	
S1.5.2	-4.5	8.1	73.8-77.2	4.18	5.36	35.8
S1.4.4	-1.4	10.8	64.2-69.3	4.00	6.39	41.7
S1.3.5	1.5	13.5	76.5-79.8	4.14	5.40	38.2
S1.3.5s	1.5	13.5	73.7-81.1	3.70	5.18	39.3
S2.4.2	-2.7	8.3	70.3	3.50	5.02	35.3
S2.3.4	0.7	12.0	63.1-68.5	3.80	5.50	35.7
S2.3.4s	0.7	12.0	58.6-	4.12	5.47	33.9
S2.2.6	4.3	15.9	65.1-75.0	3.68	5.28	39.7
S3.3.2	-1.5	8.0	71.8	3.93	4.80	38.5
S3.3.2s	-1.5	8.0	71.8-71.2	4.17	6.55	36.1
S3.2.4	2.3	12.1	73.4-74.6	4.00	6.10	37.8
S3.1.6	6.0	12.6	60.4-65.6	3.68	4.96	39.5

s Sustained load only.

(1) Average of between 3 and 7 No. 100 x 100 mm cubes tested on first and last days of test.
(2) 4 No. 300 x 150 mm cylinders tested to BS1881 Part 4 1970, on the first day of test.
(3) Between 3 and 6 No. 500 x 100 x 100 mm prisms tested to BS1881 Part 4, 1970, on first day of test.
(4) Tested to BS1881 Part 5 1970, on first day of test.

Table 6.3: Stress in Beams and Properties of Concrete

each beam varied from 60.4N/mm2 to 76.5N/mm2 on the first day of testing.

The concrete consisted of 10mm quartzite gravel, sand and Ordinary Portland Cement in the proportions 1 : 1.5 : 3 with water/cement ratio of 0.43. The concrete was found to give a strength of over 45 N/mm2 after seven days. This high strength was necessary to ensure that the maximum prestress at transfer of stresses did not exceed 50 per cent of the compressive strength.

For each mix, the concrete was proportioned by weigh-batching. The materials, in the required proportions, were fed into the mixer and turned over for about one minute before the required quantity of water was added. The concrete was then mixed for about two minutes and taken to the casting bed. The compacting factor varied between 0.85 and 0.93.

6.3.2 Steel Reinforcement

6.3.2.1 Prestressing Steel

Seven-wire strand, with a nominal diameter of 7.94mm and cross-sectional area of 37.4mm2, was used in all the test beams. Samples of the prestressing strand were subjected to tensile tests in the laboratory 'Instron' machine and a typical stress strain relationship obtained is plotted in Fig.6.2a. The 0.2 per cent proof stress, the ultimate strength and the modulus of elasticity are given in

Table 6.4.

6.3.2.2 Non-prestressed Reinforcement

The non-prestressed reinforcement consisted of 10mm cold-worked deformed bars with a guaranteed characteristic proof stress of 460 N/mm2. The steel was marketed under the trade name 'Torbar'.

Tensile tests were conducted on sample bars and a typical stress strain curve is shown in Fig.6.2b. The details of the ultimate strength and modulus of elasticity are given in Table 6.4.

6.3.2.3 Stirrups

The shear reinforcement in all the beams consisted of 6mm hot-rolled high-yield deformed bars. Nominal shear reinforcement was provided throughout the length of the beam except in the support regions where the reinforcement was doubled. Details of the stirrups are shown in Fig.6.3.

6.3.2.4 Compression Reinforcement

The beams were designed according to the British Standard CP110 and compression reinforcement was not required for all the beams. However, nominal reinforcement consisting of one 6mm mild steel bar was provided at the top to support the stirrups. Figs.6.1 and 6.3 show the details

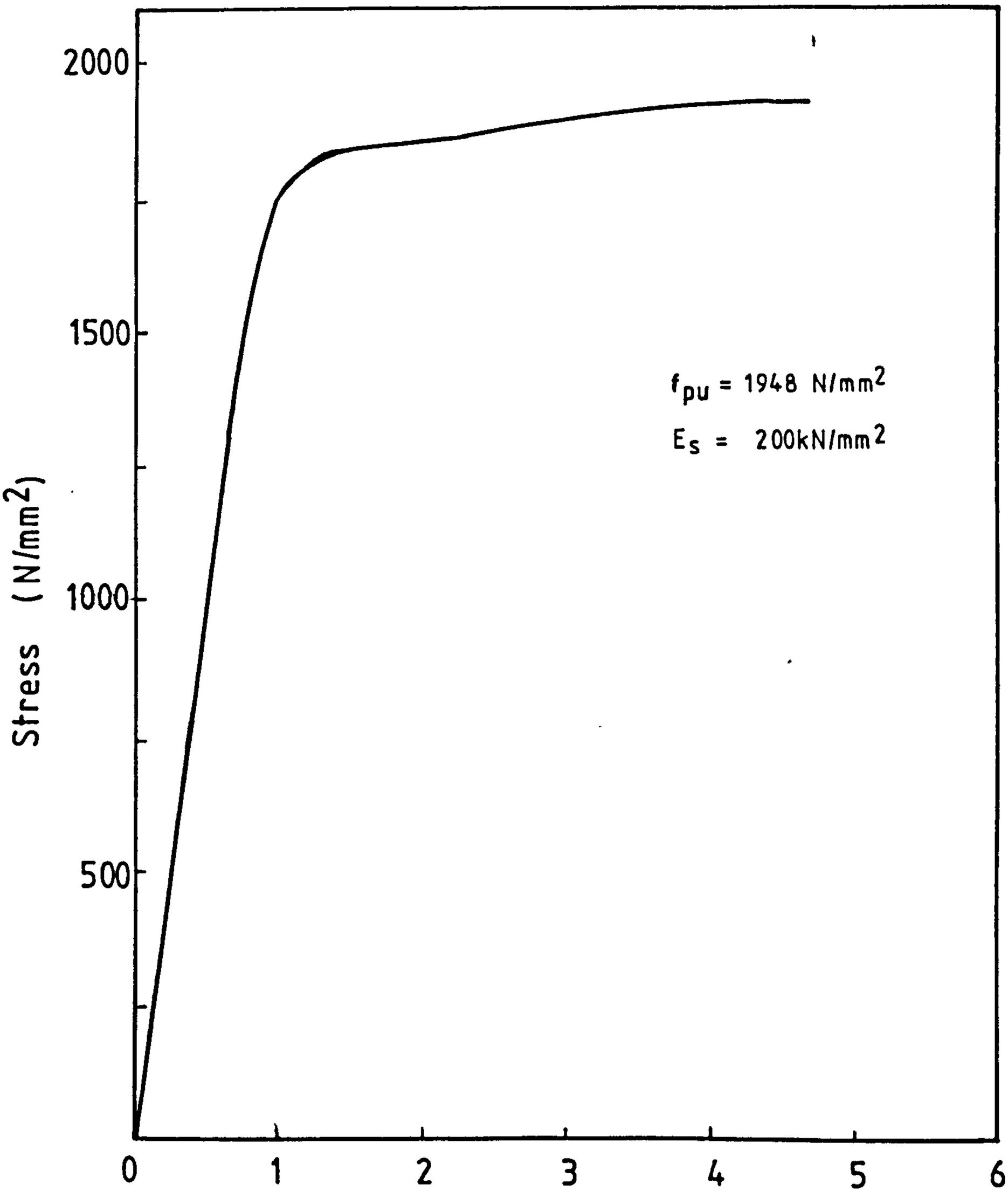

Fig.6.2a Stress Strain relationship of the 7.9mm strand

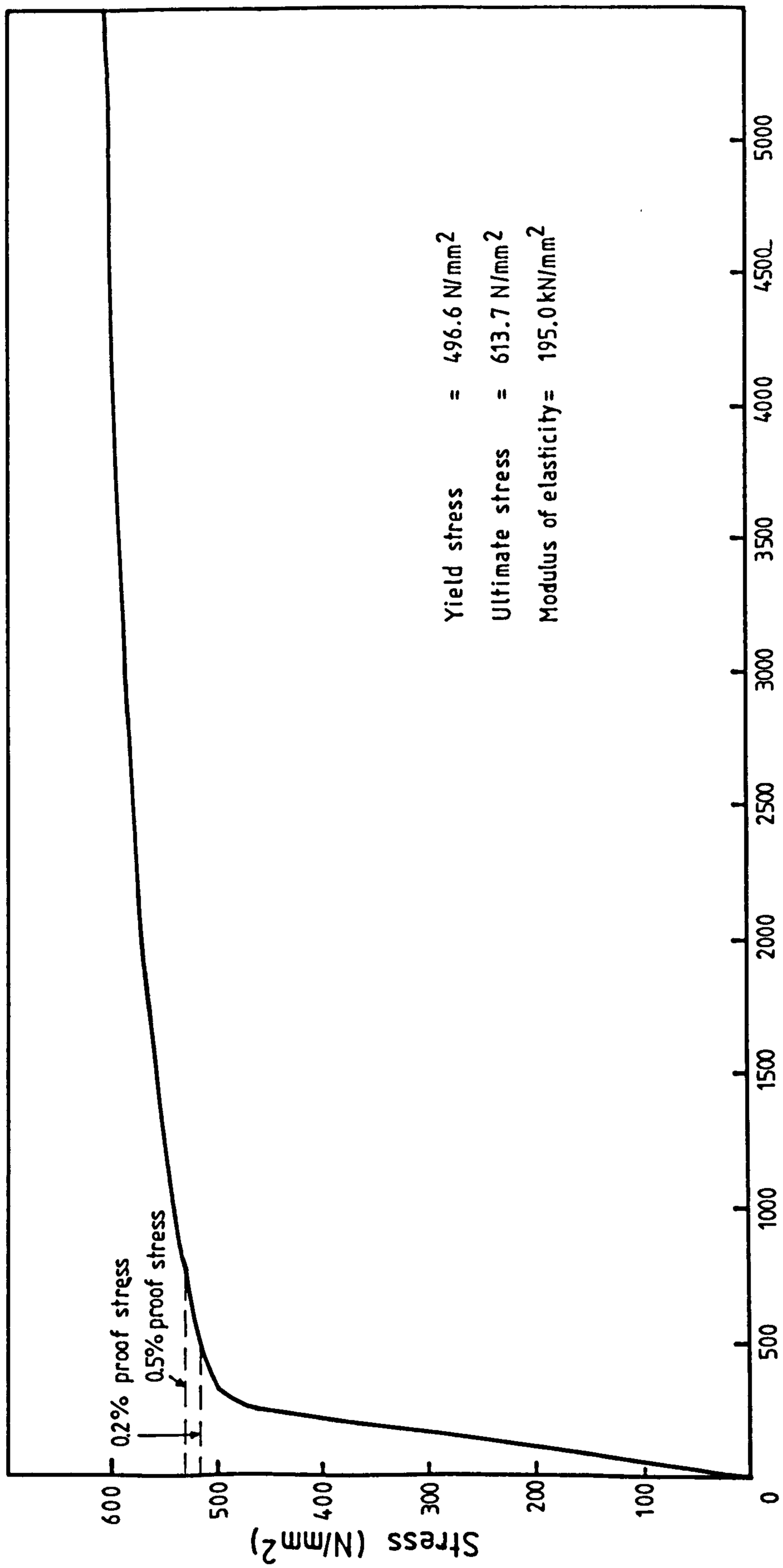

Fig. 6.2 b Typical stress-strain curve of the non-prestressed steel

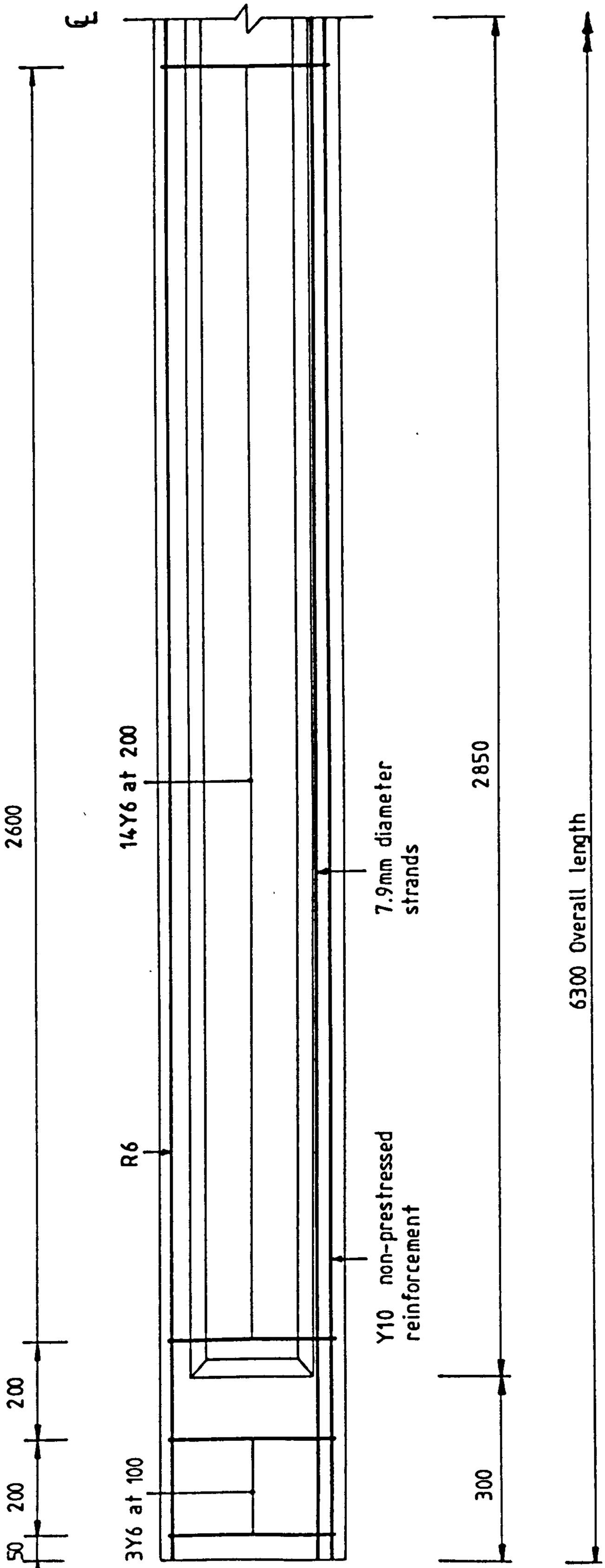

Fig. 6.3 Typical longitudinal section of the beams showing stirrups

7.94 mm Strands

Sample	0.2% Proof stress (N/mm^2)	Ultimate stress (N/mm^2)	E_s (kN/mm^2)
1	1800.5	1959.3	196.7
2	1853.4	1966.0	198.9
3	1800.5	1932.9	203.6
4	1800.5	1932.9	200.9

10 mm Cold-worked deformed bars

Sample	Yield stress (N/mm^2)	Ultimate stress (N/mm^2)	E_s (kN/mm^2)
1	496.6	604.8	197.6
2	496.6	613.7	195.0

Table 6.4: Properties of the reinforcement steels

of the reinforcement.

6.4 Fabrication of The Beams

6.4.1 Stressing the Strands

The required number of strands was inserted through the holes drilled at the designed levels in the end plates of the mould. At one end of each strand, a C.C.L. anchor grip was fixed driving the wedges hard with the grip supported against a thick anchor plate, (Fig.6.4). At the other end similar grips were placed loosely and each strand was given an equal initial tension of approximately 5 kN before the wedges of the anchoring grips were driven hard against another anchor plate about 100mm away from the end plate of the mould. The anchor plate was held in position by means of small pieces of channel section abutting the mould. All the strands, thus, had equal tension to take up the slack. This initial tensioning was done by means of a C.C.L. jack.

The total prestressing force was then applied by means of two hydraulic jacks mounted on a specially designed tensioning rig as shown in Fig.6.4. The two jacks were connected to a common gauge which was calibrated accurately and thus, the pressure in each jack was kept the same. All the strands were, therefore, stressed uniformly. The correct force in the strands was further checked by measuring the movement of the anchoring plate, which was equal to the extension of the strands, by means of dial gauges around the strands, Fig.6.4. When the correct force in each strand was

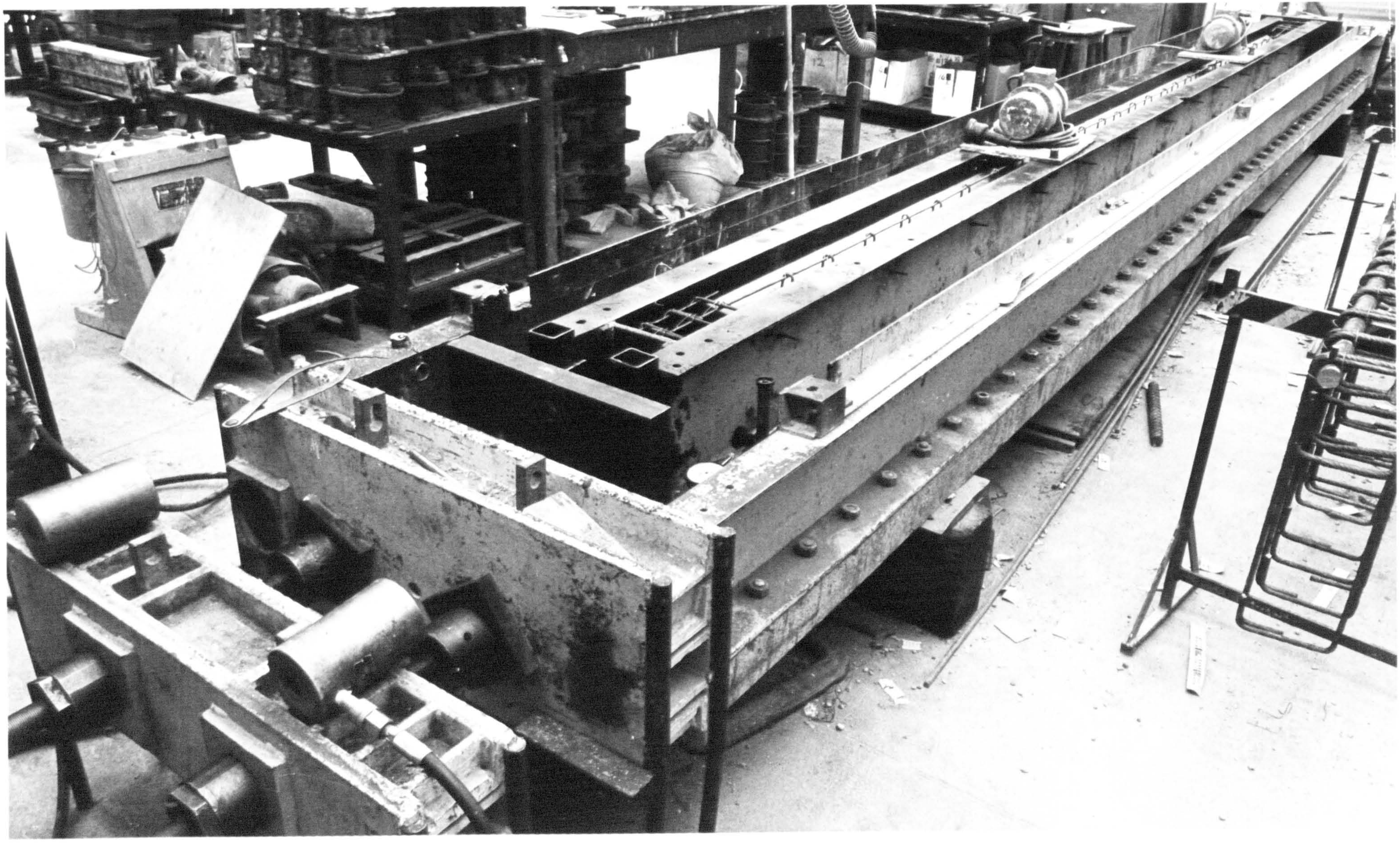

Fig.6.4 Pretensioning bed.

achieved the locknuts of the rig were tightened on to the main anchoring block at the end of the pretensioning rig. The pressure in the jacks was then slowly released.

6.4.2 Casting

The reinforcement cage, consisting of stirrups and non-prestressed bars, was placed in position on the casting bed before the strands were stressed as described in Section 6.4.1. The concrete, mixed as described in Section 6.3.1, was placed in layers and compacted by two vibrators clamped on top of the mould. All precautions were taken to ensure that concrete flowed freely between the reinforcing bars especially in the bottom flange.

Two batches of concrete were needed for each beam. From each batch of concrete six 100x100mm cubes, two 150x50mm cylinders and four 100x100x500mm prisms were cast for use as control specimens. A compacting factor test was also carried out for each batch of the concrete.

To prevent possible cracking due to shrinkage, the mould was stripped two days after casting. The beam was then covered with wet jute mats and polythene sheets. The jute mats were kept permanently wet by watering regularly

6.4.3 Transfer of Stresses

Before releasing the strands from the pretensioning rig

and transferring the stresses to the beam, strain measurements were taken by means of a demountable mechanical 'Demec' gauge on the surface of the beam. Several cubes were tested to ensure that the prestress did not exceed half the compressive strength.

The process of transfer of stresses took place seven days after casting. The jacks used to stress the strands were first operated to relieve the load on the locknuts which could then easily be loosened. The jacks were then slowly released so that the force in the strands was gradually transferred to the beam and the strands were then cut with a disc cutter. Strain measurements were taken again after the transfer of stresses and the beam was then moved into the curing room and stored until required for testing.

6.5 Instrumentation

6.5.1 Deflection

The deflection of the beams was measured at five or seven positions along the beams using 'Baty' dial gauges with a resolution of 0.025mm; the positions of the dial gauges are shown in Fig.6.5.

6.5.2 Strain

The flexural strain was measured over a gauge length of 203mm (8") using a demountable mechanical (Demec) gauge. The Demec gauge measured the change of the average strain over

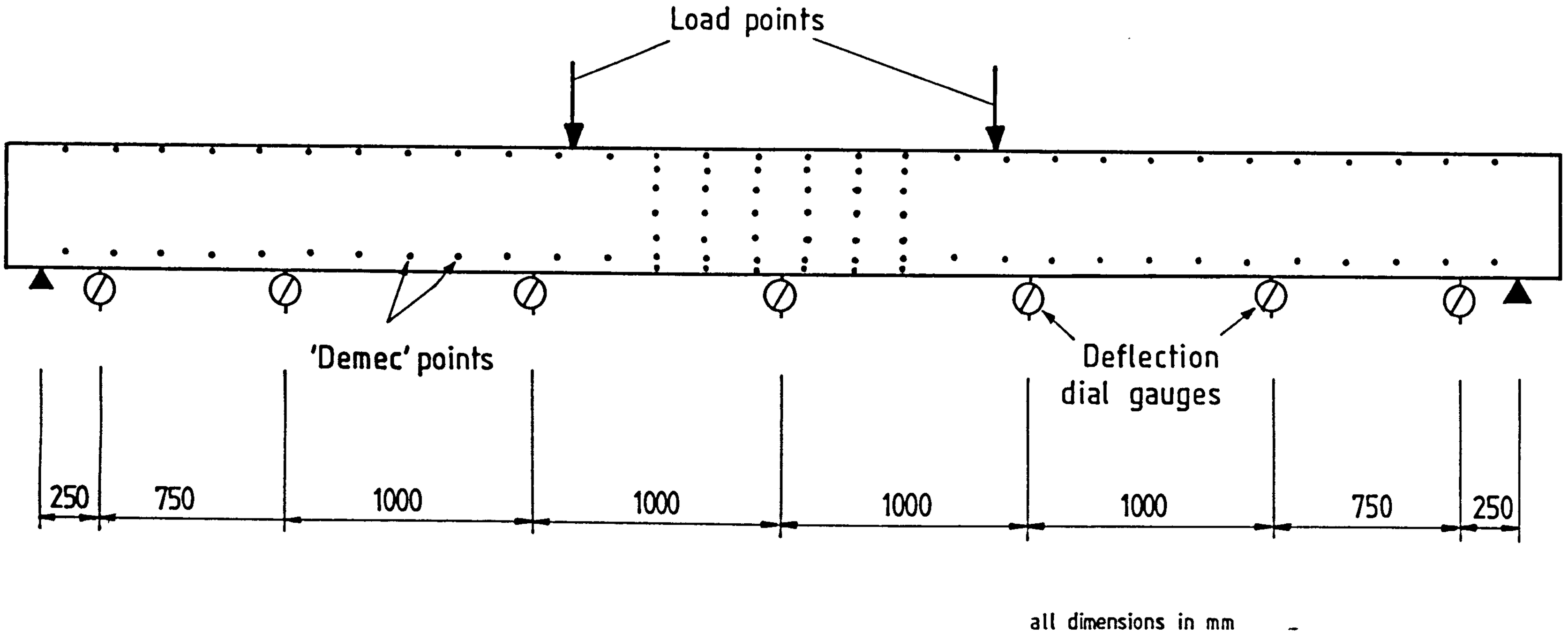

Fig. 6.5 Detail positions of Demec points and dial gauges.

the gauge length with a resolution of 10 micro-metre/metre

Strains were measured near the top and bottom of the beam over the entire span and at five additional levels in the constant moment region. The positions of the gauge lengths are shown in Fig.6.5.

6.5.3 Crack Detection and Measurements

The formation of cracks was observed by a hand-lens and the widths were measured by a 'Ultra-LOMARA 250b' microscope with magnification of 40 and resolution of 0.02mm.

6.6 Test Procedure

6.6.1 First Cycle of Loading

The general loading arrangement is shown in Figs.6.6 and 6.7. Load was applied by means of a 'Dennison-Avery' 250kN jack which acted on the beams as two symmetrical concentrated loads 1.76m apart. All the beams were tested under static loading in the first cycle and in the same rig. The beams were first loaded up to the service load under which all the beams were cracked.

Before commencing the test, the initial strain readings and the deflection dial-gauge readings were taken. The distribution beam was then placed and the loading jack was centred on it. Demec and dial gauge readings were again taken.

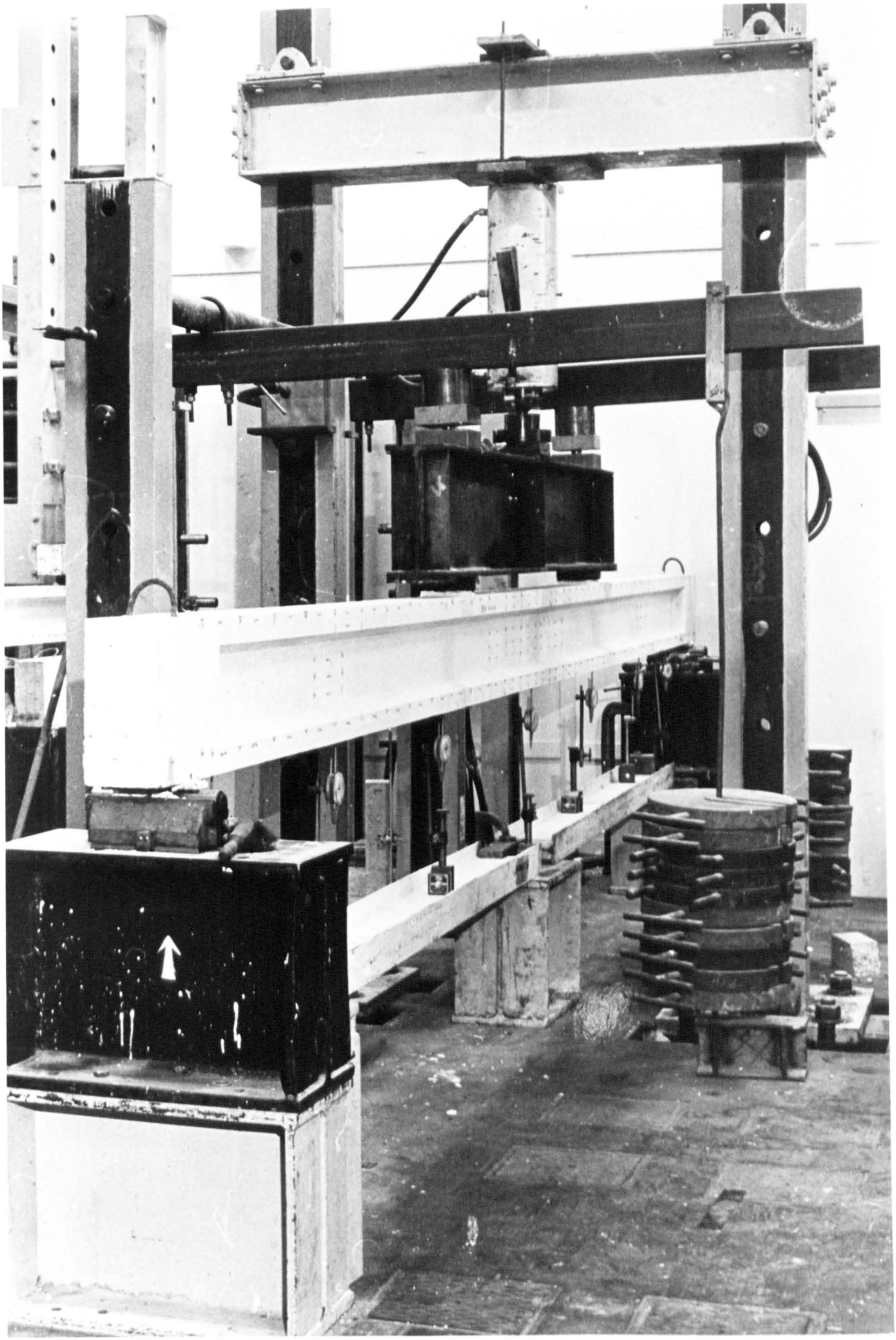

Fig.6.6 Test of beam under combined long-term and short-term cyclic loading.

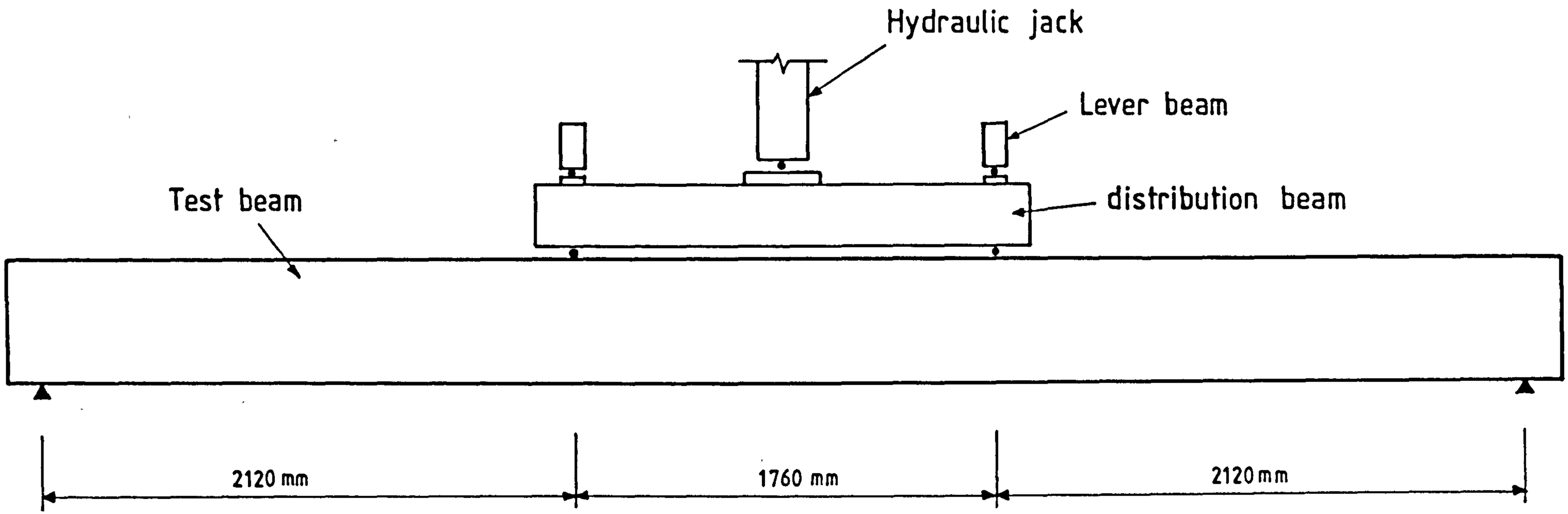

Fig. 6.7 Loading Arrangement

The load increment was between 2 to 3 kN depending on the magnitude of the service load so that a sufficient number of observations could be made for a satisfactory study of the behaviour of the beam. Deflection readings were taken at each interval and strain measurements at larger intervals. The cracking load was recorded and the widths of the cracks were measured at service load.

6.6.2 Combination of Sustained and Short-term Loading

Nine beams in the main series were subjected to combined sustained and short-term loading. After the first cycle as described in Section 6.6.1, weights, each of 100lbf, were applied to two sets of lever mechanisms acting upon the two loading points (Figs.6.6 and 6.7) until the total load on the beam was equal to half of the service load. Deflection readings were taken at each increment and strain measurements at half the service load. This load was then sustained on the beam throughout the rest of the test period.

Deflection readings were recorded every one or two days. At intervals of about five days, an intermittent cycle of additional load was applied through the jack until the total load on the beam was equal to the full service load. Strain measurements were taken before the load was added, then at service load and again at half the service load. Deflection readings were recorded at each interval of loading and unloading.

At the end of the tests (about 24 to 46 days), the beams were loaded to failure.

6.6.3 Sustained Loading Only

The three beams, S1.3.5S, S2.3.4S and S3.3.2S were subjected to static loading in the first cycle as described in Section 6.6.1. The test beam was then transferred to another rig as shown in Fig.6.8 and weights, each of 100lbs, were added onto the beam through a single lever until the total load on the beam was equivalent to half of the service load.

This load was sustained until the end of the test period. Deflection readings were taken every one or two days and strain measurements at about 10 day intervals.

At the end of the test period, the beam was totally unloaded and left on the rig to observe the recovery for about two months. Deflection readings were recorded regularly and finally the beam was loaded to failure.

6.7 Specimen Control Tests

6.7.1a Compressive Strength

The compressive strength of the concrete at the time of transfer of stresses was checked by testing at least three 100x100x100mm cubes. Generally, another four or five cubes were tested on the first day of the test and a further four

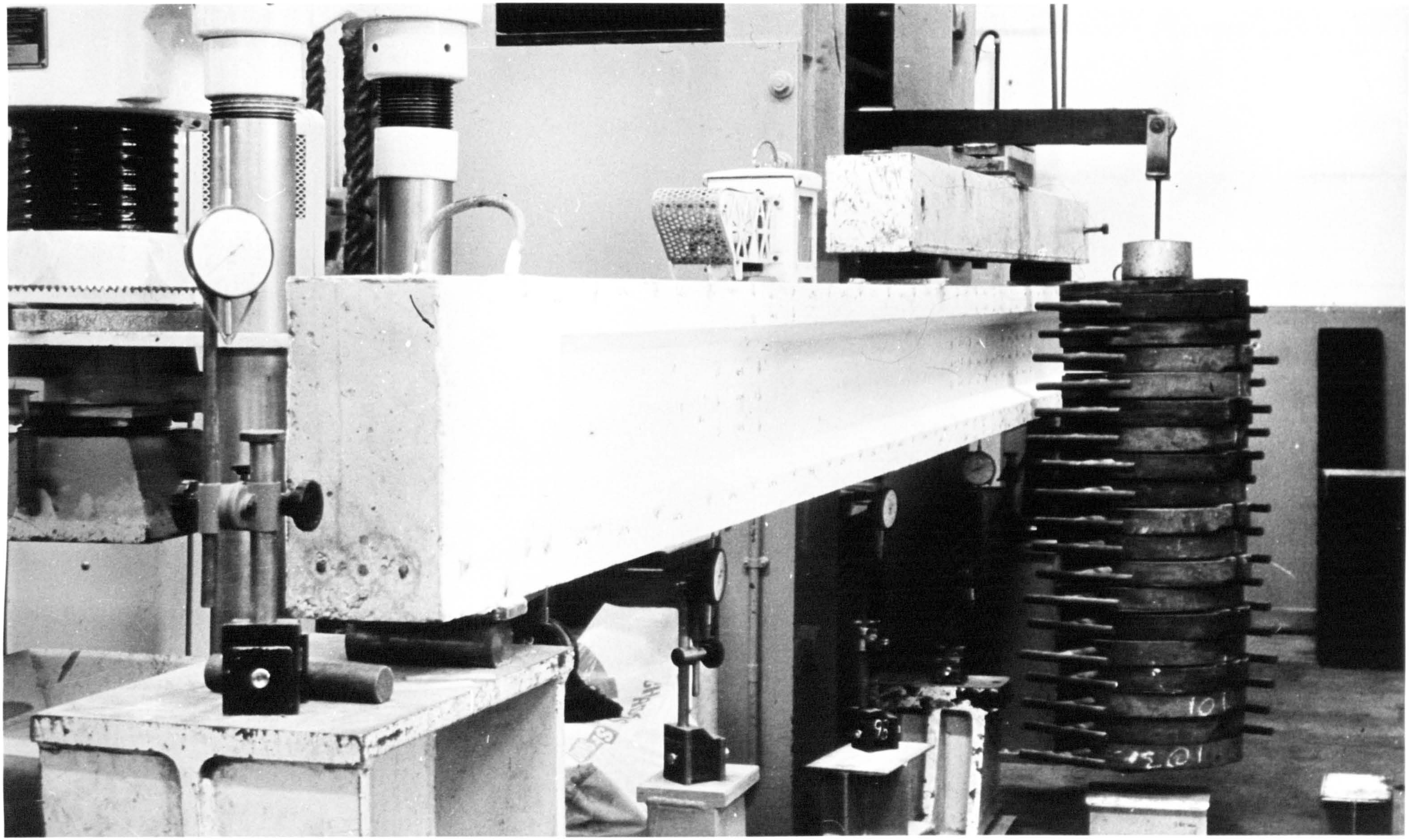

Fig.6.8 Test of beam under sustained loading alone.

or five on the day the beam was loaded to failure.

6.7.1b Flexural Strength

These tests were carried out according to B.S.1881 part 4 1970 (64) on the first day of the test. For each beam, at least four 100x100x500mm prisms were tested in a 200kN 'Avery Universal' testing machines.

6.7.1c Split Cylinder Tensile Strength

On the first day of the test, at least four 300x150mm dia. cylinders were tested according to B.S.1881 part 4, 1970 (64).

6.7.1d Modulus of Elasticity

This test was carried out according to B.S.1881 part 5, 1970 (64) on the first day of the test. The specimen used was a 500x100x100mm prism and strain was measured with a 203mm (8") 'Demec' gauge.

The properties of the concrete for all the beams obtained from these control tests are given in Table 6.3.

6.7.2 Creep Test

Cylindrical specimens for a creep test, measuring 267x76mm dia. were cast from the same materials with the

same mix ratio as the test beams. Creep test was carried out 30 days after casting and continued for 46 days. It was not possible to perform a creep test for each beam because of the time involved, however, the test which represent beam S3.3.2S, may be considered typical of all the beams tested.

The details of the test frame are shown in Figs.6.9 and 6.10. Two specimens were tested under a compressive stress of 10N/mm2 and another two under stress of 5N/mm2. The stress was applied by tightening the four nuts and checked by measuring the strain on the dynanometer which was calibrated before the test. As soon as the correct stress was achieved, the strain was measured by a 'Demec' gauge on the surface of the specimens. The test was carried out near the beam so that the specimens were under the same temperature and humidity.

On the second day and subsequently at intervals of three or four days, depending on the magnitude of the creep, the stress on the specimens was checked by measuring the strain of the dynanometer and corrected, if necessary, by tightening the nuts. The strain readings on the specimens were then taken when the stress was corrected.

Shrinkage of the concrete was monitored by measuring the strain of an unloaded plain concrete specimen using a 'Demec' gauge. The results of the test are given in Figs.6.11 and 6.12.

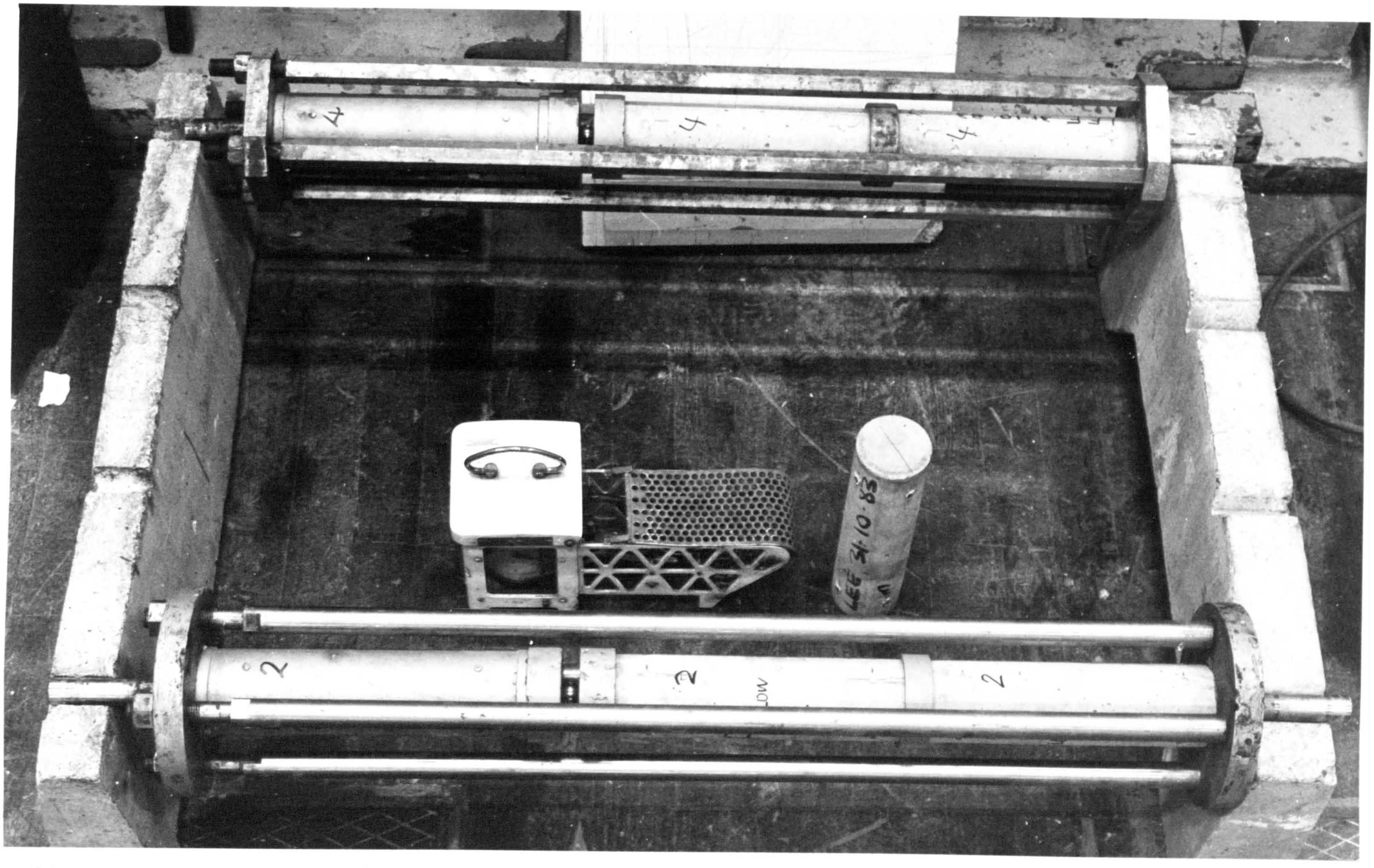

Fig.6.9 Creep specimen test.

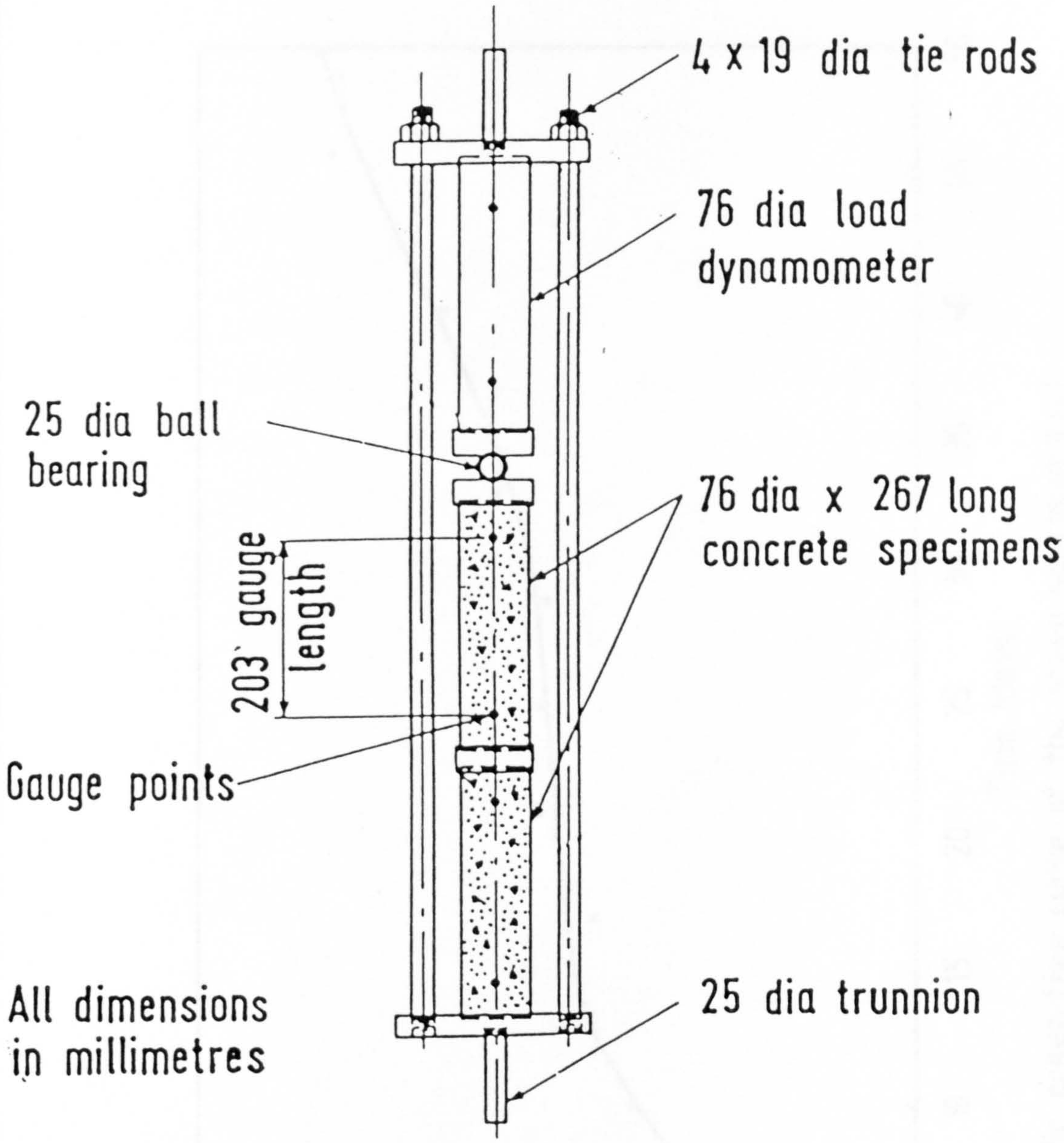

Fig. 6.10 Loading frame for creep test

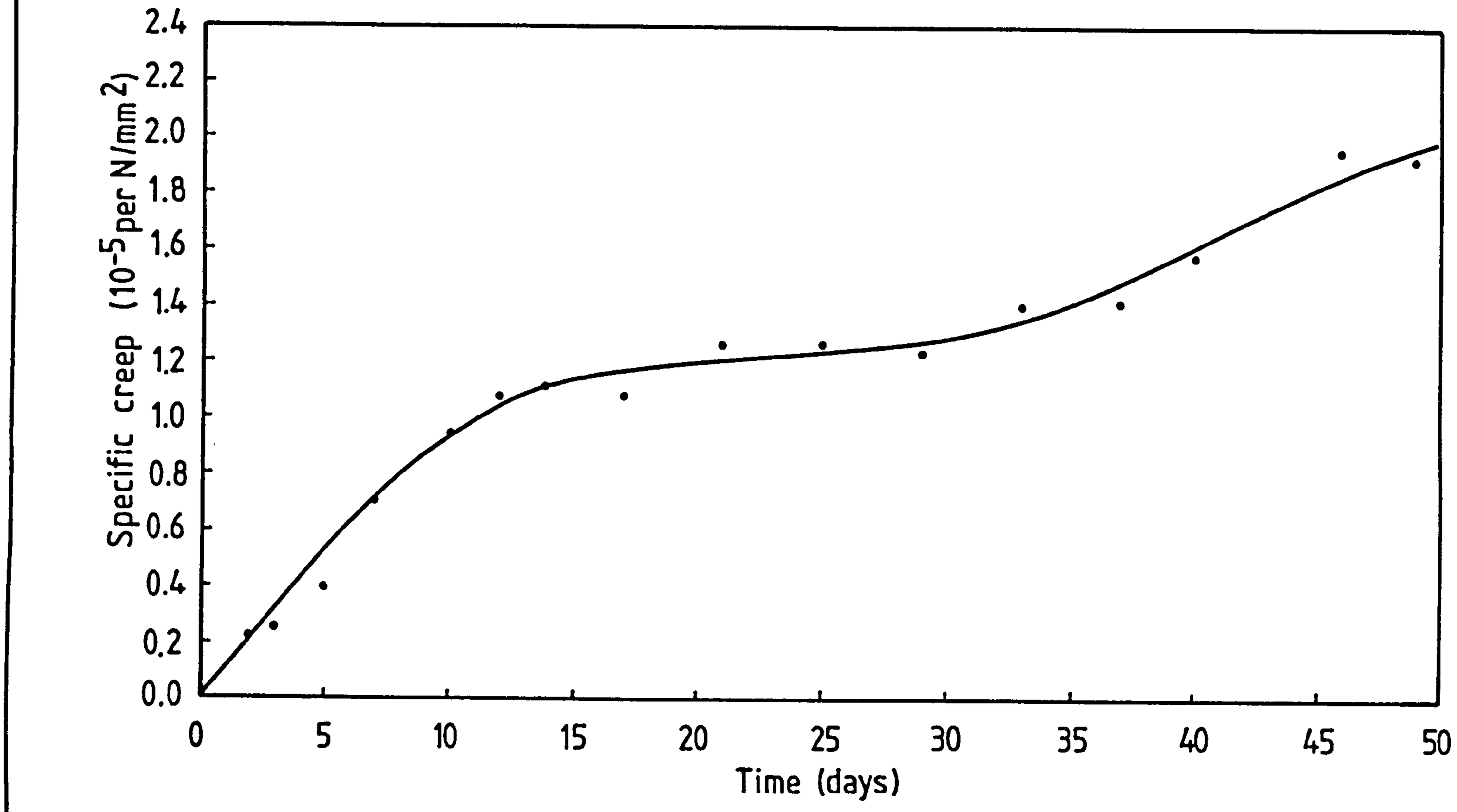

Fig. 6.11 Specific creep-time curve of the creep specimen test

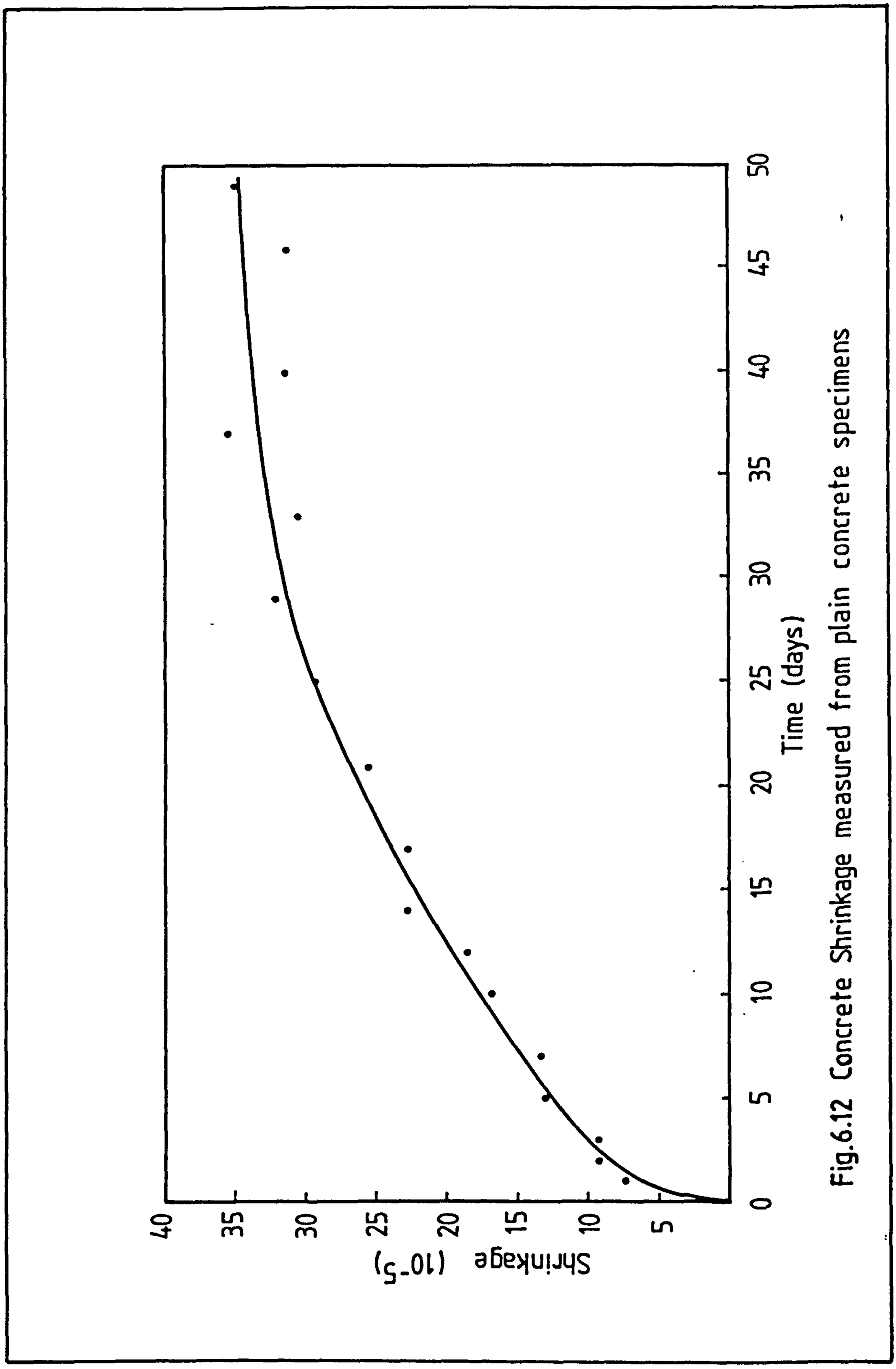

Fig.6.12 Concrete Shrinkage measured from plain concrete specimens

CHAPTER SEVEN

Discussion of Test Results and Comparisons with Theoretical Calculation

7.1 General

In this Chapter, the observations made during the tests and the results of the investigation are discussed. The first part of this Chapter deals with the general behaviour of the test beams and in the second part, the results of tests are compared with the theoretical results of the analyses described in Chapter Five and other simpler calculations.

7.2 State of Stress Before Test

It has been generally accepted that the presence of non-prestressed steel restrains the creep and shrinkage strains and thus the losses of prestressing force in the tendons are reduced. The non-elastic contraction in combination with the change of elastic strain of the beam induces compressive stresses in the non-prestressed steel. However, in partially prestressed concrete, as pointed out by Abeles (26), it is the effect of non-prestressed steel on the effective prestress in the concrete which is important, and not the effective prestressing force in the tendons. Branson (27) found that the total concrete force was "insensitive" to the provision of additional reinforcement.

Abeles (26) carried out tests on beams with different amounts of non-prestressed reinforcement but all having about the same ultimate resistance. Contrary to Branson's finding, the results of the tests showed that the effective prestress with maximum amount of non-prestressed steel was only 60 percent of that with minimum amount of non-prestressed steel.

The calculated effective prestress values in the concrete before the commencement of each of the present series of tests, are tabulated in Table 7.1. The prestress was calculated on the basis of the total effective force in the prestressed and non-prestressed reinforcement and based on the transformed section properties of the concrete area only; the areas of prestressed and non-prestressed steel were deducted from the cross-sectional area. Losses in prestressing force due to relaxation, creep, shrinkage and elastic shortening were taken into account when computing the effective force in the prestressed steel. The loss due to relaxation was taken from the results conducted by the manufacturer and the losses due to elastic deformation, creep and shrinkage were computed by measurement of surface strains at the level of prestressed steel. The effective compressive stresses present in the non-prestressed steel were computed by measurement of surface strains at that level.

The losses of prestress in the prestressed steel were generally between 7 and 12.7 percent. Since the beams were

Beam reference	Effective Prestress in concrete (N/mm²)			(2)/(1)	f_{pe} (N/mm²)	f_{se} (N/mm²)	Losses in tendons (%)
	top	bottom (1)	bottom* (2)				
S1.5.2	-2.96	16.20	16.61	1.03	-1045.9	+117.4	12.3
S1.4.4	-1.91	11.81	13.79	1.16	-1137.5	+124.1	12.0
S1.3.5	-1.43	8.70	10.26	1.18	-1178.5	+ 83.2	8.7
S1.3.5S	-1.42	8.60	10.13	1.18	-1164.5	+ 82.0	9.8
S2.4.2	-2.39	13.39	14.29	1.07	-1127.1	+133.4	12.7
S2.3.4	-1.66	9.73	10.35	1.06	-1171.3	+ 68.8	9.3
S2.3.4S	-1.67	9.77	10.33	1.06	-1171.3	+ 72.6	9.3
S2.2.6	-1.12	6.40	6.81	1.06	-1201.6	+ 39.0	7.0
S3.3.2	-1.89	10.49	11.11	1.06	-1162.2	+156.6	10.0
S3.3.2S	-1.99	10.85	11.18	1.03	-1171.7	+135.0	9.3
S3.2.4	-1.10	6.45	6.94	1.08	-1166.9	+47.1	9.6
S3.1.6	-0.59	3.39	3.33	0.98	-1199.2	+11.5	7.1

* Stresses calculated with effective prestress in tendons only and based on transformed section properties. -ve tension, tve compression

Table 7.1: Steel and concrete stresses before tests

stored in the curing room until 12 to 36 hours before testing, losses due to creep and shrinkage were therefore commonly small. The relaxation and elastic shortening were the two major causes of the losses.

The losses of stress in the prestressed steel shown in Table 7.1 indicate that the amount of loss was reduced with an increasing area of non-prestressed reinforcement. For example, the loss in the tendons amounted to 12 percent of the initial prestress for beam S1.4.4, whilst in beam S2.4.2 with a reduced area of non-prestressed reinforcement, the loss was 12.7 percent.

The calculated effective prestress in concrete (Table 7.1) consistently shows that the losses were higher in beams with a larger amount of non-prestressed reinforcement. For example, the effective prestress in beam S3.3.2 was higher than that in S2.3.4 whilst the prestress in S1.3.5 was the lowest among the three beams having the same initial prestressing force (three prestressed strands each).

The common practice in partially prestressed concrete is to calculate the effective prestress in concrete based on the transformed section properties in which the stiffness of the additional steel is taken into account, and on the effective prestressing force in the tendons, while the compressive stress induced in the non-prestressed steel is ignored. It is evident from Table 7.1 that this method generally overestimates the prestress particularly in beams

with a large amount of prestressed and non-prestressed steel where the errors are found to be more than 16 percent in some cases like S1.4.4 and S1.3.5.

7.3 Behaviour of Test Beams

7.3.1 General Behaviour (First Cycle)

7.3.1.1 Load-Deflection Relationship

The load-deflection curve normally gives a good indication of the general behaviour of the test beam. Figs.7.1 and 7.2 show the load-deflection relationships for some of the beams during the first cycle of loading up to the service load. The effect of prestress in beams with the same ultimate resistance is evident from Figs.7.1a and 7.1b. As many investigators have observed in their tests (12,21,23), the effect of prestress is to delay the formation of cracks in a virgin cycle of loading. It has been a common observation in tests that cracks are visible under the loads in which the load-deflection curves deviates from the initial straight lines when the beams are uncracked. Table 7.2 gives the loads at which cracks were first observed in the first cycle. These values include the weight of the distribution beam which was 2.3kN and should be deducted when comparisons are made with Figs.7.1. An examination of Table 7.2 and Fig.7.1a confirms the effect of prestress on the cracking load.

Fig.7.2a compares the deflection of beams with about the same level of prestress but with different amounts of

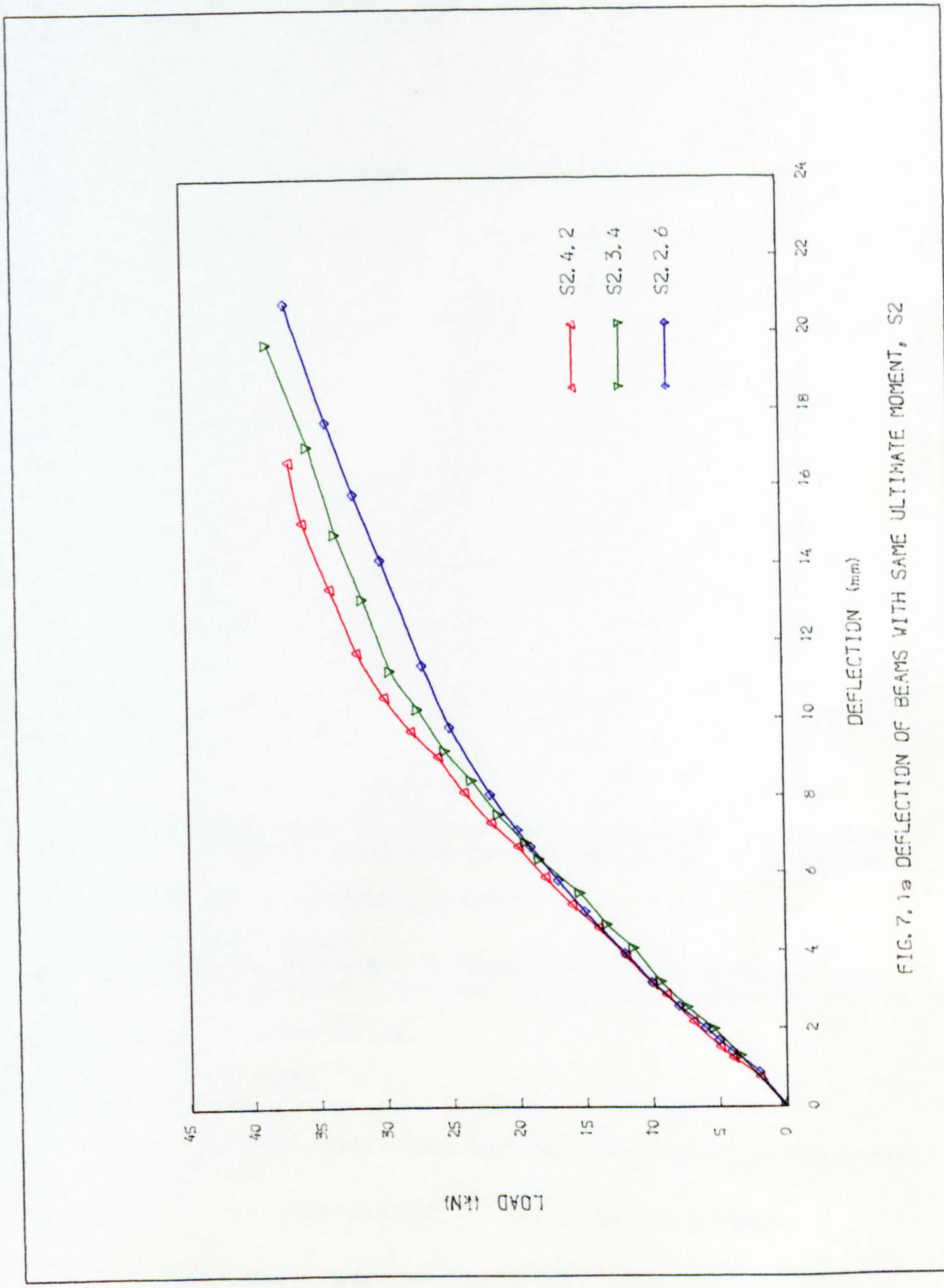

FIG. 7.1a DEFLECTION OF BEAMS WITH SAME ULTIMATE MOMENT, S2

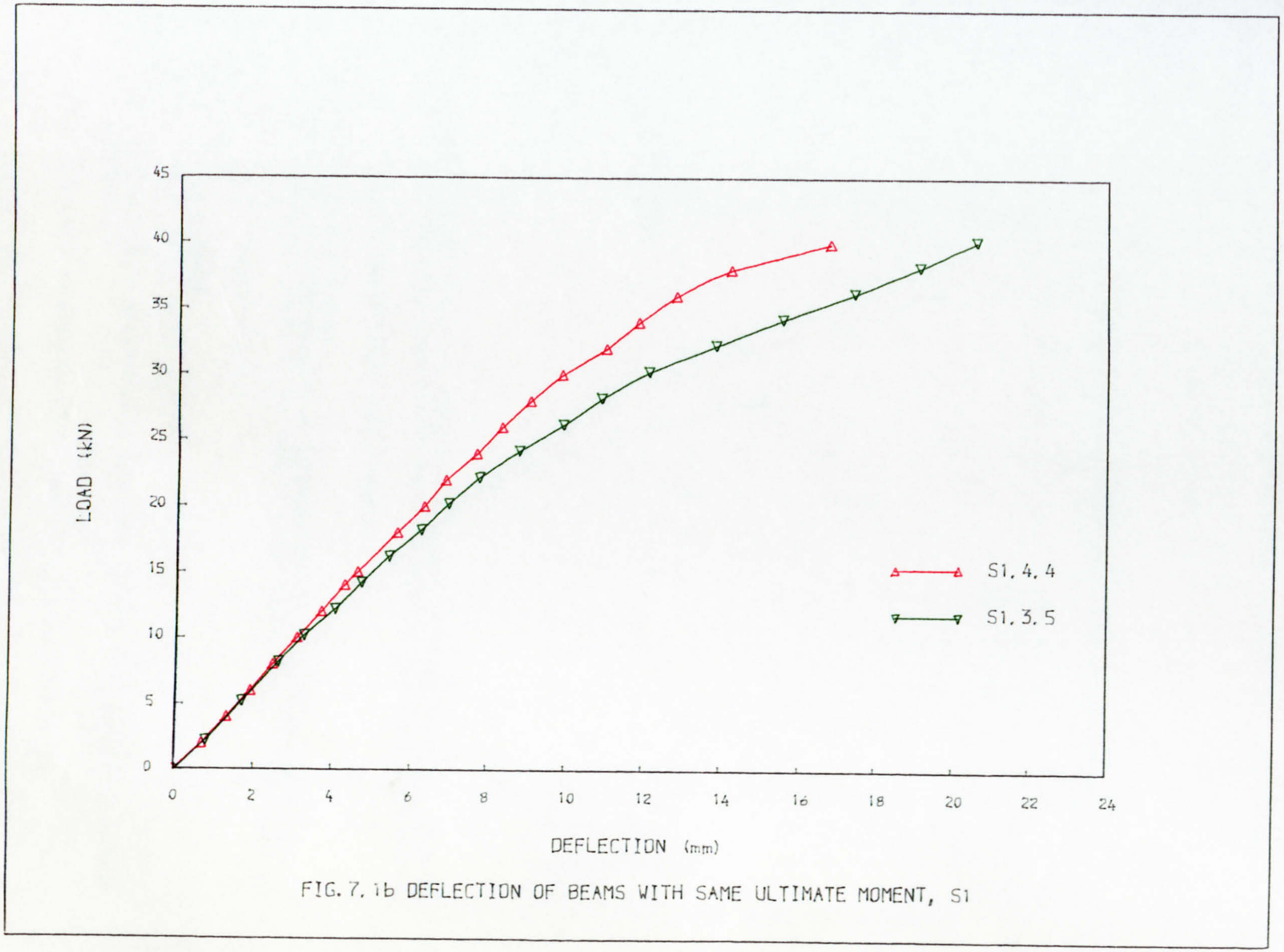

FIG. 7. 16 DEFLECTION OF BEAMS WITH SAME ULTIMATE MOMENT, S1

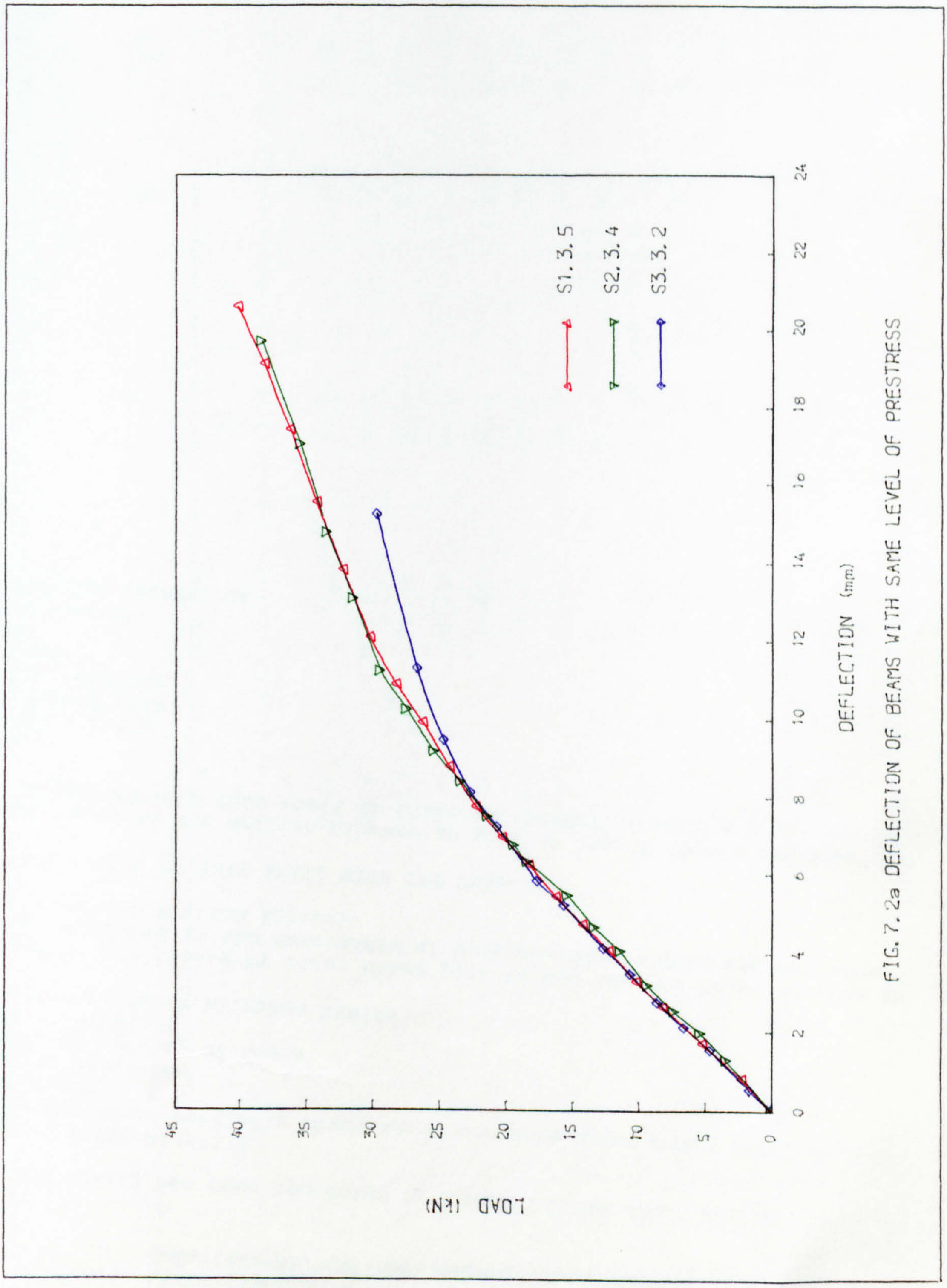

FIG. 7.2a DEFLECTION OF BEAMS WITH SAME LEVEL OF PRESTRESS

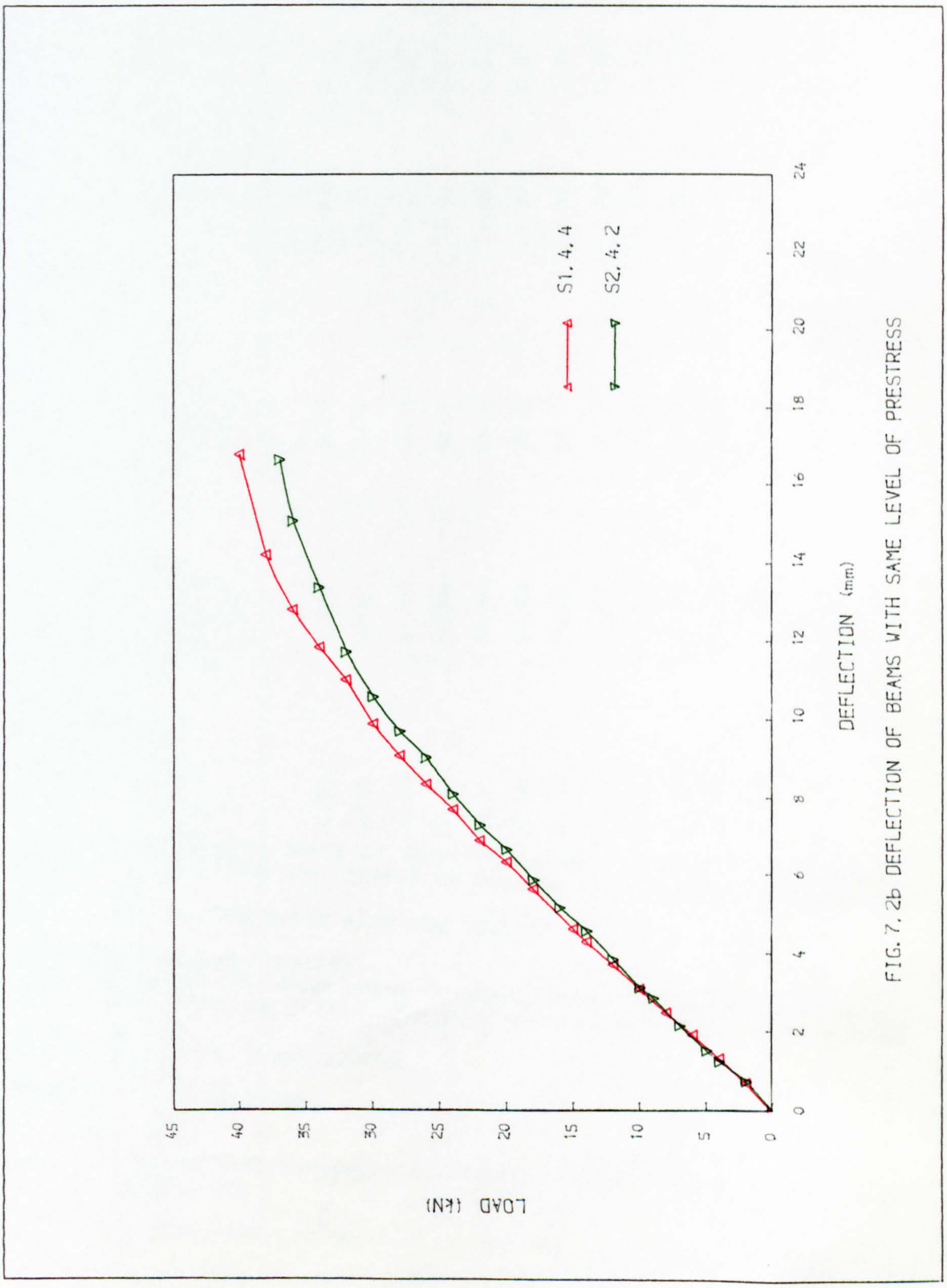

FIG. 7.2b DEFLECTION OF BEAMS WITH SAME LEVEL OF PRESTRESS

Beam Reference	Decomp. Load (kN)	Cracking Load (kN)			(3)/(1)	(3)/(2)
		Calculated based on (1) f_t	Calculated based on (2) f_{tc}	Observed (3)		
S1.5.2	31.47	40.09	42.52	38.3	0.96	0.90
S1.4.4	26.18	34.58	39.61	32.3	0.93	0.82
S1.3.5	19.43	28.40	31.13	28.3	1.00	0.91
S1.3.5S	19.17	27.19	30.40	26.3	0.97	0.87
S2.4.2	26.37	33.51	36.61	34.3	1.02	0.94
S2.3.4	19.44	27.60	31.26	30.3	1.10	0.97
S2.3.4S	19.44	28.32	29.44	29.3	1.03	0.99
S2.2.6	12.09	20.13	23.63	21.3	1.06	0.90
S3.3.2	19.42	27.29	29.03	25.3	0.93	0.87
S3.3.2S	19.62	27.98	32.76	24.3	0.87	0.74
S3.2.4	11.78	20.20	24.61	23.4	1.16	0.95
S3.1.6	4.55	12.68	15.51	17.3	1.36	1.12

Note: The loads include the weight of the spreader beam (2.3kN).

Table 7.2: Observed and calculated loads at decompression and cracking.

non-prestressed reinforcement. It is interesting to observe that the rate of increase of deflection, which is also represented by the reciprocal of the slope of the curve, after the point of cracking, was greatest in the beam with smallest amount of reinforcement (i.e.S3.3.2). The effect, however, was small before cracking occurred. For beams with the same reinforcement ratio (Fig.7.1a), the slopes of the load-deflection curve can be seen to be approximately the same. The result suggests that the rate of increase of deflection was not affected by the level of prestress, but the deflection under service load was affected because of the varying cracking loads.

On unloading, the load-deflection curve did not retrace the loading path. In completing the first cycle, the load-deflection curve formed a "loop" which can be seen to be widest in the beams such as S3.1.6, with the lowest amount of prestress (Figs.7.7 to 7.15).

Generally, the cracks did not close on unloading until the load was below the point of decompression. However, for beams like S3.1.6 with a low degree of prestress and a large amount of non-prestressed reinforcement, hair cracks remained open even when the beam was completely unloaded. This behaviour has also been observed in tests conducted by Veerasubramaniam (23).

The deflections of all the beams under service load in the first cycle are summarised in Table 7.3a, and were all

Beam Reference	Initial Deflection mm		Duration of Test days (No. of intermittent cycles)	Final Deflection mm		(2)-(1) mm	(3)-(4) mm	(4)/(1)
	$^1/_2$ SL (1)	SL (2)		SL (3)	$^1/_2$ SL (4)			
S1.5.2†	6.5†	17.1	28(5)	21.4	12.3	10.6	9.1	1.9
S1.4.4	5.8	16.8	30(6)	21.2	12.2	11.0	9.0	2.1
S1.3.5	6.4	21.5	35(7)	27.2	16.2	15.1	11.0	2.5
S1.3.5 s	6.1	20.8	35(0)	-	13.3	14.7	-	2.2
S2.4.2	5.4	16.1	26(5)	18.5	9.8	10.7	8.7	1.8
S2.3.4	5.8	19.6	46(7)	26.3	17.0	13.8	9.3	2.9
S2.3.4 s	5.8	19.5	46(0)	-	11.8	13.7	-	2.0
S2.2.6	5.5	20.7	31(6)	25.6	15.3	15.2	10.3	2.8
S3.3.2	4.1	16.0	30(5)	20.8	10.6	11.9	10.2	2.6
S3.3.2 s	4.1	15.6	30(0)	-	7.7	11.5	-	1.9
S3.2.4	4.4	18.8‡	34(6)	22.4	12.6	14.4	9.8	2.9
S3.1.6	4.9	21.6	24(5)	26.5	16.6	16.7	9.9	3.4

SL = Service Load.

* One initial cycle to SL followed by long-time load of $^1/_2$ SL.

† Strands not fully prestressed due to error in construction.

‡ In second cycle. Maximum load of first cycle was $^1/_2$ SL.

Table 7.3a: Summary of Deflections

within the CP110 limitation of L/250, which is equivalent to 24mm for these tests.

7.3.1.2 Residual Deformation

As many other investigators observed in their tests, all the beams had residual deflections after cyclic loading. In the present tests the residual deflections ranged from 2.5mm to 4.0mm at the end of the first cycle.

The principles governing residual deflection have not been well established. The amount of residual deflection was thought to be dependent on the extent to which the concrete and steel are stressed under the design load in the first cycle, when some inelastic strain may occur (12,23,52). From the observations in the present tests, the most likely causes of the residual deflection (after the first load cycle) appear to be the deterioration of the bond between the concrete and steel and a small amount of creep strain which depends on the duration of the test. It may be seen from Figs.7.7 to 7.15 that the residual deflection after the first cycle was largest in beams S3.1.6 and S2.2.6, both of which had high ratios of service load to cracking load combined with large amounts of non-prestressed reinforcement.

It is possible to explain the mechanism of the formation of the residual deflection in the first cycle, with respect to the slip and cracking of the beam. When a

prestressed beam is loaded beyond the point at which flexural cracks appear and the load is subsequently reduced, the cracks will not close completely until a sufficient compressive force has developed in the tendons and reinforcement in the crack to reverse the slip that has occurred in the formation of the crack. When the load has been completely removed, this force will be equal to the total prestressing force and will normally be sufficient to enable the crack to close, in which case the residual deflection will be small. If, however, the prestressing force is small and there is a substantial amount of non-prestressed reinforcement which requires a greater force to reverse the slip, it is possible for there to be a residual slip and width of crack after unloading as has been observed in S3.1.6 and S2.2.6. This will then result in larger residual deflection.

In the tests, several hours were required to complete one cycle of loading during which time creep strain would have occurred, and a certain proportion of the residual deflection may be due to this effect. However, it is impossible to determine numerically the proportion of the residual deflection due to this effect from the present tests. More research is needed in this area.

7.3.1.3 Crack Width

Table 10.2 shows the widths of the cracks under service load in the first cycle for all the beams tested. It is

interesting to note that all the values are within the CP110 limitations (0.1mm or 0.2mm) although in some beams the hypothetical tensile stress was in excess of the value recommended in the code. Moreover, the span/depth ratio for most of the beams was about 22 against the code maximum of 20 for simply supported reinforced concrete members.

7.3.2 Beams Under Sustained Load Alone

7.3.2.1 Deflection-Time Relationships

The three beams (S1.3.5S, S2.3.4S and S3.3.2S) tested under sustained load alone (50 percent of the total service load), were first subjected to one cycle of short-term loading up to the full service load similar to the other tests in the main series.

Limited information is available concerning the behaviour of cracked prestressed members subjected to sustained load. The results of sustained loading tests on reinforced and cracked prestressed members by a number of previous investigators (12,32,46,47) suggest that the deflection under sustained loading increases over a long period of time although at a decreasing rate. The tests carried out by Dave and Chandrasekhar (12,46,47) with sustained full design load on partially prestressed beams, showed an increase of deflection of over twice the initial deflection after about one year.

The deflection-time relationships for the present tests

are shown in Fig.7.3. The ratios of the total deflection to the initial deflection were 1.40, 1.56 and 1.38 for beams S1.3.5S, S2.3.4S and S3.3.2S respectively, after about 30 days. It should be pointed out that these values are not directly comparable with the results of the previous investigators, since these beams were subjected to lower sustained loads.

After the removal of the sustained load at the end of the test, the recovery of the residual deflection for the three beams was observed for about two months. The total residual deflection immediately after unloading varied from 2.4 to 4.5 times the amount after the first load cycle and this total was seen to have decreased by about 30 to 50 per cent after 50 days (Table 7.3b).

The beam S1.3.5S was cracked initially under the sustained load and the crack widths were re-examined at the end of the test period. There was only a small increment in the width which was generally less than 0.02mm after 30 days under sustained loading. The result therefore conforms with Abeles' (35) finding.

7.3.2.2 Curvature-Time Relationship

The upward deflection (camber) of unloaded fully prestressed concrete beams has often been observed to increase over a period of time and there is obviously an increase in the positive curvature which causes upward

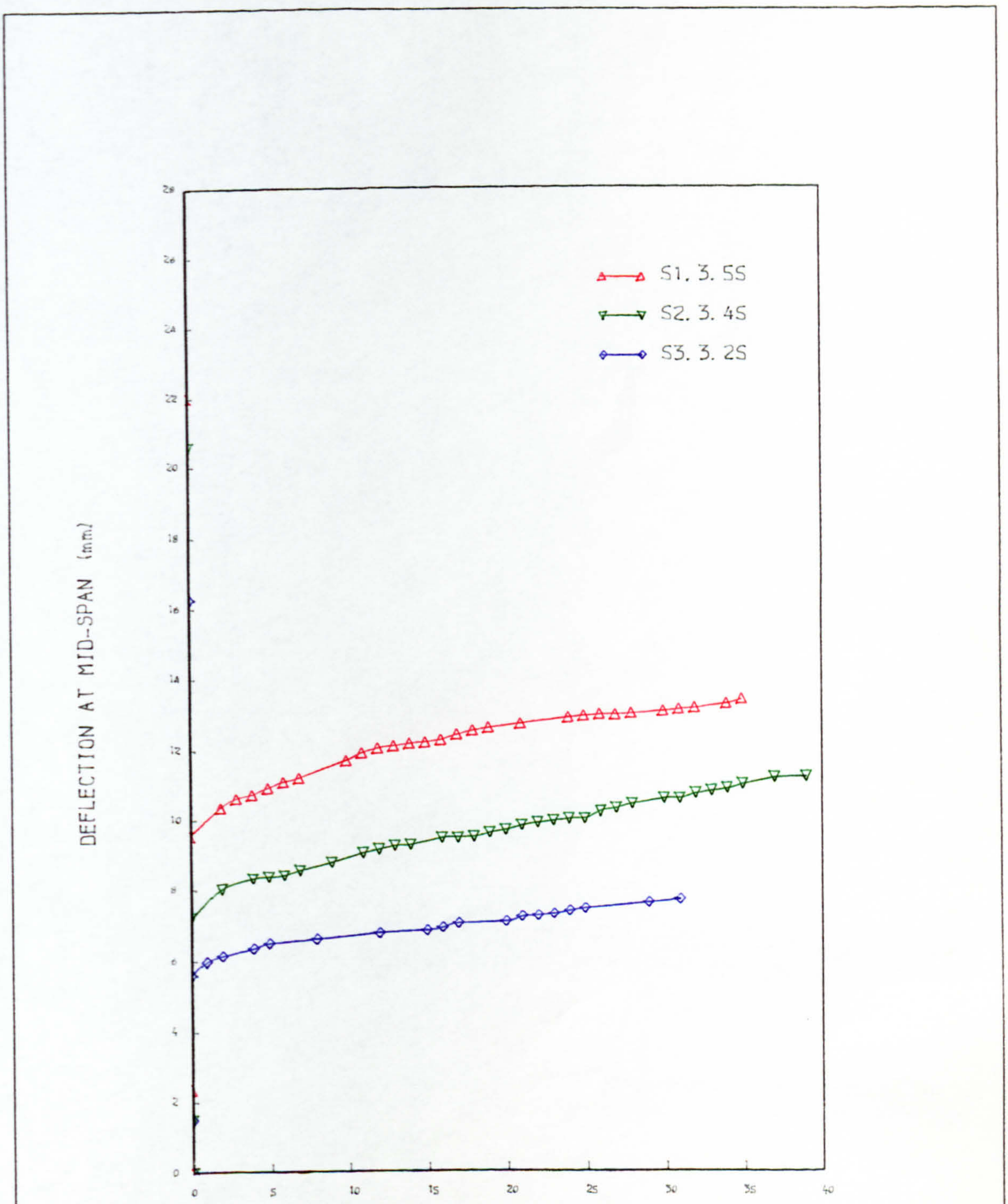

FIG. 7. 3 DEFLECTION vs TIME, (BEAMS UNDER SUSTAINED LOAD ONLY)

Beam References	Duration of tests	Total Residual Deflections (mm)				(2)/(1)	(3)/(1)	(4)/(1)
		After 1st cycle (1)	Unloaded at the end of test (2)	10 days after unloading (3)	50 days after unloading (4)			
S1.3.5S	47	2.37	6.85	4.87	4.78	2.9	2.1	2.0
S2.3.4S	38	1.48	6.70	5.38	4.92	4.5	3.6	3.3
S3.3.2S	32	1.37	3.23	2.29	1.63	2.4	1.7	1.2

TABLE 7.3b: Residual Deflection after Unloading

camber. In cracked prestressed concrete beam, however, the sections near midspan normally have negative curvature (causing downward deflection) while the sections near the supports still have positive curvature. There is limited experimental information concerning the changes of these curvatures at different sections over the whole span.

Figs.7.3b to 7.3d show the measured longitudinal curvature distribution after different periods of time under sustained load. The curvature was calculated from the strains measured near the top and bottom surfaces of the beams and over the whole span. It is evident from these diagrams that there is generally an increment in the negative curvature near the midspan. It is also clear that the positive curvatures for sections near the supports were reduced and some even changed from positive to negative curvature. There is no sign of any increase in the positive curvature, even in sections near the supports with rather large curvature. This feature is believed to be due to the change of stress and the reversal of the creep strain when the beam is loaded initially. The sudden reduction in the compressive stress at the soffit due to the additional bending stress at the commencement of the test should result in some time-dependent recovery of the compressive creep strain (i.e. tensile strain) which has already occurred since the beam was prestressed. At the top of the beam, there is a small tensile stress initially which becomes compressive after loading and therefore the strain due to creep will be compressive. Hence the change of strain

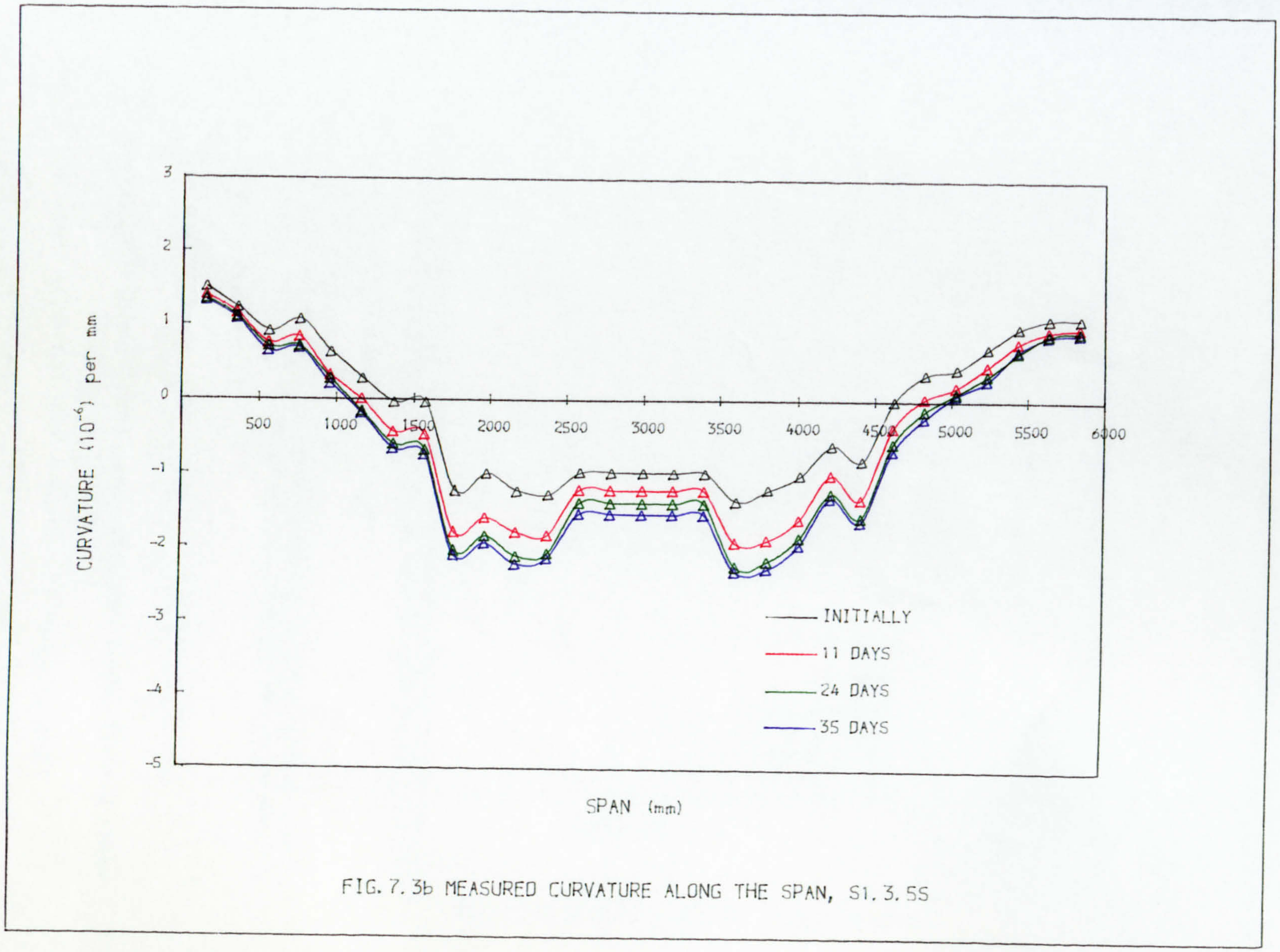

FIG. 7.3b MEASURED CURVATURE ALONG THE SPAN, S1.3.5S

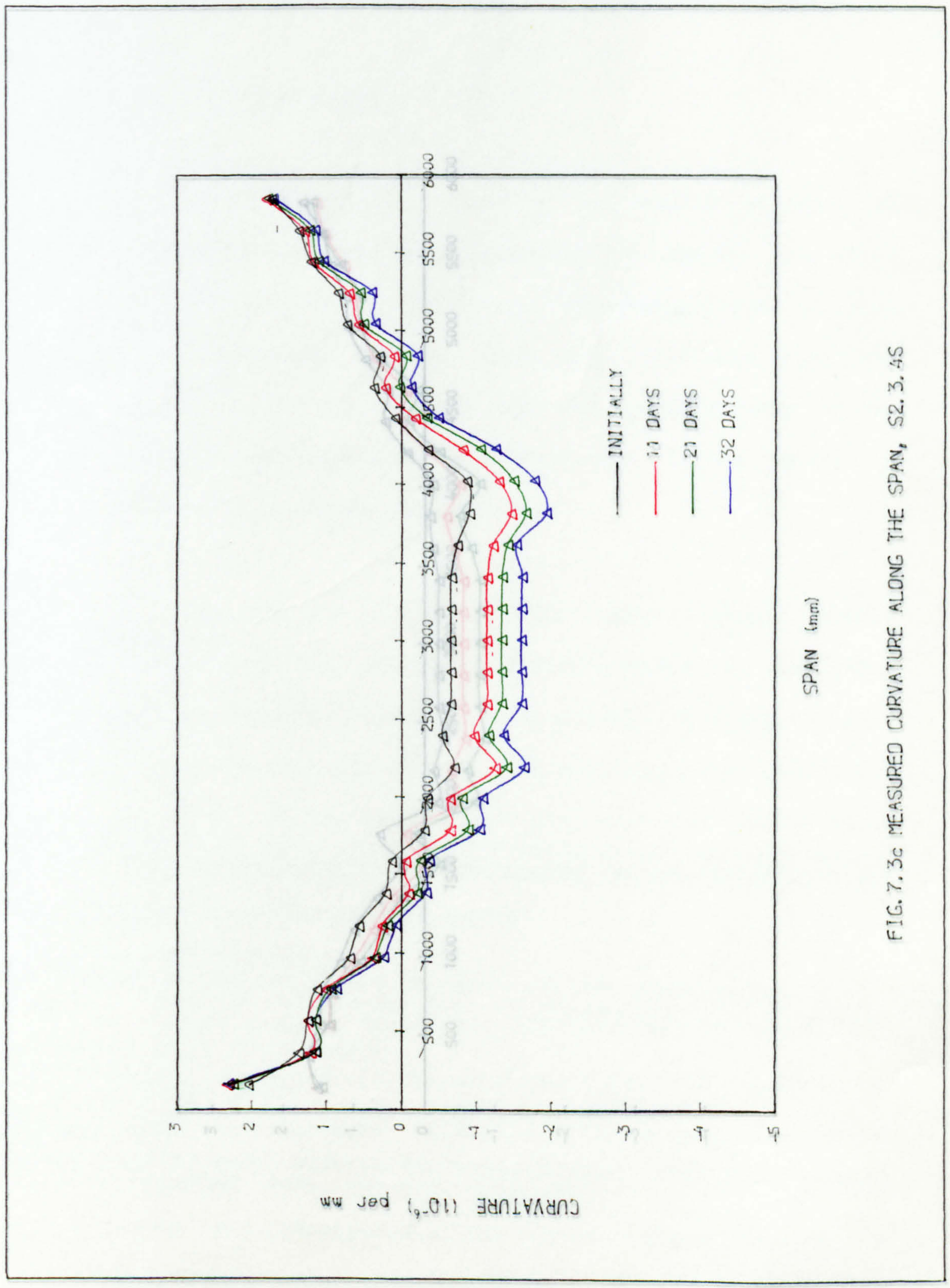

FIG. 7.3c MEASURED CURVATURE ALONG THE SPAN, S2.3.4S

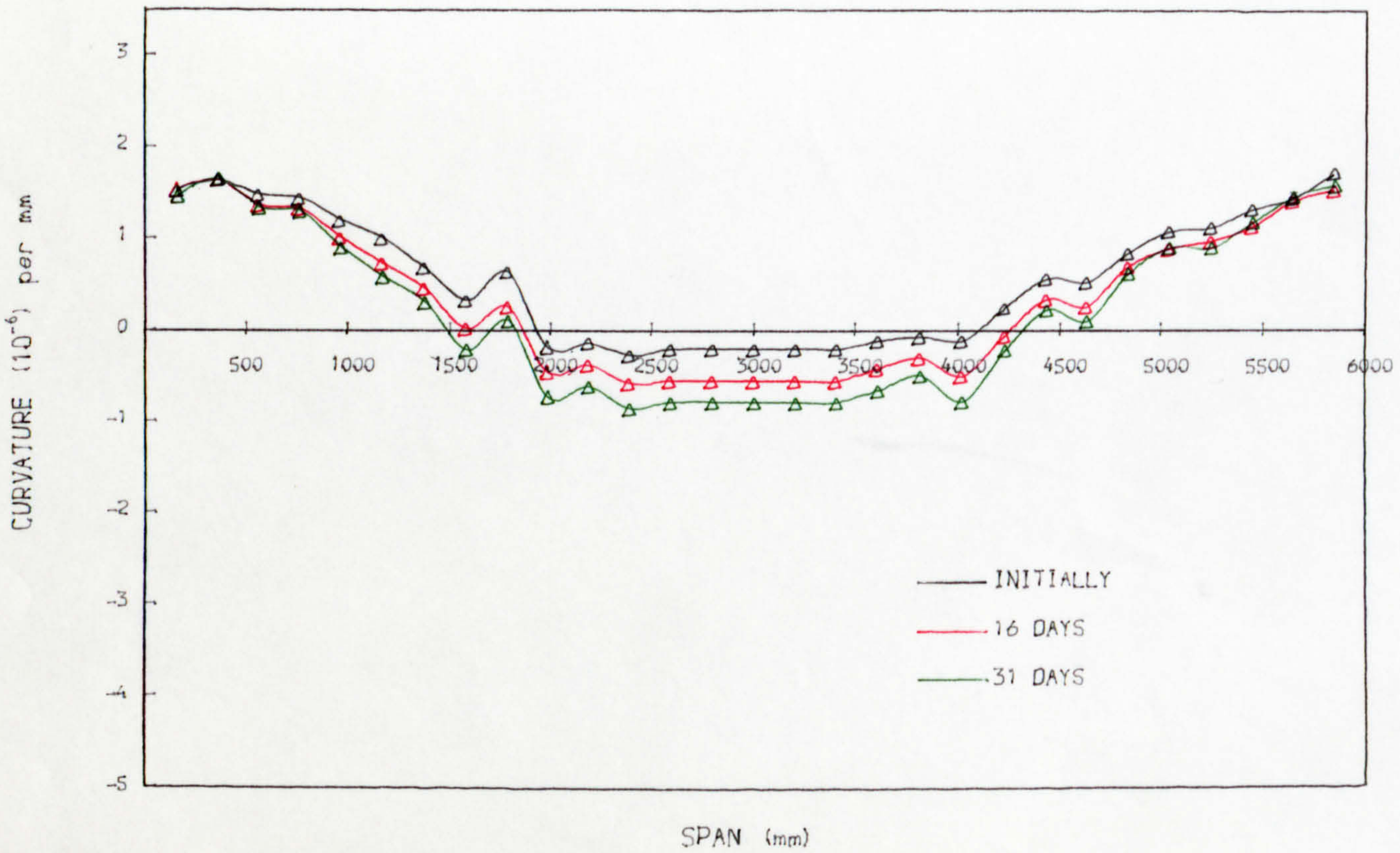

FIG. 7.3d MEASURED CURVATURE ALONG THE SPAN, S3.3.2S

distribution should result in a decrease of positive curvature as observed over the greater part of the span.

7.3.2.3 Neutral Axis

As early as 1939, based on the results of tests on reinforced concrete beams, Glanville and Thomas (32) found that the position of the neutral axis changes over a period under sustained loading. Dave (46) confirmed that the neutral axis was lowered and the reinforcement stress reduced and, interestingly, there was a case where the reinforcement stress changed sign.

Figs.7.4 to 7.6 show the total midspan strain distributions for the three beams, measured at intervals, over the periods of tests. It is evident from Fig.7.4 that the neutral axis was lowered and generally, the compressive strain at the top surface was almost doubled whilst there was only a slight reduction in the tensile strain at the soffit.

The results, therefore, can be seen to support the theory described in Chapter Four, for the analysis of reinforcement stresses under long-term loading. Due to the effects of creep and shrinkage, there is generally a small change in the reinforcement stresses which disturbs the equilibrium conditions. Equilibrium is restored when the neutral axis of stresses is, either lowered due to the effect of creep (Fig.4.4) or raised with the effect of

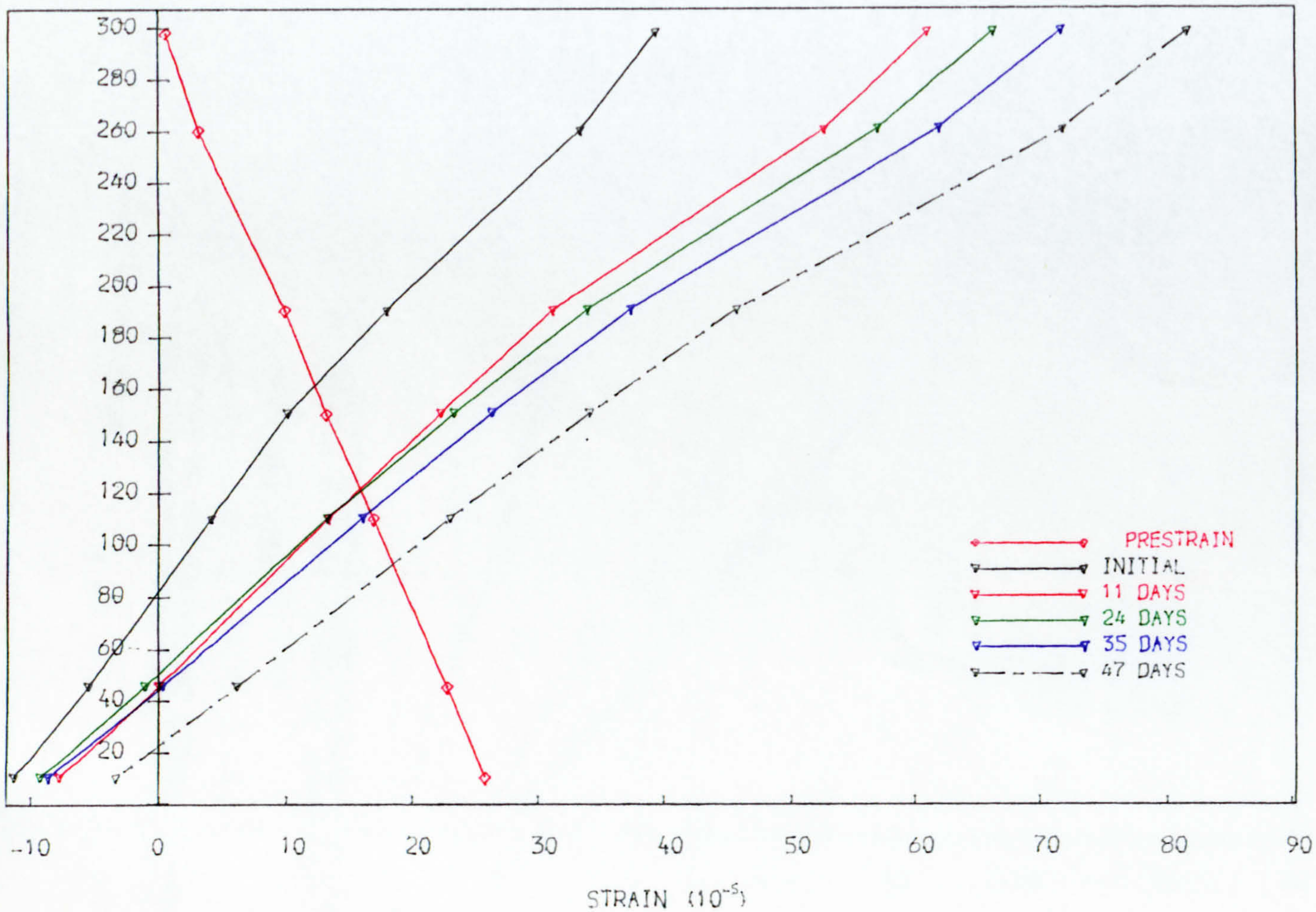

FIG. 7.4 TOTAL STRAINS UNDER SUSTAINED LOAD, BEAM S1.3.5S

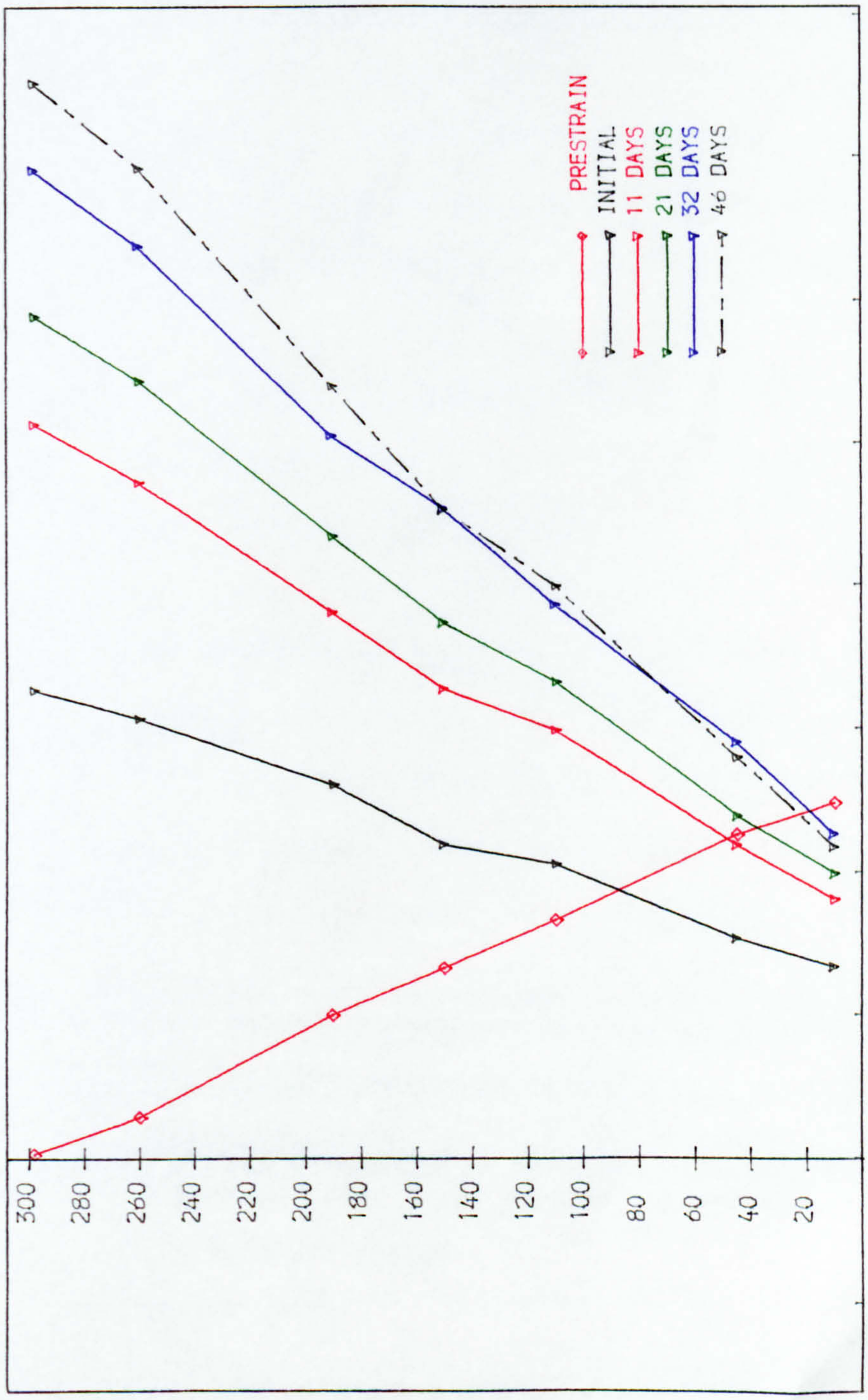

FIG. 7.5 TOTAL STRAINS UNDER SUSTAINED LOAD, BEAM S2, 3, 4S

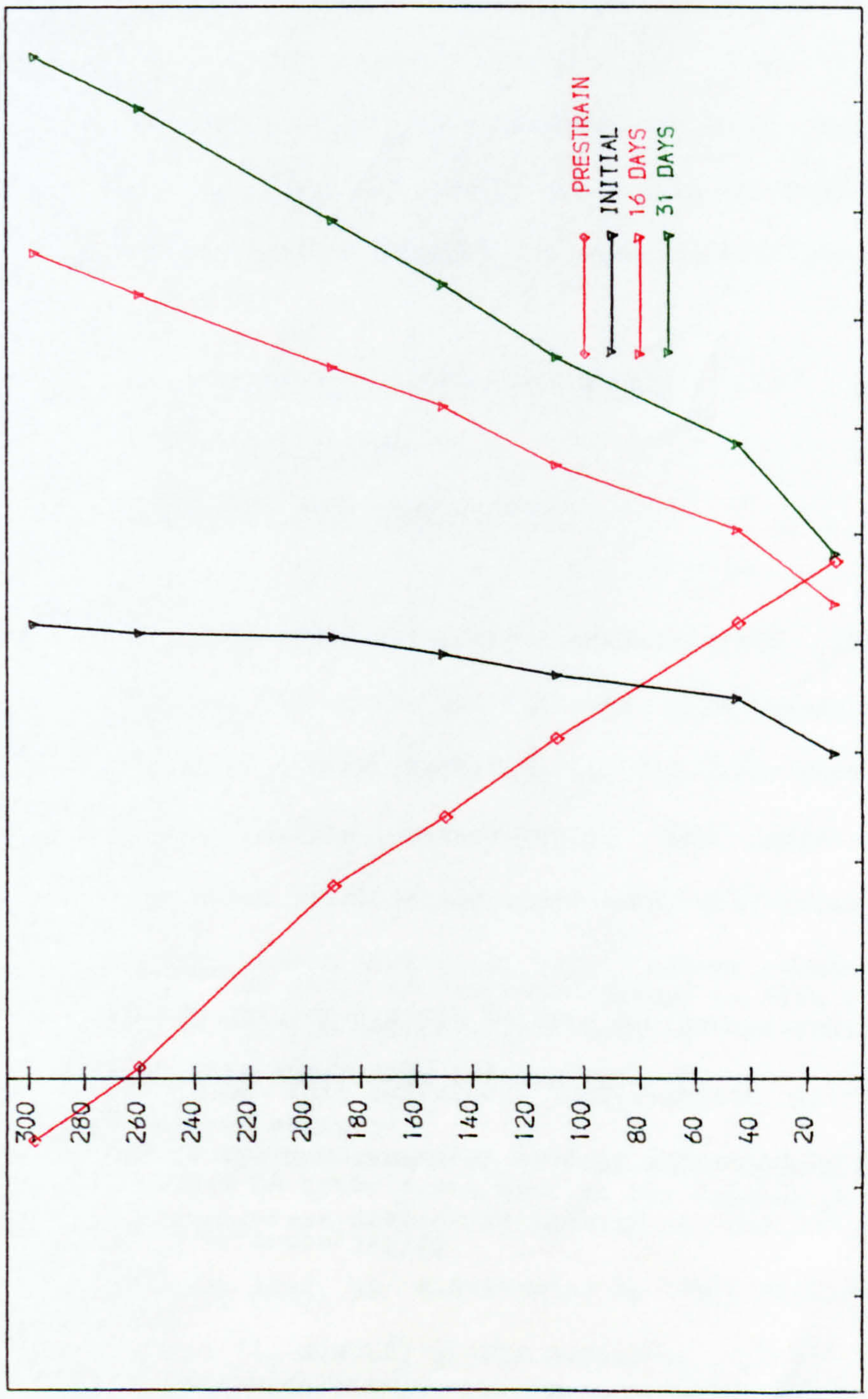

FIG. 7.6 TOTAL STRAINS UNDER SUSTAINED LOAD, BEAM S3.3.25

shrinkage (Fig.4.6). The neutral axis of strain, however, is generally lowered (Figs.7.4 to 7.6) and therefore also conforms with the analysis.

It may be of interest to note that the neutral axis/depth ratio changed from 0.74 to 0.93 after 47 days under sustained loading, as shown in Fig.7.4.

7.3.3 Beams Under Combined Loading

7.3.3.1 Deflection

Load-Deflection Relationship

The load-deflection relationship throughout the duration of tests of all the nine beams are shown in Figs.7.7 to 7.15. Referring to Fig.7.11, which is a typical load-deflection relationship, the point marked (1) represents the load and short-term deflection at 50 percent of the service load (i.e. total moment equals to 50 percent of the service moment). The long-term deflection due to the effect of this sustained load together with 8 short-term cycles up to the service load is indicated by the point (4). The short-term deflection between 50 and 100 percent of the service load is represented by the horizontal distance between (1) and (2) at the beginning and (3) and (4) at the end of the test. This basic data is given for all the tests in Table 7.3a. It may be seen that the increase of deflection between 50 and 100 percent of the service load is greatest in the first cycle.

It can also be seen from Figs.7.7 to 7.15 that the slope of the curve, generally, is smallest in the first load cycle and became constant and steeper after two or three cycles of short-term loading, indicating that the rate of increase of deflection is smaller than in the first cycle.

Deflection-Time Relationship

The results may also be presented as a deflection-time relationship. Figs.7.16 to 7.24 show the deflection-time relationship for all the beams tested. The deflection of S1.3.5, S2.3.4 and S3.3.2 under permanent and intermittent short-term load, as shown in Figs.7.18, 7.20 and 7.22 respectively, are compared with that of the companion beams which were subjected only to the permanent loads after the initial short-term cycle up to 100 percent of the service loads. Up to the fifth day, as shown in Fig.7.18, under the same loading condition, the deflections of the two beams were almost the same but with the application of successive short-term load cycles, the long-term deflection of one beam is seen to have become progressively greater than that of the other, which was subjected only to the permanent long-term loading. This result is also reflected in Figs.7.20 and 7.22 although there was a slight difference in the initial deflections. The downward concave slope of the deflection time curves (Figs.7.16 to 7.24) immediately after each intermittent load cycle clearly indicates some recovery of the residual deflection for at least one or two days, but the general divergence of the two curves (Figs.7.18, 7.20

and 7.22) suggests an element of non-recovarable residual deflection resulting from each cycle of short-term loading, which is indicated at the end of the test by the vertical distance (4)-(4´) on Fig.7.18.

It is interesting to note from Figs.7.16 to 7.24 that the residual deflection after each short-term load cycle was greatest in the first two cycles but became progressively smaller and then remain constant in the last few cycles. This constant residual deflection was about 0.3mm to 0.4mm and was partly recoverable with time under the sustained load in all the tests. Figs.7.24b, 24c and 24d show the curves of the increase of residual deflection (after the first cycle) after each cycle of intermittent short-term loading. This residual deflection, corrected to account for the difference in the initial deflections between the two companion beams, corresponds to the vertical distance (4)-(4´) in Fig.7.18 for each cycle of loading. It is evident from these three curves, for beams S1.3.5, S2.3.4 and S3.3.2, that the residual deflection due to the cyclic loading effect and hence the total deflection would progressively approach a constant value if the cyclic loading were continued.

At the end of the test on beam S3.3.2, instead of one cycle of intermittent cycle of loading from 50 to 100 percent service load, eight cycles of short-term loading were applied successively to observe the total residual deflection. It is interesting to see from Fig.7.22 that the

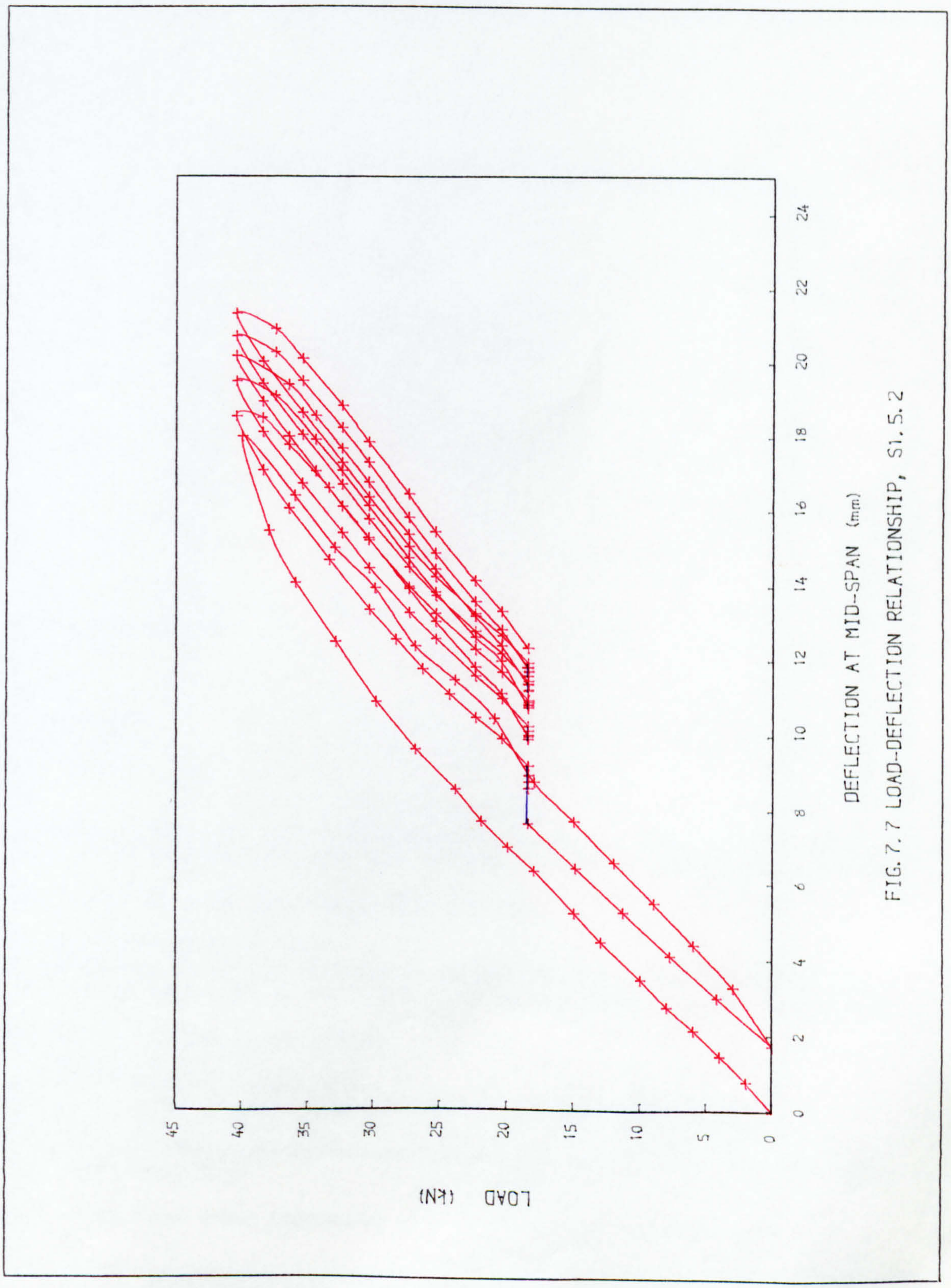

FIG. 7.7 LOAD-DEFLECTION RELATIONSHIP, S1.5.2

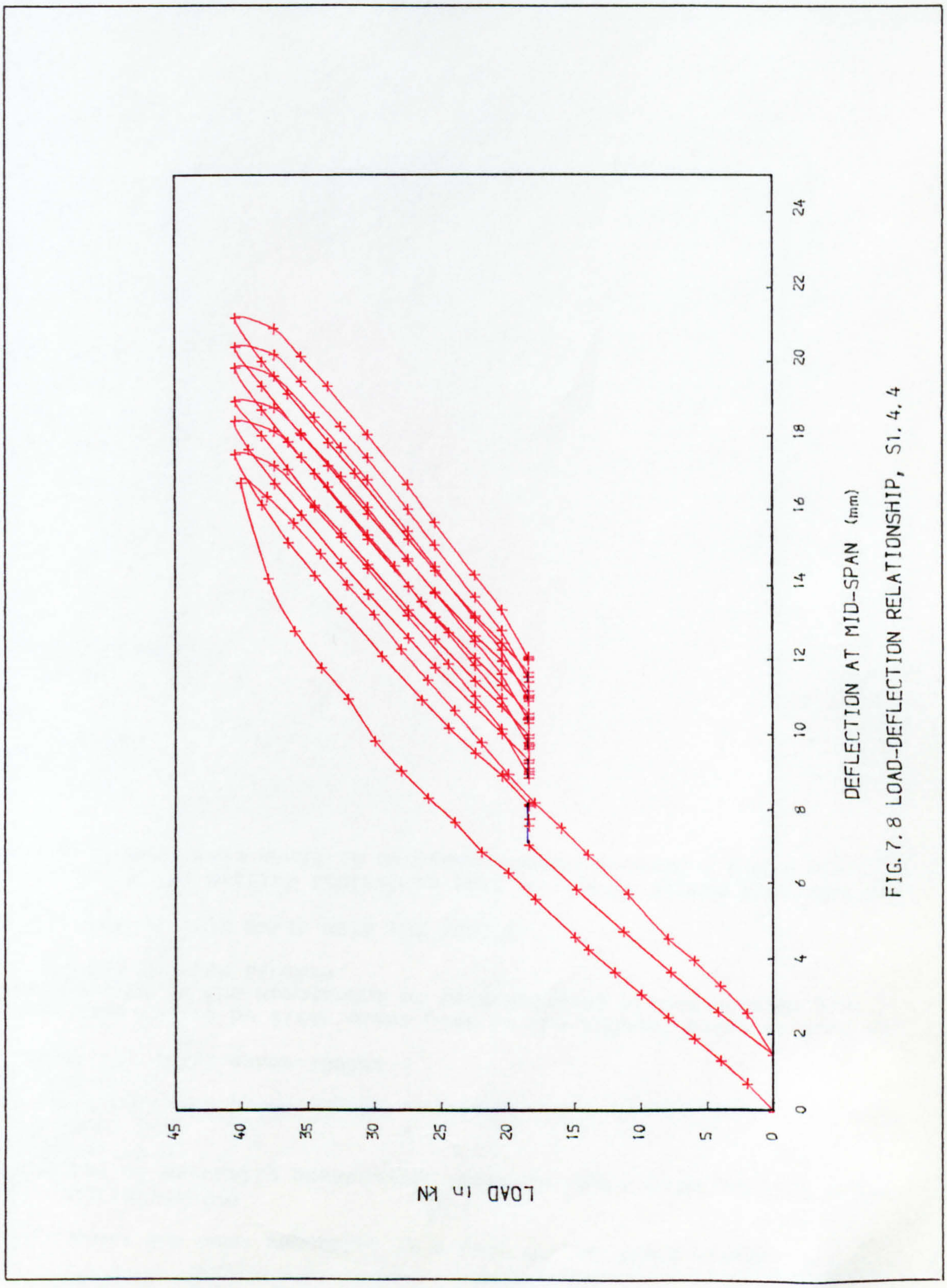

FIG. 7.8 LOAD-DEFLECTION RELATIONSHIP, S1.4.4

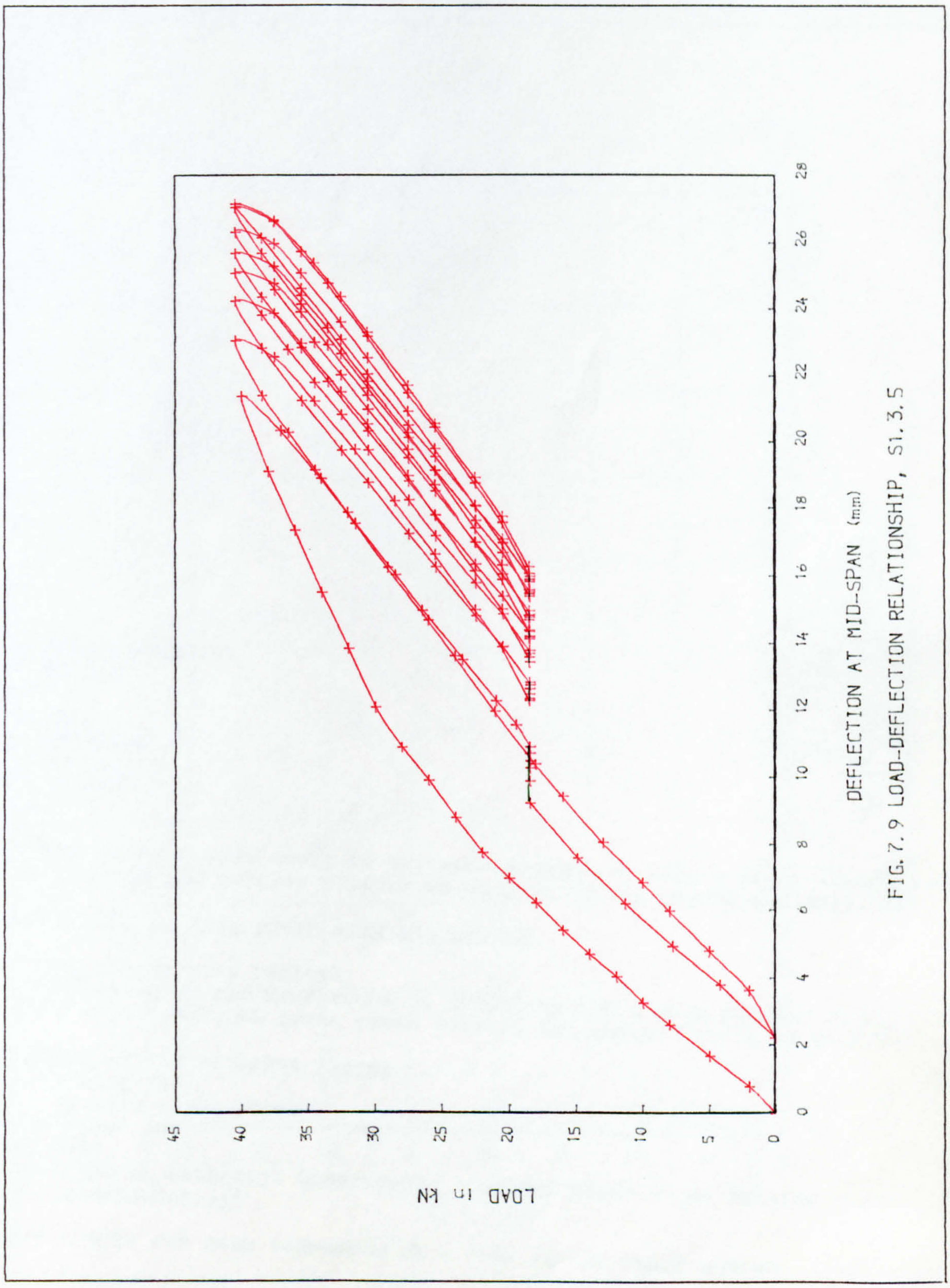

FIG. 7.9 LOAD-DEFLECTION RELATIONSHIP, S1.3.5

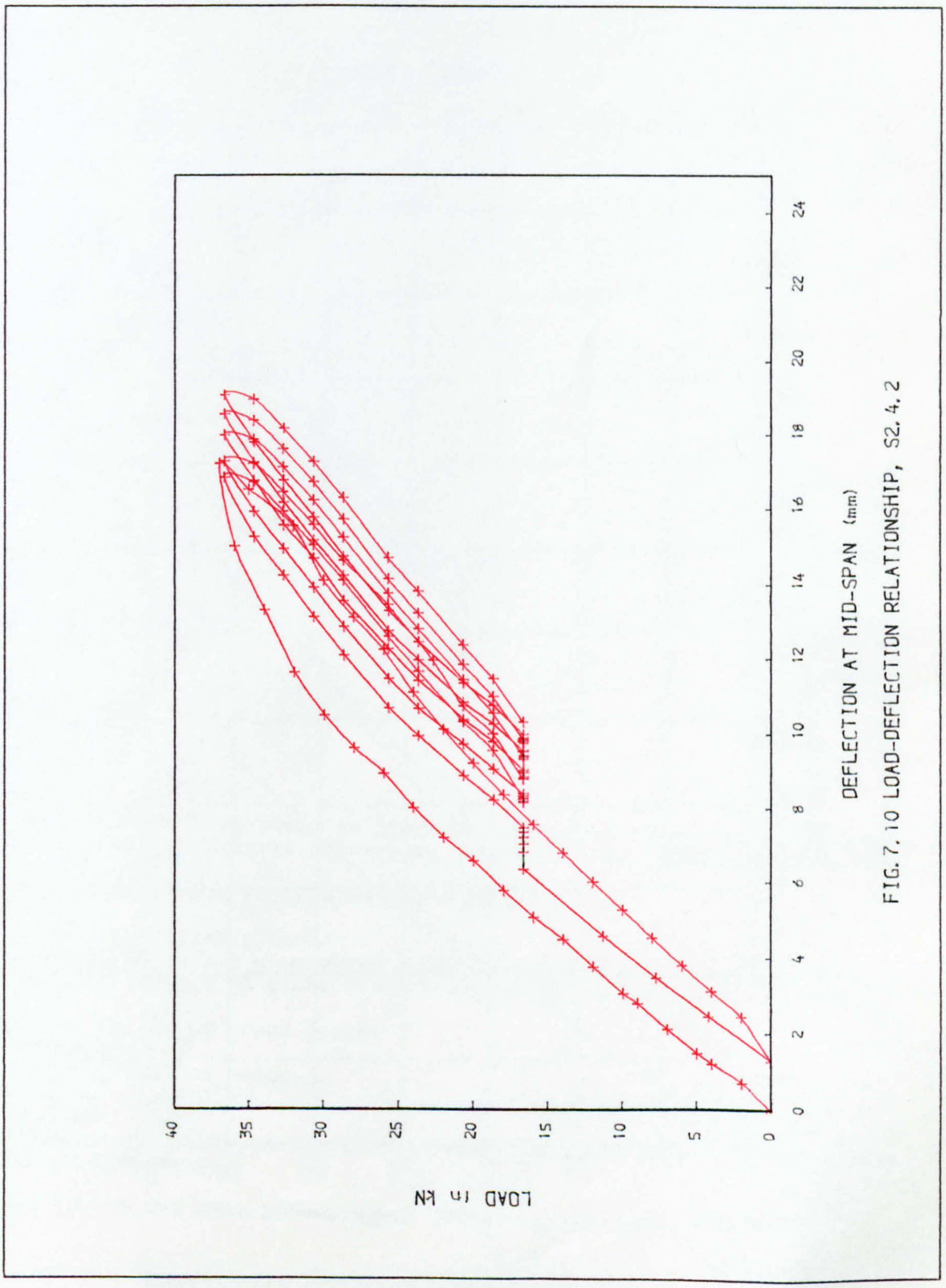

FIG. 7.10 LOAD-DEFLECTION RELATIONSHIP, S2.4.2

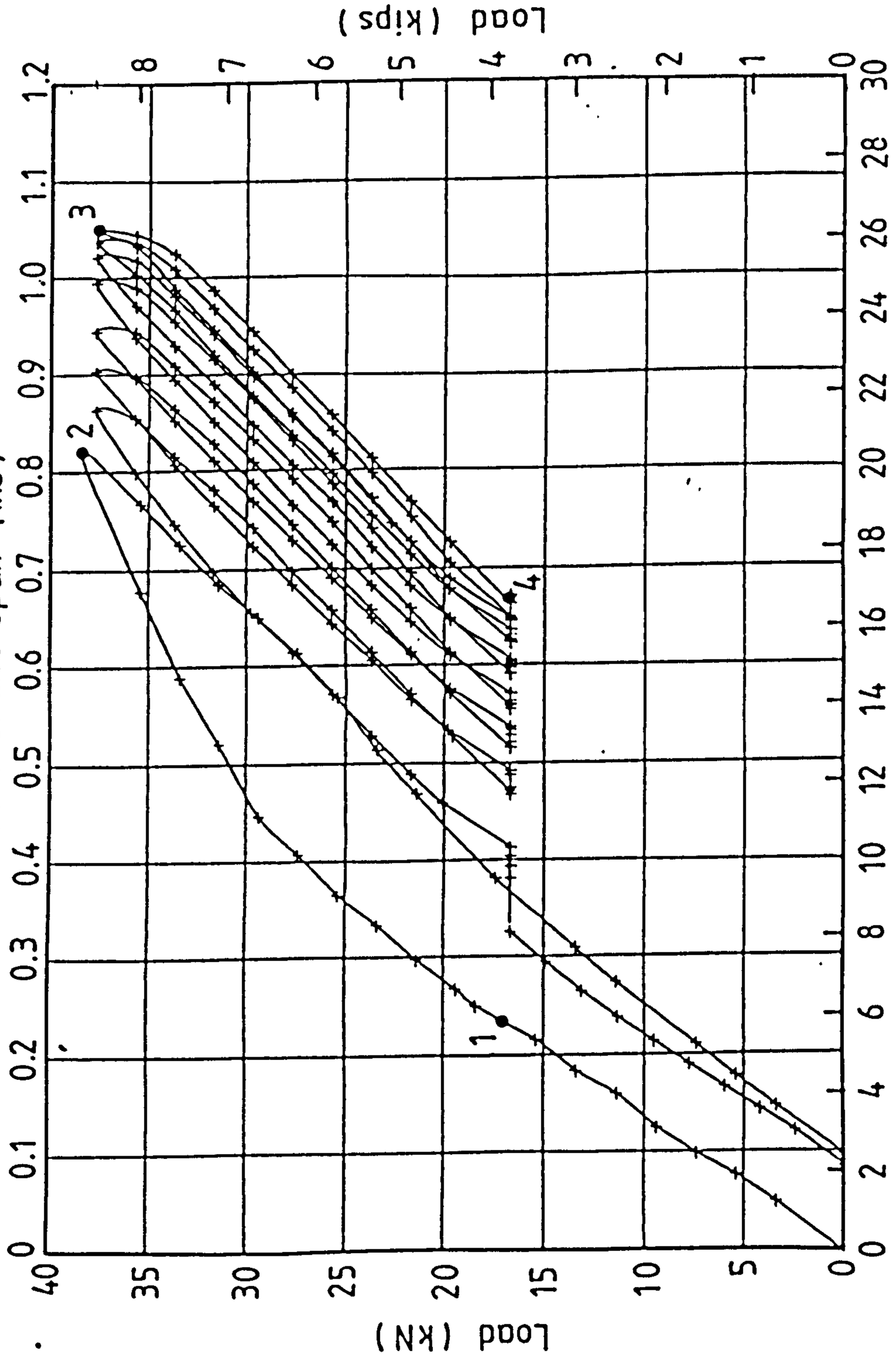

Fig.7.11 Load-deflection curves. Beam S2.3.4

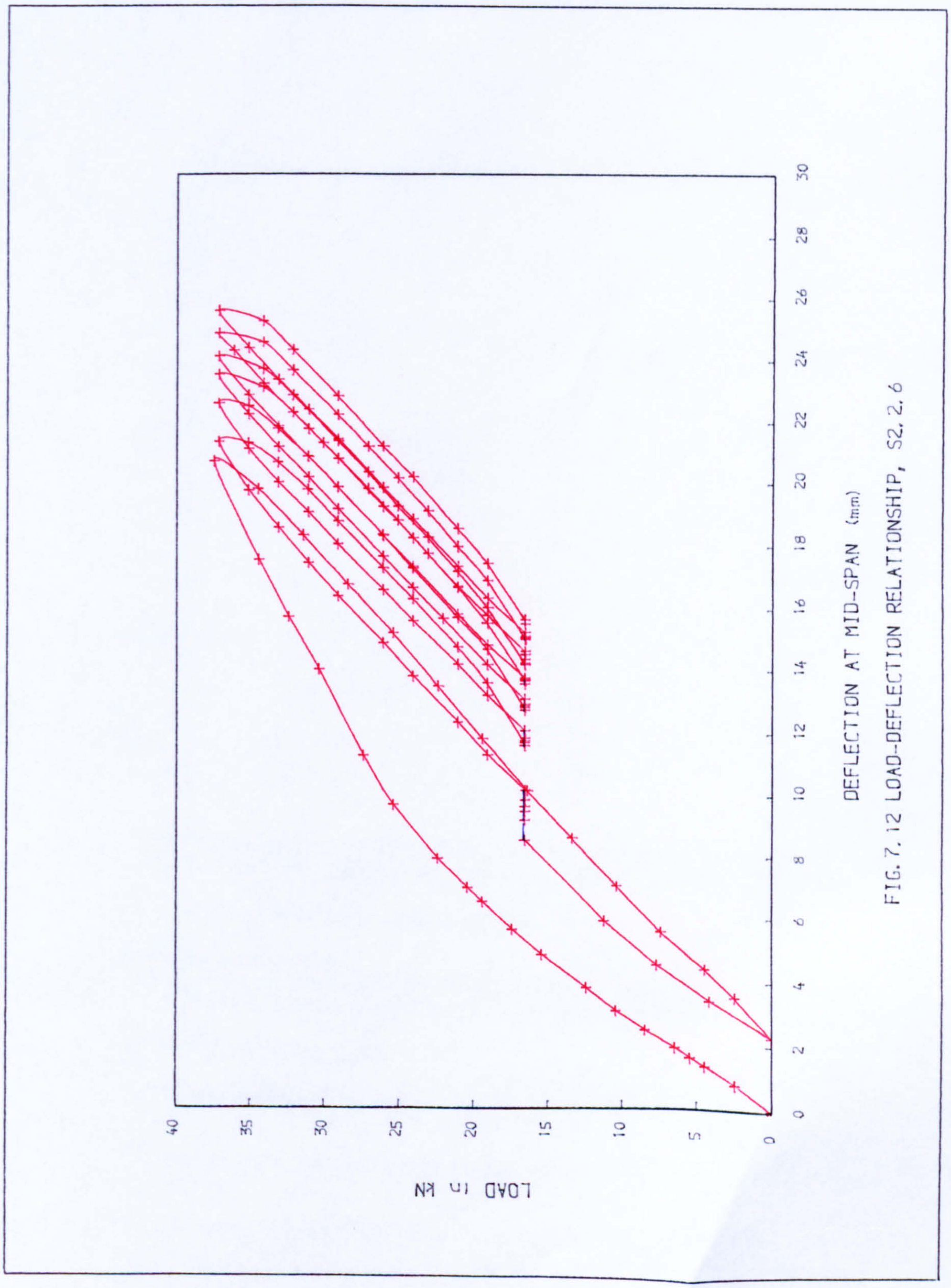

FIG. 7.12 LOAD-DEFLECTION RELATIONSHIP, S2.2.6

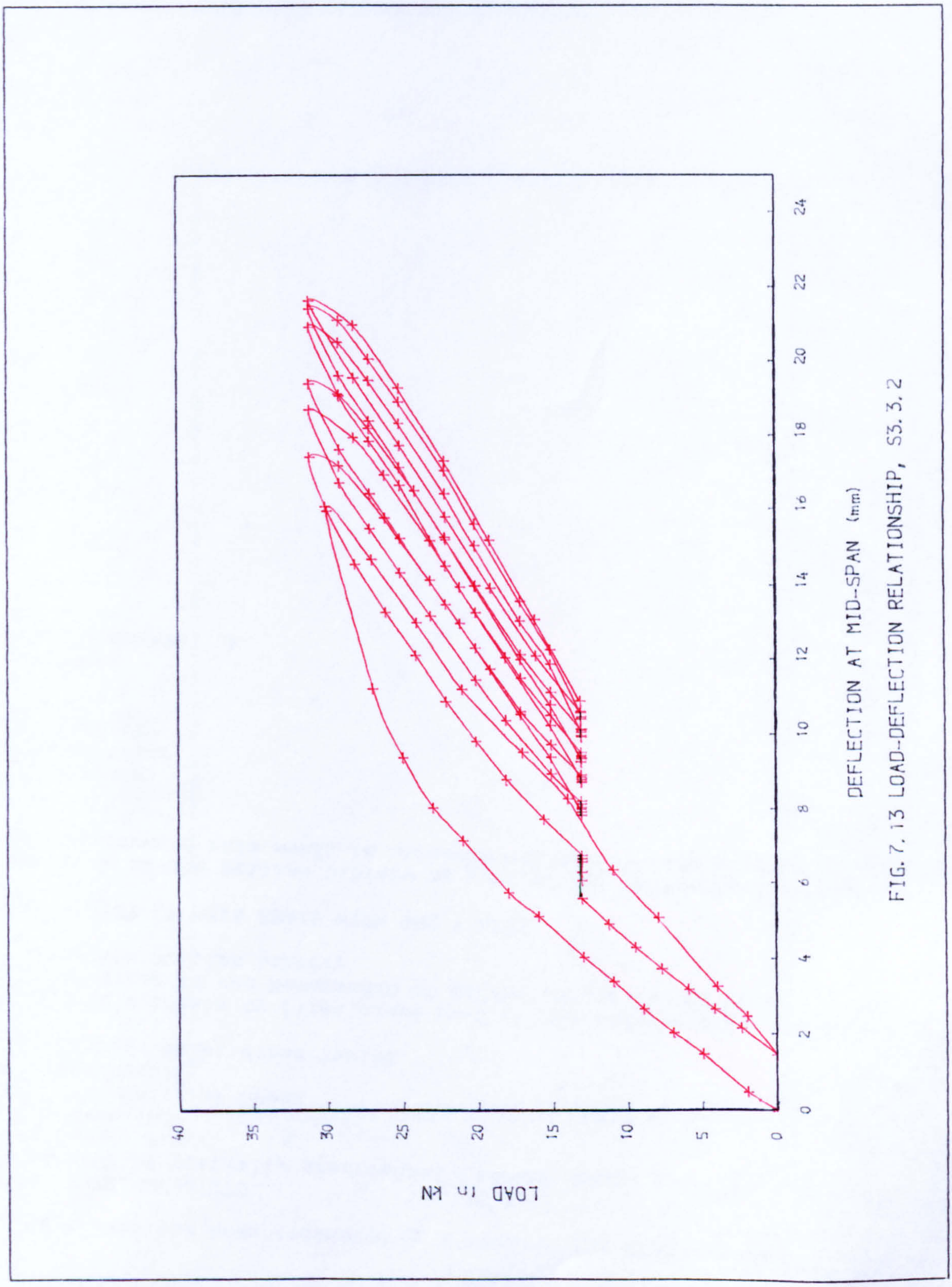

FIG. 7.13 LOAD-DEFLECTION RELATIONSHIP, S3.3.2

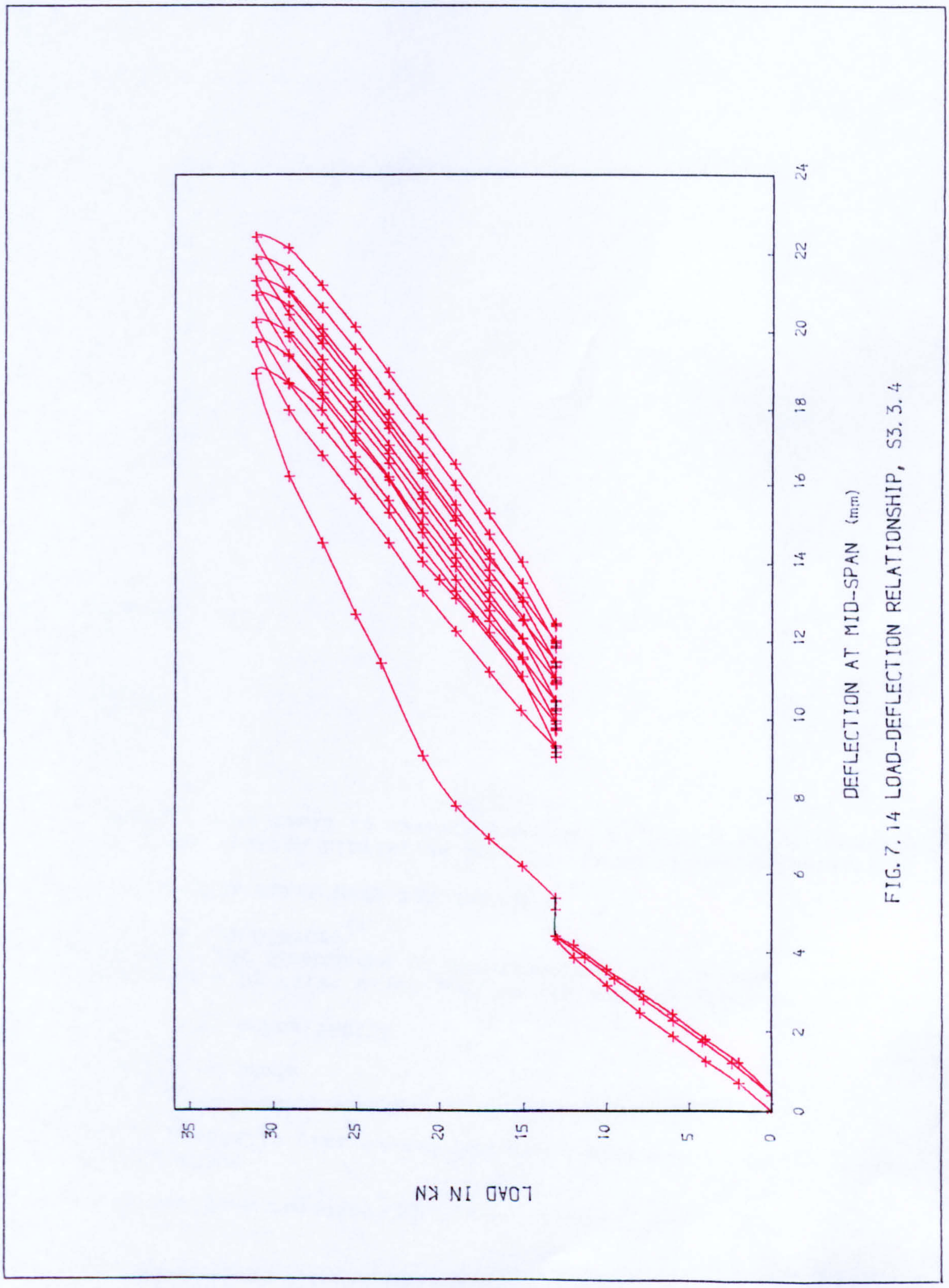

FIG. 7.14 LOAD-DEFLECTION RELATIONSHIP, S3.3.4

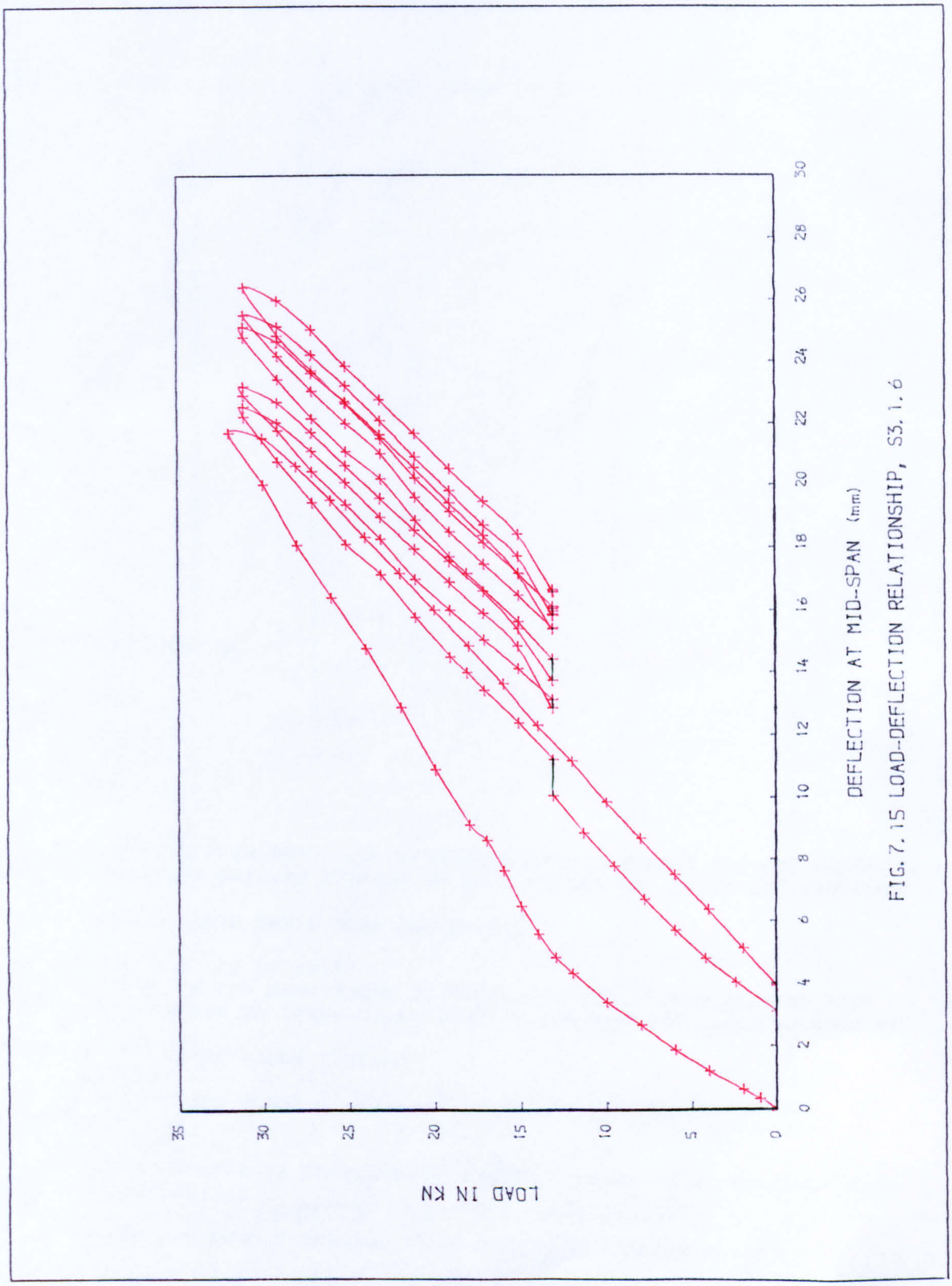

FIG. 7.15 LOAD-DEFLECTION RELATIONSHIP, S3.1.6

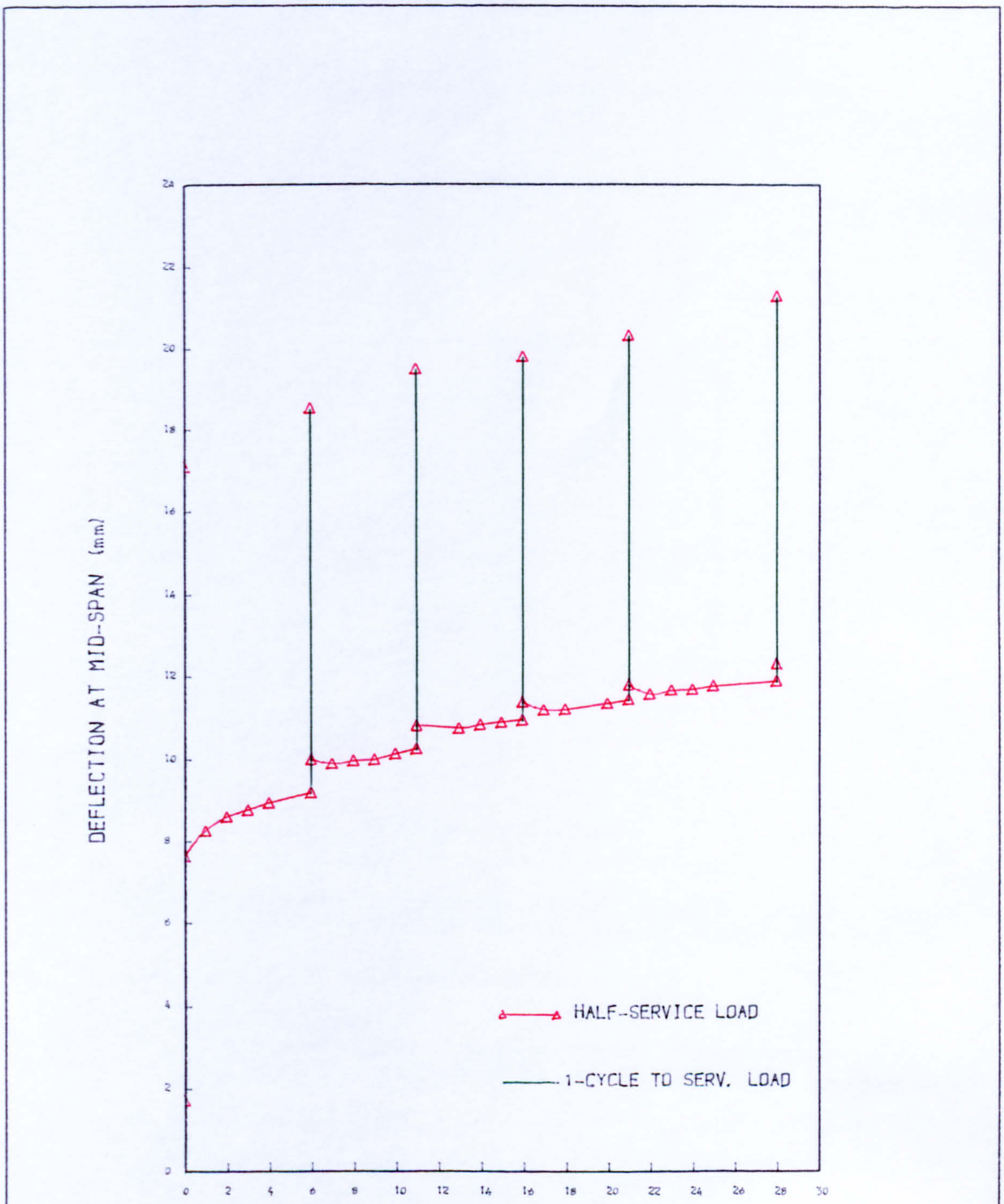

FIG. 7.16 DEFLECTION-TIME RELATIONSHIP, S1.5.2

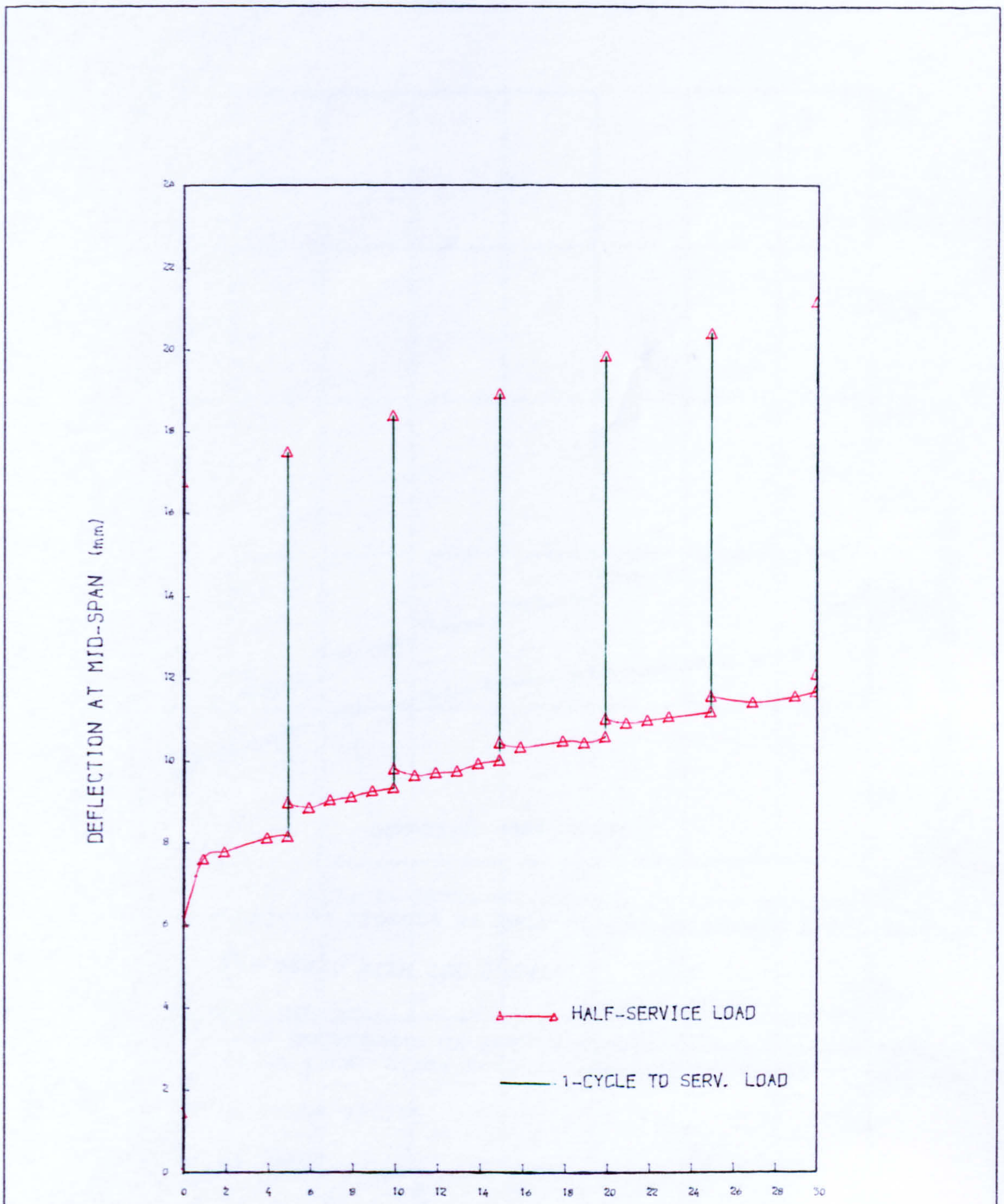

FIG. 7.17 DEFLECTION-TIME RELATIONSHIP, S1.4.4

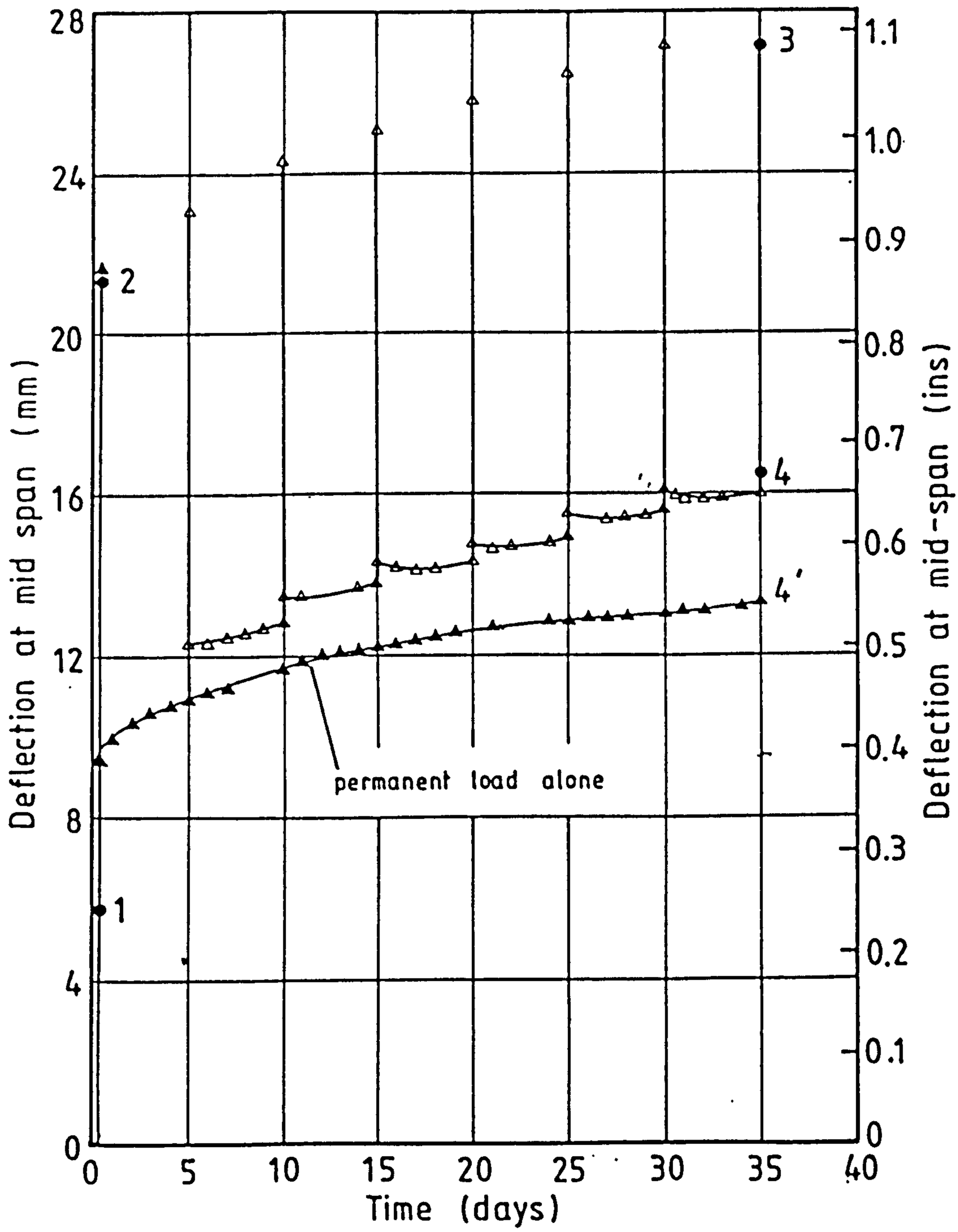

Fig.7.18 Deflection-time curve. Beam S1.3.5

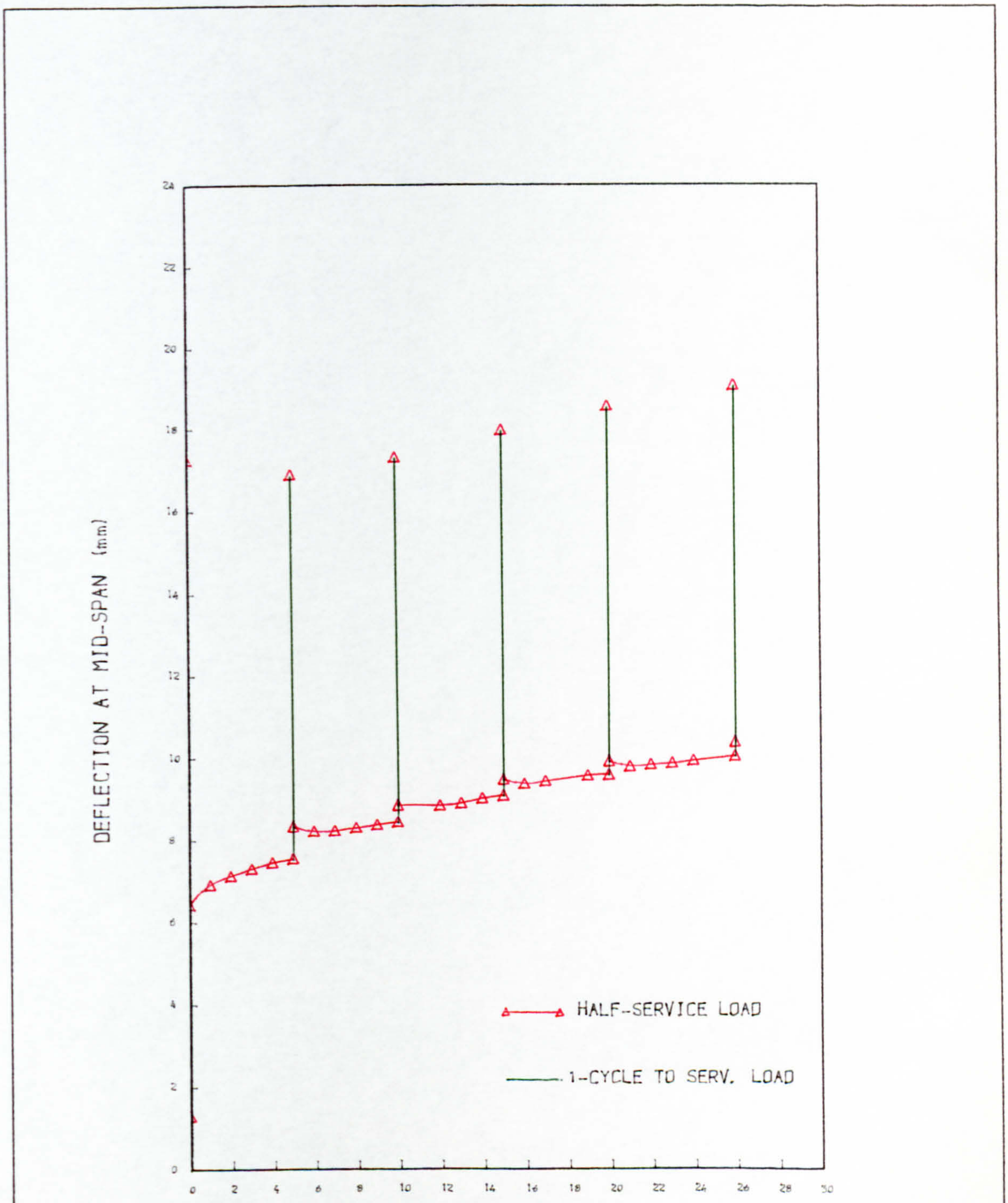

FIG. 7.19 DEFLECTION-TIME RELATIONSHIP, S2.4.2

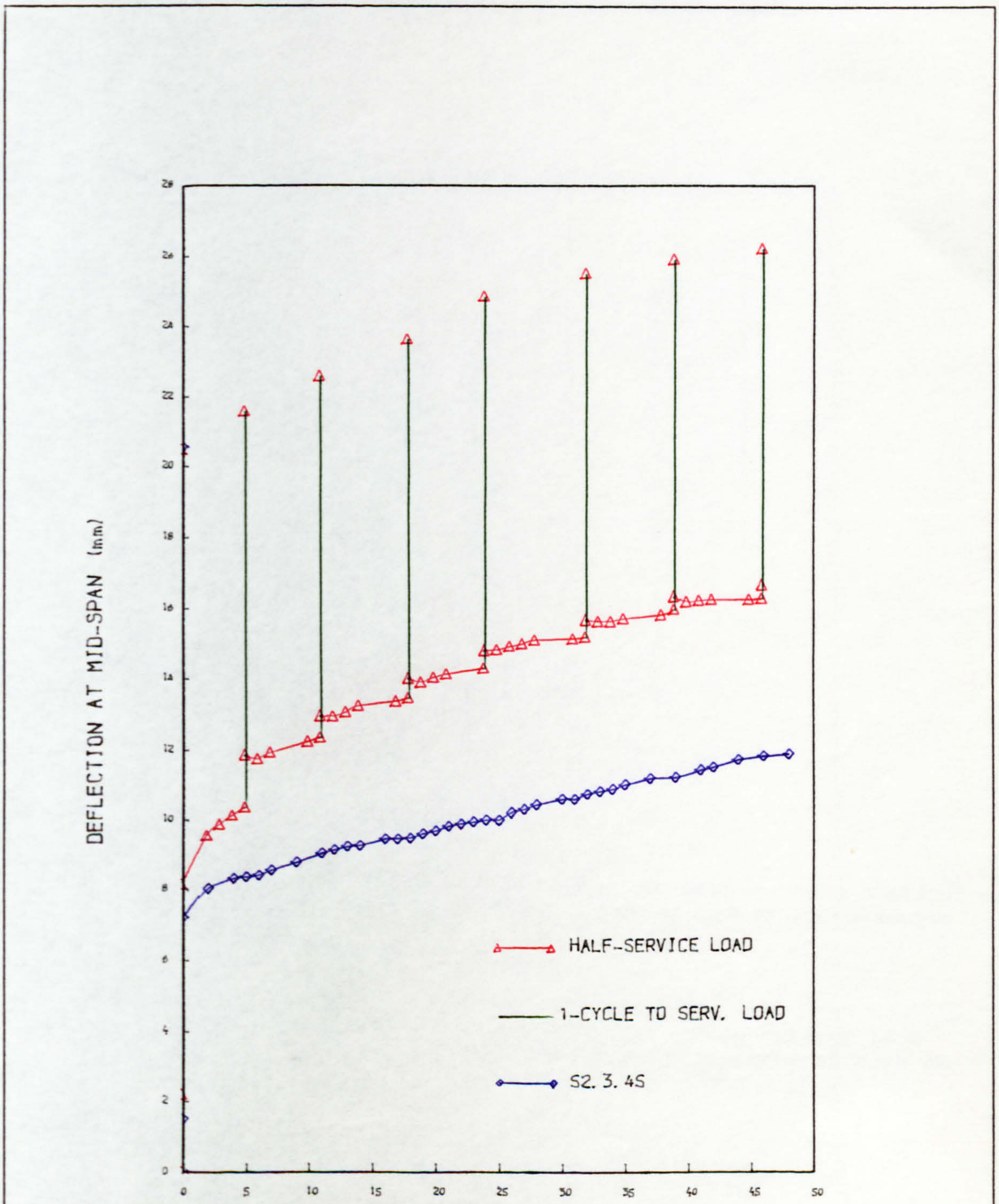

FIG. 7.20 DEFLECTION-TIME RELATIONSHIP, S2.3.4 AND S2.3.4S

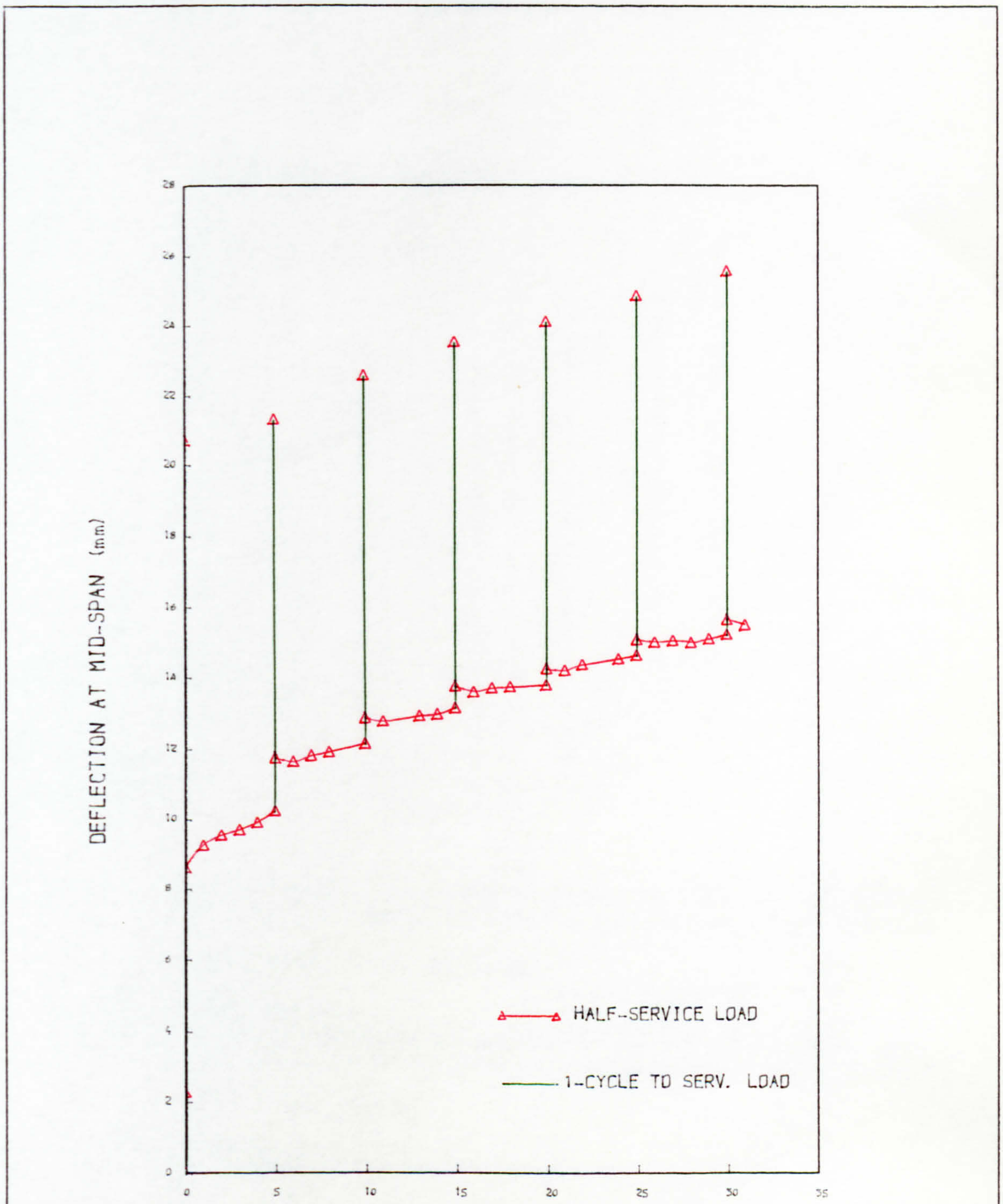

FIG. 7.21 DEFLECTION-TIME RELATIONSHIP, S2.2.6

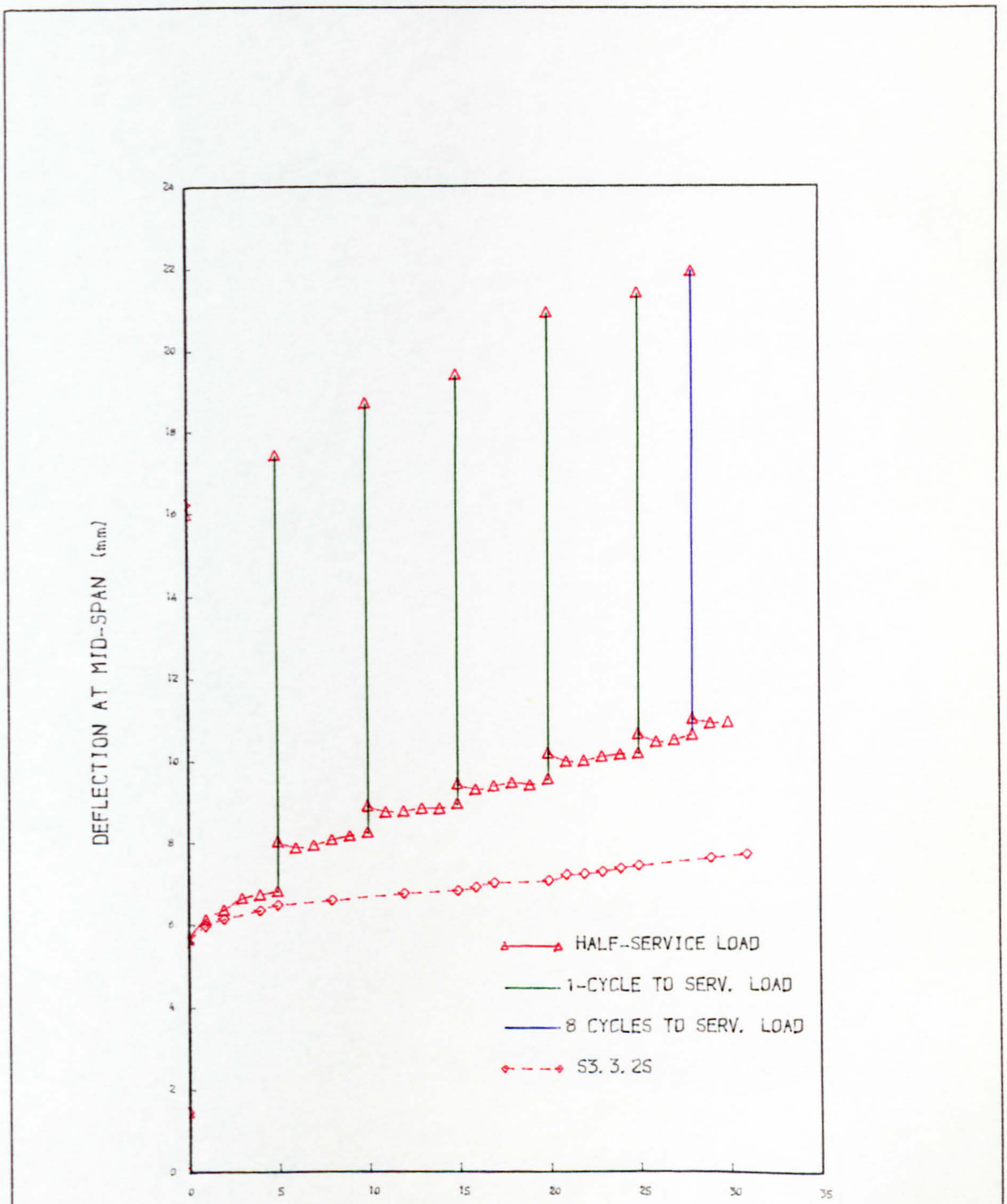

FIG. 7.22 DEFLECTION-TIME RELATIONSHIP, S3.3.2 AND S3.3.2S

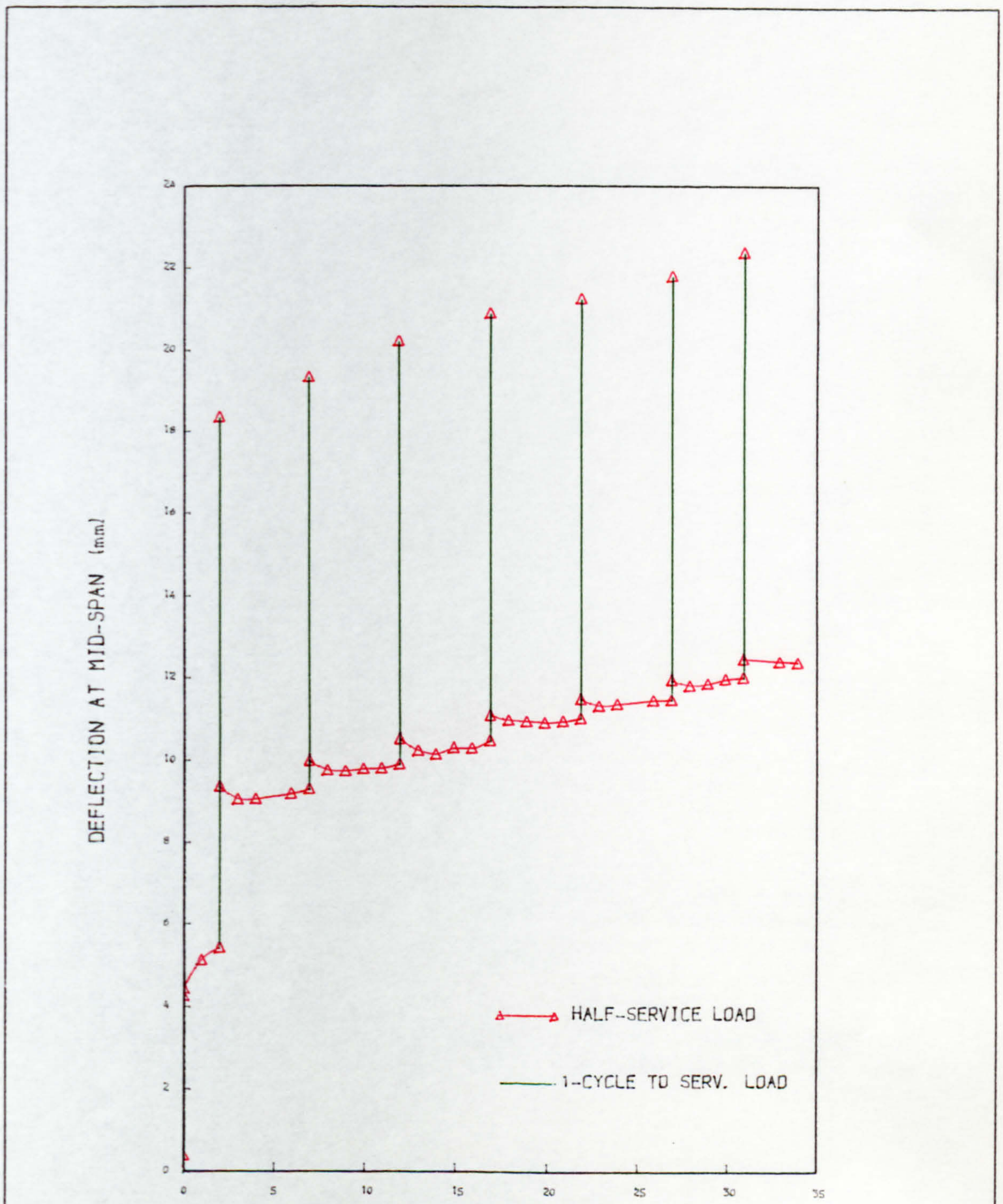

FIG. 7.23 DEFLECTION-TIME RELATIONSHIP, S3.3.4

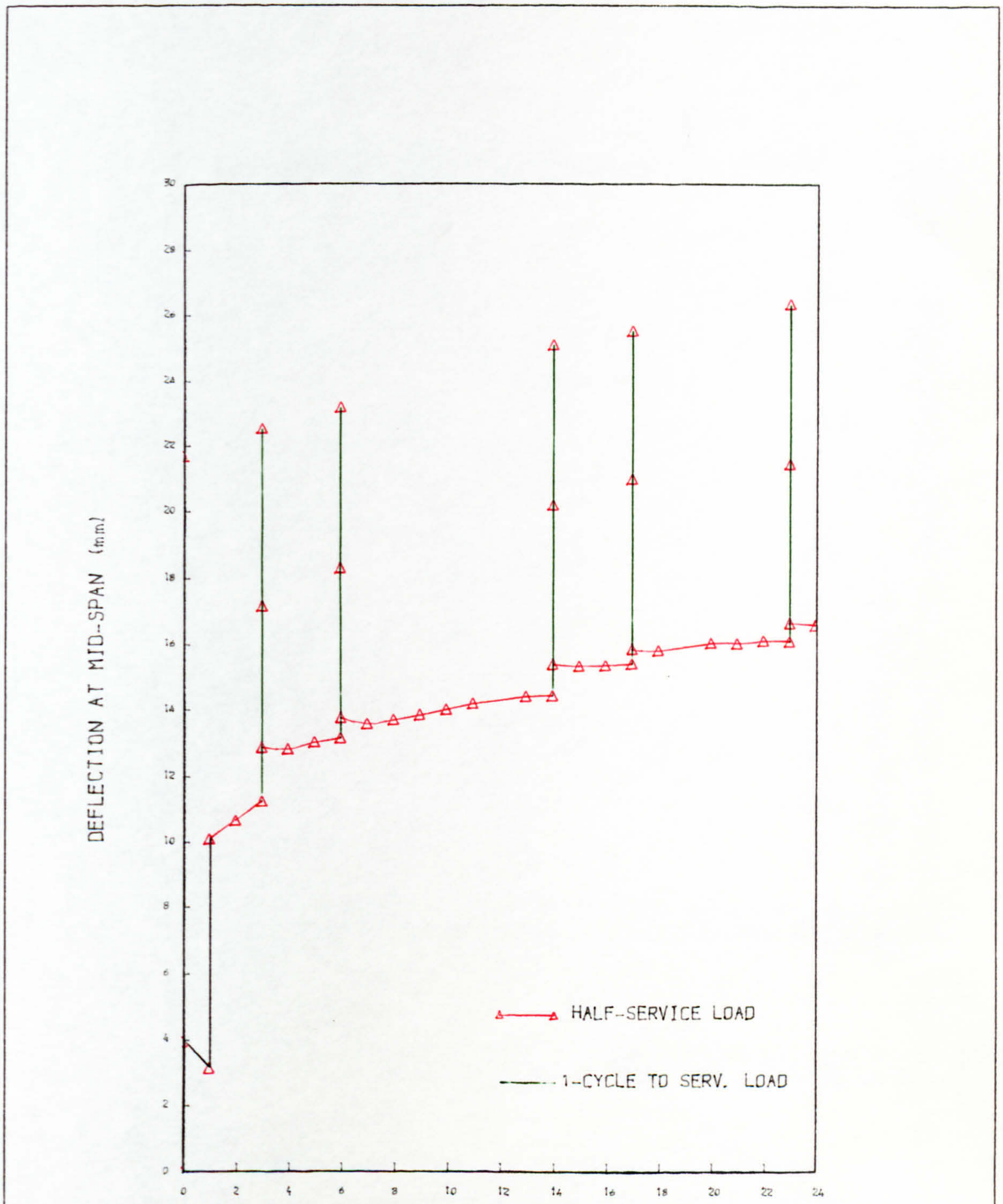

FIG. 7.24 DEFLECTION-TIME RELATIONSHIP, S3.1.6

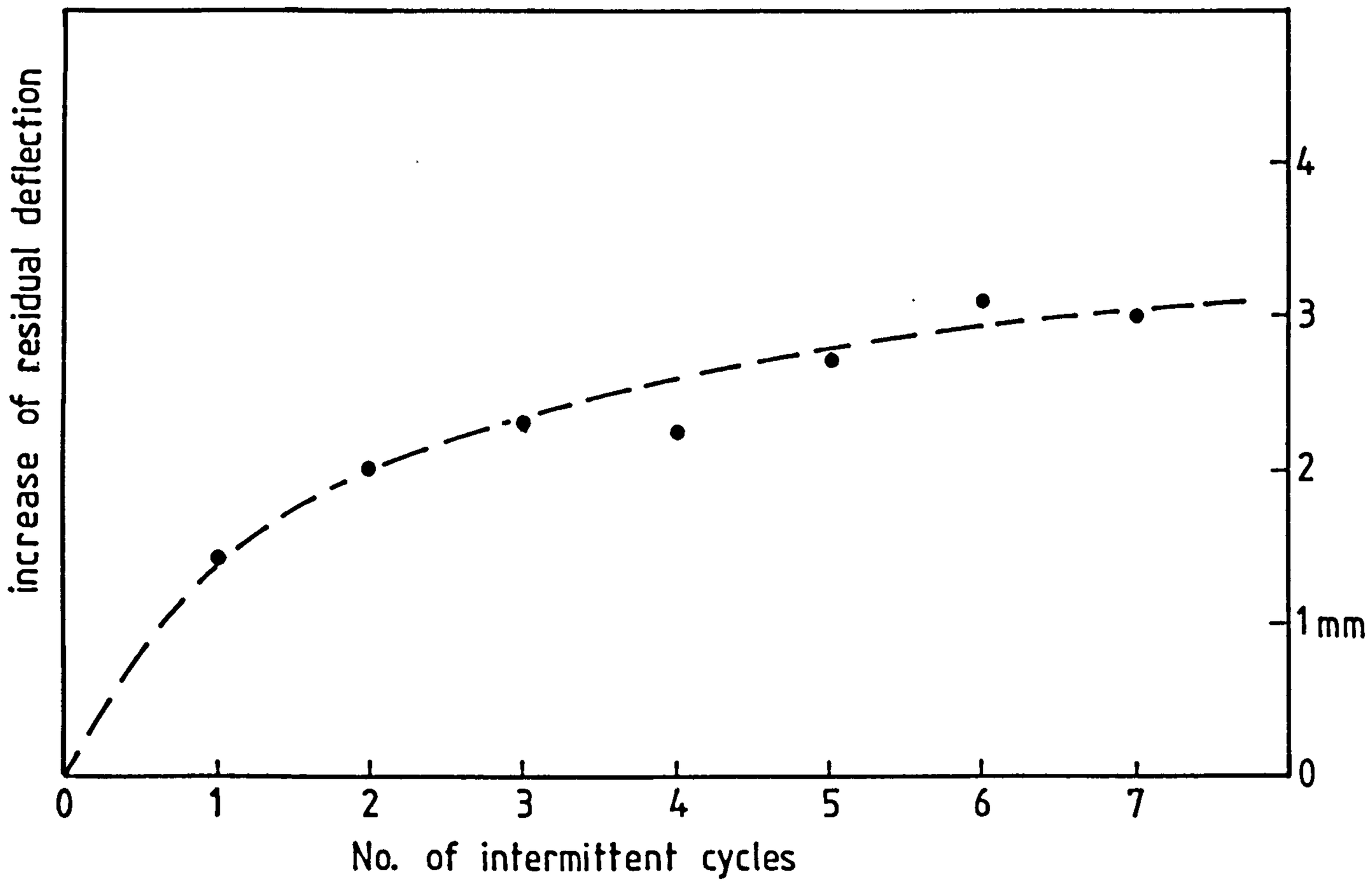

Fig. 24 b Increase of residual deflection due to short-term cycles of loading S1.3.5

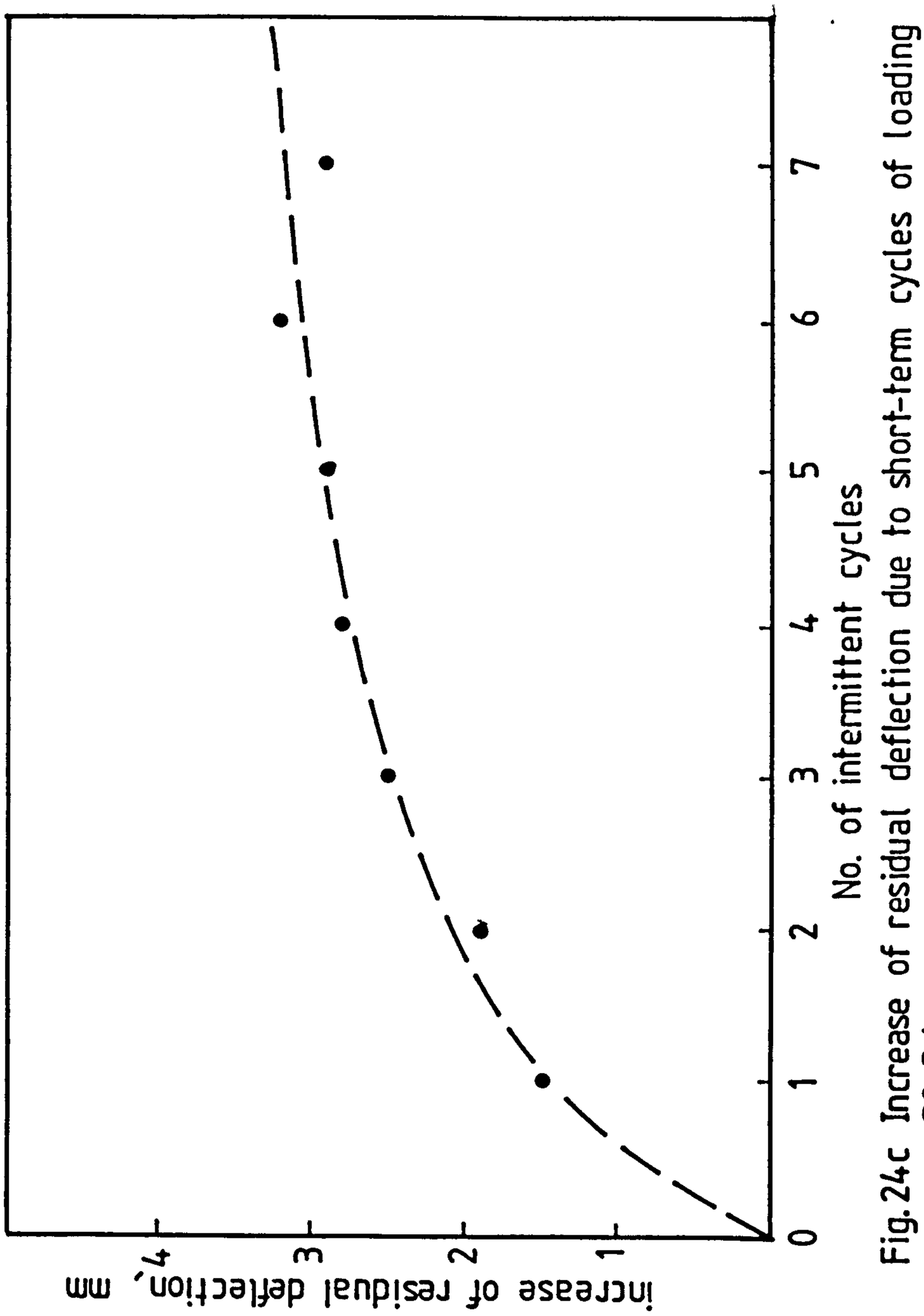

Fig.24c Increase of residual deflection due to short-term cycles of loading S2.3.4

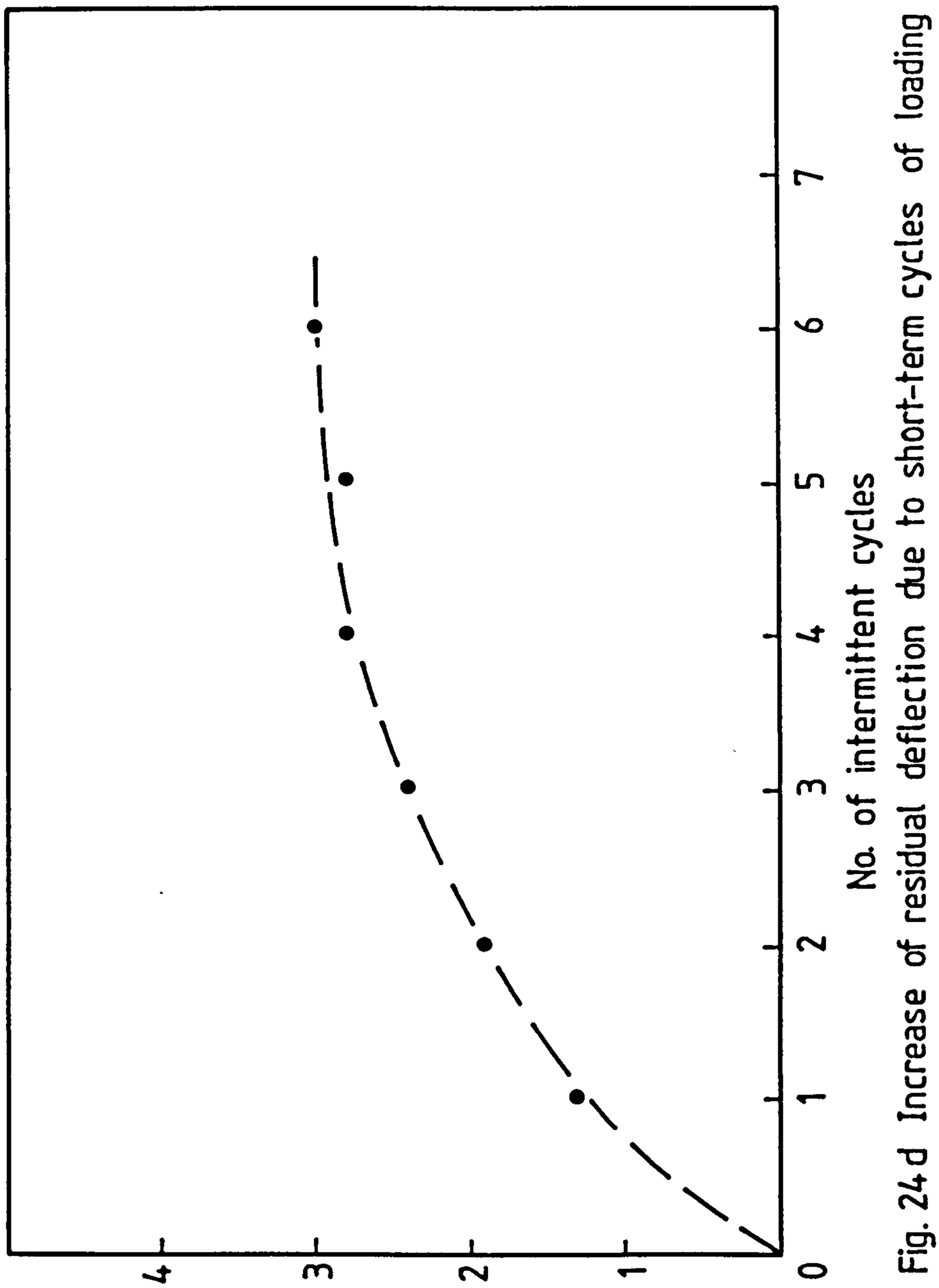

Fig. 24 d Increase of residual deflection due to short-term cycles of loading
S3.3.2

total residual deflection still remained at about 0.3mm to 0.4mm. It therefore reveals that most of the residual deflection occurred during the first of the eight cycles of loading.

An examination of Figs.7.11 and 7.18 shows that the short-term deflection between 50 and 100 percent of the service load was greatest in the first load cycle and became approximately constant after the first two or three intermittent cycles. This feature is summarised for the whole series by the columns (2)-(1) and (3)-(4) in Table 7.3a.

An examination of Table 7.3a column (3), reveals that most of the deflections under service load exceeded the CP110 limit of L/250 (24mm), at the end of each test. It is also interesting to note that the increase of deflection under the permanent load was greatest in beams with a low degree of prestress and a large amount of non-prestressed reinforcement. For example, the final deflection of beam S3.1.6 was about 3.4 times the initial deflection under 50 percent service load.

McHenry's Hypothesis

It will be noticed that the deflection under the combined loading resembles the form of deflection which would be expected to result from the addition of the deflection due to the short-term cycles alone to the long-

term deflection under the permanent load alone. Although this similarity cannnot be verified numerically without additional tests, it may be considered analogous to McHenry's hypothesis for the superposition of creep strain (48). McHenry stated the principle as follows:

"The strains produced in concrete at any time t by a stress increment applied at any time t_0 are independent of the effects of any stress applied either earlier or later than t_0." The stress increment may be positive or negative but stresses which approach ultimate strength are excluded.

It may be possible to apply McHenry's hypothesis to the deflection curves of beams subjected to permanent load with intermittent load cycles. Fig.7.25 illustrates the principle of superposition when a load is added and then removed after a short period. When a load increment is applied at time t_0, the creep strain after a given period is increased by P, which is equal to the creep strain caused by the same load applied alone at t_0. When the same load is removed at time t_1, then the curve will be similar to the reverse creep curve and Q will be equal to the creep strain caused by the load increment at time t_1. It will be noticed that Q' is then the residual strain when compared with the original curve under the permanent load alone. This may be seen to be the strain that causes the non-recoverable deflection shown in the deflection-time curves (Figs.7.16 to 7.24) of all the tests.

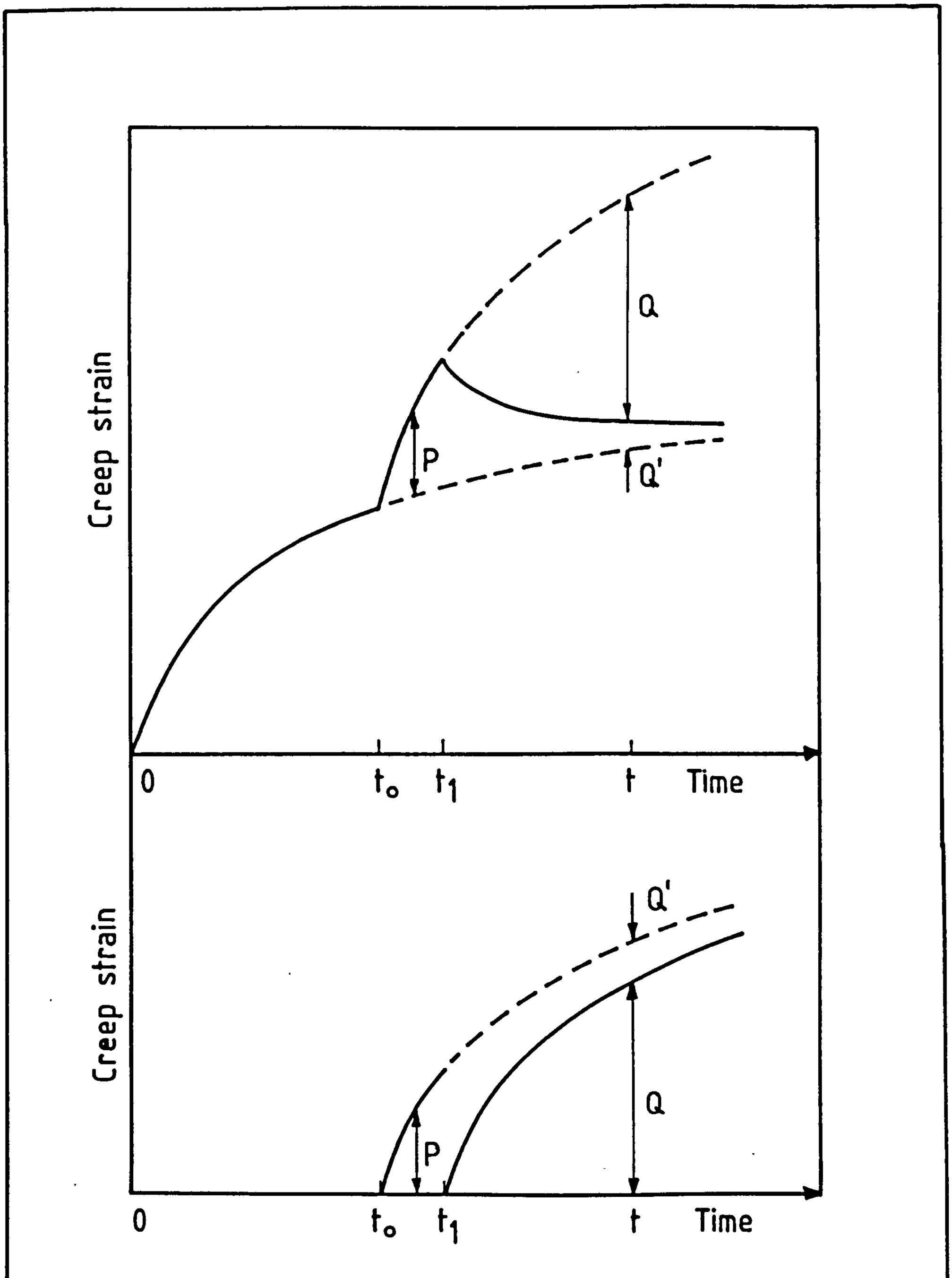

Fig. 7.25 Principle of superposition

7.3.3.2 Strain Distribution

Figs.7.26 to 7.28 show the midspan strain distributions of beams S1.3.5, S2.3.4 and S2.2.6 respectively, at increasing increments of load up to the service load. These are "elastic" value from which the creep strains before testing have been deducted. Cracking was first observed in S1.3.5 at a load of 28.3kN (Fig.7.26). It is interesting to note that before the point of cracking, the behaviour of the beams conforms with the elastic theory; all the lines cut the line, which represents the "prestrain", at about the same level (100mm from the soffit for S1.3.5 and about 140mm for S2.3.4). This may be seen to be the level which is commonly known as the bending axis of the uncracked section. This axis was seen to have risen progressively to a new level as soon as the beam cracked. The neutral axis of stress and strain can be seen to be lower than the bending axis.

The change of strain distributions under the service loads and 50 per cent of the service loads in successive cycles of intermittent short-term loading are shown in Figs.7.29 to 7.37. Referring to Fig.7.31 which is typical of all the tests, it may be seen that while there is little change of strain at the level of the reinforcement, the effect of creep and shrinkage of the concrete under the action of the permanent load is to cause a progressive lowering of the position of the neutral axis of strain. It may, therefore, be concluded from the observation that there

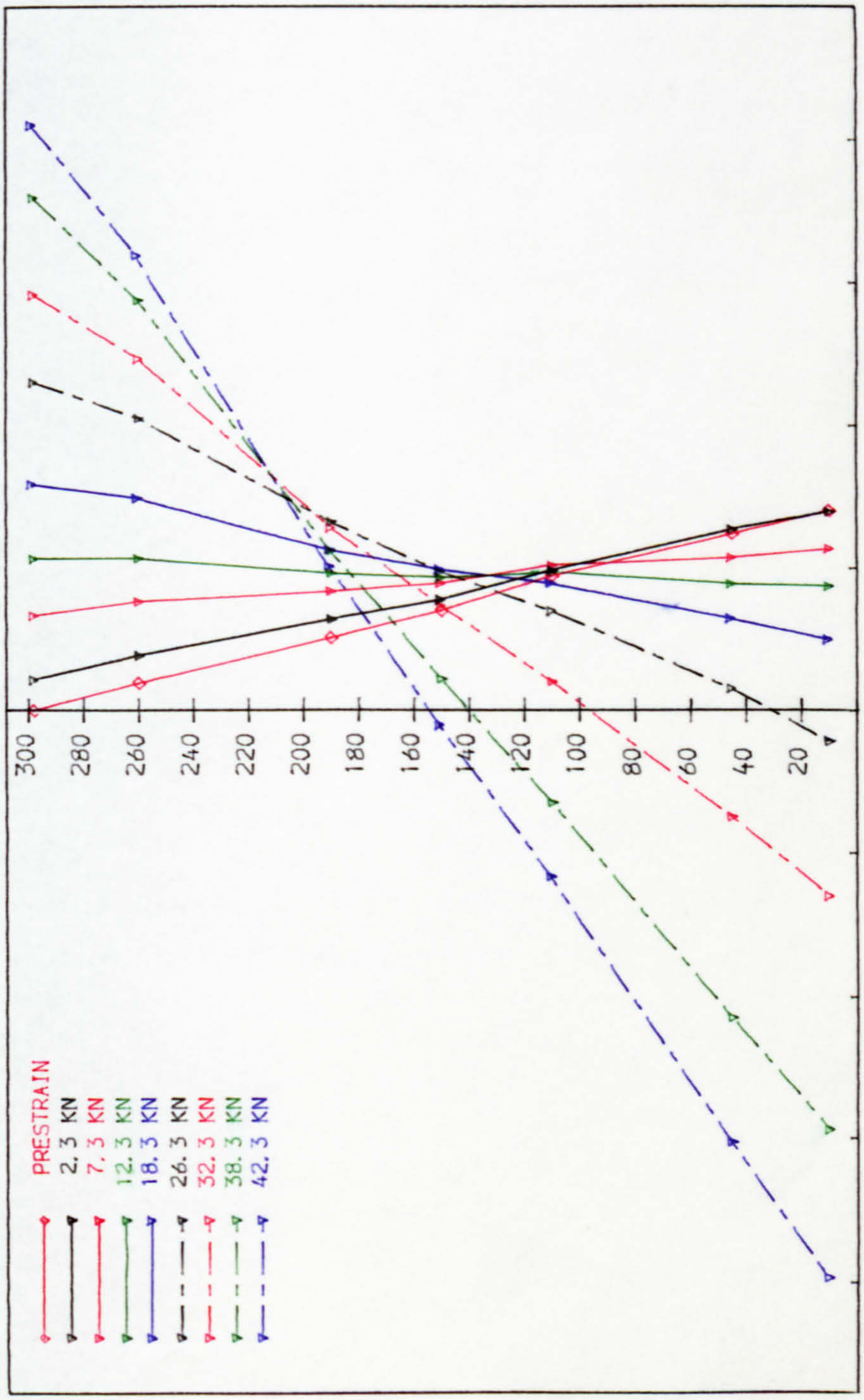

FIG. 7.26 SHORT-TERM STRAIN DISTRIBUTION AT MIDSPAN. S1.3.5 (FIRST LOAD CYCLE)

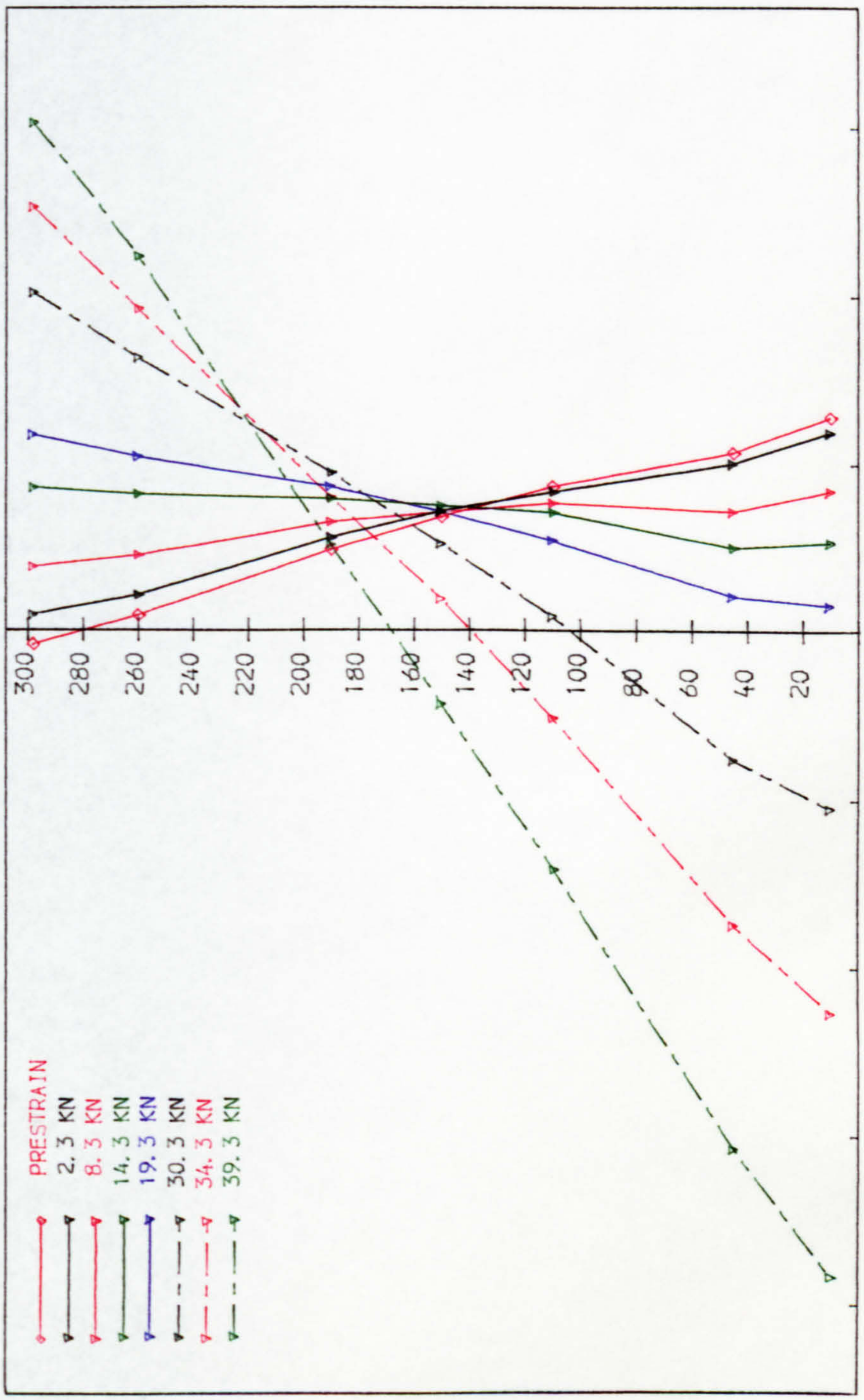

FIG. 7.27 SHORT-TERM STRAIN DISTRIBUTION AT MIDSPAN. S2.3.4 (FIRST LOAD CYCLE)

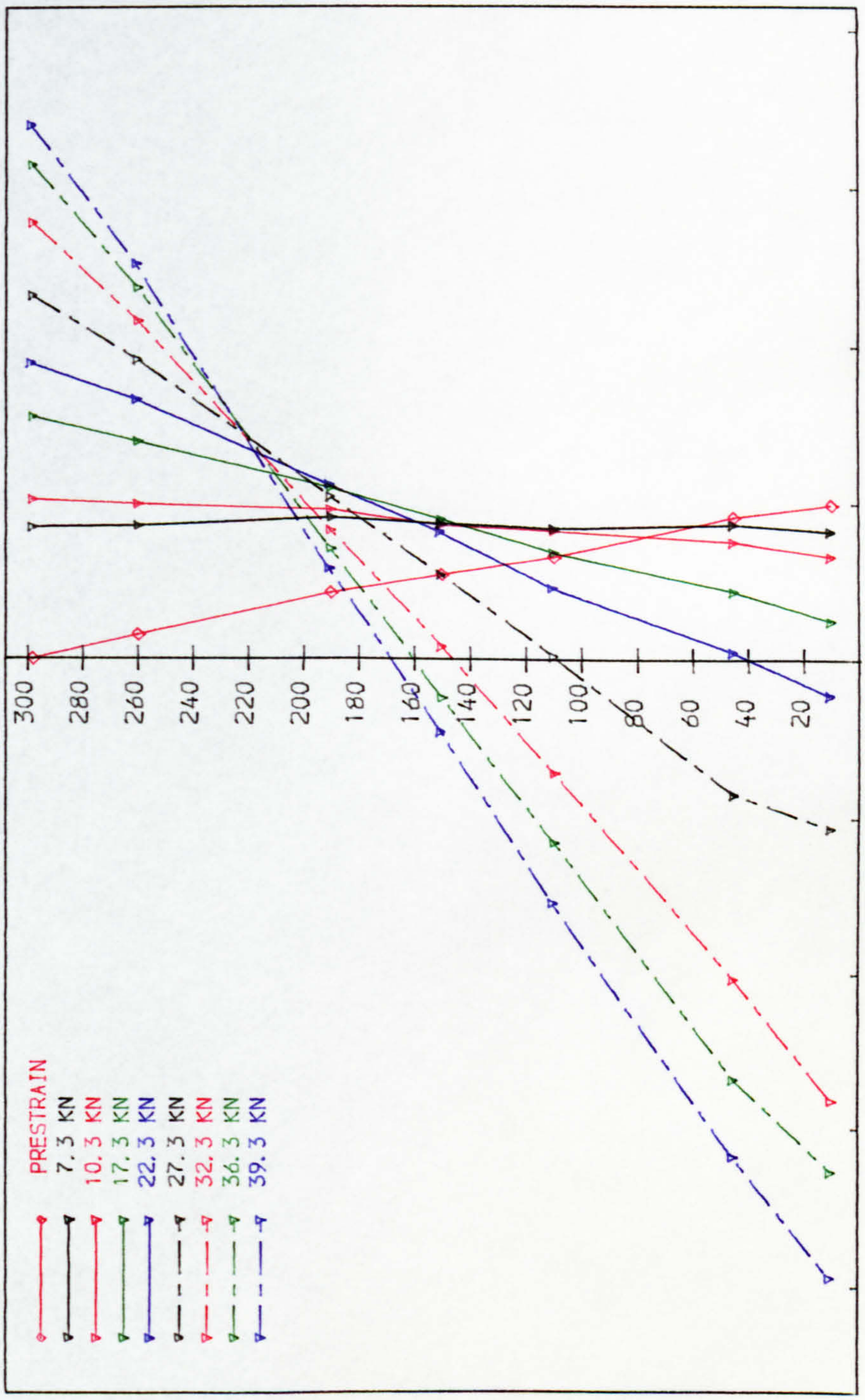

FIG. 7.28 SHORT-TERM STRAIN DISTRIBUTION AT MIDSPAN. S2.2.6 (FIRST LOAD CYCLE)

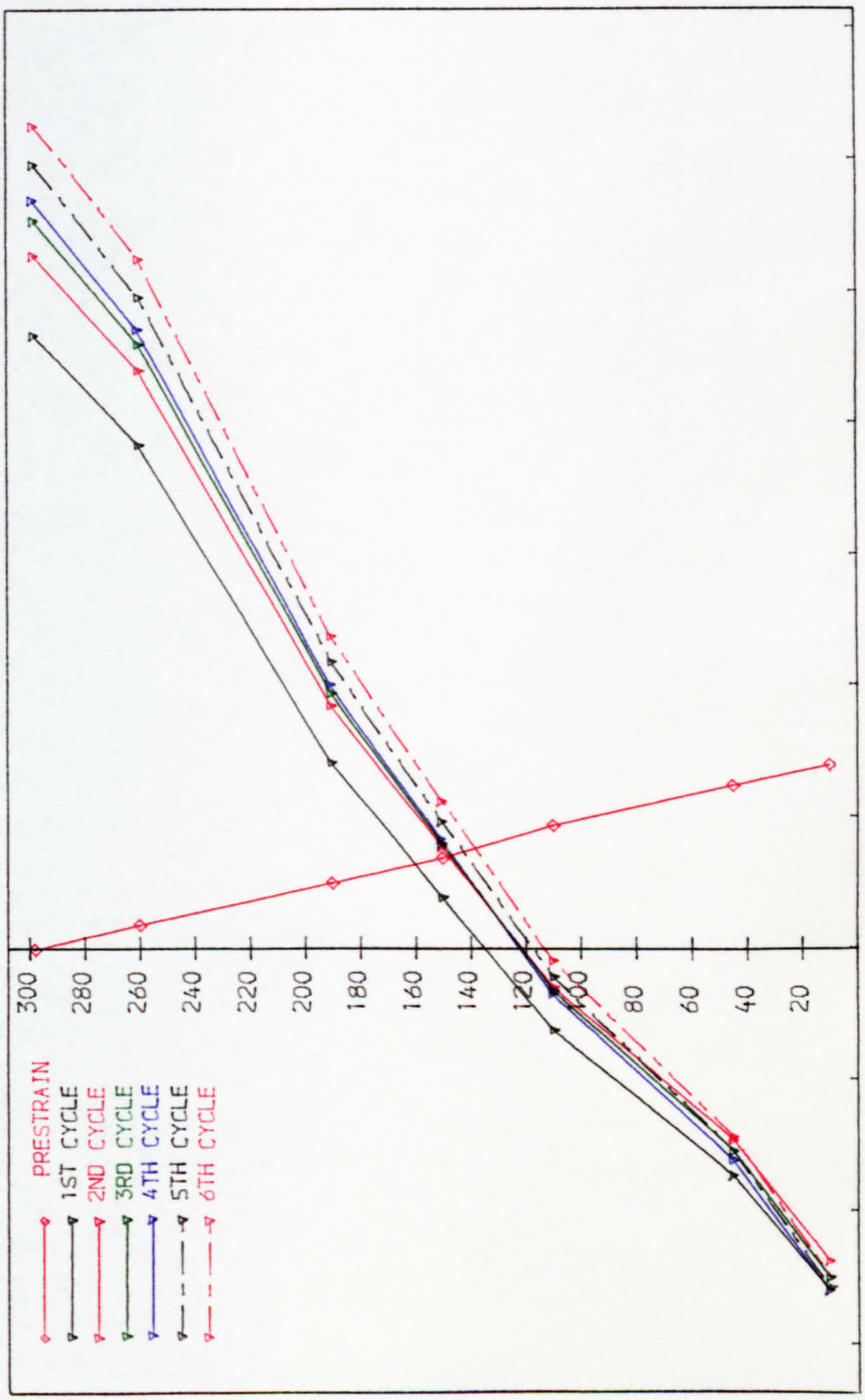

FIG. 7.29 TOTAL STRAIN DISTRIBUTION AT MIDSPAN AT SERVICE LOAD. S1.3.5

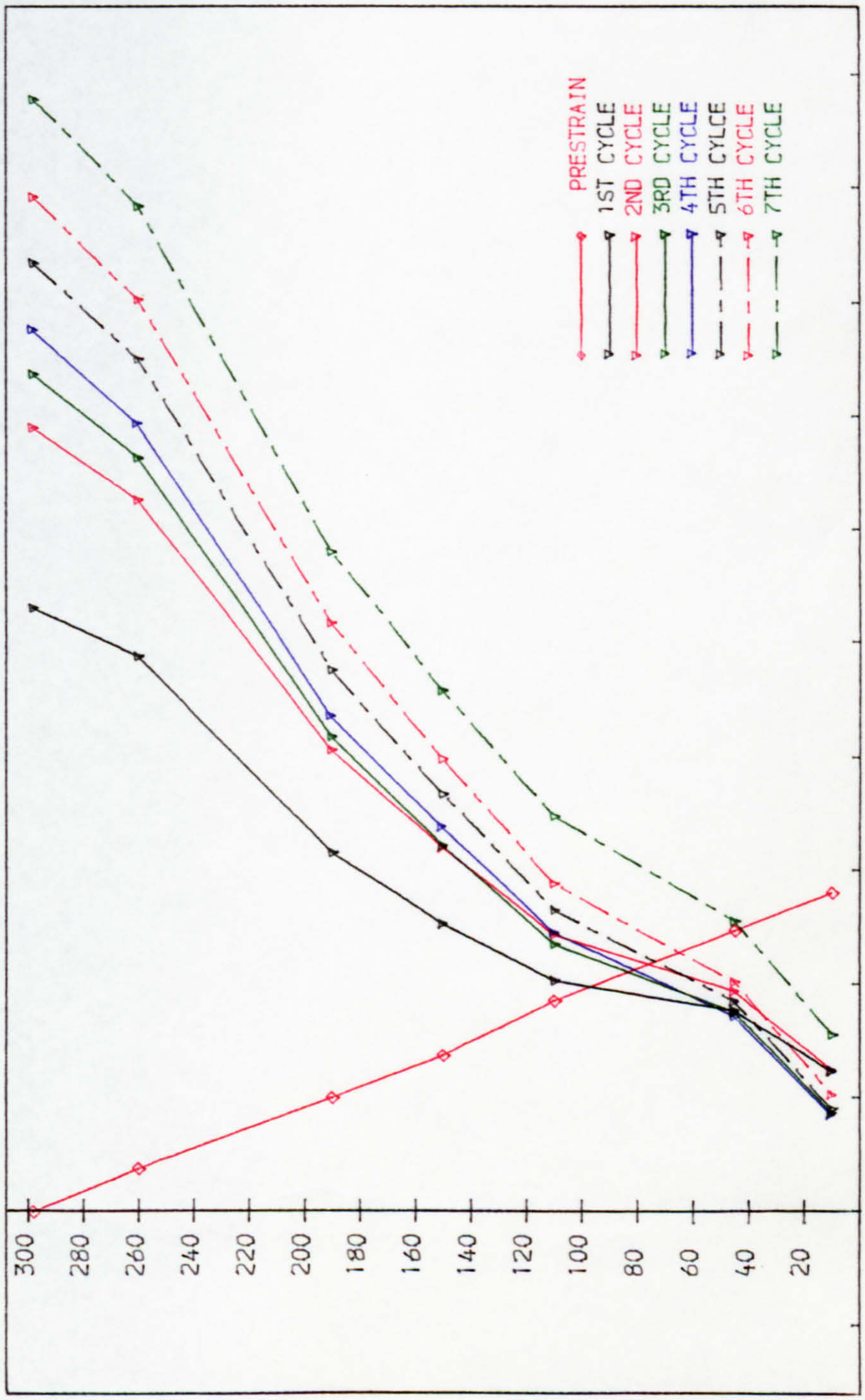

FIG. 7.29b TOTAL STRAIN DISTRIBUTION AT MIDSPAN AT HALF-SERVICE LOAD. S1.3.5

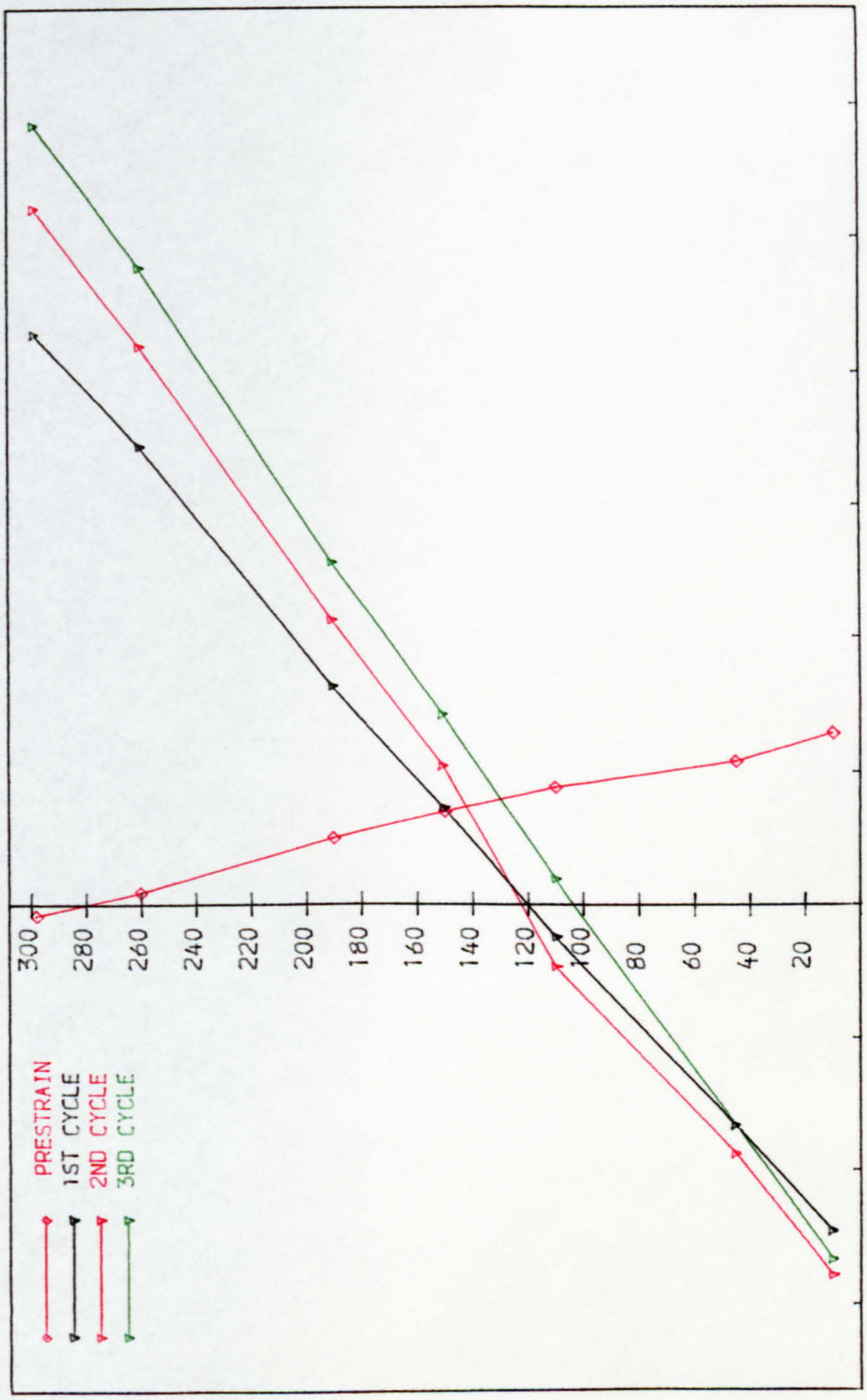

FIG. 7.30 TOTAL STRAIN DISTRIBUTION AT MIDSPAN AT SERVICE LOAD. S2.3.4

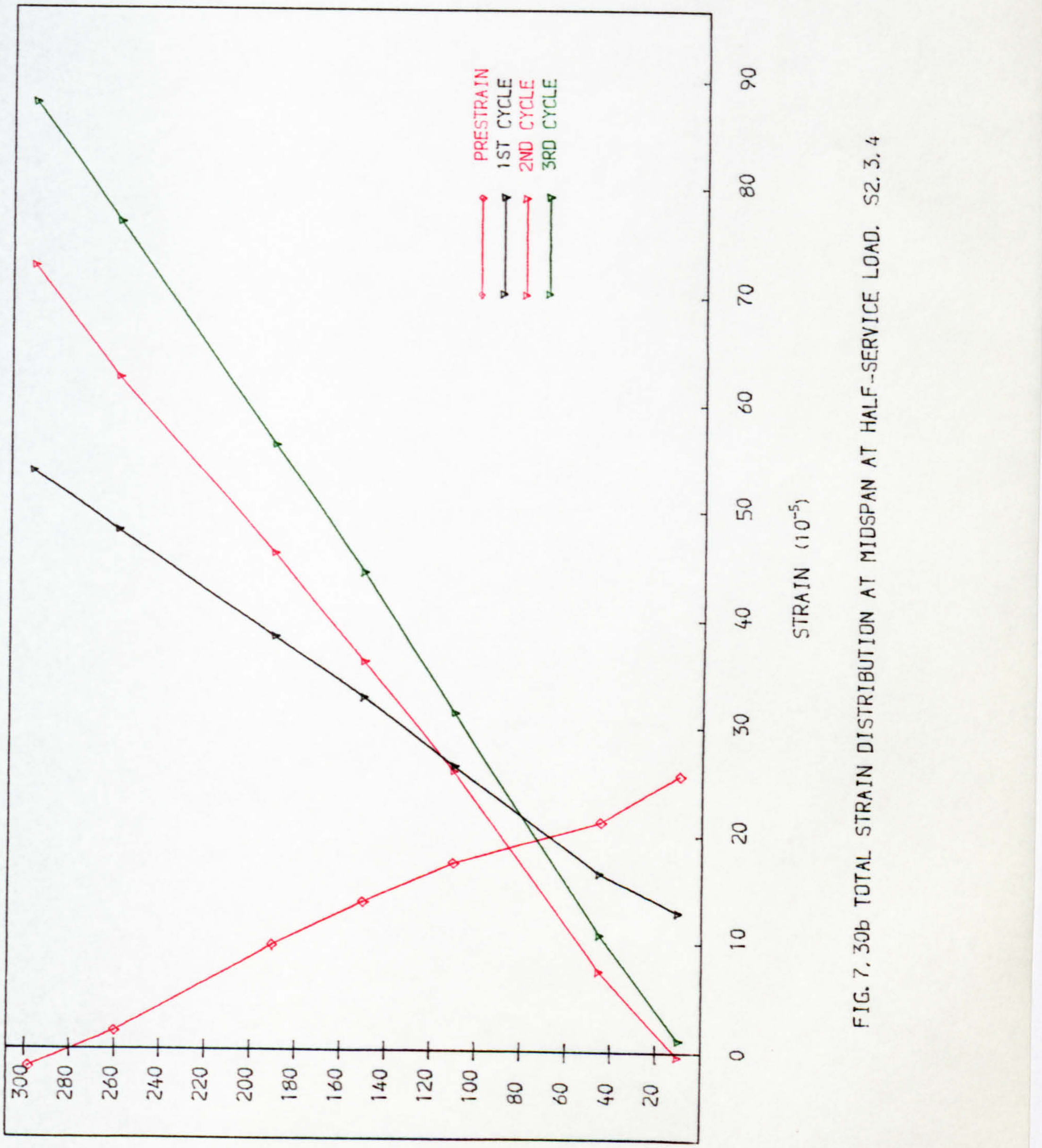

FIG. 7.30b TOTAL STRAIN DISTRIBUTION AT MIDSPAN AT HALF-SERVICE LOAD. S2.3.4

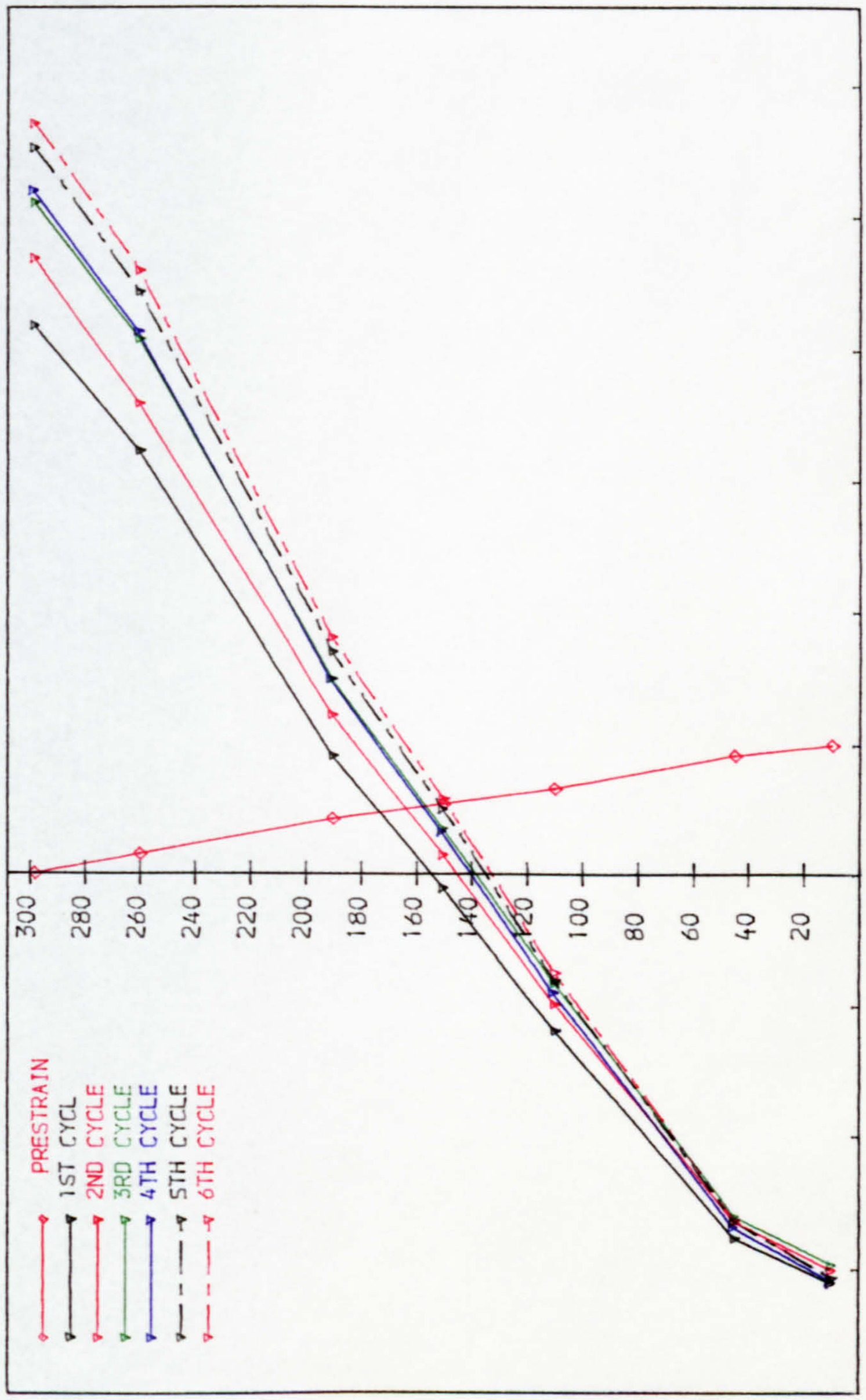

FIG. 7.31 TOTAL STRAIN DISTRIBUTION AT MIDSPAN AT SERVICE LOAD, S2.2.6

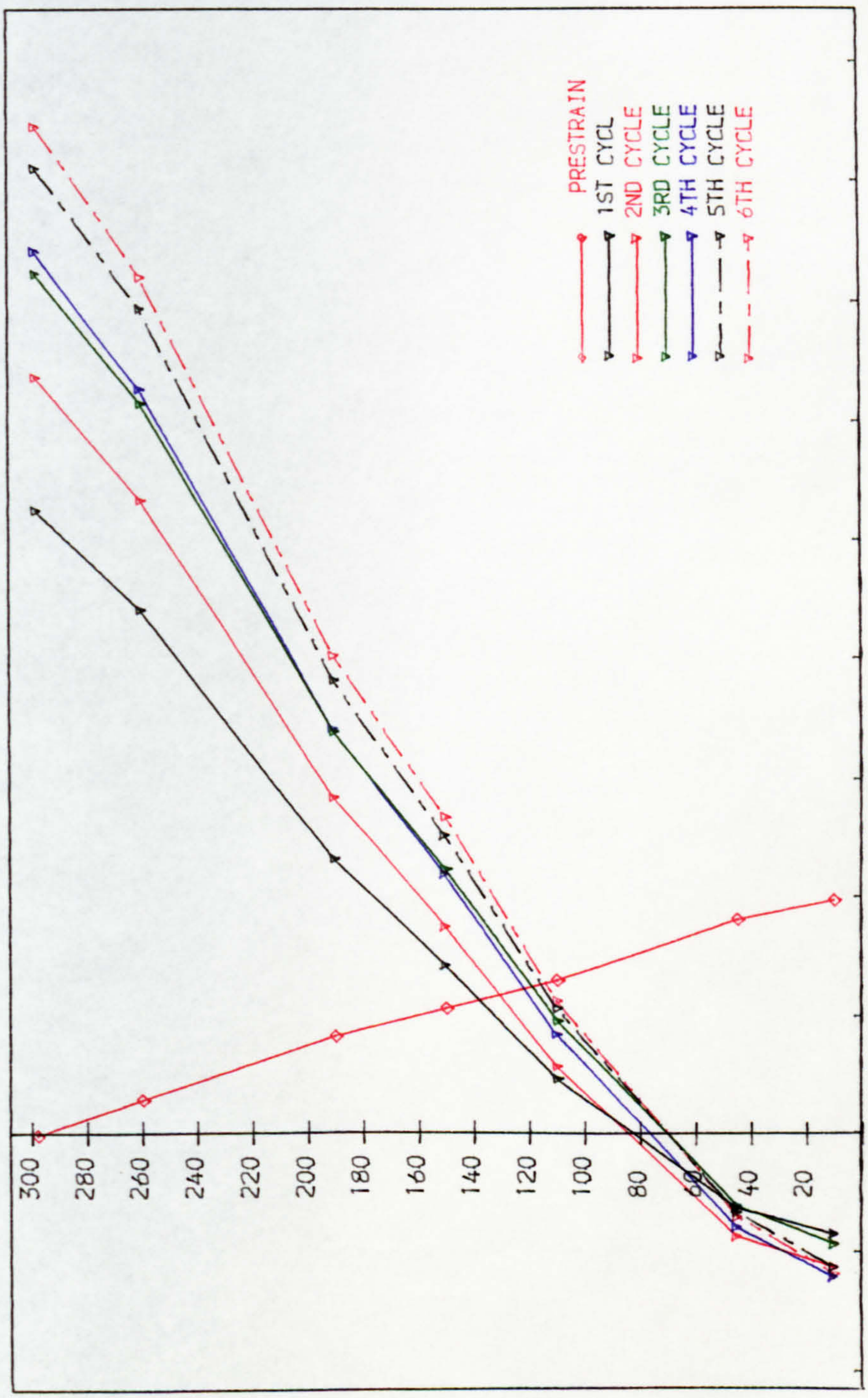

FIG. 7.31b TOTAL STRAIN DISTRIBUTION AT MIDSPAN AT HALF-SERVICE LOAD. S2.2.6

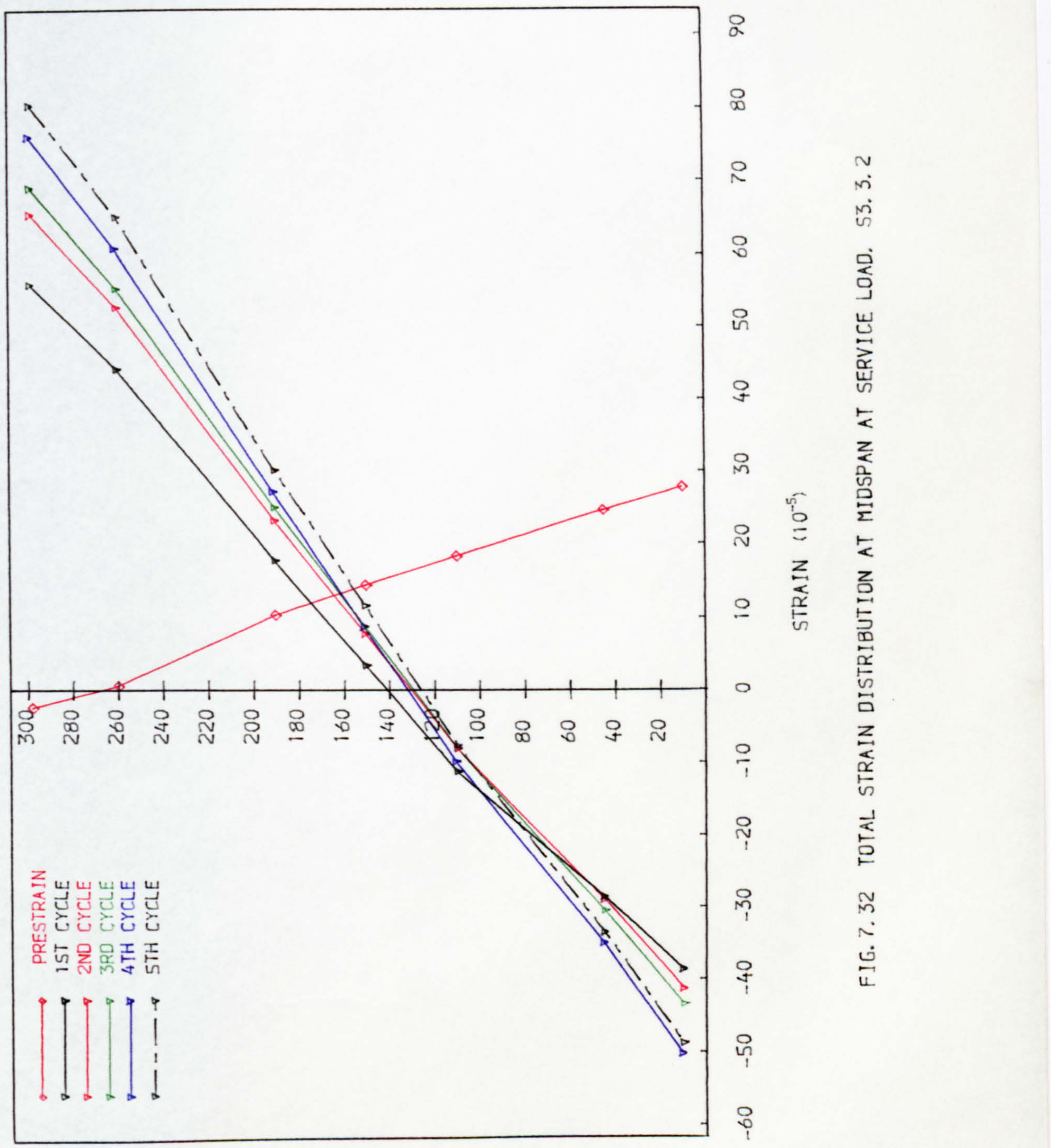

FIG. 7.32 TOTAL STRAIN DISTRIBUTION AT MIDSPAN AT SERVICE LOAD. S3.3.2

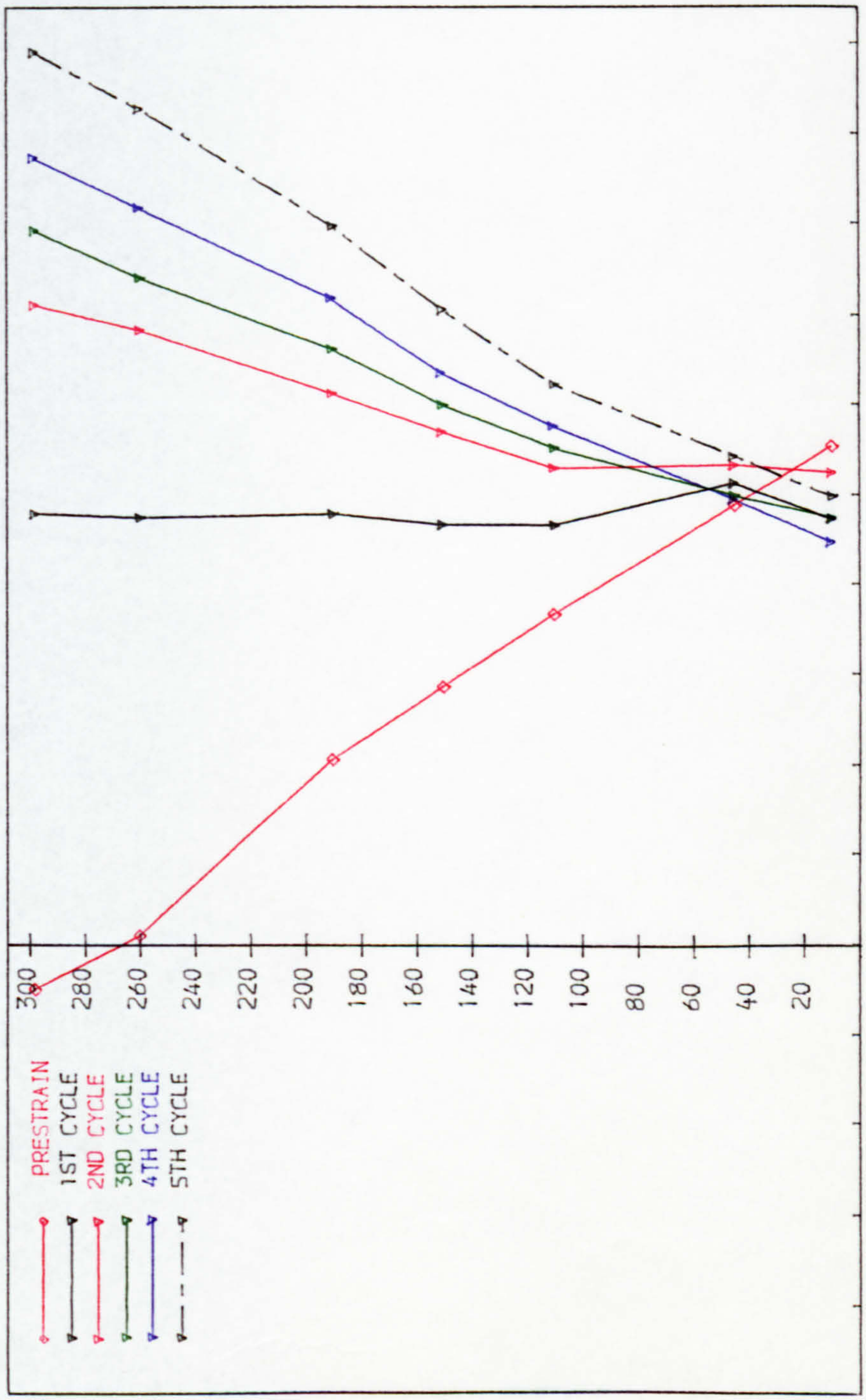

FIG. 7.32b TOTAL STRAIN DISTRIBUTION AT MIDSPAN AT HALF-SERVICE LOAD. S3.3.2

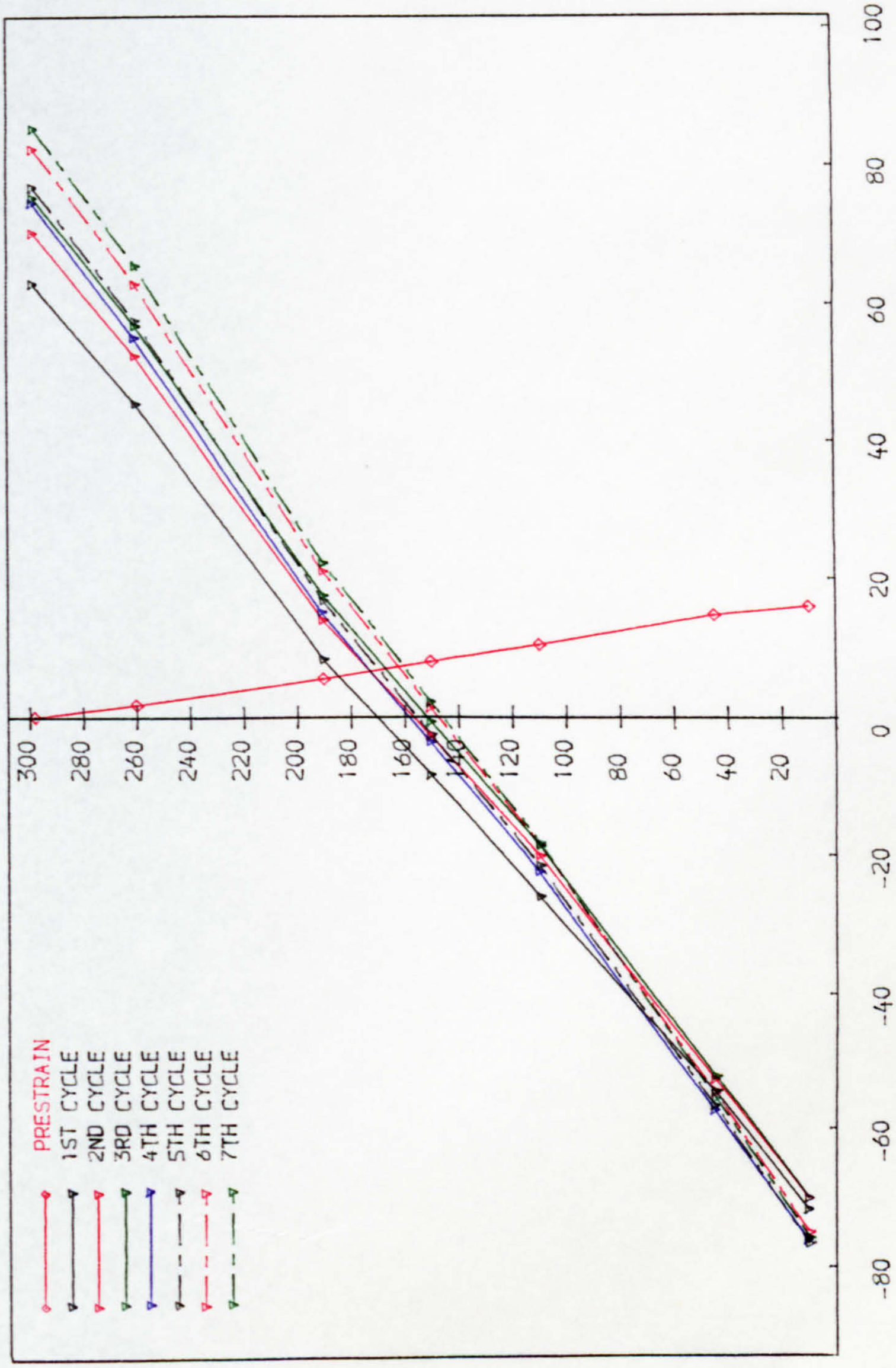

FIG. 7.33 TOTAL STRAIN DISTRIBUTION AT MIDSPAN AT SERVICE LOAD. S3.2.4

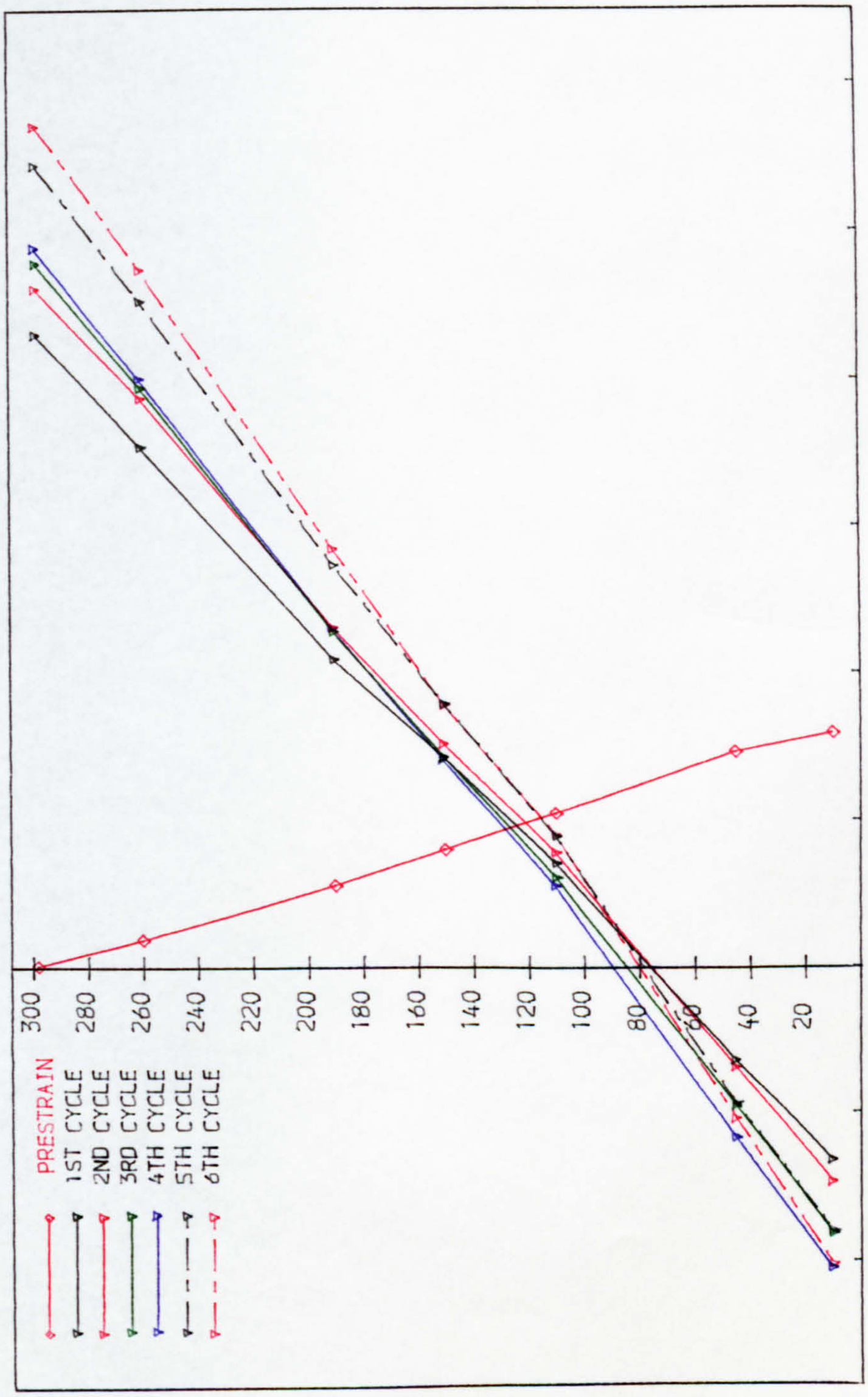

FIG. 7.33b TOTAL STRAIN DISTRIBUTION AT MIDSPAN AT HALF-SERVICE LOAD. S3.2.4

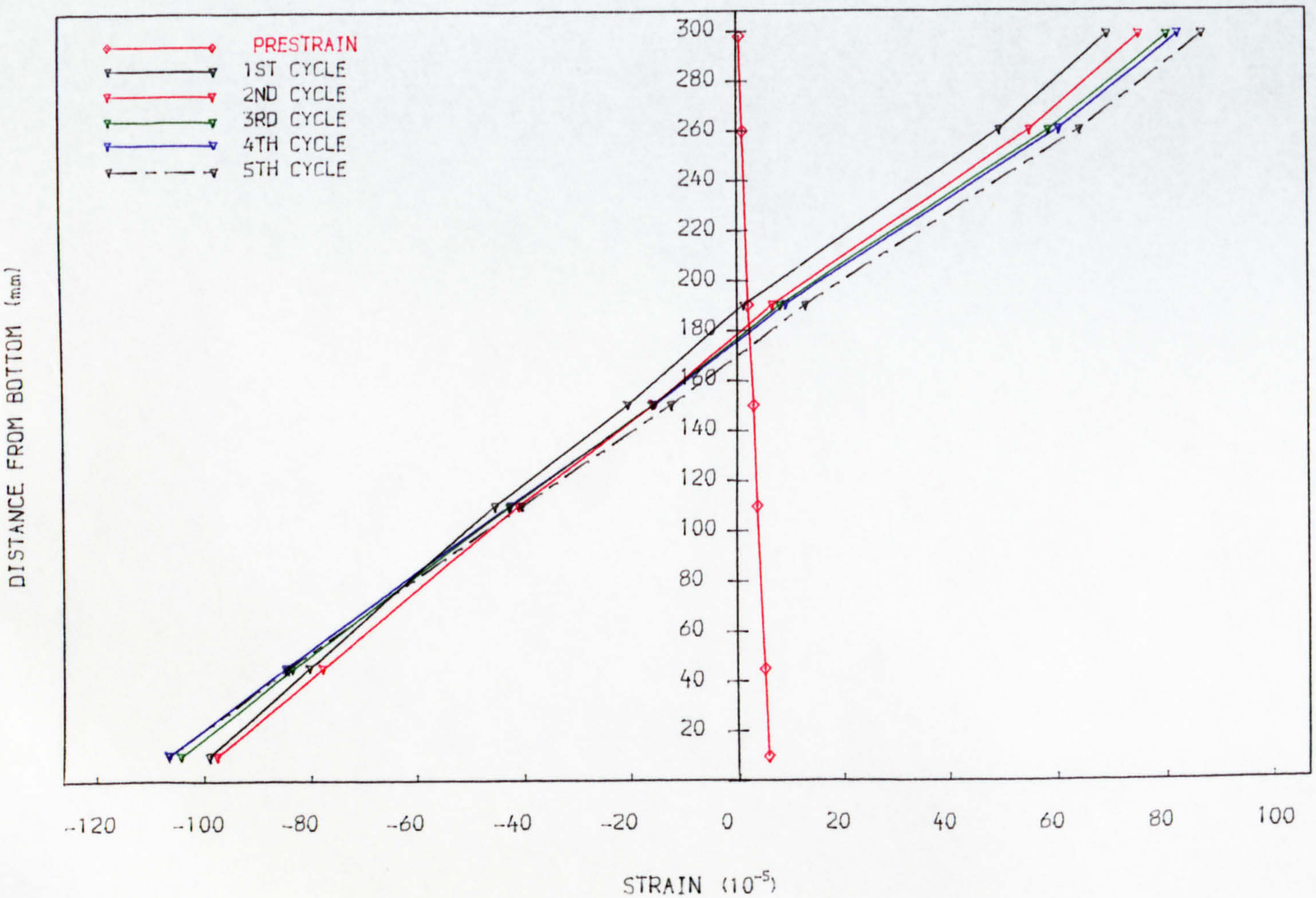

FIG. 7.34 TOTAL STRAIN DISTRIBUTION AT MIDSPAN AT SERVICE LOAD. S3.1.6

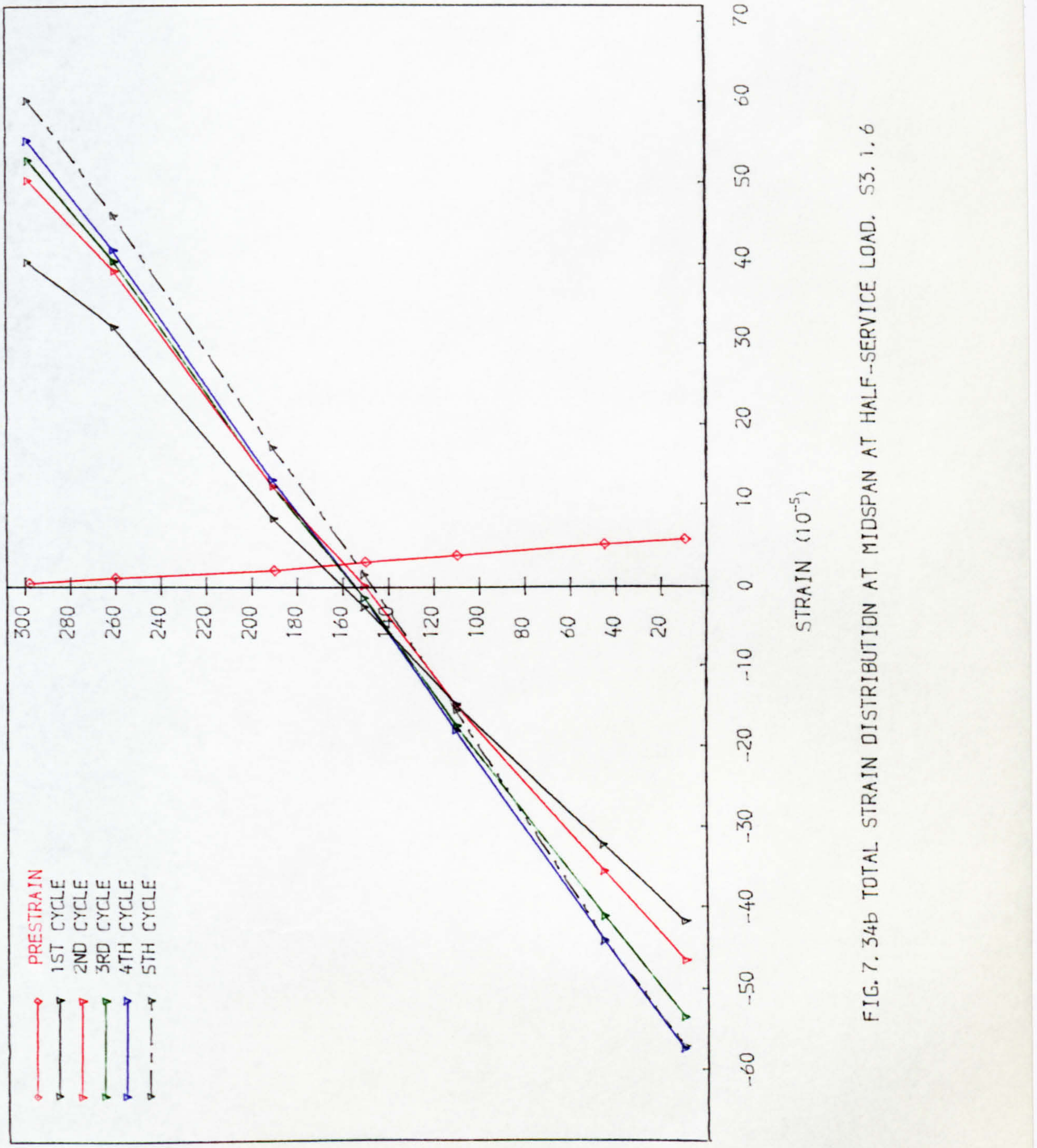

FIG. 7. 34b TOTAL STRAIN DISTRIBUTION AT MIDSPAN AT HALF--SERVICE LOAD. S3.1.6

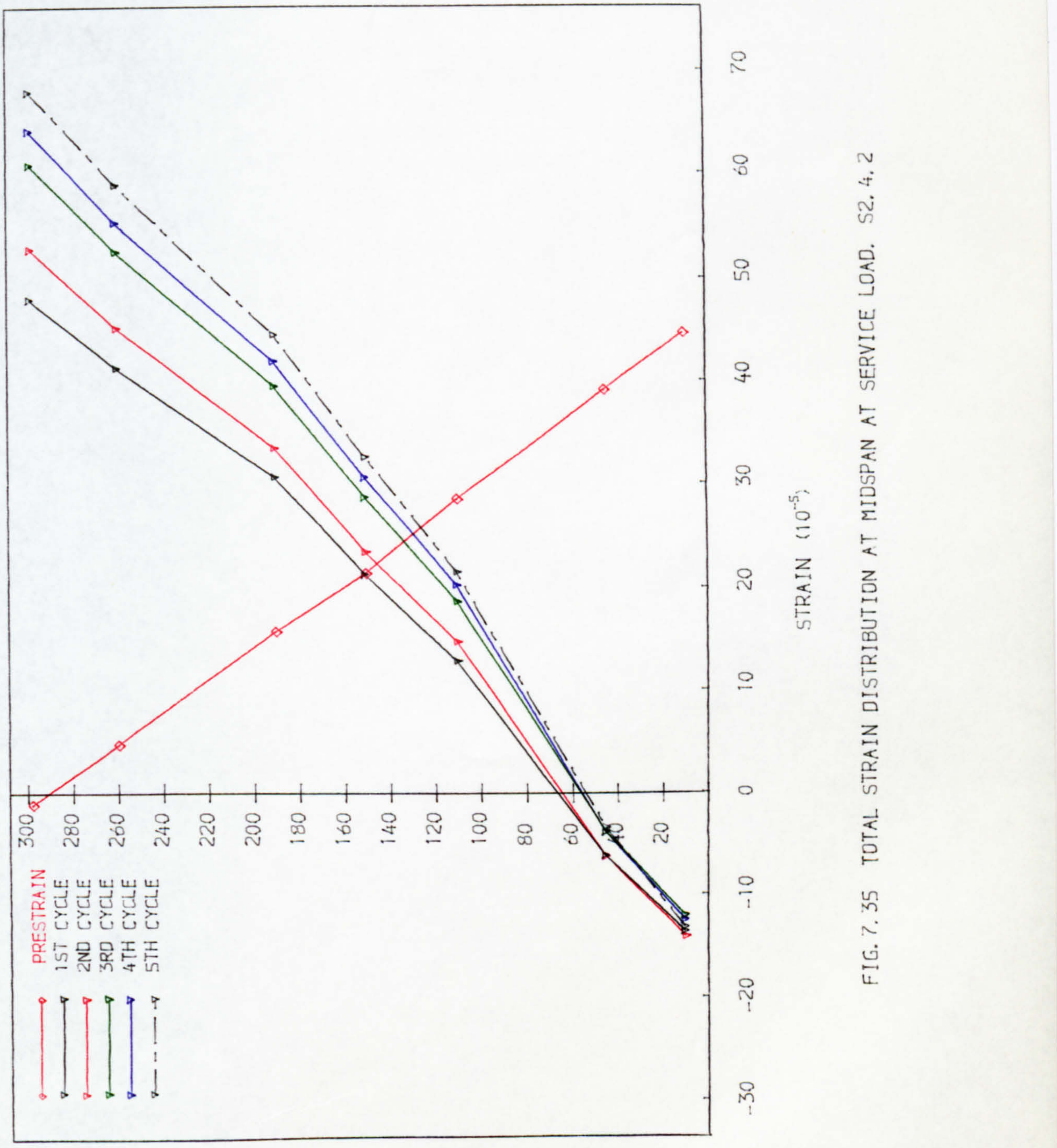

FIG. 7.35 TOTAL STRAIN DISTRIBUTION AT MIDSPAN AT SERVICE LOAD. S2.4.2

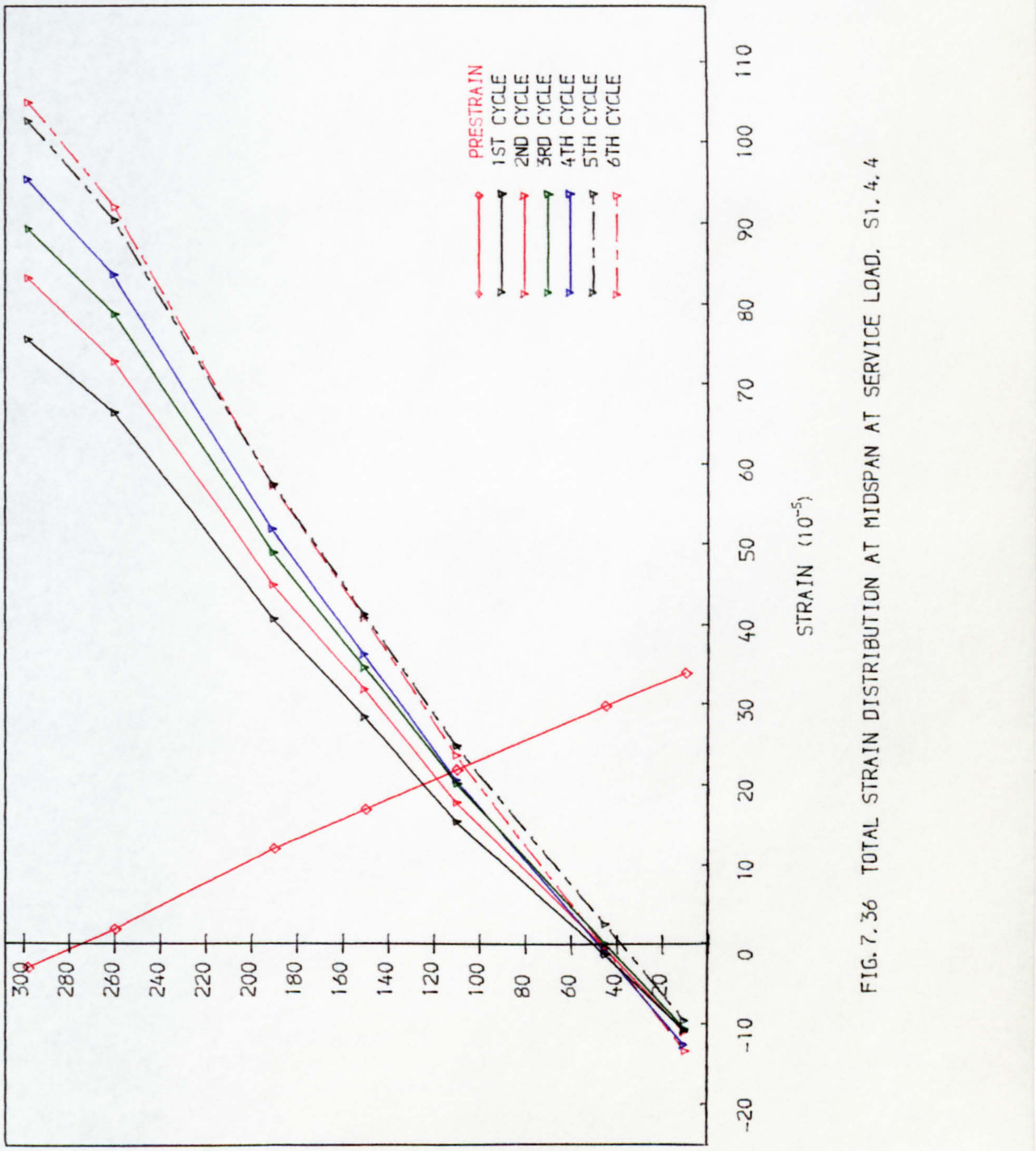

FIG. 7.36 TOTAL STRAIN DISTRIBUTION AT MIDSPAN AT SERVICE LOAD. S1.4.4

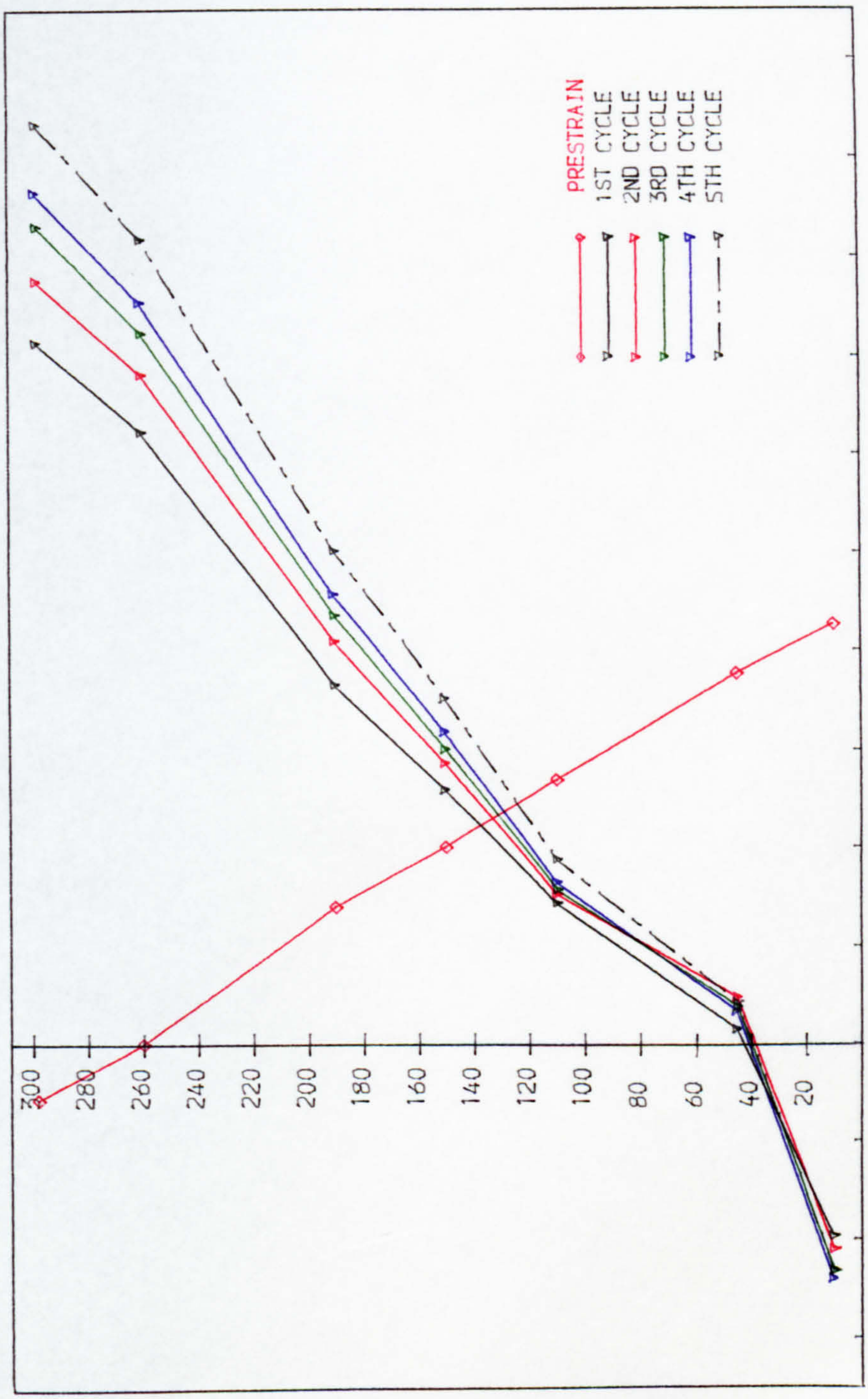

FIG. 7.37 TOTAL STRAIN DISTRIBUTION AT MIDSPAN AT SERVICE LOAD. S1.5.2

was only a small change in the reinforcement stresses under the permanent load.

Since the strains were measured near the top and bottom surfaces and over the whole span of the beam, the average curvature at each gauge position could be calculated from the expression:-

$$\frac{1}{r} = \frac{\varepsilon_{top} + \varepsilon_{bottom}}{h}$$

where r = radius of curvature

h = depth of beam

This enabled the deflection y at any point at a distance x along the beam, and hence the deflected profile, to be calculated by numerical integration of the curvature equation:-

$$\frac{1}{r} = \frac{d^2y}{dx^2}$$

Figs.7.38 and 7.39 show the short-term deflected profile calculated from the measured strains by this method accords with the readings of the deflection dial gauges in the tests. It may be seen from the diagrams that the agreement between the deflected profiles calculated by integration of curvature based on the measured strains and the deflection measured on the dial gauges, is excellent. This result, therefore, indicates that the deflection calculated by integration of curvature can be very accurate provided the calculated curvature at each section is accurate.

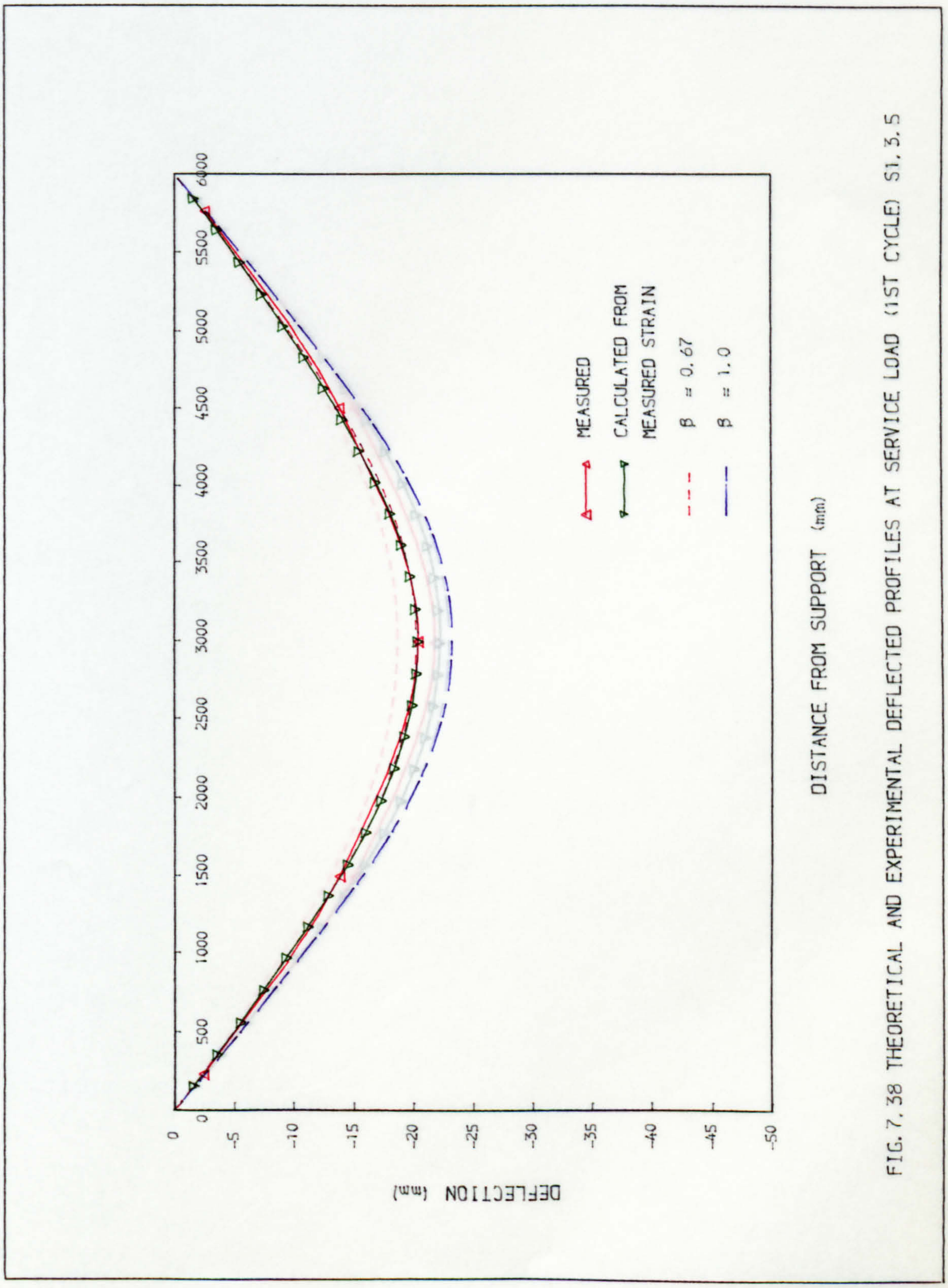

FIG. 7.38 THEORETICAL AND EXPERIMENTAL DEFLECTED PROFILES AT SERVICE LOAD (1ST CYCLE) S1.3.5

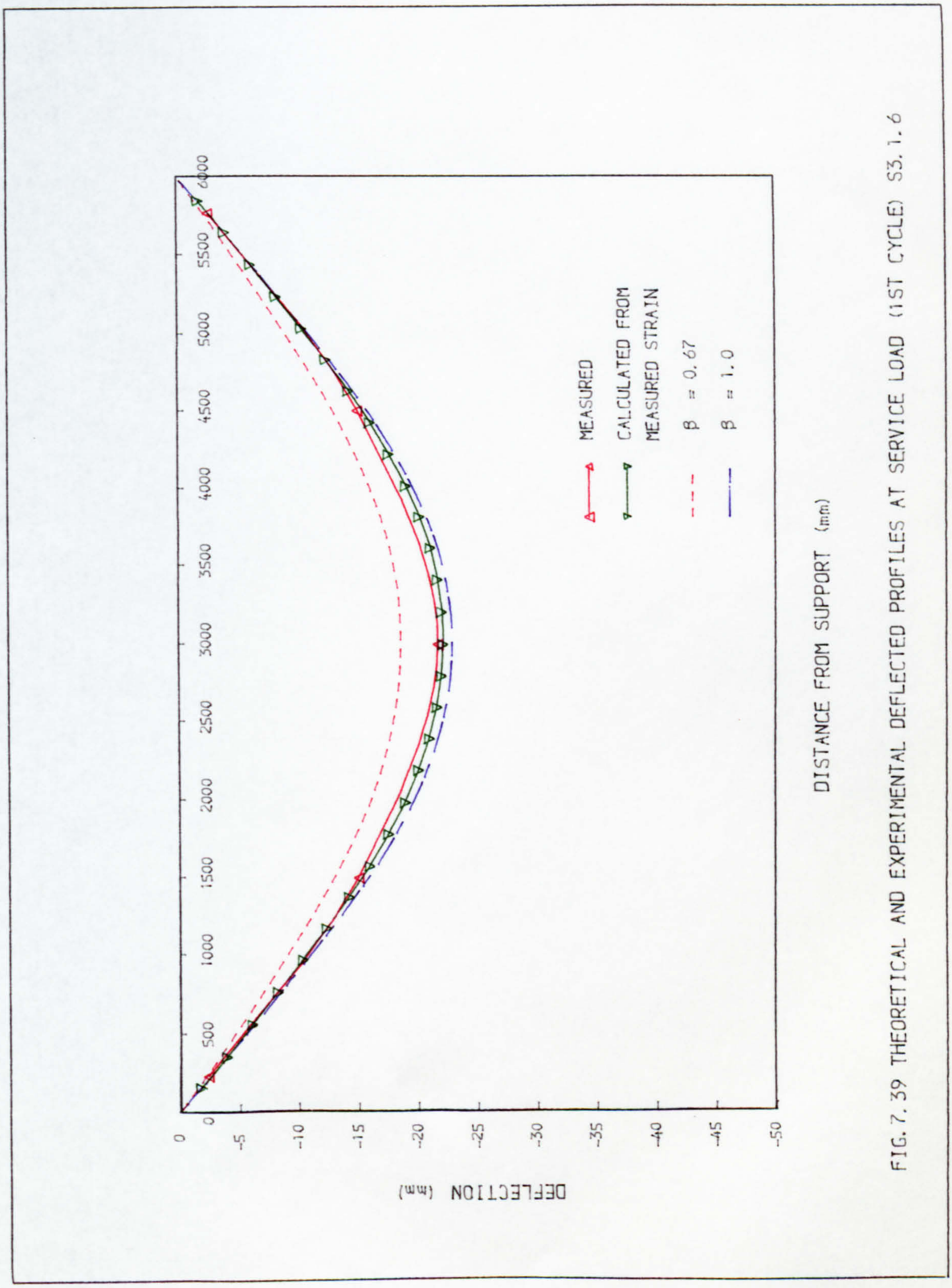
FIG. 7.39 THEORETICAL AND EXPERIMENTAL DEFLECTED PROFILES AT SERVICE LOAD (1ST CYCLE) S3.1.6
DISTANCE FROM SUPPORT (mm)
DEFLECTION (mm)
MEASURED
CALCULATED FROM MEASURED STRAIN
β = 0.67
β = 1.0
0
500
1000
1500
2000
2500
3000
3500
4000
4500
5000
5500
6000
0
-5
-10
-15
-20
-25
-30
-35
-40
-45
-50

7.3.4 Behaviour at Ultimate Limit State

Figs.7.40 to 7.43 show some of the midspan strain distributions of the beams at increasing increments of load up to near failure. It can be interpreted from these diagrams that at loads corresponding to the last recorded strain measurements, the stress in the non-prestressed reinforcement was generally above the 0.2% proof stress. The ultimate moment of resistance was calculated based on the British Code CP110 recommendation using the experimental mean strengths of concrete and steel. Table 7.4 gives the details of the calculated and observed values of the ultimate load. The ultimate strength was calculated without the materials safety factors of 1.15 and 1.5 for steel and concrete respectively. The two proof stresses used in the calculation were 0.2% and 0.5%.

It is clear from Table 7.4 that the calculated ultimate strength based on the 0.5% proof stress consistently gives the better correlation to the actual strength.

7.4 Comparisons of Experimental and Theoretical Deflections

7.4.1 Integration of Curvature Based on CP110

7.4.1.1 Short-term Deflection

An analytical method of calculating deflection is outlined in Appendix A of CP110, whereby the strain at each section is obtained from the calculated stress distribution and the deflection is then obtained by integration of

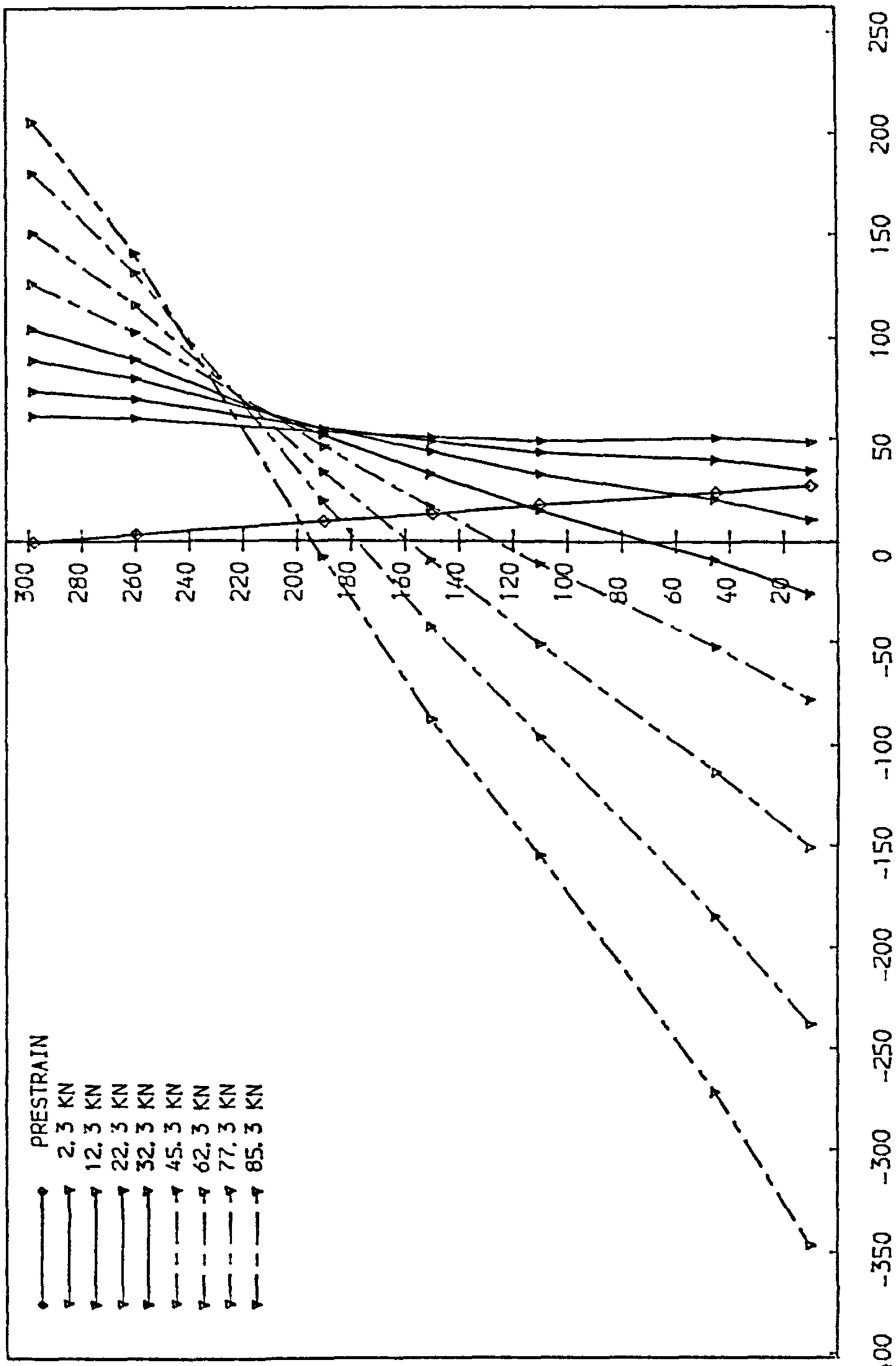

FIG. 7.40 TOTAL STRAIN DISTRIBUTION AT MIDSPAN S1.3.5 (LAST CYCLE)

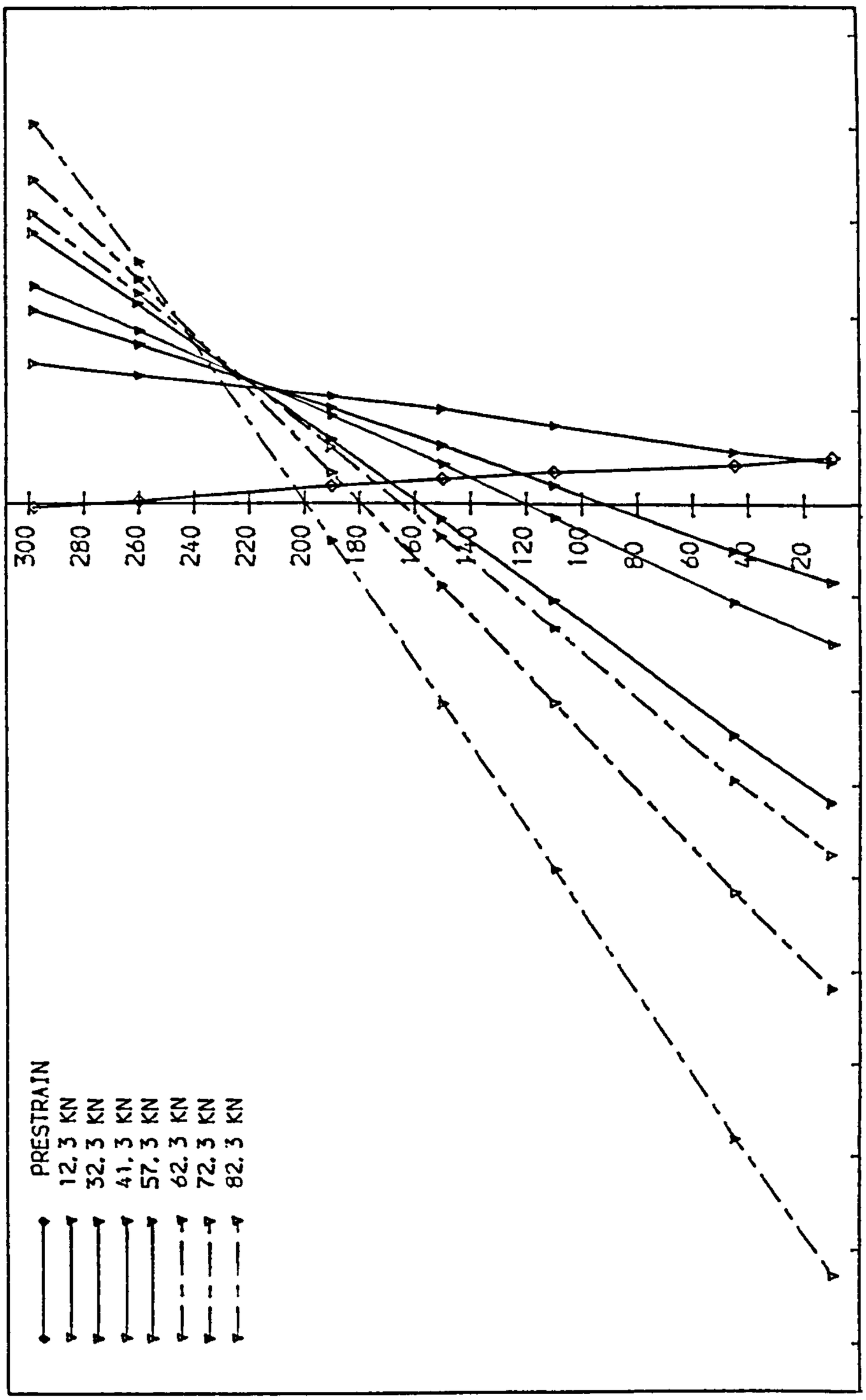

FIG. 7.41 TOTAL STRAIN DISTRIBUTION AT MIDSPAN S2.3.4 (LAST CYCLE)

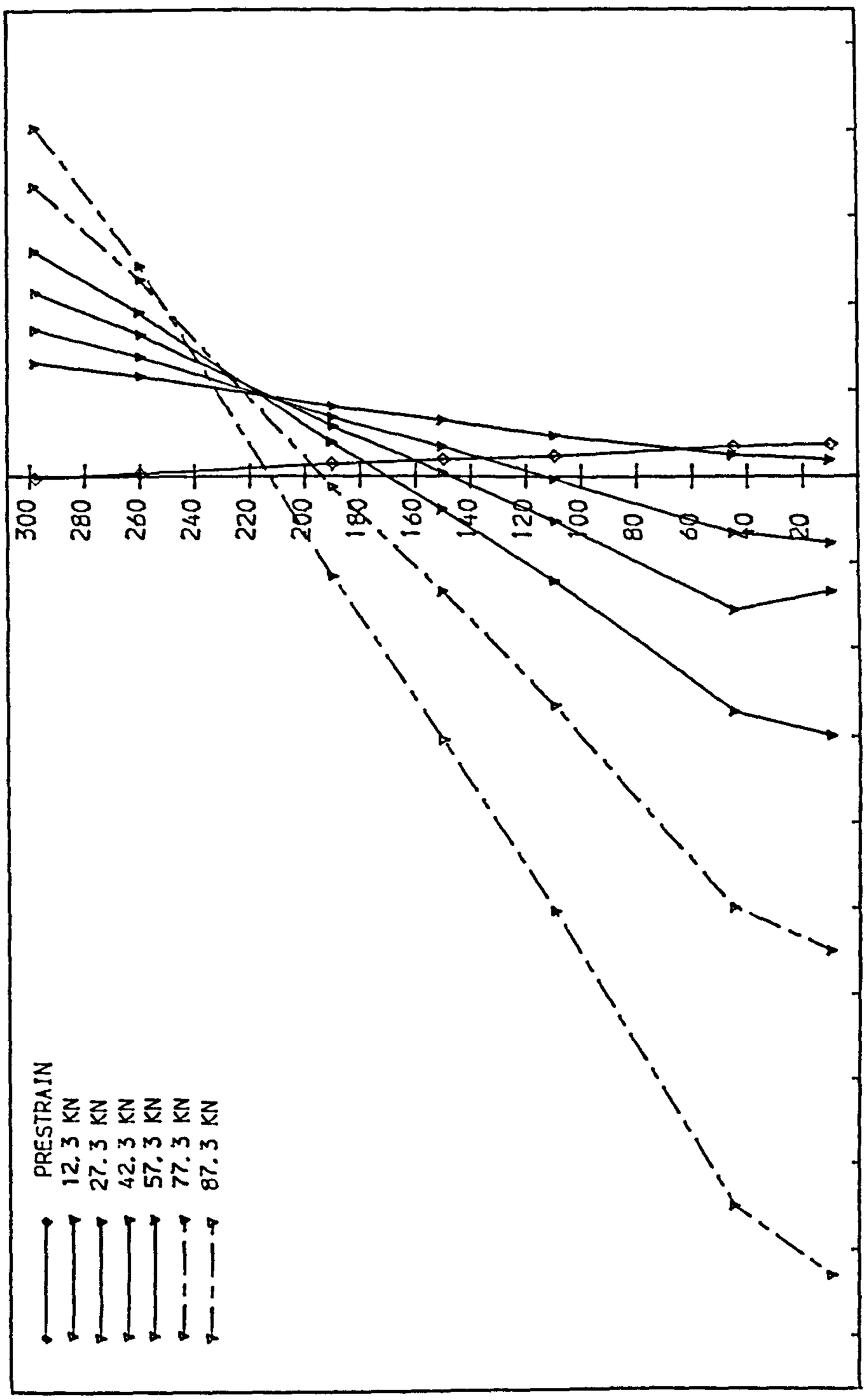

FIG. 7.42 TOTAL STRAIN DISTRIBUTION AT MIDSPAN S2.2.6 (LAST CYCLE)

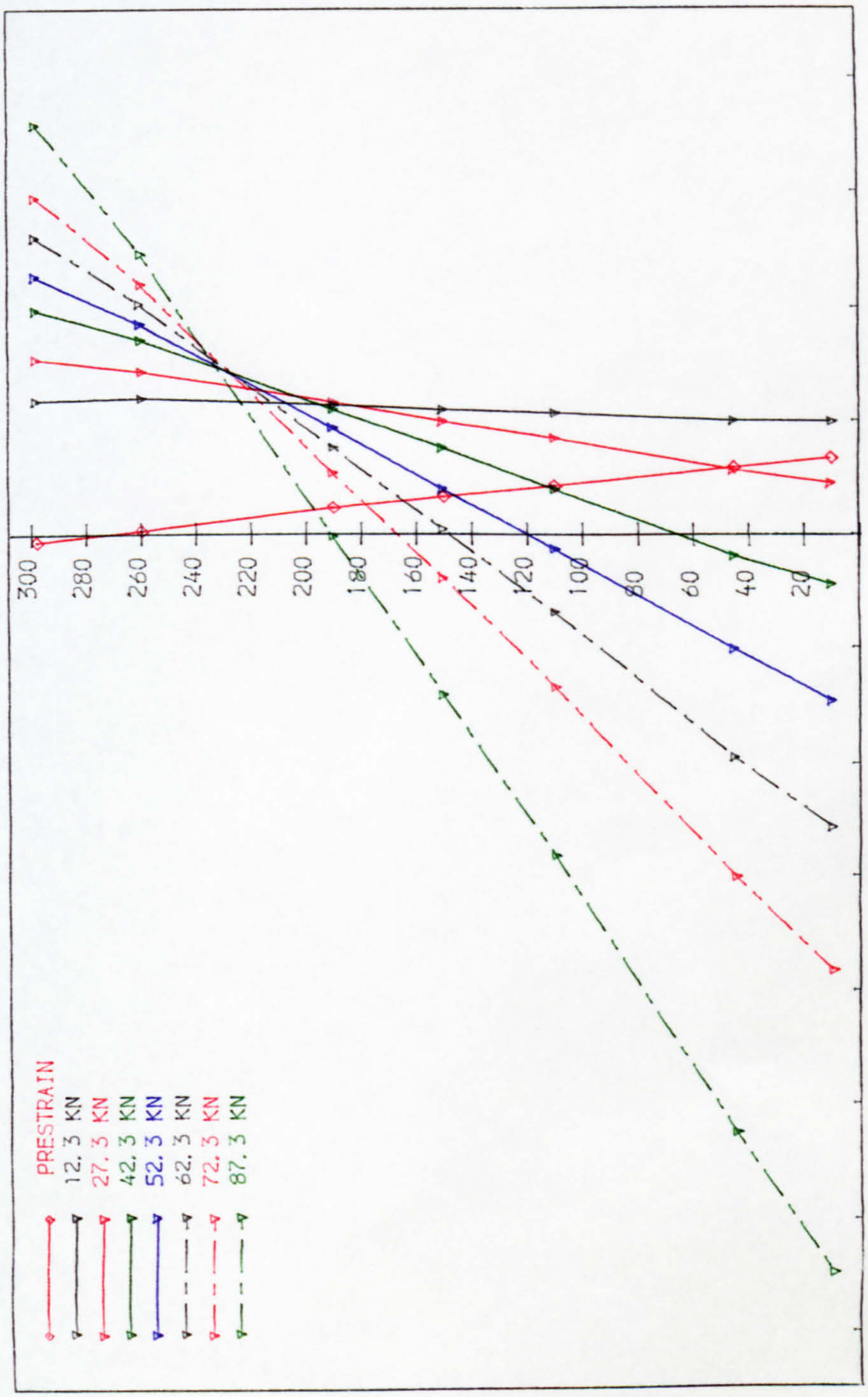

FIG. 7.43 TOTAL STRAIN DISTRIBUTION AT MIDSPAN S1.4.4 (LAST CYCLE)

Beam Reference	Actual ult. load (kN) (1)	Calculated ult. load (kN) (2)	Calculated ult. load (kN) (3)	(2)/(1)	(3)/(1)
S1.5.2	96.0	94.0	94.4	0.98	0.98
S1.4.4	103.5	95.8	96.6	0.93	0.93
S1.3.5	99.2	93.0	94.1	0.94	0.95
S1.3.5S	96.0	93.2	94.3	0.97	0.98
S2.4.2	84.5	79.4	79.8	0.94	0.94
S2.3.4	92.2	82.6	83.5	0.90	0.91
S2.3.4S	87.6	82.6	83.5	0.94	0.95
S2.2.6	73.5	85.4	86.7	1.16	1.18
S3.3.2	80.0	65.4	65.9	0.82	0.82
S3.3.2S	72.5	65.4	65.8	0.90	0.91
S3.2.4	80.0	69.4	70.3	0.87	0.88
S3.1.6	86.5	70.3	71.7	0.81	0.83

Note: Column (2) and (3) are ultimate loads calculated according to CP 110 but without the material safety factors and based on 0.2% and 0.5% proof stresses for non-prestressed steel respectively.

Table 7.4: Experimental and calculated ultimate loads

curvature. In applying this method to partially prestressed beams, the stress distribution was first calculated for the cracked region of the beam as described in Chapter Four. This enabled the curvature to be calculated for the section at a crack. However, to obtain the deflection, the average curvature is required which will be less than that at a crack on account of the "tension stiffening" effect of the concrete between cracks. The recommendation of CP110 is that the tensile stress in concrete at the centroid of the tensile steel be assumed to have a value of 1.0N/sq.mm under short-term loading.

A distribution coefficient β , as defined in Eqn.(5.3) has been introduced in Chapter Five to obtain the average curvature in the cracked region. Bennett (7,8) originally proposed a linear distribution which is equivalent to β = 0.5 while β = 1.0 represents complete loss of tension stiffening.

Figs.7.44 to 7.50 compare the deflections computed with varying values of β , with the experimental results. In order to obtain a true comparison, correct values of the modulus of elasticity and tensile strength of concrete are essential in the theoretical computation. It was, therefore, decided to obtain the modulus of elasticity and tensile strength based on the deflection before the point of cracking and the observed cracking load.

Referring to Fig.7.46 (S1.3.5), for increasing loads in

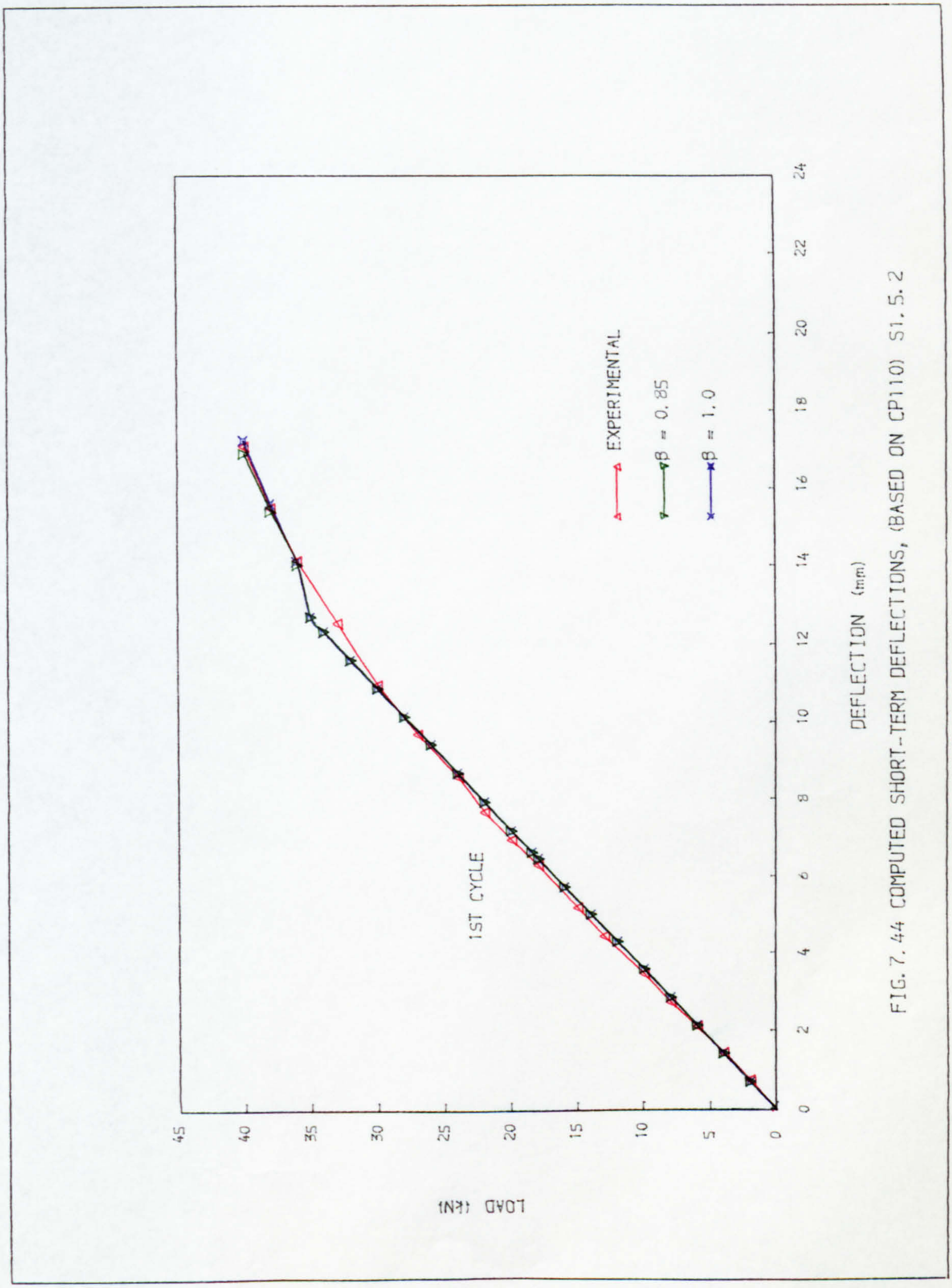

FIG. 7.44 COMPUTED SHORT-TERM DEFLECTIONS, (BASED ON CP110) S1.5.2

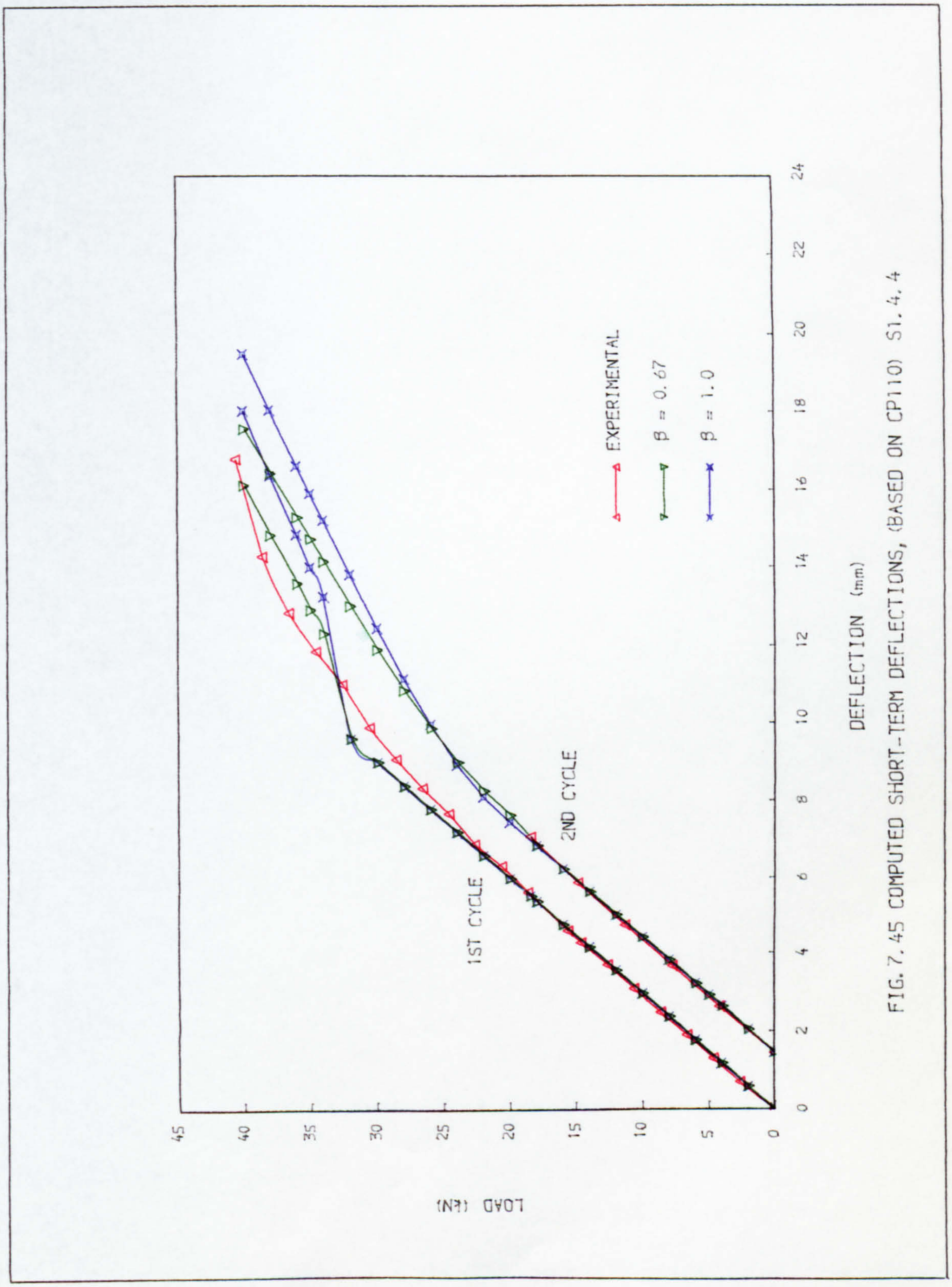

FIG. 7.45 COMPUTED SHORT-TERM DEFLECTIONS, (BASED ON CP110) S1.4.4

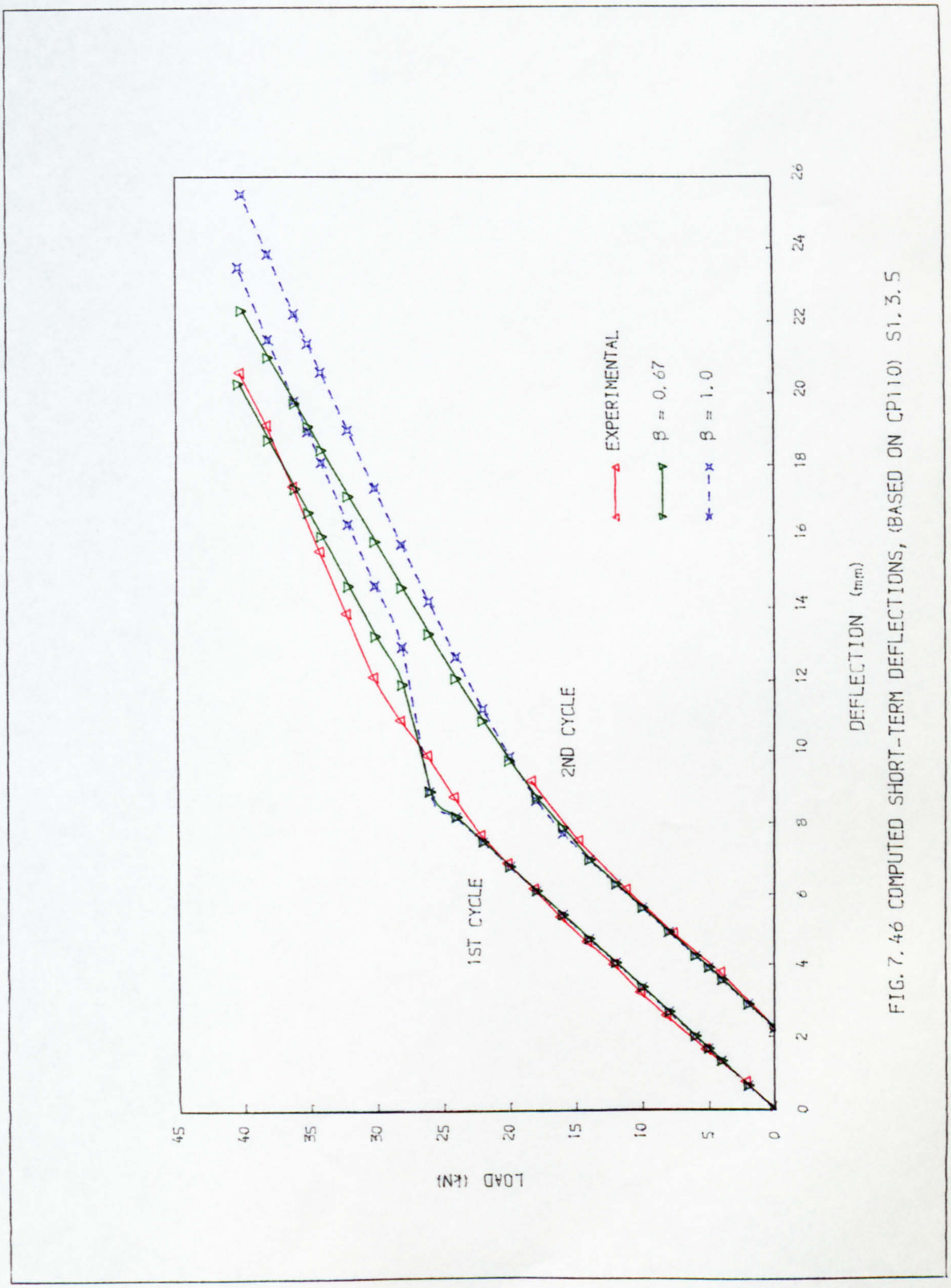

FIG. 7.46 COMPUTED SHORT-TERM DEFLECTIONS, (BASED ON CP110) S1, 3.5

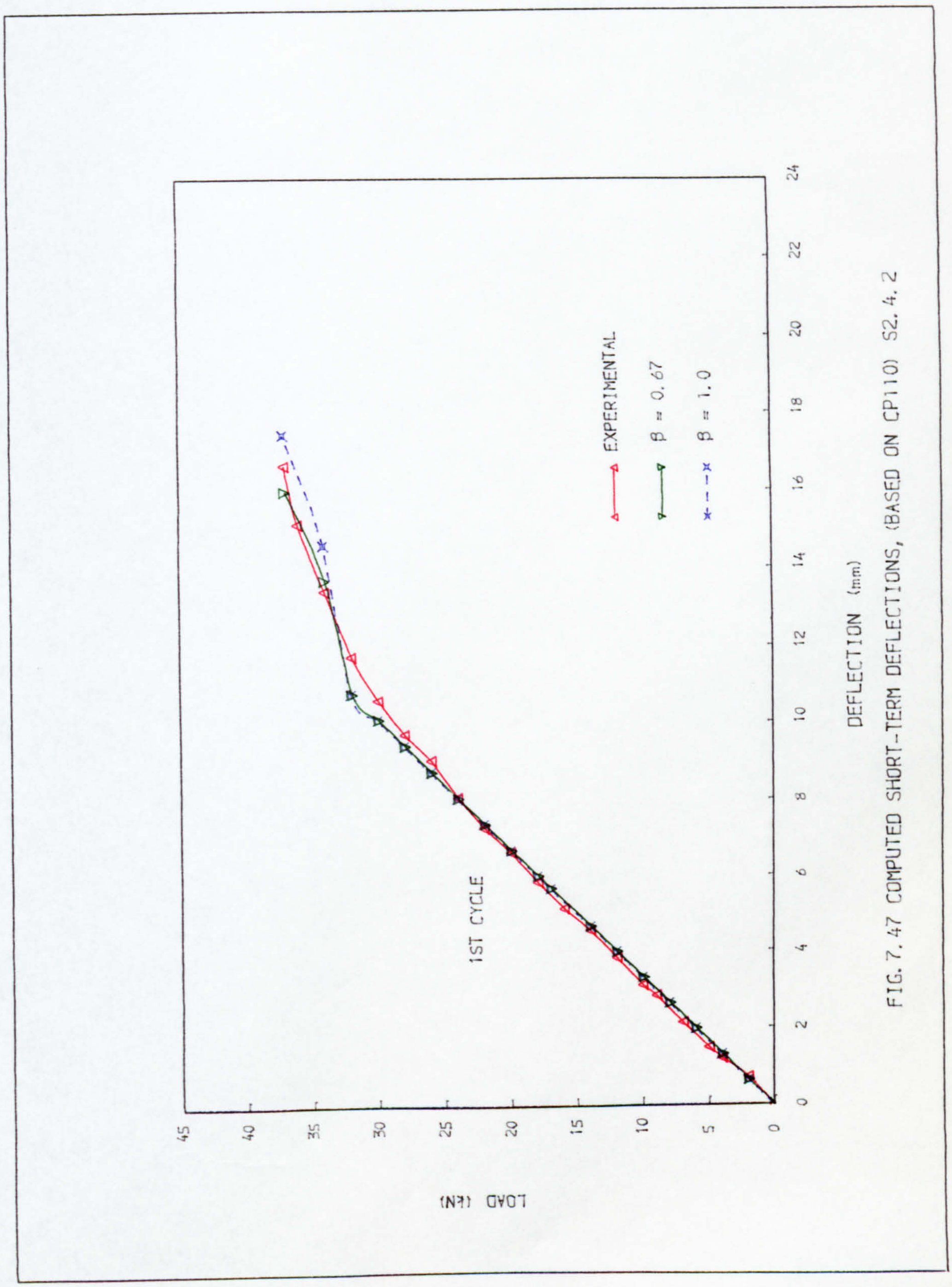

FIG. 7.47 COMPUTED SHORT-TERM DEFLECTIONS, (BASED ON CP110) S2.4.2

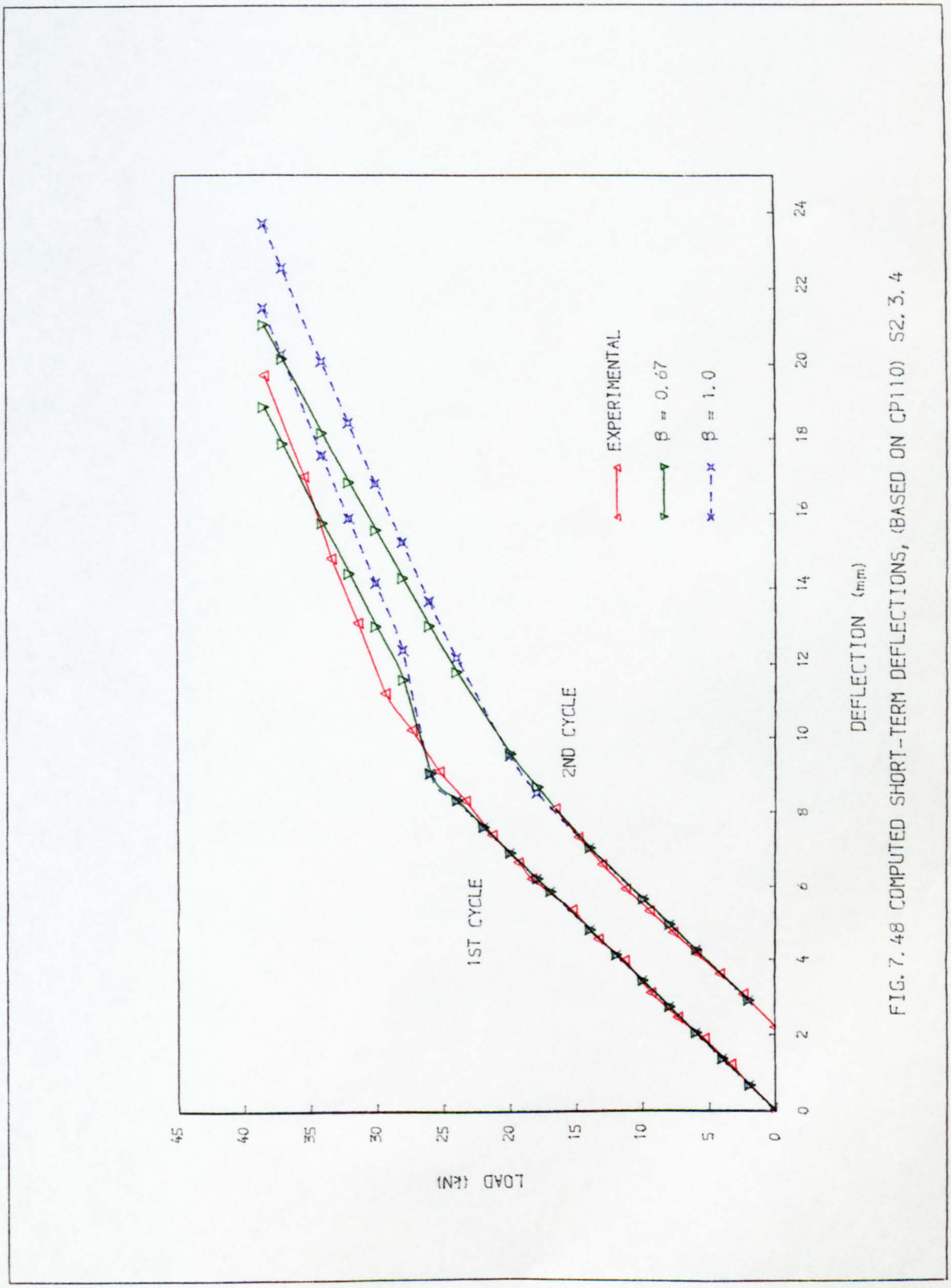

FIG. 7.48 COMPUTED SHORT-TERM DEFLECTIONS, (BASED ON CP110) S2, 3, 4

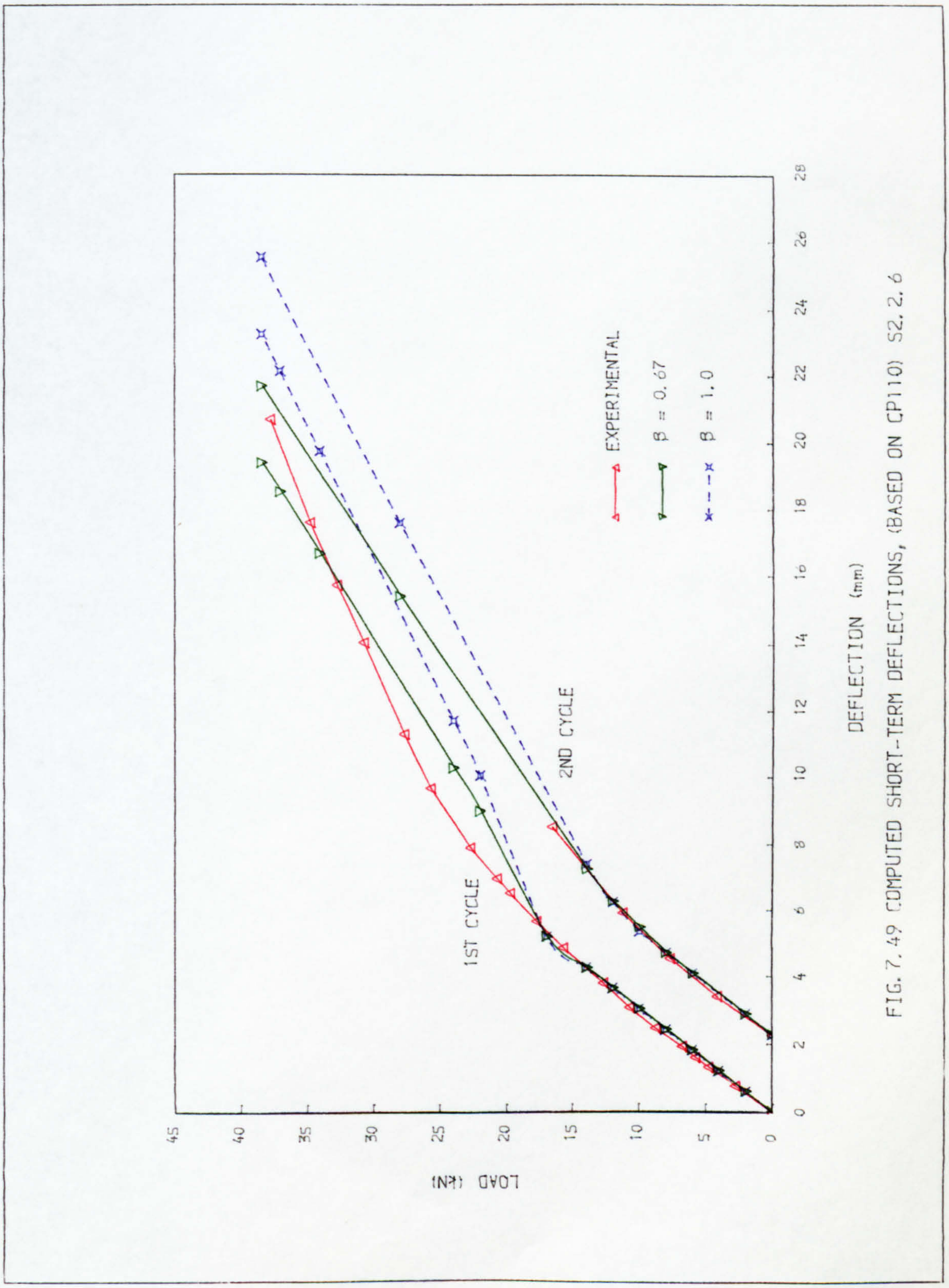

FIG. 7.49 COMPUTED SHORT-TERM DEFLECTIONS, (BASED ON CP110) S2.2.6

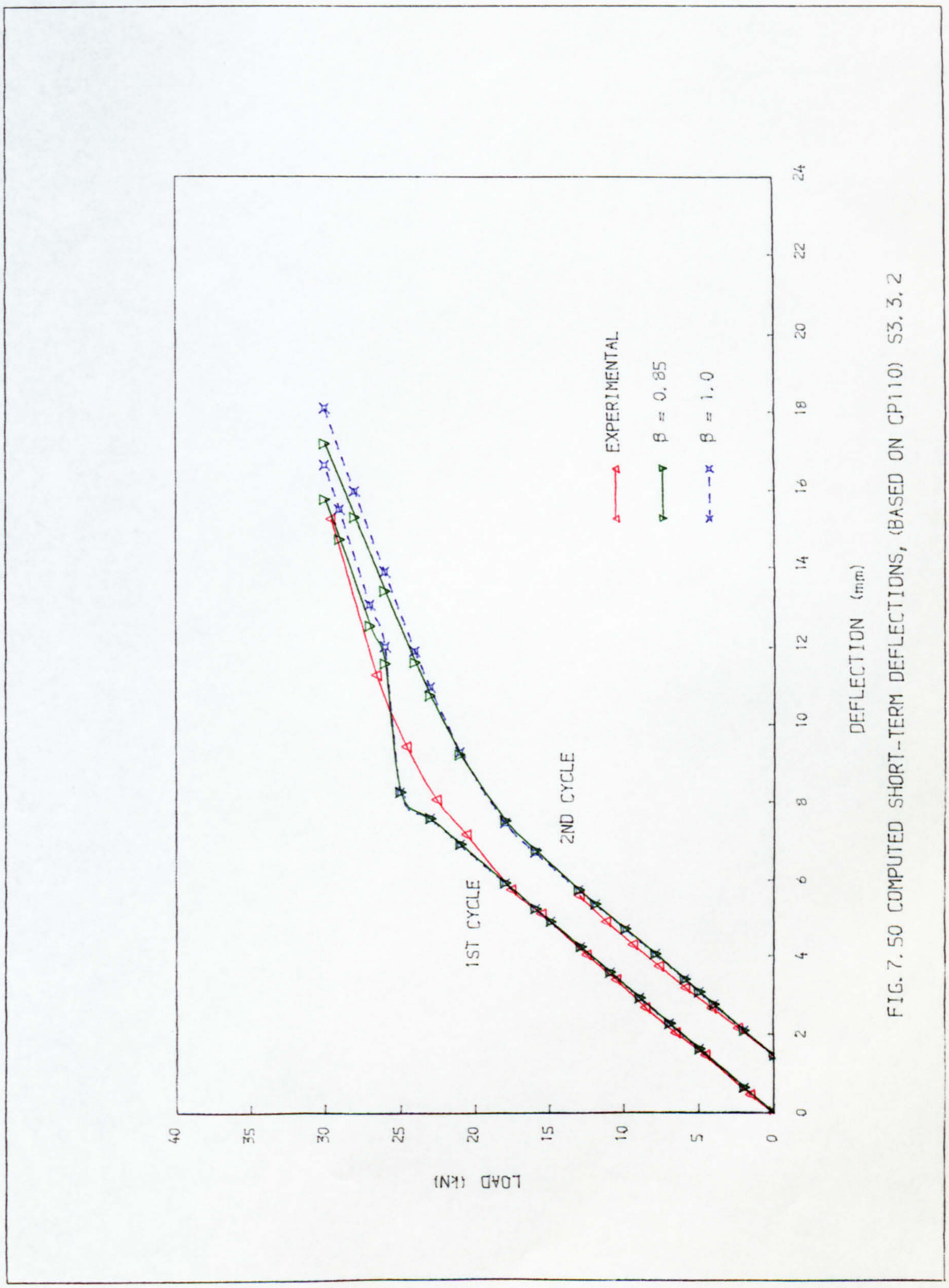

FIG. 7.50 COMPUTED SHORT-TERM DEFLECTIONS, (BASED ON CP110) S3.3.2

the first cycle where correct value of β is used, the excellent agreement obtained for all points on the beam at maximum load (Fig.7.38) is seen to be maintained over the full range of load except in the region of the cracking load, where the convention of neglecting the whole tensile resistance of the concrete when the maximum tensile stress has exceeded the tensile strength results in a discontinuity between the two parts of the theoretical curve. No such sudden transition occurs in the second cycle in which the tensile resistance is neglected throughout, as is appropriate for a partially prestressed member in which cracking has already occurred.

Although the beams were loaded up to 50 percent of the service load in the second cycle of incremental loading, the slope of the curve for increasing loads, is also fairly accurately represented by the theoretical analysis, when the observed residual deflection (after the first cycle) is added to the computed deflection. In Figs.7.44 to 7.50, the results of the theoretical analyses are compared with the experimental deflections for most of the tests.

Table 7.5 summarises the computed deflections with varying values of β for all the beams under service loads. It can be seen that the experimental deflections are consistently underestimated by putting $\beta = 0.5$, sometimes by more than 20 percent. On the other hand, with $\beta = 1.0$, the theoretical analysis overestimates the experimental deflection by more than 10 percent in some cases. The

Beam reference	Computed Deflection (mm)				(4)-(1)	Approximate experimental value of β
	β=0.5 (1)	β=0.67 (2)	β=0.85 (3)	β=1.0 (4)		
S1.5.2	16.10 (0.94)	16.49 (0.96)	16.90 (0.99)	17.23 (1.01)	1.13	0.93
S1.4.4	15.10 (0.90)	16.09 (0.96)	17.14 (1.02)	18.01 (1.07)	2.91	0.79
S1.3.5	18.42 (0.86)	20.24 (0.94)	22.02 (1.02)	23.49 (1.09)	5.07	0.81
S1.3.5S	17.15 (0.82)	18.71 (0.90)	20.36 (0.98)	21.75 (1.05)	4.60	0.89
S2.4.2	15.18 (0.94)	15.95 (0.99)	16.77 (1.04)	17.45 (1.08)	2.27	0.71
S2.3.4	17.45 (0.89)	18.82 (0.96)	20.27 (1.03)	21.48 (1.10)	4.03	0.77
S2.3.4S	18.08 (0.93)	19.47 (1.00)	20.94 (1.07)	22.18 (1.14)	4.10	0.67
S2.2.6	17.42 (0.84)	19.41 (0.94)	21.52 (1.04)	23.28 (1.12)	5.86	0.78
S3.3.2	13.61 (0.85)	14.63 (0.91)	15.73 (0.98)	16.64 (1.04)	3.03	0.90
S3.3.2S	13.37 (0.86)	14.27 (0.91)	15.21 (0.98)	15.99 (1.03)	2.62	0.91
S3.2.4	15.88 (0.84)	17.56 (0.93)	19.45 (1.03)	21.02 (1.12)	5.14	0.80
S3.1.6	16.36 (0.76)	18.56 (0.86)	20.89 (0.97)	22.83 (1.06)	6.47	0.90

Figures in brackets are $\frac{\text{computed deflection}}{\text{experimental deflection}}$

Table 7.5+ Computed deflection by integration of curvatures based on CP110

approximate experimental values of β, given in Table 7.5 were obtained by interpolation.

A careful study of Table 7.5 reveals that the effect of varying the distribution coefficient β, on the deflection was small for beams with 5 and 4 strands (i.e. higher degree of prestress), in which case the cracked region was small. For example, in the beam S1.5.2, the difference in the deflections calculated with $\beta = 0.5$ and $\beta = 1.0$ was only approximately 7 percent (1.13mm) of the actual deflection. The effect, however, was significant for beams with a low degree of prestress and high degree of cracking, (high ratio of service to cracking load) and in which case, the cracked region was wider. It is not possible to establish the effect of the amount of reinforcement on the value of β, since the beams with the same degree of prestress but with varying amounts of non-prestressed reinforcement were subjected to different service loads. The results, however, indicate that the distribution coefficient is related to the reinforcement stress which in turn is related to the degree of cracking.

The approximate correct values of the distribution coefficient for all the beams, as shown in Table 7.5, vary from 0.67 to 0.93. It is, therefore, probably safer to adopt $\beta = 1.0$ (i.e. neglect tension stiffening effect) in design. The error involved would be insignificant particularly for beams with a higher degree of prestress.

7.4.1.2 Long-term Deflection

An analytical method for computing long-term deflection by integration of curvature has been described in Chapter Five. Based on CP110 recommendation, the concrete stress between cracks at the level of the centroid of steel is assumed to have a value of 0.55 N/sq.mm.

Fig.7.51 shows the experimental and the computed long-term deflections for the three beams tested under sustained load alone. The total increase of deflection was taken to be the sum of the increments due to the effects of creep and shrinkage computed separately. The observed residual deflection after the first cycle was added to the computed deflection in order to give a true comparison. It should be pointed out that the approximate correct values of β (Table 7.5) had been used in the calculation. The ratios of the final to the initial computed deflections were 1.25, 1.47 and 1.26 respectively for beams S1.3.5S, S2.3.4S and S3.3.2S, against the ratios of the final to the initial experimental deflections of 1.38, 1.54 and 1.38.

The computation of the long-term deflection was based on the data obtained from the creep test described in Chapter Six. It can be seen from Fig.7.51 that the agreement between the calculated and the experimental deflection is fairly good for S3.3.2S, throughout the period of test. The calculated deflection for beams S1.3.5S and S2.3.4S, however, was consistently smaller than the actual deflection

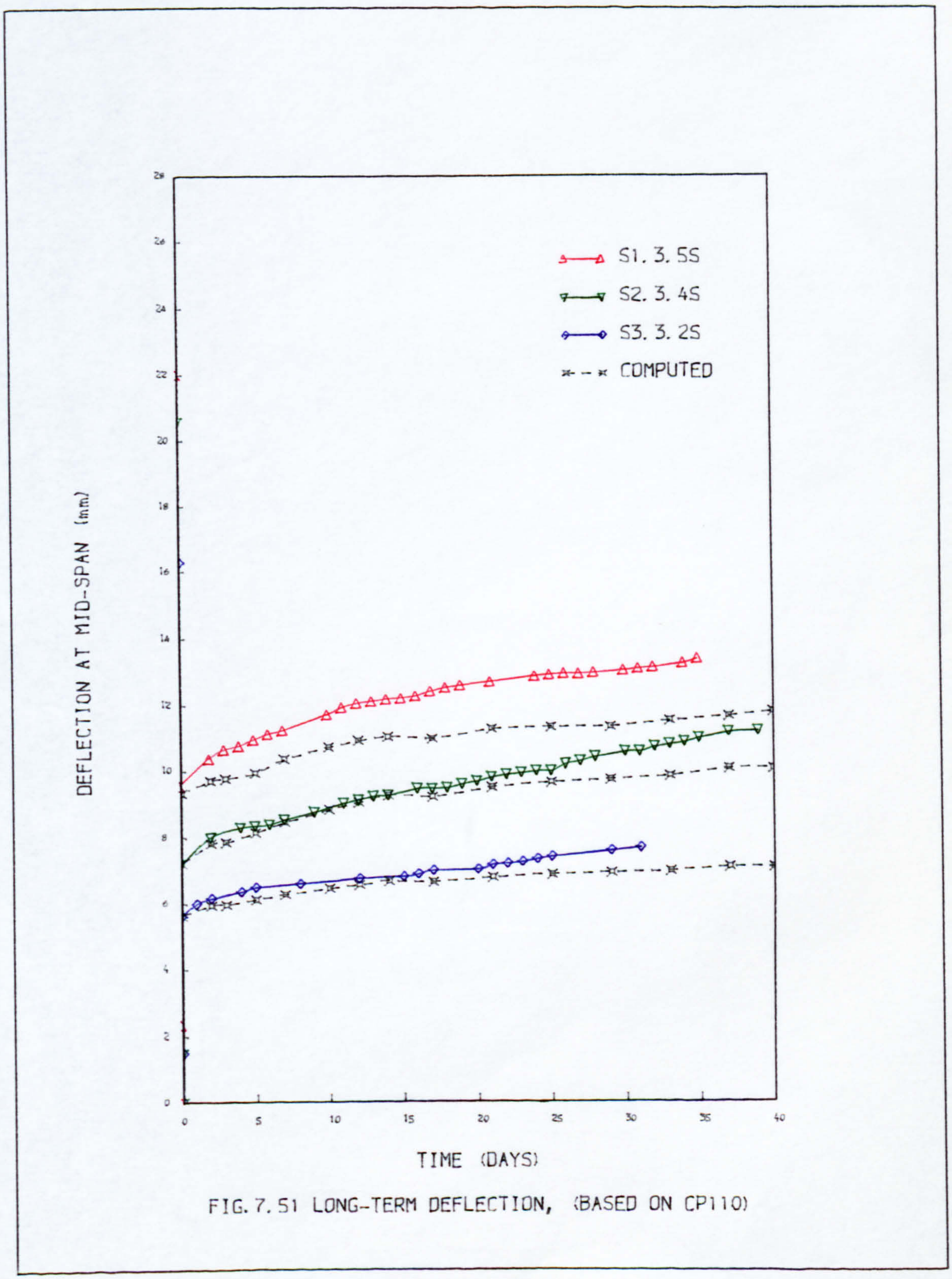

FIG. 7. 51 LONG-TERM DEFLECTION, (BASED ON CP110)

throughout the duration of tests. It should be noted that the creep specimen tests were conducted at the time parallel with the test of S3.3.2S, which was in winter months whilst S1.3.5S was tested during the hot summer months. It is commonly known (31) that a higher temperature normally leads to a higher creep and this may be the main reason for such a difference between the actual and computed deflection particularly for beam S1.3.5S. The error may also be attributed to some of the assumptions made in the theoretical analysis described in Chapter Four, in which the increase in the reinforcement stresses at the cracks, due to the effect of creep and shrinkage on the adjacent uncracked sections, was ignored.

The effect of shrinkage on the calculated deflection was found to be small compared to that due to creep.

It is, therefore, possible to conclude that the analytical calculation of long-term deflection described in Chapters Four and Five should give fairly good agreement with the actual deflection provided the correct creep data is available. More research is needed to develop a more rigorous analytical method of calculating long-term deflection.

7.4.2 Integration of Curvature according to Model Code (36)

The CEB/FIP Model Code (36) also recommends that the deflection of partially prestressed concrete member is to be

calculated by integration of curvature. The approach is similar to CP110 recommendations except that a different expression is given to account for the "tension stiffening" effect. The average reinforcement steel strain in the cracked region is given as:-

$$\varepsilon_{sm} = \frac{f_s}{E_s}\left[1 - \beta_1\beta_2\left(\frac{f_{cr}}{f_s}\right)^2\right] \nless 0.4\,\frac{f_s}{E_s}$$

(the notations have been given in Chapter Five)

It will be noticed that the average strain is expressed as a function of the degree of cracking which in turn varies with the load.

Table 7.6 shows that the short-term deflections computed according to the Model Code are in excellent agreement with the experimental results, provided the correct cracking moments are used. The deflections were calculated based on the observed cracking loads. As shown in Table 7.6, the calculated deflections are all within 8 percent error when compared to the actual deflections under service loads.

Figs.7.52 to 7.60 show the deflections for most of the beams at increasing loads in the first cycle up to the service loads. The agreement between the computed and experimental deflection curves was excellent for most of the cases (S1.5.2, S1.3.5S, S2.4.2, S2.3.4 and S3.3.2) for the whole range of loads up to the service load levels. It is interesting to note from the other figures, Figs.7.57 and 7.59, in which the computed deflections deviate from the

Beam references	Deflection	
	Calculated	Calculated / Experimental
S1.5.2	16.84	0.99
S1.4.4	17.38	1.03
S1.3.5	21.92	1.02
S1.3.5S	20.89	1.00
S2.4.2	16.10	1.00
S2.3.4	19.50	1.00
S2.3.4S	20.60	1.06
S2.2.6	22.06	1.07
S3.3.2	16.09	1.00
S3.3.2 S	16.15	1.04
S3.2.4	17.86	0.95
S3.1.6	19.84	0.92

Table 7.6: Computed deflection according to Model Code[36]

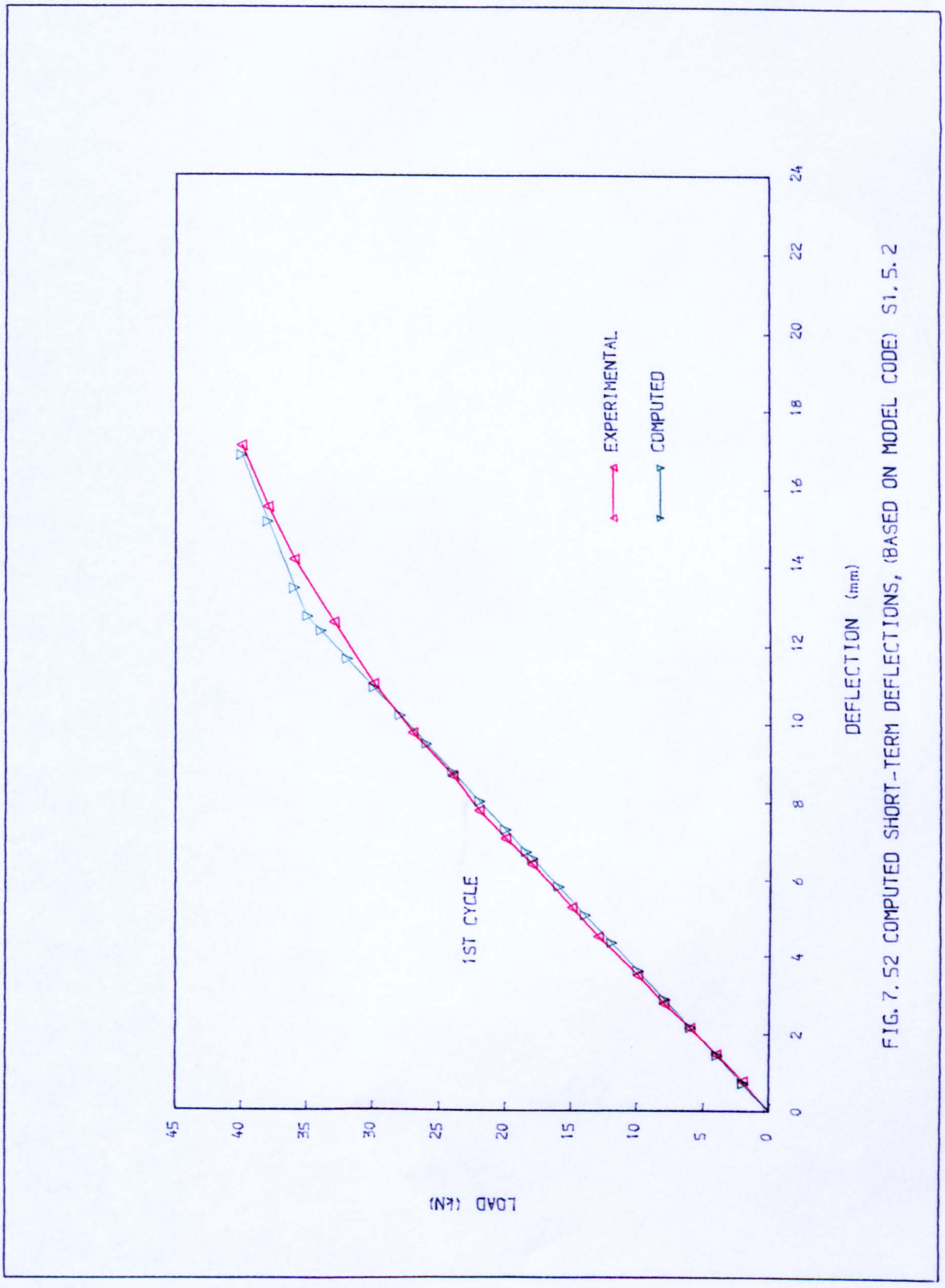

FIG. 7.52 COMPUTED SHORT-TERM DEFLECTIONS, (BASED ON MODEL CODE) S1.5.2

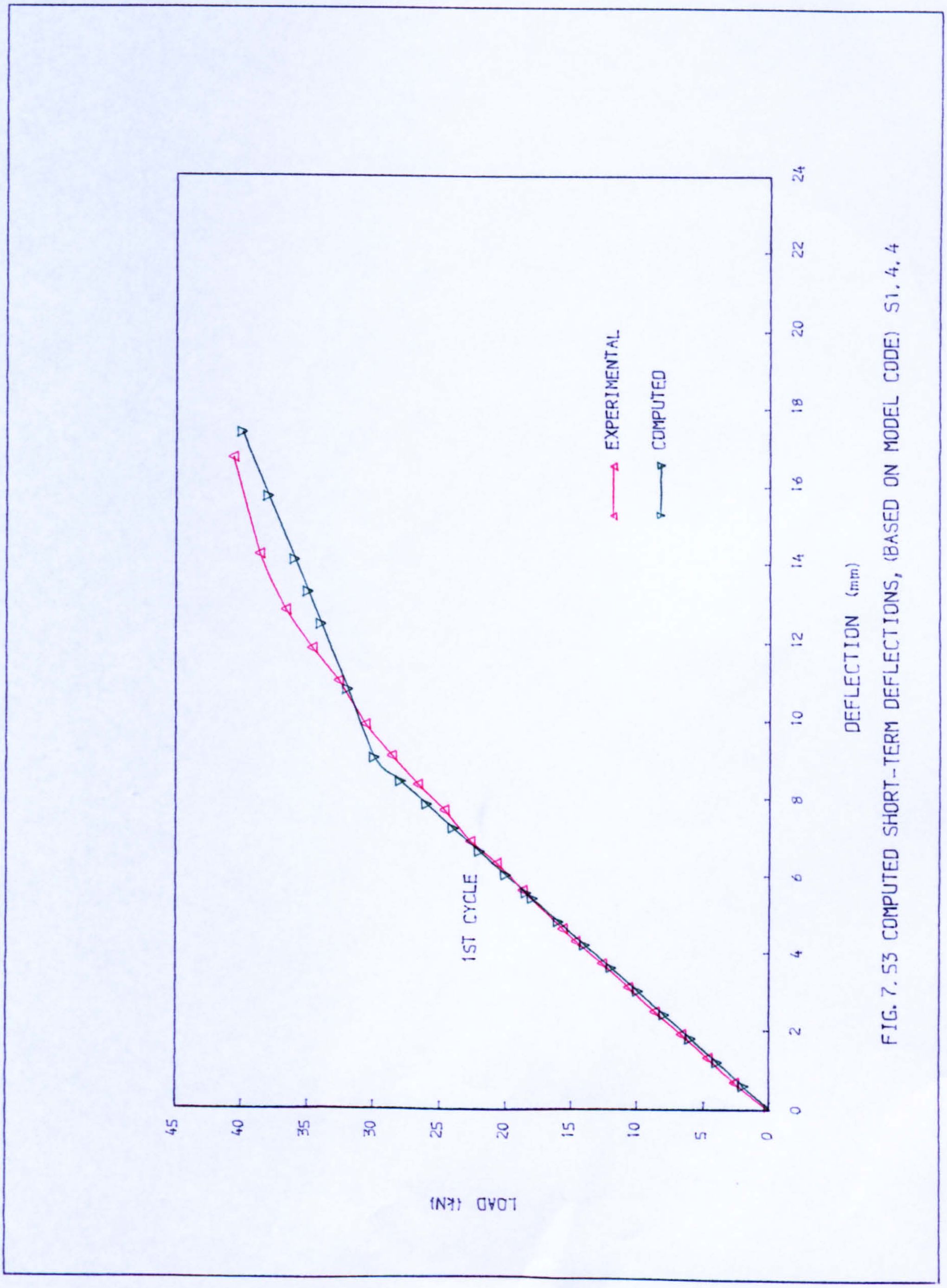

FIG. 7.53 COMPUTED SHORT-TERM DEFLECTIONS, (BASED ON MODEL CODE) S1.4.4

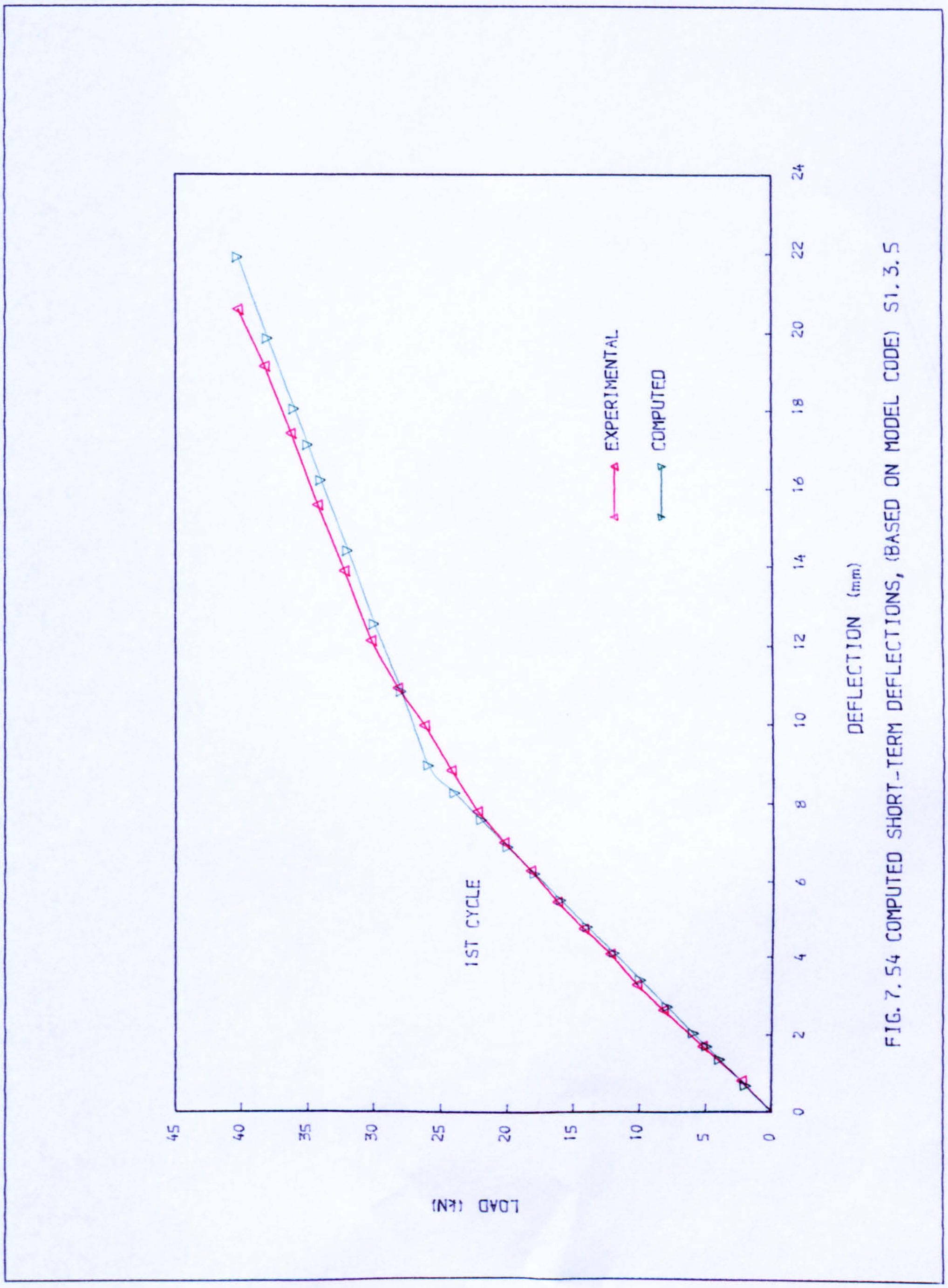

FIG. 7.54 COMPUTED SHORT-TERM DEFLECTIONS, (BASED ON MODEL CODE) S1.3.5

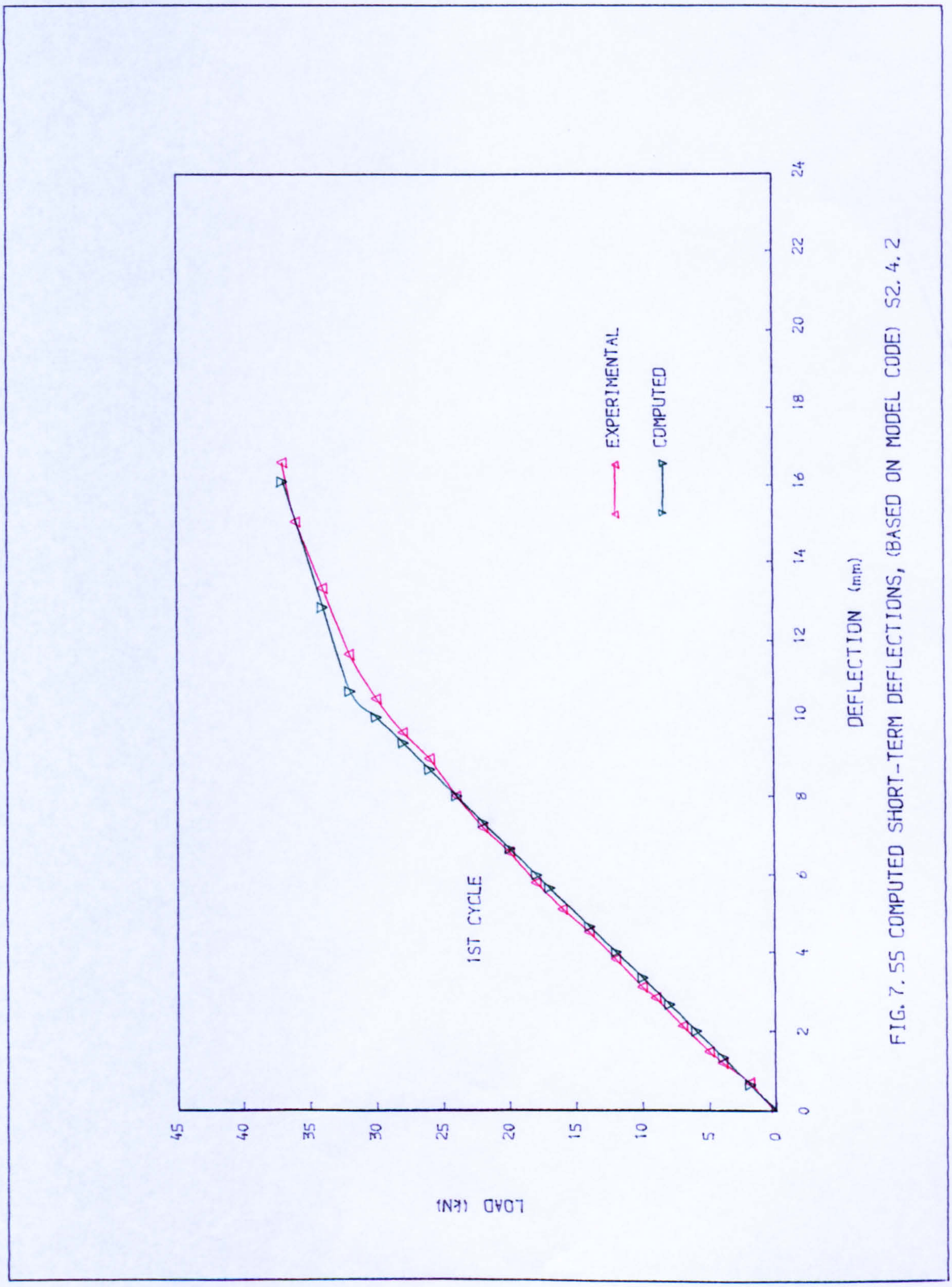

FIG. 7.55 COMPUTED SHORT-TERM DEFLECTIONS, (BASED ON MODEL CODE) S2.4.2

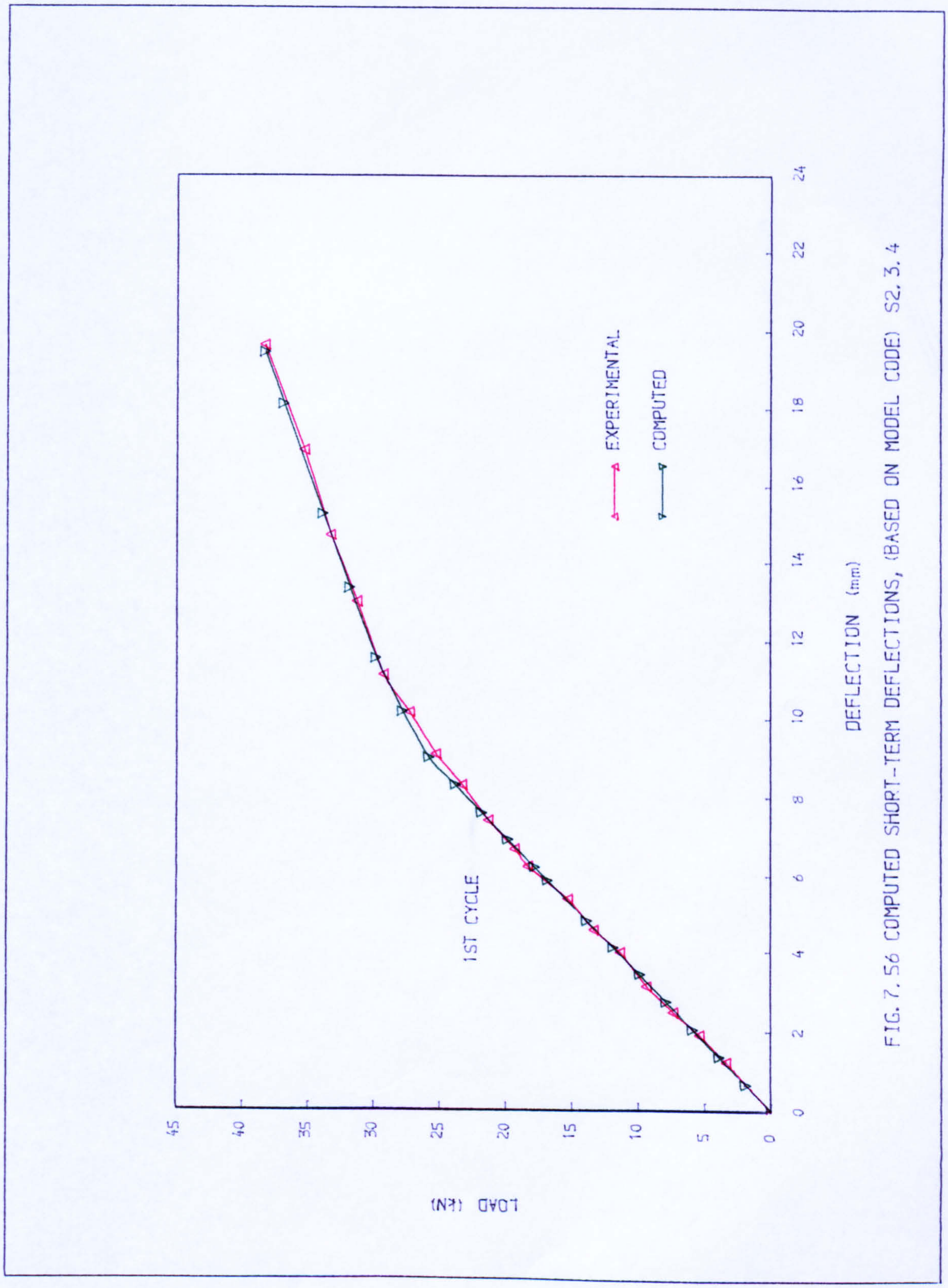

FIG. 7.56 COMPUTED SHORT-TERM DEFLECTIONS, (BASED ON MODEL CODE) S2, 3, 4

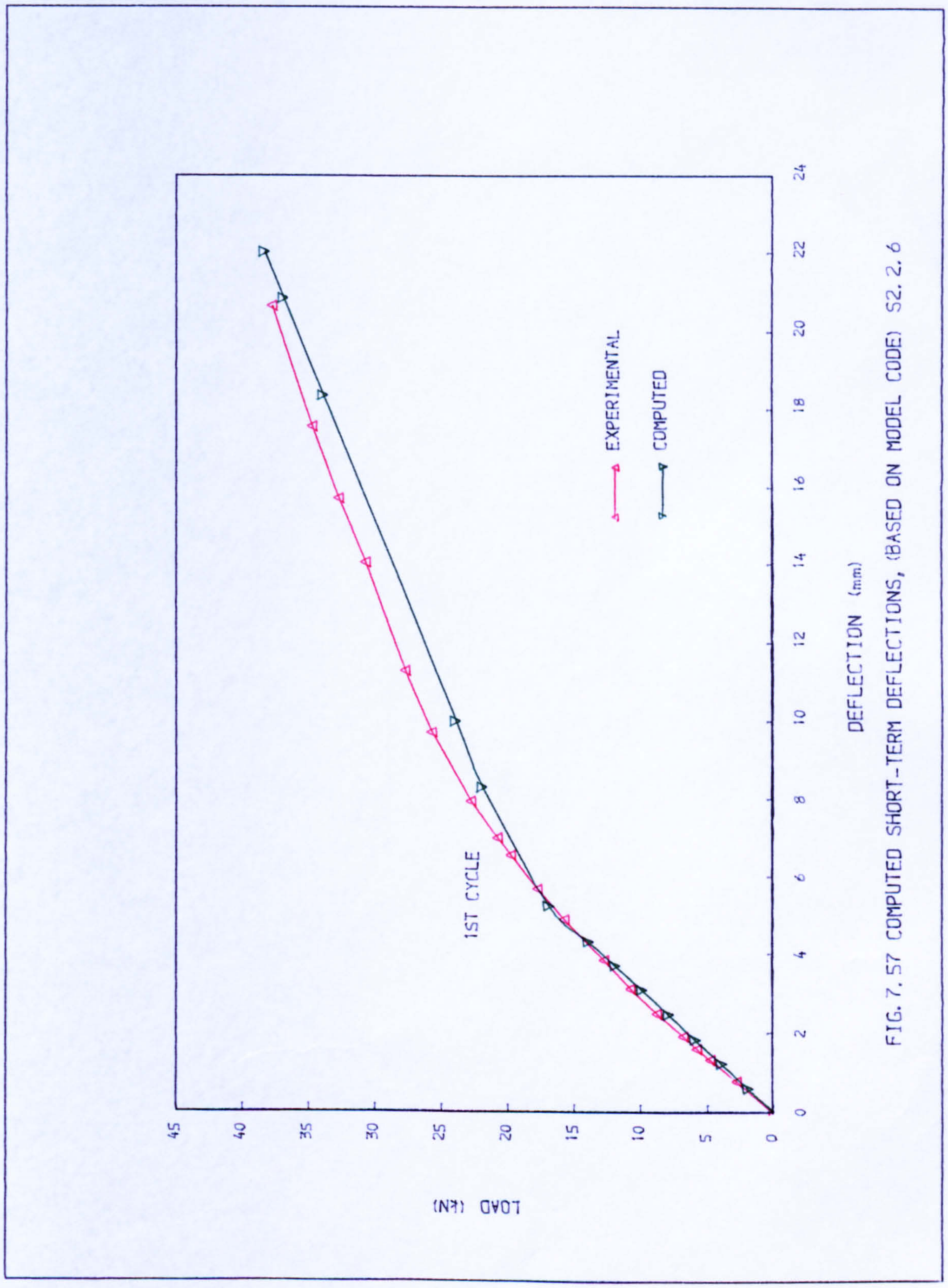

FIG. 7.57 COMPUTED SHORT-TERM DEFLECTIONS, (BASED ON MODEL CODE) S2.2.6

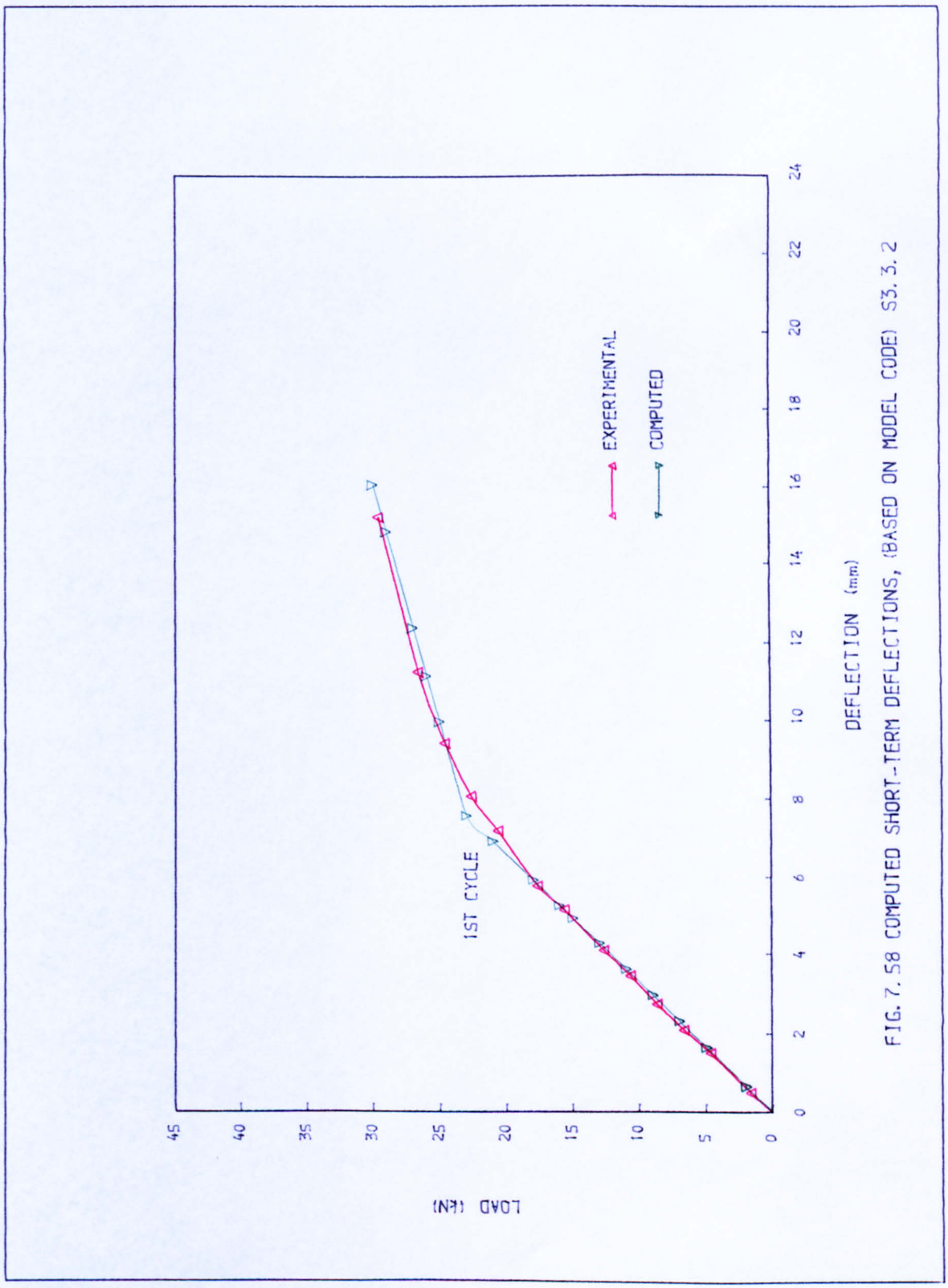

FIG. 7.58 COMPUTED SHORT-TERM DEFLECTIONS, (BASED ON MODEL CODE) S3.3.2

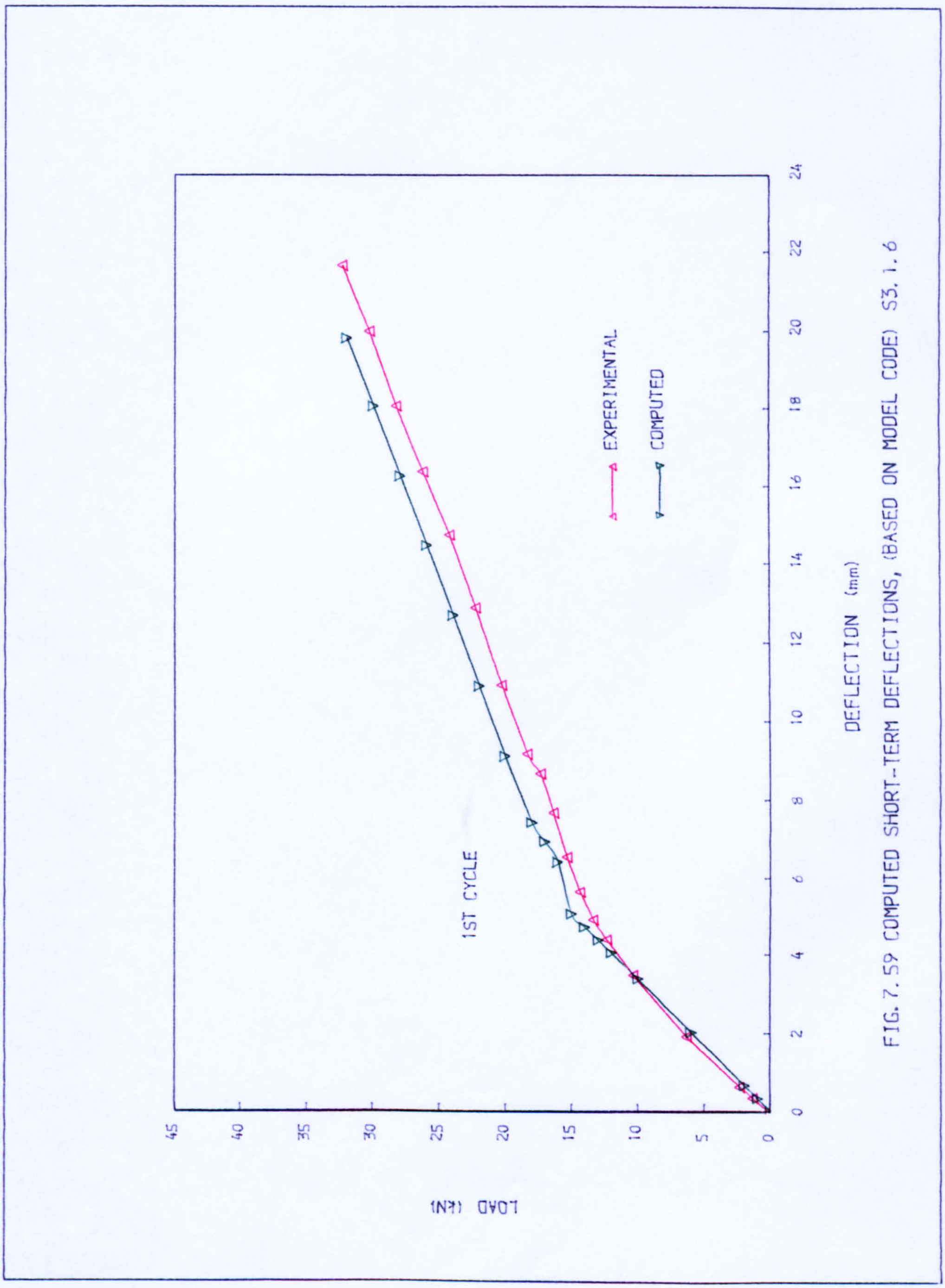

FIG. 7.59 COMPUTED SHORT-TERM DEFLECTIONS, (BASED ON MODEL CODE) S3.1.6

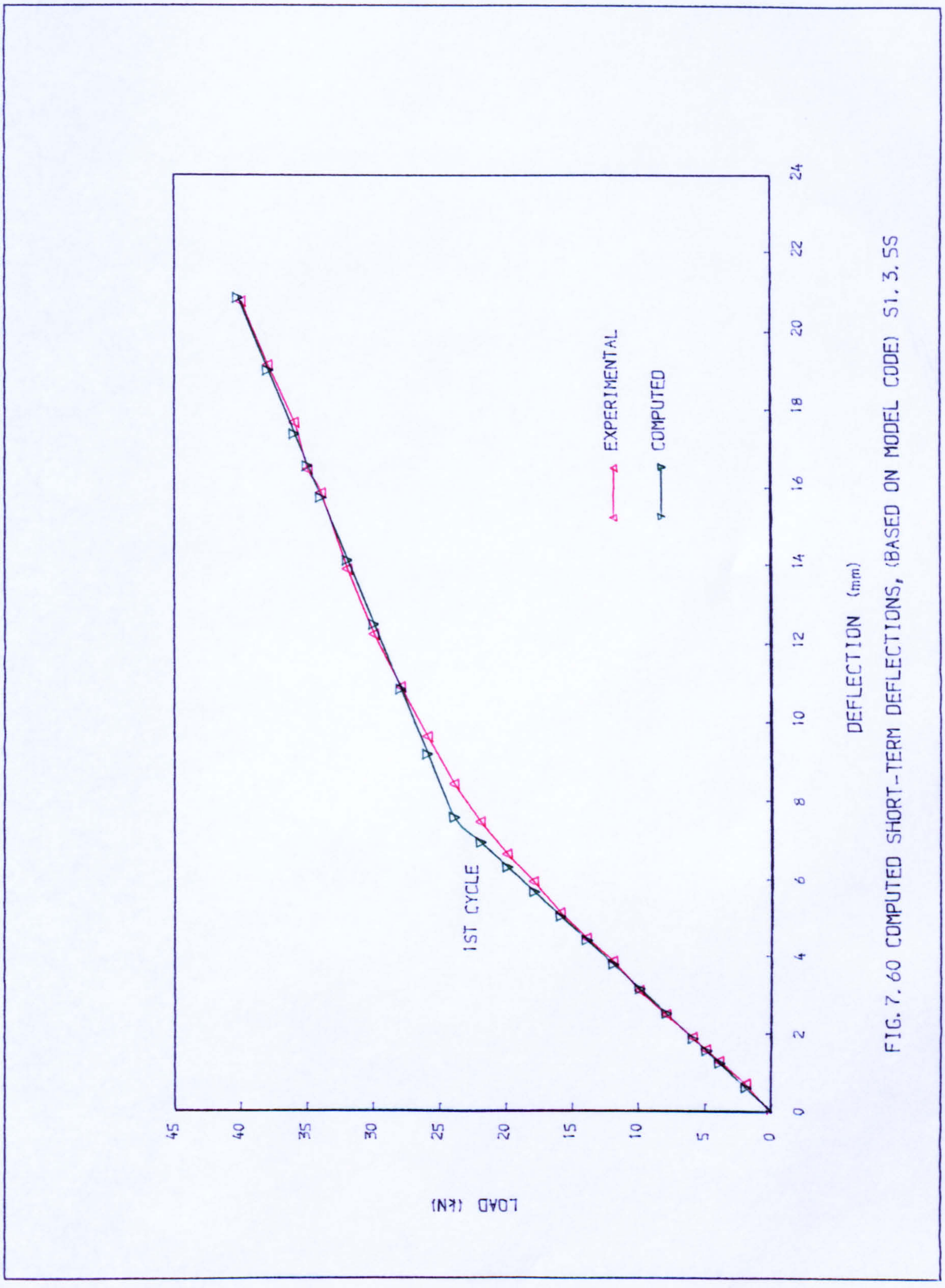

FIG. 7.60 COMPUTED SHORT-TERM DEFLECTIONS, (BASED ON MODEL CODE) S1.3.55

experimental results, the computed curves are parallel to the experimental curves after cracking has occurred. This, therefore, suggests that the results might be better if the correct cracking load had been used.

It can be concluded that the deflection analysed according to the Model Code (36) was in excellent agreement with experimental results for the whole range of loads below the service load levels.

7.4.3 ACI - 318 83 (57)

The ACI "I-effective" method of calculating deflection of conventional reinforced concrete members is well known. This method has been recommended by Branson and others (14,15,30,43,45,49) to be extended to partially prestressed concrete members. The recommended modified expression for "I-effective" is defined as follows:-

$$I_e = \left[\frac{M_{cr} - Pe}{M_{max} - Pe}\right]^3 I_g + \left[1 - \left(\frac{M_{cr} - Pe}{M_{max} - Pe}\right)^3\right] I_{cr}$$

The deflection can then be calculated by the normal expression:-

$$a = K \frac{M_{max}}{E_c I_e}$$

where K is a load distribution factor.

The effective moment of inertia method (I-effective) is claimed to provide a transition value between well-defined

limits in the uncracked (I_g) and fully cracked (I_{cr}) states. As it was originally derived empirically for ordinary reinforced concrete, its application to prestressed concrete has been somewhat different according to the value of I_{cr} adopted. Recently, there has been open discussion (43,45,49) amongst some of the experts regarding the appropriate value of I_{cr}. Branson (30,49) who proposed the original formula, recommends that I_{cr} should be calculated based on the conventional reinforced concrete section, in which case, the effect of axial prestressing force on the second moment of area of the section is ignored. Branson in the discussion of Ref.(45) argued that the I-effective was originally derived for reinforced concrete and its accuracy has been proved by many other investigators (30,58) who had calculated deflection according to his proposal. Naaman (14,15), however, has suggested the use of a cracked moment of inertia, I_{cr} to be determined with respect to the neutral axis, in which case the effect of prestressing force is taken into account. Tadros (45) went on further to suggest that I_{cr} should be calculated with respect to the centroid of the cracked prestressed concrete section. The present Author basically agrees with Tadros' proposal, since this centroid is the true bending axis of a cracked prestressed section which changes with the applied moment. It should be pointed out that the calculation based on Tadros' proposal is complicated and requires the analysis of the position of the neutral axis.

The ACI code recommends that the additional long-term

deflection resulting from creep and shrinkage of flexural members is to be calculated by multiplying the short-term deflection caused by the sustained load considered, by the factor:-

$$\lambda = \frac{\xi}{1 + 50\rho'}$$

where ρ' = ratio of non-prestressed compression reinforcement

ξ = Time dependent factor for sustained loads and may be taken equal to 0.67 for approximately one month.

The deflections calculated based on the I-effective method for all the test beams are tabulated in Table 7.7. The two basic methods of calculating I_{cr} as suggested by Branson and Tadros are also compared in Table 7.7. The calculated complete short-term deflection curves (I_{cr} was calculated based on Tadros' proposal) for the first and final cycle are shown against the test results in Figs.7.61 to 7.65. The final cycle was calculated by adopting the common practice of adding the short-term to the long-term deflection.

The calculated initial short-term deflections under service loads are all within 20 percent error when compared to the experimental values in most cases. The biggest error as shown in S3.3.2S is largely due to the cracking moment used, as has been pointed out by Branson (30). The deflections were calculated based on the flexural strength

Beam Reference	Initial Deflection (mm)		Final Deflection after approx. one month (mm)		Initial Deflection calculated according to Branson
	$^1/_2$ S.L. (1)	S.L. (2)	S.L. (3)	$^1/_2$ S.L. (4)	S.L. (5)
S1.5.2	6.68(1.03)	14.5 (0.85)	18.78(1.10)	10.98(0.89)	14.48(0.85)
S1.4.4	5.62(0.97)	13.85(0.83)	17.48(0.82)	9.25(0.76)	13.90(0.82)
S1.3.5	6.48(1.00)	23.11(1.07)	27.28(1.00)	10.64(0.66)	23.22(1.08)
S1.3.5S	5.79(0.94)	21.54(1.04)	-	9.83(0.74)	21.23(1.02)
S2.4.2	6.02(1.11)	15.54(0.96)	19.43(1.05)	9.91(1.01)	15.70(0.98)
S2.3.4	5.81(0.94)	21.02(1.07)	24.78(0.94)	9.57(0.56)	21.16(1.08)
S2.3.4S	6.06(1.04)	21.33(1.09)	-	9.96(0.84)	21.33(1.09)
S2.2.6	5.19(0.94)	23.50(1.14)	26.84(1.05)	8.53(0.56)	23.54(1.14)
S3.3.2	4.39(1.07)	12.90(0.81)	18.64(0.90)	7.21(0.68)	13.01(0.81)
S3.3.2S	4.66(1.13)	10.67(0.68)	-	7.66(0.99)	10.67(0.68)
S3.2.4	4.4 (1.0)	19.38**	22.2 (0.99)	7.25(0.58)	19.42
S3.1.6	5.7 (1.16)	24.7 (1.14)	28.38(1.07)	9.37(0.56)	24.74 (1.14)

S.L. = Service Load

Figures in brackets are ratios of $\frac{\text{Calculated deflection}}{\text{Experimental deflection}}$

* One initial cycle to S.L. followed by long-time load of $^1/_2$ S.L.

** In second cycle. Maximum load of first cycle was $^1/_2$ S.L.

TABLE 7.7: Deflections calculated according to ACI 318-83

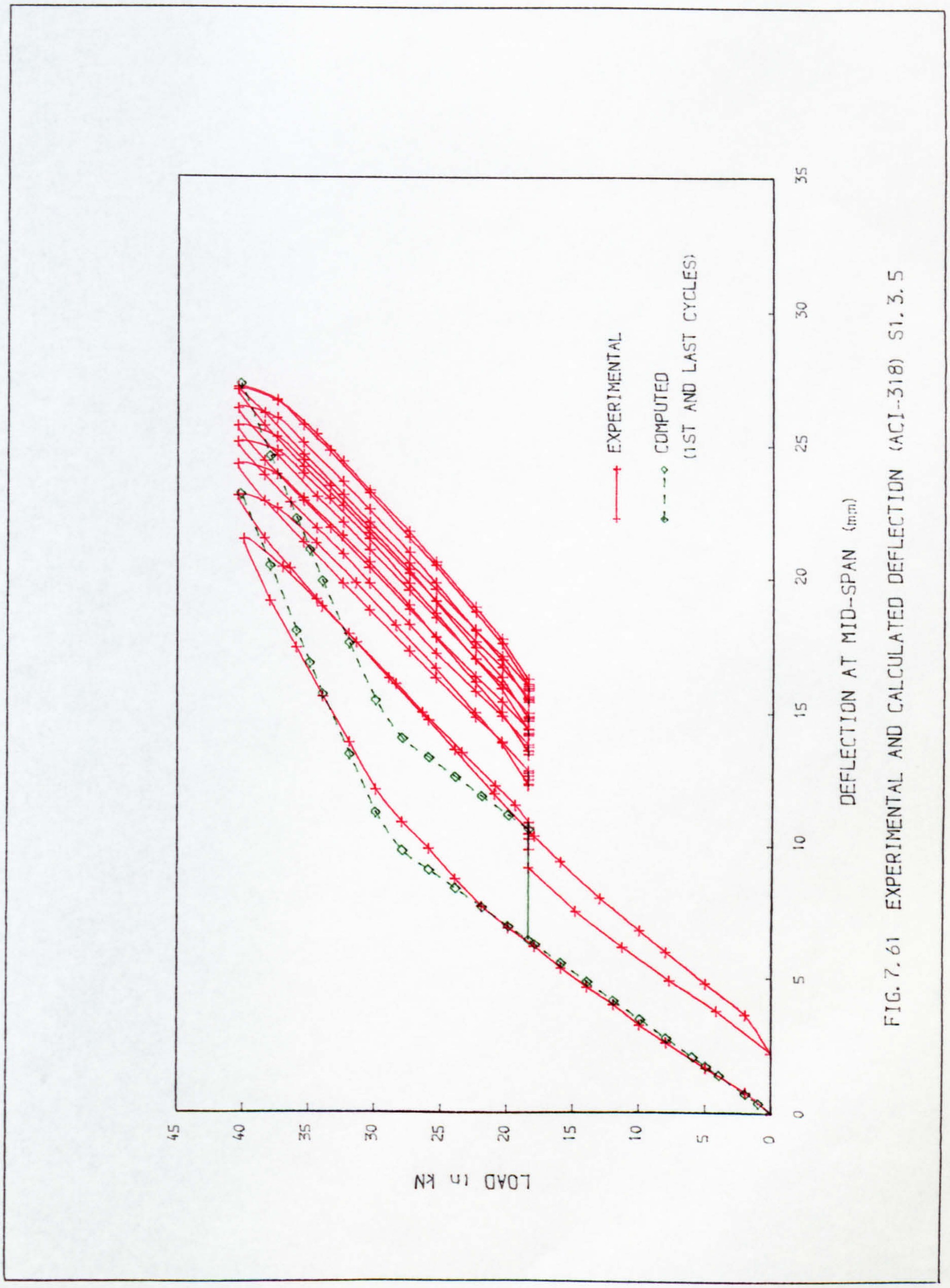

FIG. 7.61 EXPERIMENTAL AND CALCULATED DEFLECTION (ACI-318) S1.3.5

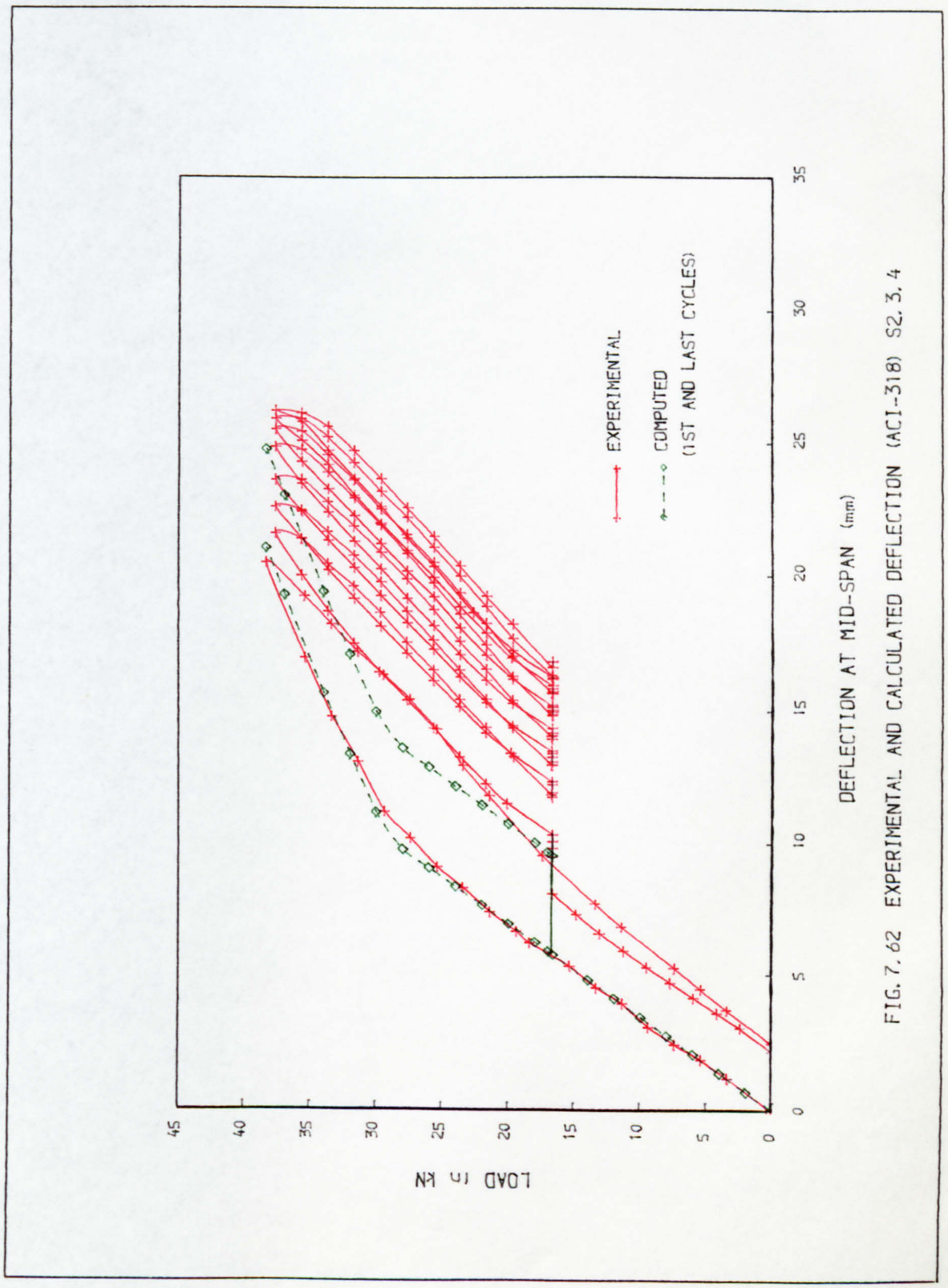

FIG. 7.62 EXPERIMENTAL AND CALCULATED DEFLECTION (ACI-318) S2, 3, 4

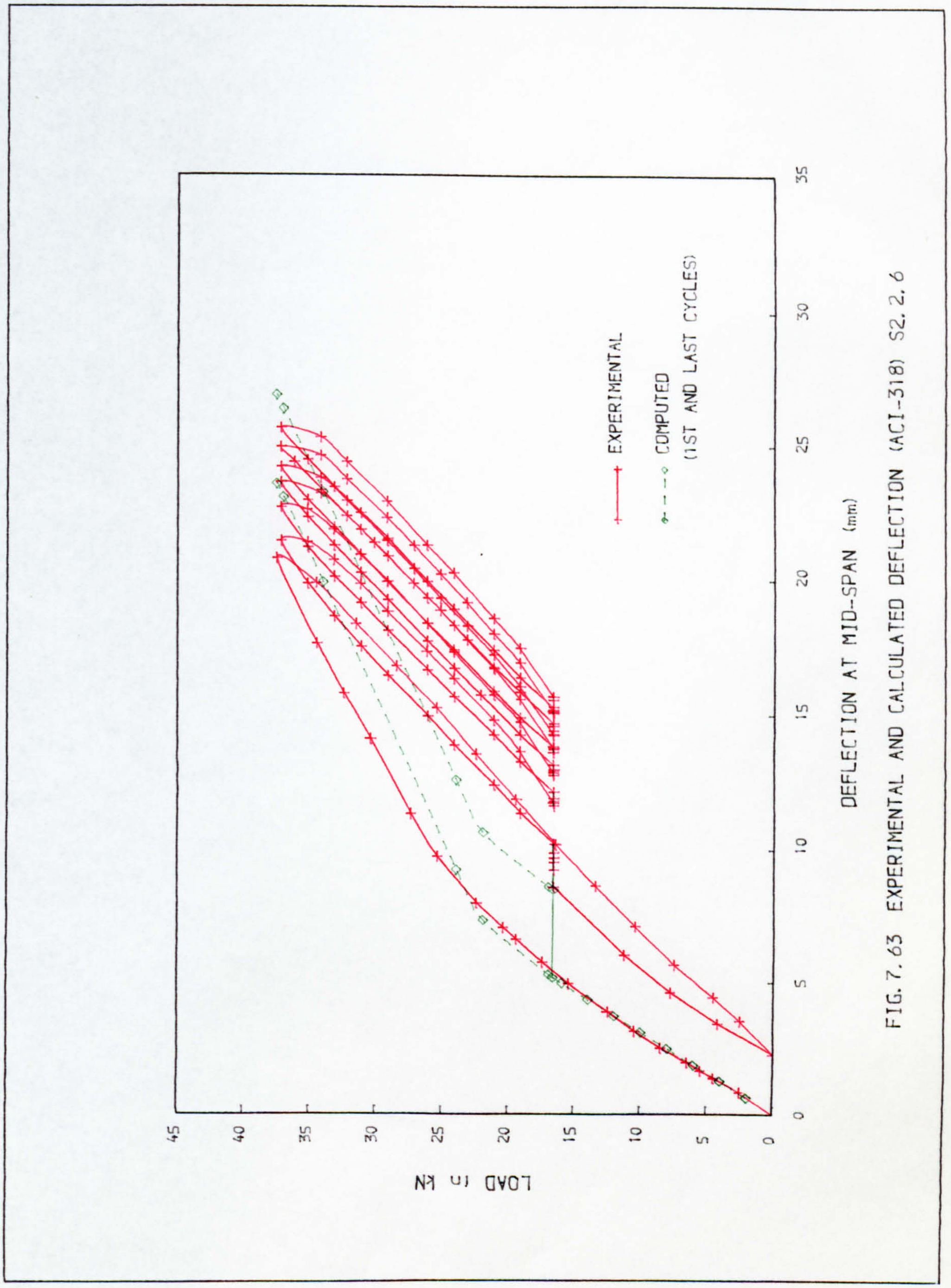

FIG. 7.63 EXPERIMENTAL AND CALCULATED DEFLECTION (ACI-318) S2.2.6

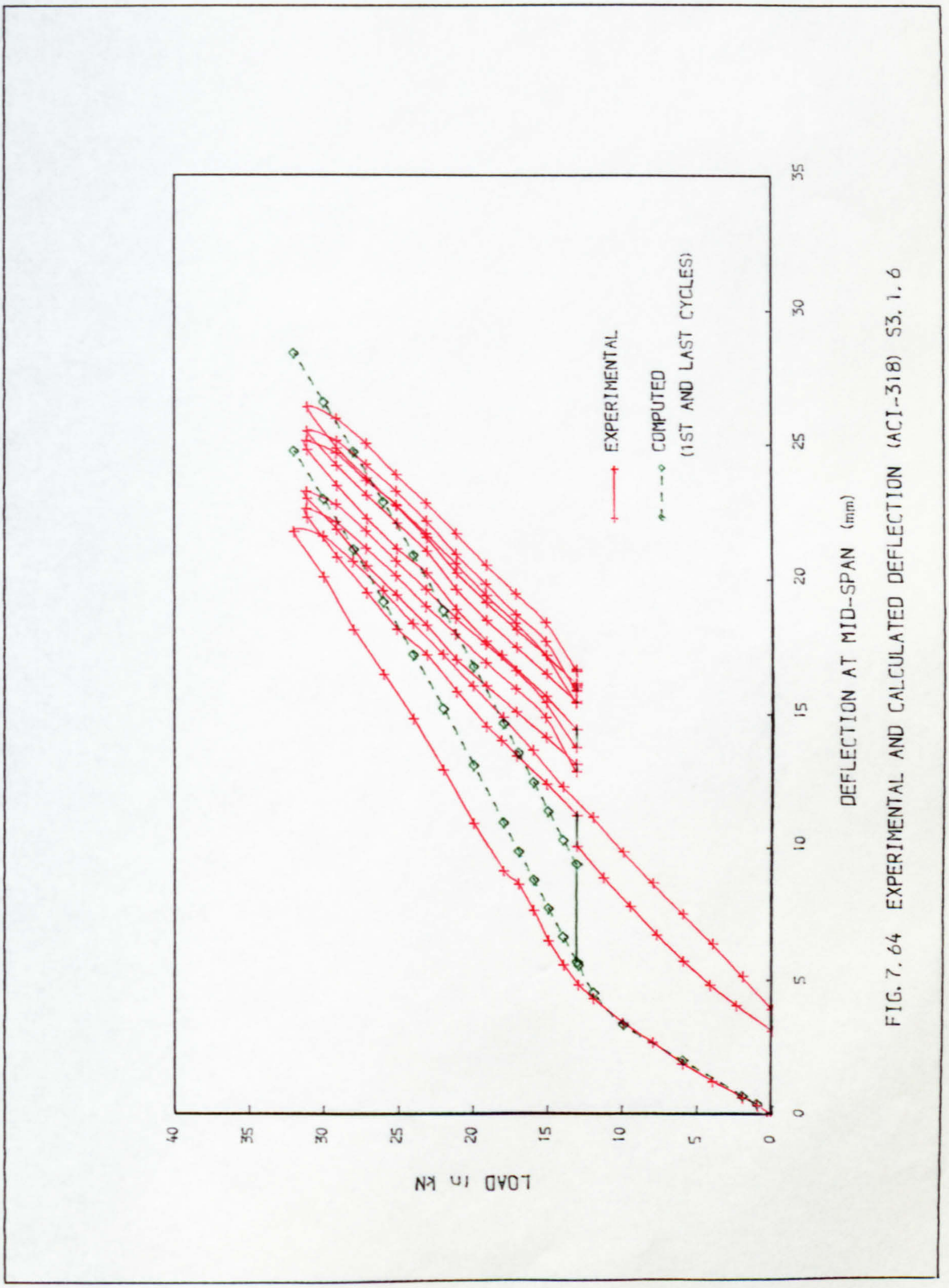

FIG. 7.64 EXPERIMENTAL AND CALCULATED DEFLECTION (ACI-318) S3.1.6

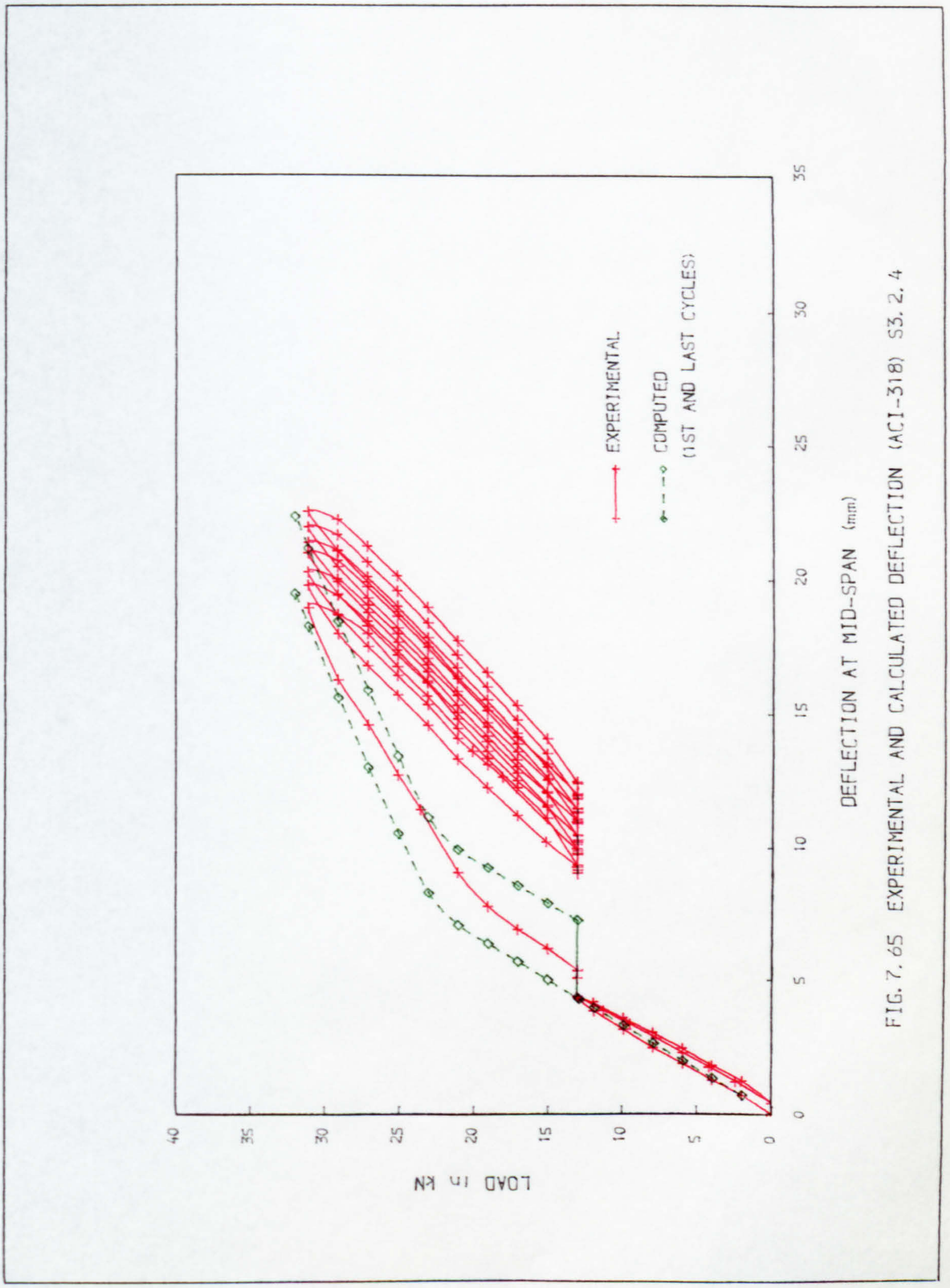

FIG. 7.65 EXPERIMENTAL AND CALCULATED DEFLECTION (ACI-318) S3.2.4

obtained from tests on plain concrete specimens which was somewhat higher than the observed cracking stress (Table 7.2).

The calculated final deflections at half the service load, under the permanent load plus a number of cycles of short-term load can be seen to be mostly unconservative, sometimes by more than 40 percent. An examination of the test results, of which Fig.7.61 is typical, reveals that the inaccuracy is almost entirely accounted for by the cumulative residual deflection after successive cycles of short-term load.

Branson and Trost (30,58) have proposed an additional factor applied to the initial deflection to represent the effect of cracking under repeated cycles of load and although in the present tests of partially prestressed beams, the additional deflection appears to be the results of non-recoverable creep, it could be represented by a similar factor. The value of this factor (which is defined as a multiple of the initial deflection) can be deduced from Table 7.7 to be not less than 0.44 for these beams, in order not to underestimate the deflection.

The shape of the short-term load deflection curve given by the "I-effective" method appears to be appropriate for the first cycle only, but when compared to the subsequent cycles, the slope of the curve appears to be smaller than the experimental results. It may be remarked that the

overestimation of the short-term deflection (final cycle) by the "I-effective" method has contributed to the fairly good agreement with the experimental final deflection at service load (Fig.7.61 and Table 7.7 column 3), by compensating for the non-inclusion of the residual deflection after cyclic loading.

The computed deflections based on I_{cr} calculated for a conventional reinforced concrete section, are shown in Table 7.7 column (5). The results when compared with column (2) of Table 7.7, indicate that the difference on the calculated deflection at service load between the two methods of calculating I_{cr} is not significant. It is therefore possible to conclude that for design purposes, I_{cr} may be calculated as for a reinforced concrete section as proposed by Branson.

CHAPTER EIGHT

Conclusions and Recommendations for Further Research

8.1 Summary

Nine tests were carried out on partially prestressed beams, in which 50 per cent of the service load was sustained for a period of up to 46 days during which time the load was increased to the full service load up to seven times in intermittent short-term cycles. Three additional beams were tested under the long-term load alone. These were designed to study the effect of the intermittent short-term cycles of loading on the permanent deflection.

Two analytical methods have been derived for calculating short-term and long-term deflections, respectively, of partially prestressed concrete beams by integration of curvature according to the CP110 (6) recommendation. A third analytical method of calculating deflection by integration of curvature according to the Model Code (36) has been studied and compared with the experimental results.

8.2 General Behaviour of Test Beams

8.2.1 Losses of Prestress

The losses of prestress in the prestressed steel were less in beams with larger amount of non-prestressed

reinforcement. The loss of prestress in the concrete which is likely to cause more concern in practice, however, was higher in these beams.

The effect on the calculated prestress of ignoring the compressive stresses in the non-prestressed reinforcement, as is commonly done, can be significant particularly in beams with a large proportion of this type of steel.

8.2.2 Deflection in First Cycle

The rate of increase of deflection after the point of cracking was larger in beams with smaller amounts of non-prestressed reinforcement. In the design of partially prestressed concrete members the deflection can therefore be controlled by varying the amount of reinforcement.

Although the rate of increase after cracking was the same for beams with the same reinforcement ratio (same ultimate moment of resistance), the deflection of beams with a lower degree of prestress was larger than that of other beams with the same reinforcement ratio.

The residual deflection was largest in beams with the greatest degree of cracking (i.e. ratio of service load to decompression load) and with the largest amount of non-prestressed reinforcement.

8.3 Beams Under Sustained Load

The deflections of the three beams subjected to sustained loading alone increased by about 50 per cent of the initial value, after about 30 days. There was only a small increment in the crack width within that period of time.

The neutral axis of strain moved downwards under the sustained load and generally, the compressive strain at the top was approximately doubled by the end of the tests whilst there was only a slight reduction in the tensile strain at the levels of reinforcement.

8.4 Beams Under Combined Loading

The rate of increase of deflection was greatest in the first cycle, became progressively smaller and then remained at a constant value after two or three intermittent cycles of short-term loading.

The effect of the intermittent cycles of short-term loading was to increase the residual deflection under the permanent load. Only part of this increase was recoverable.

In all tests, the residual deflection after each cycle of intermittent short-term cycle of loading remained at a constant value (about 0.3mm to 0.4mm) after two or three cycles.

The form of the deflection curve resulting from a combined permanent load and intermittent cycles of short-term loading appeared to be similar to the sum of the deflections due to two types of loading applied separately. This similarity may be considered analogous to McHenry's hypothesis for the superposition of creep strains (48).

The final deflection of most of the test beams under service load exceeded the CP110 (6) limit although the span/depth ratio was near the maximum allowable in the code. About half of the increase of deflection above the initial value was due to the effect of the intermittent cycles of short-term loading. The common practice of calculating long-term deflection which allows for the effects of creep and shrinkage under the permanent load alone seems to be unconservative.

The neutral axis of strain at service load moved downwards under the combined effects of the permanent load and intermittent cycles of loading. This was accompanied by a substantial increase in the compressive strain at the top surface but only a slight change in the strain (and stress) in the reinforcement under the same load.

The deflected profile could be accurately determined by integration of the curvature obtained from the measured surface strain over the whole span.

8.5 Integration of Curvature Based on CP110

An analytical method, based on the recommendations in CP110 Appendix A (6), was developed for calculating the short-term deflection of partially prestressed concrete beams, as described in Chapter Five.

The deflections calculated by the above method were in good agreement with the experimental results for various values of β (as defined in Eqn.5.3) between 0.67 and 1.0. In all the beams, the deflections were overestimated by adopting $\beta = 1.0$ (i.e. neglecting the stiffening effect of the concrete).

The effect of "tension stiffening" on the calculated deflection was found to be insignificant for beams with relatively high prestress where the cracked region was small. The effect was more important in beams with a low degree of prestress (i.e. a high ratio of service to cracking load). The deflection could be predicted conservatively and fairly accurately by neglecting the tension stiffening effect, particularly in highly prestressed beams.

The analytical method of calculating long-term deflection of beam under permanent load alone as described in Chapter Five, gave fairly good agreement with the experimental deflection depending on the accuracy of the creep and shrinkage data available.

8.6 Integration of Curvature According to Model Code

The deflection calculated by integration of curvature according to the CEB/FIP Model Code was found to be accurate to within 10 per cent compared with the experimental deflection in all the tests. The deflection was also accurately predicted below the service load level in most cases.

The accuracy of the predicted deflection under any load depends on the correct value of the cracking load used.

8.7 Simplified Calculation - ACI-318 83

The "I-effective" method of calculating deflection of cracked prestressed concrete beam as recommeded in ACI-318 83 and modified by Branson and Trost (30) gave good results for the first cycle of short-term load but were unconservative for long-term load combined with intermittent cycles of short-term loading.

The present method of calculating long-term deflection does not consider the effect of intermittent cycles of short-term loading on the permanent deflection which was found to be significant. Better agreement could be obtained by the introduction of a factor to represent the non-recoverable residual deflection after successive cycles of short-term loading.

It is suggested that the I-effective should be calculated by the method proposed by Branson, based on I_{cr} for a cracked reinforced concrete section. This was found to be the simpler of two alternatives considered which gave approximately the same values.

8.8 Recommendations for Further Research

The experimental results presented in this thesis showed that the residual deflection after the first cycle of loading (mainly due to cracking) was considerable in most of the tests, and largely contributed to the unconservative results predicted by the ACI "I-effective" method. More research is therefore needed in this area.

The effect of tension stiffening on the deflection has been shown to be significant in beams with a low degree of prestress, but not well predicted by the recommendation of CP110. Further research is required to analyse the concrete stresses and also to investigate the distribution of curvature or the average steel strain between the adjacent cracks. This could be done by adopting a suitable model.

The form of the deflection resulting from the combined permanent and intermittent short-term loading was found to be similar to the sum of the deflections due to two types of loading applied separately. This may be analogous to the McHenry hypothesis of the superposition of creep strain and may form a basis for a new theoretical analysis of long-term

deflection with intermittent cycles of short-term loading.

PART III

STUDY OF PARTIAL PRESTRESSING PARAMETERS

CHAPTER NINE

Object and Method of Study

9.1 Object of Study

A recent international survey conducted by Bachmann (17) showed that partial prestressing has so far been included only in a few national codes and that these contain widely varying design requirements. The British Code CP110 is among some of the national codes in which the design criterion is the calculated tensile stresses in an uncracked section. In several countries, such as Hungary and Sweden, design is based on the behaviour of the cracked section under service loads as specified by the permissible crack widths. In the Swiss and the Dutch codes, however, the design specification is based on the calculated stress increments in the non-prestressed and prestressed reinforcement in the cracked section. Generally, according to the survey, two or three main classes of prestressing are defined in various national codes. The classification in the British Code has been described in Chapter One.

Many experts are convinced that partial prestressing has many advantages. However, it has not been widely accepted in practice and this was the general concern among those present at two recent international symposiums, namely the 1980 FIP Symposium in Bucharest and the 1983 International Symposium on Non-linearity and Continuity in

Prestressed Concrete in Waterloo, Canada. According to Bachmann (38), the experience of wide application of partial prestressing in Switzerland since 1968, proves that a simple and effective design procedure is essential; otherwise, "partial prestressing has no chance of acceptance in practice".

Several design parameters have been proposed over the last few years. The three most commonly discussed are: the Partial Prestressing Ratio (16), the Degree of Prestress (18) and the Hypothetical Tensile Stress (6,8).

The object of the study is to investigate the correspondence of each of the above proposed partial prestressing parameters to the serviceability criteria. Based on the results of the study, a simple design procedure is proposed.

The three proposed parameters have been defined in Chapter Two. Brief definitions are given below:

(a) Partial Prestressing Ratio (PPR)

The Partial Prestressing Ratio is defined as the ratio of the ultimate moment of resistance provided by the prestressing steel alone to the total ultimate moment provided by the two types of reinforcement together.

$$PPR = \frac{(M_u)_p}{(M_u)_{p+s}} \simeq \frac{A_p f_{pu}}{A_p f_{pu} + A_s f_y} \quad \ldots \text{ Eqn (9.1)}$$

This parameter is based on the ultimate limit state in which the behaviour of partially prestressed concrete members is similar to other types of concrete structures. According to Naaman (16), it is because of this similarity that the PPR approach should be adopted as a unified design procedure for all types of concrete structures especially partially prestressed concrete members.

(b) Degree of Prestress (DEG)

The degree of prestress is defined as the ratio of the moment when concrete ceases to be compressive, to the total service moment.

$$DEG = \frac{M_d}{M_{g+q}} \qquad \ldots \text{Eqn (9.2)}$$

This parameter has the advantage that it is based on serviceability conditions in which the advantages of partial prestressing lie. The values of the degree of prestress lie between zero (conventional reinforced concrete) and unity (fully prestressed concrete) and any values in between represent partial prestressing.

(c) Hypothetical Tensile Stress (HYP)

The Hypothetical tensile stress is the fictitious tensile stress of the concrete at the soffit if the section is assumed to remain uncracked under service load when the tensile strength of the concrete has been exceeded. It is

defined as:

$$HYP = \frac{M_{g+q}}{Z_{inf}} - f_{inf}$$

$$Hyp = \frac{M_{\mathcal{L}}}{Z_{inf}} - f_{inf}$$ ... Eqn (9.3)

measured from str
before loading
composite
composite

In this case shrinkage and creep a
included in the strain measurement

This approach has been adopted in CP110 (6) and has the advantage of its simplicity in design. The procedures in design for prestressed concrete can be easily extended to partially prestressed concrete by using Hypothetical Tensile Stress.

9.2 Method of Study

9.2.1 Introduction

It is generally accepted that the main advantage of partial prestressing lies in its superior structural behaviour under service load. Partial prestressing enables the undesirable excessive camber of fully prestressed members or excessive deflection and crack width in reinforced concrete members with small percentages of high strength reinforcement, to be limited by introducing a suitable proportion of prestressed reinforcement so as to maintain the same ultimate load. There is no appreciable difference in the structural behaviour of a fully prestressed, partially prestressed or an ordinary reinforced concrete beam at ultimate limit state.

The relative usefulness of the partial prestressing design parameters will, therefore, depend on how closely each relates to the serviceability criteria, since these are

the important controlling factors in the design of partially prestressed members. Ideally, the most suitable parameter would have a unique relationship with the serviceability criteria, independently of other variables such as reinforcement ratio, level of prestress or the shape of the section.

The major serviceability criteria and variables closely related to them are discussed in Sections 9.2.2 and 9.2.3. The analytical procedures developed for this investigation are described in Section 9.2.4. The complicated calculation was facilitated by a computer program which is given in full in Appendix C.

9.2.2 Serviceability Criteria

The most commonly considered criteria for the design of partially prestressed beams under service load conditions are as follows:

(a) The allowable compressive stress in the concrete must not be exceeded under the application of temporary loads (such as those occurring during erection and transportation) or full service load.

(b) The deflection or camber (short and long-term) due to the combined effect of the prestressing force and full service load must satisfy the code requirements. Where the dead load is more than 25 percent of the total

service load, CP110 specifies that the span/depth ratio should not exceed the maximum allowable values for reinforced concrete.

(c) The maximum crack width under the effect of full service load must be limited to a specified value, depending on the probable environment of the member.

(d) Where there are frequent repetitions of part of the live load, the increase of the reinforcement stress must be less than the permissible ranges for the respective types of steel. Research over the last fifteen years (11,12,37) has shown that flexural crack width is related to the increase of the reinforcement stresses after the point of decompression at the level of the steel. For example, the crack width was found by Bennett and Nilson (10,11) to be related to the stresses by the expression:-

$$w = \beta_1 + \beta_2 \frac{f_s}{E_s} C$$

where β_1 and β_2 are constants, c is the cover to the reinforcement and f_s is the increase of stresses. The fatigue strength has also been shown experimentally to be related to the calculated ranges of stresses in the reinforcement (39,40,41). According to the CEB/FIP Model Code (36), the maximum ranges should be limited to 150N/sq.mm for bonded deformed tendons and bars.

The deflection of a member uniformly loaded, is a function of the curvature at all sections and may be approximately related to the curvature at the section of maximum moment, irrespective of whether the section is cracked or uncracked. It has been demonstrated in Part II of this thesis how the deflection of a cracked or uncracked prestressed beam can be calculated by integration of curvature over the whole span.

9.2.3 Other Parameters

In addition to the range of stress in the reinforcement and the curvature, the other major variables that affect the deflection, crack width and fatigue strength of partially prestressed concrete members are:

1) Reinforcement ratio
2) Level of prestress
3) Shape of the section
4) Modulus of elasticity of concrete and steel
5) Distribution of reinforcement in the tension zone
6) Cover to the reinforcement
7) Type of prestressing

It was decided to study the performance of the three partial prestressing design parameters in relation to the first three variables listed above. The other variables were kept to constant values as follows:

(a) The ratio of the modulus of elasticity of steel to that of concrete, $\alpha = 6.0$

(b) The prestressed and non-prestressed reinforcement were assumed to be located at the same level and at 0.9 times the depth of the section

(c) In calculating the ultimate moment the tendons were assumed to be pretensioned.

(d) The strength of the tendons and the yield stress of the steel was:

f_{pu} = 1600 N/sq.mm f_y = 400 N/sq.mm

9.2.4 Method of Analysis

The relative usefulness of the three parameters to be compared will depend on how closely each relates to the serviceability criteria, which have been shown above to be closely associated with the increase of stress in the reinforcement and the increase in curvature at the section where the moment is a maximum, both calculated for the service load.

In the following analysis, the increase of stress and curvature is therefore calculated for each of the design parameters for sections of different shape and with varying ratios of prestressed and non-prestressed steel.

The procedure for the analysis is as follows:

(1) Shape and Reinforcement Ratio

The shape of the section is defined by the ratios of web breadth to the total breadth and flange depth to total

depth. The other data required is the equivalent reinforcement ratio, A_{eq} /bd, where A_{eq} is the area of prestressed reinforcement that would have the same strength as the actual combined strength of the prestressed and non-prestressed reinforcement.

$$A_{eq} = A_p + \frac{f_y}{f_{pu}} A_s \quad \text{... Eqn (9.4)}$$

The ultimate moment is calculated according to CP110 and thus the service moment, M_{g+q} which is assumed to be equal to 0.65 times the ultimate moment.

(2) Varying Ratios of Prestressed and non-prestressed Steel

A chosen proportion of the reinforcement represented by the equivalent reinforcement ratio (A_{eq}) is assumed to be prestressed. The area of non-prestressed steel is calculated and hence, the Partial Prestressing Ratio (PPR) by Eqn.(9.1). The transformed section properties can then be calculated.

(3) Losses of Prestress

The losses of prestress are calculated according to CP110 assuming specific creep of 50×10^{-6} per N/sq.mm initial stress under dead load, and concrete shrinkage of 250×10^{-6}. Shrinkage is assumed to occur with any level of prestress but creep losses only occur when the prestress at the level of the reinforcement is larger than the bending stress due to the dead load moment, assuming the latter to be 0.35 times the ultimate moment.

(4) Reference Force

The reference force, F_o, which is defined as the total force in all the reinforcement when the concrete ceases to be compressive at that level, is calculated by the expression:

$$F_o = F_e + \alpha f_{cpe}(A_p + A_s)$$

where F_e is the total effective force (after losses) in the reinforcement

f_{cpe} is the corresponding effective prestress at the level of reinforcement

(5) Lever arm

The depth of the neutral axis and the lever arm, z, of the cracked section are then calculated by the method of analysis described in Chapter Four, Section 4.2.

(6) Calculation of Parameters

The Degree of prestress and the Hypothetical tensile stress for the amounts of prestressed and non-prestressed reinforcement, are calculated by Eqns.9.2 and 9.3 respectively.

(7) Increase of Stress in Reinforcement

The increase of stress in the reinforcement, measured from the point of decompression at that level, is calculated from the expression:

$$f_s = \frac{1}{A_p + A_s}\left(\frac{M}{z} - F_o\right)$$

(8) Increase of Curvature

The calculated stress and strain in the reinforcement and the strain at the top of the cracked section enable the total curvature to be calculated from the expression given in Eqn.(5.1). The curvature increment is then the difference of the total curvature and the curvature when the concrete ceases to be compressive at the level of the reinforcement.

The procedure is repeated from step (2) for varying levels of prestress. In this calculation, the area of prestressed reinforcement was varied from zero (ordinary reinforced concrete) to unity (fully prestressed) in steps of 0.05 times the equilavent area as defined in Eqn.(9.4).

All the steps, from (1) to (8) are then repeated for other reinforcement ratios and also for cross-sections of different shape.

CHAPTER TEN

Discussion of Results

10.1 General

In this Chapter, the results of the analyses of stress and curvature, in relation to the three partial prestressing parameters, are presented and discussed. The range of data used in the investigation and the concrete section references are given in the following two sections.

10.2 Shapes and Reference Numbers of Sections

The three most common shapes with varying cross-sectional areas were studied. These sections were:-

a) Rectangular section

b) A range of symmetrical I-sections with varying ratios of h_f/h and b_w/b between 0.1 and 0.3

c) A range of symmetrical T-sections with varying ratios of h_f/h and b_w/b between 0.1 and 0.3

The actual unit dimensions of all the sections investigated are given in Table 10.1.

A simple reference system has been adopted for all the sections studied. The first letter designates the shape of the section, T, I and R indicating T-section, I-section and rectangular section respectively. The last two numerals

Section References	$\frac{b_w}{b}$	$\frac{b_i}{b}$	$\frac{h_f}{h}$	$\frac{h_b}{h}$	Reinforcement Ratio $\frac{A_{eq}}{bd}$		
					Max.	Med.	Min.
R-1.0	1.0	1.0	1.0	1.0	0.0075	0.0045	0.0015
T-0.1	0.1	0.1	0.1	0.0	0.0019	0.0o1	0.00015
T-0.2	0.2	0.2	0.2	0.0	0.00355	0.0019	0.0003
T-0.3	0.3	0.3	0.3	0.0	0.004939	0.0027	0.00045
I-0.1	0.1	1.0	0.1	0.1	0.0019	0.0011	0.0003
I-0.2	0.2	1.0	0.2	0.2	0.00355	0.002	0.0006
I-0.3	0.3	1.0	0.3	0.3	0.004939	0.0029	0.0009

Table 10.1: Section references and data of investigation

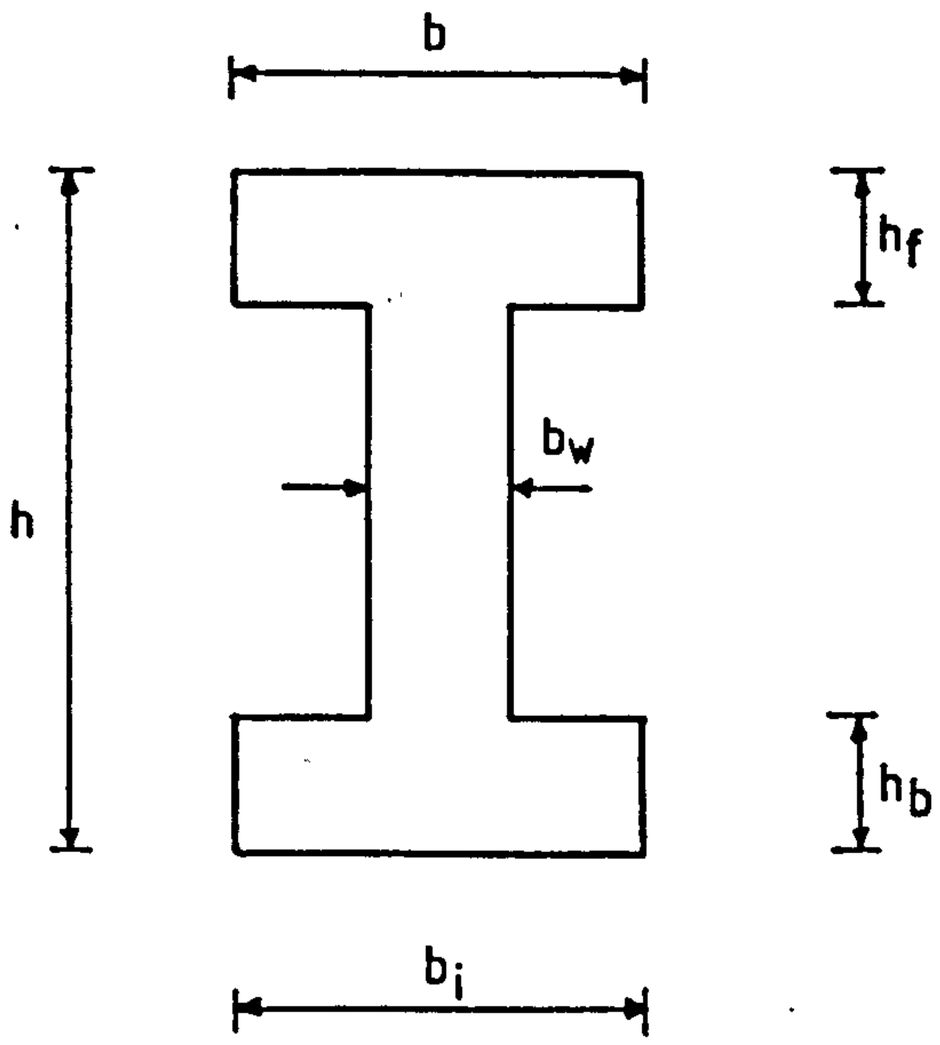

represent the web breadth to overall breadth ratio which is also equal to the flange depth to overall depth ratio in these examples. Hence, T-0.1 refers to a T-section with flange depth to overall depth and web breadth to overall breadth ratios of 0.1. The full range of section references is given in Table 10.1 which shows the corresponding flange depth and web breadth ratios for a generalised I-section.

10.3 Reinforcement Ratio

As pointed out in Chapter Nine, the reinforcement ratio is one of the major parameters affecting the curvature and reinforcement stresses in a section. Thus, in this series of investigations, three levels of reinforcement namely, the maximum, medium and minimum reinforcement ratios, were studied for each section, so as to cover the full range of practical design cases.

The 'design' ultimate moments of the sections were calculated according to CP110 with materials safety factors of 1.15 and 1.5 for steel and concrete respectively. The reinforcement ratios were expressed as the ratios of the equivalent reinforcement areas to the total areas, the flange breadth multiply by the effective depth (bd).

The maximum reinforcement ratios are the ratios for which at the ultimate load, the neutral axis/effective depth ratio is equal to 0.655, the maximum allowable in CP110 for members with pretensioned tendons. The minimum

reinforcement ratios were taken as 0.15% b_t d in accordance with CP110 Section 3.11.4.1, where d is the effective depth and b_t is the breadth of the section. For I and T sections, b_t was taken as the average breadth below the upper flange. In the analysis, b_t was calculated by dividing the concrete area below the top flange by the depth below the same level. The medium reinforcement ratio for a section, was the mean of the maximum and the minimum values. The calculated ratios used in the investigation are given in Table 10.1.

10.4 Discussion of Results

10.4.1 Reinforcement Stresses - Parameters Relationships

Figs.10.1 to 10.7 show the relationships between the Partial Prestressing Ratio (PPR) and the increase of reinforcement stress (f_s), for varying amounts of reinforcement and shapes of section. Generally, the curves show that f_s decreases as the value of PPR increases towards one, which denotes the section without non-prestressed reinforcement, defined as "fully prestressed" (16). The results indicate that the reinforcement stresses and hence the crack width, can be controlled by varying the value of PPR, although the relationship is not linear.

For values of PPR less than about 0.15, for example between points (1) and (2) in Fig.10.2, generally, there is an increase of stress in the reinforcement as the value of PPR increases. With such low values of PPR and hence low prestress, the calculated shrinkage loss was more than the

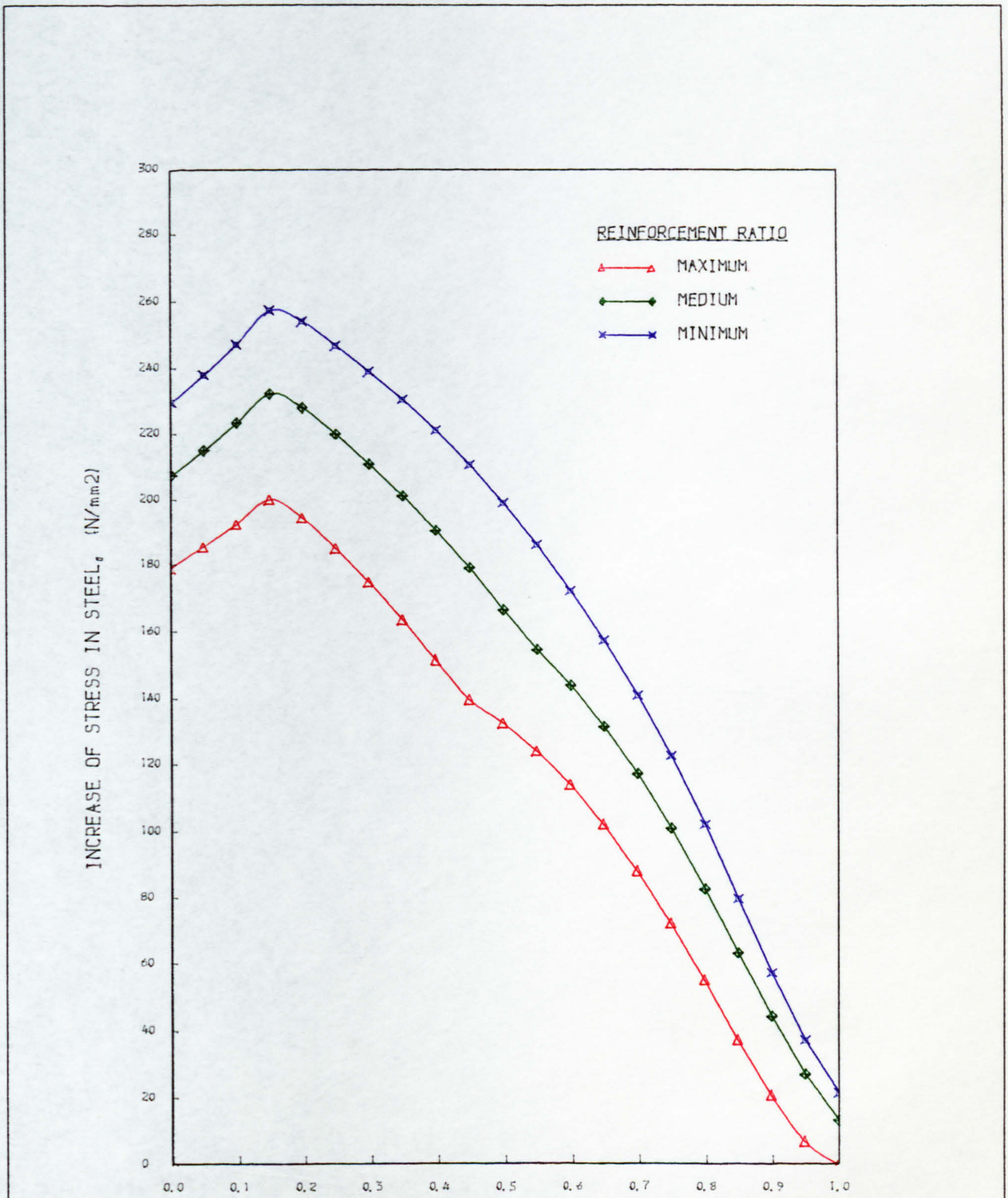

Fig. 10.1 PPR - REINFORCEMENT STRESSES RELATIONSHIP

SECTION R-1.0

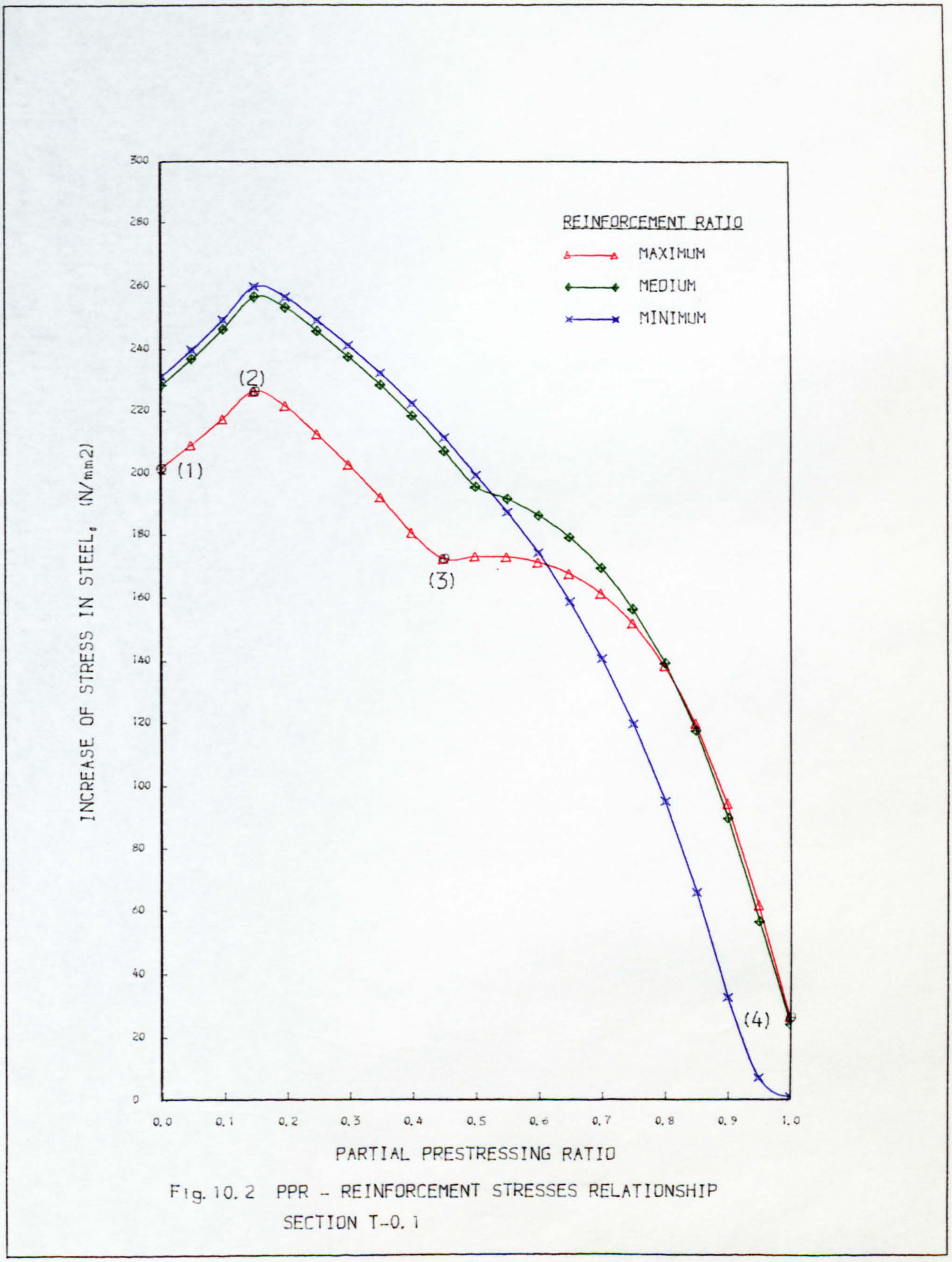

Fig. 10.2 PPR - REINFORCEMENT STRESSES RELATIONSHIP
SECTION T-0.1

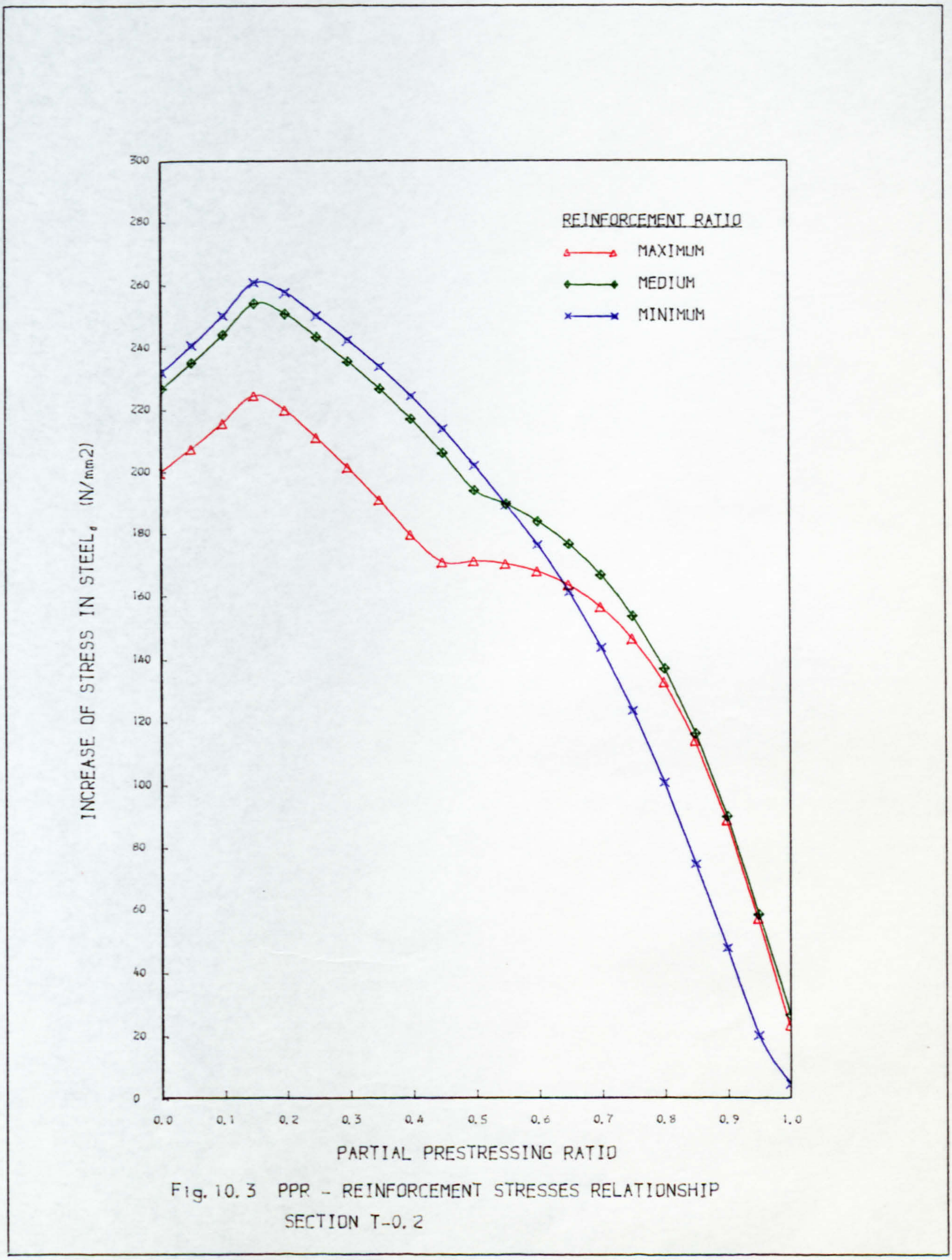

Fig. 10.3 PPR - REINFORCEMENT STRESSES RELATIONSHIP

SECTION T-0.2

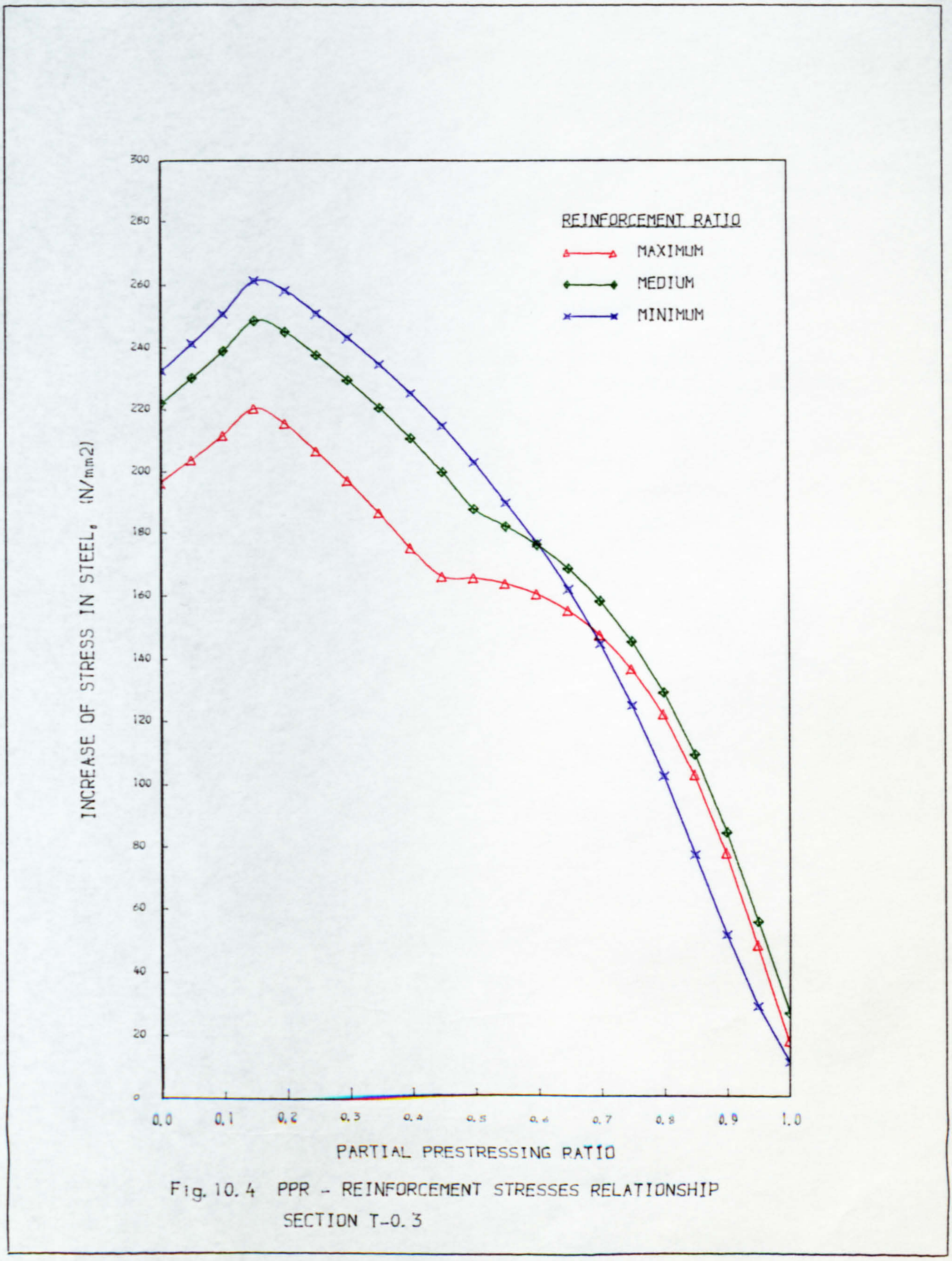

Fig. 10.4 PPR - REINFORCEMENT STRESSES RELATIONSHIP
SECTION T-0.3

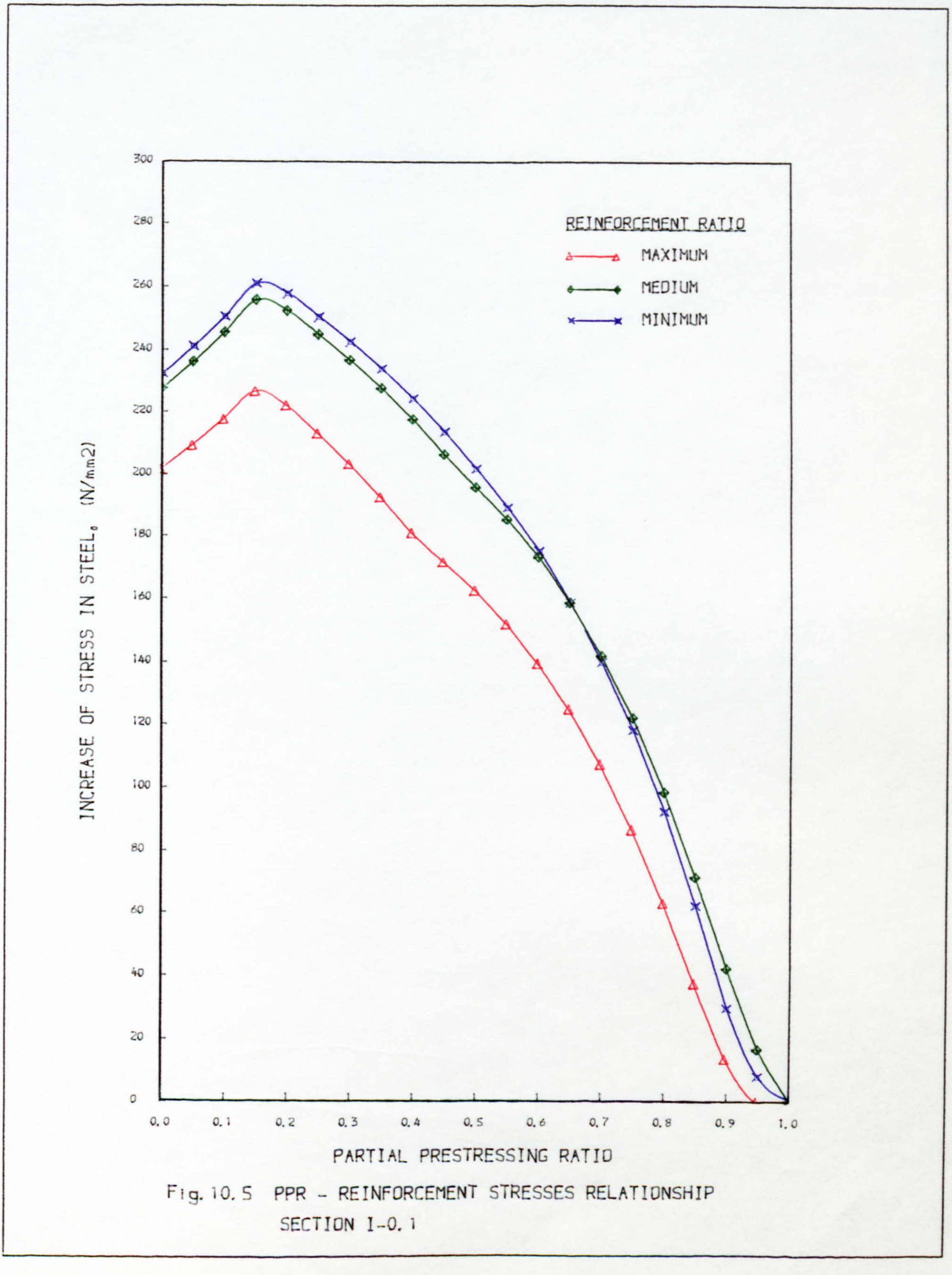

Fig. 10.5 PPR - REINFORCEMENT STRESSES RELATIONSHIP
SECTION I-0.1

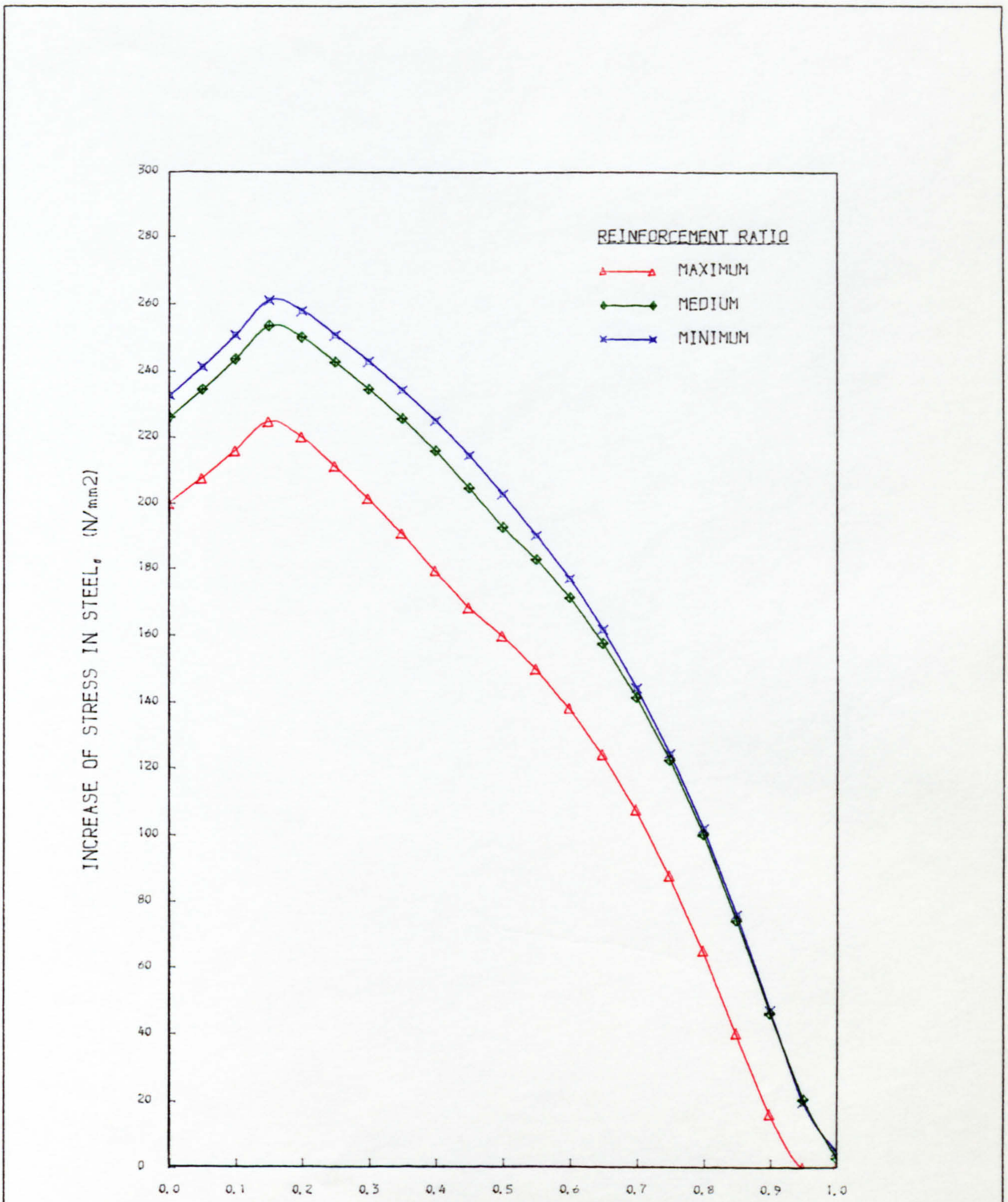

Fig. 10.6 PPR - REINFORCEMENT STRESSES RELATIONSHIP
SECTION I-0.2

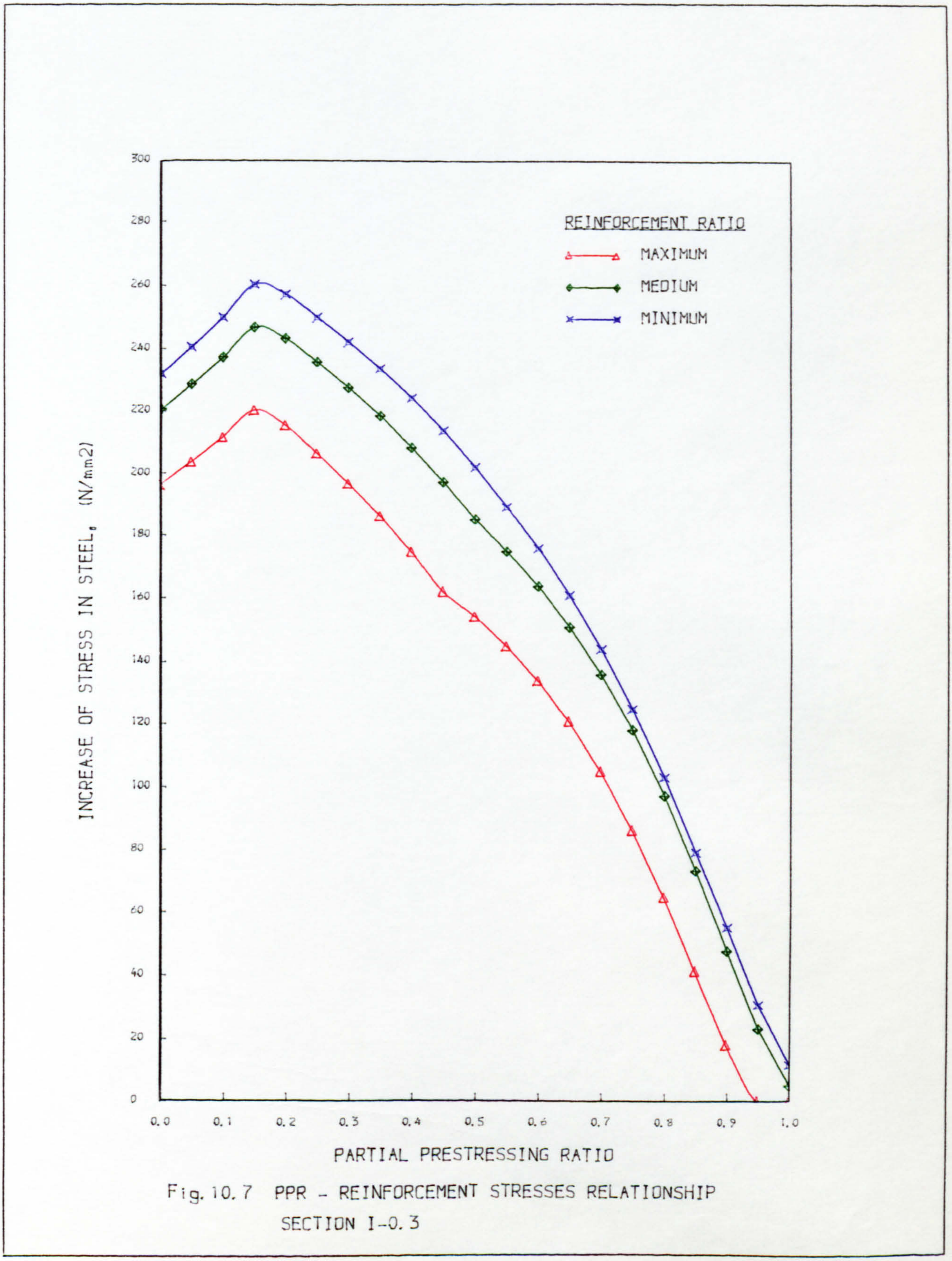

Fig. 10.7 PPR - REINFORCEMENT STRESSES RELATIONSHIP
SECTION I-0.3

prestress in the steel and it was therefore decided to ignore the prestressing force and treat the sections as ordinary reinforced concrete. Thus, in these cases, f_s would be expected to increase as PPR increases and the total area of reinforcement required for the ultimate moment becomes less.

Referring again to Fig.10.2, for all the sections between points (2) and (4), losses due to creep and shrinkage (calculated according to CP110), were taken into account when the reinforcement stresses were calculated except between points (2) and (3) where the prestress was less than the bending stress due to dead load alone and hence, creep loss was ignored. The sudden change of slope in the curve at point (3) in which the losses due to creep were taken into account, is more obvious in sections with smaller concrete areas and therefore higher prestress. For example, in Section T-0.1 (smaller concrete area), the creep losses were larger than Sections I-0.1 or R-1.0 (larger concrete area) at the corresponding values of PPR and reinforcement ratio.

For smaller values of PPR, generally, the higher the reinforcement ratio (higher prestressing force), the lower are the values of f_s under service loads. For higher values of PPR where losses due to creep were significant, sections with higher reinforcement ratios sometimes show higher increments of steel stress than other sections with low reinforcement ratios and the same value of PPR. The results,

therefore, indicate that the reinforcement stresses and hence the crack width, are affected by the amount of reinforcement, but the effect seems to diminish at higher values of PPR when the losses due to creep are higher in sections with larger amounts of reinforcement.

Figs.10.8 to 10.14 show the relationships of the Degree of Prestress (DEG) and the increase of reinforcement stresses (f_s) with varying ratios of reinforcement and shapes of section. The relationships are very similar to the results for the Partial Prestressing Ratio (PPR). Generally, the curves show that f_s decreases as the value of DEG increases towards unity, when the decompression moment is equal to the service moment and the section is defined as "fully prestressed" (18). This indicates that the reinforcement stresses and crack width can also be controlled by varying the values of DEG.

The effect of losses of prestress due to creep and shrinkage is similar to that observed from the analysis based on the Partial Prestressing Ratio. For the part of the curve between points (1) and (2) in Fig.10.9, when under dead load alone the concrete was in tension at the level of the reinforcement, losses due to creep were ignored.

The results shown in Figs.10.8 to 10.14 clearly indicate that sections with high reinforcement ratios generally have lower incremental stresses than the corresponding sections with lower reinforcement ratios

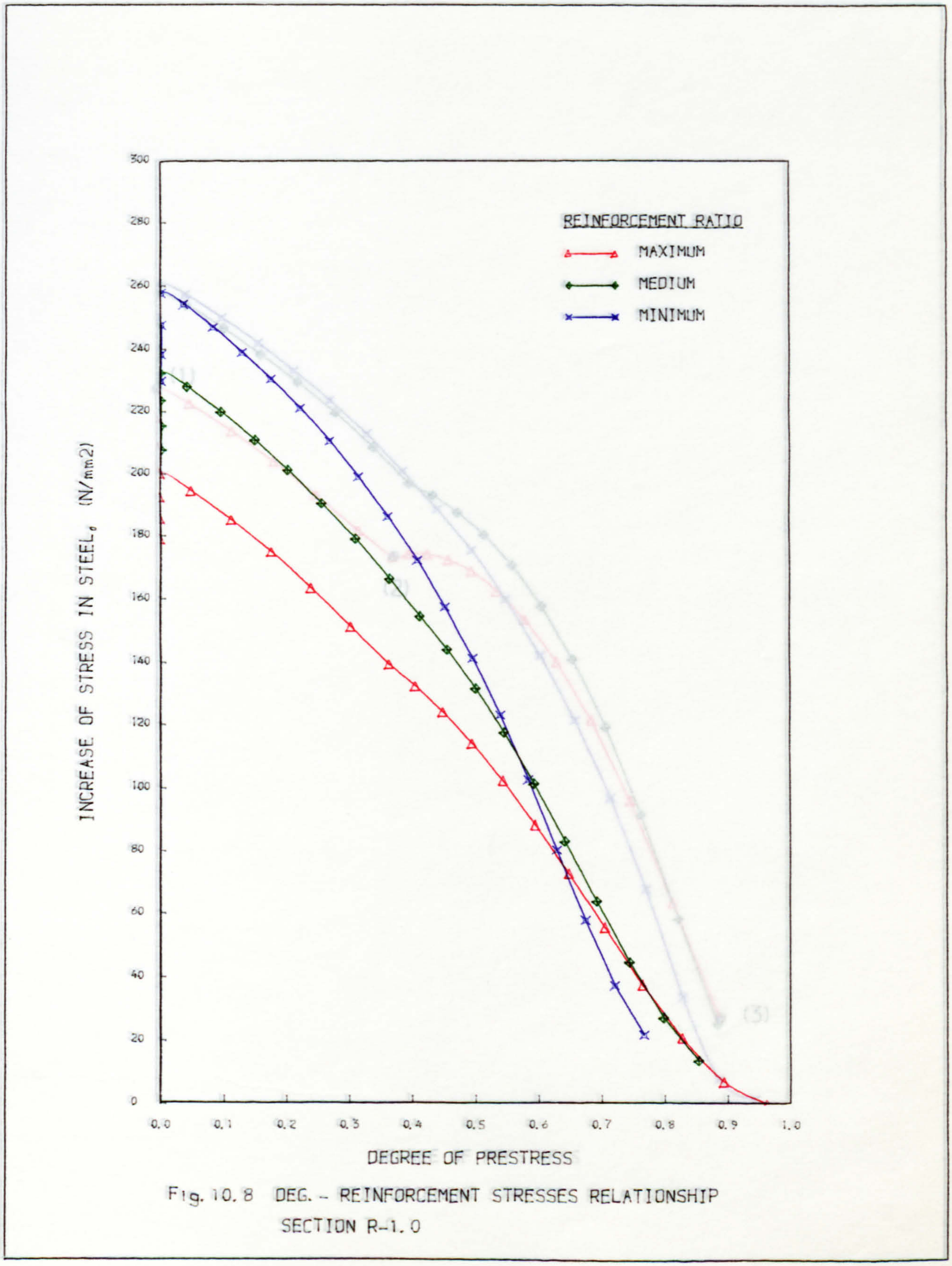

Fig. 10.8 DEG. - REINFORCEMENT STRESSES RELATIONSHIP
SECTION R-1.0

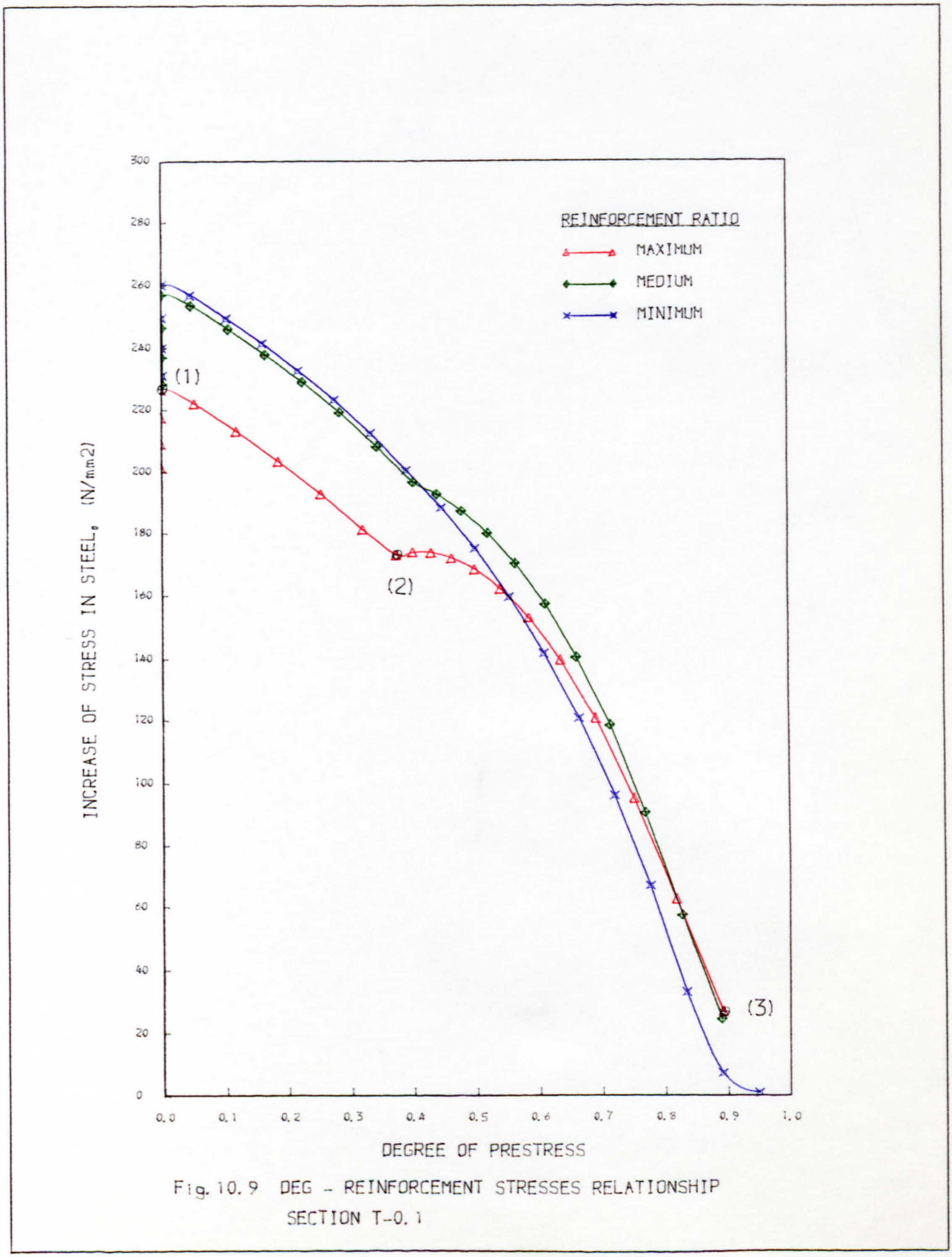

Fig. 10.9 DEG - REINFORCEMENT STRESSES RELATIONSHIP
SECTION T-0.1

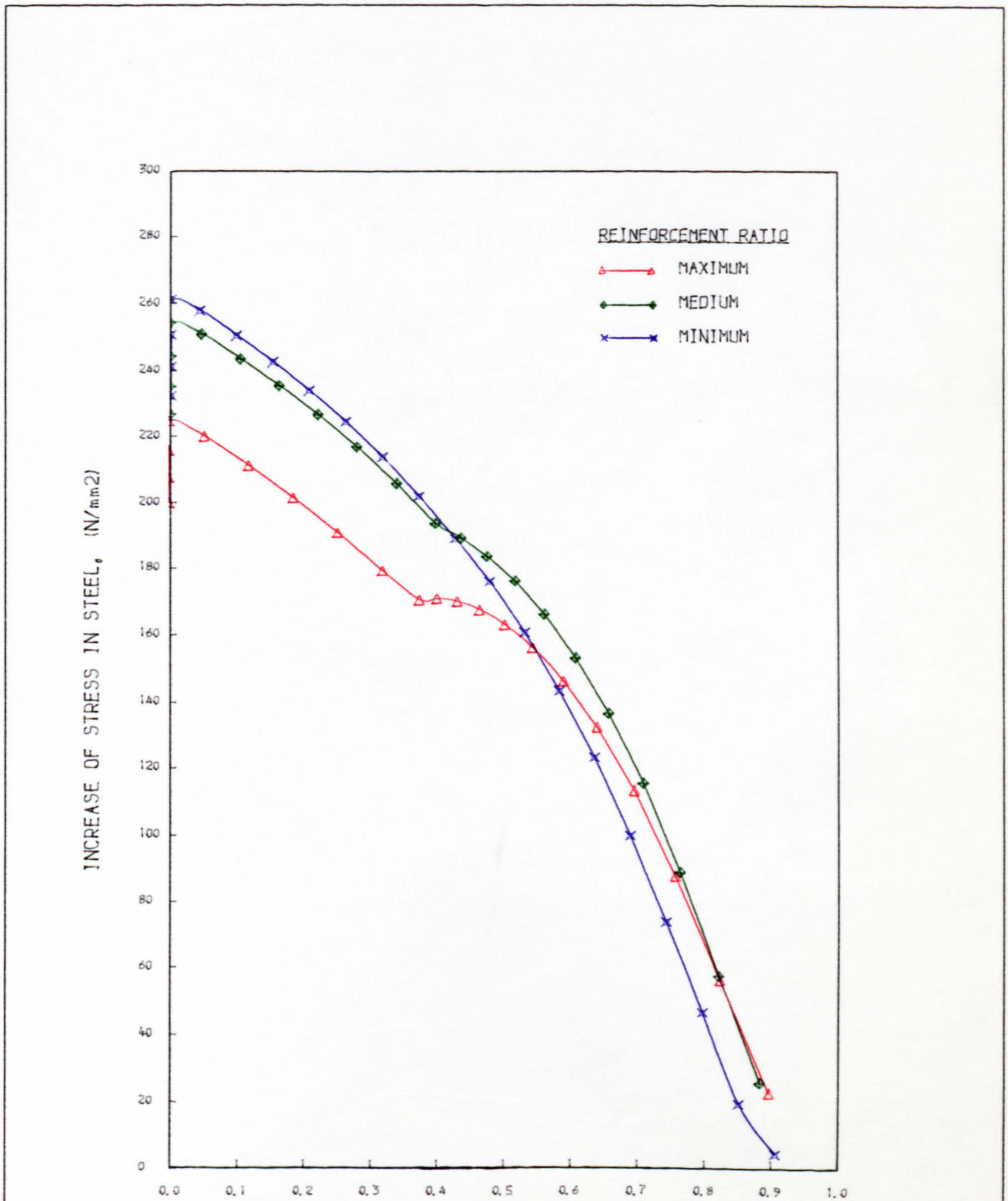

Fig. 10.10 DEG. - REINFORCEMENT STRESSES RELATIONSHIP
SECTION T-0.2

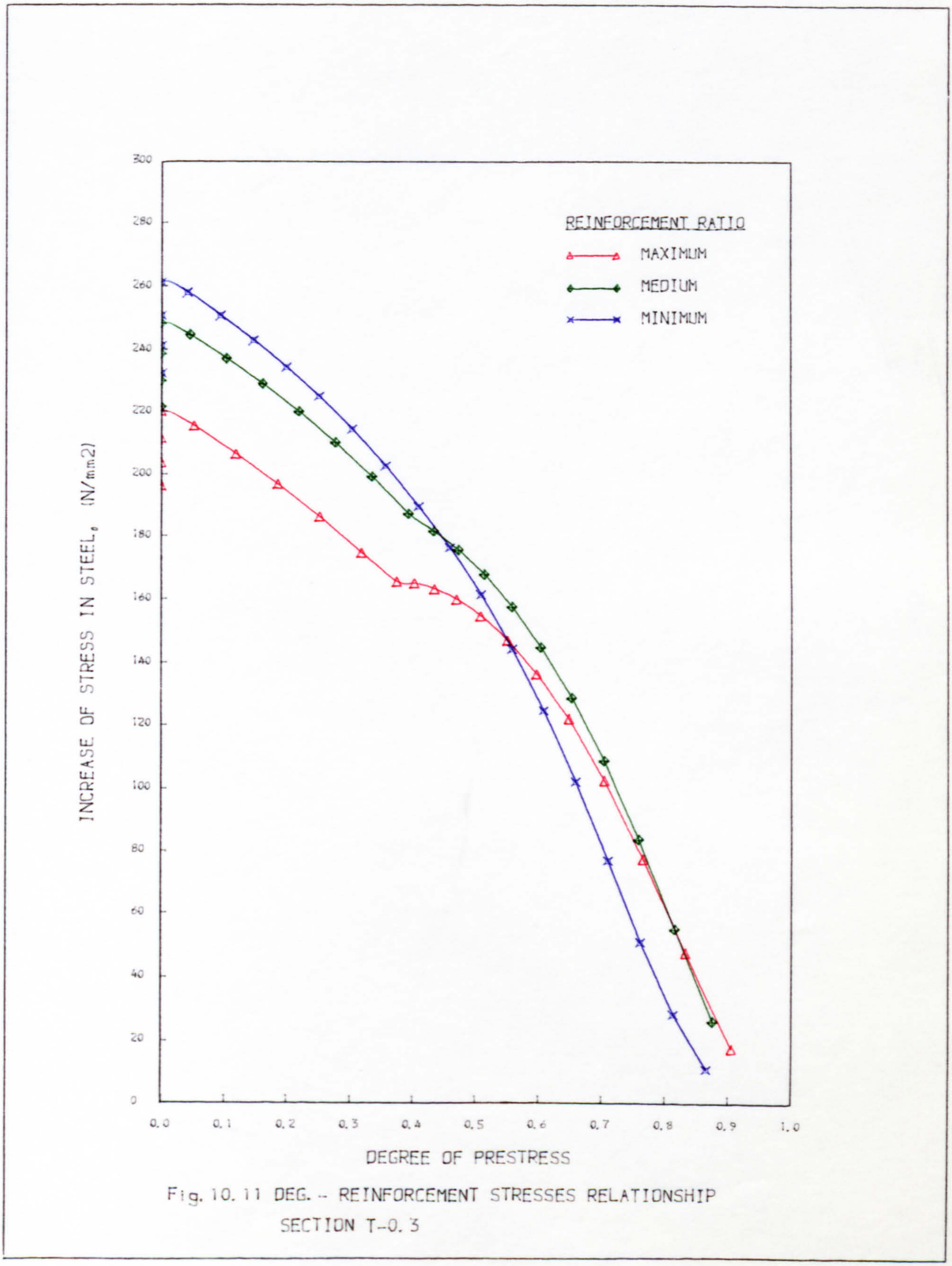

Fig. 10.11 DEG. - REINFORCEMENT STRESSES RELATIONSHIP
SECTION T-0.3

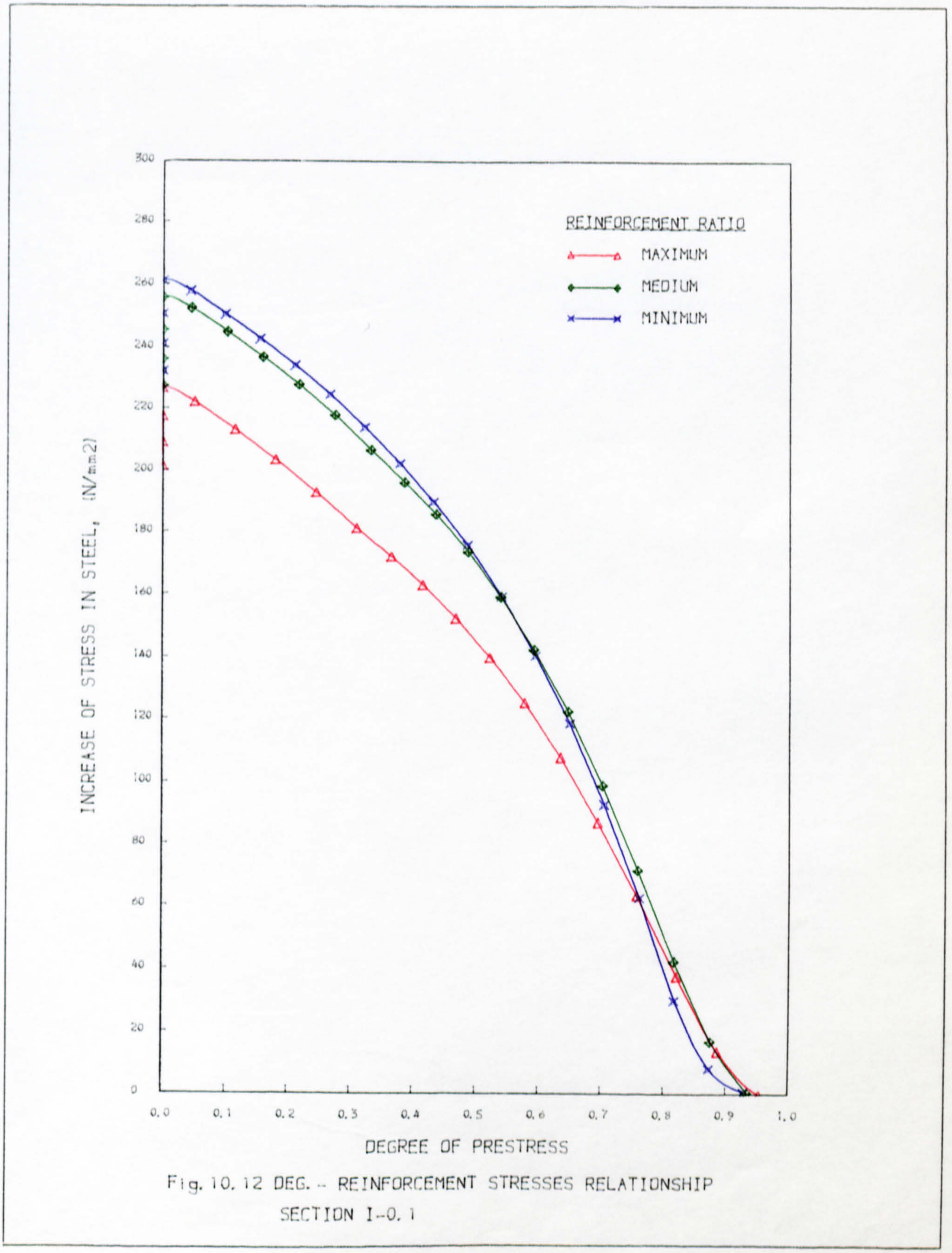

Fig. 10.12 DEG. - REINFORCEMENT STRESSES RELATIONSHIP
SECTION I-0.1

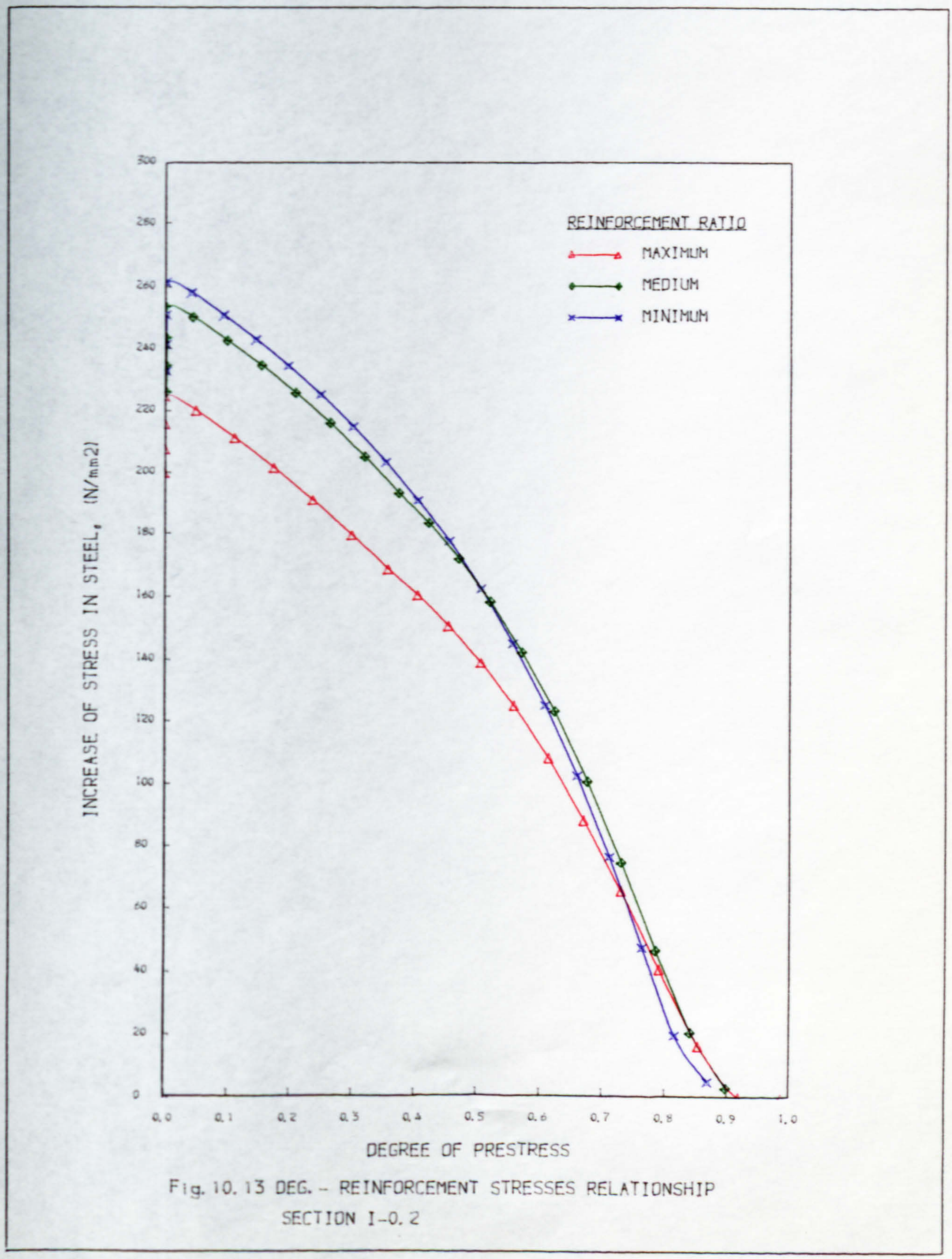

Fig. 10.13 DEG. - REINFORCEMENT STRESSES RELATIONSHIP
SECTION I-0.2

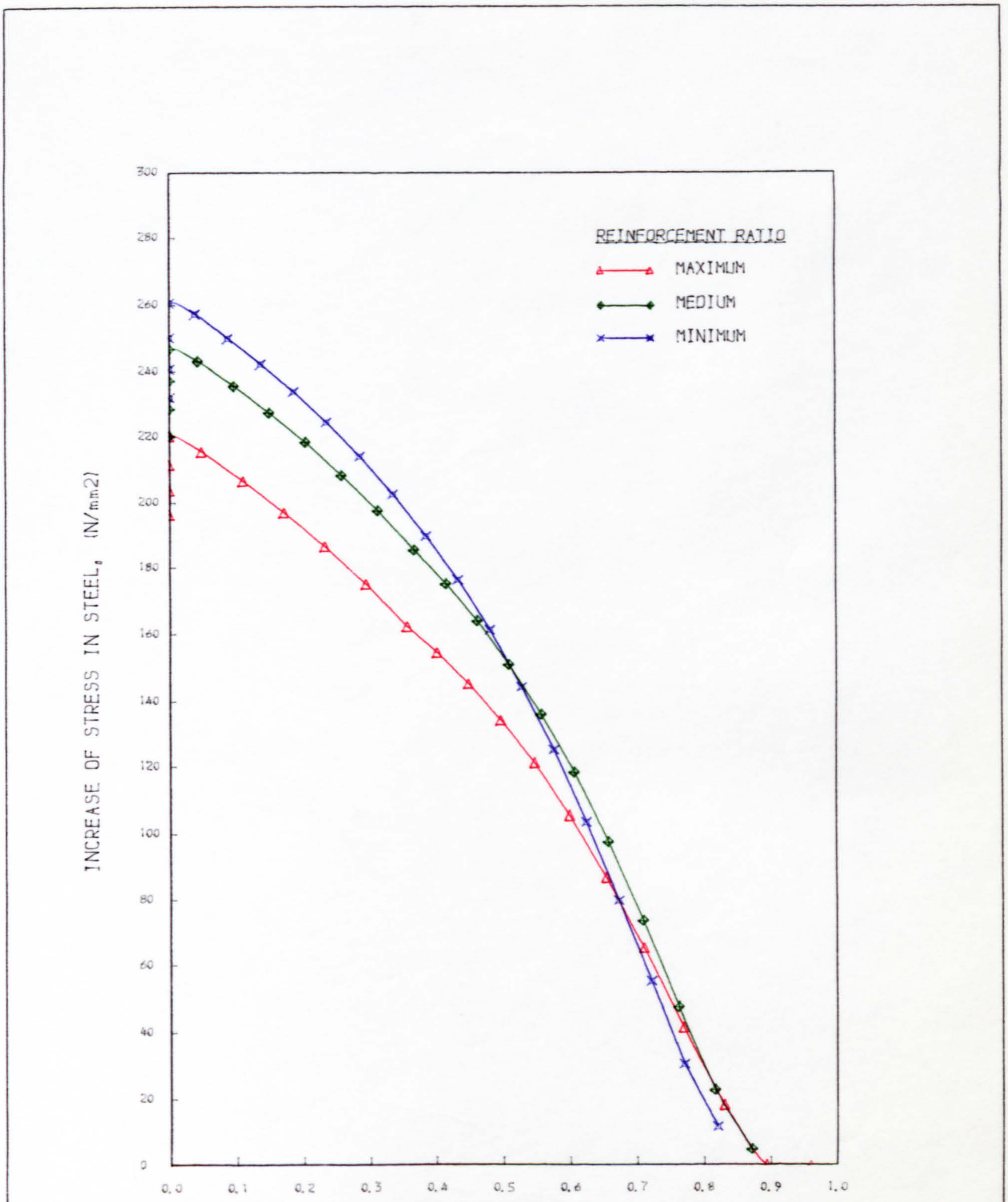

Fig. 10.14 DEG. - REINFORCEMENT STRESSES RELATIONSHIP
SECTION I-0.3

having the same values of DEG. This effect diminishes at higher degrees of prestress when the increased effect of creep, which is greater with high reinforcement ratios, appears to have compensate for the smaller increase of stress. Therefore, at higher values of DEG, the effect of the reinforcement ratio on the incremental steel stress is small.

The relationships between f_s and the hypothetical tensile stress (HYP) with varying ratios of reinforcement and shapes of sections are shown in Figs.10.15 to 10.21. Generally, the value of f_s increases as the fictitious concrete tensile stress increases (under service loads). The slopes of the curves or the rate of increase of f_s, however, depend on the reinforcement ratios. The results, therefore, indicate that f_s is very sensitive to a small change of the hypothetical tensile stress, especially for sections with lower reinforcement ratios. For example, in Fig.10.17, a small change of tensile stress from 0.5 N/sq.mm to 4.0 N/sq.mm in sections with minimum reinforcement, would have increased the value of f_s by about 250 N/sq.mm, but for other sections with maximum reinforcement ratios, a change of tensile stress from 4.0 N/sq.mm to 24 N/sq.mm only increased the value of f_s by about 200 N/sq.mm. The behaviour of the test beams described in Part II of this thesis confirms the above results. The crack widths under service loads only increased by 0.02mm when the hypothetical tensile stresses increased from 7.4 N/sq.mm to 13.52 N/sq.mm. for beams (S1.5.2 and S1.3.5) with high

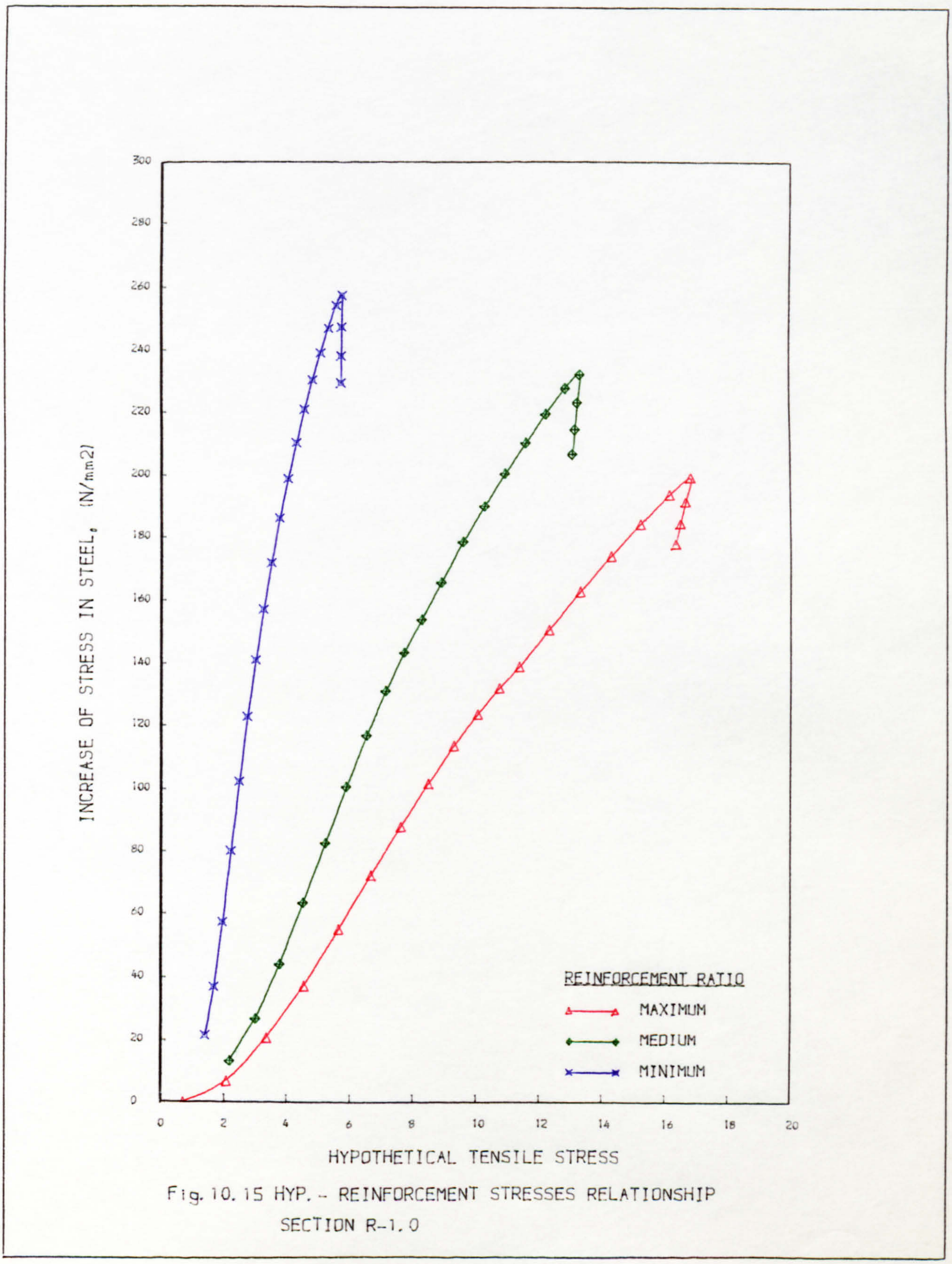

Fig. 10.15 HYP. - REINFORCEMENT STRESSES RELATIONSHIP
SECTION R-1.0

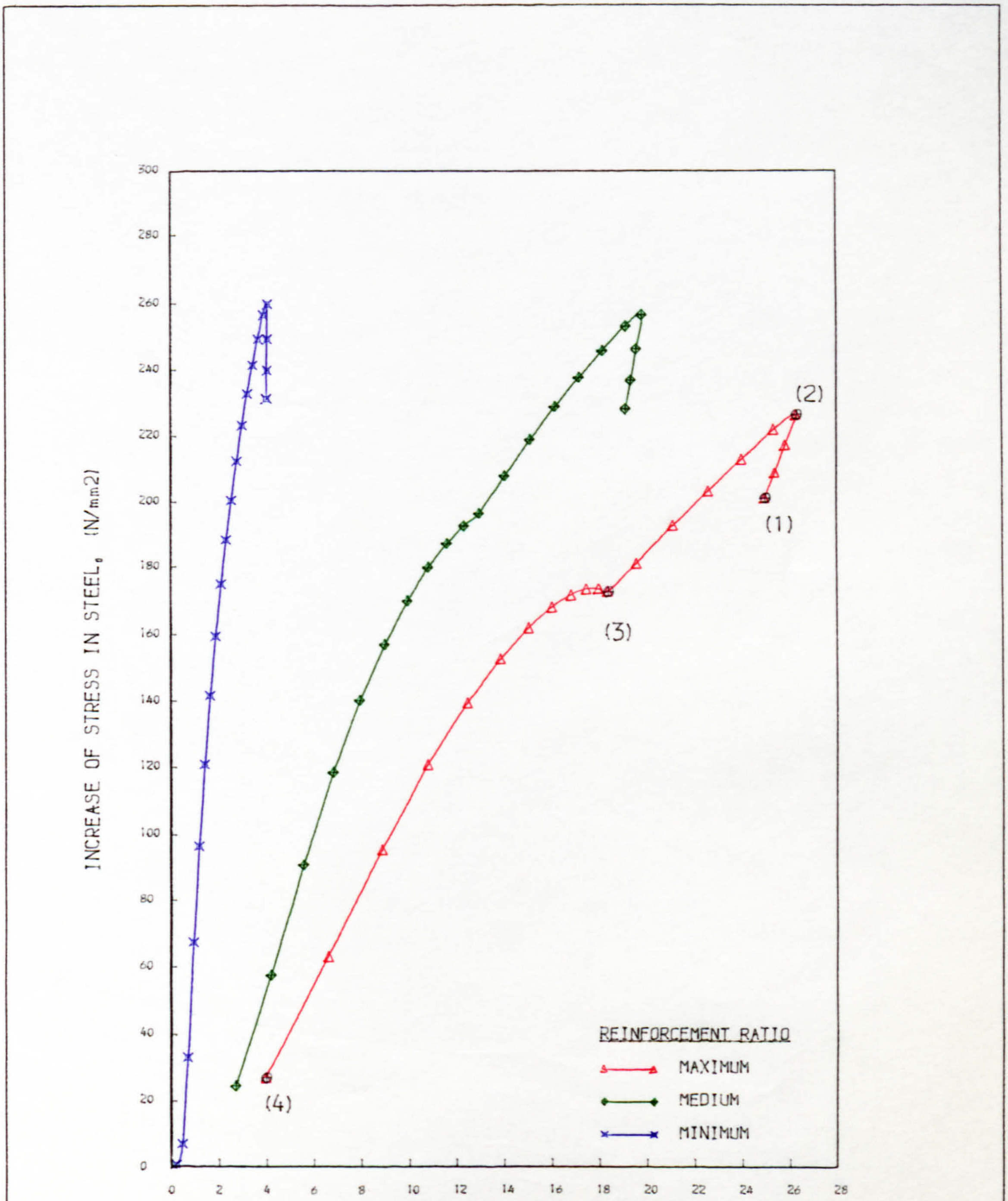

Fig. 10.16 HYP. - REINFORCEMENT STRESSES RELATIONSHIP

SECTION T-O.1

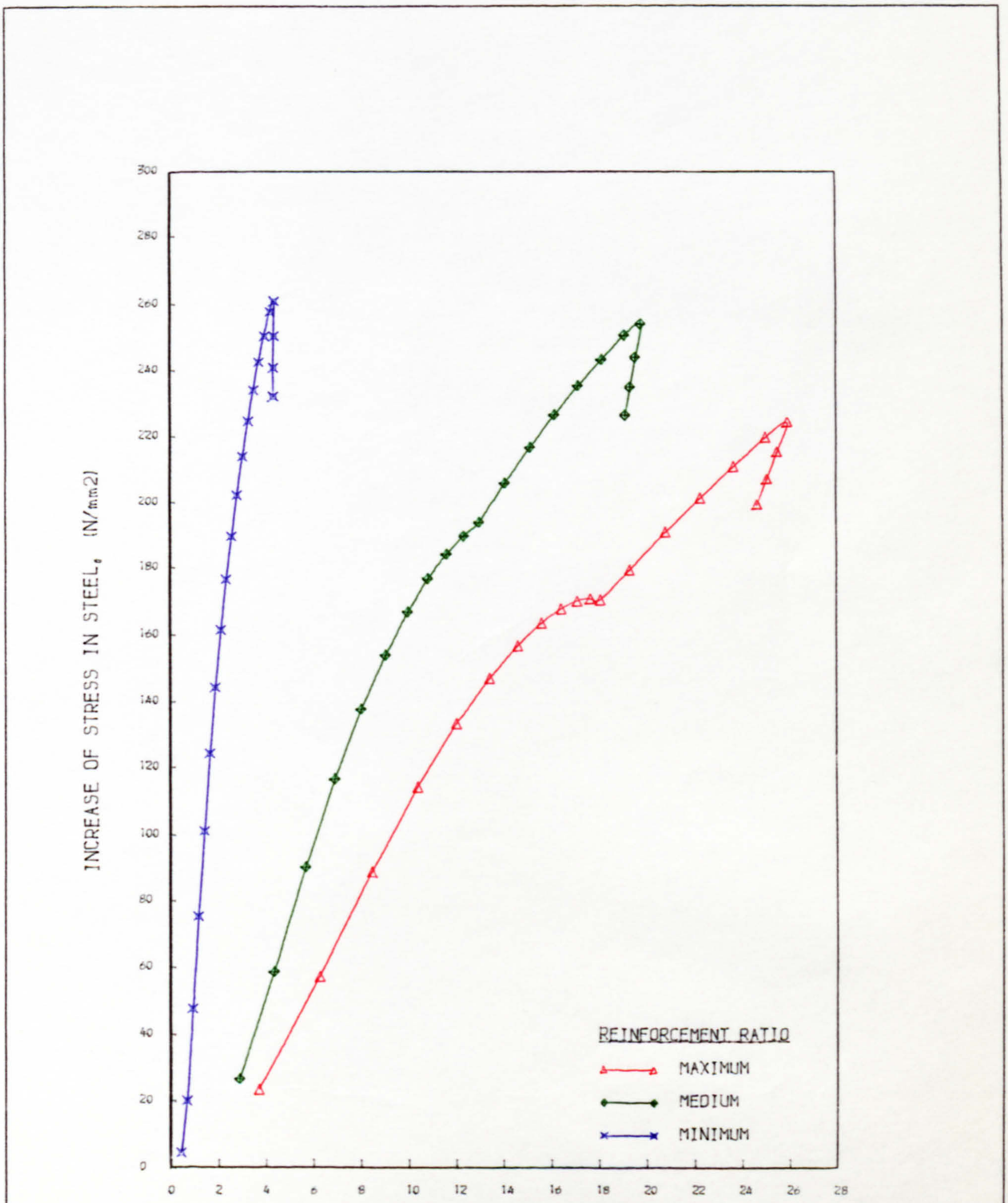

Fig. 10.17 HYP. - REINFORCEMENT STRESSES RELATIONSHIP

SECTION T-0.2

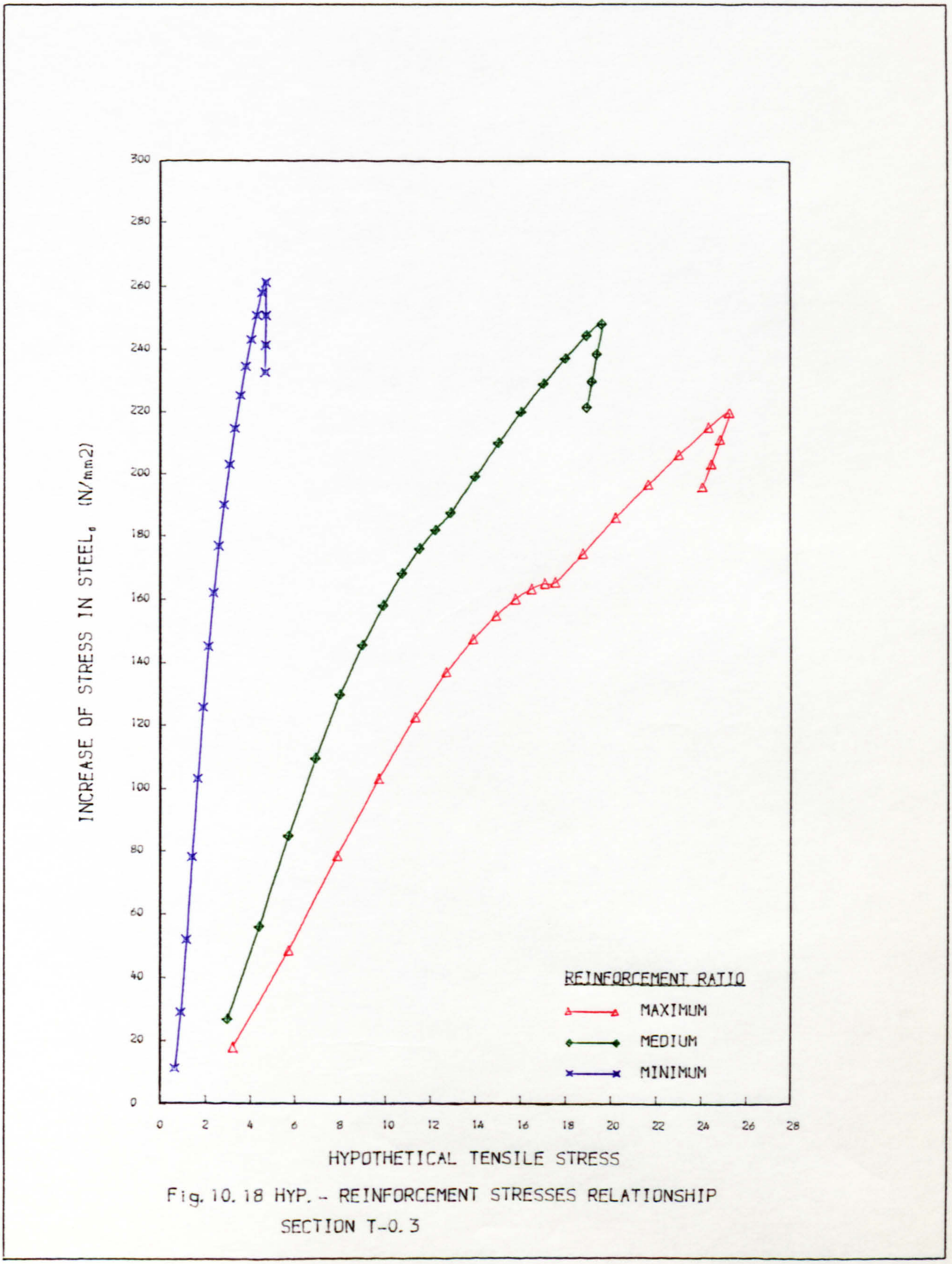

Fig. 10.18 HYP. - REINFORCEMENT STRESSES RELATIONSHIP

SECTION T-0.3

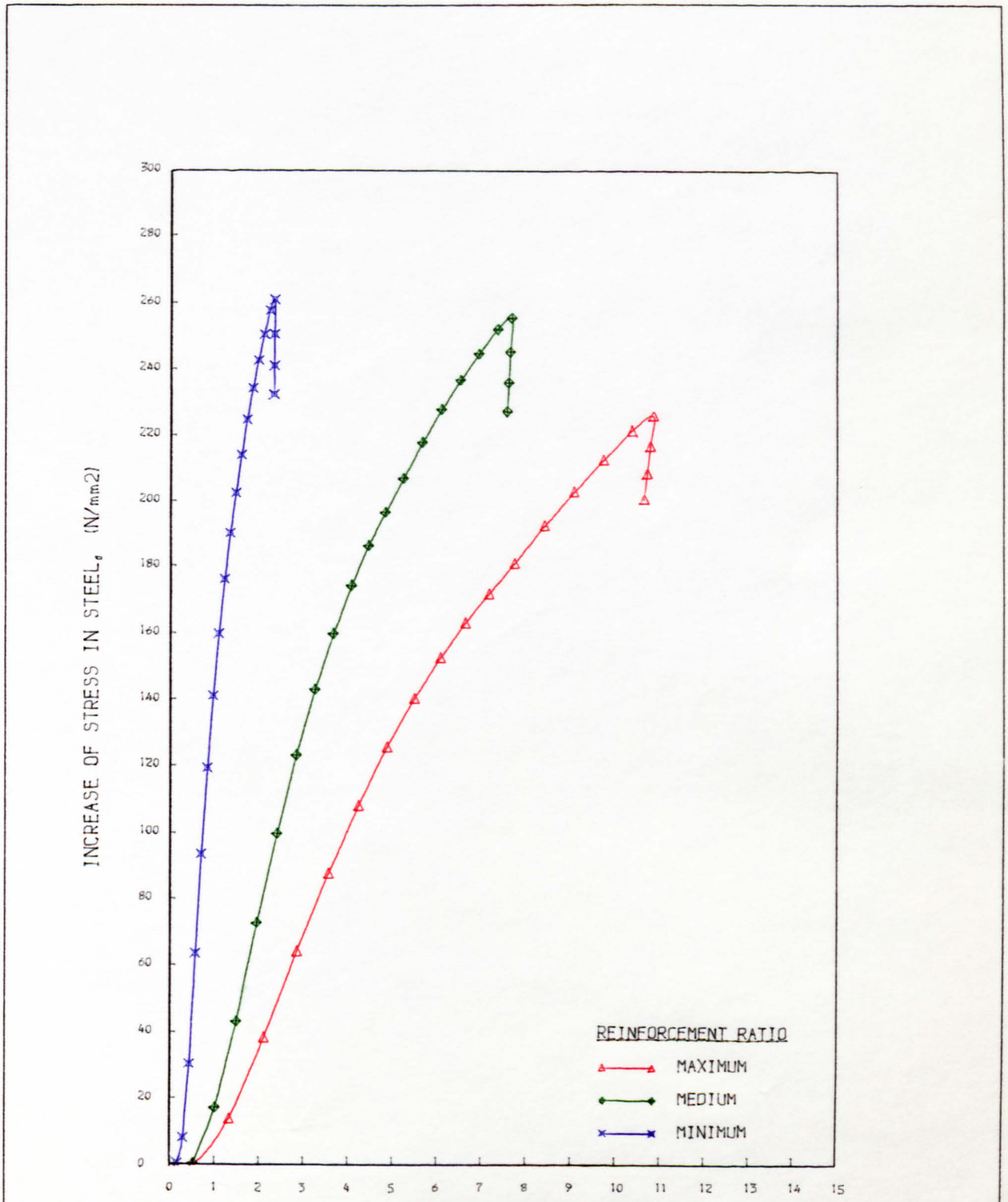

Fig. 10.19 HYP. - REINFORCEMENT STRESSES RELATIONSHIP

SECTION I-0.1

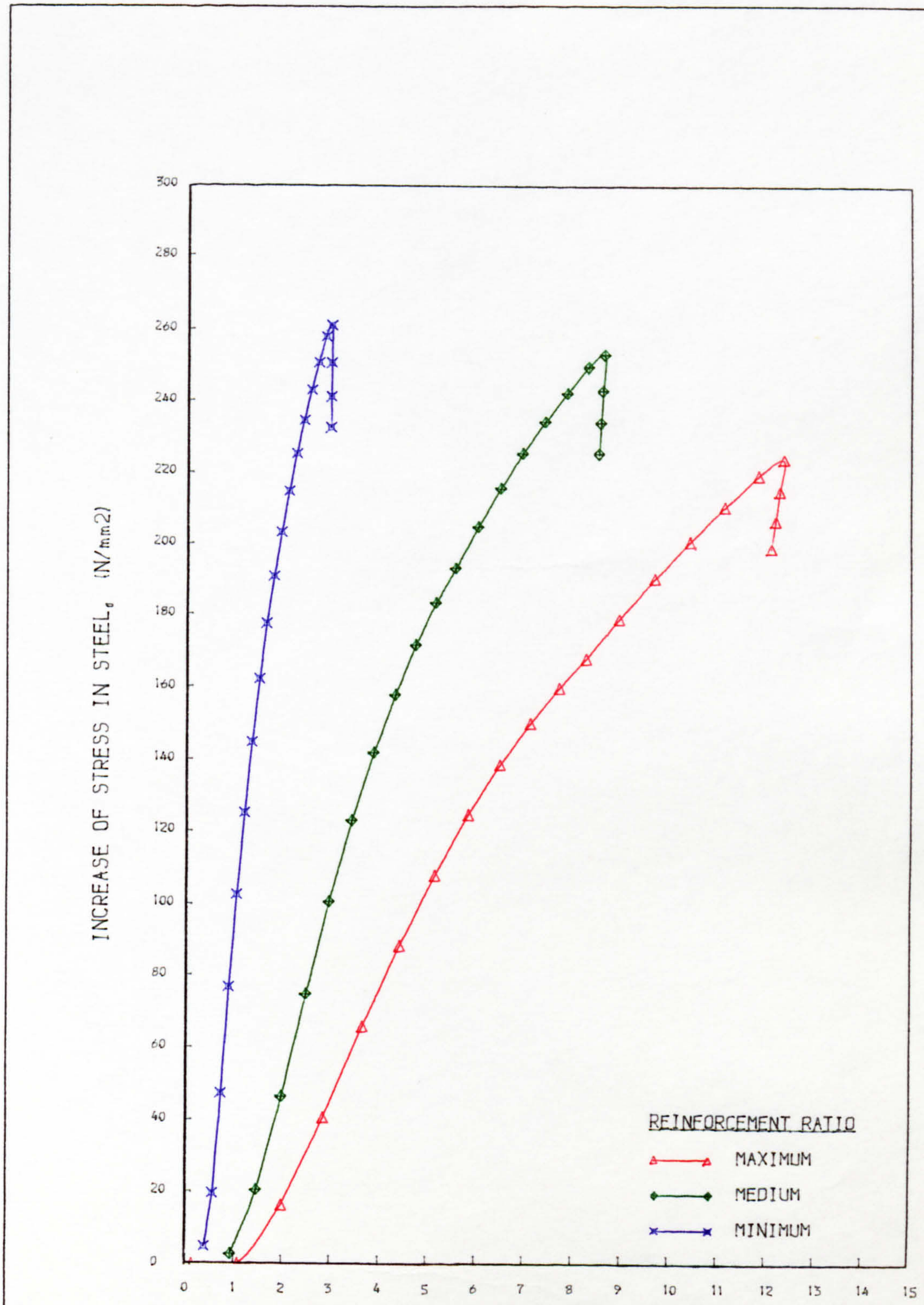

Fig. 10.20 HYP. - REINFORCEMENT STRESSES RELATIONSHIP

SECTION I-0.2

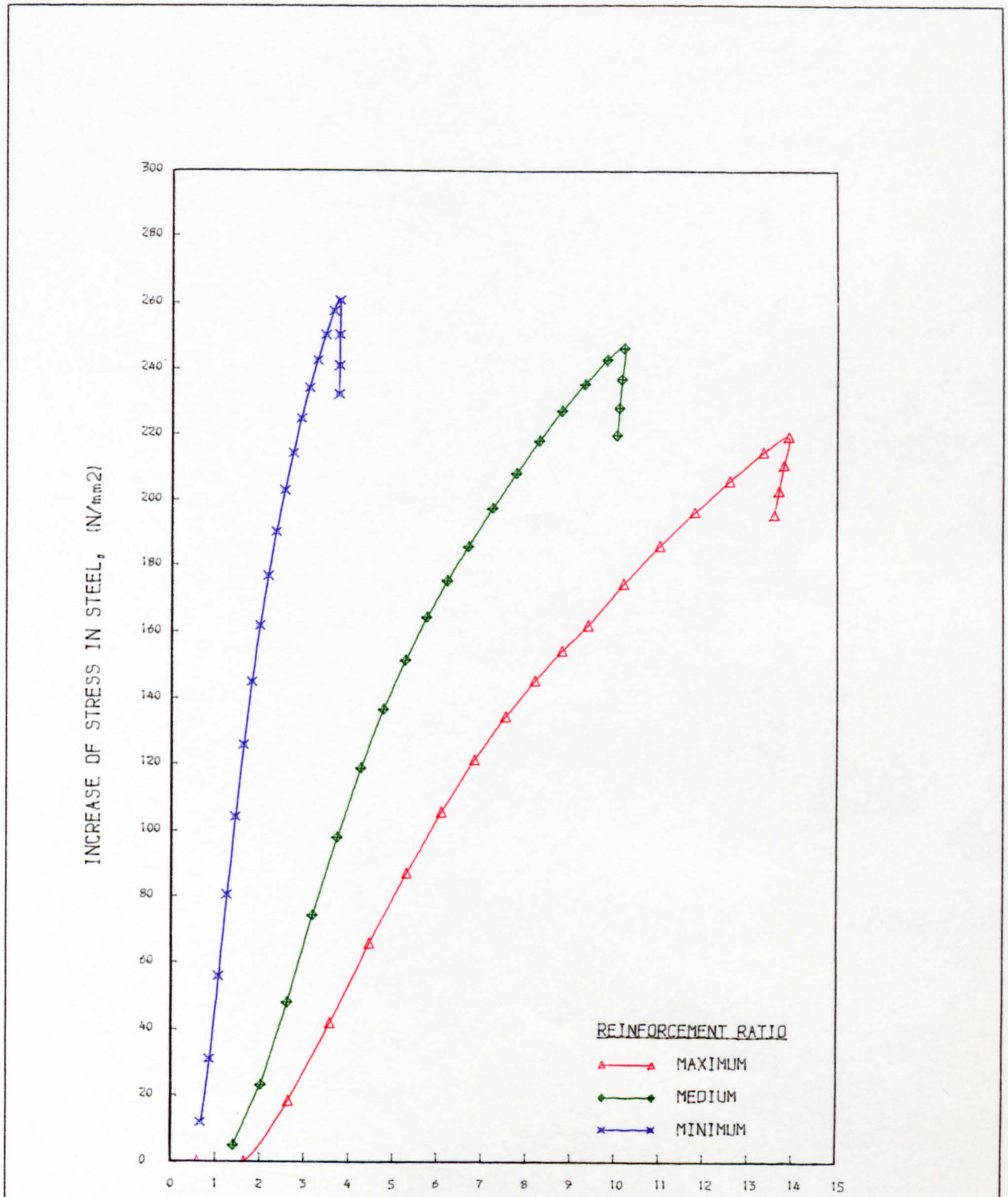

Fig. 10.21 HYP. - REINFORCEMENT STRESSES RELATIONSHIP
SECTION I-0.3

reinforcement ratios whilst in beams with low reinforcement ratios like S3.3.2 and S3.1.6, the crack widths increased by about 0.03mm when the tensile stresses increased from 7.98 N/sq.mm to 12.65 N/sq.mm., (Table 10.2).

In those sections between points (1) and (2) in Fig.10.16, the prestressing forces were smaller than the calculated losses due to shrinkage and hence these sections were analysed as ordinary reinforced concrete. Between points (2) and (3), the concrete at the level of the reinforcement was in tension under the combined effect of prestress and dead load moment and the losses due to creep were therefore ignored.

10.4.2 Curvature - Parameters Relationships

The relationships of the increase in curvature after decompression at the level of reinforcement (1/r), with each of the three parameters are similar to the corresponding relationships with the incremental steel stress, f_s. Figs.10.22 to 10.28, Figs.10.29 to 10.35 and Figs.10.36 to 10.42 show the relationships of 1/r with Partial Prestressing Ratio (PPR), Degree of Prestress (DEG) and Hypothetical Tensile Stress (HYP) respectively. Generally, the results indicate that the curvature and hence, deflection of a member, can be controlled by varying the ratios of PPR or DEG. Unlike reinforcement stresses, however, the values of 1/r are generally larger with higher reinforcement ratios than other sections, with the

Beam References	PPR	DEG	HYP (N/mm^2)	Crack width mm at S.L. (1st cycle)
S1.5.2*	0.83	0.69	7.4	0.04
S1.4.4	0.65	0.56	10.88	0.04
S1.3.5	0.53	0.44	13.52	0.06
S2.4.2	0.79	0.62	8.28	0.06
S2.3.4	0.59	0.47	12.00	0.06
S2.2.6	0.39	0.32	15.88	0.08
S3.3.2	0.74	0.58	7.98	0.05
S3.2.4	0.49	0.38	12.06	-
S3.1.6	0.24	0.20	12.65	0.08

* Strands not fully prestressed due to error in construction

S.L. Service Load

Table 10.2: Partial Prestressing Parameters and crack widths under service loads

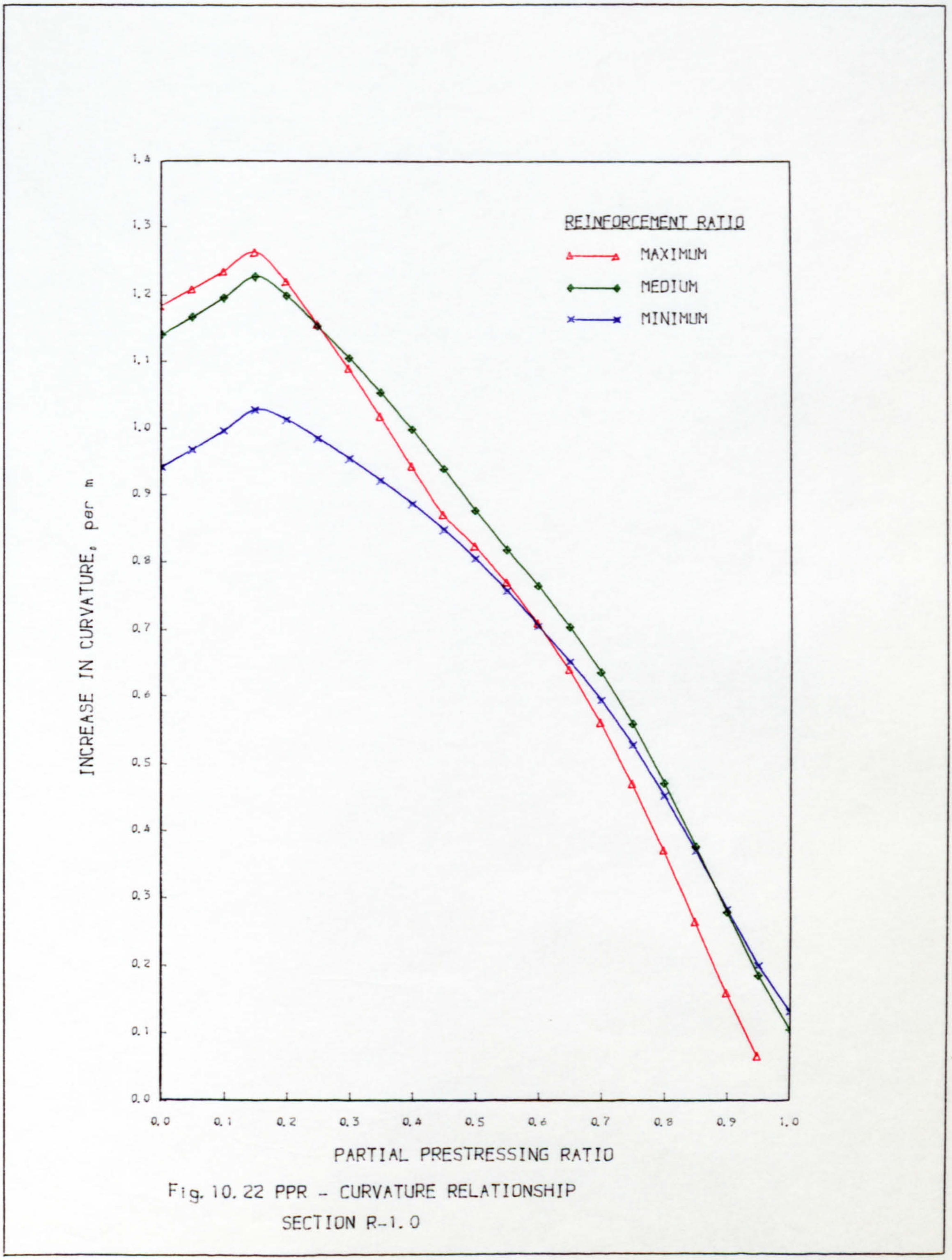

Fig. 10.22 PPR - CURVATURE RELATIONSHIP

SECTION R-1.0

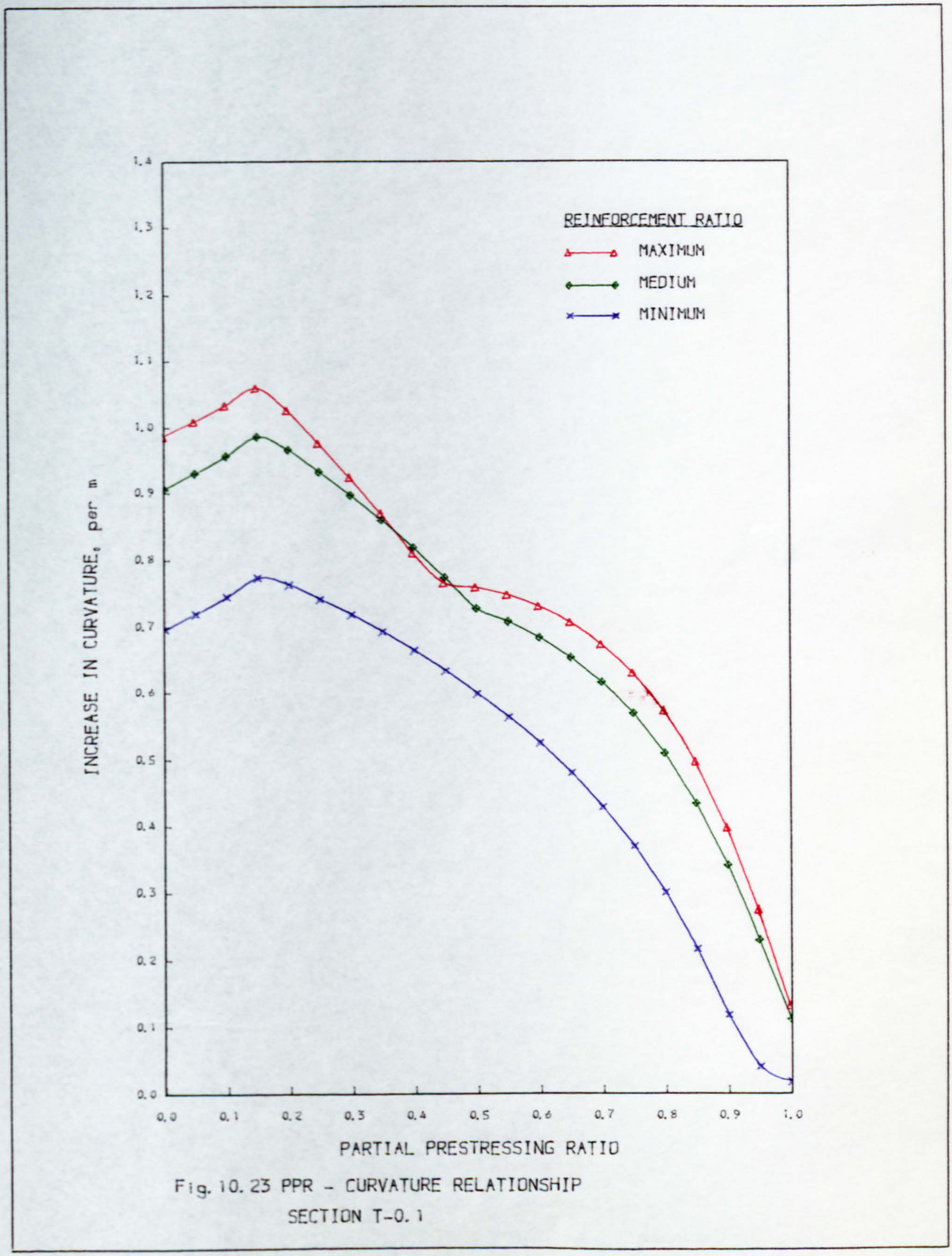

Fig. 10.23 PPR - CURVATURE RELATIONSHIP

SECTION T-0.1

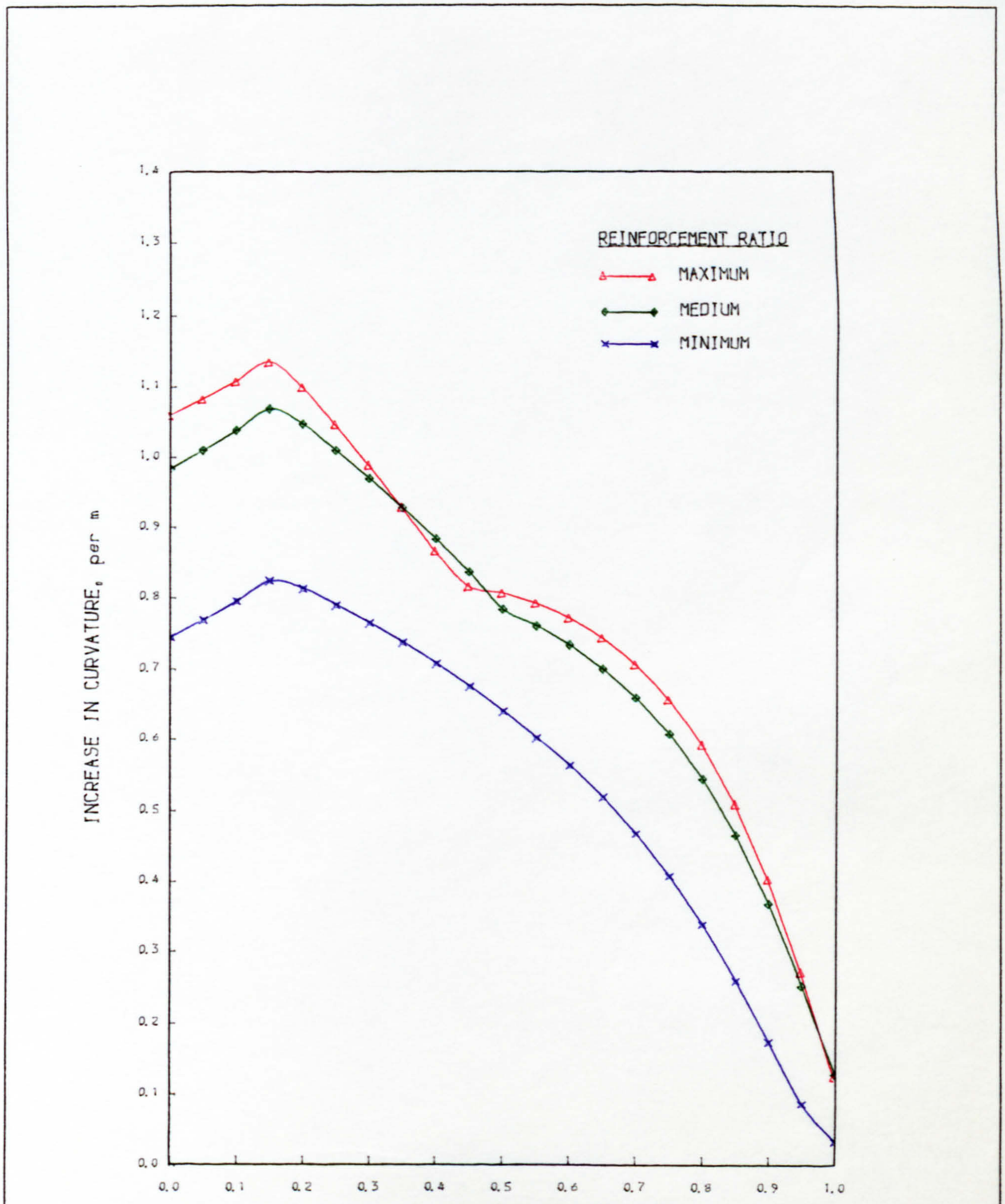

Fig. 10.24 PPR - CURVATURE RELATIONSHIP

SECTION T-0.2

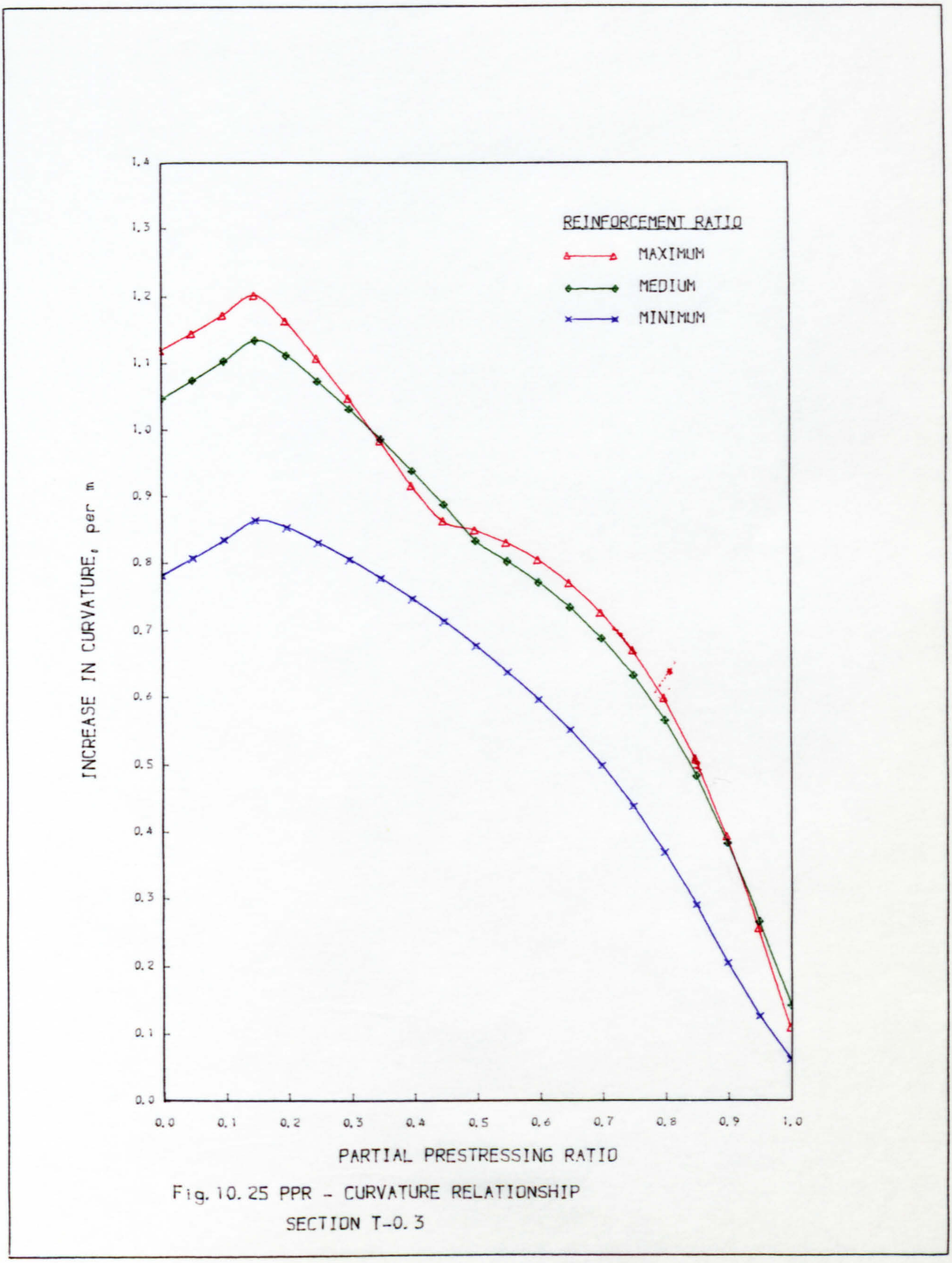

Fig. 10.25 PPR - CURVATURE RELATIONSHIP

SECTION T-0.3

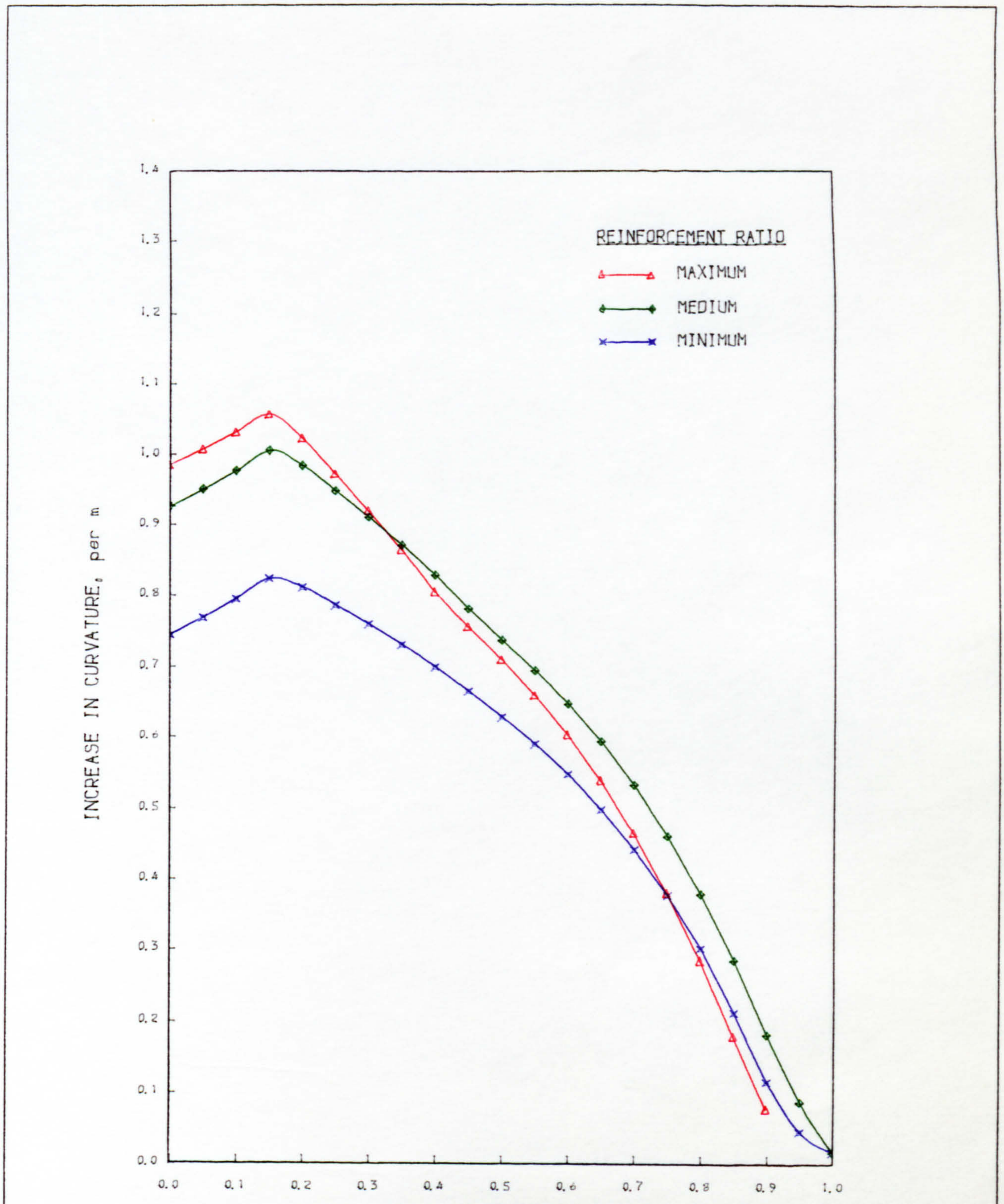

Fig. 10.26 PPR - CURVATURE RELATIONSHIP

SECTION I-0.1

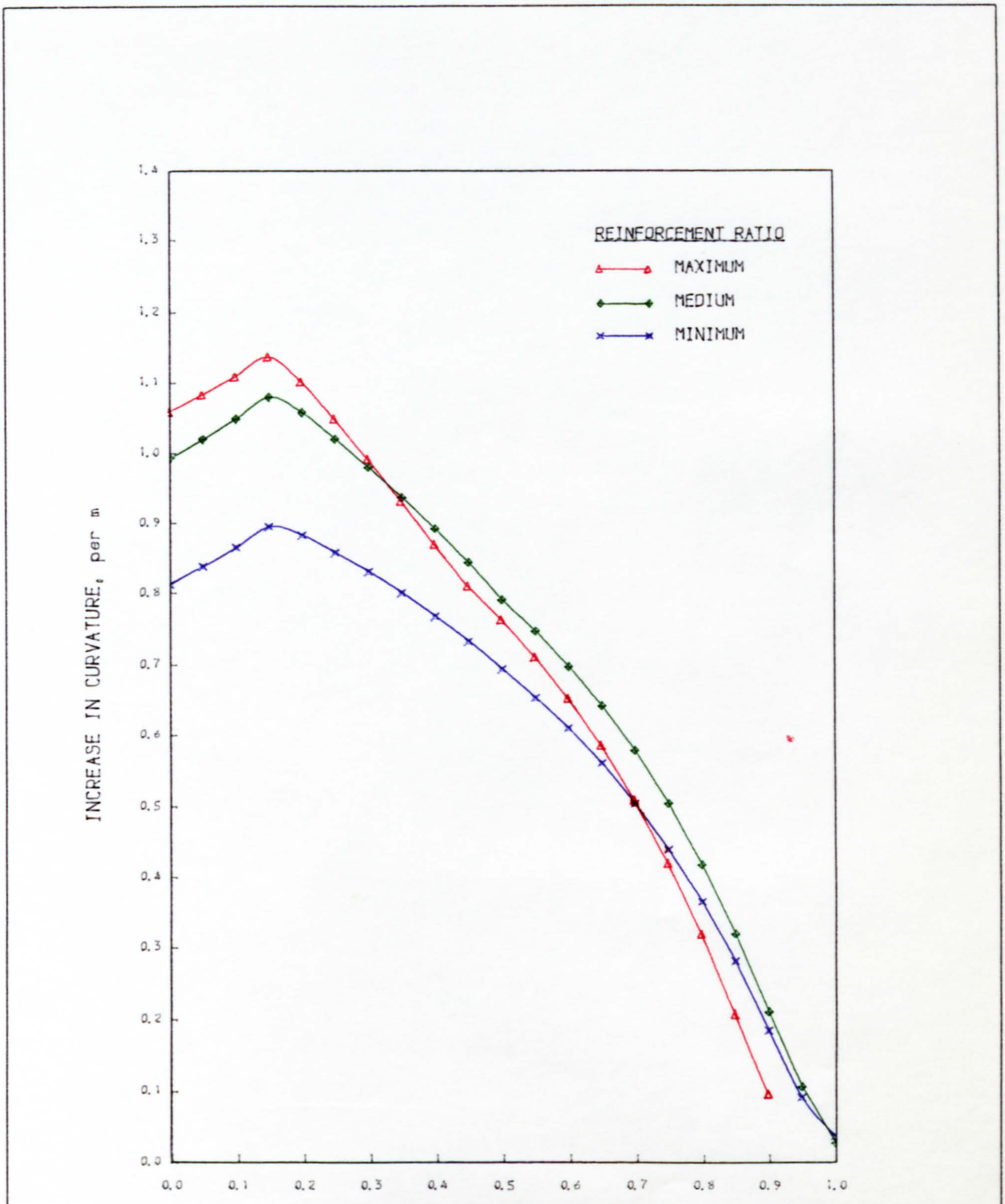

Fig. 10.27 PPR - CURVATURE RELATIONSHIP

SECTION I-0.2

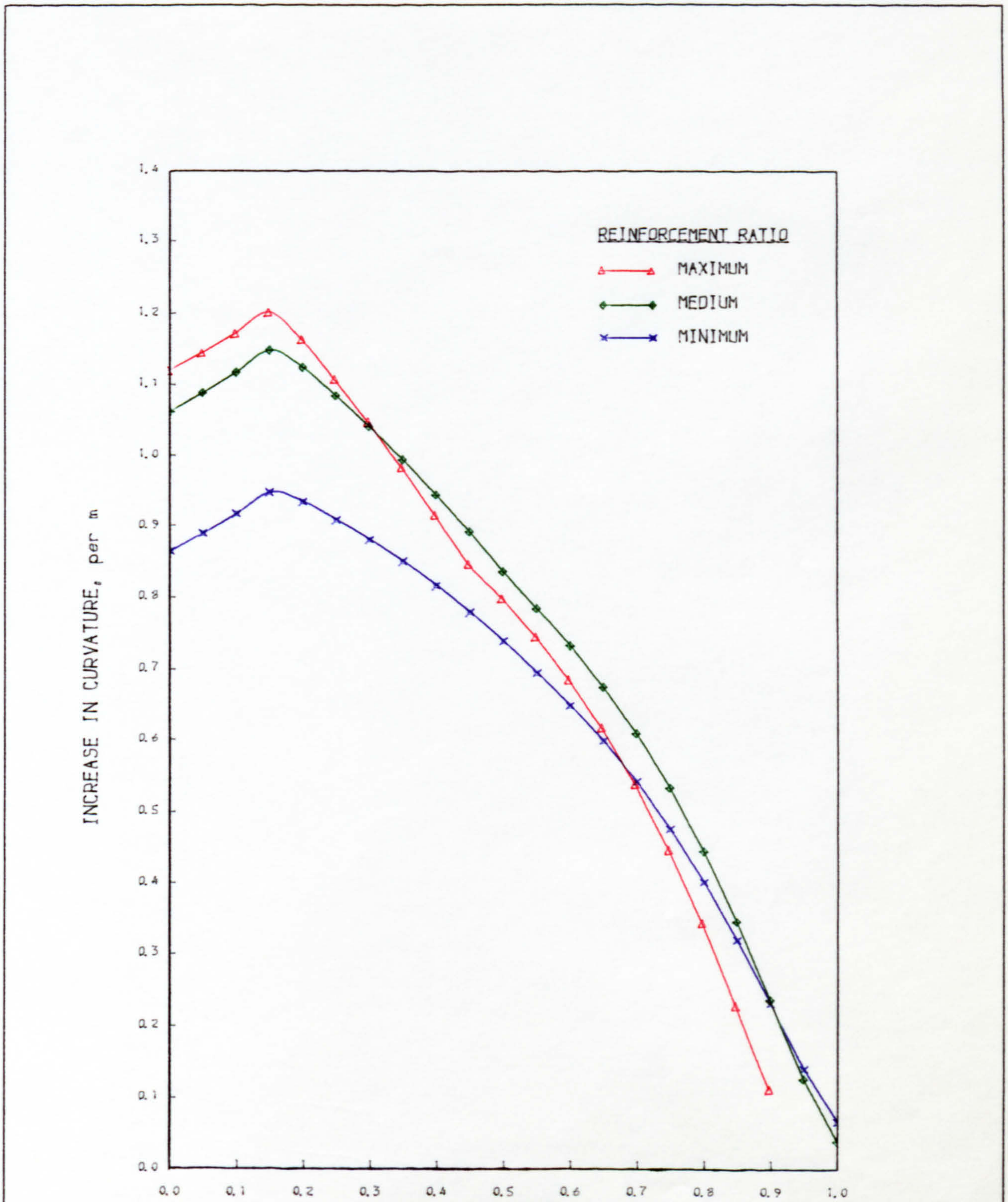

Fig. 10.28 PPR - CURVATURE RELATIONSHIP

SECTION I-0.3

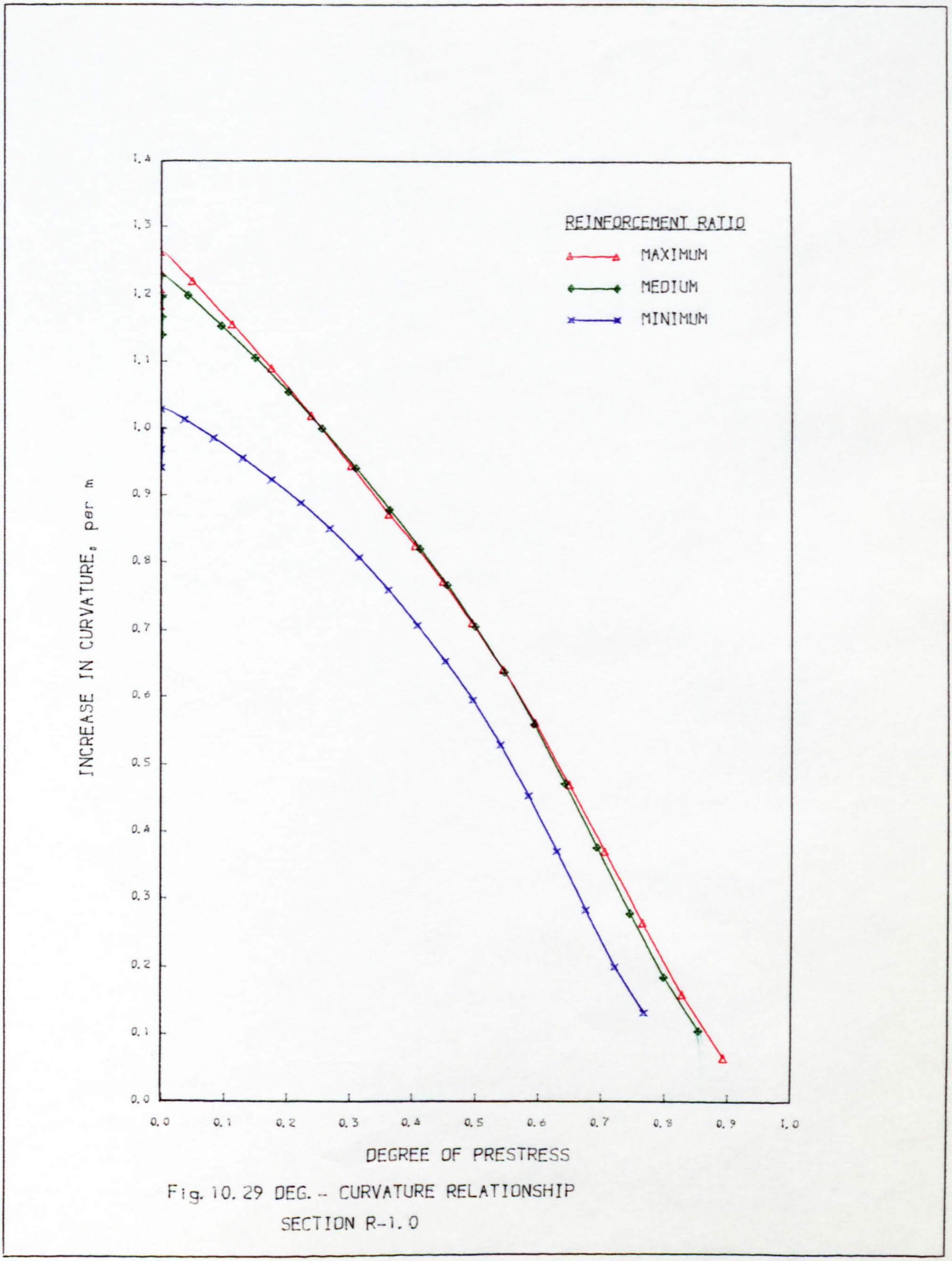

Fig. 10.29 DEG. - CURVATURE RELATIONSHIP

SECTION R-1.0

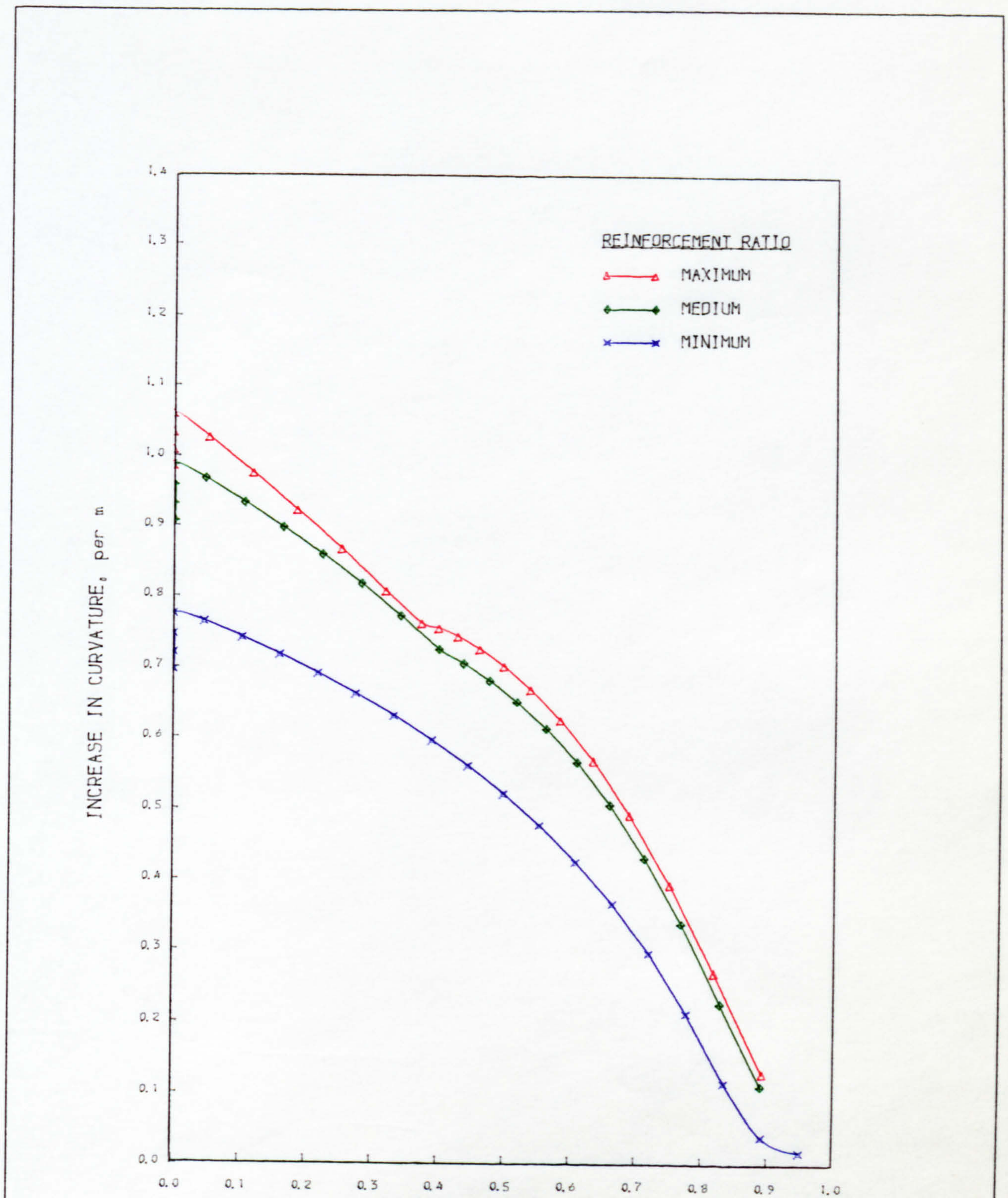

Fig. 10.30 DEG - CURVATURE RELATIONSHIP

SECTION T-0.1

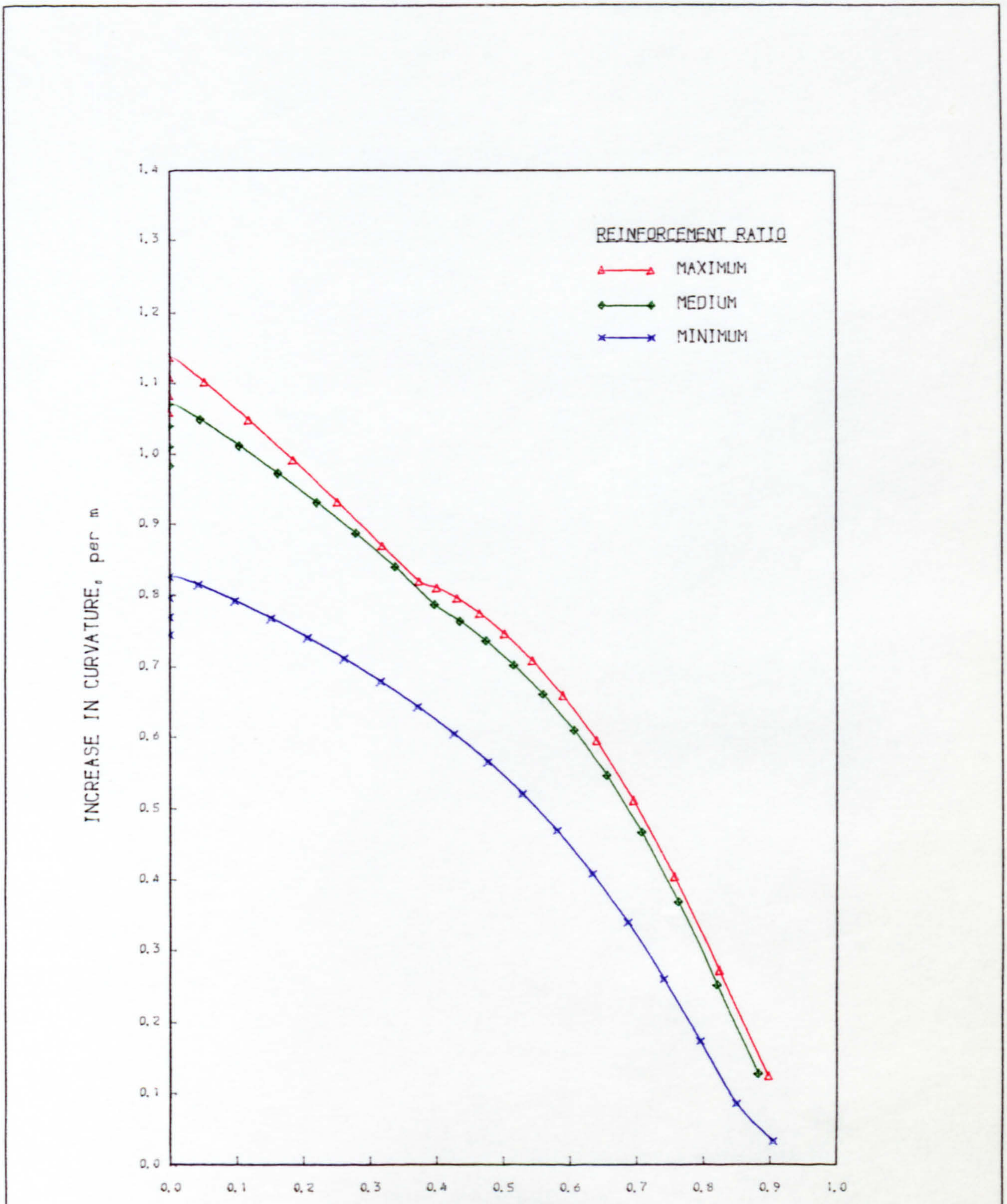

Fig. 10.31 DEG. - CURVATURE RELATIONSHIP
SECTION T-0.2

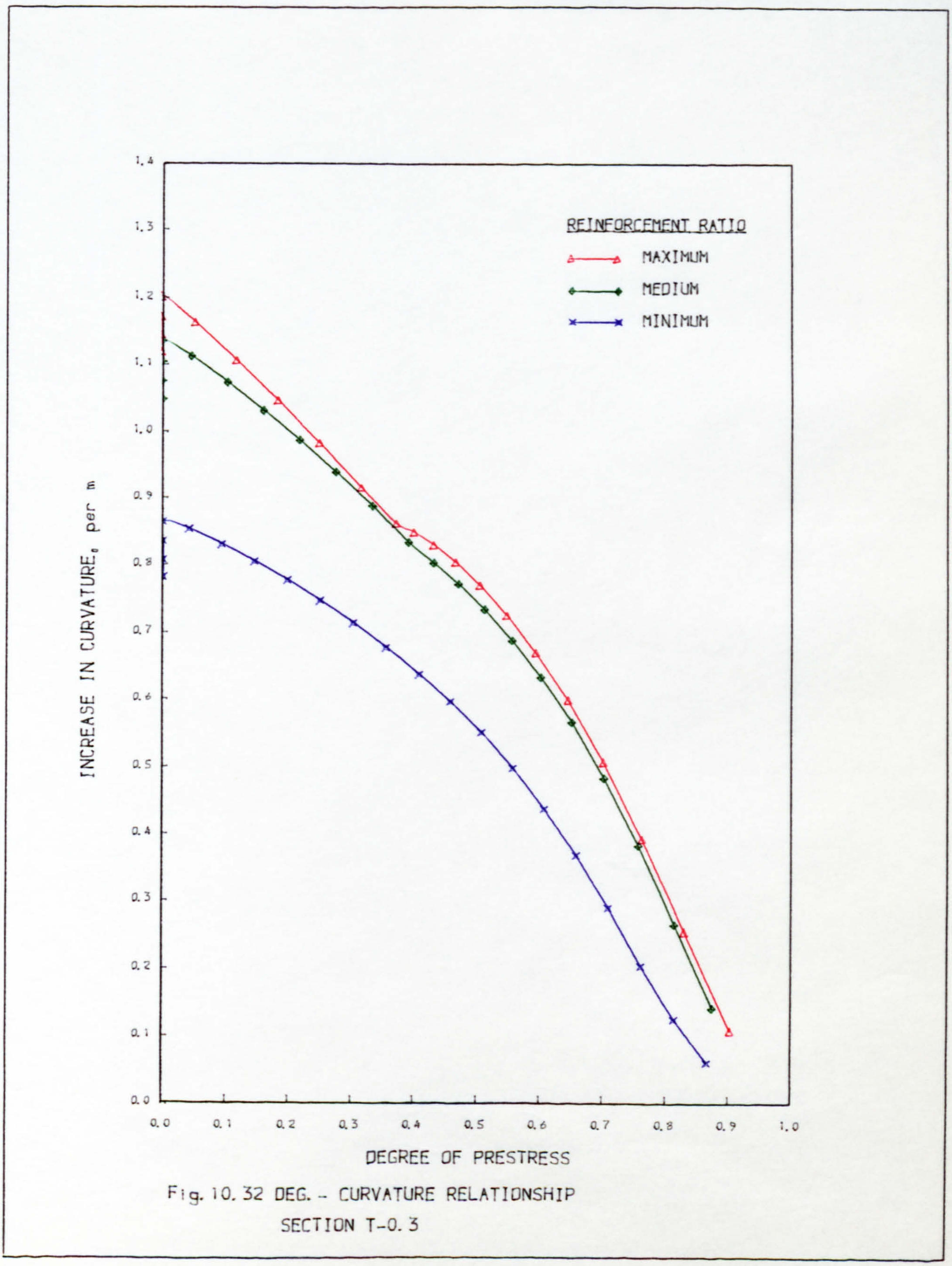

Fig. 10.32 DEG. - CURVATURE RELATIONSHIP

SECTION T-0.3

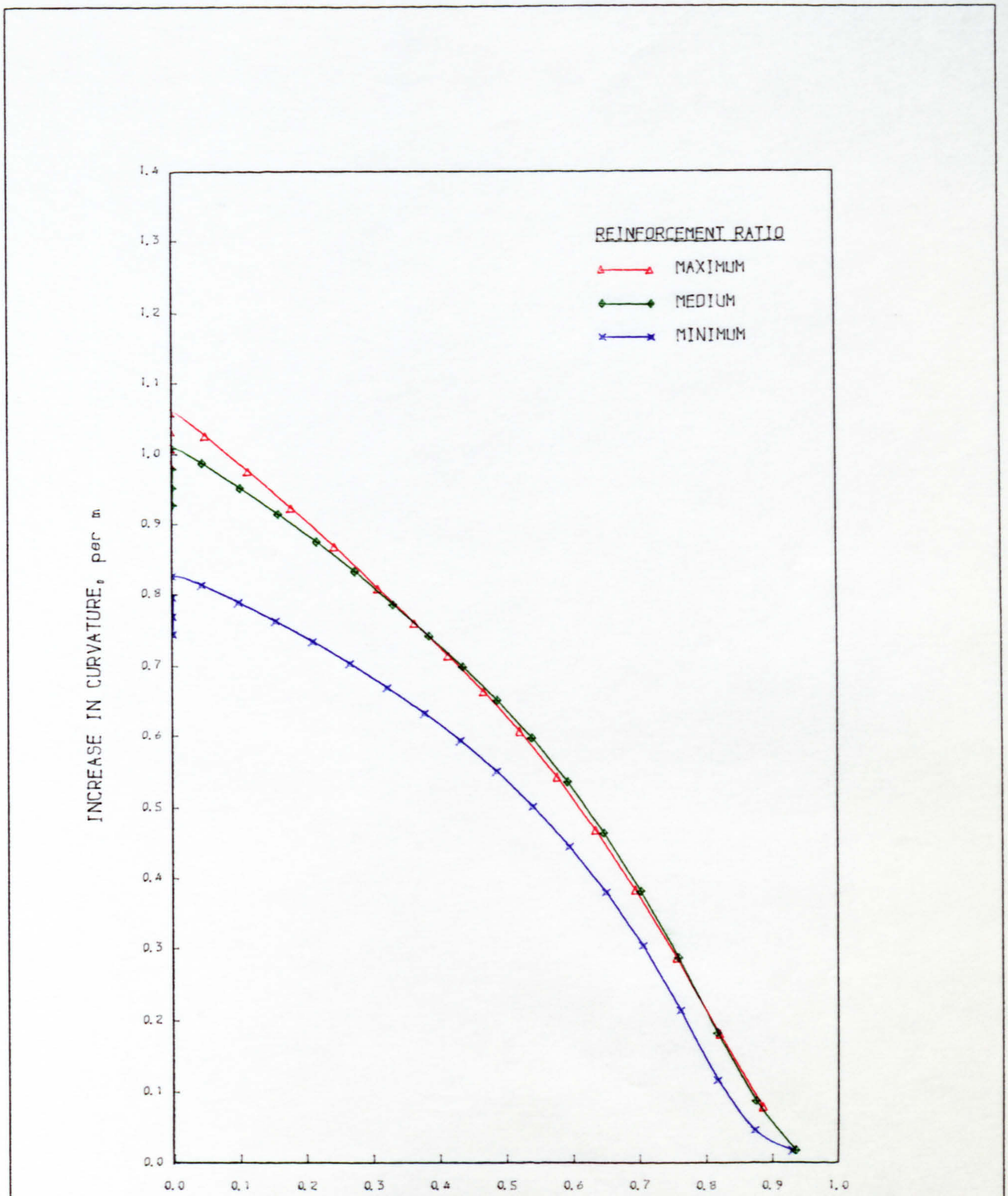

Fig. 10.33 DEG. - CURVATURE RELATIONSHIP

SECTION I-0.1

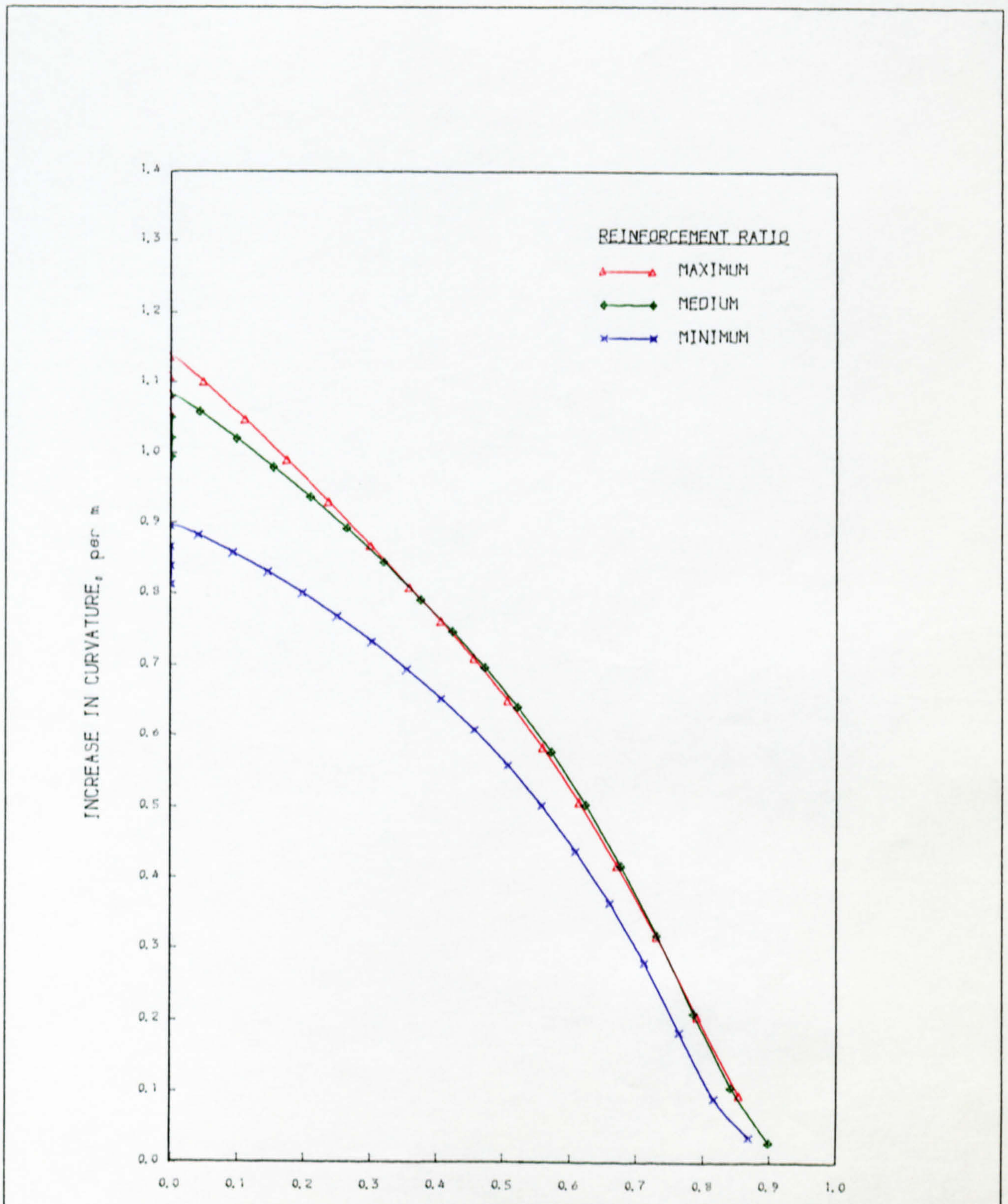

Fig. 10.34 DEG. - CURVATURE RELATIONSHIP

SECTION I-0.2

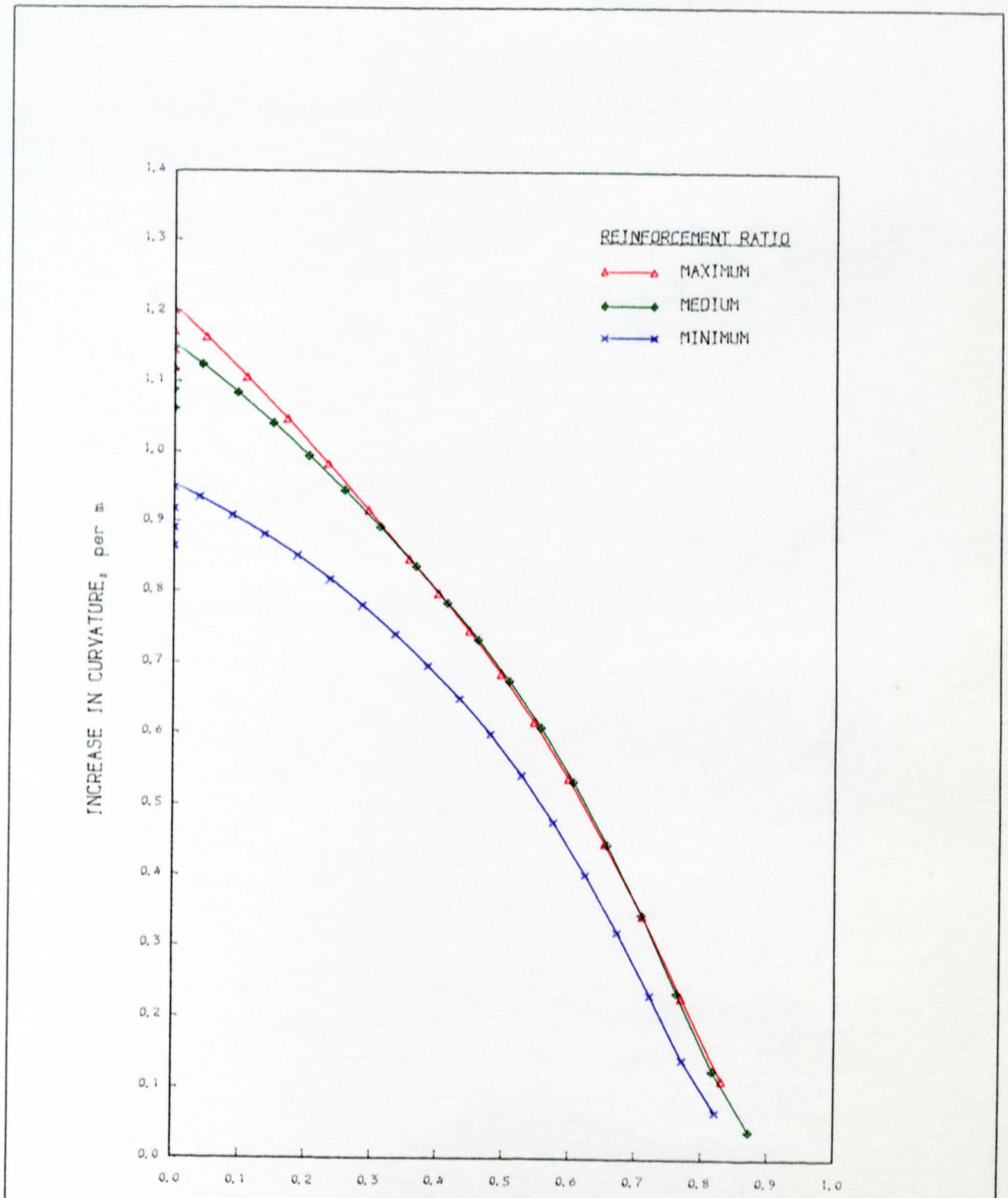

Fig. 10.35 DEG. - CURVATURE RELATIONSHIP

SECTION I-0.3

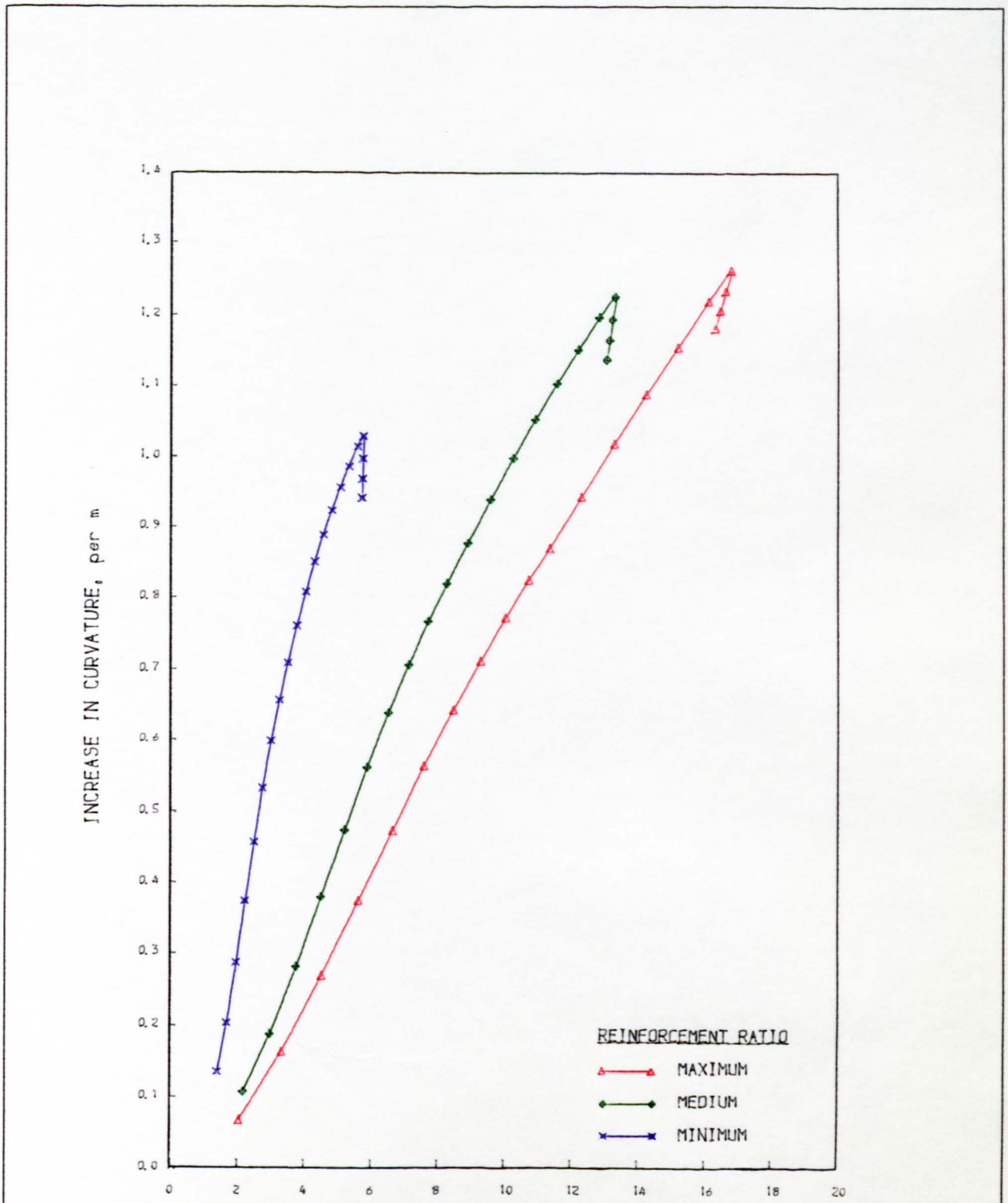

Fig. 10.36 HYP. - CURVATURE RELATIONSHIP
SECTION R-1.0

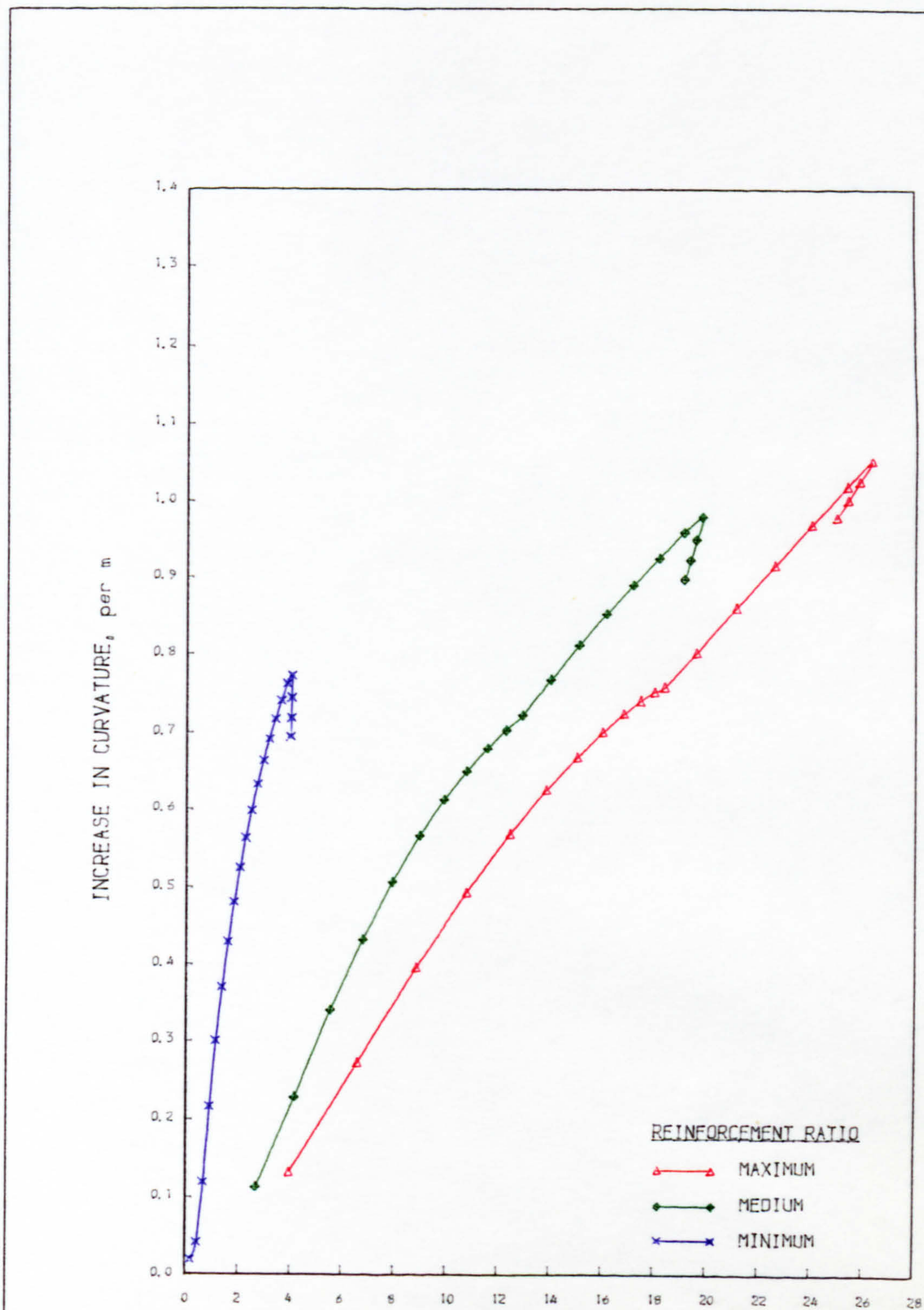

Fig. 10.37 HYP. - CURVATURE RELATIONSHIP

SECTION T-0.1

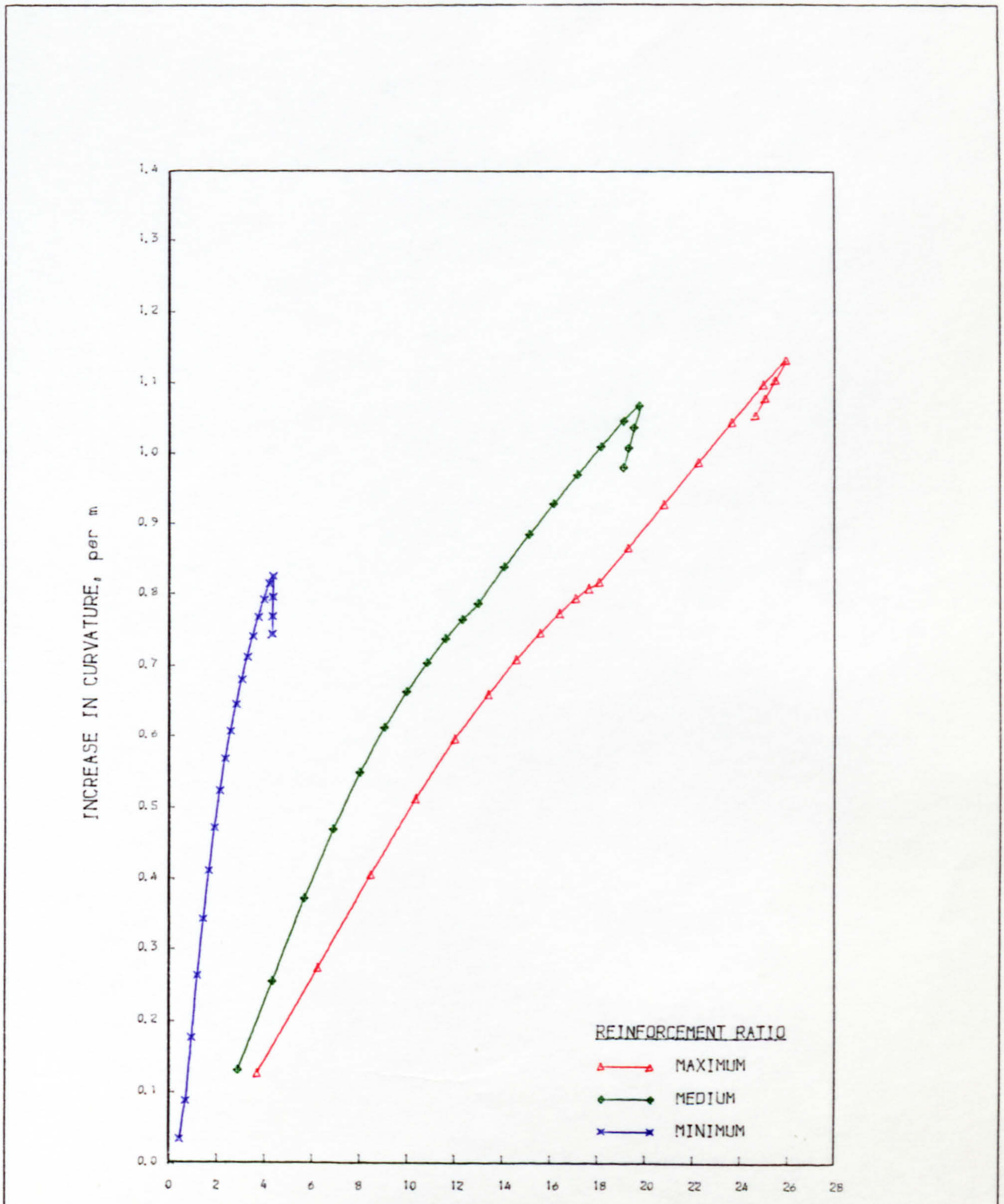

Fig. 10.38 HYP. - CURVATURE RELATIONSHIP

SECTION T-0.2

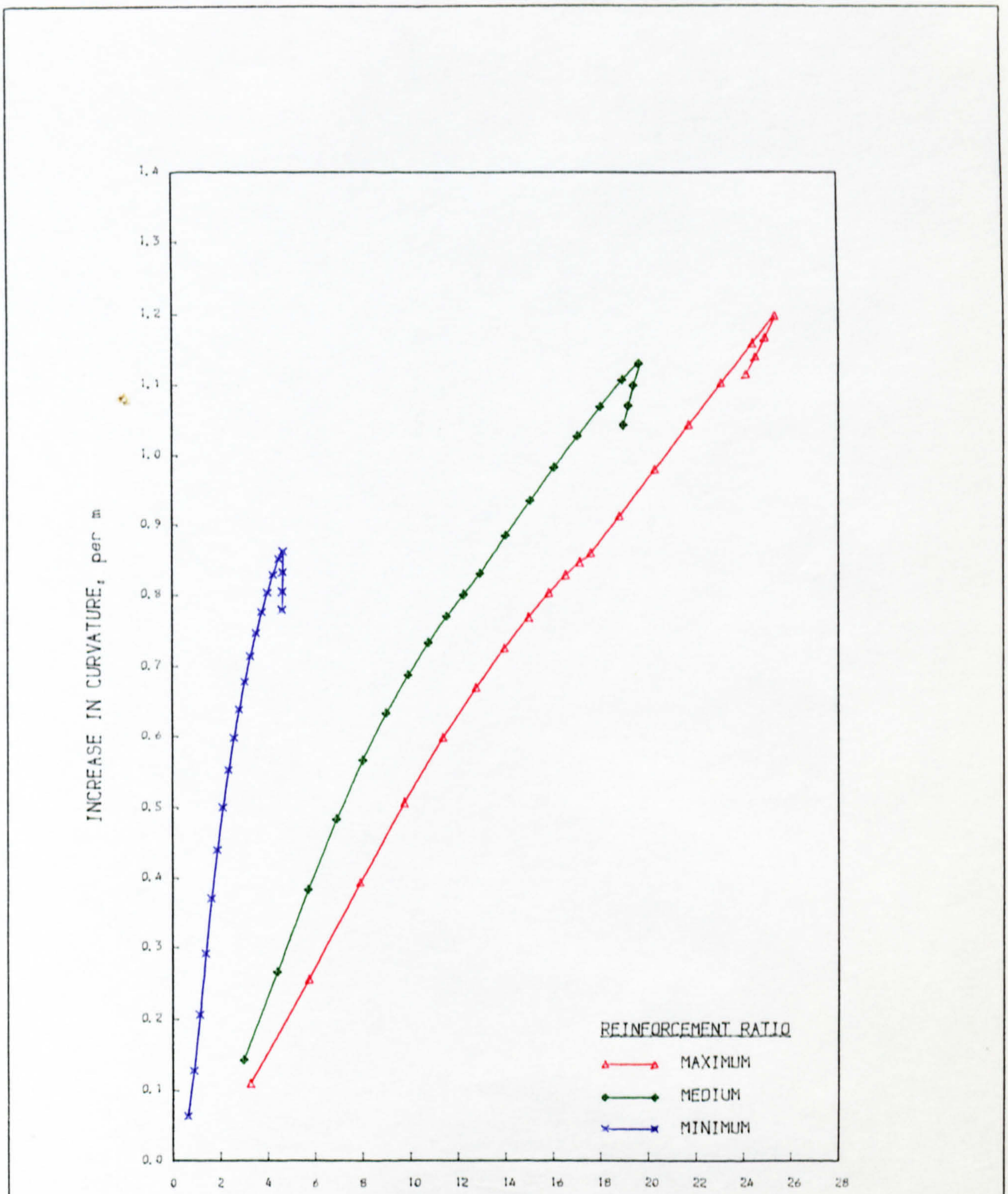

Fig. 10.39 HYP. - CURVATURE RELATIONSHIP

SECTION T-0.3

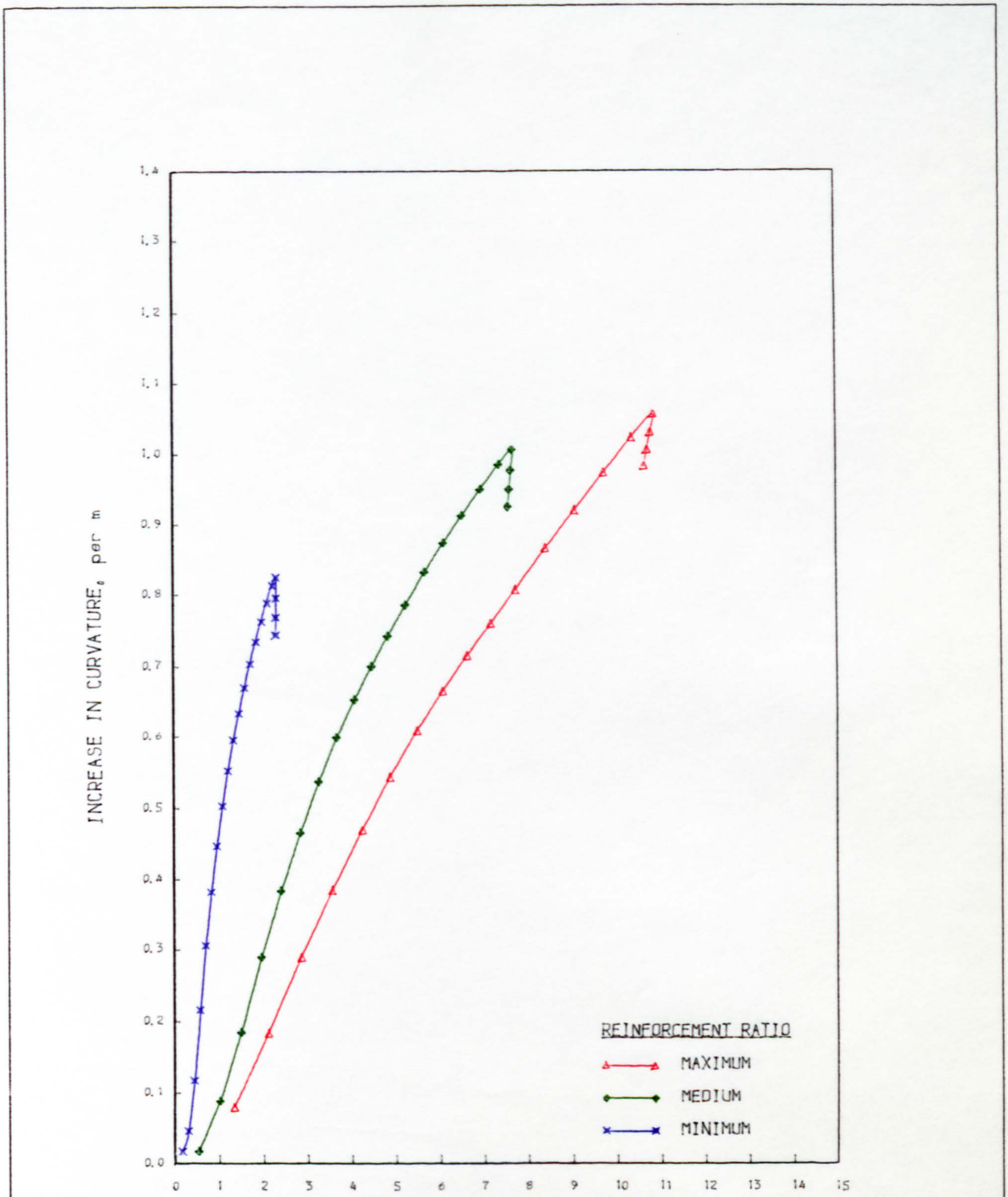

Fig. 10.40 HYP. - CURVATURE RELATIONSHIP

SECTION I-0.1

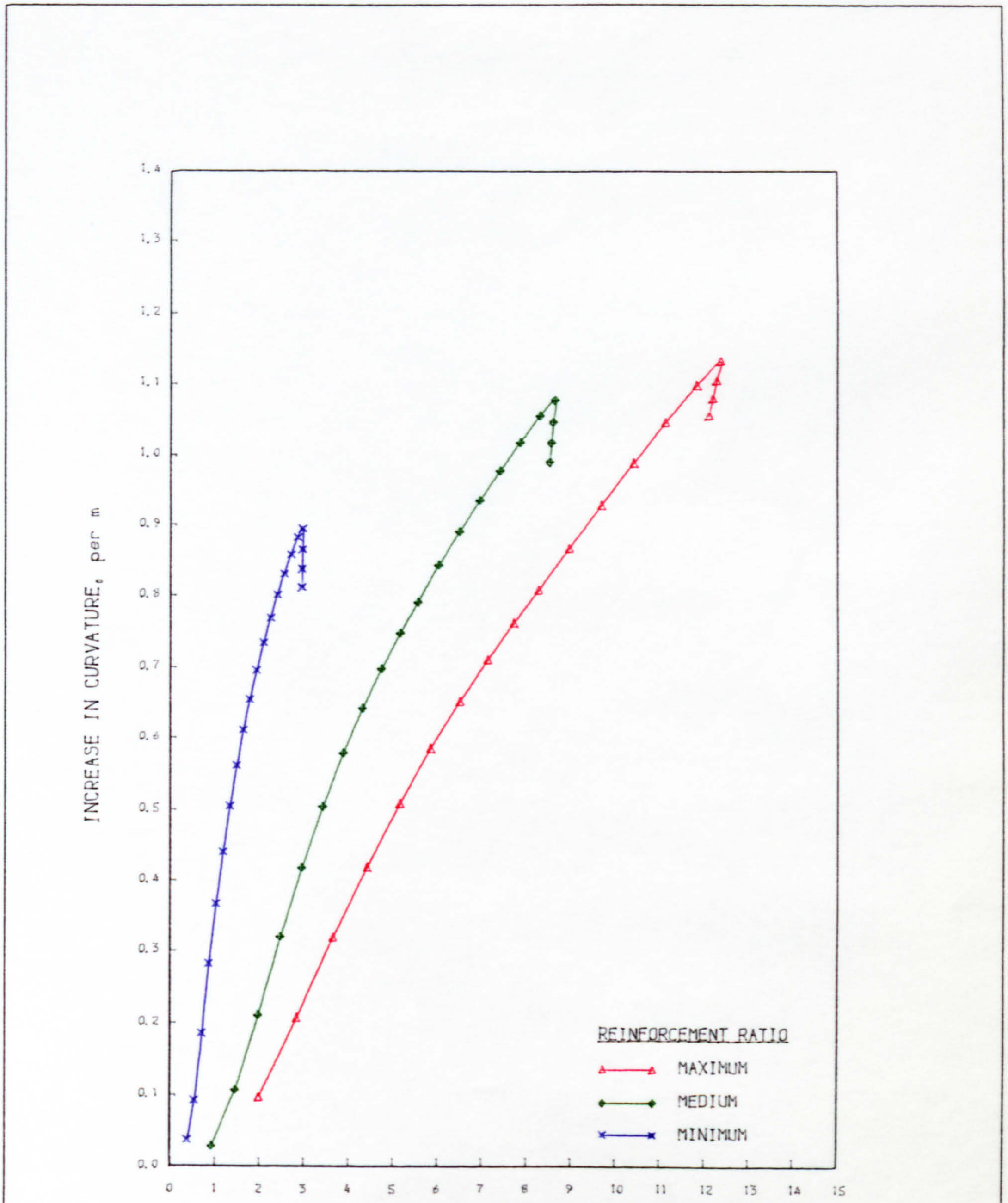

Fig. 10.41 HYP. - CURVATURE RELATIONSHIP
SECTION I-0.2

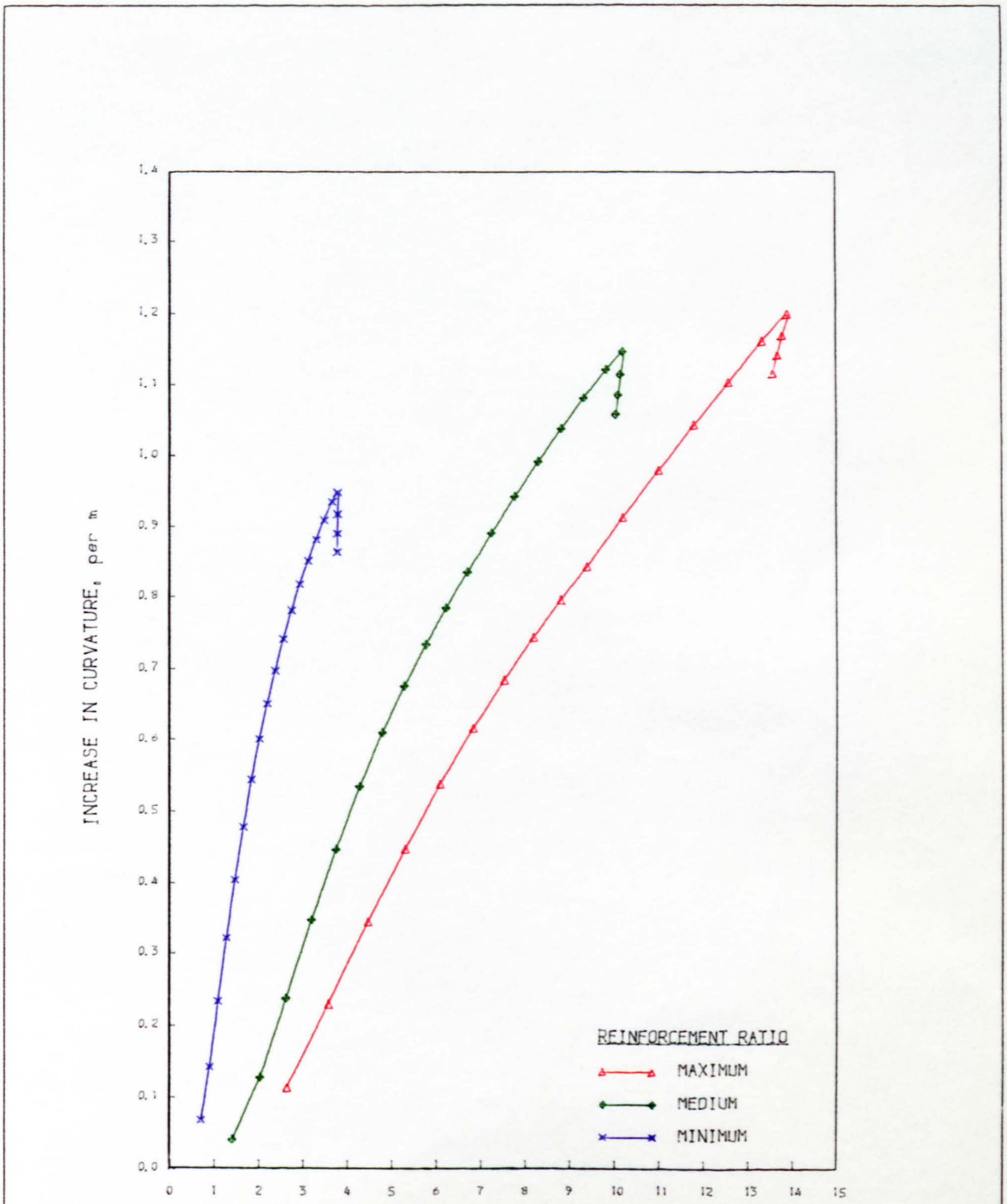

Fig. 10.42 HYP. - CURVATURE RELATIONSHIP

SECTION I-0.3

corresponding values of PPR or DEG.

It is again evident from the analyses that the effect of reinforcement ratios was greater on the relationship with the Hypothetical tensile stress than with the other two parameters.

10.4.3 Comparisons of The Parameters

The British Code CP110 specifies 0.2mm as the limiting crack width for Class 3 members under normal exposure conditions. This value also corresponds to an increase of reinforcement stress, f_s , of 150 N/sq.mm, calculated according to the equation proposed by Bennett et al (11) and modified by Martino and Nilson (10). Table 10.3 shows the values of each of the parameters corresponding to the limiting steel stress of 150 N/sq.mm under service loads.

Referring to Table 10.3, it can be deduced that for all the shapes and reinforcement ratios studied, the value of PPR lies between 0.41 and 0.77 when f_s = 150 N/sq.mm, whilst the value of DEG lies between 0.31 and 0.64. These ranges can be seen to be smaller within each of the shapes of section. For example, in T-sections, the values of PPR lie between 0.54 and 0.64 whilst values of DEG lie between 0.68 and 0.77. However, the Hypothetical tensile stress (HYP) varies from 1.0 N/sq.mm to 14.13 N/sq.mm with the same increment of reinforcement stresses (150 N/sq.mm) under service loads. Therefore, it reflects the result of

Parameters	"Standard section" (Medium reinforcement ratio) I-0.2	Variation of the values of parameters corresponding to f_s = 150 N/mm²							Maximum	Maximum variation (percentage with respect to the "standard section"
		Reinforcement Ratio (I-0.2) min. max.	R-1.0	T-0.1	T-0.2	T-0.3	I-0.1	I-0.3		
DEG	0.55	-0.01 -0.1	+0.0 -0.24	+0.09 -0.0	+0.06 -0.0	+0.03 -0.01	+0.02 -0.07	+0.0 -0.13	+0.09 -0.24	+16.4 -43.6
PPR	0.67	+0.01 -0.12	+0.0 -0.26	+0.1 -0.0	+0.09 -0.0	+0.07 -0.0	+0.11 -0.12	+0.01 -0.15	+0.11 -0.26	+16.4 -38.8
HYP (N/mm²)	4.14	+2.93 -2.74	+8.06 -1.14	+9.17 -2.33	+9.61 -2.14	+9.99 -1.89	+1.79 -3.14	+4.26 -2.24	+9.99 -3.14	241.3 -75.8
Allowable HYP in CP110 N/mm²	6.80	+2.60 -1.28	+3.20 -1.09	+1.64 -1.43	+1.94 -1.42	+2.57 -1.40	+2.48 -1.30	+2.87 -1.23	+3.20 -1.43	47.0 -21.0

Table 10.3: Variation of the values of the parameters for different shapes and reinforcement ratios.

investigation carried out by Naaman (14,15) in which he found that the fictitious tensile stress can vary from 3 N/sq.mm to 23 N/sq.mm under service loads.

The reinforcement ratio appears to have only a small effect on the values of PPR and DEG, but the effect is extremely important for hypothetical tensile stress.

The permissible hypothetical tensile stresses specified in the Code CP110 are given in Table 10.3 for sections with pretensioned tendons, grade 40 concrete and limiting crack width of about 0.2mm allowing for the amount of non-prestressed reinforcement and assuming the depth of the section to be 400mm. It can be seen that these allowable stresses are generally higher and therefore unconservative compared with the calculated values for a stress f_s = 150 N/sq.mm in sections with minimum reinforcement. More specifically, the permissble values are adequate for rectangular and T-sections with maximum reinforcement, but unconservative for all the I-sections.

It should be noted that CP110 specifies that the allowable hypothetical tensile stress is to be increased in proportion to the ratio of the non-prestressed reinforcement which is expressed as the area of the steel to the cross-sectional area of the concrete. The Code BS5400 (63), however, expresses this ratio as the area of the non-prestressed steel to the cross-sectional area of the 'tensile concrete'. This difference between the two codes in

the interpretation of the ratio means that the allowable hypothetical tensile stresses are higher according to BS5400 and even more unconservative than CP110.

The three parameters were also compared in another way as tabulated in Tables 10.4 to 10.9. A typical symmetrical I-section (section I-0.2) with medium amount of reinforcement and f_s = 150 N/sq.mm under service load was taken as a standard case to compare the values of the reinforcement stresses when the shapes and reinforcement ratios were varied, (Table 10.5). This was repeated for other values of f_s ; 120 N/sq.mm and 180 N/sq.mm and the results are tabulated in Tables 10.4 and 10.6 respectively. Similar comparisons were made for the other serviceability criteria i.e. the increase of curvature after the point of decompression, 1/r, for the values of 1/r equal to 0.49, 0.73 and 0.608 (per metre depth) in sections I-0.2 (Tables 10.7 to 10.9).

The results (Table 10.4 to 10.6) show that the first two parameters, the Partial Prestressing Ratio and the Degree of Prestress, have almost the same maximum differences for the three limiting values of stress increments. The maximum differences were all within 32 percent of the limiting values in the standard section (I-0.2). The third parameter, the Hypothetical tensile stress, however, has maximum differences of well over 100 percent. The relative performance of each of the three parameters in relation to the other serviceability criteria

(deflection or the increase in curvature) is again similar to the steel stress increments. This clearly suggests that the hypothetical tensile stress approach is relatively unreliable to be used as a design parameter as compared to Partial Prestressing Ratio and the Degree of Prestress.

An examination of the results, however, shows that there is no appreciable difference in the performance and hence reliability of the latter two parameters. The fact that the Degree of Prestress is serviceability based and the advantages of partial prestressing lies in its superior behaviour at this limit state, whilst the Partial Prestressing Ratio is based on the ultimate limit state, may therefore, favour the former parameter as the most suitable design parameter.

Parameters	Section I-0.2 f_s (N/mm²)	Difference in f_s (N/mm²) with other variables							Maximum difference (N/mm²)	Maximum difference (%)
		Reinforcement Ratio (I-0.2) min. max.	R-1.0	T-0.1	T-0.2	T-0.3	I-0.1	I-0.3		
DEG =0.63	120	- 5.5 -19.1	-34.2	+29.1	+25.5	+14.5	+5.5	-11.8	+29.1 -34.2	+24.3 -28.5
PPR =0.76	120	+ 0.0 -38.2	-21.8	+33.6	+30.0	+22.7	+0.0	- 5.5	+33.6 -38.2	+28.0 -31.8
HYP =3.41 (N/mm²)	120	+140.9* - 61.8	-86.4	-80.0	-79.5	-83.6	+29.1	-35.5	+140.9* - 86.4	+117* - 72

A symmetrical standard I-section of $\frac{b_w}{b} = \frac{h_f}{h} = 0.2$ with medium amount of reinforcement and f_s = 120 N/mm² under service load, is compared with other variables with the same values of design parameters and level of reinforcement.

* No values can be obtained, the values given are the minimum.

Table 10.4: Comparison of I-0.2 (f_s = 120 N/mm²) with other variables.

Parameters	Section I-0.2 f_s (N/mm²)	Difference in f_s (N/mm²) with other variables							Maximum difference (N/mm²)	Maximum difference (%)
		Reinforcement Ratio (I-0.2) min. max.	R-1.0	T-0.1	T-0.2	T-0.3	I-0.1	I-0.3		
DEG =0.55	150	- 1.8 -23.6	-35.5	+20.9	+18.2	+ 8.2	+ 4.5	-12.7	+20.9 -35.5	+13.9 -23.7
PPR =0.68	150	+ 2.7 -35.5	-26.4	+24.5	+20.9	+12.7	+ 0.9	- 6.4	+24.5 -35.5	+16.3 -23.7
HYP =4.14 (N/mm²)	150	+110.9* - 70.0	-96.4	-94.5	-97.3	-100.0	+27.3	-38.2	+110.9* -100.0	+73.9* -66.7

A symmetrical standard I-section of $\frac{b_w}{b} = \frac{h_f}{h} = 0.2$ with medium amount of reinforcement and $f_s = 150$ N/mm² under service load is compared with other sections with the same values of design parameters and level of reinforcement.

* No value can be obtained, the values given are the minimum.

Table 10.5: Comparison of I-0.2 ($f_s = 150$ N/mm²) with other variables.

Parameters	Section I-0.2 f_s (N/mm²)	Difference in f_s (N/mm²) with other variables							Maximum difference (N/mm²)	Maximum difference (%)
		Reinforcement Ratio (I-0.2) min. max.	R-1.0	T-0.1	T-0.2	T-0.3	I-0.1	I-0.3		
DEG =0.43	180	+1.8 -26.0	-31.8	+12.7	+10.0	+ 0.9	+ 5.5	-10.0	+12.7 -31.8	+ 7.1 -17.7
PPR =0.56	180	+5.5 -34.5	-29.1	+10.0	+ 6.4	+ 0.0	+ 2.7	- 9.1	+10.0 -34.5	+ 5.6 -19.2
HYP = 5.07 (N/mm²)	180	+80.9* -72.7	-96.4	-104.5	-105.5	-110.9	+22.7	-34.5	+80.9* -110.9	+44.9* -61.6

A symmetrical standard I-section of $\frac{b_w}{b} = \frac{h_f}{h} = 0.2$ with medium amount of reinforcement and $f_s = 180$ N/mm² under service load, is compared with other variables with the same values of design parameters and amount of reinforcement.

* No value can be obtained, the values given are the minimum.

Table 10.6: Comparison of I-0.2 ($f_s = 180$ N/mm²) with other variables.

Parameters	Section I-0.2 $\frac{1}{r}$ (per m)	Difference in $\frac{1}{r}$ (per m depth) with other variables							Maximum difference (per m)	Maximum difference (%)
		Reinforcement Ratio (I-0.2) min. max.	R-1.0	T-0.1	T-0.2	T-0.3	I-0.1	I-0.3		
DEG =0.63	0.490	-0.09 -0.015	+0.018	+0.052	+0.085	+0.102	-0.013	+0.01	+0.102 -0.015	+ 20.8 - 3.1
PPR =0.76	0.490	-0.057 -0.094	+0.056	+0.068	+0.11	+0.127	-0.04	+0.027	+0.127 -0.094	+ 25.9 - 19.2
HYP =3.41 (N/mm^2)	0.490	+0.398* -0.198	-0.265	-0.315	-0.302	-0.298	+0.068	+0.085	+0.398* -0.315	+ 81.2* -64.3

A symmetrical standard I-section, $\frac{b_w}{b} = \frac{h_f}{h} = 0.2$ with medium amount of reinforcement and $\frac{1}{r} = 0.49$ (per metre depth) under service load, is compared with other sections with the same values of design parameter and amount of reinforcement ratios.

* No value can be obtained, the values given are the minimum.

Table 10.7: Comparison of I-0.2 ($\frac{1}{r} = 0.49$) with other variables.

Parameters	Section I-0.2 $\frac{1}{r}$ (per m)	Difference in $\frac{1}{r}$ (per m depth) with other variables							Maximum difference (per m)	Maximum difference (%)
		Reinforcement Ratio (I-0.2) min. max.	R-1.0	T-0.1	T-0.2	T-0.3	I-0.1	I-0.3		
DEG =0.43	0.73	-0.109 -0.013	+0.058	-0.022	+0.028	+0.07	-0.03	+0.024	+0.07 -0.109	+ 9.6 -14.9
PPR =0.56	0.73	-0.097 -0.038	+0.074	-0.03	+0.028	+0.062	-0.051	+0.037	+0.074 -0.097	+10.1 -13.3
Hyp =5.07 (N/mm^2)	0.730	-0.158* -0.222	-0.255	-0.43	-0.417	-0.409	-0.045	-0.076	+0.045 -0.43	+ 6.2 -58.9

A symmetrical standard I-section, $\frac{b_w}{b} = \frac{h_f}{h} = 0.2$ with medium amount of reinforcement and $\frac{1}{r} = 0.73$ (per metre depth) under service load is compared with other sections with the same amount of design parameters and amount of reinforcement.

* No value can be obtained, the values given are the minimum.

Table 10.8: Comparison of I-0.2 ($\frac{1}{r} = 0.73$) with other variables.

Parameters	Section I-0.2 $\frac{1}{r}$ (per m)	Difference in $\frac{1}{r}$ (per m depth) with other variables							Maximum difference (per m)	Maximum difference (%)
		Reinforcement Ratio (I-0.2) min. max.	R-1.0	T-0.1	T-0.2	T-0.3	I-0.1	I-0.3		
DEG =0.55	0.608	-0.108 -0.025	+0.009	+0.013	+0.059	+0.08	-0.031	+0.0	+0.08 -0.108	+13.2 -17.8
PPR =0.68	0.608	-0.075 -0.071	+0.063	+0.025	+0.071	+0.1	-0.05	+0.03	+0.071 -0.075	+11.7 -12.3
HYP =4.14 (N/mm^2)	0.608	+0.28* -0.22	-0.275	-0.377	-0.366	-0.358	+0.055	-0.1	+0.28* -0.377	+46.1* -62.0

A symmetrical standard I-section of $\frac{b_w}{b} = \frac{h_f}{h} = 0.2$ with medium amount of reinforcement and $\frac{1}{r} = 0.608$ (per metre depth) under service load is compared with other sections with the same values of design parameters and amount of reinforcement.
*No value can be obtained, the values given are the minimum.

Table 10.9: Comparison of I-0.2 ($\frac{1}{r} = 0.608$) with other variables.

CHAPTER ELEVEN

Conclusions and Design Recommendation

11.1 General

The results of the investigations and the relationships of each of the proposed design parameters with the serviceability criteria and other variables, are summarised in this Chapter. The conclusions are given in Section 11.2.4.

Based on the results of the investigations, a simple design procedure for partially prestressed concrete beams is recommended at the end of the Chapter.

11.2 Summary and Conclusions

11.2.1 Partial Prestressing Ratio

The results discussed in Chapter Ten showed that the Partial Prestressing Ratio is a possible design parameter. The incremental steel stress and the curvature can be controlled by varying the values of PPR.

In order to achieve the same limiting stress, the variation of the values of PPR was considerable (from 0.41 to 0.78) with varying shapes of the sections, but the effect of the reinforcement ratio was small under the same conditions.

The minimum values of PPR that would probably satisfy the serviceability criteria described in Section 9.2.2, irrespective of the reinforcement ratios, are given below for some of the common shapes of cross section:

Rectangular Section	0.67
T-section	0.76
I-section	0.78

11.2.2 Degree of Prestress

There was no appreciable difference between the performance of the Degree of Prestress and the Partial Prestressing Ratio. The variation of the values of DEG was also considerable (from 0.31 to 0.64) with varying shapes of the sections, but the effect of reinforcement ratio was similarly small particularly at higher degree of prestress.

The minimum values of DEG that would probably satisfy the serviceability criteria, irrespective of the reinforcement ratios, are as follows:-

Rectangular Section	0.47
T-section	0.64
I-section	0.57

Leonhardt (19) also found that these values would produce lowest cost sections.

11.2.3 Hypothetical Tensile Stress

The hypothetical tensile stress approach, as currently recommended in CP110, was found to be least satisfactory of the three parameters investigated.[1] The tensile stress can vary from 1.0 N/sq.mm to 14 N/sq.mm, depending on the amount of reinforcement, for the same increment of reinforcement stress.

The allowable hypothetical tensile stresses specified in CP110 were found to be higher and therefore unconservative compared with the calculated values for crack widths of about 0.2mm with minimum reinforcement ratio. The values specified in BS5400 were even more unconservative than in CP110.

It is recommended that the allowable hypothetical tensile stress should be reduced to as low as 1.0 N/sq.mm for sections with low reinforcement ratios for a crack width of about 0.2mm. This is possible either by specifying a smaller basic value or by introducing a reduction factor for decreasing reinforcement ratios.

11.2.4 Conclusions

The object of the investigation was to study the relative usefulness of the three proposed parameters. The relative usefulness depends on how closely each of these parameters is related to the serviceability criteria and

other variables such as the reinforcement ratio and shape of section. It can be concluded from the results that the most suitable design parameter for partially prestressed concrete is the Degree of Prestress. Although the Partial Prestressing Ratio and the Degree of Prestress have similar relationships with the serviceability criteria, the fact that the latter is serviceability based favour it as the most suitable parameter for this type of structures.

It was also clear from the investigation that the Hypothetical tensile stress approach was the least sound parameter of the three studied.

The limiting values of the hypothetical tensile stress specified in CP100 can be unconservative for sections with low reinforcement ratios. These limiting values should be reduced for sections lightly reinforced.

It appeared from the results that the limiting values of hypothetical tensile stress as specified in Table 34 of CP110 should be reduced to as low as 1.0 N/sq.mm for members with low reinforcement ratios unless the designer is confident that cracks will not appear under any circumstances.

11.3 Recommended Design Procedures

The Degree of Prestress has been found to be the most useful parameter of the three proposed. The recommended

design procedures using the Degree of Prestress are listed in the following steps:-

1) Choice of the Degree of Prestress

A desired degree of prestress is chosen based on the design requirements. Its value, for example, can be chosen on the basis that a certain proportion of the total design moment (or dead load) is to be counteracted or "balanced" by the prestress.

The degree of prestress can also be chosen from the recommended values given in Section 11.2.2 for different shapes of the sections. According to Leonhardt (19), these are also the values that would result in the most economic designs.

The decompression moment, M_d, can then be calculated from the expression:-

$$M_d = (DEG) . M_{g+q}$$

2) Choice of the Section

The section can either be selected from the standard precast unit available in the manufacturers' catalogue or with the guide of the following expression:-

$$z \geq \frac{M_d - \eta M_{min}}{\eta f_{cpadm}} \quad \text{or} \simeq \frac{M_d(1 - \eta)}{\eta f_{cpadm}}$$

where z = section modulus

η = loss ratio

f_{cpadm} = allowable prestress during prestressing

3) Determination of area of prestressing steel

The required prestress (after losses) which together with bending stress due to the decompression moment, M_d, produces zero stress at the soffit, can be easily calculated by the elastic theory when the section properties are known. The prestressing force and hence the area of the prestressing steel can then be calculated by the usual prestressed concrete formulae available in the standard text books (13,55,56).

4) Determination of the area of non-prestressed steel

The ultimate conditions are satisfied by providing additional non-prestressed reinforcement. This can be calculated according to CP110, whereby the ultimate tensile resistance are provided by both the prestressed and non-prestressed reinforcement and with materials safety factors of of 1.5 and 1.15 for concrete and steel respectively.

5) Checks at Serviceability Limit State

The concrete and steel stresses and the deflection are to be checked to satisfy the requirements specified in the codes. The increase of steel stresses (after the point of decompression in concrete) can be calculated by the method described in Chapter Four or simply estimated from the design charts available in the Concrete Society Report (9). These design charts are reproduced in Figs.11.1 to 11.8. The neutral axis under service load can be found from Figs.11.1 to 11.4 (depending on the

shape of the section) and the incremental steel stress can be estimated from Figs.11.5 to 11.8. If necessary, the crack width can be calculated by using the formulae proposed by Bennett et al and Nilson (10,11).

The deflection, if necessary, can be predicted by the ACI's "I-effective" method (57) or if more rigorous analysis is required, the method by integration of curvature described in Chapter Five can be used. However, the latter method may be laborious and is best handled by computer.

If found to be unsatisfactory, the deflection and the increase of reinforcement stresses (or crack width) may be reduced by increasing the value of the Degree of Prestress.

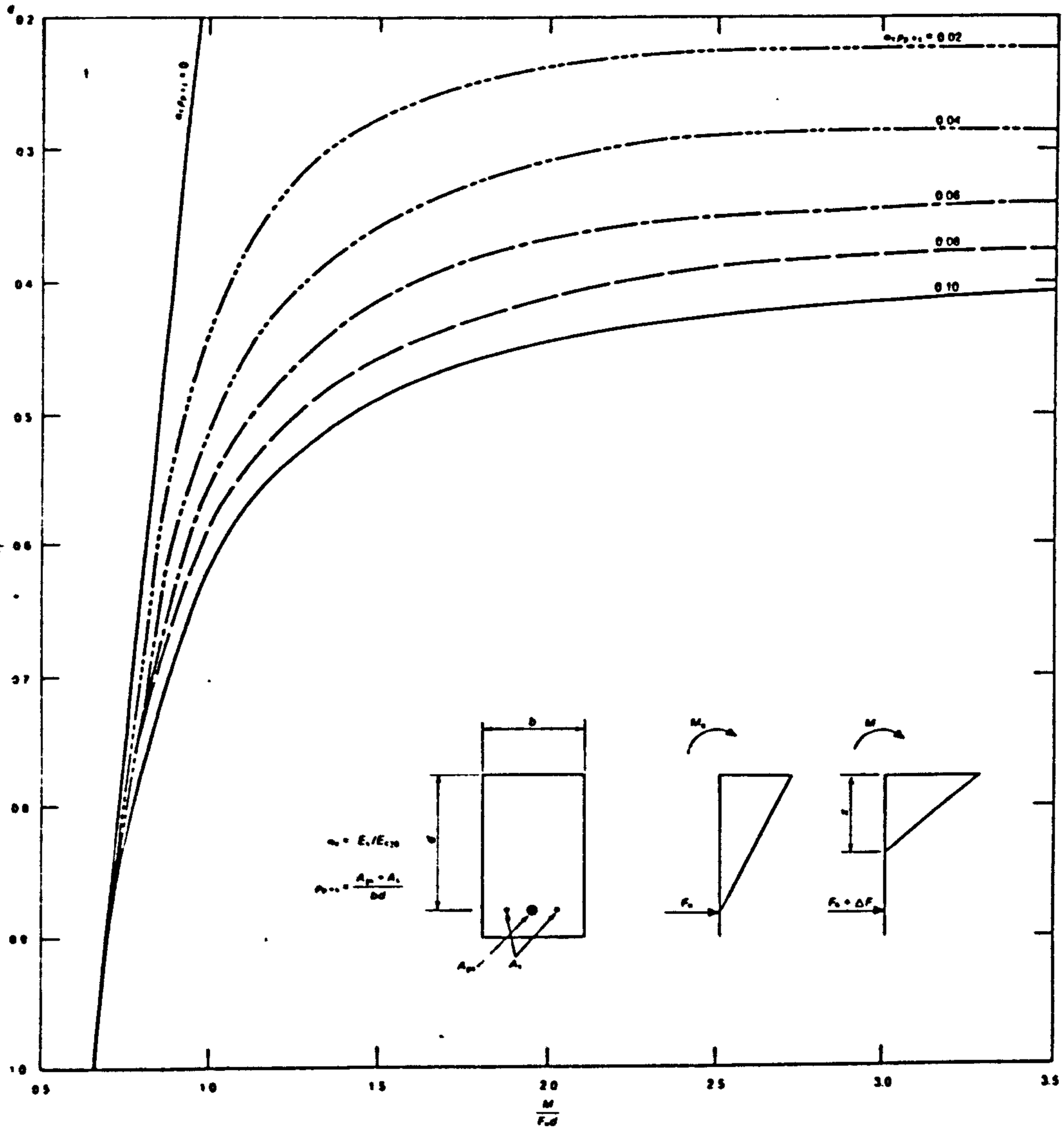

Fig.11.1 Neutral axis depth for rectangular section (9)

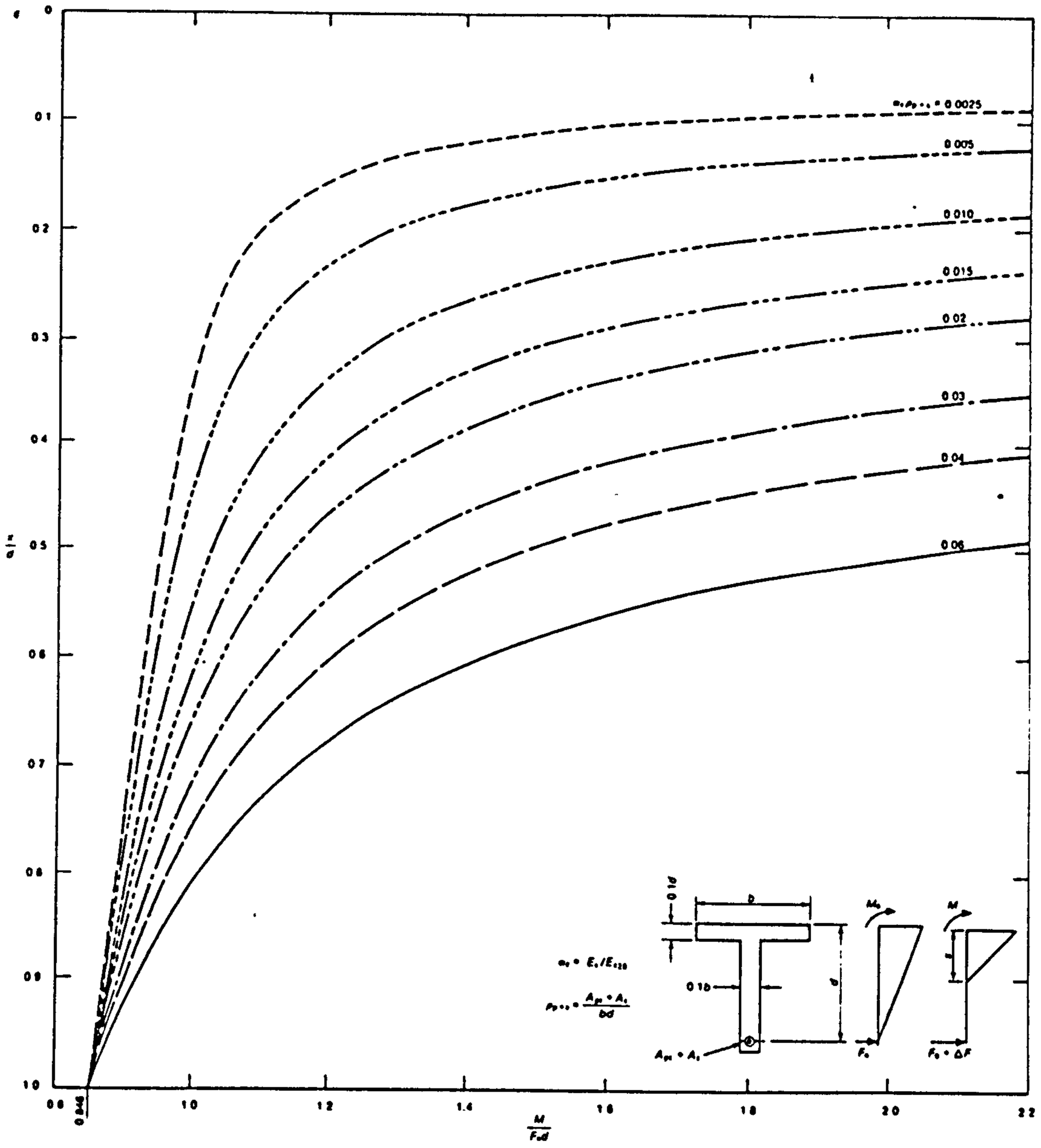

Fig.11.2 Neutral axis depth for flanged section ($h_f = 0.1d$, $b_w = 0.1b$)

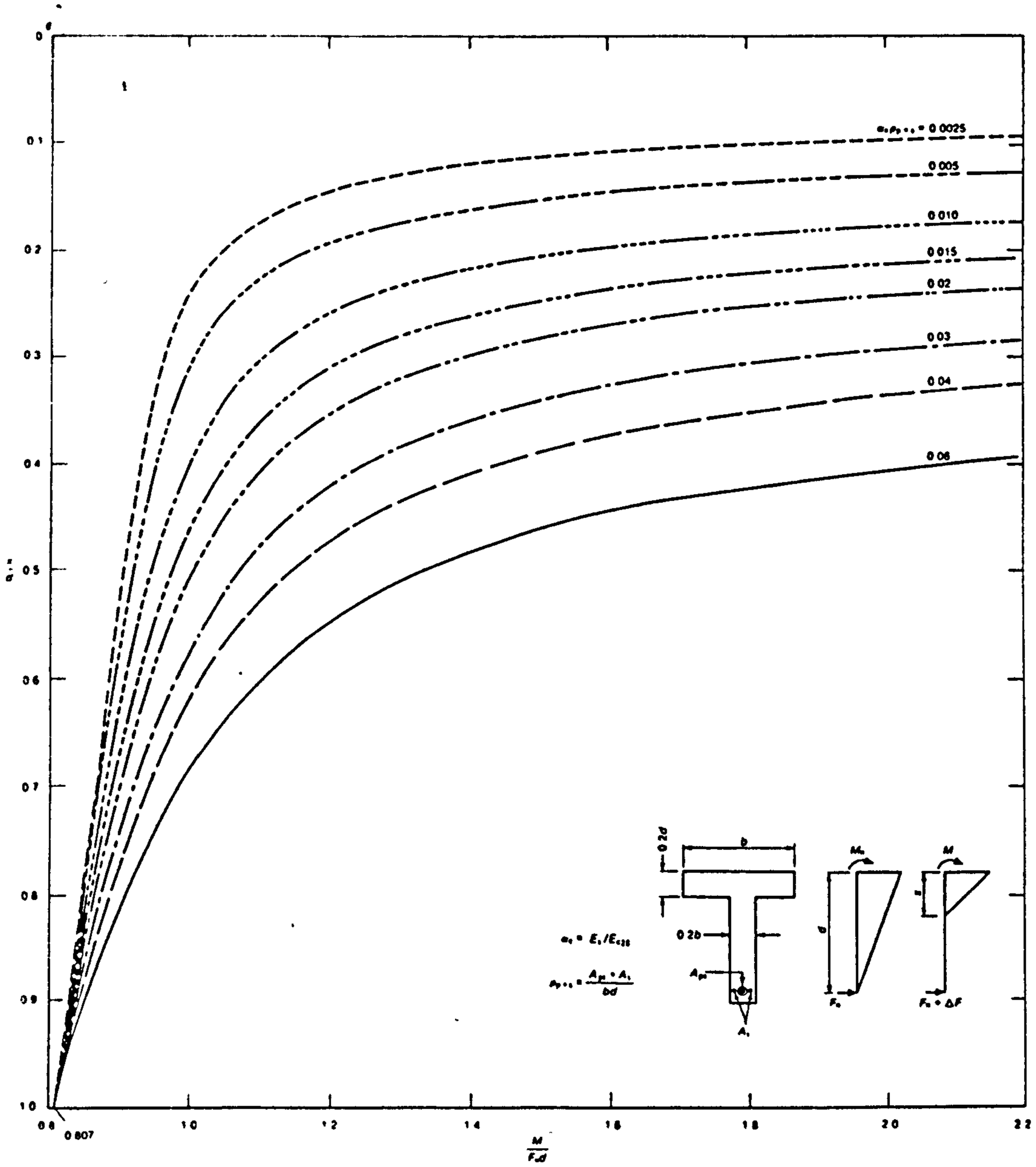

Fig. 11.3 Neutral axis depth for flanged section ($h_f = 0.2d$, $b_w = 0.2b$)

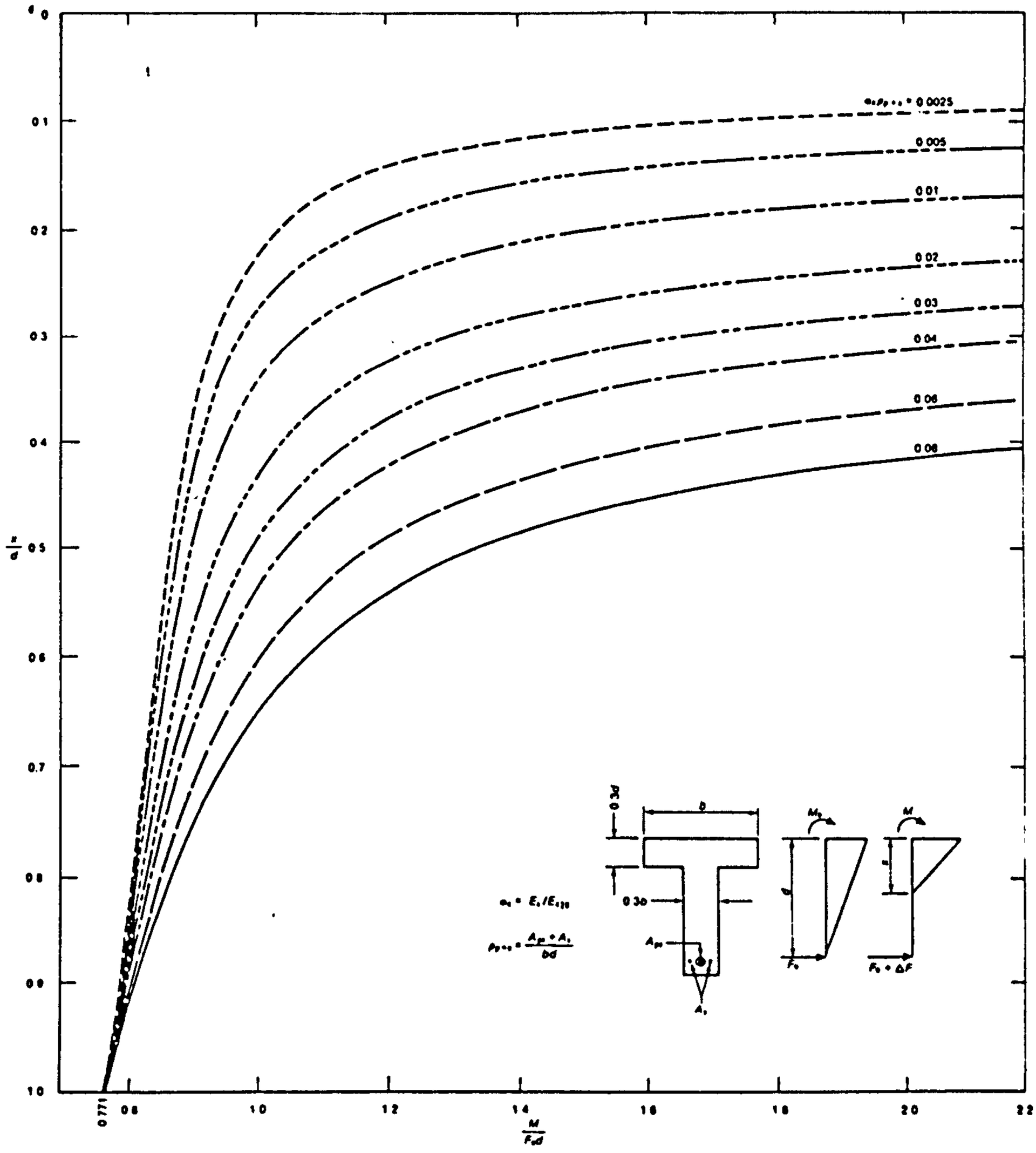

Fig.11.4 Neutral axis depth for flanged section ($h_f = 0.3d$, $b_w = 0.3b$)

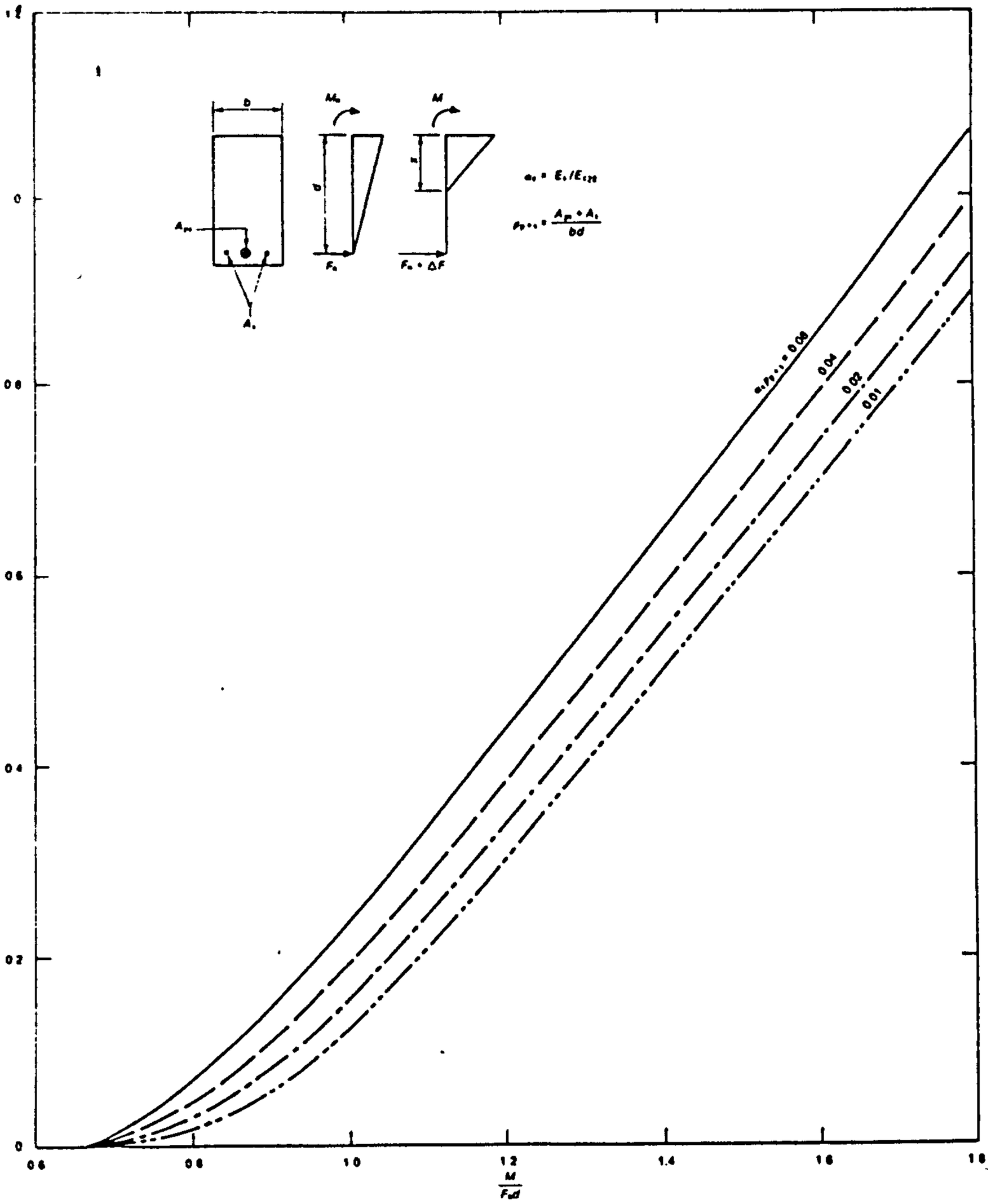

Fig.11.5 Increase of total reinforcement force in rectangular section after cracking

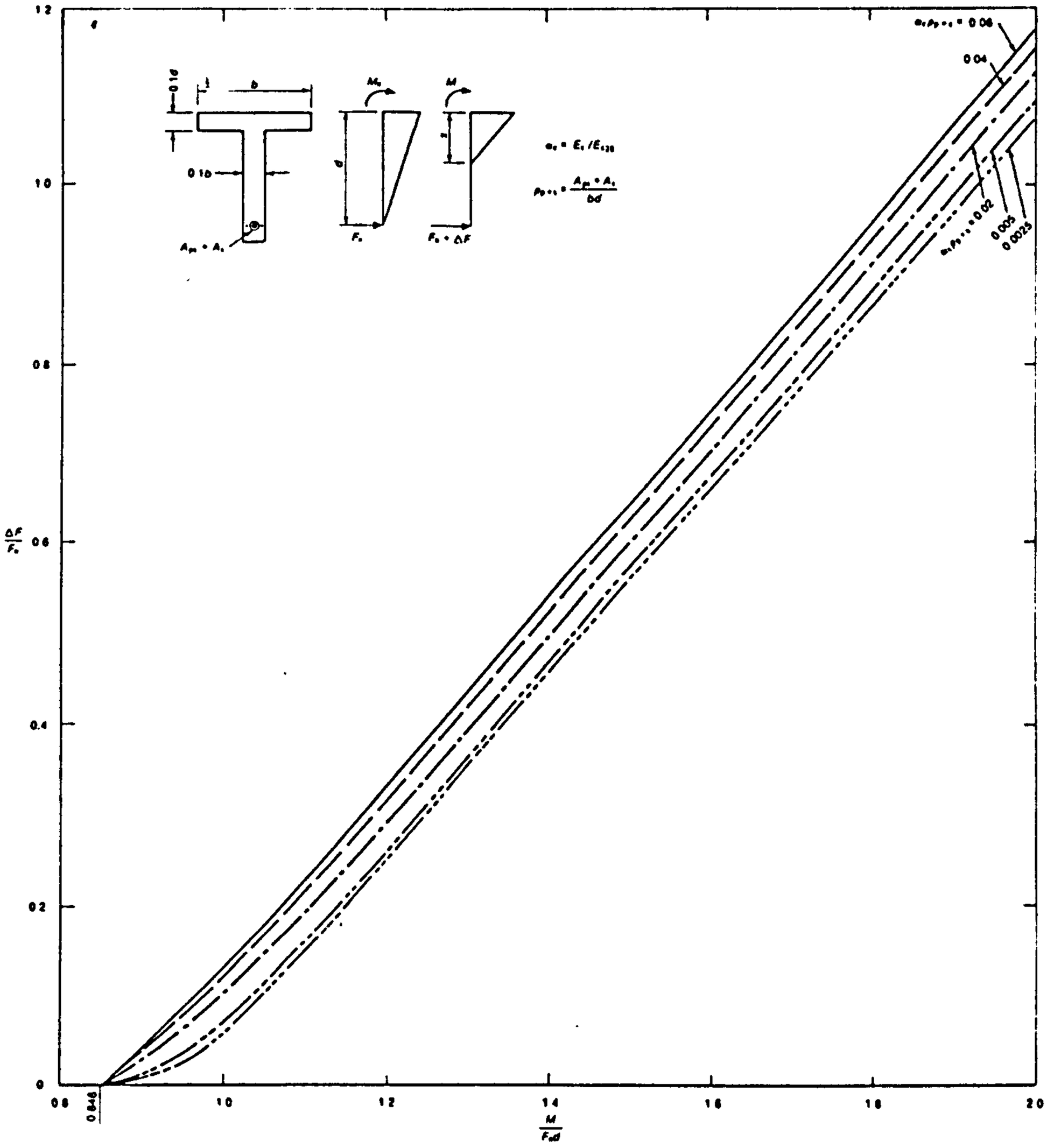

Fig.11.6 Increase of total reinforcement force in flanged section ($h_f = 0.1d$, $b_w = 0.1b$) after cracking

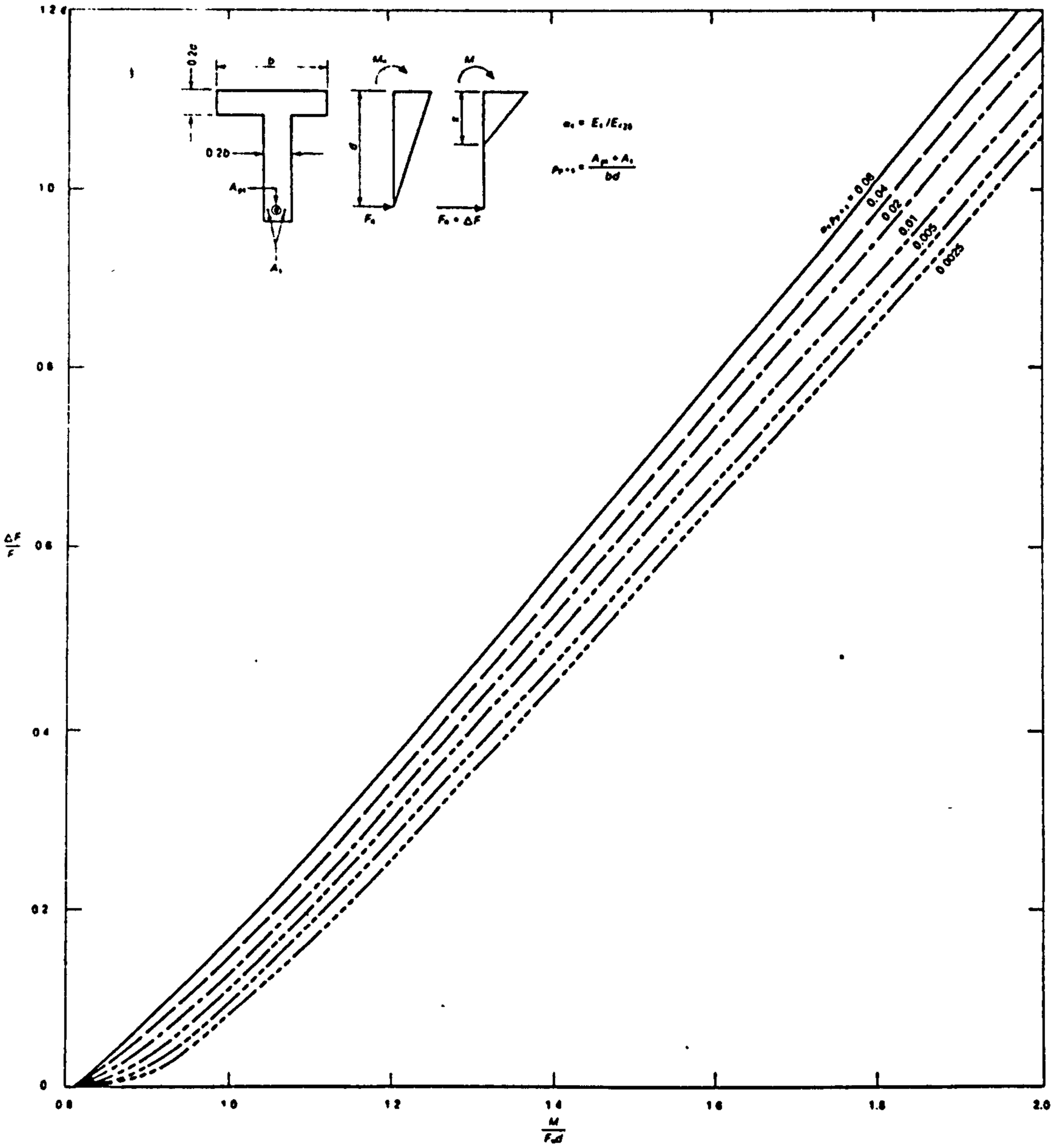

Fig.11.7 Increase of total reinforcement force in flanged section ($h_f = 0.2d$, $b_w = 0.2b$) after cracking

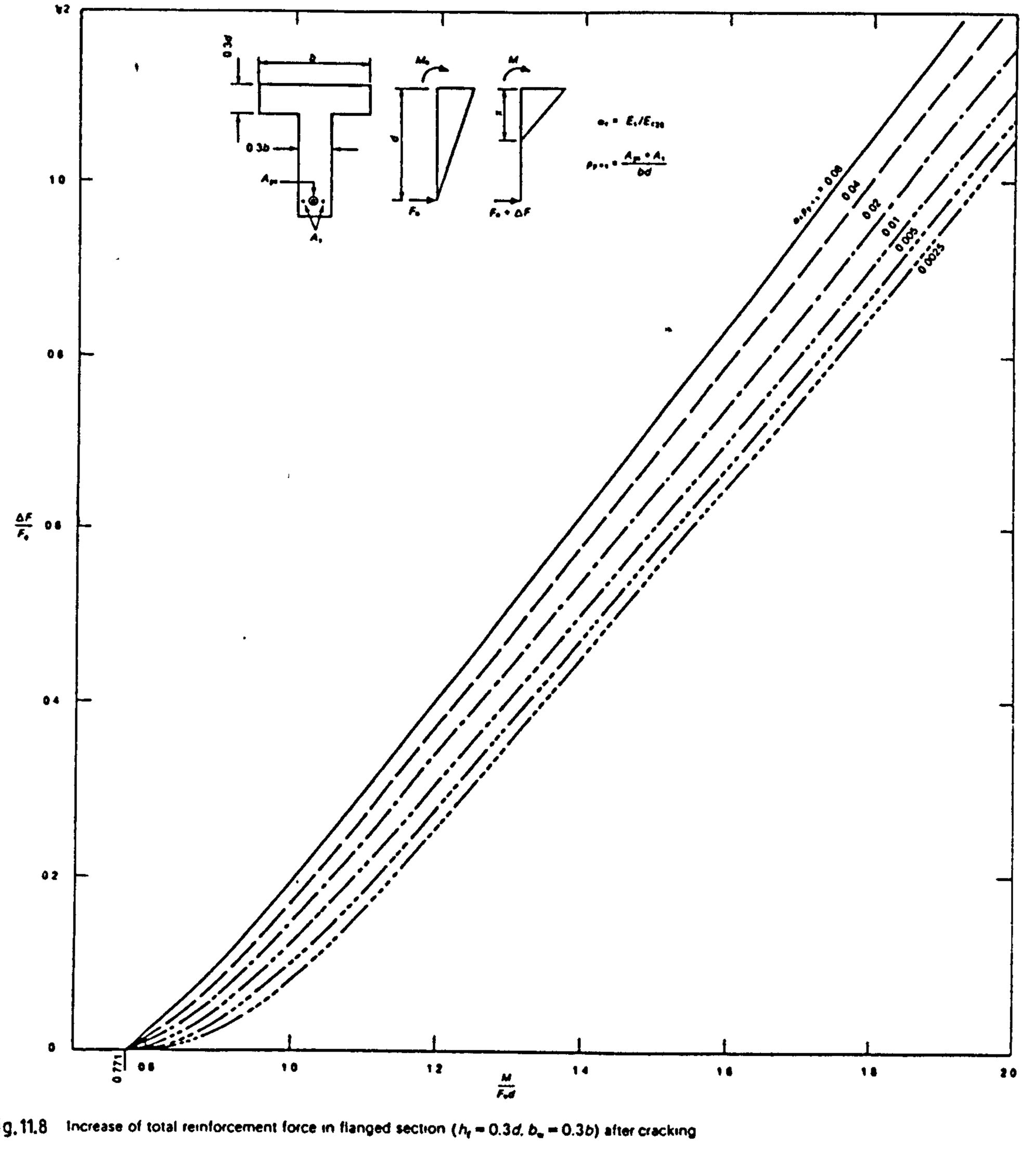

Fig. 11.8 Increase of total reinforcement force in flanged section ($h_f = 0.3d$, $b_w = 0.3b$) after cracking

REFERENCES

1. ABELES, P.W., "Fully and Partly Prestressed Concrete", Journal of ACI, Vol. 16, No. 3, Jan. 1945, pp. 181-214.

2. ABELES, P.W., "Saving Reinforcement by Prestressing", Concrete & Constructional Engineering, Vol. 35, No. 7, July 1940, pp. 328-333.

3. ABELES, P.W., "Saving Reinforcement by Prestressing", Discussion Paper, Concr. Const. Eng., Vol. 36, Feb., 1941.

4. FREYSSINET, E., "Prestressed Concrete - Principles and Applications", Journal, Inst. of Civil Engineers, Vol. 33, No. 4, Feb. 1950, pp. 331-380.

5. ABELES, P.W., "Design of Partially Prestressed Concrete Beams", Journal, ACI, Vol. 64, No. 10, Oct. 1967, pp. 669-677.

6. BRITISH STANDARDS INSTITUTION, "Code of Practice for the Structural Use of Concrete. Part 1: Design, Materials and Workmanship", London, pp. 156, CP100: Part 1: 1972.

7. BENNETT, E.W., "Partial Prestressing - Developments in Prestressed Concrete - 1." Sawko, F. (Editor) London, Applied Science Publishers, 1978, pp. 125-147.

8. BENNETT, E.W., "Design of partially prestressed concrete with reference to the CEB/FIP Model Code", FIP Proceedings of a Symposium on Partial Prestressing, Sept. 1980, Vol. 1, Bucharest pp. 207-235.

9. THE CONCRETE SOCIETY, "Partial Prestressing", Report of a Concrete Society Working Party, 1983, pp. 27, Technical Report No. 23, Publication 53.040.

10. MARTINO, N.E. and NILSON, A.H. "Crack Widths in Partially Prestressed Concrete Beams", Ithaca, New York, Cornell University.

11. BENNETT, E.W. and CHANDRASEKHAR, C.S., "Calculation of width of cracks in Class 3 prestressed beams", Proc. Inst. of Civil Engrs. Vol. 49, 1972, pp. 333-346.

12. CHANDRAVEKHAR, C.S., "A study of the influence of the properties and distribution of the reinforcement of the behaviour of beams with limited prestress. PhD Thesis, University of Leeds, 1970.

13. BENNETT, E.W., "Structural Concrete Elements", Chapman & Hall, London 1973.

14. NAAMAN, A.E. and SIRIAKSORN, A., "Serviceability based design of partially prestressed beams. Part 1: Analytical formulation", Journal, PCI, Vol. 24, No. 2, March/April 1979, pp. 64-89.

15. NAAMAN, A.E. and SIRIAKSORN, A., "Servicability based design of partially prestressed beams. Part 2: Computerized design and evaluation of major parameters", Journal PCI, Vol. 24, No. 3, May/June 1979, pp. 40-60.

16. NAAMAN, A.E., "Partially prestressed beams: A unified design procedure for strength and serviceability", FIP proceeding of a symposium on Partial Prestressing, Sept. 1980, Vol. 1, Bucharest, pp. 2360249.

17. BACHMANN, H., "Partial Prestressing of Concrete Structures, IABSE Survey", S-11/79, International Association for Bridge and Structural Engineering, Nov. 1979.

18. BACHMANN, H., "10 Thesis on Partial Prestressing", FIP proceeding of a symposium on Partial Prestressing, Sept. 1980, Vol. 1, Bucharest, pp. 92-103.

19. LEONHARDT, F., "Partial Prestressing Improves Serviceability", FIP Proceeding of a Symposium on Partial Prestressing, Sept. 1980, Vol. 1, Bucharest, pp. 250-257.

20. ABELES, P.W., "Partial prestressing and its suitability for limit states design", Structural Engr., Vol. 49, No. 2, Feb. 1971, pp. 67-86.

21. STEVEN, R.F., "Tests on prestressed reinforced concrete beams", Concrete, Vol. 3, No. 11, Nov. 1969, pp. 457-462.

22. Cement and Concrete Association, "Handbook on the Unified Code ofr Structural Concrete CCP110:1972), London.

23. VEERASWBRAMANIAN, N., "Effect of shape of cross-section on the flexural behaviour of 'Class 3' prestressed concrete beams", PhD Thesis, University of Leeds.

24. BENNETT, E.W. and VEERASWBRAMANIAN, N., "Behaviour of non-rectangular beams with limited prestress after flexural cracking", Journal ACI, Vol. 69, No. 9, Sept. 1972, pp. 533-542.

25. ABELES, P.W., "Studies of crack widths and deformation under sustained and fatigue loading", Journal PCI, Vol. 10, Dec. 1965, pp. 43-52.

26. ABELES, P.W. and KUNG, R., "Prestress losses due to the effect of shrinkage and creep on non-tensioned steei", Journal ACI, Vol. 70, No. 4, Jan. 1973, pp. 19-27.

27. SHEIKH, A.F. and BRANSON, D.E., "Non-tensioned steel in prestressed concrete beams", Journal, Prestressed Concrete Institute, Vol. 15, No. 1, Feb. 1970, pp. 14-36.

28. BRANSON, D.E., "Design Procedures for computing deflection", ACI Journal, Vol. 65, No. 9, Sept. 1968, pp. 730-742.

29. KRIPAHARAYANAN, K.M. and BRANSON, D.E., "Short-time deflections of beams under single and repeated load cycles", ACI Journal Vol. 69, No. 2, Feb. 1972, pp. 110-117.

30. BRANSON, D.E. and TROST, H., "Unified procedures for predicting the deflection and centroidal axis location of partially cracked non-prestressed and prestressed concrete members", ACI Journal, Vol. 79, No. 2, March/April 1982, pp. 119-130.

31. NEVILLE, A.M., "Properties of concrete", Pitman Publishing Limited, London, 3rd Edition, 1981.

32. GLANVILLE, W.H. and THOMAS, F.G., "Further investigations on the creep or flow of concrete under load", D.S.I.R., Building Research, Technical Paper No. 21, (London H.M.S.O) 1939.

33. GOTO, Y. "Cracks formed in concrete around deformed tension bars", Proc. ACI Journal, Vol. 68, April 1971, pp. 244-251.

34. RAO, P.S. and SUBRAHMANYAM, B.V., "Trisegmental moment-curvature relations for einforced concrete members", Proc. ACI Journal, Vol. 70, May 1973, pp. 346-351.

35. CLARK, L.A. and SPEIRS, D.M., "Tension stiffening in reinforced concrete beams and slabs under short-term load", London, Cement and Concrete Association, Report 42.251, July 1978.

36. COMITE EURO-INTERNATIONAL DU BETON, "CEB/FIP Model Code for Concrete Structures", International System for Unified Standard Codes of Practice for Structures, Vol. 2, London, Comite Euro-International du Beton.

37. NAWY, E.G. and HUANG, P.T., "Crack and deflection control of pretensioned prestressed beams", Journal, PCI, Vol. 22, No. 3, May/June 1977, pp. 30-47.

38. BACHMANN, H., "Partially prestressed concrete: Simplified design based on Swiss practice since 1968", International Symposium: Non-Linearity and Continuity in Prestressed Concrete, Preliminary Publication, Vol. 1, University of Waterloo, Ontario, Canada, July, 1983.

39. BENNETT, E.W. and JOYNES, H.W., "Fatigue strength of cold-worked non-prestressed reinforcement in prestressed concrete beams", Magazine of Concrete Research, Vol. 31, No. 106, pp. 13-18, March 1979.

40. BENNETT, E.W. and JOYNES, H.W., "Fatigue resistance of the reinforcement in partially prestressed beams", Journal, PCI, Vol. 22, No. 2, pp. 78-88, March/April 1977, Discussion, Vol. 22, No. 6, pp. 116-118, Nov/Dec, 1977.

41. JOYNES, H.W., "Fatigue of reinforcement in beams with limited prestress", PhD Thesis, Leeds University, July, 1975.

42. NILSON, A.H., "Flexural stresses after cracking in partially prestressed beams", PCI Journal, Vol. 21, No. 4, July/Aug. 1976, pp. 72-81.

43. MONSTAFA, S.E., "Design of partially prestressed concrete flexural members", PCI Journal, Vol. 22, No. 3, May/June 1977, pp. 12-29, Discussion: PCI Journal, Vol. 23, No. 3, May/June 1978, pp. 72-94.

44. BRØNDUM-NIELSEN, T., "Stress Analysis of concrete sections under service load", ACI Journal, Vol. 76, No. 2, Feb. 1979, pp. 195-211.

45. TADROS, M.K., "Expedient service load analysis of cracked prestressed concrete sections", PCI Journal, Vol. 27, No. 6, Nov/Dec. 1982, pp. 86-111. Discussion: PCI Journal, Vol. 28, No. 6, Nov/Dec. 1983, pp. 137-158.

46. DAVE, N.J., "Limited prestressing as a means of economy in structural concrete", PhD Thesis, Leeds University, 1967.

47. BENNETT, E.W. and DAVE, N.J., "Test performance and design of concrete beams with limited prestress". Structural Engineers, Vol. 47, No. 12, Dec. 1969, pp. 487-496.

48. McHENRY, D., "A new aspect of creep in concrete and its application to design", ASTM, Proc. 43, 1943, pp. 1069-1084.

49. BRANSON, D.E., and TROST, H., "Application of I-effective method in calculating deflections of partially prestressed tendons", PCI Journal, Vol.27, No.5, Sep/Oct.1982, pp.62-77.
Discussion: PCI Journal, Vol.28, No.6, Nov/Dec 1983, pp. 131-137.

50. MOOSECKER, W. and GRASSER, E., "Evaluation of tension stiffening effects in reinforced concrete linear members", Colloquium on Advanced Mechanics of Reinforced Concrete (Delft, June 1981), International Association for Bridge and Structural Engineering, Zurich, 1981, pp. 1-10.

51. NEVILLE, A.M., "Creep of concrete: plain, reinforced and prestressed", North-Holland Publishing Company, Amsterdam, 1970.

52. BENNETT, E.W., "A theory for the movement of cracks in concrete members with plain bar reinforcement or plain wire tendons", Mag. of Concrete Research, Vol. 26, No. 87, June 1974, pp. 83-92.

53. BENNETT, E.W. and CHANDRASEKHAR, C.S., "Supplementary tensile reinforcement in prestressed concrete beams", Concrete, Vol. 6, Oct. 1972, pp. 35-39.

54. BENNETT, E.W. and CHANDRASEKHAR, C.S., "Stresses in tendons and supplement reinforcement of 'class 3' prestressed concrete beams", Building Science, Vol. 6, pp. 123-131, 1971.

55. NAAMAN, A.E., "Prestressed concrete analysis and design", McGraw-Hill Book Company, New York, 1982.

56. BATE, S.C.C. and BENNETT, E.W. "Design of prestressed concrete", Surrey University Press, 138 pp. London 1976.

57. ACI Committee 318, "Building Code Requirements for Reinforced Concrete (ACI 318-83)", Detroit, 1983.

58. BRANSON, D.E. and TROST, H., "Unified procedures for predicting the deflection and centroidal axis location for non-prestressed and partially prestressed members", Lehrstuhl und Institut fur Massivban, Technische Hochschule (RWTH), Aachen, June 1981.

59. BRANSON, D.E., "Deformation of concrete structures", McGraw-Hill International Book Company, 1977.

60. LIN, T.Y., "Partial prestressing design - philosophy and approach", ACI Special Publication SP-59, 1979, pp. 257-267.

61. ABELES, P.W., "Philosophy of design of partial prestressing", ACI Special Publication, SP-59, 1979, pp. 287-304.

62. STANDARDS ASSOCIATION OF AUSTRALIA, "Rules for the Use of Prestressed Concrete in Structures - SAA Prestressed Concrete Code", North Sydney, New South Wales, Australia.

63. BRITISH STANDARDS INSTITUTE, "Steel, concrete and composite bridges, BS 5400: Part 4, 1978 (as revised 1982), Code of Practice for the Design of Concrete Bridges.

64. BRITISH STANDARDS INSTITUTION, BS1881:Part 4 & Part 5, 1970, Method of Testing Concrete, 1970, London.

Appendix A

```
C  Program to calculate the deflection of an uncracked or cracked
C  prestressed beam.
C
C  The method of calculation is based on the CP110 Appendix A
C  recommendation in which the deflection is calculated by integration
C  of curvature.
C
C  Basically this program can be used to calculate short-term and
C  long-term deflections. The effect of creep on the stress distribution
C  is considered in the analysis of reinforcement stresses.
C
      CHARACTER*4 INAS
      COMMON /CRKMOM/ AMCRK
      COMMON /LEVEL/D,DP,DS
      COMMON /BMT/BMOML(100),BMOMD(100)
      COMMON /CRK/ICK(100)
      COMMON /CURVER/CURV1(100),CURV2(100),CURV22(100)
      COMMON /SECT/AREAE,AREAC,ECI,CCI,YEP,YES,YCP,YCS,
     * AREAP,PCI,YPP,YPS
      COMMON /SHAPE/B,BI,BW,H,HF,HB,AP,AS
      COMMON /LD/PLOAD,WLOAD
      COMMON /LCP2/ DEFDD(100),DEFLI(100),DEFTO(100),PAXIS1(100),
     * PAXIS2(100),PAXIS3(100),SFP1(100),SFP2(100),SFS1(100),SFS2(100)
C
10    WRITE(6,20)
C
20    FORMAT('0','**********************************************',
     1 '**********')
C
      WRITE(6,22)
22    FORMAT('0',5X,'INDEX',40X,'TYPE',/6X,'=====',40X,'====')
      WRITE(6,24)
24    FORMAT('0','1.  First cycle of loading',25X,'1ST')
      WRITE(6,25)
25    FORMAT('0','2.  further increment of load in 1st cycle',9X,'1ST2')
      WRITE(6,26)
26    FORMAT('0','3.  Second or subsequent cycle of loading',10X,'2ND',/
     1  5X,'OR   Unloading',//,
     *           ' 4.  Long-term deflections                    ',10X,'LTM')
      WRITE(6,28)
28    FORMAT('0','5.  Neutral Axis of cracked section',16X,'NAX')
      WRITE(6,30)
30    FORMAT('0','6.  End Job',40X,'END')
      WRITE(6,20)
      WRITE(6,32)
32    FORMAT('0','*** Choose one option from the above index ***')
      READ(5,FMT=40,ERR=10)INAS
40    FORMAT(A4)
C
      IF(INAS.EQ.'2ND'.OR.INAS.EQ.'LTM') GOTO 190
      IF(INAS.EQ.'END') GOTO 260
C
      IF(INAS.EQ.'1ST') GOTO 99
      IF(INAS.EQ.'NAX') GOTO 99
```

```
      IF(INAS.EQ.'1ST2') GOTO 199
C
      GOTO 10
C
99    WRITE(6,100)
100   FORMAT(' Dimensions of the beam')
      WRITE(6,110)
110   FORMAT(' b, bw, bi, H, Hf, Hb, Span   (all in mm)')
      READ(5,*)B,BW,BI,H,HF,HB,SPAN
      WRITE(6,120)
120   FORMAT('0Area of tendons, Area of ordinary reinforcement')
      WRITE(6,130)
130   FORMAT(' Ap,  As   (mm2)')
      READ(5,*)AP,AS
C
      WRITE(6,140)
140   FORMAT('0Levels of reinforcement : Dp,  Ds  (mm)')
      READ(5,*)DP,DS
      WRITE(6,150)
150   FORMAT('0Mod. of elas. of concrete : Ec   (N/mm2)')
      READ(5,*)EC
      WRITE(6,160)
160   FORMAT('0Ratio of  Es/Ec   : Alpha')
      READ(5,*)ALPHA
C
      WRITE(6,170)
170   FORMAT('0Eff. force in tendons after losses  (N)')
      READ(5,*)PE
C
      WRITE(6,175)
175   FORMAT('0Corresponding force in ord. reinf. (- for compr.)')
      READ(5,*)FSE
C
      IF(INAS.NE.'NAX') GOTO 176
C
      CALL NEUTRL (PE,FSE,ALPHA,EC)
C
      GOTO 10
176   WRITE(6,180)
180   FORMAT('0Tensile strength of concretr : fcr   (N/mm2)',/,
     *' OR Observed cracking moment : Mcr  Nmm',/,
     *' INPUT (-1) for unwanted option')
      READ(5,*)FCR,AMCRK
C
C -----------------------------------------------------------------
C Assumed Data.
C The beam is arbitrarily divided into 81 elements in half span.
C
      NELEM = 81
      WELEM = SPAN/(2*NELEM - 1)
C     NRELEM = 21
C
C -----------------------------------------------------------------
C
      CALL PROPT (ALPHA)
C
199   DO 200 I=1,NELEM
      ICK(I)=0
```

```
200    CONTINUE
C
190    CALL MOMENT (SPAN,NELEM,WELEM)
C
C ==========================================================
C
       DO 220  II = 1,NELEM
C
C Position of neutral-axis is arbitrarily assigned a value.
C
       PAXIS1(II)=-1.0
       AMOM = BMOMD(II)
       CALL UNCRAK (II,AMOM,ALPHA,PE,FSE,FCR,EC,FP,FS,SMCUR)
C
       IF (SMCUR.NE.0.0) GOTO 210
C
C
       WRITE(6,201)II
201    FORMAT(' II = ',I3)
       CALL STRESS (II,FCR,PE,FSE,AMOM,ALPHA,EC,AXIS,FP,FS,SMCUR)
C
       PAXIS1(II)=AXIS
210    SFP1(II)  =FP
       SFS1(II)  =FS
C
       CURV1(II) = SMCUR
C
220    CONTINUE
C
C ***************
C
C  Bending moment is set to the TOTAL moment due to prestress, dead
C  and live load.
C  The CURVATURES calculated will be the total due to all loads.
C
C ***************
C
       DO 400  II=1,NELEM
       PAXIS2(II)=-1.0
       AMOM = BMOML(II)+BMOMD(II)
C
       CALL UNCRAK (II,AMOM,ALPHA,PE,FSE,FCR,EC,FP,FS,SMCUR)
       IF (SMCUR.NE.0.0) GOTO 450
       WRITE(6,401)II
401    FORMAT(' II = ',I3)
C
       CALL STRESS (II,FCR,PE,FSE,AMOM,ALPHA,EC,AXIS,FP,FS,SMCUR)
C
       PAXIS2(II)=AXIS
450    SFP2(II)  =FP
       SFS2(II)  =FS
C
       CURV2(II)=SMCUR
C
400    CONTINUE
C
       IF (INAS.EQ.'LTM') THEN
       CALL LONG (ALPHA,NELEM,WELEM,SPAN,PE,FSE,EC)
```

```
      GOTO 10
      END IF
C
C =============================================================================
C
      DO 225  NRELEM = 1,NELEM
      CALL DEFLEC (WELEM,NELEM,NRELEM,SPAN,DEF1,DEF2)
C
      DEFDD(NRELEM) = DEF1
      DEFTO(NRELEM) = DEF2
      DEFLI(NRELEM) = DEF2-DEF1
225   CONTINUE
C
      PLOAD2=PLOAD*2.0
      WRITE(7,312)PLOAD2
312   FORMAT(' APPLIED LOAD = ',F7.1)
C
C -----------------------------------------------------------------------------
C
C     WRITE(7,300)
C300   FORMAT(30X,'DEFLECTIONS CAUSED BY :   (ALL IN MM)')
C     WRITE(7,310)
C310   FORMAT(3X,'DIST. FR. SUPPORT',7X,'PRESTRESS & DEAD LOAD',7X,
C    1  'LIVE LOAD',7X,'TOTAL')
C     WRITE(7,315)
C315   FORMAT(3X,'================',7X,'====================',7X,
C    2  '========',7X,'=====')
C
C     DO 350 I=1,NELEM
C     WRITE(7,500)
C500   FORMAT('   ')
C     IXX = WELEM*(I-0.5)
C     WRITE(7,320)IXX,DEFDD(I),DEFLI(I),DEFTO(I)
C320   FORMAT(9X,I4,21X,F7.3,15X,F7.3,7X,F7.3)
C350  CONTINUE
C     WRITE(7,230)DEFTO(41)
C230   FORMAT(' Central deflection is : ',F7.2,'  (mm)')
C
C     DO 231  N=1,NELEM
C      WRITE(4,232)CURV1(N),CURV2(N)
C232   FORMAT('0',F12.8,F12.8)
231   CONTINUE
C
C
C
C -----------------------------------------------------------------------------
C
      WRITE(7,300)
300   FORMAT(' D.F.SPT',12X,'Effect of prestress + Dead Load',20X,
     * 'Effect of Prestress + Total Load',15X,'Live Load Def.')
      WRITE(7,315)
315   FORMAT(' -------',4X,'-------------------------------------
     *--',
     *3X,'-----------------------------------------------------',2X,
     *'--------------')
      WRITE(7,500)
500   FORMAT('   ')
      WRITE(7,310)
```

```
310   FORMAT(12X,'T.STRESS',3X,'UTS STRESS',3X,'CURVATURE',3X,
     *'DEFLECTION',3X,
     * 'N-AXIS',3X,'T.STRESS',3X,'UTS STRESS',3X,'CURVATURE',3X,
     * 'DEFLECTION')
      WRITE(7,500)
      DO 350 I=1,NELEM
      IXX =WELEM*(I-0.5)
      WRITE(7,320)IXX,SFP1(I),SFS1(I),CURV1(I),DEFDD(I),PAXIS2(I),
     *SFP2(I),SFS2(I),CURV2(I),DEFTO(I),DEFLI(I)
320   FORMAT(2X,I5,5X,F7.2,4X,F7.2,5X,E10.3,4X,F7.3,5X,F6.3,3X,F7.2,
     * 5X,F7.2,
     * 4X,E10.3,4X,F7.3,5X,F7.3)
C
350   CONTINUE
      WRITE(9,352)PLOAD2,DEFLI(81)
352   FORMAT(F10.3,5X,F10.4)
C
      GOTO 10
C
260   STOP
      END
C
C ***************************************************************************
C
C  Subroutine to calculate neutral axis and level arm of a cracked
C  section.
C
      SUBROUTINE NEUTRL (PE,FSE,ALPHA,EC)
C
      COMMON /LEVEL/D,DP,DS
      COMMON /SECT/ AREAE,AREAC,ECI,CCI,YEP,YES,YCP,YCS,
     * AREAP,PCI,YPP,YPS
      COMMON /SHAPE/B,BI,BW,H,HF,HB,AP,AS
      COMMON /ZAXIS/ZARM
C
      WRITE(6,10)
10    FORMAT('0BENDING MOMENT ?')
      READ(5,*)AMOM
C
      CALL PROPT (ALPHA)
C
      CALL STRESS (II,FCR,PE,FSE,AMOM,ALPHA,EC,AXIS,FP,FS,SMCUR)
C
      WRITE(6,20)AXIS
20    FORMAT('0NEUTRAL AXIS,    x/d = ',F6.4)
      WRITE(6,30)ZARM
30    FORMAT('0LEVEL ARM,       z/d = ',F6.4)
C
      RETURN
      END
C
C ***************************************************************************
C
      SUBROUTINE MOMENT (SPAN,NELEM,WELEM)
C
      COMMON /BMT/BMOML(100),BMOMD(100)
      COMMON /LD/PLOAD,WLOAD
C
```

```
C  This subroutine computes the bending moment at all the sections
C  along the beam.
C  The bending moment is the sum of moment of two types of loading,
C  Uniformly Distributed AND Two-point loads with equal distant
C  from the ends.
C  Each point load should have same load P.
C
      ,WRITE(6,20)
20     FORMAT('0Distributed load     (N/mm)')
       READ(5,*)WLOAD
       WRITE(6,25)
25     FORMAT('0Each two-point load     (N)')
       READ(5,*)PLOAD
       WRITE(6,30)
30     FORMAT('0Distant of the point load from the support   (mm)')
       READ(5,*)ADIST
C
C
       DO 40 I=1,NELEM
C
       XDIST  = WELEM*(I-0.5)
       BMUNI  = 0.5*WLOAD*XDIST*(SPAN-XDIST)
       XL     = SPAN-ADIST
C
       IF (XDIST.GT.ADIST) GOTO 50
       BMPTS = PLOAD*XDIST
       GOTO 100
C
50     IF (XDIST.GT.XL) GOTO 60
       BMPTS = PLOAD*ADIST
       GOTO 100
C
60     BMPTS = PLOAD*(SPAN-XDIST)
100    BMOMD(I) = BMUNI
       BMOML(I) = BMPTS
C
40     CONTINUE
C
       RETURN
       END
C
C ***************************************************************************
C
       SUBROUTINE PROPT (ALPHA)
C  THIS SUBROUTINE COMPUTE THE SECTION PROPERTIES.
C  THE DATA REQUIRED ARE THE DIMENSIONS OF THE SECTION, THE AREA OF
C  TENDONS AND ORDINARY REINFORCEMENT, AND THE LEVELS OF BOTH TYPE
C  OF STEELS.
C
C  BW   : BREADTH OF WEB
C  B    : BREADTH OF TOP FLANGE
C  BI   : BREADTH OF BOTTOM FLANGE
C  H    : OVERALL DEPTH OF SECTION
C  HF   : DEPTH OF TOP FLANGE
C  HB   : DEPTH OF BOTTOM FLANGE
C
C
       COMMON /LEVEL/D,DP,DS
```

```
      COMMON /SECT/AREAE,AREAC,ECI,CCI,YEP,YES,YCP,YCS,
     * AREAP,PCI,YPP,YPS
      COMMON /SHAPE/B,BI,BW,H,HF,HB,AP,AS
C
C
      B8 = BW/B
      B9 = BI/B
      H8 = HF/H
      H9 = HB/H
C
C
      TERM = (1.0-B8)*(1.0-H8-H9) + (1.0-B9)*H9
C
C  AREA, *BH
C
      AREA = (1.0-TERM)
      RT2  = (1.0-B8)*(2.0-H8)*H8
      RT3  = (B9-B8)*(H9**2.0)
C
C  SUBROUTINE TO CALCULATE REINFORCEMENT STRESSES IN TENDONS AND
C  YIF, Y INFERIOR *H
C
      YIF = 0.5*(B8+RT2+RT3)/(AREA)
      YSUP = (1.0-YIF)
      GIGG = (1.0-B8)*(H8**3.0) + (B9-B8)*(H9**3.0) + B8
      AYSQ = 3.0*(B8+(1.0-B8)*(H8)*((2.0-H8)**2.0) +
     2      (B9-B8)*(H9**3.0))
      AYIFSQ =  AREA*(YIF**2.0)*12.0
C
C  CI, SECOND MOMENT OF AREA ABOUT CENTROID,  *BH**3/12
C
      CI = GIGG + AYSQ - AYIFSQ
C
C  Z AT TOP AND BOTTOM SOFFITS,  *(BH)**2/6
C
      ZIF  = (CI/YIF)*0.5
      ZSUP = 0.5*CI/(1.0-YIF)
C
C  EP : ECCENTRICITY OF TENDONS FROM CENTROID    IN  MM
C  ES : ECCENTRICITY OF ORDINARY REINFORCEMENT FROM CENTROID IN MM
C
      EP = DP - (1.0-YIF)*H
      ES = DS - (1.0-YIF)*H
C
C  COMPUTE THE EFFECTIVE SECTION PROPERTIES.
C  THE STIFFENESS OF BOTH TENDONS AND ORDINARY REINFORCEMENT ARE TAKEN
C  INTO ACCOUNT.
C  BOTH TYPE OF STEELS ARE AT DIFFERENT LEVELS.
C  USE THESE PROPERTIES FOR CALCULATION OF STRESSES BY BENDING.
C
C  AREAE, IN MM2
C  ECI   , IN MM4
C
      AREAE = AREA*B*H + (ALPHA-1.0)*(AP+AS)
      DE    = (ALPHA-1.0)*(AP*EP+AS*ES)/AREAE
      ECI   = (CI*B*(H**3.0)/12.0) + AREA*B*H*(DE**2.0) +
     3     (ALPHA-1.0)*AP*((EP-DE)**2.0)+(ALPHA-1.0)*AS*((ES-DE)**2.0)
      YEP = EP - DE
```

```
      YES = ES - DE
C
C  EFFECTIVE SECTION PROPERTIES.
C  ONLY THE STIFFENESS OF ORDINARY REINFORCEMENT IS TAKEN INTO ACCOUNT.
C  USE THESE PROPERTIES FOR CALCULATIONS OF PRESTRESS.
C
C  AREAC, IN MM2
C  CCI ,  IN MM4
C
      AREAC = AREA*B*H + ALPHA*AS - AP - AS
      CDE = (ALPHA*AS*ES-AS*ES-AP*EP)/AREAC
      CCI = (CI*B*(H**3.0)/12.0) + (AREA*B*H)*(CDE**2.0) +
     4     (ALPHA*AS*((ES-CDE)**2.0)) - AP*((EP-CDE)**2.0)
      YCP = EP - CDE
      YCS = ES - CDE
C
C Transformed section properties based on the concrete area only,
C the reinforcement areas are deducted.
C
      AREAP = AREA*B*H - (AP+AS)
      PDE   = -(AP*EP+AS*ES)/AREAP
      PCI   = (CI*B*(H**3)/12.0)+ AREA*B*H*ABS(PDE**2)
     * - AS*((ES-PDE)**2) - AP*((EP-PDE)**2)
      YPP = EP-PDE
      YPS = ES-PDE
C
      RETURN
      END
C
C ***********************************************************
C
      SUBROUTINE UNCRAK(II,AMOM,ALPHA,PE,FSE,FCR,EC,FP,FS,SMCUR)
C
C  This subroutine computes the curvature of the uncracked sections
C  The curvature is calculated based on the strain values at the
C  top and bottom extreme fibres.
C
      COMMON /CRKMOM/AMCRK
      COMMON /LEVEL/D,DP,DS
      COMMON /SHAPE/B,BI,BW,H,HF,HB,AP,AS
      COMMON /SECT/AREAE,AREAC,ECI,CCI,YEP,YES,YCP,YCS,
     * AREAP,PCI,YPP,YPS
      COMMON /CRK/ICK(100)
      COMMON /SUMSTR/ SMST1(100),SMST2(100),SMST3(100),SMST4(100)
C
C  1  : refer to extreme top fibre
C  2  : refer to extreme bottom fibre
C  3  : refer to the level of tendons
C  4  : refer to the level of non-prestressed reinforcement
C  P  : due to prestress
C  B  : due to bending stress
C
      YSUPP = DP-YCP
      YINFP = H-DP+YCP
C
C  compute prestress at the extreme top and bottom fibres.
C
      YP1 = DP-YPP
```

```
      YP2 = H-DP+YPP
      FINFP2 = (PE/AREAP)+(PE*YP2*YPP/PCI)+(FSE/AREAP)+(FSE*YP2*YPS/PCI)
      FINFP1 = (PE/AREAP)-(PE*YP1*YPP/PCI)+(FSE/AREAP)-(FSE*YP1*YPS/PCI)
      FINFP3 = (PE/AREAP)+(PE*YPP*YPP/PCI)+(FSE/AREAP)+(FSE*YPP*YPS/PCI)
      FINFP4 = (PE/AREAP)+(PE*YPP*YPS/PCI)+(FSE/AREAP)+(FSE*YPS*YPS/PCI)
C
      YSUPB = DP-YEP
      YINFB = H-DP+YEP
C
C  Compute cracking Moment, AMCRK i.e. the moment causing stresses
C  equal to concrete tensile strength at the soffit.
C
      IF (FCR.LT.0.0) THEN
      FCR = (AMCRK*YINFB/ECI)-FINFP2
      PRINT *,' FCR = ',FCR
      ELSE
      AMCRK = (FCR+FINFP2)*ECI/YINFB
      END IF
C
C  Compute stresses due to bending.
C
      FINFB2 = AMOM*YINFB/ECI
      FINFB1 = AMOM*YSUPB/ECI
      FINFB3 = AMOM*YEP/ECI
      FINFB4 = AMOM*YES/ECI
C
C  SMFIN2 : sum of stresses at extreme bottom fibre
C           + ve tension ; -ve compression
C
      SMFIN2 = FINFB2-FINFP2
C
      SMFIN1 =  FINFB1+FINFP1
      SMFIN3 =  FINFB3-FINFP3
      SMFIN4 =  FINFB4-FINFP4
C
C Convert the sign convention to
C +ve compression ; -ve tension
C
      SMST1(II) = SMFIN1
      SMST2(II) = 0.0-SMFIN2
      SMST3(II) = 0.0-SMFIN3
      SMST4(II) = 0.0-SMFIN4
C
      IF (SMFIN2.LT.0.0) GOTO 30
      IF (ICK(II).EQ.1) GOTO 40
      IF (SMFIN2.GT.FCR) GOTO 40
C
C  FCR, The tensile stress that concrete can withstand and it must
C  be given as positive value. SMFIN2  : will be positive if the
C  total stresses is in tension.
C
C  CURP : curvature due to prestress
C  CURB : curvature due to bending stress
C
30    CURP = (FINFP2-FINFP1)/(EC*H)
      CURB = (FINFB1+FINFB2)/(EC*H)
      FP   = (PE/AP) + (ALPHA*FINFB3)
      FS   = (FSE/AS) + (ALPHA*FINFB4)
```

```
C
      SMCUR = CURB-CURP
C
C
      GOTO 50
C
C  Section is cracked, thus curvature is arbitrary assigned a
C  value and return to the main program.
C
40    SMCUR = 0.0
      ICK(II)=1
      FP = 0.0
      FS = 0.0
C
C     WRITE(6,45)
45    FORMAT(' TOTAL STRESS AT BOTTOM SOFFIT EXCEED ALLOWABLE ! ')
C     WRITE(6,46)
46    FORMAT(' THE SECTION IS THUS CONSIDERED CRACKED.')
C
50    IF(II.EQ.81) THEN
      WRITE(6,47)FINFP1,FINFP2
47    FORMAT(' EFFECTIVE PRESTRESS: TOP,BOTTOM = ',F6.2,5X,F6.2)
      END IF
      RETURN
      END
C
C ***********************************************************************
C
C
      SUBROUTINE STRESS (II,FCR,PE,FSE,AMOM,ALPHA,EC,AXIS,FP,FS,SMCUR)
      REAL *8 IMZ,REZ,AR,TOL
C
C ***************
C
C  This subroutine computes the CURVATURE, STRESSES in both tendons
C  and non-prestressed reinforcement at the cracked section and also
C  the average stresses at the cracked region.
C
C ***************
C
      COMMON /CRKMOM/AMCRK
      COMMON /LEVEL/D,DP,DS
      COMMON /SHAPE/B,BI,BW,H,HF,HB,AP,AS
      COMMON /SECT/AREAE,AREAC,ECI,CCI,YEP,YES,YCP,YCS,
     * AREAP,PCI,YPP,YPS
      COMMON /ZAXIS/ZARM
      COMMON /POLYN/ AR(4),REZ(4),IMZ(4)
      COMMON /LCP/ FCTOP(100),PNOT(100),FSNOT(100),FC11(100),FC22(100)
C
      ASR = AS/(B*H)
      APR = AP/(B*H)
      ASPR = APR+ASR
      ASPRR = (AP+AS)/AREAE
      WEB = (H-HB)/H
      FLGT= HF/H
C
C ***************
C
```

```
C  The reference level of the section and the neutral axis is taken
C  as the total depth of the section, H.
C
C  DAVE, is the centroidal level of the total steel area or the
C  average level of the steel in this program.
C
C ***************
C
C  FCP : Prestress after losses in concrete at the level of tendons.
C  FCS : Prestress after losses in concrete at the level of non-
C        prestressed reinforcement.
C  FSO and PO : (+ tension, - compression)
C  FSO : FORCE  in non-prestressed steel at the point of decompression
C        at the level of non-prestressed reinforcement, Ds
C  PO  : FORCE  in the tendons at the point of decompression at the
C        level of the tendons, Dp
C  PE  : Effective FORCE in the tendons (+ tension)
C  FSE : Effective FORCE in the non-prestressed reinforcement
C        (+ tension, - compression)
C
C ***************
C
      FCP = (PE/AREAP)+(PE*YPP*YPP/PCI)+(FSE/AREAP)+(FSE*YPS*YPP/PCI)
      FCS = (PE/AREAP)+(PE*YPP*YPS/PCI)+(FSE/AREAP)+(FSE*YPS*YPS/PCI)
C
      FSO = FSE + (ALPHA*FCS)*AS
      PO = PE + ALPHA*FCP*AP
C
      CK = (AMOM+FSO*(DP-DS))/((PO+FSO)*H)
C
      H1 = HF/H
      H2 = HB/H
      D2 = DP/H
      D3 = DS/H
C
      B1 = 1.0-(BW/B)
      B2 = (BI/B)-(BW/B)
C
C ***************
C
C  Compute the coefficients of the cubic equation :
C     AA*(x/d)**3 + BB*(x/d)**2 + CC*(x/d) + DD = 0
C
C ***************
C
C  FIRST, assume the neutral axis lies above the bottom flange, so
C  set bi = bw  or B2=0.0
C
      B2 = 0.0
C ***************
C
      N = 0
10    N = N+1
C
C
C                    ****************************
C
C  The following cubic equation is to compute the neutral-axis of
```

```
C  stresses.  Prestressed tendons and non-prestressed reinforcement
C  may be located at different levels.
C  This equation takes into account the COMPRESSIVE stress in the
C  bottom flange  if the  neutral axis  is at the  bottom flange
C  This cubic equation is solved by a routine C02AEF available in
C  the NAG library packages.
C
C  AAA, BBB, CCC are the sub-coefficients within the coefficients
C  and they must be set to ZERO if the neutral axis is above the
C  bottom flange.
C
C                        ***************************
C
      AAA =  B2
      BBB = 3.0*B2*(CK-D2)
      CCC =  B2*( 6.0*CK*(H2-1.0) - 3.0*(H2**2.0)  + 6.0*H2 - 3.0 -
     1  6.0*D2*H2 + 6.0*D2)
      DDD =  3.0*B2*CK*((H2**2.0)-2.0*H2+1.0) + (B2*(6.0*(H2**2.0)-
     1  6.0*H2-2.0*(H2**3.0)+2.0+6.0*D2*H2-3.0*D2*(H2**2.0)-3.0*D2))
C
C COEFFICIENTS :
C
      AA = (1.0-B1)+ AAA
      BB = 3.0*(1.0-B1)*(CK-D2) + BBB
      CC = B1*(6.0*H1*CK+3.0*(H1**2.0)-6.0*D2*H1) + 6.0*ALPHA*CK*
     1 (ASR+APR) - 6.0*ALPHA*ASR*(D2-D3) + CCC
      DD = B1*((H1**2.0)*(3.0*D2-2.0*H1-3.0*CK)) - 6.0*ALPHA*CK*
     1 (ASR*D3+APR*D2) + 6.0*ALPHA*ASR*(D2-D3)*D3 + DDD
C
C ***************
C
C  The cubic equation is solved by calling the NAG routine C02AEF
C  NAG routine C02AEF employs the Newton's method to calculate all
C  the roots both complex and real.  The roots are then stored in
C  the arrays REZ and IMZ respectively for real and complex roots.
C  The required root is the one with complex root equal ZERO and
C  lies within the web, that is between top and bottom flanges.
C  Otherwise, if the root lies in the bottom flange or slightly
C  lower than the bottom soffit, there will be values for AAA,BBB,
C  CCC,DDD.
C  If the root lies within the top flange, the coefficients of the
C  equation will have to be modified automatically to rectangular
C  shape and roots are than recalculated again.
C  N9 is the number of coefficients in the cubic equation, including
C  the constant.
C
C ****************
C
      N9 = 4
      AR(1) = AA
      AR(2) = BB
      AR(3) = CC
      AR(4) = DD
      N91 = N9-1
C
      TOL = 1.0*10.0**(-11.0)
      IFAIL = 0
C
```

```
      CALL CO2AEF (AR,N9,REZ,IMZ,TOL,IFAIL)
C
      IF (N.GT.1) GOTO 110
      IFLGT=0
      IFLGB=0
C
C ***************
C
C  Is Neutral-axis within the WEB ?
C
      DO 20 I = 1,3
      IF (IMZ(I).NE.0.00000) GOTO 20
      IF (REZ(I).LE.WEB.AND.REZ(I).GE.FLGT) GOTO 100
20    CONTINUE
C
C ***************
C
C  Is Neutral-axis within TOP FLANGE ?
C
      DO 30 I = 1,3
C
      IF (IMZ(I).NE.0.0000) GOTO 30
      IF (REZ(I).LT.WEB.AND.REZ(I).GE.0.0000) GOTO 90
30    CONTINUE
C
C ***************
C
C  Is Neutral-axis in the BOTTOM FLANGE ?
C
      DO 40 I = 1,3
      IF (IMZ(I).NE.0.00000) GOTO 40
      IF (REZ(I).GT.WEB) GOTO 80
40    CONTINUE
C
C ***************
C
C  Neutral-axis is within TOP FLANGE
C  Set BW/B = 1.0   i.e. rectangular equation
C
90    Bl = 0.0
      IFLGT = 1
      GOTO 10
C
C ***************
C
C  Neutral-axis is within BOTTOM FLANGE
C  Set BI/B  to its original value.
C
80    B2 = (BI/B)-(BW/B)
      IFLGB = 1
      GOTO 10
C
C ***************
C
110   IF (IFLGB.EQ.1) GOTO 140
      DO 120 I = 1,3
C
      IF (IMZ(I).NE.0.0000) GOTO 120
```

```
      IF (REZ(I).LE.FLGT.AND.REZ(I).GT.0.0000) GOTO 100
120   CONTINUE
C
      GOTO 200
140   DO 150 I = 1,3
      IF (IMZ(I).NE.0.0000) GOTO 150
      IF (REZ(I).GE.WEB.AND.REZ(I).LE.H) GOTO 100
150   CONTINUE
C
      GOTO 200
C
100   X1 = REZ(I)
      AXIS = X1
C
C ***************
C
      IF (X1.GT.1.0) THEN
      WRITE(6,101)II
101   FORMAT(I3,'WARNING ! N-AXIS GREATER THAN 1')
      END IF
C
      T1 = H2-1.0+X1
      T2 = X1-H1
C
      IF (T2.GT.0.000) THEN
      ZTOP1 = (X1**3.0)-B1*(T2**2.0)*(X1+2.0*H1)
      ZTOP2 = 3.0*((X1**2.0)-B1*(T2**2.0))
      ZTOP  = ZTOP1/ZTOP2
      END IF
C
      IF (T1.GT.0.000) THEN
      ZTOP1 = (X1**3.0)-B1*(T2**2.0)*(X1+2.0*H1)+(B2*(T1**2.0)*(X1-
     1   2.0*H2+2.0))
      ZTOP2 = 3.0*((X1**2.0)-B1*(T2**2.0)+B2*(T1**2.0))
      ZTOP  = ZTOP1/ZTOP2
      END IF
C
      ZTOP = ZTOP*H
C
      ZP = DP - ZTOP
      ZS = DS - ZTOP
C
      DAVE = (AS*DS+AP*DP)/(AS+AP)
C
      RS = (D3-X1)/(1.0-X1)
      RP = (D2-X1)/(1.0-X1)
      RAVE = ((DAVE/H)-X1)/(1.0-X1)
C
      FAV = (AMOM-PO*ZP-FSO*ZS)/(AP*RP*ZP+AS*RS*ZS)
      FAVE= FAV*RAVE
      FIP = FAV*RP
C ***************
C
C  Computes the STRESSES in the tendons and non-prestressed reinforce-
C  ment.
C  Tensile strain in the concrete is assumed to be proportional to the
C  distant from the neutral axis.
C
```

```
C  FAV : STRESS at the reference level, H                    (in steel units)
C  FAVE: STRESS at the average level, DAVE
C  FS  : STRESS in the non-prestressed steel                  (in steel units)
C  FP  : STRESS in the tendons                                (in steel units)
C
C ***************
      FP = (PO/AP)+(RP*FAV)
      FS = (FSO/AS)+(RS*FAV)
      FC = (FAV*X1)/(ALPHA*(1.0-X1))
C ***************
C
C  CUR  : total CURVATURE
C  CUR1 : CURVATURE due to prestress and dead load
C  CUR2 : CURVATURE due to live load
C  FC   : Stress of the concrete at top fibre
C
C **************
C
C  Curvature is the sum of the strain at the top fibre and the strain
C  at the  average  level i.e. total depth.
C  Since the section is cracked, the strain at the average level is
C  the average strain, at the crack and section between adjacents.
C  i.e. tension-stiffening effect.
C  The following CUR does include the effect which is taken as equal
C  to 1.0 N/mm2. Therefore, the average strain at the average level
C  is ((FAVE/Es)+(1.0/Ec)).
C
C **************
C
C  BETA :  curvature distribution coefficient
C
      BETA = 0.67
C
      CUR = (FC + 1.0 + BETA*((FIP/ALPHA) - 1.0))/(EC*DP)
      SMCUR = CUR
C
      FCTOP(II) = FC
      PNOT(II)  = PO
      FSNOT(II) = FSO
C
      GOTO 220
200   WRITE(6,62)
62    FORMAT(' Error in Neutral-axis, Warning !  ')
220   RETURN
      END
C
C ***********************************************************************
C
C
C                          **********************
C
C
C  Subroutine to calculate deflection at any particular section of the
C  beam, X  by CONJUGATE BEAM theory and by INTEGRATION of CURVATURES
C  along the beam.
C
C  The beam is divided into elements ans it is required to have
C  curvatures of all the elements in that half span of the beam.
C  it is then possible to find the deflection of the beam at any
```

```
C  particular section or R th element.
C
C                        **********
C
C
      SUBROUTINE DEFLEC (WELEM,NELEM,NRELEM,SPAN,DEF1,DEF2)
C
      COMMON /CURVER/CURV1(100),CURV2(100),CURV22(100)
C
C  WELEM  : WIDTH OF EACH ELEMENT
C  NELEM  : NUMBER OF ELEMENTS IN HALF SPAN OF THE BEAM
C  NRELEM : THE R TH ELEMENT WHERE THE DEFLECTION IS REQUIRED
C  SPAN   : SPAN OF THE BEAM
C
C  CONJUGATE BEAM THEORY
C  Subscripts : 1 : due to prestress and dead load
C               2 : due to total load
C
C
      RA = 0.0
      RA1 = 0.0
C
C
      DO 20  N =1,NELEM
C
      IF (N.NE.NELEM) GOTO 5
      DRA = WELEM*(CURV2(N))*0.5
      DRA1 = WELEM*(CURV1(N))*0.5
      GOTO 10
C
5      DRA = WELEM*(CURV2(N))
       DRA1 = WELEM*(CURV1(N))
10     RA = RA + DRA
       RA1 = RA1 + DRA1
C
20    CONTINUE
C
C  DEFLECTION AT R TH ELEMENT IS THE MOMENT OF THE CONJUGATE BEAM.
C
      DMOM = 0.0
      DMOM1 = 0.0
C
      DO 30  N =1,NRELEM
C
      DDMOM = WELEM*(CURV2(N))*(WELEM*(NRELEM-N))
      DDMOM1 = WELEM*(CURV1(N))*(WELEM*(NRELEM-N))
       DMOM = DMOM + DDMOM
       DMOM1 = DMOM1 + DDMOM1
C
30    CONTINUE
C
C  DEF : DEFLECTION
C
      DEF2 = WELEM*(NRELEM-0.5)*RA - DMOM
      DEF1 = WELEM*(NRELEM-0.5)*RA1 - DMOM1
C
      RETURN
      END
C
```

```
C ***********************************************************************
C
      SUBROUTINE LONG (ALPHA,NELEM,WELEM,SPAN,PE,FSE,EC)
C
C  Subroutine to calculate long-term deflection with the effect of
C  creep only.
C
      COMMON /WRITE/FX3(100),FP22(100),FS22(100)
      COMMON /LCP/ FCTOP(100),PNOT(100),FSNOT(100),FC11(100),FC22(100)
      COMMON /LCP2/DEFDD(100),DEFLI(100),DEFTO(100),PAXIS1(100),
     * PAXIS2(100),PAXIS3(100),SFP1(100),SFP2(100),SFS1(100),SFS2(100)
      COMMON /BMT/ BMOML(100),BMOMD(100)
      COMMON /CRK/ ICK(100)
      COMMON /SUMSTR/ SMST1(100),SMST2(100),SMST3(100),SMST4(100)
      COMMON /CURVER/ CURV1(100),CURV2(100),CURV22(100)
      COMMON /LTERM/SCREEP(50)
C
      DO 40 I = 1,NELEM
40    CURV22(I)=CURV2(I)
C
      PRINT *,' No. of Specific Creep data '
      READ(5,*)NO
C
      PRINT *,' All values of Specific Creep'
      READ(5,*)(SCREEP(I),I=1,NO)
C
      DO 20 ITIME=1,NO
C
      DO 10 II=1,NELEM
      IF (SMST2(II).GE.0.0) THEN
C
      PAXIS3(II)= -1.0
      FCTOP(II) = -1.0
      FX3(II)   = -1.0
      FP22(II)  = -1.0
      FS22(II)  = -1.0
C
      X3 = 0.0
      CALL UCREEP (ITIME,II,EC,ALPHA,PE,FSE,X3)
      ELSE
      AMOM = BMOML(II)+BMOMD(II)
      CALL CREEP (ITIME,II,ALPHA,AMOM,EC)
      END IF
10    CONTINUE
C
      DO 30 NRELEM=1,NELEM
      CALL DEFLEC (WELEM,NELEM,NRELEM,SPAN,DEF1,DEF2)
      DEFDD(NRELEM) = DEF1
      DEFTO(NRELEM) = DEF2
      DEFLI(NRELEM) = DEF2-DEF1
30    CONTINUE
      CALL WRITG (ITIME,NELEM,WELEM)
C
20    CONTINUE
      RETURN
      END
C
C ***********************************************************************
```

```
C
      SUBROUTINE UCREEP (ITIME,II,EC,ALPHA,PE,FSE,X3)
C
C  Analysis of uncracked sections under sustained load.
C
      COMMON /SECT/ AREAE,AREAC,ECI,CCI,YEP,YES,YCP,YCS,
     * AREAP,PCI,YPP,YPS
      COMMON /LEVEL/ D,DP,DS
      COMMON /SHAPE/ B,BI,BW,H,HF,HB,AP,AS
      COMMON /CURVER/ CURV1(100),CURV2(100),CURV22(100)
      COMMON /SUMSTR/ SMST1(100),SMST2(100),SMST3(100),SMST4(100)
      COMMON /LTERM/SCREEP(50)
      COMMON /GTHAN1/STT3,STT4
C
      YSUP  = DP-YEP
      YINF  = H-DP+YEP
C
C  Subscripts 1 : refers to extreme top fibre
C             2 : refers to extreme bottom fibre
C             3 : refers to the level of the tendons.
C
      CCREEP = SCREEP(ITIME)*EC
C
C Imaginary forces
C
      IF(X3.GE.1.0) THEN
        IF(SMST3(II).LT.0.0) STT3 = 0.0
        IF(SMST4(II).LT.0.0) STT4 = 0.0
      DFP = ALPHA*CCREEP*STT3*AP
      DFS = ALPHA*CCREEP*STT4*AS
      ELSE
      DFP = ALPHA*CCREEP*SMST3(II)*AP
      DFS = ALPHA*CCREEP*SMST4(II)*AS
      END IF
C
C  FBL :    Total balancing forces.
C  BLM :    Total balancing moment.
C
      FBL = DFP + DFS
      BLM = DFP*YEP + DFS*YES
C
C Differential stresses : +ve tension
C
      DFINF = (FBL/AREAE)+(BLM*YINF/ECI)
      DFSUP = (FBL/AREAE)-(BLM*YSUP/ECI)
C
C  Increase in curvatures : +ve compression
C
      DSTN1 = (CCREEP*SMST1(II)/EC)-(DFSUP/EC)
      DSTN2 = (CCREEP*SMST2(II)/EC)-(DFINF/EC)
C
      CURV2(II) = CURV22(II)+((DSTN1-DSTN2)/H)
C
      RETURN
      END
C
C ***********************************************************************
C
```

```
      SUBROUTINE CREEP (ITIME,II,ALPHA,AMOM,EC)
C
C  Analysis of cracked sections under sustained load.
C
      COMMON /WRITE/FX3(100),FP22(100),FS22(100)
      COMMON /LEVEL/D,DP,DS
      COMMON /SHAPE/B,BI,BW,H,HF,HB,AP,AS
      COMMON /CURVER/ CURV1(100),CURV2(100),CURV22(100)
      COMMON /LCP/ FCTOP(100),PNOT(100),FSNOT(100),FC11(100),FC22(100)
      COMMON /LCP2/ DEFDD(100),DEFLI(100),DEFTO(100),PAXIS1(100),
     * PAXIS2(100),PAXIS3(100),SFP1(100),SFP2(100),SFS1(100),SFS2(100)
      COMMON /LTERM/SCREEP(50)
      COMMON /GTHAN1/STT3,STT4
C
      DIMENSION AR(4),REZ(4)
      REAL *8 IMZ(4),REZ,AR,TOL
C
      ASR = AS/(B*H)
      APR = AP/(B*H)
      WEB = (H-HB)/H
      FLGT= (HF/H)
C
      FC1 = FCTOP(II)
      P0  = PNOT(II)
      FS0 = FSNOT(II)
      X1  = PAXIS2(II)
C     CCREEP = 48.0*(10.0**(-6.0))*EC
      CCREEP =  SCREEP(ITIME)*EC
C
C FC1  : the short-term concrete stress at the extreme top fibre.
C FC2  : the new concrete stress at the extreme top fibre after taking
C        creep effect into account, plus the creep
C        fc2' = fc2 + Cc*fc1
C
C
C  B1   : (1.0-bw/b)
C  B2   : (bi/b)-(bw/b)
C
      H1 = HF/H
      H2 = HB/H
      D2 = DP/H
      D3 = DS/H
C
      T1 = H2-1.0+X1
      T2 = X1-H1
      DAVE = (AS*DS+AP*DP)/(AP+AS)
      D = DAVE
      NN = 0
C
      B1 = 1.0 - (BW/B)
      B2 = (BI/B) - (BW/B)
C
C Iteration for D
C
160   D1 = 3.0*D/H
C
C  CK    is the K    as derived in the original equation
C  CK1   is the K1   as derived in the original equation
```

```
C  CK2  is the K2  as derived in the original equation
C
      CK1 = X1
      CK2 = X1*(D1-X1)
C
      IF (T2.GT.0.000) THEN
      CK1 = CK1-(B1*(T2**2.0)/X1)
      CK2 = CK2 - (B1*(T2**2.0)*(D1-X1-2.0*H1)/X1)
      END IF
C
      IF (T1.GT.0.000) THEN
      CK1 = CK1 + (B2*(T1**2.0)/X1)
      CK2 = CK2 + (B2*(T1**2.0)*(D1-X1+2.0*H2-2.0)/X1)
      END IF
C
      CK1 = CK1*CCREEP*FC1*B*H/2.0
      CK2 = CK2*CCREEP*FC1*B*(H**2.0)/(3.0*2.0)
      CK = 3.0*(AMOM+CK2)/((FSO+PO+CK1)*H)
C
C  Assume Neutral-axis lies above the bottom flange.
C  Set bi = bw  or B2 = 0
C
      B2 = 0.0
C
      N = 0
10    N = N+1
C
C  Coefficients of the cubic equation : AA, BB, CC, DD
C  sub-coefficients : AAA, BBB, CCC, DDD,    within the coefficients
C
      AAA = B2
      BBB = B2*(CK-D1)
      CCC = B2*((2.0*H2*D1)-2.0*CK*(H2-1.0)+(3.0*(H2**2.0))-(6.0*H2)
     1   -(2.0*D1)+3.0)
      DDD = B2*(CK*(2.0*H2-(H2**2.0)-1.0)+((H2**2.0)*D1)-(2.0*H2*D1)
     1   +(2.0*(H2**3.0))-(6.0*(H2**2.0))+(6.0*H2)+D1-2.0)
C
      AA  = (1.0-B1) + AAA
      BB  = CK - B1*(CK-D1) - D1 + BBB
      CC  = B1*((2.0*H1*CK)+(3.0*(H1**2.0))-(2.0*H1*D1))
     1  + 2.0*ALPHA*CK*(ASR+APR) - CCC
      DD  = B1*((H1**2.0)*D1-2.0*(H1**3.0)-(H1**2.0)*CK)
     1  - (2.0*ALPHA*CK*(APR*D2+ASR*D3)) - DDD
      N9 = 4
      AR(1) = AA
      AR(2) = BB
      AR(3) = CC
      AR(4) = DD
      TOL = 1.0*10.0**(-11.0)
      IFAIL = 0
C
      CALL C02AEF (AR,N9,REZ,IMZ,TOL,IFAIL)
C
      IF (N.GT.1) GOTO 110
      IFLGT = 0
      IFLGB = 0
C
C  Is neutral-axis within the web ?
```

```
C
      DO 20 I=1,3
      IF(IMZ(I).NE.0.0000) GOTO 20
      IF(REZ(I).LE.WEB.AND.REZ(I).GE.FLGT) GOTO 100
20    CONTINUE
C
C  Is neutral-axis within top flange ?
C
      DO 30 I=1,3
      IF (IMZ(I).NE.0.0000) GOTO 30
      IF (REZ(I).LT.WEB.AND.REZ(I).GE.0.0000) GOTO 90
30    CONTINUE
C
C  Is neutral-axis in the bottom flange ?
C
      DO 40 I=1,3
      IF (IMZ(I).NE.0.0000) GOTO 40
      IF (REZ(I).GT.WEB) GOTO 80
40    CONTINUE
C
C  Neutral-axis is within the top flange,
C  Set bw/b = 1.0  i.e. to use rectangular section equation.
C
90    B1 = 0.0
      IFLGT = 1
      GOTO 10
C
C  Neutral-axis is within bottom flange,
C  Set bi/b  to its original value
C
80    B2 = (BI/B)-(BW/B)
      IFLGB = 1
      GOTO 10
C
110   IF ( IFLGB.EQ.1) GOTO 140
      DO 120 I=1,3
      IF (IMZ(I).NE.0.000) GOTO 120
      IF (REZ(I).LE.FLGT.AND.REZ(I).GT.0.0000) GOTO 100
120   CONTINUE
C
      GOTO 200
140   DO 150 I=1,3
      IF  (IMZ(I).NE.0.0000 ) GOTO 150
      IF (REZ(I).GE.WEB.AND.REZ(I).LE.H) GOTO 100
150   CONTINUE
      GOTO 200
C
C  X3  : the new position of neutral-axis of stresses.
C        this stress distribution is assumed to be bi-linear.
C        Neutral axis of total strain also coincides with this axis
C        of stresses
C
C
100   X3 = REZ(I)
C
      IF (X3.GE.1.0) THEN
      WRITE(6,101)II,ITIME,X3
101   FORMAT(I3,I3,F6.2, ' WARNING ! Neutral-axis greater than 1...')
```

```
      CALL UCREEP (ITIME,II,EC,ALPHA,PE,FSE,X3)
      GOTO 220
      END IF
C
C Substitute X3 into the equation of moment equilibrium and get FC2
C or fc2´ as in the original equation.
C
C  Find the new strain at the level of the centroid of the total steel
C  area.
C
      T3 = H2-1.0+X3
      T4 = X3-H1
C
      CK3 = 3.0*(AMOM+CK2)/(B*(H**2.0))
      FC2 = 2.0*CK3/(X3*(D1-X3))
C
      IF (T4.GT.0.000) THEN
      FC2 = 2.0*CK3/(X3*(D1-X3)-(B1*(T4**2.0)*(D1-X3-2.0*H1)/X3))
      END IF
C
      IF (T3.GT.0.000) THEN
      FC2 = 2.0*CK3/(X3*(D1-X3)-(B1*(T4**2.0)*(D1-X3-2.0*H1)/X3)
     1    + (B2*(T3**2.0)*(D1-X3+2.0*H2-2.0)/X3) )
      END IF
C
C  FP2    is the new increase of stress in tendon after P0
C  FS2    is the new increase of stress in non-prestressed steel
C         after FS0
C  FPP    is the total stress in the tendon
C  FSS    is the total stress in the non-prestressed steel
C
      FP2  = ALPHA*FC2*(D2-X3)/X3
      FS2  = ALPHA*FC2*(D3-X3)/X3
      FAVE = ALPHA*FC2*((DAVE/H)-X3)/X3
C
      FPP = (P0/AP) + FP2
      FSS = (FS0/AS) + FS2
C
      IF(FAVE.LE.0.0) THEN
      CUR = (FC2+(FAVE/ALPHA))/(EC*DAVE)
      ELSE
      BETA = 0.89
      CUR = (FC2 + 0.55+ BETA*((FAVE/ALPHA) - 0.55))/(EC*DAVE)
      END IF
C
      DNEW = (FPP*AP*DP+FSS*AS*DS)/(AP*FPP+AS*FSS)
C
      NN = NN+1
      IF (ABS((DNEW-D)/H).GT.0.005.AND.NN.LT.50 ) THEN
      D = DNEW
      GOTO 160
      END IF
C
      IF (NN.GE.50) THEN
      WRITE(6,206)
206   FORMAT(´ Error in the iteration process for D ....´)
      END IF
C
```

```
      CURV2(II) = CUR
      PAXIS3(II)= X3
C
      FP22(II) = FP2
      FS22(II) = FS2
      FX3(II)  = FC2
C
      GOTO 220
200   WRITE(6,205)
205   FORMAT(' WARNING ! Error in neutral-axis.')
C
220   RETURN
      END
C
C ***********************************************************
C
      SUBROUTINE WRITG (ITIME,NELEM,WELEM)
C
      COMMON /LCP/FCTOP(100),PNOT(100),FSNOT(100),FC11(100),FC22(100)
      COMMON /WRITE/FX3(100),FP22(100),FS22(100)
      COMMON /LCP2/ DEFDD(100),DEFLI(100),DEFTO(100),PAXIS1(100),
     * PAXIS2(100),PAXIS3(100),SFP1(100),SFP2(100),SFS1(100),SFS2(100)
      COMMON /CURVER/ CURV1(100),CURV2(100),CURV22(100)
      COMMON /LTERM/SCREEP(50)
C
      IF (ITIME.EQ.1) THEN
      WRITE(8,10)
10    FORMAT(' LONG-TERM DEFLECTIONS',/,' ====================',//)
      END IF
C
      WRITE(8,20)SCREEP(ITIME)
20    FORMAT(' Specific creep =  ',E8.1,//)
C
      DO 30  I=1,NELEM
      IXX = WELEM*(I-0.5)
30    WRITE(8,40)IXX,DEFDD(I),DEFLI(I),DEFTO(I),PAXIS3(I),FCTOP(I),
     1 FX3(I),FP22(I),FS22(I),CURV1(I),CURV2(I)
40    FORMAT(2X,I5,5X,F7.2,4X,F7.2,5X,F7.2,5X,F6.3,5X,F7.3,5X,F7.3,
     1 5X,F7.2,5X,F7.2,4X,E10.3,4X,E10.3,/)
C30   WRITE(8,40)IXX,DEFDD(I),DEFLI(I),DEFTO(I),PAXIS3(I),CURV1(I),
C     * CURV22(I)
C40   FORMAT(2X,I5,5X,F7.2,4X,F7.2,5X,F7.2,5X,F6.3,5X,E10.3,5X,E10.3)
      RETURN
      END
```

Appendix B

Program to calculate long-term deflection with shrinkage effect alone

The first part of this program is similar to that listed in Appendix A. Therefore, only the necessary subroutines are listed here.

```
      SUBROUTINE LONG (ALPHA,NELEM,WELEM,SPAN,PE,FSE,EC)
C
C  Calculate the long-term deflection in which the effect of shrinkage
C  alone is considered.
C
      COMMON /WRITE/AXIS2(100),FX3(100),FP22(100),FS22(100)
      COMMON /LCP/ FCTOP(100),PNOT(100),FSNOT(100),FC11(100),FC22(100)
      COMMON /LCP2/DEFDD(100),DEFLI(100),DEFTO(100),PAXIS1(100),
     * PAXIS2(100),PAXIS3(100),SFP1(100),SFP2(100),SFS1(100),SFS2(100)
      COMMON /BMT/ BMOML(100),BMOMD(100)
      COMMON /CRK/ ICK(100)
      COMMON /CURVER/ CURV1(100),CURV2(100),CURV22(100)
      COMMON /SUMSTR/SMST1(100),SMST2(100),SMST3(100),SMST4(100)
      COMMON /LTERM/SHR(50)
C
      DO 40 I = 1,NELEM
40    CURV22(I)=CURV2(I)
C
      PRINT *,' No. of Shrinkage data'
      READ(5,*)NO
C
      PRINT *,' All the values of Shrinkage'
      READ(5,*)(SHR(I),I=1,NO)
C
      DO 20 ITIME=1,NO
C
      DO 10 II=1,NELEM
      IF (SMST2(II).GE.0.0) THEN
C
      PAXIS3(II)= -1.0
      FCTOP(II) = -1.0
      FX3(II)   = -1.0
      FP22(II)  = -1.0
      FS22(II)  = -1.0
      AXIS2(II) = -1.0
C
      CALL USHRNK (ITIME,II,EC,ALPHA,PE,FSE)
      ELSE
      AMOM = BMOML(II)+BMOMD(II)
      CALL SHRINK(ITIME,II,ALPHA,AMOM,EC)
      END IF
10    CONTINUE
C
      DO 30 NRELEM=1,NELEM
      CALL DEFLEC (WELEM,NELEM,NRELEM,SPAN,DEF1,DEF2)
      DEFDD(NRELEM) = DEF1
```

```
      DEFTO(NRELEM) = DEF2
      DEFLI(NRELEM) = DEF2-DEF1
30    CONTINUE
      CALL WRITG (ITIME,NELEM,WELEM)
C
20    CONTINUE
      RETURN
      END
C
C ***********************************************************************
C
      SUBROUTINE USHRNK (ITIME,II,EC,ALPHA,PE,FSE)
C
C  Analysis of uncracked section
C
      COMMON /SECT/ AREAE,AREAC,ECI,CCI,YEP,YES,YCP,YCS
      COMMON /LEVEL/ D,DP,DS
      COMMON /SHAPE/ B,BI,BW,H,HF,HB,AP,AS
      COMMON /CURVER/ CURV1(100),CURV2(100),CURV22(100)
      COMMON /SUMSTR/ SMST1(100),SMST2(100),SMST3(100)
      COMMON /LTERM/ SHR(50)
C
      YSUP  = DP-YEP
      YINF  = H-DP+YEP
C
C  Subscripts 1 : refers to extreme top fibre
C             2 : refers to extreme bottom fibre
C             3 : refers to the level of the tendons.
C
      CSHRNK = SHR(ITIME)
C
C  Imaginary forces
C
      DFP = CSHRNK*AP*ALPHA*EC
      DFS = CSHRNK*AS*ALPHA*EC
C
C  FBL : total balancing force
C  BLM : total balancing moment
      FBL = (AS+AP)*CSHRNK*ALPHA*EC
      BLM = DFP*YEP+DFS*YES
C
C Differential stresses.
C
      DFINF = (FBL/AREAE)+(BLM*YINF/ECI)
      DFSUP = (FBL/AREAE)-(BLM*YSUP/ECI)
C
C Increase of strain : +ve compression
C
      DSTN1 = CSHRNK - (DFSUP/EC)
      DSTN2 = CSHRNK - (DFINF/EC)
      CURV2(II) = CURV22(II)+((DSTN1-DSTN2)/H)
C
      RETURN
      END
C
C ***********************************************************************
C
      SUBROUTINE SHRINK(ITIME,II,ALPHA,AMOM,EC)
```

```
C
C  Analysis of cracked section under sustained load and concrete
C  undergoing shrinkage.
C
      COMMON /WRITE/AXIS2(100),FX3(100),FP22(100),FS22(100)
      COMMON /LEVEL/D,DP,DS
      COMMON /SHAPE/B,BI,BW,H,HF,HB,AP,AS
      COMMON /CURVER/ CURV1(100),CURV2(100),CURV22(100)
      COMMON /LCP/ FCTOP(100),PNOT(100),FSNOT(100),FC11(100),FC22(100)
      COMMON /LCP2/ DEFDD(100),DEFLI(100),DEFTO(100),PAXIS1(100),
     * PAXIS2(100),PAXIS3(100),SFP1(100),SFP2(100),SFS1(100),SFS2(100)
      COMMON /LTERM/ SHR(50)
C
      DIMENSION AR(4),REZ(4)
      REAL *8 IMZ(4),REZ,AR,TOL
C
      ASR = AS/(B*H)
      APR = AP/(B*H)
      WEB = (H-HB)/H
      FLGT= (HF/H)
C
      FC1 = FCTOP(II)
      PO  = PNOT(II)
      FSO = FSNOT(II)
      X1  = PAXIS2(II)
C     CCREEP = 48.0*(10.0**(-6.0))*EC
      CSHRNK = SHR(ITIME)
C
C FC1  : the short-term concrete stress at the extreme top fibre.
C FC2  : the new concrete stress at the extreme top fibre after taking
C        shrinkage effect into account
C
C  B1   : (1.0-bw/b)
C  B2   : (bi/b)-(bw/b)
C
      H1 = HF/H
      H2 = HB/H
      D2 = DP/H
      D3 = DS/H
C
      B1 = 1.0 - (BW/B)
      B2 = (BI/B) - (BW/B)
C
C  CK   is the K   as derived in the original equation
C
      CK1 = AMOM + (FSO-AS*ALPHA*EC*CSHRNK)*(DP-DS)
      CK2 = (PO + FSO - ALPHA*EC*CSHRNK*(AP+AS))*H
      CK  = CK1/CK2
C
C  Assume Neutral-axis lies above the bottom flange.
C  Set bi = bw  or B2 = 0
C
      B2 = 0.0
C
      N = 0
10    N = N+1
C
C  Coefficients of the cubic equation : AA, BB, CC, DD
```

```
C  sub-coefficients : AAA, BBB, CCC, DDD,    within the coefficients
C
       AAA = B2
       BBB = 3.0*B2*(CK-D2)
       CCC = B2*(6.0*CK*(H2-1.0)-3.0*(H2**2.0)+6.0*H2-3.0-6.0*D2*H2 +
      1  6.0*D2)
       DDD = 3.0*B2*CK*((H2**2.0)-2.0*H2+1.0) + (B2*(6.0*(H2**2.0)-
      1  6.0*H2-2.0*(H2**3.0)+2.0+6.0*D2*H2-3.0*D2*(H2**2.0)-3.0*D2))
C
       AA = (1.0-B1) + AAA
       BB = 3.0*(1.0-B1)*(CK-D2) + BBB
       CC = B1*(6.0*H1*CK+3.0*(H1**2.0)-6.0*D2*H1) +
      1  6.0*ALPHA*CK*(ASR+APR)-6.0*ALPHA*ASR*(D2-D3) + CCC
       DD = B1*((H1**2.0)*(3.0*D2-2.0*H1-3.0*CK)) -
      1  6.0*ALPHA*CK*(ASR*D3+APR*D2)+6.0*ALPHA*ASR*D3*(D2-D3) + DDD
C
       N9 = 4
       AR(1) = AA
       AR(2) = BB
       AR(3) = CC
       AR(4) = DD
       TOL = 1.0*10.0**(-11.0)
       IFAIL = 0
C
       CALL C02AEF (AR,N9,REZ,IMZ,TOL,IFAIL)
C
       IF (N.GT.1) GOTO 110
       IFLGT = 0
       IFLGB = 0
C
C  Is neutral-axis within the web ?
C
          DO 20 I=1,3
          IF(IMZ(I).NE.0.0000) GOTO 20
          IF(REZ(I).LE.WEB.AND.REZ(I).GE.FLGT) GOTO 100
20        CONTINUE
C
C  Is neutral-axis within top flange ?
C
          DO 30 I=1,3
          IF (IMZ(I).NE.0.0000) GOTO 30
          IF (REZ(I).LT.WEB.AND.REZ(I).GE.0.0000) GOTO 90
30        CONTINUE
C
C  Is neutral-axis in the bottom flange ?
C
          DO 40 I=1,3
          IF (IMZ(I).NE.0.0000) GOTO 40
          IF (REZ(I).GT.WEB) GOTO 80
40        CONTINUE
C
C  Neutral-axis is within the top flange,
C  Set bw/b = 1.0  i.e. to use rectangular section equation.
C
90        B1 = 0.0
          IFLGT = 1
          GOTO 10
C
```

```
C  Neutral-axis is within bottom flange,
C  Set bi/b  to its original value
C
80     B2 = (BI/B)-(BW/B)
       IFLGB = 1
       GOTO 10
C
110    IF ( IFLGB.EQ.1) GOTO 140
       DO 120 I=1,3
       IF (IMZ(I).NE.0.000) GOTO 120
       IF (REZ(I).LE.FLGT.AND.REZ(I).GT.0.0000) GOTO 100
120    CONTINUE
C
       GOTO 200
140    DO 150 I=1,3
       IF  (IMZ(I).NE.0.0000 ) GOTO 150
       IF (REZ(I).GE.WEB.AND.REZ(I).LE.H) GOTO 100
150    CONTINUE
       GOTO 200
C
C  X2   : the new position of neutral-axis of stresses.
C         this stress distribution is assumed to be linear.
C  X3   : Neutral axis of the final total strain.
C
100    X2 = REZ(I)
C
       IF (X2.GE.1.0) THEN
       WRITE(6,101)II,ITIME
101    FORMAT(I3,I3,' WARNING ! Neutral-axis greater than 1...')
       END IF
C
C
       T1 = H2-1.0+X2
       T2 = X2-H1
C
       IF (T2.GT.0.000) THEN
       ZTOP1 = (X2**3.0)-B1*(T2**2.0)*(X2+2.0*H1)
       ZTOP2 = 3.0*((X2**2.0)-B1*(T2**2.0))
       ZTOP  = ZTOP1/ZTOP2
       END IF
C
       IF (T1.GT.0.000) THEN
       ZTOP1 = (X2**3.0)-B1*(T2**2.0)*(X2+2.0*H1)+(B2*(T1**2.0)*(X2-
      1  2.0*H2+2.0))
       ZTOP2 = 3.0*((X2**2.0)-B1*(T2**2.0)+B2*(T1**2.0))
       ZTOP  = ZTOP1/ZTOP2
       END IF
C
       ZTOP = ZTOP*H
C
       ZP = DP - ZTOP
       ZS = DS - ZTOP
C
C  FP2    is the new increase of stress in tendon after P0
C  FS2    is the new increase of stress in non-prestressed steel
C         after FS0
C  FPP    is the total stress in the tendon
C  FSS    is the total stress in the non-prestressed steel
```

```
C
      DAVE = (AS*DS+AP*DP)/(AS+AP)
C
      FC21= AMOM-(PO-AP*ALPHA*EC*CSHRNK)*ZP-(FSO-AS*ALPHA*EC*CSHRNK)*ZS
      FC211= (ALPHA*AP*ZP*(D2-X2)/X2)+(ALPHA*AS*ZS*(D3-X2)/X2)
      FC2 = FC21/FC211
C
      FP2  = (ALPHA*FC2*(D2-X2)/X2) - ALPHA*EC*CSHRNK
      FS2  = (ALPHA*FC2*(D3-X2)/X2) - ALPHA*EC*CSHRNK
C
      X3 = ((ALPHA*FC2+ALPHA*EC*CSHRNK)/(ALPHA*FC2))*X2
C
      IF(X3.GE.1.0) THEN
      PRINT 102,II,ITIME,X3,' WARNING! Strain N.A. greater than 1 !'
102   FORMAT(I3,I3,F6.2)
      END IF
C
      FAVE = (ALPHA*FC2+ALPHA*EC*CSHRNK)*((DAVE/H)-X3)/X3
C
      FPP = (PO/AP) + FP2
      FSS = (FSO/AS) + FS2
C
      IF(FAVE.LE.0.0) THEN
      CUR = (FC2+(FAVE/ALPHA))/(EC*DAVE)
      ELSE
      BETA = 0.67
      CUR = (FC2 + 0.5 + BETA*((FAVE/ALPHA) - 0.5))/(EC*DAVE)
      END IF
C
      CURV2(II) = CUR
      PAXIS3(II)= X3
      FP22(II) = FP2
      FS22(II) = FS2
      FX3(II)  = FC2
      AXIS2(II)= X2
C
      GOTO 220
200   WRITE(6,205)
205   FORMAT(' WARNING ! Error in neutral-axis.')
C
220   RETURN
      END
```

Appendix C

```
C Analysis of Partial Prestressing Parameters
C
C ***********************************************************************
C
C  Assumptions :-
C
C  1.  Prestressed and non-prestressed steels are both located at the
C      same level: 0.9 H
C  2.  Service load = 0.65x(design ultimate load)
C  3.  Concrete Grade 40
C  4.  Ratio of mod. of elasticity of steel to concrete = 6.0
C  5.  Stress in tendon at transfer = 1100 N/mm2
C  6.  Characteristic ultimate strength of tendon, fcu = 1600 N/mm2
C  7.  Characteristic yield strength of non-prestressed steel
C      = 400 N/MM2
C
C ***********************************************************************
      CHARACTER*4 IQES
      COMMON /NAX/F1
      COMMON /PERINF/APR,ASR,ASPR,AEQP
1     PRINT *,' INDEX'
      PRINT *,' ====='
      PRINT *,'  '
5     PRINT *,' PPR    -    PARTIAL PRESTRESS RATIO'
      PRINT *,' DEG    -    DEGREE OF PRESTRESS AND HYP'
      PRINT *,' AXIS   -    FIND NEUTRAL AXIS OF A CRACKED SECTION'
      PRINT *,' QUIT   -    END THE ANALYSIS JOB'
      PRINT *,' CHOOSE ONE OPTION FROM THE INDEX'
      READ(5,30)IQES
30    FORMAT(A4)
      IF (IQES.EQ.'DEG') CALL KEPAL
      IF (IQES.EQ.'QUIT') GOTO 100
      IF (IQES.EQ.'PPR') CALL PART
      IF (IQES.EQ.'AXIS') GOTO 50
      GOTO 1
50    PRINT *,' HF/H,   BW/B,   M/FD,   ALPHA-RHO'
      READ(5,*)HF,BW,RM1,ARX2
      APR = 0.1
C
      CALL NAXIS(HF,BW,RM1,ARX2,AXIS,ZARM)
C
      WRITE(6,60)
60    FORMAT(' M/FD',7X,'AL-RHO',7X,'BW/B',10X,'HF/H',10X,
     3       'X/D',10X,'DF/F')
      WRITE(6,65)RM1,ARX2,BW,HF,AXIS,F1
65    FORMAT(1X,6F12.6)
100   STOP
      END
C
C =======================================================================
C
      SUBROUTINE PART
C
C  Analysis of Partial Prestressing Ratio
C
```

```
      DIMENSION STRESS(3,100),FPRES(3,100),FSRES(3,100),CURVE(3,100)
      DIMENSION Z(3,100),A(3,100),F(3,100)
      COMMON /SMAREA/AREAE,AREAC,ZIFE,ZIFC,EES,CES,AREAP,PES,PESINF,AREA
      COMMON /PERINF/APR,ASR,ASPR,AEQP
      COMMON /DINF/ZIFEP
      AMW = 0.65
C
1     PRINT *,' bw/b , bi/b , hf/h , hb/h'
      READ(5,*)BW,BI,HF,HB
      PRINT *,' How many values of Equivalent area, curves'
      READ(5,*)NCUR
C
      DO 50 K = 1,NCUR
      PRINT *,' Total reinforcement ratio when fully prestressed'
      READ(5,*)AREAMI
      PRINT *,' PPR'
C
      WRITE(4,41)
41    FORMAT(17X,'P P R',4X,'DSTRESS',7X,'ULT.MOM.',5X,
     1  'Z-VALUE',5X,'  FO',8X,'ASPR',9X,'NAXIS')
C
C  Analysing Partial Prestressing Ratio
C  Increase the Ratio in steps of 0.05 with initial value of zero
C
      DO 50 I=1,21
      PPR = (I-1.0)*0.05
C
      CALL AREARF (PPR,AREAMI,APR,ASR,ASPR,AEQP)
C
      CALL PROPT (BW,BI,HF,HB)
C
      CALL MOMENT (AEQP,BW,HF,AMU)
C
      CALL LOSS (AMU,ZIFEP,FO,FPO,FSO)
      IF (FO.EQ.0.0) GOTO 28
C
C MEW,U = 0.65
      AMW = 0.65
      RM1  = (AMW*AMU)/FO
      GOTO 29
28    RM1 = 0.0
      GOTO 15
29    IF (HF.GT.0.9) GOTO 30
      HFC = (1.0/0.9)*HF
      GOTO 31
30    HFC =1.0
31    Z1 = 1.0-(1.0-BW)*((1.0-HFC)**3.0)
      Z2 = 1.0-(1.0-BW)*((1.0-HFC)**2.0)
      ZO = (2.0/3.0)*(Z1/Z2)
      IF (RM1.LE.ZO) GOTO 20
15    ARX2 = 6.0*ASPR
C
C RM1  IN TERM OF *BD
C
      CALL NAXIS (HF,BW,RM1,ARX2,AXIS,ZARM)
C
      GOTO 25
20    ZARM = AMU*AMW/FO
```

```
      AXIS = 1.0
C
C Calculate the increase of stress in the reinforcement
C
25    DFS3 = (AMW*AMU/ZARM)-FO
      IF (APR.EQ.0.0) GOTO 26
      DFS2 = PPR/((4.0-3.0*PPR)*APR)
      GOTO 27
26    DFS2 = 4*(1.0-PPR)/((4.0-3.0*PPR)*ASR)
27    DFS  = DFS2*DFS3
C
C FP :  stress in the prestressed reinforcement
C FS :  stress in the non-prestressed reinforcement
C
      FP = FPO + DFS
      FS = FSO + DFS
C
      STRESS(K,I)=DFS
      FPRES (K,I) = FP
      FSRES (K,I) = FS
C
      CALL DEFLEC (DFS,AXIS,RM1,BW,HF,FO,ACURV)
      CURVE (K,I) = ACURV
C     WRITE(6,17)DFS
17    FORMAT(' INCREASE IN STRESS = ',F12.4)
C     WRITE(6,18)DFS
18    FORMAT(F20.4)
      Z(K,I) = ZARM
      F(K,I) = FO
      A(K,I) = APR
      WRITE(4,40)PPR,DFS,AMU,ZARM,FO,ASPR,AXIS,RM1
40    FORMAT(10X,8F12.4)
50    CONTINUE
C
      WRITE(4,60)
60    FORMAT(' PPR      DSTRESS      CURVATU      FPSTESS      FSTRESS')
      DO 70 K = 1,3
C
C
      DO 70 I=1,21
C     WRITE(6,100)
100   FORMAT(' ')
      PPR = (I-1.0)*0.05
      WRITE(4,62)PPR,STRESS(K,I),CURVE(K,I),FPRES(K,I),FSRES(K,I)
62    FORMAT(1X,F4.2,5X,F6.2,5X,F7.3,5X,F8.3,5X,F8.3)
      WRITE(11,63)PPR,STRESS(K,I)
70    CONTINUE
C
C
      DO 80 K = 1,3
      DO 80 I = 1,21
      PPR = (I-1.0)*0.05
      WRITE(7,63)PPR,Z(K,I)
      WRITE(11,63)PPR,CURVE(K,I)
63    FORMAT(2F12.6)
80    CONTINUE
      DO 81 K=1,1
      DO 81 I=1,21
```

```
      PPR = (I-1.0)*0.05
81    WRITE(7,63)PPR,F(K,I)
      DO 82 K=1,1
      DO 82 I=1,21
      PPR =(I-1.0)*0.05
82    WRITE(7,63)PPR,A(K,I)
      DO 91 I = 1,21
      PPR =(I-1.0)*0.05,
91    WRITE(7,63)PPR,Z(3,I)
      DO 92 I = 1,21
      PPR =(I-1.0)*0.05
92    WRITE(7,63)PPR,F(3,I)
      DO 93 I=1,21
      PPR =(I-1.0)*0.05
93    WRITE(7,63)PPR,A(3,I)
C
      RETURN
      END
C
C ==========================================================
C
C  Analysis of The Degree of Prestress and
C              The Hypothetical Tensile Stress
C
      SUBROUTINE KEPAL
C
      DIMENSION DSTRES(3,100),DEGR(3,100),SRES(3,100)
      DIMENSION CURVED(3,100),PRES(3,100)
      DIMENSION FHT(3,100),FHTCP(3,100)
      COMMON /SMAREA/AREAE,AREAC,ZIFE,ZIFC,EES,CES,AREAP,PES,PESINF,AREA
      COMMON /PERINF/APR,ASR,ASPR,AEQP
      COMMON /STINF/FCPAL,FINFAL
      COMMON /DINF/ZIFEP
C
C
      AMW = 0.65
5     PRINT *,' bw/b, bi/b, hf/h, hb/h'
      READ (5,*)BW,BI,HF,HB
      PRINT *,' How many values of Equivalent area, curve'
      READ(5,*)NCUR
C
      DO 200 K = 1,NCUR
      PRINT *,' Total reinforcement ratio when fully prestressed'
      READ(5,*)AREAMI
C
      AEQP = AREAMI
C
      CALL MOMENT (AEQP,BW,HF,AMU)
C
      DO 200 I = 1,21
      APR = (I-1.0)*0.05*AREAMI
      ASR = 4.0*(AREAMI-APR)
      ASPR= APR + ASR
C
      CALL PROPT (BW,BI,HF,HB)
C
      CALL LOSS (AMU,ZIFEP,FO,FPO,FSO)
      IF (FO.EQ.0.0) GOTO 40
```

```
C
      RM1 = (AMW*AMU)/FO
      GOTO 50
C
40    RM1 = 0.0
      GOTO 60
C
50    IF (HF.GT.0.9) GOTO 70
      HFC = (1.0/0.9)*HF
      GOTO 75
C
70    HFC = 1.0
C
75    Z1 = 1.0-(1.0-BW)*((1.0-HFC)**3.0)
      Z2 = 1.0-(1.0-BW)*((1.0-HFC)**2.0)
      Z0 = (2.0/3.0)*(Z1/Z2)
C
      IF (RM1.LE.Z0) GOTO 80
C
60    ARX2 = 6.0*ASPR
C
      CALL NAXIS (HF,BW,RM1,ARX2,AXIS,ZARM)
      GOTO 90
C
80    ZARM = AMU*AMW/FO
      AXIS = 1.0
C
C DPR : Degree of Prestress
C
90    DPR = FINFAL*ZIFE/(6.0*AMW*AMU*0.81)
      FHTST = (6.0*AMW*AMU*0.81/ZIFE) - FINFAL
      FHTSCP = 5.0 + 4.0*ASR*0.9/(AREA*0.01)
      DFS3 = (AMW*AMU/ZARM)-FO
      DFS  = (1.0/ASPR)*DFS3
C
      FP = FPO + DFS
      FS = FSO + DFS
C
      DEGR(K,I) = DPR
      FHT(K,I) = FHTST
      FHTCP(K,I) = FHTSCP
      DSTRES(K,I) = DFS
      PRES(K,I)   = FP
      SRES(K,I)   = FS
C
      CALL DEFLEC (DFS,AXIS,RM1,BW,HF,FO,ACURV)
      CURVED(K,I) = ACURV
C
200   CONTINUE
C
      DO 210 K = 1,3
      DO 210 I = 1,21
      WRITE(4,220)
220   FORMAT(' ')
      WRITE(4,230)DEGR(K,I),DSTRES(K,I),CURVED(K,I),PRES(K,I)
     1           ,SRES(K,I)
230   FORMAT(1X,F5.3,5X,F6.2,5X,F7.3,5X,F8.3,5X,F8.3)
      WRITE(12,231)DEGR(K,I),DSTRES(K,I)
```

```
      WRITE(13,231)FHT(K,I),FHTCP(K,I),DSTRES(K,I)
231   FORMAT(3F12.6)
210   CONTINUE
C
      DO 250 K = 1,3
      DO 250 I = 1,21
      WRITE(4,220)
      WRITE(4,240)FHT(K,I),DSTRES(K,I),CURVED(K,I),PRES(K,I),
     2            SRES(K,I)
240   FORMAT(1X,F8.3,5X,F8.3,5X,F8.3,5X,F8.3,5X,F8.3)
      WRITE(12,231)DEGR(K,I),CURVED(K,I)
      WRITE(13,231)FHT(K,I),CURVED(K,I)
250   CONTINUE
      RETURN
      END
C ================================================================
C
C  Calculate the Curvature
C
      SUBROUTINE DEFLEC (DFS,AXIS,RM1,BW,HF,FO,ACURV)
      HF1 = HF/0.9
      IF (HF1.LT.1.0) GOTO 5
      HF1 = 1.0
5     IF (AXIS.GE.1.0) GOTO 10
C
      FC = (DFS*AXIS)/(6.0*(1.0-AXIS))
C
C 1/R : curvature per m if depth of section is 1 metre
C
      CUR = (2.0*FC+(DFS/6.0)+1.0)/(2.0*33.3333333)
C
      TE = 1.0 - (1.0-BW)*((1.0-HF1)**2.0)
      CCUR = (2.0*FO*6.0)/(200.0*TE)
      ACURV= CUR-CCUR
C
      GOTO 20
10    ACURV = -1.0
20    RETURN
      END
C
C ================================================================
C
C  Calculate the Section Properties
C
      SUBROUTINE PROPT (BW,BI,HF,HB)
      COMMON /SMAREA/AREAE,AREAC,ZIFE,ZIFC,EES,CES,AREAP,PES,PESINF,AREA
      COMMON /PERINF/APR,ASR,ASPR,AEQP
      COMMON /DINF/ZIFEP
      COMMON /STINF/FCPAL,FINFAL
      COMMON /AINF/CESINF
C
      REAL IGG
      TERM = (1.0-BW)*( X4571912) + ((1.0-BI)*HB)
C
C AREA in term of BH
C
      AREA = (1.0-TERM)
      RT2  = (1.0-BW)*(2.0-HF)*(HF)
```

```
      RT3  = (BI-BW)*(HB)**2.0
C
C YIF, Y INFERIOR IN TERM OF H
C
      YIF = 0.5*(BW+RT2+RT3)/(AREA)
      E = YIF - 0.1
      IGG = (1.0-BW)*(HF)**3.0 + (BI-BW)*(HB)**3.0 + BW
      AYSQ=3.0*(BW+(1.0-BW)*(HF)*((2.0-HF)**2.0)+
     2       (BI-BW)*(HB)**3.0)
      AYIFSQ = (AREA*(YIF)**2.0)*12.0
C
C CI, SECOND MOMENT OF AREA ABOUT CENTROID, IN TERM OF (BH**3/12)
C
      CI = IGG + AYSQ - AYIFSQ
C
C Z  IN TERM OF (BH)**2/6
C
      ZIF = (CI/YIF)*0.5
      ZSUP= 0.5*CI/(1.0-YIF)
C
C EFFECTIVE AREA, AREAE *BH
C THE STIFFENESS OF BOTH TENDONS AND ORDINARY REINFORCEMENT ARE TAKEN
C INTO ACCOUNT.
C USE THESE VALUES FOR CALCULATION OF STRESSES OF BENDING.
C
      AREAE = AREA + (5.0*ASPR*0.9)
      DE = (5.0*0.9*ASPR*E)/AREAE
      ECI = CI + (AREA*E*DE*12.0)
      ZIFE = (0.5*ECI)/(E-DE+0.1)
      ZIFEP = (0.5*ECI)/(E-DE)
C
C TO FIND (1+E2/I2)
C
      EES = 1.0+12.0*((AREAE*(E-DE)**2.0)/ECI)
C
C TRANSFORMED AREA, AREAC *BH
C THE STIFFENESS OF ORDINARY REINFORCEMENT ONLY IS TAKEN INTO ACCOUNT.
C USE THESE VALUES FOR CALCULATION OF PRESTRESS.
C
      AREAC = AREA + (6.0*0.9*ASR)-(0.9*ASPR)
      CDE   = (6.0*ASR-ASPR)*0.9*E/AREAC
      CCI   = CI + (AREA*E*CDE)*12.0
      ZIFC  = (0.5*CCI)/(E-CDE+0.1)
C
C TO FIND 1+E2/I2
C
      CES = 1.0+12.0*((AREAC*(E-CDE)**2.0)/CCI)
      CESINF = 1.0+12.0*((AREAC*(E-CDE+0.1)*(E-CDE))/CCI)
C
C Transformed area, AREAP , in term of *BH
C In this section, the section properties are calculated based on the
C concrete section only ; both the area of tendons and area of non-
C prestressed reinforcement are deducted.
C These properties are used when the forces in the tendon and non-
C prestressed steel are both taken in the calculation together.
C
      AREAP = AREA - 0.9*ASPR
      PDE   = -(0.9*ASPR*E)/AREAP
```

```
      PCI    = CI + (AREA*E*PDE*12.0)
C
C PES : 1+e2/i2
C PESINF : 1+eYinf/i2
C
      PES    = 1.0 + 12.0*((AREAP*(E-PDE)**2.0)/PCI)
      PESINF= 1.0 + 12.0*((AREAP*(E-PDE)*(E-PDE+0.1))/PCI)
C
      RETURN
      END
C
C ================================================================
C
C SUBROUTINE TO CALCULATE THE VALUES OF RHO S
C
      SUBROUTINE AREARF (PPR,AREAMI,APR,ASR,ASPR,AEQP)
      APR    = PPR*AREAMI
C
C AREAMI IS THE AREA OF REINFORCEMENT WHEN FULLY PRESTRESSED,PPR=1
C
      ASR    = 4.0*(AREAMI - APR)
      ASPR   = APR + ASR
      AEQP   = AREAMI
      RETURN
      END
C
C ================================================================
C
C Subroutine to calculate the ultimate moment
C
      SUBROUTINE MOMENT (AEQP,BW,HF,AMU)
C     XD = 87.0*AEQP*(1.0/BW) - ((1.0/BW)-1.0)*HF
      XH = 87.0*AEQP*(1.0/BW)*0.9-((1.0/BW)-1.0)*HF
      XD = XH/0.9
C
      IF (XH.LE.HF) GOTO 5
      GOTO 10
5     XH = 87.0*AEQP*0.9
      AMU = 0.4*40.0*XH*(0.9-0.5*XH)
      GOTO 30
C ULTIMATE MOMENT OF DESIGN * 1/BH2
C
10    AMU = (BW*XH*(0.9-0.5*XH)+(1.0-BW)*HF*(0.9-0.5*HF))*0.4*40.0
C
C CONVERT TO *BD2
C
30    AMU = AMU/0.81
      RETURN
      END
C
C ================================================================
C
C SUBROUTINE TO CALCULATE LOSSES OF PRESTRESS
C ASSUMED SP. CREEP = 50.0*10**-6
C         SHRINKAGE = 250 *10**-6
C
      SUBROUTINE LOSS (AMU,ZIFEP,FO,FPO,FSO)
      COMMON /SMAREA/AREAE,AREAC,ZIFE,ZIFC,EES,CES,AREAP,PES,PESINF,AREA
```

```
      COMMON /PERINF/APR,ASR,ASPR,AEQP
      COMMON /STINF/ FCPAL,FINFAL
      COMMON /AINF/CESINF
C
C Assumed initial prestress in tendon  1100 N/mm2
C
C   ** At transfer **
C FT   : total force in both prestressed and non-prestressed reinforce-
C        ment, *BH
C PT   : prestressing in tendon, *BH
C FST  : force in the non-prestressed reinforcement, *BH
C FCP  : prestress in concrete at the level of reinforcement, N/mm2
C
      FT  = 0.9*(1100.0*APR)/(1.0+(6.0*0.9*ASPR*PES/AREAP))
      FCP = (FT/AREAP)*PES
      PT  = (1100.0-6.0*FCP)*APR*0.9
      FST = -6.0*FCP*ASR*0.9
C
C Assumed MG = 0.35 MU
C DM       : dead load moment
C DLOSS    : loss of stress in reinforcement
C
      DM = 0.35*AMU*0.81*6.0/ZIFEP
      IF (FCP.LE.DM) THEN
      DLOSS = 50.0
        ELSE
      DLOSS= (FCP-(0.35*AMU*0.81*6.0/ZIFEP))*50.0*0.2+0.2*250.0
      END IF
C
C    ** After loss ; effective forces **
C DF  : loss of total force in both types of reinforcement, *BH
C FE  : effective total force, *BH
C PE  : effective force in tendon, *BH
C FSE : effective force in non-prestressed reinforcement, *BH
C FCPE: effective prestress in concrete, N/mm2
C
      DF  = 0.9*ASPR*DLOSS/(1.0+(6.0*0.9*ASPR*PES/AREAP))
      FE  = FT - DF
      PE  = PT - DF*APR/ASPR
      FSE = FST - DF*ASR/ASPR
      IF ( FE.LE.0.0) THEN
      FE = 0.0
      PE = 0.0
      FSE = 0.0
      END IF
C
      FCPE = FE*PES/AREAP
      FCPAL= FCPE
      FINFAL = FE*PESINF/AREAP
C
C FO  : total decompression force at the level of reinforcement, *BD
C PO  : decompression stress in tendon, N/mm2
C FSO : decompression stress in non-prestressed reinforcement, N/mm2
C
      FO  = (FE/0.9) + 6.0*FCPE*ASPR
      IF(APR.NE.0.0) THEN
      FPO = (PE/(APR*0.9)) + (6.0*FCPE)
      ELSE
```

```
      FPO = 0.0
      END IF
      IF (ASR.NE.0.0) THEN
      FSO = (FSE/(ASR*0.9)) + (6.0*FCPE)
      ELSE
      FSO = 0.0
      END IF
C
      WRITE(9,11)PPR,DLOSS,FE,FO,FPO,FSO,APR,ASR,AEQP,FCP,FCPE
11    FORMAT(E10.3,4X,F7.2,4X,F7.3,4X,F7.3,4X,F9.3,4X,F9.3,E8.2,4X,E8.2,
     *4X,E8.2,4X,F6.2,4X,F6.2)
      RETURN
      END
C
C ================================================================
C
      SUBROUTINE NAXIS (HF,BW,RM1,ARX2,AXIS,ZARM)
C
C  This subroutine is to find the position of neutral axis and the
C  lever arm under any bending moment.
C  The cubic equation is solved by NEWTON-RAPHSON'S method.
C  If the neutral axis lies within the top flange, the neutral axis
C  is solved again assuming that the section is rectangular.
C  If it is an ordinary reinforced concrete, the netrual axis is
C  then solved by the quadratic equation.
C
      COMMON /PERINF/APR,ASR,ASPR,AEQP
      COMMON /NAX/F1
C H1  IS HF/H AND THEN CONVERT TO HF/D HERE
C
      B1 = BW
      H1 = HF
      IF (HF.GT.0.9) GOTO 10
      H1 = (1.0/0.9)*HF
      GOTO 20
10    H1 = 1.0
20    Z1 = 1.0-(1.0-B1)*((1.0-H1)**3.0)
      Z2 = 1.0-(1.0-B1)*((1.0-H1)**2.0)
      Z0 = (2.0/3.0)*(Z1/Z2)
C
      N = 0
25    N = N+1
      IF (APR.EQ.0.0) GOTO 55
      IF (RM1.EQ.0.0) GOTO 55
C
      H8=(3.0-2*H1)
      H9=(3.0*H1)-6.0+(6.0*RM1)
      C1=3.0*(RM1-1.0)*B1
      C2=(6.0*ARX2*RM1) + ((1.0-B1)*H1*H9)
      C3=(H1**2*(1.0-B1)*H8) - (6.0*ARX2*RM1)
      C4=3.0*RM1*(1.0-B1)*(H1)**2
C
      X1=0.5
C
40    FN1 = ((X1)**3*B1)+((X1)**2*C1)+((X1)*C2)+C3-C4
      FN2 = 3.0*(X1)**2*B1 + 2.0*(X1)*C1 +C2
      FN3 = FN1/FN2
      X1  = X1-(FN1/FN2)
```

```
      SP = ABS(FN3)
      IF (SP.LE.0.001) GOTO 50
      GOTO 40
C
50    IF (X1.GT.0.000) GOTO  51
      X1 = 0.90
      GOTO 40
55    X91 = ((1.0-B1)*H1 + ARX2)**2.0 +
     1       B1*((1.0-B1)*(H1)**2.0 +  2.0*ARX2)
      X9  = SQRT(X91)
      X1  = (-(1.0-B1)*H1-ARX2+(X9))/B1
51    AXIS = X1
C
      IF (N.GT.1) GOTO 52
      IF (X1.GT.H1) GOTO 52
      B1 = 1.0
      GOTO 25
52    IF (X1.LE.H1) GOTO 90
      WRITE(6,42)AXIS
42    FORMAT(' NEUTRAL AXIS = ',F7.3)
C
      C5 = (1.0-B1)*((X1)**2.0+H1**2.0-2.0*(X1)*(H1))
      C6 = (1.0-B1)*((X1)**2+H1**2-2.0*(X1)*H1)
     1     *(3.0-2.0*H1-X1)
      C7 = (X1)**2*(3.0-X1)-C6
C
      F1 =(3.0*RM1*((X1)**2-C5)/C7)-1.0
C
C LEVER-ARM, ZARM IN TERM OF D
      ZARM = C7/(3.0*((X1)**2.0-C5))
      GOTO 100
90    ZARM = (X1**2.0*(3.0-X1))/(3.0*(X1)**2.0)
C
100   RETURN
      END
```